Basics of Foundation Design

Electronic Edition, November 2009

Bengt H. Fellenius

Dr. Tech., P. Eng.

www.Fellenius.net

Reference:
Fellenius, B.H., 2009. Basics of foundation design.
Electronic Edition. www.Fellenius.net, 346 p.

Basics of Foundation Design

Electronic Edition, November 2009

Bengt H. Fellenius

Dr. Tech., P. Eng.

9658 First Street
Sidney, British Columbia
Canada, V8L 3C9

E-address: <Bengt@Fellenius.net>
Web site: **www.Fellenius.net**

BASICS OF FOUNDATION DESIGN

TABLE OF CONTENTS

P R E F A C E

This copy of the "Red Book" is an update of previous version completed in January 2009 with amendments in March and November of, primarily Chapters 7 and 8. The text is available for free downloading from the author's web site, [**www.Fellenius.net**] and dissemination of copies is encouraged. The author has appreciated receiving comments and questions triggered by the earlier versions of the book and hopes that this revised and expanded text (now consisting of 346 pages as opposed to 275 pages) will bring additional questions and suggestions. Not least welcome are those pointing out typos and mistakes in the text to correct in future updated versions. Note that the web site downloading link includes copies several technical articles that provide a wider treatment of the subject matters.

The "Red Book" presents a background to conventional foundation analysis and design. The origin of the text is two-fold. First, it is a compendium of the contents of courses in foundation design given by the author during his years as Professor at the University of Ottawa, Department of Civil Engineering. Second, it serves as a background document to the software developed by former students and marketed in UniSoft Ltd. in collaboration with the author.

The text is not intended to replace the much more comprehensive 'standard' textbooks, but rather to support and augment these in a few important areas, supplying methods applicable to practical cases handled daily by practicing engineers.

The text concentrates on the static design for stationary foundation conditions, though the topic is not exhaustively treated. However, it does intend to present most of the basic material needed for a practicing engineer involved in routine geotechnical design, as well as provide the tools for an engineering student to approach and solve common geotechnical design problems. Indeed, the author makes the somewhat brazen claim that the text actually goes a good deal beyond what the average geotechnical engineer usually deals with in the course of an ordinary design practice.

The text emphasizes two main aspects of geotechnical analysis, the use of effective stress analysis and the understanding that the vertical distribution of pore pressures in the field is fundamental to the relevance of any foundation design. Indeed, foundation design requires a solid understanding of the in principle simple, but in reality very complex interaction of solid particles with the water and gas present in the pores, as well as an in-depth recognition of the most basic principle in soil mechanics, the *principium* of effective stress.

To avoid the easily introduced errors of using buoyant unit weight, the author recommends to use the straight-forward method of calculating the effective stress from determining separately the total stress and pore pressure distributions, finding the effective stress distribution quite simply as a subtraction between the two. The method is useful for the student and the practicing engineer alike.

The text starts with a brief summary of phase system calculations and how to determine the vertical distribution of stress underneath a loaded area applying the methods of 2:1, Boussinesq, and Westergaard.

The author holds that the piezocone (CPTU) is invaluable for the engineer charged with determining a soil profile and estimating key routine soil parameters at a site. Accordingly, the second chapter gives a background to the soil profiling from CPTU data. This chapter is followed by a summary of methods of routine settlement analysis based on change of effective stress. More in-depth aspects, such as creep and lateral flow are very cursorily introduced or not at all, allowing the text to expand on the influence of adjacent loads, excavations, and groundwater table changes being present or acting simultaneously with the foundation analyzed.

Consolidation analysis is treated sparingly in the book, but for the use and design of acceleration of consolidation by means of vertical drains, which is a very constructive tool for the geotechnical engineers that could be put to much more use than is the current case.

Earth stress – earth pressure – is presented with emphasis on the Coulomb formulae and the effect of sloping retaining walls and sloping ground surface with surcharge and/or limited area surface or line loads per the requirements in current design manuals and codes. Bearing capacity of shallow foundations is introduced and the importance of combining the bearing capacity design analysis with earth stress and horizontal and inclined loading is emphasized. The Limit States Design or Load and Resistance Factor Design for retaining walls and footings is also presented in this context.

The design of piles and pile groups is only very parsimoniously treated in most textbooks. This text, therefore, spends a good deal of effort on presenting the static design of piles considering capacity, negative skin friction, and settlement, emphasizing the interaction of load-transfer and settlement (downdrag), which the author has termed "the Unified Piled Foundation Design", followed by a separate chapter on the analysis of static loading tests. The author holds the firm conviction that the analysis is not completed until the results of the test in terms of load distribution is correlated to an effective stress analysis.

Basics of dynamic testing is presented. The treatment is not directed toward the expert, but is intended to serve as background to the general practicing engineer.

Frequently, many of the difficulties experienced by the student in learning to use the analytical tools and methods of geotechnical engineering, and by the practicing engineer in applying the 'standard' knowledge and procedures, lie with a less than perfect feel for the terminology and concepts involved. To assist in this area, a brief chapter on preferred terminology and an explanation to common foundation terms is also included.

Everyone surely recognizes that the success of a design to a large extent rests on an equally successful construction of the designed project. However, many engineers appear to oblivious that one key prerequisite for success of the construction is a dispute-free interaction between the engineers and the contractors during the construction, as judged from the many acutely inept specs texts common in the field. The author has added a strongly felt commentary on the subject at the end of the book.

A relatively large portion of the space is given to presentation of solved examples and problems for individual practice. The problems are of different degree of complexity, but even when very simple, they intend to be realistic and have some relevance to the practice of engineering design.

Finally, most facts, principles, and recommendations put forward in this book are those of others. Although several pertinent references are included, these are more to indicate to the reader where additional information can be obtained on a particular topic, rather than to give professional credit. However, the author is well aware of his considerable indebtedness to others in the profession from mentors, colleagues, friends, and collaborators throughout his career, too many to mention. The opinions and sometimes strong statements are his own, however, and the author is equally aware that time might suggest a change of these, often, but not always, toward the mellow side.

The author is indebted to Dr. Mauricio Ochoa, PE, for his careful review of the new version after it was first uploaded in January, and for his informing the author about the many typos in need of correction as well as making many most pertinent and much appreciated suggestions for clarifications and add-ons.

Sidney November 2009

Bengt H. Fellenius

9658 First Street
Sidney, British Columbia
V8L 3C9

Tel: (778) 426-0775
E: <Bengt@Fellenius.net>
[www.Fellenius.net]

CHAPTER 1

CLASSIFICATION, EFFECTIVE STRESS, and STRESS DISTRIBUTION

1.1 Introduction

Before a foundation design can be embarked on, the associated soil profile must be well established. The soil profile is compiled from three cornerstones of information**:**

- in-situ testing results, particularly continuous tests, such as the CPTU
  and laboratory classification and testing of recovered soil samples
- pore pressure (piezometer) observations
- assessment of the overall site geology

Projects where construction difficulties, disputes, and litigations arise often have one thing in common**:** borehole logs were thought sufficient when determining the soil profile.

The essential part of the foundation design is to devise a foundation type and size that will result in acceptable values of deformation (settlement) and an adequate margin of safety to failure (the degree of utilization of the soil strength). Deformation is ***due to change*** of effective stress and soil strength is ***proportional*** to effective stress. Therefore, all foundation designs must start with determining the effective stress distribution of the soil around and below the foundation unit. That distribution then serves as basis for the design analysis.

Effective stress is the total stress minus the pore pressure (the water pressure in the voids). Determining the effective stress requires that the basic parameters of the soil are known. That is, the pore pressure distribution and the Phase Parameters, such as water content[1] and total density. Unfortunately, far too many soil reports lack adequate information on both pore pressure distribution and phase parameters.

1.2 Phase Parameters

Soil is an “interparticulate medium”. A soil mass consists of a heterogeneous collection of solid particles with voids in between. The solids are made up of grains of minerals or organic material. The voids contain water and gas. The water can be clean or include dissolved salts and gas. The gas is similar to ordinary air, sometimes mixed with gas generated from decaying organic matter. The ***solids***, the ***water***, and the ***gas*** are termed the three **phases** of the soil.

To aid a rational analysis of a soil mass, the three phases are “disconnected”. Soil analysis makes use of basic definitions and relations of volume, mass, density, water content, saturation, void ratio, etc., as indicated in Fig. 1.1. The definitions are related and knowledge of a few will let the geotechnical engineer derive all the others.

---

1 The term "moisture content" is sometimes used in the same sense as "water content". Most people, even geotechnical engineers, will consider that calling a soil "moist", "damp", or "wet" signifies different conditions of the soils (though undefined). It follows that laymen, read lawyers and judges, will believe and expect that "moisture content" is something different to "water content", perhaps thinking that the former indicates a less than saturated soil. However, there is no difference, It is only that saying "moisture" instead of "water" implies a greater degree of sophistication of the User, and, because the term is not immediately understood by the layman, its use sends the message that the User is in the "know", a specialist of some stature. Don't fall into that trap. Use "water content". Remember, we should strive to use simple terms that laymen can understand. (Quoted from Chapter 10).

The need for phase systems calculation arises, for example, when the engineer wants to establish the effective stress profile at a site and does not know the total density of the soil, only the water content. Or, when determining the dry density and degree of saturation from the initial water content and total density in a Proctor test. Or, when calculating the final void ratio from the measured final water content in an oedometer test. While the water content is usually a measured quantity and, as such, a reliable number, many of the other parameters reported by a laboratory are based on an assumed value of solid density, usually taken as 2,670 kg/m^3 plus the assumption that the tested sample is saturated. The latter assumption is often very wrong and the error can result in significantly incorrect soil parameters.

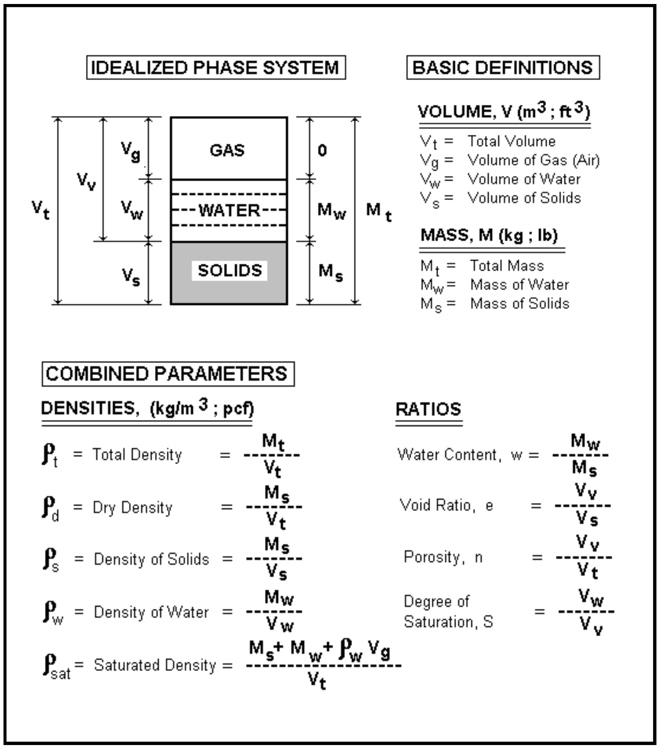

Fig. 1.1 The Phase System definitions

Starting from the definitions shown In Fig. 1.1, a series of useful formulae can be derived, as follows:

(1.1) $$S = \frac{w}{\rho_w} \times \frac{\rho_s \rho_d}{\rho_s - \rho_d} = \frac{w}{e} \times \frac{\rho_s}{\rho_w}$$

(1.2) $$w = S \rho_w \times \frac{\rho_s - \rho_d}{\rho_s \rho_d} = \frac{\rho_t}{\rho_d} - 1$$

(1.3) $$\rho_{SAT} = \frac{M_w + \rho_w V_g + M_s}{V_t} = \rho_d + \rho_w (1 - \frac{\rho_d}{\rho_s}) = \frac{\rho_d}{\rho_s}(\rho_s + e\rho_w) = \rho_s \frac{1+w}{1+e}$$

(1.4) $$\rho_d = \frac{\rho_s}{1+e} = \frac{\rho_t}{1+w} = \frac{\rho_w\, S}{w + \dfrac{\rho_w}{\rho_s} S}$$

(1.5) $$\rho_t = \frac{\rho_s(1+w)}{1+e} = \rho_d(1+w)$$

(1.6) $$e = \frac{n}{1-n} = \frac{\rho_s}{\rho_d} - 1 = \frac{w}{S} \times \frac{\rho_s}{\rho_w}$$

(1.7) $$n = \frac{e}{1 = e} = 1 - \frac{\rho_d}{\rho_s}$$

When performing phase calculations, the engineer normally knows or assumes the value of the density of the soil solids, ρ_t. Sometimes, the soil can be assumed to be fully saturated (however, presence of gas in fine-grained soils may often result in their not being fully saturated even well below the groundwater table; organic soils are rarely saturated and fills are almost never saturated). Knowing the density of the solids, ρ_t, and one more parameter, such as the water content, all other relations can be calculated using the above formulae (they can also be found in many elementary textbooks, or easily be derived from the basic definitions and relations*).

The density of water is usually 1,000 kg/m^3. However, temperature and, especially, salt content can change this value by more than a few percentage points. For example, places in Syracuse, NY, have groundwater that has a salt content of up to 16 % by weight. Such large salt content cannot be disregarded when determining distribution of pore pressure and effective stress.

While most silica-based clays can be assumed to made up of particles with a solid density of 2,670 kg/m^3 (165 pcf), the solid density of other clay types may be quite different. For example, calcareous clays can have a solid density of 2,800 kg/m^3 (175 pcf). However, at the same time, calcareous soils, in particular coral sands, can have such a large portion of voids that the bulk density is quite low compared to that of silica soils. Indeed, mineral composed of different material can have a very different mechanical response to load. For example, just a few percent of mica in a sand will make the sand weaker and more compressible, all other aspects equal (Gilboy 1928).

---

*) The program UniPhase provides a fast and easy means to phase system calculations. The program is available for free downloading as "176 UniPhase.zip" from the author's web site [www.Fellenius.net]. When working in UniPile and UniSettle, or some other geotechnical program where input is total density, the User normally knows the water content and has a good feel for the solid density. The total density value to input is then the calculated by UniPhase. When the User compiles the result of a oedometer test, the water content and the total density values are normally the input and UniPhase is used to determine the degree of saturation and void ratio.

Organic materials usually have a solid density that is much smaller than inorganic material. Therefore, when soils contain organics, their average solid density is usually smaller than for inorganic materials.

Soil grains are composed of minerals and the solid density varies between different minerals. Table 1.1 below lists some values of solid density for minerals that are common in rocks and, therefore, common in soils. (The need for listing the densities in both units could have been avoided by giving the densities in relation to the density of water, which is called "relative density" in modern international terminology and "specific gravity" in old, now abandoned terminology. However, presenting instead the values in both systems of units avoids the conflict of which of the two mentioned terms to use; either the correct term, which many would misunderstand, or the incorrect term, which all understand, but the use of which would suggest ignorance of current terminology convention. Shifting to a home-made term, such as "specific density", which sometimes pops up in the literature, does not make the ignorance smaller).

Table 1.1 Solid Density for Minerals

Mineral Type	**Solid Density** kg/m^3	pcf
Amphibole	≅3,000+	190
Calcite	2,800	180
Quartz	2,670	165
Mica	2,800	175
Pyrite	5,000	310
Illite	2,700	170

Depending on the soil void ratio and degree of saturation, the total density of soils can vary within wide boundaries. Tables 1.2 and 1.3 list some representative values.

Table 1.2 Total saturated density for some typical soils

Soil Type	**Saturated** Total Density Metric (SI) units kg/m^3	English units pcf
Sands; gravels	1,900 - 2,300	118 - 144
Sandy Silts	1,700 - 2,200	105 - 138
Clayey Silts and Silts	1,500 - 1,900	95 - 120
Soft clays	1,300 - 1,800	80 - 112
Firm clays	1,600 - 2,100	100 - 130
Glacial till	2,100 - 2,400	130 - 150
Peat	1,000 - 1,200	62 - 75
Organic silt	1,200 - 1,900	75 - 118
Granular fill	1,900 - 2,200	118 - 140

Table 1.3 Total saturated density for uniform silica sand

"Relative" Density	Total Saturated Density kg/m^3	Water Content %	Void Ratio (**subjective**)
Very dense	2,200	15	0.4
Dense	2,100	19	0.5
Compact	2,050	22	0.6
Loose	2,000	26	0.7
Very loose	1,900	30	0.8

1.3 Soil Classification by Grain Size

All languages describe "clay", "sand", "gravel", etc., which are terms primarily based on grain size. In the very beginning of the 20th century, Atterberg, a Swedish scientist and agriculturalist, proposed a classification system based on specific grain sizes. With minor modifications, the Atterberg system is still used and are the basis of the International Geotechnical Standard, as listed in Table 1.4

Table 1.4 Classification of Grain Size Boundaries (mm)

Clay		<	0.002
Silt			
Fine silt	0.002	<	0.006
Medium silt	0.006	<	0.002
Coarse silt	0.002	<	0.06
Sand			
Fine sand	0.06	<	0.2
Medium sand	0.2	<	0.6
Coarse sand	0.6	<	2.0
Gravel			
Fine gravel	2	<	6
Medium gravel	6	<	20
Coarse gravel	20	<	60
Cobbles	60	<	200
Boulders	200	<	

Soil is made up of grains with a wide range of sizes and is named according to the portion of the specific grain sizes. Several classification systems are in use, e.g., ASTM, AASHTO, and International Geotechnical Society. Table 1.5 indicates the latter, which is also the Canadian standard (CFEM 1992).

The International (and Canadian) naming convention differs in some aspects from the AASHTO and ASTM systems which are dominant in US practice. For example, the boundary between silt and sand in the international standard is at 0.060 mm, whereas the AASHTO and ASTM standards place that boundary at Sieve #200 which has an opening of 0.075 mm. Table 1.5 follows the International standard. For details and examples of classification systems, see Holtz and Kovacs (1981).

Table 1.5 Classification of Grain Size Boundaries (mm)

"Noun" (Clay, Silt, Sand, Gravel)	35	<	100 %
"and" plus noun	20 %	<	35 %
"adjective" (clayey, silty, sandy)	10%	<	20%
"trace" (clay, silt, sand, gravel)	1 %	<	10 %

The grain size distribution for a soil is determined using a standard set of sieves. Conventionally, the results of the sieve analysis are plotted in diagram drawn with the abscissa in logarithmic scale as shown in Fig. 1.2. The three grain size curves, A, B, and C, shown are classified according to Table 1.5 as A: "*Sand trace gravel*". B: Sandy clay some silt, and C: would be named clayey sandy silt some gravel. Samples A and B are alluvial soils and are suitably named. However, Sample C, having 21 %, 44 %, 23 %, and 12 % of clay, silt, sand, and gravel size grains, is from a glacial till for which soil all grain size portions are conventionally named as adjective to the noun "till", i.e., the sample is a "*clayey sandy silty glacial till*".

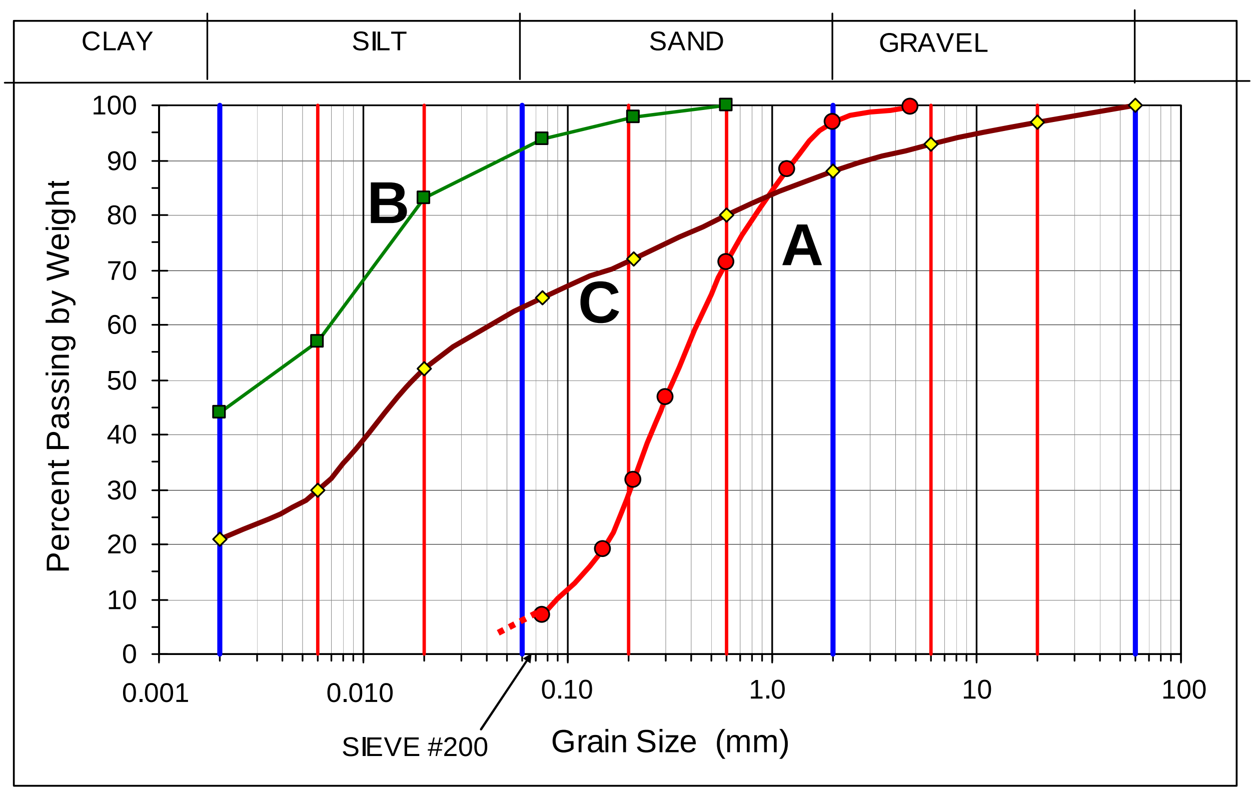

Fig. 1.2 Grain size diagram

Sometimes grain-size analysis results are plotted in a three-axes diagram called "ternary diagram" as illustrated in Fig. 1.3, which allows for a description according to grain size portions to be obtained at a glance.

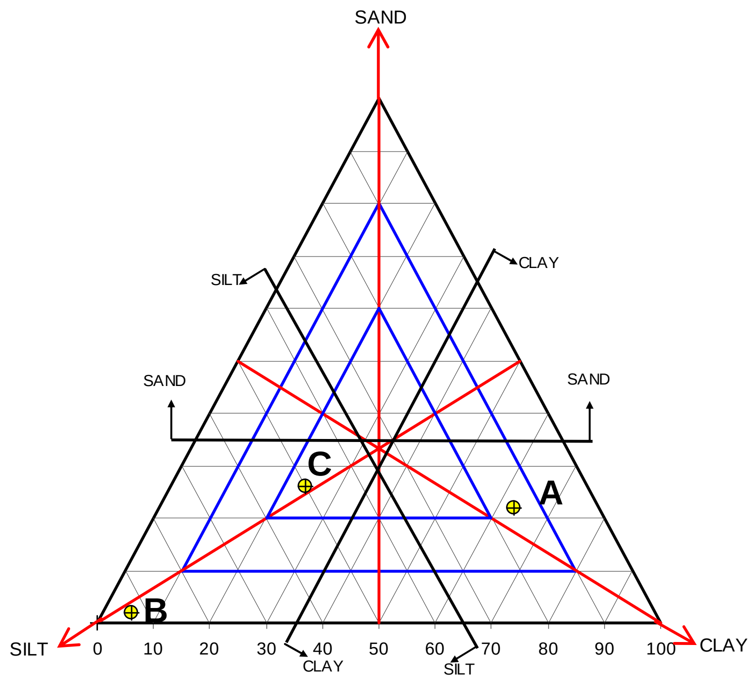

Fig. 1.3 Example of a ternary diagram

1.4. Effective Stress

As mentioned, effective stress is the total stress minus the pore pressure (the water pressure in the voids). Total stress at a certain depth is the easiest of all values to determine as it is the summation of the total unit weight (total density times gravity constant) and height. If the distribution of pore water pressure at the site is hydrostatic, then, the pore pressure at that same point is the height of the water column up to the **groundwater table**, which is defined as the uppermost level of zero pore pressure. (Notice, the soil can be partially saturated also above the groundwater table. Then, because of capillary action, pore pressures in the partially saturated zone above the groundwater table may be negative. In routine calculations, pore pressures are usually assumed to be zero in the zone above the groundwater table).

Notice, however, the pore pressure distribution is not always hydrostatic, far from it actually. Hydrostatic pore water pressure has a vertical pressure gradient that is equal to unity (no vertical flow). Similarly, a site may have a downward gradient from a perched groundwater table, or an upward gradient from an **aquifer** down below (an aquifer is a soil layer containing free-flowing water).

Frequently, the common method of determining the effective stress, $\Delta\sigma'$ contributed by a soil layer is to multiply the buoyant unit weight, γ', of the soil with the layer thickness, Δh, as indicated in Eq. 1.8a.

(1.8a) $$\Delta\sigma' = \gamma'\Delta h$$

The effective stress at a depth, σ'_z is the sum of the contributions from the soil layers, as follows.

(1.8b) $$\sigma'_z = \sum(\gamma'\Delta h)$$

The buoyant unit weight, γ', is often thought to be equal to the total unit weight (γ_t) of the soil minus the unit weight of water (γ_w) which presupposes that there is no vertical gradient of water flow in the soil, $i = 0$, defined below. However, this is only a special case. Because most sites display either an upward flow, maybe even artesian (the head is greater than the depth), or a downward flow, calculations of effective stress must consider the effect of the gradient — the buoyant unit weight is a function of the gradient in the soil as follows.

(1.8c) $$\gamma' \;=\; \gamma_t - \gamma_w(1 - i)$$

where
σ' = effective overburden stress
Δh = layer thickness
γ' = buoyant unit weight
γ_t = total (bulk) unit weight
γ_w = unit weight of water
i = upward gradient

The **gradient**, ***i***, is defined as the difference in head between two points divided by the distance the water has to flow between these two points. Upward flow gradient is negative and downward flow gradient is positive. For example, if, for a particular case of artesian condition, the gradient is nearly equal to -1, then, the buoyant weight is nearly zero. Therefore, the effective stress is close to zero, too, and the soil has little or no strength. This is the case of “quick sand”, which is not a particular type of sand, but a soil, usually a silty fine sand, subjected to a particular pore pressure condition.

The gradient in a non-hydrostatic condition is often awkward to determine. However, the difficulty can be avoided, because the effective stress is most easily found by calculating the total stress and the pore water pressure separately. The effective stress is then obtained by simple subtraction of the latter from the former.

Note, the difference in terminology—effective *stress* and pore *pressure*—which reflects the fundamental difference between forces in soil as opposed to in water. Stress is directional, that is, stress changes depending on the orientation of the plane of action in the soil. In contrast, pressure is omni-directional, that is, independent of the orientation. Don't use the term "*soil pressure*", it is a misnomer.

The soil stresses, total and effective, and the water pressures are determined, as follows: The **total vertical stress** (symbol σ_z) at a point in the soil profile (also called “total overburden stress”) is calculated as the stress exerted by a soil column determined by multiplying the soil total (or bulk) unit weight times the height of the column (or the sum of separate weights when the soil profile is made up of a series of separate soil layers having different unit weights). The symbol for the total unit weight is γ_t (the subscript “t” stands for “total”).

(1.9) $$\sigma_z = \gamma_t\, z \qquad \text{or:} \qquad \sigma_z = \Sigma\, \Delta\sigma_z = \Sigma\, (\gamma_t\, \Delta h)$$

Similarly, the **pore pressure** (symbol u), if measured in a stand-pipe, is equal to the unit weight of water, γ_w, times the height of the water column, h, in the stand-pipe. (If the pore pressure is measured directly, the head of water is equal to the pressure divided by the unit weight of the water, γ_w).

(1.10) $$u = \gamma_w\, h$$

The height of the column of water (the head) representing the water pressure is usually not the distance to the ground surface nor, even, to the groundwater table. For this reason, the height is usually referred to as the “phreatic height” or the “piezometric height” to separate it from the depth below the groundwater table or depth below the ground surface.

The pore pressure distribution is determined by applying the fact that (in stationary situations) the pore pressure distribution can be assumed linear in each individual, or separate, soil layer, and, in pervious soil layers that are "sandwiched" between less pervious layers, the pore pressure is hydrostatic (that is, the vertical gradient is unity). (Note, if the pore pressure distribution within a specific soil layer is not linear, then, the soil layer is undergoing consolidation).

The **effective overburden stress** (symbol σ'_z), also called "effective vertical stress", is then obtained as the difference between total stress and pore pressure.

(1.11) $\sigma'_z = \sigma_z - u_z = \gamma_t z - \gamma_w h$

Usually, the geotechnical engineer provides a unit density, ρ, instead of the unit weight, γ. The unit density is mass per volume and unit weight is force per volume. Because in the customary English system of units, both types of units are given as lb/volume, the difference is not clear (that one is pound-mass and the other is pound-force is not normally indicated). In the SI-system, unit density is given in kg/m^3 and unit weight is given in N/m^3. Unit weight is unit density times the gravitational constant, g. (For most foundation engineering purposes, the gravitational constant can be taken to be 10 m/s^2 rather than the overly exact value of 9.81 m/s^2).

(1.12) $\gamma = \rho g$

Many soil reports do not indicate the bulk or total soil density, ρ_t, and provide only the water content, w, and the dry density, ρ_d. Knowing the dry density, the total density of a saturated soil can be calculated as:

(1.5) $\rho_t = \rho_d (1 + w)$

1.5 Stress Distribution

Load applied to the surface of a body distributes into the body over a successively wider area. The simplest way to calculate the stress distribution is by means of the 2:1 method. This method assumes that the load is distributed over an area that increases in width in proportion to the depth below the loaded area, as is illustrated in Fig. 1.4. Since the same vertical load, Q, acts over the increasingly larger area, the stress (load per surface area) diminishes with depth. The mathematical relation is as follows.

(1.14) $$q_z = q_0 \times \frac{B \times L}{(B+z) \times (L+z)}$$

where q_z = stress at Depth z
z = depth where q_z is considered
B = width (breadth) of loaded area
L = length of loaded area
q_0 = applied stress = Q/B L

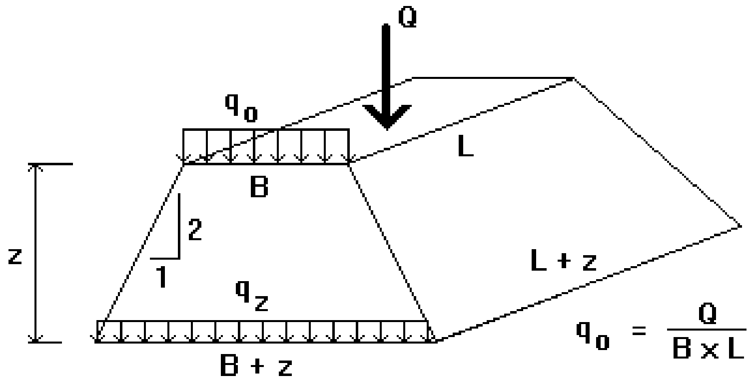

Fig. 1.4 The 2:1 method

Note, the 2:1 distribution is only valid inside (below) the footprint of the loaded area and must never be used to calculate the stress outside the footprint.

Example 1.1 The principles of calculating effective stress and stress distribution are illustrated by the calculations involved in the following soil profile**:** An upper 4 m thick layer of normally consolidated sandy silt is deposited on 17 m of soft, compressible, slightly overconsolidated clay, followed by, 6 m of medium dense silty sand and, hereunder, a thick deposit of medium dense to very dense sandy ablation glacial till. The densities of the four soil layers and the earth fill are: 2,000 kg/m^3, 1,700 kg/m^3, 2,100 kg/m^3, 2,200 kg/m^3, and 2,000 kg/m^3, respectively. The groundwater table lies at a depth of 1.0 m. For "original conditions", the pore pressure is hydrostatically distributed from the groundwater table throughout the soil profile. For "final conditions", the pore pressure in the sand is changed. Although still hydrostatically distributed (which is the case in a more pervious soil layer sandwiched between less pervious soils—a key fact to consider when calculating the distribution of pore pressure and effective stress), it has increased and has now a phreatic height above ground of 5 m; the phreatic height reaching above ground makes the pressure condition "artesian". Moreover, the pore pressure in the clay has become non-hydrostatic. Note, however, that it is linear, assuming that the "final" condition is long-term, i.e., the pore pressure has stabilized. The pore pressure in the glacial till is assumed to remain hydrostatically distributed. For those "final conditions", a 1.5 m thick earth fill has been placed over a square area with a 36 m side.

Calculate the distribution of total and effective stresses, and pore pressure underneath the center of the earth fill before and after placing the earth fill. Distribute the earth fill, by means of the 2:1-method, that is, distribute the load from the fill area evenly over an area that increases in width and length by an amount equal to the depth below the base of fill area (Eq. 1.14).

Table 1.6 presents the results of the stress calculation for the Example 1.1 conditions. The calculation results are presented in the format of a spread sheet "hand calculation" format to ease verifying the computer calculations. Notice that performing the calculations at every metre depth is normally not necessary. The table includes a comparison between the non-hydrostatic pore pressure values and the hydrostatic, as well as the effect of the earth fill, which can be seen from the difference in the values of total stress for "original" and "final" conditions.

TABLE 1.6
STRESS DISTRIBUTION (2:1 METHOD) BELOW CENTER OF EARTH FILL
[Calculations by means of UniSettle]

ORIGINAL CONDITION (no earth fill)				**FINAL CONDITION** (with earth fill)		
Depth (m)	σ_0 (KPa)	u_0 (KPa)	σ_0' (KPa)	σ_1 (KPa)	u_1 (KPa)	σ_1' (KPa)
Layer 1	**Sandy silt**	**ρ = 2,000 kg/m^3**				
0.00	0.0	0.0	0.0	30.0	0.0	30.0
1.00 (**GWT**)	20.0	0.0	20.0	48.4	0.0	48.4
2.00	40.0	10.0	30.0	66.9	10.0	56.9
3.00	60.0	20.0	40.0	85.6	20.0	65.6
4.00	80.0	30.0	50.0	104.3	30.0	74.3
Layer 2	**Soft Clay**	**ρ = 1,700 kg/m^3**				
4.00	80.0	30.0	50.0	104.3	30.0	74.3
5.00	97.0	40.0	57.0	120.1	43.5	76.6
6.00	114.0	50.0	64.0	136.0	57.1	79.0
7.00	131.0	60.0	71.0	152.0	70.6	81.4
8.00	148.0	70.0	78.0	168.1	84.1	84.0
9.00	165.0	80.0	85.0	184.2	97.6	86.6
10.00	182.0	90.0	92.0	200.4	111.2	89.2
11.00	199.0	100.0	99.0	216.6	124.7	91.9
12.00	216.0	110.0	106.0	232.9	138.2	94.6
13.00	233.0	120.0	113.0	249.2	151.8	97.4
14.00	250.0	130.0	120.0	265.6	165.3	100.3
15.00	267.0	140.0	127.0	281.9	178.8	103.1
16.00	284.0	150.0	134.0	298.4	192.4	106.0
17.00	301.0	160.0	141.0	314.8	205.9	109.0
18.00	318.0	170.0	148.0	331.3	219.4	111.9
19.00	335.0	180.0	155.0	347.9	232.9	114.9
20.00	352.0	190.0	162.0	364.4	246.5	117.9
21.00	369.0	200.0	169.0	381.0	260.0	121.0
Layer 3	**Silty Sand**	**ρ = 2,100 kg/m^3**				
21.00	369.0	200.0	169.0	381.0	260.0	121.0
22.00	390.0	210.0	180.0	401.6	270.0	131.6
23.00	411.0	220.0	191.0	422.2	280.0	142.2
24.00	432.0	230.0	202.0	442.8	290.0	152.8
25.00	453.0	240.0	213.0	463.4	300.0	163.4
26.00	474.0	250.0	224.0	484.1	310.0	174.1
27.00	495.0	260.0	235.0	504.8	320.0	184.8
Layer 4	**Ablation Till**	**ρ = 2,200 kg/m^3**				
27.00	495.0	260.0	235.0	504.8	320.0	184.8
28.00	517.0	270.0	247.0	526.5	330.0	196.5
29.00	539.0	280.0	259.0	548.2	340.0	208.2
30.00	561.0	290.0	271.0	569.9	350.0	219.9
31.00	583.0	300.0	283.0	591.7	360.0	231.7
32.00	605.0	310.0	295.0	613.4	370.0	243.4
33.00	627.0	320.0	307.0	635.2	380.0	255.2

The stress distribution below the center of the loaded area shown in Table 1.1 was calculated by means of the 2:1-method. However, the 2:1-method is rather approximate and limited in use. Compare, for example, the vertical stress below a loaded footing that is either a square or a circle with a side or diameter of B. For the same contact stress, q_0, the 2:1-method, strictly applied to the side and diameter values, indicates that the vertical distributions of stress, [$q_z = q_0/(B + z)^2$] are equal for the square and the circular footings. Yet, the total applied load on the square footing is $4/\pi = 1.27$ times larger than the total load on the circular footing. Therefore, if applying the 2:1-method to circles and other non-rectangular areas, they should be modeled as a rectangle of an equal size ('equivalent') area. Thus, a circle is modeled as an equivalent square with a side equal to the circle radius times $\sqrt{\pi}$.

Notice, the 2:1-method is inappropriate to use for determining the stress distribution below a point at any other location than the center of the loaded area. For this reason, it cannot be used to combine stress from two or more loaded areas unless the areas have the same center. To calculate the stresses induced from more than one loaded area and/or below an off-center location, more elaborate methods, such as the Boussinesq distribution, are required.

1.6 Boussinesq Distribution

The Boussinesq distribution (Boussinesq, 1885; Holtz and Kovacs, 1981) assumes that the soil is a homogeneous, isotropic, linearly elastic half sphere (Poisson's ratio equal to 0.5). The following relation gives the vertical distribution of the stress resulting from the point load. The location of the distribution line is given by the radial distance to the point of application (Fig. 1.5) and calculated by Eq. 1.15.

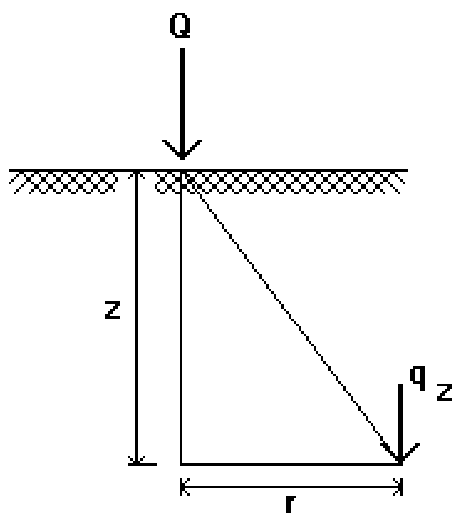

Fig. 1.5. Definition of terms used in Eq. 1.15.

$$q_z = Q \frac{3z^3}{2\pi\,(r^2 + z^2)^{5/2}} \qquad (1.15)$$

where Q = the point load (total load applied)
q_z = stress at Depth z
z = depth where q_z is considered
r = radial distance to the point of application

A footing is usually placed in an excavation and often a fill is placed next to the footing. When calculating the stress increase from one or more footing loads, the changes in effective stress from the excavations and fills must be included, which, therefore, precludes the use of the 2:1-method (unless all such excavations and fills are concentric with the footing).

By means of integrating the point load relation (Eq. 1.15) along a line, a relation for the stress imposed by a line load, P, can be determined as given in Eq. 1.16.

$$(1.16) \qquad q_z = P \frac{2z^3}{\pi\,(r^2 + z^2)^2}$$

where
P = line load (force/ unit length)
q_z = stress at Depth z
z = depth where q_z is considered
r = radial distance to the point of application

1.7 Newmark Influence Chart

Newmark (1935) integrated Eq. 1.15 over a finite area and obtained a relation, Eq. 1.17, for the stress under the **corner of a uniformly loaded rectangular** area, for example, a footing.

$$(1.17) \qquad q_z = q_0 \times I = \frac{A \times B + C}{4\pi}$$

where

$$A = \frac{2mn\sqrt{m^2 + n^2 + 1}}{m^2 + n^2 + 1 + m^2 n^2}$$

$$B = \frac{m^2 + n^2 + 2}{m^2 + n^2 + 1}$$

$$C = \arctan\left[\frac{2mn\sqrt{m^2 + n^2 + 1}}{m^2 + n^2 + 1 - m^2 n^2}\right]$$

and
m = x/z
n = y/z
x = length of the loaded area
y = width of the loaded area
z = depth to the point under the corner where the stress is calculated

Notice that Eq. 1.17 provides the stress in only one point; for stresses at other points, for example when determining the vertical distribution at several depths below the corner point, the calculations have to be performed for each depth. To determine the stress below a point other than the corner point, the area has to be split in several parts, all with a corner at the point in question and the results of multiple calculations summed up to give the answer. Indeed, the relations are rather cumbersome to use. Also restricting the usefulness in engineering practice of the footing relation is that an irregularly shaped area has to be broken up in several smaller rectangular areas. Recognizing this, Newmark (1942) published diagrams called influence charts by which the time and effort necessary for the calculation of the stress below a point was considerably shortened even for an area with an irregularly shaped footprint.

Until the advent of the computer and spread-sheet programs, the influence chart was faster to use than Eq. 1.17, and the Newmark charts became an indispensable tool for all geotechnical engineers. Others developed the Boussinesq basic equation to apply to non-rectangular areas and non-uniformly loaded areas, for example, a uniformly loaded circle or a the trapezoidal load from a sloping embankment. Holtz and Kovacs (1981) include several references to developments based on the Boussinesq basic relation.

A detailed study of the integration reveals that, near the base of the loaded area, the formula produces a sudden change of values. Fig. 1.6 shows the stress distribution underneath the center of a 3-m square footing exerting a contact stress of 100 KPa. Below a depth of about one third of the footing width, the stress diminishes in a steady manner. However, at about one third of the width, there is a kink and the stress above the kink decreases whereas a continued increase would have been expected. The kink is due to the transfer of the point load to stress, which no integration can disguise.

For the same case and set of calculations, Fig. 1.7 shows the influence factor, *I* for the corner of an 1.5 m wide square footing. The expected influence factor immediately below the footing is 0.25, but, for the same reason of incompatibility of point load and stress, it decreases from m = n = about 1.5 (side of "corner" footing = 0.67z; side of "square" footing = 0.33z). Newmark (1935) resolved this conflict by extending the curve, as indicated by the extension lines in Figs. 1.7 and 1.7. by means of adjusting Eq. 1.17 to Eq. 1.17a. The relation shown below the equations, indicates when each equation controls. Although Newmark (1935) included the adjustment, it is not normally included in textbooks (Codetta 1994 being an exception).

(1.17a) $$q_z \quad = \quad q_0 \times I = \frac{A \times B + \pi - C}{4\pi}$$

which is valid where: $\mathbf{m^2 + n^2 + 1 \leq m^2\, n^2}$

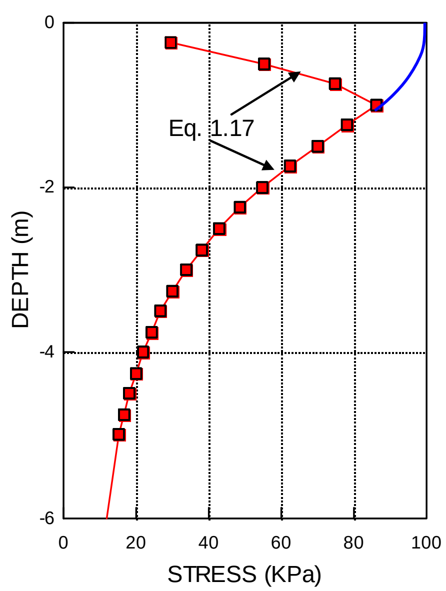

Fig. 1.6. Calculated stress distribution

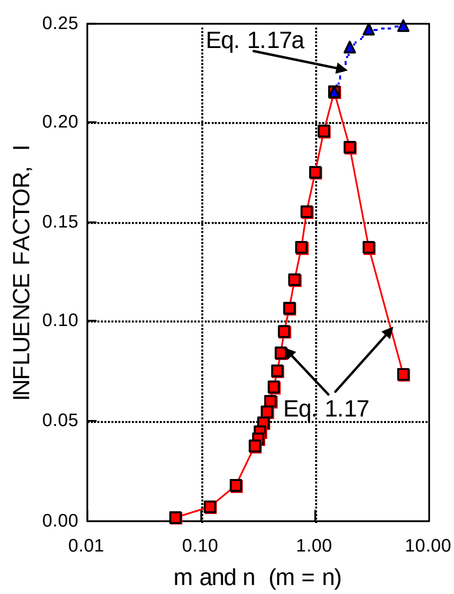

Fig. 1.7. Influence factor

1.8 Westergaard Distribution

Westergaard (1938) suggested that in soil with horizontal layers that restrict horizontal expansion, it would appropriate to assume that the soil layers are rigid horizontally (Poisson's ratio equal to zero) allowing only vertical compression for an imposed stress. Westergaard's solution for the stress caused by a point load is given in Eq. 1.18.

(1.18) $$q_z = \frac{Q}{\pi z^2} = \frac{1}{\left[1+2(r/z)^2\right]^{3/2}}$$

where Q = total load applied
q_z = stress at Depth z
z = depth where q_z is considered
r = radial distance to the point of application

An integration of the Westergaard relation similar to the integration of the Boussinesq relation (Eq. 1.16) results in Eq. 1.19 (Taylor, 1948). For the same reason of incompatibility of dimensions between Load and Stress, a “kink” appears also for the Westergaard solution.

(1.19) $$q_z = q_0 \times I = q_0 \frac{1}{2\pi} \arctan\left[\frac{1}{\sqrt{D+E+F}}\right]$$

where $$D = \frac{1}{2m^2} \qquad E = \frac{1}{2n^2} \qquad F = \frac{1}{4m^2 n^2}$$

and m = x/z
n = y/z
x = length of the loaded area
y = width of the loaded area
z = depth to the point under the corner for where the stress is calculated

Influence charts similar to the Newmark charts for the Boussinesq relation have been developed also for the Westergaard relation. The difference between stresses calculated by one or the other method is small and considered less significant than the differences between reality and the idealistic assumptions behind either theory. The Westergaard method is often preferred over the Boussinesq method when calculating stress distribution in layered soils and below the center portion of wide areas of flexible load.

A small diameter footing, of about 1 metre width, can normally be assumed to distribute the contact stress evenly over the footing contact area. However, this cannot be assumed to be the case for wider footings. Both the Boussinesq and the Westergaard distributions assume ideally flexible footings (and ideally elastic soil), which is not the case for real footings, which are neither fully flexible nor absolutely rigid. Kany (1959) showed that below a so-called **characteristic point**, the vertical stress distribution is equal for flexible and rigid footings. The characteristic point is located at a distance of 0.37 B and 0.37 L from the center of a rectangular footing of sides B and L and at a radius of 0.37 R from the center of a circular footing of radius R. When applying Boussinesq method of stress distribution to regularly shaped footings, the stress below the characteristic point is normally used rather than the stress below the center of the footing to arrive at a representative contact stress to distribute. In fact, with regard to vertical stress distribution, we can normally live with the fact that natural soils are far from perfectly elastic.

The calculations by either of Boussinesq or Westergaard methods are time-consuming. The 2:1 method is faster to use and it is therefore the most commonly used method in engineering practice. Moreover, the 2:1 distribution lies close to the Boussinesq distribution for the characteristic point. However, for calculation of stress imposed by a loaded area outside its own footprint, the 2:1 method cannot be used. Unfortunately, the work involved in a "hand calculation" of stress distribution according the Boussinesq or Westergaard equations for anything but the simplest case involves a substantial effort. To reduce the effort, calculations are normally restricted to involve only a single or very few loaded areas. Stress history, that is, the local preconsolidation effect of previously loaded areas at a site, is rarely included.

Computer programs are now available which greatly simplify and speed up the calculation effort. In particular, the advent of the UniSettle program has drastically reduced the calculation effort even for the most complex conditions and vastly increased the usefulness of the Boussinesq and Westergaard methods.

1.9 Examples

Example 1.2. Fig. 1.8 illustrates the difference between the three stress calculation methods for a square flexible footing with a side equal to "b" and loaded at its center. Forestalling the presentation in Chapter 3, Fig. 1.9 shows the distribution of settlement for the three stress distribution shown in Fig. 1.5. The settlement values have been normalized to the settlement calculated for the distribution calculated according to the Boussinesq method. Figs. 1.10 and 1.11 shows the same for when the load is applied at the so-called characteristic point (0.37b from the center of the footing), below which the stress distributions are the same for a flexible as for a rigid footing.

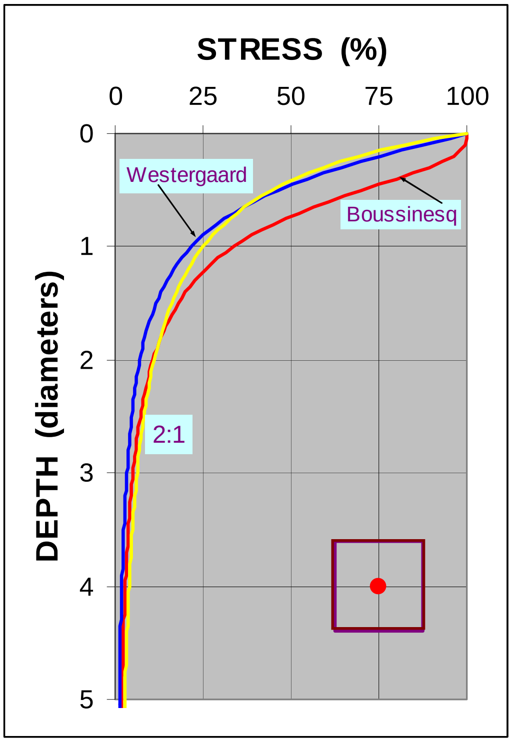

Fig. 1.8 Comparison between the methods

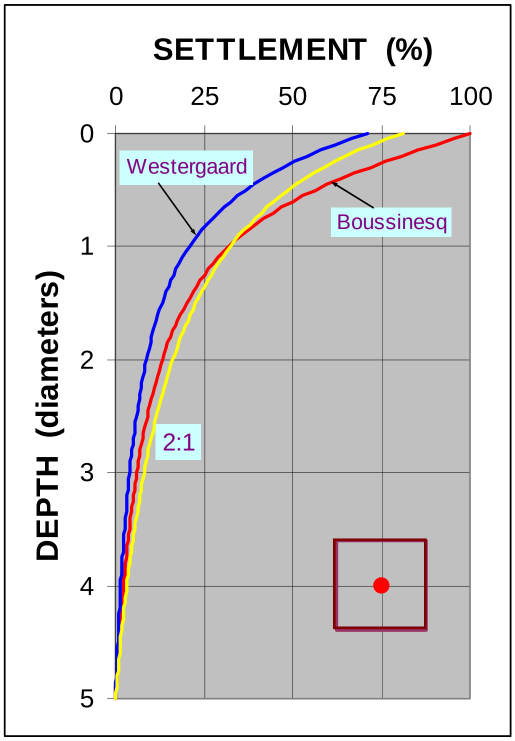

Fig. 1.9 Settlement distributions

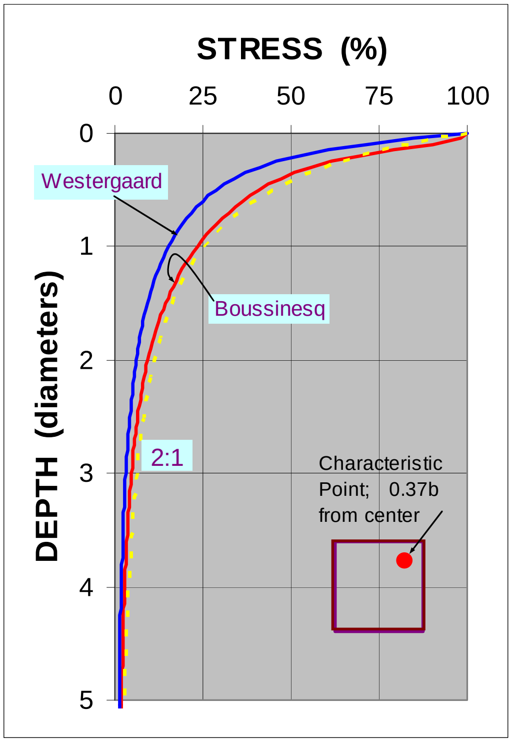

Fig. 1.10 Comparison between the methods

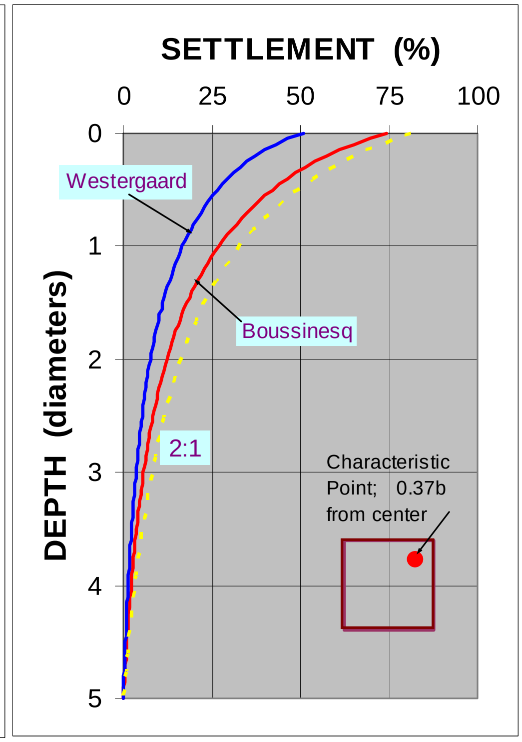

Fig. 1.11 Settlement distributions

As illustrated in Fig. 1.12, calculations using Boussinesq distribution can be used to determine how stress applied to the soil from one building may affect an adjacent existing building.

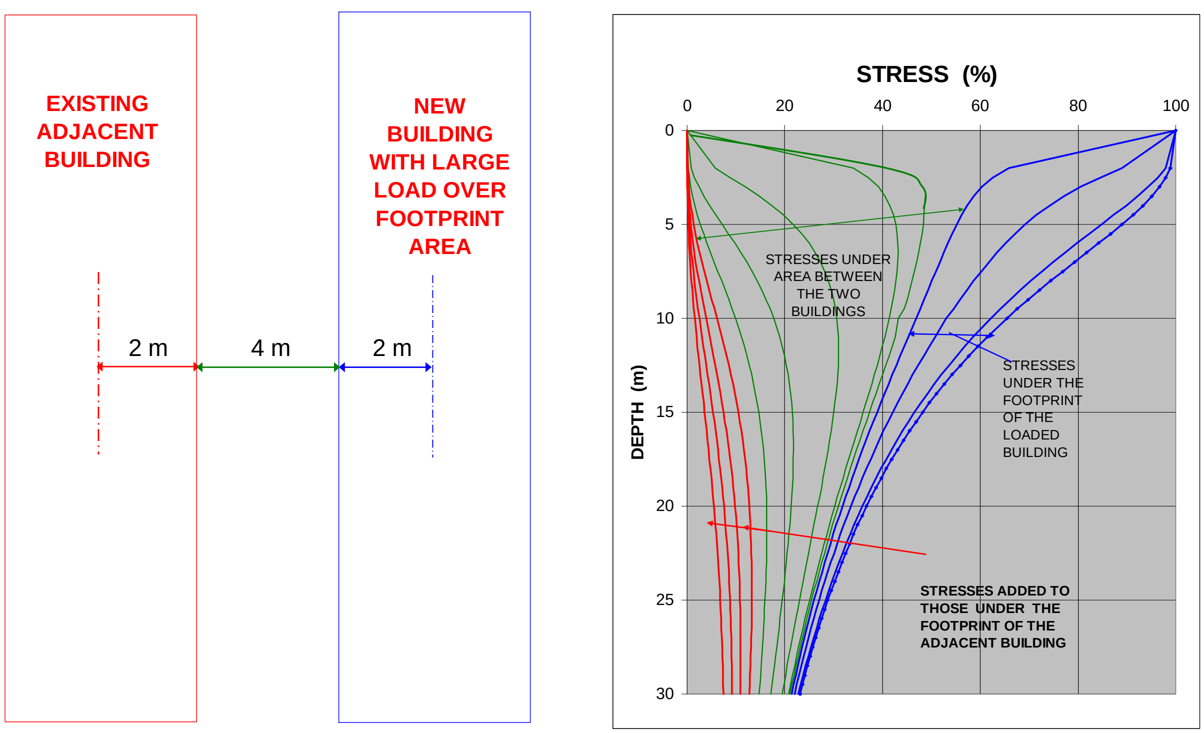

Fig. 1.12 Influence on stress from one building over to an adjacent building.

The load from the existing building is quite close to the preconsolidation margin of the soil, which means that the settlement for the load is small. The new building exerts the same stress on the soil, and the new stress adds to the stress from the existing building resulting in that the virgin compressibility has become engaged. Consequently, the new building will settle more than the existing did. Moreover, the construction of the new building will cause the existing one to undergo additional settlement. The simple stress calculations will make the problem and potential undesirable effect very clear. (For aspects on settlement analysis, see Chapter 3).

CHAPTER 2

USE OF THE CONE PENETROMETER

2.1 Introduction

Design of foundations presupposes that the soil conditions (profile and parameters) at the site have been established by a geotechnical site investigation. Site investigations employ soil sampling and in-situ sounding methods. Most methods consist of intermittent sampling, e.g., the standard penetration test with split-spoon sampling and probing for density—the N-index. Other intermittent methods are the vane, dilatometer, and pressuremeter tests. The only continuous in-situ test is the cone penetrometer test.

In-situ sounding by standardized penetrometers came along early in the development of geotechnical engineering. For example, the Swedish weight-sounding device (Swedish State Railways Geotechnical Commission, 1922), which still is in common use in Sweden and Finland. The cone resistance obtained by this device and other early penetrometers included the influence of soil friction along the rod surface. In the 1930's, a "mechanical cone penetrometer" was developed in the Netherlands where the rods to the cone point were placed inside an outer pipe (a sleeve), separating the cone rods from the soil (Begemann 1963). The mechanical penetrometer was advanced by first pushing the entire system to obtain the combined resistance. Intermittently, every even metre or so, the cone point was advanced a small distance while the outer tubing was held immobile, thus obtaining the cone resistance separately. The difference was the total shaft resistance.

Begemann (1953) introduced a short section sleeve, immediately above the cone point. The sleeve arrangement enabled measuring the shaft resistance over a short distance ("sleeve friction") near the cone. Sensors were placed in the cone and the sleeve to measure the cone resistance and sleeve friction directly (Begemann, 1963). This penetrometer became known as the "electrical cone penetrometer".

In the early 1980's, piezometer elements were incorporated with the electrical cone penetrometer, leading to the modern cone version, "the piezocone", which provides values of cone resistance, sleeve friction, and pore pressure at close distances, usually every 25 mm, but frequently every 10 mm. (The shear resistance along the sleeve, the "sleeve friction" is regarded as a measure of the undrained shear strength—of a sort—the value is recognized as not being accurate; e. g., Lunne et al. 1986, Robertson 1990). Fig. 2.1 shows an example of a piezocone to a depth of 30 m at the site where the soil profile consists of three layers: an upper layer of soft to firm clay, a middle layer of compact silt, and a lower layer of dense sand. The groundwater table lies at a depth of 2.5 m. The CPT values shown in the diagram have been determined at every 50 mm rather than the standardized spacing of 20 mm to 25 mm. (Note, nothing is gained by widening distance between measuring points. Instead valuable information may be lost.).

While a CPT sounding is always aimed vertical, it will bend in the soil, which will cause the cone point to deviate from below the starting point. The bending will also mean that sounding depth becomes shorter; the cone point "lifts". For most cone soundings, deviation from the exact horizontal location and the depth is inconsequential. However, for deep soundings, the deviation can be substantial. Modern CPT equipment will always measure the deviation from the vertical in two directions, which allows the evaluation of the deviation from the ideal. Curiously, the inclination measurements are often not included with a final report. They should be.

The cone penetrometer does not provide a measurement of static resistance, but records the resistance at a certain penetration rate (now standardized to 20 mm/s). Therefore, pore water pressures develop in the soil at the location of the cone point and sleeve that add to the "neutral" pore water pressure. In dense fine sands, which are prone to dilation, the induced pore pressures can significantly reduce the neutral pressure. In pervious soils, such as sands, the pore pressure changes are small, while in less pervious soils, such as silts and clays, they can be quite large. Measurements with the piezocone showed that the cone resistance must be corrected for the pore pressure acting on the cone shoulder (Baligh et al. 1981; Campanella et al. 1982). See Section 2.26 and Eq. 2.1 below.

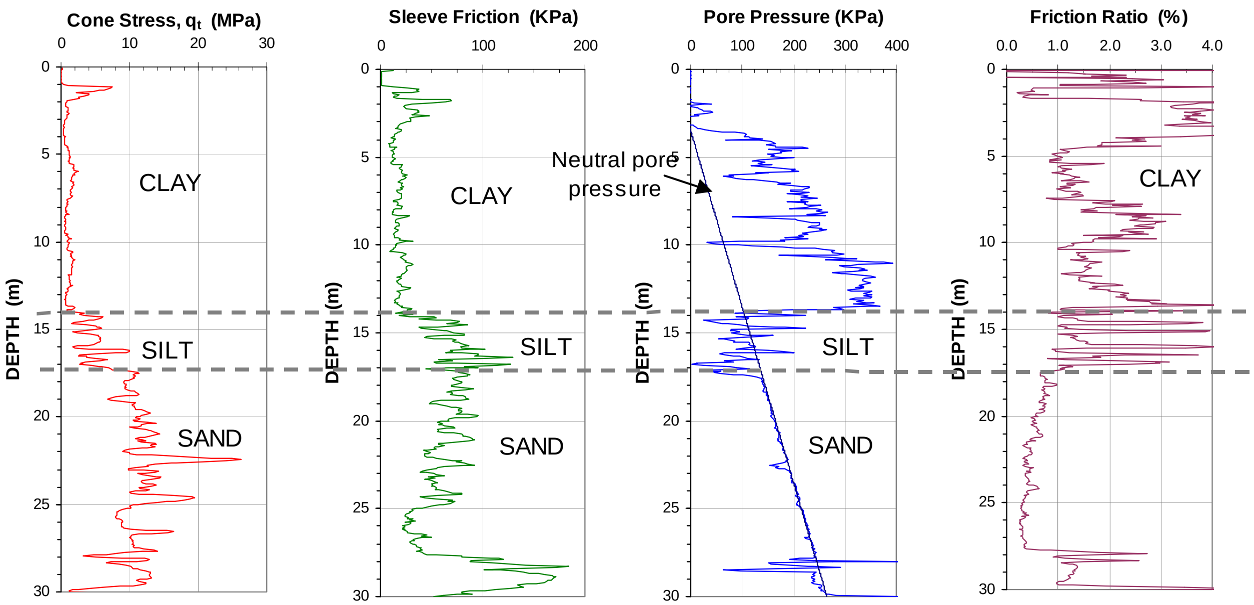

Fig. 2.1 Results from a piezocone to a depth of 30 m

The cone penetrometer test, is simple, fast to perform, economical, supplies continuous records with depth, and allows a variety of sensors to be incorporated with the penetrometer. The direct numerical values produced by the test have been used as input to geotechnical formulae, usually of empirical nature, to determine capacity and settlement, and for soil profiling.

Early cone penetrometers gave limited information that could be used for determining soil type and were limited to determining the location of soil type boundaries. The soil type had to be confirmed from the results of conventional borings. Empirical interpretations were possible but they were limited to the geological area where they had been developed. Begemann (1965) is credited with having presented the first rational soil profiling method based on CPT soundings. With the advent of the piezocone, the CPTU, the cone penetrometer was established as an accurate site investigation tool.

This chapter is a summary to indicate some of the uses of the cone penetrometer test. For a more thorough account the reader is directed to the many reports and papers by Lunne, Mayne, and Robertson, specifically, Robertson and Campanella (1983), Kulhawy and Mayne (1990), Lunne et al. (1997), Mayne et al. (2001), Mayne et al. (2002).

2.2 Brief Survey of Soil Profiling Methods

2.21 Begemann (1965)

Begemann (1965) pioneered soil profiling from the CPT, showing that, while coarse-grained soils generally demonstrate larger values of cone resistance, q_c, and sleeve friction, f_s, as opposed to fine-grained soils, the soil type is not a strict function of either cone resistance or sleeve friction, but of the combination of the these values.

Figure 2.2 presents the Begemann soil profiling chart, showing (linear scales) q_c as a function of f_s. Begemann showed that the soil type is a function of the ratio, the "friction ratio", f_R, between the sleeve friction and the cone resistance, as indicated by the slope of the fanned-out lines. Table 2. shows the soil types for the Begemann data base correlated to friction ratio. The Begemann chart and table were derived from tests in Dutch soils with the mechanical cone. That is, the chart is site-specific, i.e., directly applicable only to the specific geologic locality where it was developed. For example, the cone tests in sand show a friction ratio smaller than 1 %. A distinction too frequently overlooked is that Begemann did not suggest that the friction ratio alone governs the soil type. Aspects, such as overconsolidation, whether a recent or old sedimentary soil, or a residual soil, mineralogical content, etc. will influence the friction ratio, and, therefore, the interpretation, as will a recent fill or excavation. However, the chart is of an important general qualitative value.

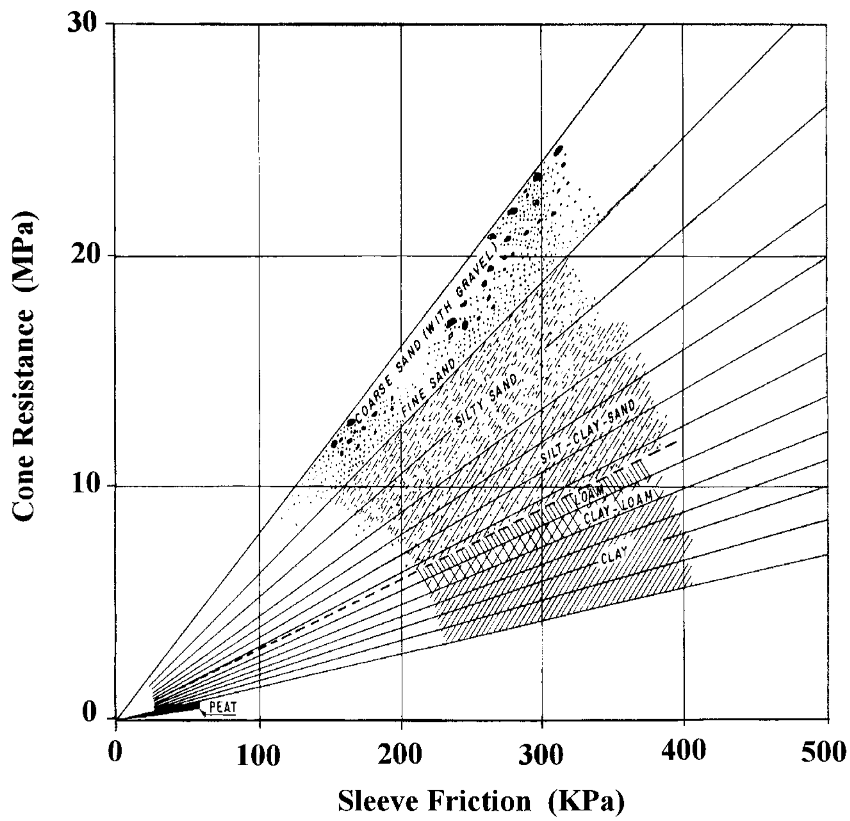

Fig. 2.2 The Begemann original profiling chart (Begemann, 1965)

Soil Type as a Function of Friction Ratio (Begemann, 1965)

Coarse sand with gravel through fine sand	1.2 %	-	1.6 %
Silty sand	1.6 %	-	2.2 %
Silty sandy clayey soils	2.2 %	-	3.2 %
Clay and loam, and loam soils	3.2 %	-	4.1 %
Clay	4.1 %	-	7.0 %
Peat		>7 %	

2.22 Sanglerat et al. (1974)

Sanglerat et al. (1974) proposed the chart shown in Fig. 2.3A presenting cone stress, q_c, values from soundings using a 80 mm diameter research penetrometer. The chart plots the cone resistance (logarithmic scale) versus the friction ratio (linear scale). The change from Begemann's type of plotting to plotting against the friction ratio is unfortunate. This manner of plotting has the apparent advantage of combining the two important parameters, the cone resistance and the friction ratio. However, plotting the cone resistance versus the friction ratio implies, falsely, that the values are independent of each other; the friction ratio would be the independent variable and the cone resistance the dependent variable. In reality, the friction ratio is the inverse of the ordinate and the values are patently not independent—the cone resistance is plotted against its own inverse self, multiplied by a variable that ranges, normally, from a low of about 0.01 through a high of about 0.07.

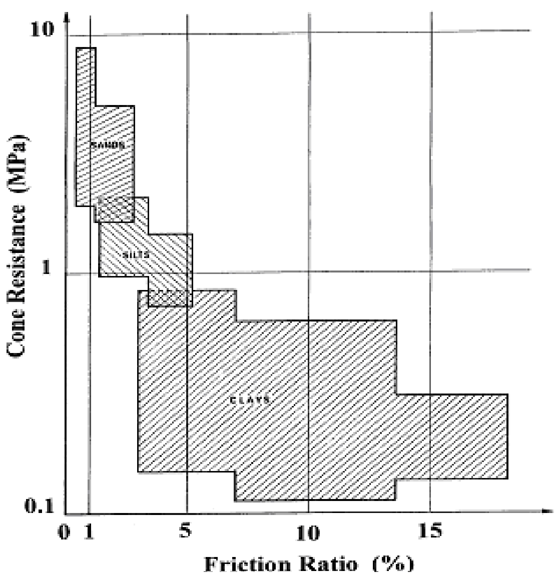

Fig. 2.3A Plot of data from research penetrometer (Sanglerat et al. 1974)

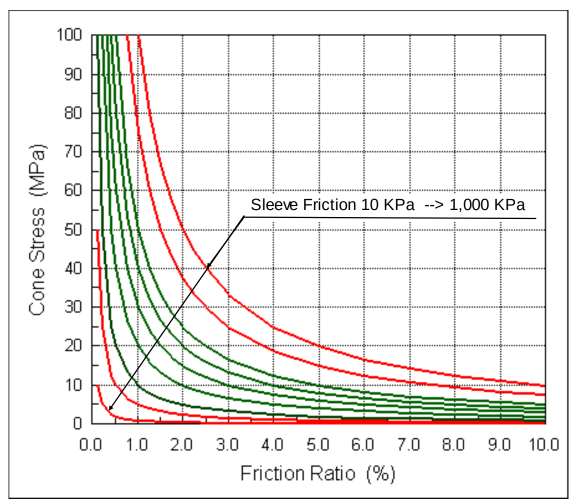

Fig. 2.3B Cone Stress Plotted against Friction Ratio for a Range of values of Sleeve Friction

As is very evident in Fig. 2.3A, regardless of the actual values, the plotting of data against own inverse values will predispose the plot to a hyperbolically shaped zone ranging from large ordinate values at small abscissa values through small ordinate values at large abscissa values. The resolution of data representing fine-grained soils is very much exaggerated as opposed to the resolution of the data representing coarse-grained soils. Simply, while both cone resistance and sleeve friction are important soil profiling parameters, plotting one as a function of the other distorts the information. To illustrate the hyperbolic trend obtained when a value is plotted against its inverse self, Fig. 2.3B presents a series of curves of Cone Stress, q_C, plotted against the Friction Ratio, f_R, for values of Sleeve Friction, f_s, ranging from 10 KPa through 1,000 KPa. The green curves indicate the range of values ordinarily encountered. Obviously, plotting against the Friction Ratio restricts the usable area of the graph, and, therefore, the potential resolution of the test data.

Notice, however, that Fig. 2.3A defines the soil type also by its upper and lower limit of cone resistance and not just by the friction ratio. The boundary between compact and dense sand is usually placed at a cone stress of 10 MPa, however. Obviously, the soils at the particular geologic localities did not exhibit a cone resistance larger than about 1 MPa in clays and about 9 MPa in sands.

From this time on, the Begemann manner of plotting the cone stress against the sleeve friction was discarded in favor of Sanglerat's plotting cone stress against the friction ratio. However, this development—plotting the cone stress against itself (its inverted self) modified by the sleeve friction value—is unfortunate.

2.23 Schmertmann (1978)

Schmertmann (1978) proposed the soil profiling chart shown in Fig. 2.4A. The chart is based on results from mechanical cone data in "North Central Florida" and incorporates Begemann's CPT data. The chart indicates envelopes of zones of common soil type. It also presents boundaries for density of sands and consistency (undrained shear strength) of clays and silts, which are imposed by definition and not related to the soil profile interpreted from the CPT results.

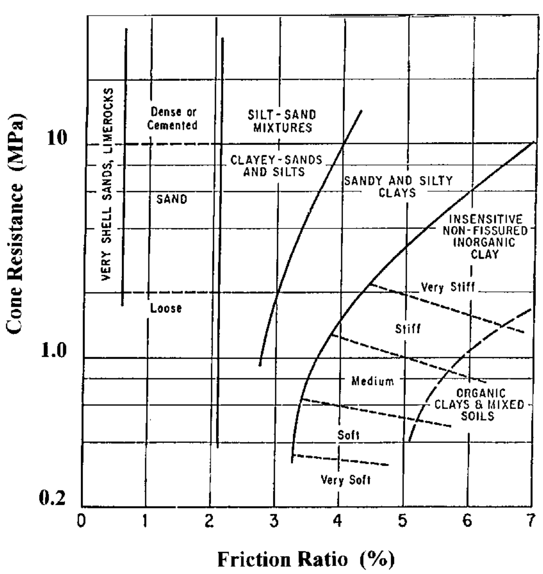

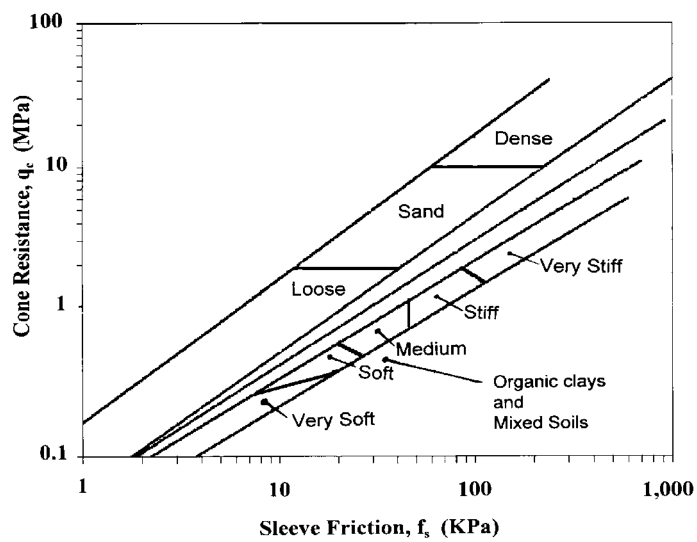

Fig. 2.4A The Schmertmann profiling chart (Schmertmann, 1978)

Fig. 2.4B The Schmertmann profiling chart converted to a Begemann type profiling chart

Also the Schmertmann (1978) chart (Fig. 2.4A) presents the cone resistance as a plot against the friction ratio, that is, the data are plotted against their inverse self. Fig. 2.4B shows the Schmertmann chart converted to a Begemann type graph (logarithmic scales), re-plotting the Fig. 2.4A envelopes and boundaries as well as text information. When the plotting of the data against own inverse values is removed, a qualitative, visual effect comes forth that is quite different from that of Fig. 2.4A. Note also that the consistency boundaries do not any longer appear to be very logical.

Schmertmann (1978) states that the correlations shown in Fig. 2.4A may be significantly different in areas of dissimilar geology. The chart is intended for typical reference and includes two warnings: "*Local correlations are preferred*" and "*Friction ratio values decrease in accuracy with low values of* q_c". Schmertmann also mentions that soil sensitivity, friction sleeve surface roughness, soil ductility, and pore pressure effects can influence the chart correlation. Notwithstanding the caveat, the Schmertmann chart is very commonly applied "as is" in North American practice.

2.24 Douglas and Olsen (1981)

Douglas and Olsen (1981) proposed a soil profiling chart based on tests with the electrical cone penetrometer. The chart, which is shown in Fig. 2.5A, appends classification per the unified soil classification system to the soil type zones. The chart also indicates trends for liquidity index and earth stress coefficient, as well as sensitive soils and "metastable sands". The Douglas and Olsen chart envelopes several zones using three upward curving lines representing increasing content of coarse-grained soil and four lines with equal sleeve friction. This way, the chart distinguishes an area (lower left corner of the chart) where soils are sensitive or "metastable".

Comparing the Fig. 2.5A chart with the Fig. 2.3A chart, a difference emerges in implied soil type response**:** while in the Schmertmann chart the soil type envelopes curve downward, in the Douglas and Olsen chart they curve upward. Zones for sand and for clay are approximately the same in the two charts, however.

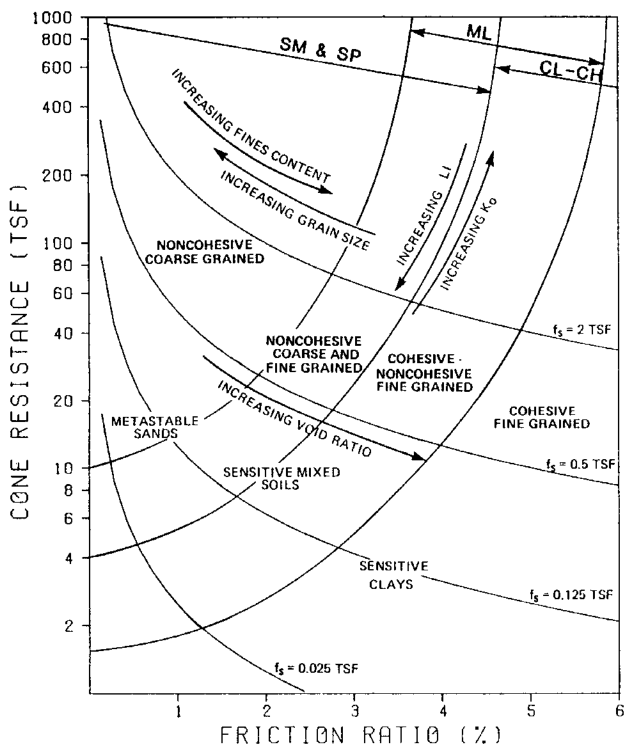

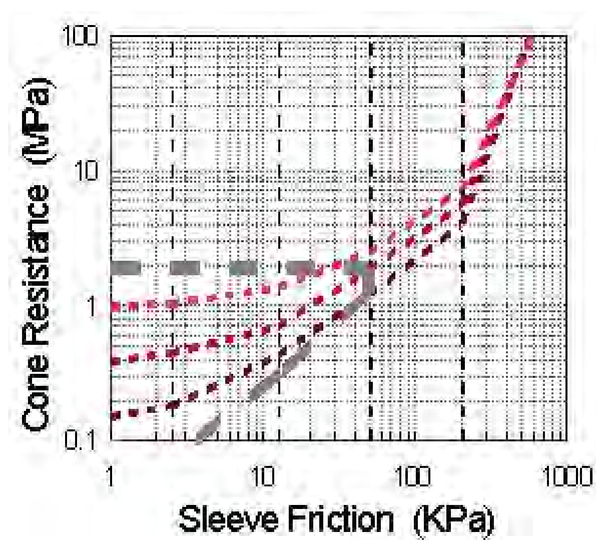

Fig. 2.5A   Profiling chart per Douglas and Olsen (1981)

Fig. 2.5B   The Douglas and Olsen profiling chart converted to a Begemann type chart

A comparison between the Schmertmann and Douglas and Olsen charts (Figs. 2.4A and 2.5A) is more relevant if the charts are prepared per the Begemann type of presentation. Thus, Fig. 2.5B shows the Douglas and Olsen chart converted to a Begemann type graph. The figure includes the three curved envelopes and the four lines with equal sleeve friction and a heavy dashed line which identifies an approximate envelop of the zones indicated to represent “metastable” and “sensitive” soils.

The Douglas and Olsen chart (Fig. 2.5A) offers a smaller band width for dense sands and sandy soils (q_c > 10 MPa) and a larger band width in the low range of cone resistance (q_c < 1 MPa) as opposed to the Schmertmann chart (Fig. 2.4a).

2.25 Vos (1982)

Vos (1982) suggested using the electrical cone penetrometer for Dutch soils to identify soil types from the friction ratio, as shown below. The percentage values are similar but not identical to those recommended by Begemann (1965).

Soil Behavior Categories as a Function of Friction Ratio (Vos, 1982)

Coarse sand and gravel		<1.0%
Fine sand	1.0 %-	1.5 %
Silt	1.5 %-	3.0 %
Clay	3.0%-	7.0%
Peat	>7 %	

2.26 Robertson et al. (1986)

Robertson et al. (1986) and Campanella and Robertson (1988) presented a chart, which was the first chart to be based on the piezocone, i.e., the first to include the correction of cone resistance for pore pressure at the shoulder according to Eq. 2.1.

(2.1) $$q_t = q_c + U2(1 - a)$$

where q_t = cone resistance corrected for pore water pressure on shoulder
q_c = measured cone resistance
$U2$ = pore pressure measured at cone shoulder
a = ratio between shoulder area (cone base) unaffected by the pore water pressure to total shoulder area

The Robertson et al. (1986) profiling chart is presented in Fig. 2.6. The chart identifies numbered areas that separate the soil behavior categories in twelve zones, as follows.

1. Sensitive fine-grained soil
2. Organic soil
3. Clay
4. Silty clay to clay
5. Clayey silt to silty clay
6. Sandy silt to clayey silt
7. Silty sand to sandy silt
8. Sand to silty sand
9. Sand
10. Sand to gravelly sand
11. Very stiff fine-grained soil
12. Overconsolidated or cemented sand to clayey sand

A novel information in the profiling chart is the delineation of Zones 1, 11, and 12, representing somewhat extreme soil responses, enabling the CPTU to uncover more than just soil grain size. The rather detailed separation of the in-between zones, Zones 3 through 10 indicate a gradual transition from fine-grained to coarse-grained soil.

As mentioned above, plotting of cone stress value against the friction ratio is plotting the cone stress against itself (its inverted self) modified by the sleeve friction value, distorting the results. Yet, as indicated in Fig. 2.7B, the measured values of cone stress and sleeve friction can just as easily be plotted separately. The friction ratio is a valuable parameter and it is included as an array of lines ranging from a ratio of 0.1 % through 25 %.

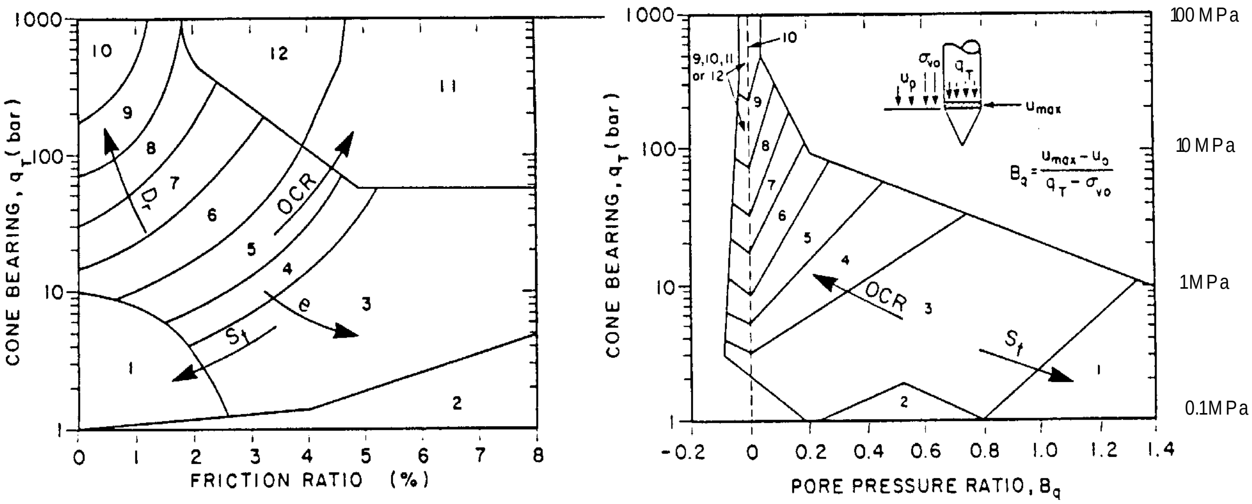

Fig. 2.6 Profiling chart per Robertson et al. (1986)

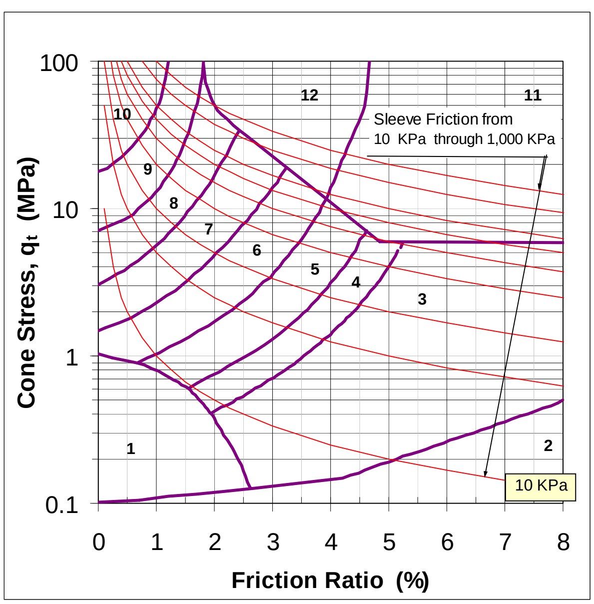

Fig. 2.7A The profiling chart shown in Fig. 2.6

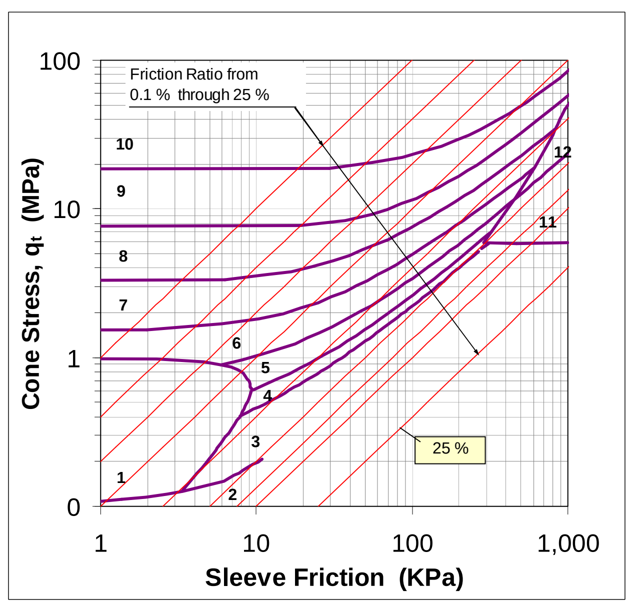

Fig. 2.7B The profiling chart plotted as Cone Stress vs. Sleeve Friction

The Robertson et al. (1986) profiling chart (Fig. 2.6) introduced a pore pressure ratio, B_q, defined by Eq. 2.2, as follows.

(2.2) $$B_q = \frac{u2 - u_0}{q_t - \sigma_v}$$

where B_q = pore pressure ratio
u_2 = pore pressure measured at cone shoulder
u_0 = in-situ pore pressure
q_t = cone resistance corrected for pore water pressure on shoulder
σ_v = total overburden stress

Essentially, the B_q-value shows the change of pore pressure divided by the cone stress, q_t (the cone stress is very much larger than the total stress). Directly, the B_q-chart (Fig. 2.8) shows zones where the U2 pore pressures become smaller than the neutral pore pressures (u_0) in the soil during the advancement of the penetrometer, resulting in negative B_q-values. Otherwise, the B_q-chart appears to be an alternative rather than an auxiliary chart; one can use one or the other depending on preference. However, near the upper envelopes, a CPTU datum plotting in a particular soil-type zone in the friction ratio chart will not always appear in the same soil-type zone in the B_q-chart. Robertson et al. (1986) points out that "occasionally soils will fall within different zones on each chart" and recommends that the users study the pore pressure rate of dissipation (if measured) to decide which zone applies to questioned data.

The pore pressure ratio, B_q, is an inverse function of the cone stress, q_t. Therefore, also the B_q-plot represents the data as a function of their own self values.

Eslami and Fellenius (1996) proposed a pore pressure ratio, B_E, defined, as follows.

(2.3) $$B_E = \frac{u2 - u_0}{u_0}$$

where B_E = pore pressure ratio
u_0 = neutral pore pressure
$u2$ = pore pressure measured at the cone shoulder

The B_E-value shows the relative change of pore pressure introduced by pushing the cone.

There is little information obtained from the pore pressure ratios that is not available directly from the measured pore pressure (U2) and friction ratio, f_R.

2.27 Robertson (1990)

Robertson (1990) proposed a development of the Robertson et al. (1986) profiling chart, shown in Fig. 2.8, plotting a "normalized cone resistance", q_{cnrm}, against a "normalized friction ratio", R_{fnrm}, in a cone resistance chart. The accompanying pore pressure ratio chart plots the "normalized cone resistance" against the pore pressure ratio, B_q, defined by Eq. 2.2 applying the same B_q-limits as the previous chart (Zone 2 is not included in Fig. 2.8).

The normalized cone resistance is defined by Eq. 2.4.

(2.4) $$q_{cnrm'} = \frac{q_t - \sigma'_v}{\sigma_v}$$

where $q_{cnrm'}$ = cone resistance normalized according to Robertson (1990)
q_t = cone resistance corrected for pore water pressure on shoulder
σ_v = total overburden stress
σ'_v = effective overburden stress
$(q_t - \sigma_v)$ = net cone resistance

The normalized friction ratio is defined as the sleeve friction over the net cone resistance, as follows.

(2.5) $$R_{fnrm'} = \frac{f_s}{q_t - \sigma_v}$$

where f_s = sleeve friction
q_t = cone resistance corrected for pore water pressure on shoulder
σ_v = total overburden stress

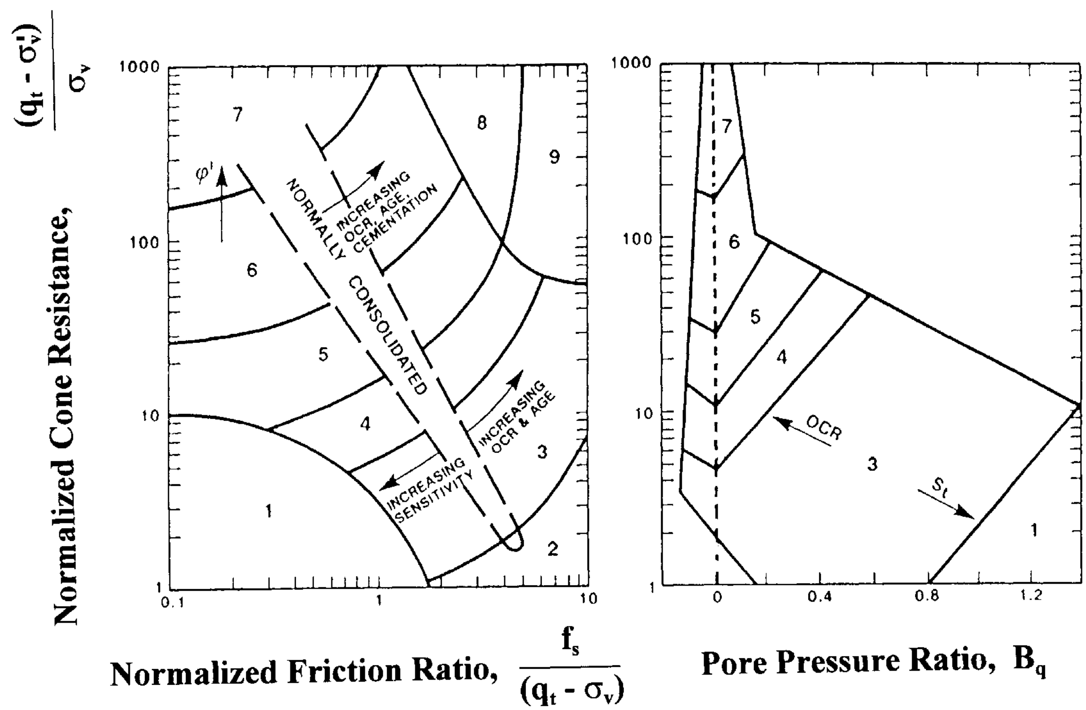

Fig. 2.8 Profiling chart per Robertson (1990)

The numbered areas in the profiling chart separate the soil behavior categories in nine zones, as follows.

1. Sensitive, fine-grained soils
2. Organic soils and peat
3. Clays [clay to silty clay]
4. Silt mixtures [silty clay to clayey silt]
5. Sand mixtures [sandy silt to silty sand]
6. Sand [silty sand to clean sand]
7. Sand to gravelly sand
8. Sand – clayey sand to "very stiff" sand
9. Very stiff, fine-grained, overconsolidated or cemented soil

The two first and two last soil types are the same as those used by Robertson et al. (1986) and Types 3 through 7 correspond to former Types 3 through 10. The Robertson (1990) normalized profiling chart has seen extensive use in engineering practice (as has the Robertson et al. 1986 chart).

The normalization is professedly to compensate for that the cone resistance is influenced by the overburden stress. Therefore, when analyzing deep CPTU soundings (i.e., deeper than about 30 m), a profiling chart developed for more shallow soundings does not apply well to the deeper sites. At very shallow depths, however, the proposed normalization will tend to lift the data in the chart and imply a coarser soil than necessarily the case. Moreover, where soil types alternate between light-weight and soils (which soil densities can range from 1,400 kg/m^3 through 2,100 kg/m^3) and/or where upward or downward pore pressure gradients exist, the normalization is unwieldy. For these reasons, it would appear that the normalization merely exchanges one difficulty for another.

More important, the chart still includes the plotting of data against the inverse of own self. This is not necessary. A chart with the same soil zones could just as well have been produced with normalized cone resistance against a normalized sleeve friction.

Accepting the Robertson (1990) normalization, Figs. 2.9A and 2.9B show the envelopes of the Robertson (1990) chart (Fig. 2.8) converted to a Begemann type chart. The ordinate is the same and the abscissa is the multiplier of the normalized cone resistance and the normalized friction factor of the original chart (the normalized sleeve friction is the sleeve friction divided by the effective overburden stress). Where needed, the envelopes have been extended with a thin line to the frame of the diagram.

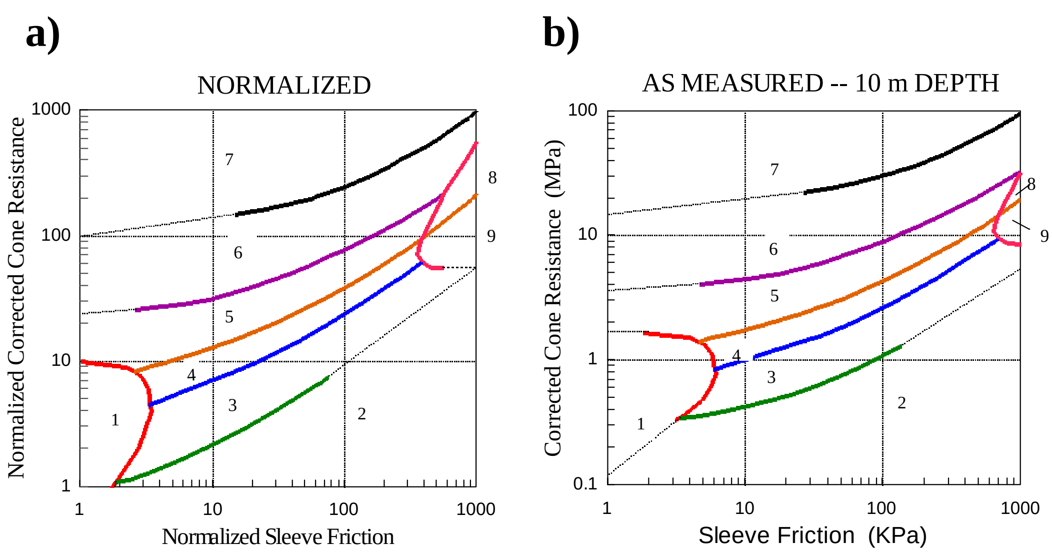

Fig. 2.9A Normalized corrected cone resistance vs. normalized sleeve friction

Fig. 2.9B Pore-pressure corrected cone resistance vs. sleeve friction

As reference to Figs. 2.4B and 2.5B, Fig. 2.9b presents the usual Begemann type profiling chart converted from Fig. 2.8 under the assumption that the data apply to a depth of about 10 m at a site where the groundwater table lies about 2 m below the ground surface. This chart is approximately representative for a depth range of about 5 m to 30 m. Comparing the "normalized" chart with the "as measured" chart does not indicate that normalization would be advantageous.
Other early profiling charts were proposed by Searle (1979), Jones and Rust (1982), Olsen and Farr (1986), Olsen and Malone (1988), Erwig (1988). CPTU charts similar to similar to that of Robertson (1990) were proposed by Larsson and Mulabdic (1991), Jefferies and Davies (1991, 1993), and Olsen and Mitchell (1995).

2.3 The Eslami-Fellenius CPTU Profiling and Soil Behavior Type Classification Method

To investigate the use of cone penetrometer data in pile design, Eslami and Fellenius (1997) compiled a database consisting of CPT and CPTU data linked with results of boring, sampling, laboratory testing, and routine soil characteristics. The cases are from 18 sources reporting data from 20 sites in 5 countries. About half of the cases are from piezocone tests, CPTU, and include pore pressure measurements (U2). Non-CPTU tests are from sand soils and were used with the assumption that the U2-values are approximately equal to the neutral pore pressure (u_0). The database values are separated on five main soil behavior categories as follows.

1. Very soft Clay or
   Sensitive and Collapsible Clay and/or Silt
2. Clay and/or Silt
3. Silty Clay and/or Clayey Silt

4a. Sandy Silt
4b. Silty Sand
5. Sand and/or Sandy Gravel

The data points were plotted in a Begemann type profiling chart and envelopes were drawn enclosing each of the five soil types. The envelopes are shown in Fig. 2.10. The database does not include cases with cemented soils or very stiff clays, and, for this reason, no envelopes for such soil types are included in the chart.

$$q_E = (q_t - u2) \tag{2.6}$$

where q_E = "effective" cone resistance
q_t = cone resistance corrected for pore water pressure on shoulder (Eq. 2.1)
$u2$ = pore pressure measured at cone shoulder

Plotting an "effective" cone resistance defined by Eq. 2.6 was found to provide a more consistent delineation of envelopes than a plot of only the cone resistance. (Note, subtracting the pore pressure does not make the value an effective stress. It was only found that the subtraction made the data come together in more easily delineated zones. The subscript "E" can also be thought to be a short for "Eslami").

The q_E-value was shown to be a consistent value for use in relation to soil responses, such as pile shaft and pile toe resistances (Eslami 1996, Eslami and Fellenius 1995; 1996; 1997). Notice again that, as mentioned by Robertson (1990), the measured pore water pressure is a function of where the pore pressure gage is located. Therefore, the q_E-value is by no means a measurement of effective stress in conventional sense. Because the sleeve friction is a rather approximate measurement, no similar benefit was found in producing an "effective" sleeve friction. In dense, coarse-grained soils, the q_E-value differs only marginally from the q_t-value. In contrast, cone tests in fine-grained soils could generate substantial values of excess pore water pressure causing the q_E-value to be much smaller than the q_t-value, indeed, even negative, in which case the value should be taken as equal to zero.

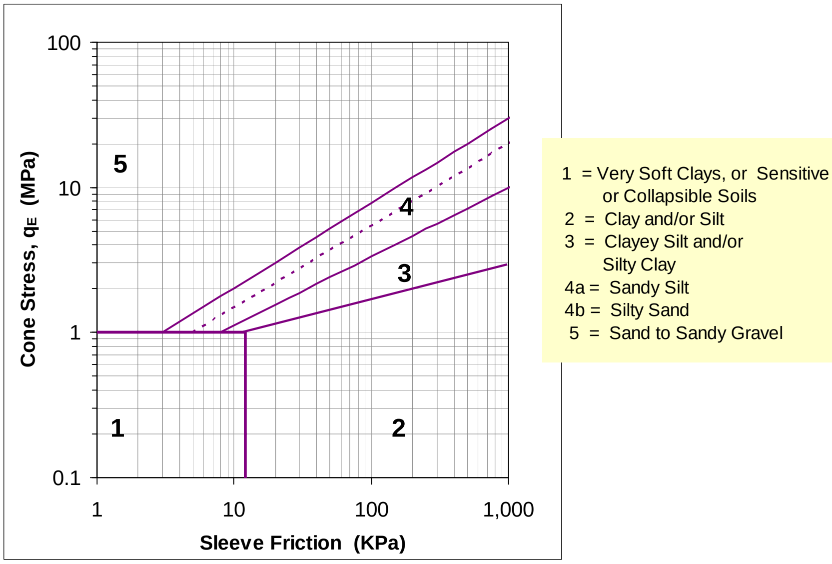

Fig. 2.10 The Eslami-Fellenius profiling chart (Eslami 1996; Eslami and Fellenius, 1997)

The Eslami-Fellenius chart is simple to use and requires no adjustment to estimated value of the overburden stresses. The chart is primarily intended for soil type (profiling) analysis of CPTU data. With regard to the grain-size boundaries between the main soil fractions (clay, silt, sand, and gravel), international and North American practices agree. In contrast, differences exist with regard to how soil-type names are modified according to the contents of other than the main soil fraction. The chart assumes the name convention summarized in Section 1.3 as indicated in the Canadian Foundation Engineering Manual (1992, 2006).

The data from the CPT diagrams presented in Fig. 2.1 are presented in the chart shown in Fig. 2.11. The three layers are presented with different symbols.

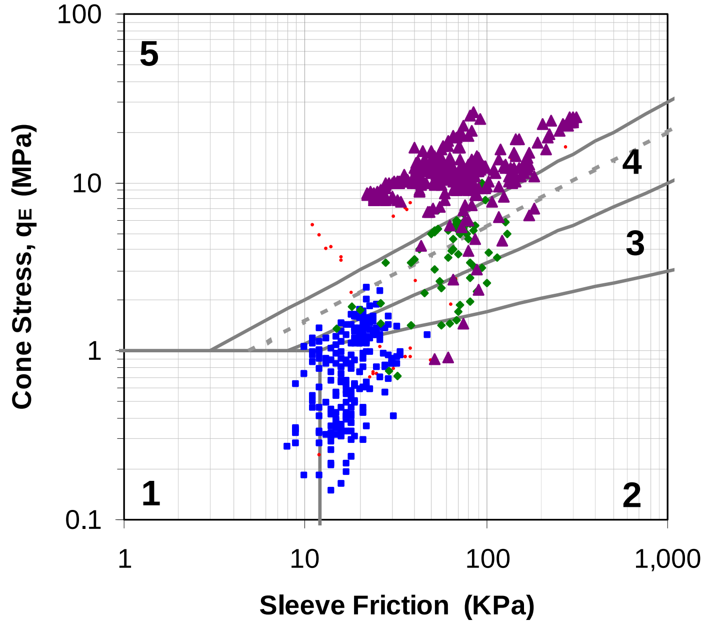

Fig. 2.11 The CPT sounding shown in Fig. 2.1 plotted in a Eslami-Fellenius profiling chart.

2.4. Comparison between the Eslami-Fellenius and Robertson (1990) Methods

To provide a direct comparison between the Robertson (1990) profiling chart and the Eslami-Fellenius chart, three short series of CPTU data were compiled from sites with very different geologic origin where the soil profiles had been established independently of the CPTU. The borehole information provides soil description and water content of recovered samples. For one of the cases, the grain size distribution is also available. The CPTU-diagrams from the site are shown in Fig. 2.12. The soil and CPTU information for the specific points are compiled in Table 1. The three sites are:

1. North Western University, **Evanston**, Illinois (Finno 1989). CPTU data were obtained in a soil profile consisting of 7 m of sand deposited on normally consolidated silty clay. The piezometer was attached to the cone face (u_1) and not behind the shoulder (u_2). The method of converting the pore pressure measurement to the u_2-value presented by Finno (1989) has been accepted here, although the conversion is disputed. For comments, see Mayne et al. (1990).
2. Along the shore of Fraser River, **Vancouver**, British Columbia (personal communication, V. Sowa, 1998). A 20 m thick mixed soil profile of deltaic deposits of clay, silt, and sand. The first four data points are essentially variations of silty clay or clayey silt. The fifth is a silty sand.
3. University of Massachusetts, **Amherst**, Massachusetts (personal communication, P. Mayne, 1998). A soil profile (Lutenegger and Miller 1995) consisting of 5 m of a thick homogeneous overconsolidated clayey silt. This case includes also information on grain size distribution. The borehole records show the soil samples for data points Nos. 3 through 7 to be essentially identical. Notice that the u_2-measurements indicate substantial negative values, that is, the overconsolidated clay dilates as the cone is advanced.

For each case, the soil information in Table 1 is from depths where the CPTU data were consistent over a 0.5 m length. Then, the CPTU data from 150 mm above and below the middle of this depth range were averaged using geometric averaging, preferred over the arithmetic average as it is less subject to influence of unrepresentative spikes and troughs in the data (a redundant effort, however, as the records contain no such spikes and troughs). The CPTU data were analyzed by the Eslami-Fellenius (1996) and the Robertson (1990) profiling methods and the results are shown in Fig. 2.13.

Evanston data: The first three samples of the are from a sand soil and both methods identify the CPTU data accordingly. The remaining data points (Nos. 4 through 7) given as Silty Clay in the borehole records are identified as Clay/Silt by the Eslami-Fellenius and as Clay to Silty Clay by the Robertson method, that is, both methods agree with the independent soil classification.

Vancouver data: Both methods properly identify the first four data points to range from Clayey Silt to Silty Clay in agreement with the independent soil classification. The fifth sample (Silty Sand) is identified correctly by the Eslami-Fellenius method as a Sand close to the boundary to Silty Sand and Sandy Silt. The Robertson method identifies the soil as a Sandy Silt to Clayey Silt, which is essentially correct, also.

Amherst data: Both methods identify the soils to be silt or clay or silt and clay mixtures. Moreover, both methods place Points 3 through 7 on the same soil type boundary line, that is, confirming the similarity between the soil samples. However, the spread of plotted points appear to be larger for the Robertson method; possibly due that its profiling does not consider the pore pressures developed by the advancing penetrometer (but for the pore pressure on the shoulder, of course), while the Eslami-Fellenius method does account for the substantial negative pore pressures that developed.

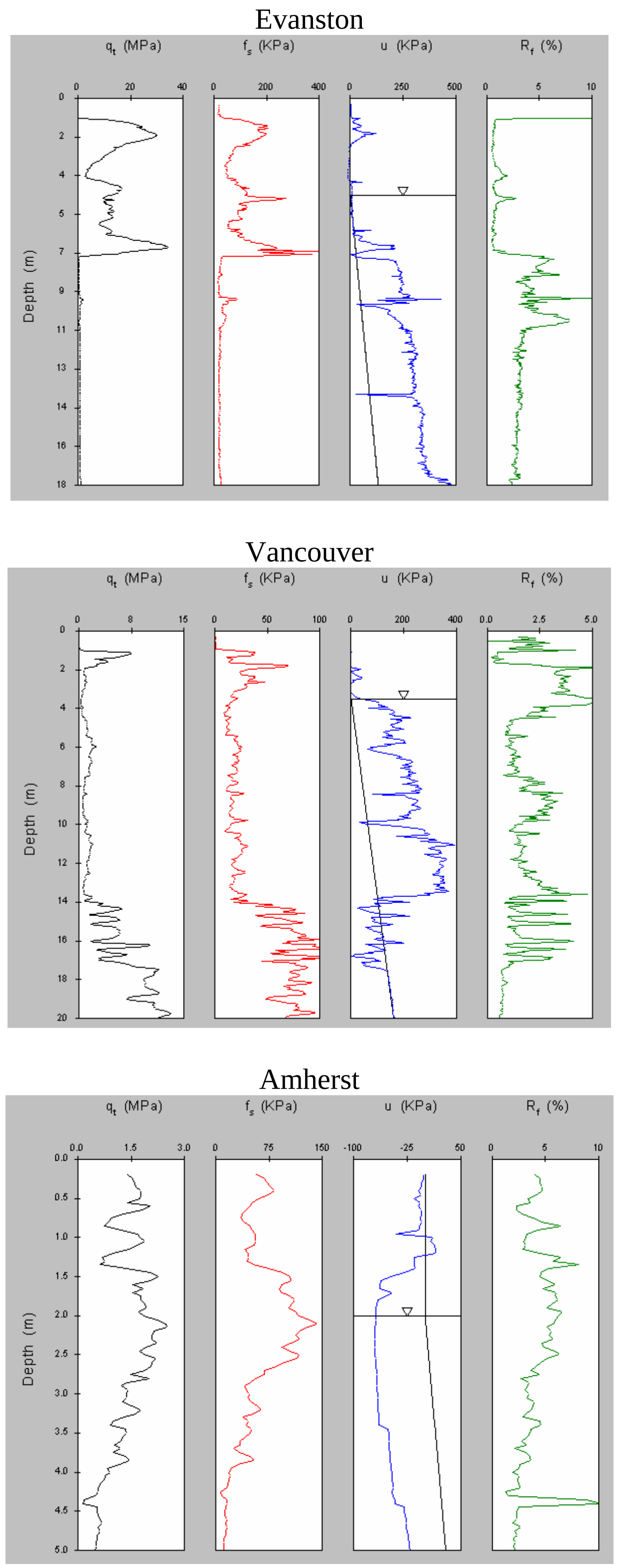

Fig. 2.12 CPTU diagram from the three sites

No.	Depth (m)	Description	Water Content (%)	Soil Fractions (%) Clay	Silt	Sand	CPTU Data q_t (MPa)	f_s (KPa)	U2 (KPa)
Evanston, IL (Groundwater table at 4.5 m)									
1	1.5	SAND, Fine to medium, trace gravel	29				25.08	191.5	49.8
2	3.4	SAND, Medium, trace gravel	16				3.48	47.9	-16.0
3	6.7	SAND, Fine, trace silt, organics	26				32.03	162.8	111.7
4	8.5	Silty CLAY, trace sand	28				0.51	21.1	306.4
5	9.5	Silty CLAY, little gravel	22				0.99	57.5	39.6
6	12.8	Silty CLAY, little gravel	23				0.69	19.2	383.0
7	16.5	Silty CLAY, little gravel	24				0.77	17.2	427.1
Vancouver, BC (Groundwater table at 3.5 m)									
1	3.7	CLAY to Clayey SILT	52				0.27	16.1	82.5
2	5.8	Clayey SILT to SILT	34				1.74	20.0	177.1
3	10.2	Silty CLAY	47				1.03	13.4	183.5
4	14.3	Silty CLAY	40				4.53	60.2	54.3
5	17.5	Silty SAND	25				10.22	77.8	118.5
Amherst, MA (Groundwater table at 2.0 m)									
				Clay	Silt	Sand			
1	0.6	SAND and SILT, trace clay	20	10	30	60	2.04	47.5	- 9.4
2	1.5	Clayey SILT, trace sand	28	23	67	10	2.29	103.3	-47.3
3	2.0	Clayey SILT, trace sand	36	21	75	4	1.87	117.0	-69.5
4	2.5	Clayey SILT, trace sand	29	33	65	2	1.86	117.0	-70.3
5	3.0	Clayey SILT, trace sand	40	36	62	2	1.37	46.8	-66.3
6	3.5	Clayey SILT, trace sand	53	40	58	2	1.38	48.9	-50.7
7	4.0	Clayey SILT, trace sand	60	40	58		0.91	17.9	-46.9
8	4.5	Clayey SILT	30	42	57	1	0.55	12.9	-29.3

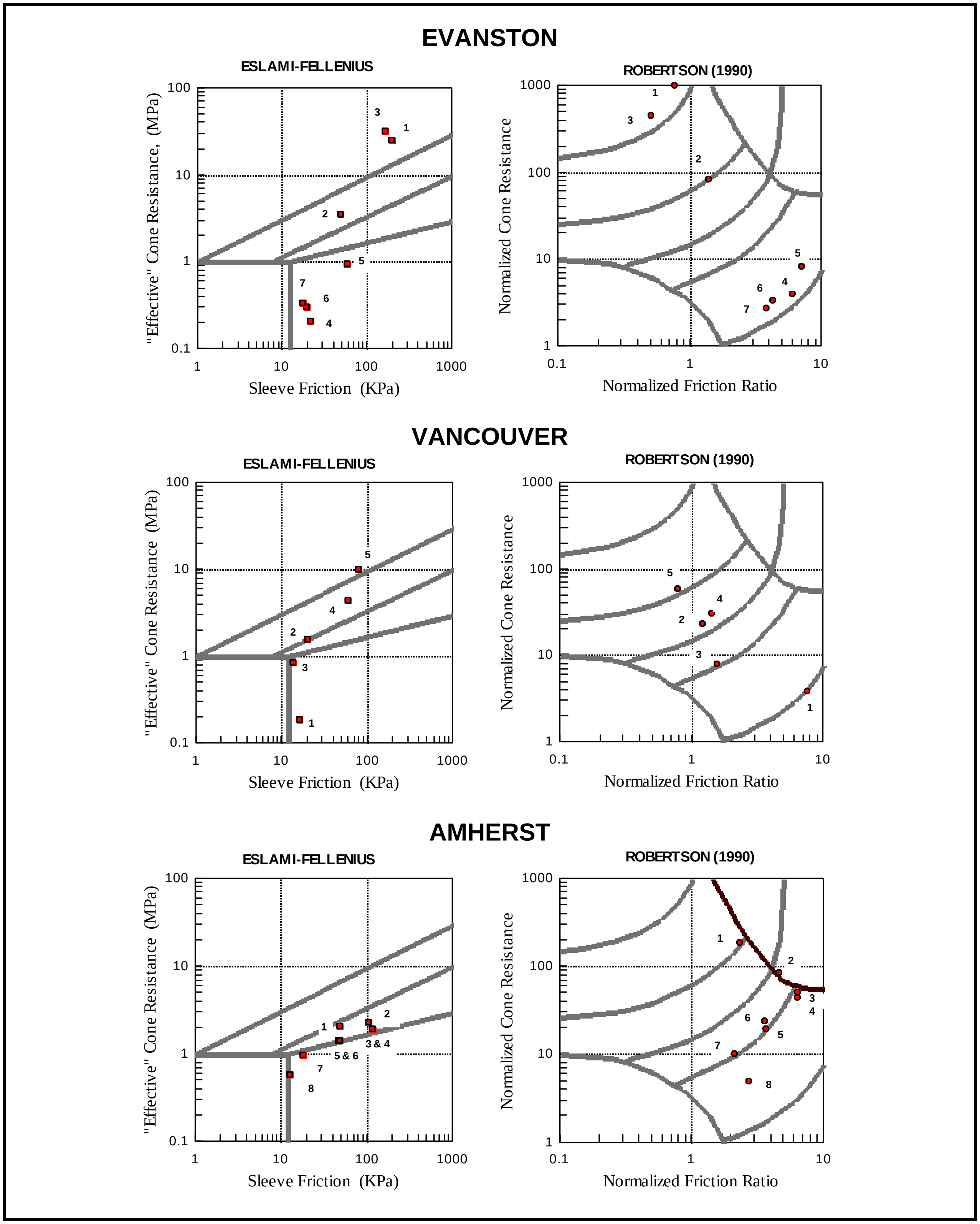

Fig. 2.13 Comparison between the Table 1 data plotted in Eslami-Fellenius and Robertson profiling charts

2.5 Comparisons

I. The CPT methods (mechanical cones) do not correct for the pore pressure on the cone shoulder and the profiling developed based on CPT data may not be relevant outside the local area where they were developed. The error due to omitting the pore water pressure correction is large in fine-grained soils and small in coarse-grained soils.

II. Except for the profiling chart by Begemann (1965) and Eslami-Fellenius (1997), all of the referenced soil profiling methods plot the cone resistance versus its own inverse value in one form or another. This generates data distortion and violates the rule that dependent and independent variables must be rigorously separated.

III. Some profiling methods, e. g., Robertson (1990), include normalization which require unwieldy manipulation of the CPT data. For example, in a layered soil, should a guesstimated "typical" density value be used in determining the overburden stress or a value that accurately reflects the density? Moreover, regardless of soil layering, determining the effective overburden stress (needed for normalization) requires knowledge of the pore pressure distribution, which is not always hydrostatic but can have an upward or downward gradient and this information is rarely available.

IV. The normalization by division with the effective overburden stress does not seem relevant. For example, the normalized values of fine-grained soils obtained at shallow depth (where the overburden stress is small) will often plot in zones for coarse-grained soil.

V. The Robertson (1990) and the Eslami-Fellenius (1997) CPTU methods of soil profiling were applied to data from three geographically apart sites having known soils of different types and geologic origins. Both methods identified the soil types accurately.

VI. Eslami-Fellenius (1996) method has the advantage over the Robertson (1990) that it avoids the solecism of plotting data against their own inverted values and associated distortion of the data.

VII. Eslami-Fellenius (1997) method has the additional advantage over other referenced piezocone methods in that it allows the user to directly assess a value without first having to determine distribution of total and effective stress to use in a subtraction and multiplication effort in calculating a "normalized" set of values.

VIII. A soil profiling chart based on a Begemann type plot, such as the Eslami-Fellenius (1996) method can easily be expanded by adding delineation of strength and consistency of fine-grained soils and relative density and friction angle of coarse-grained soils per the user preferred definitions or per applicable standards.

IX. No doubt, CPTU sounding information from a specific area or site can be used to further detail a soil profiling chart and result in delineation of additional zones of interest. However, there is a danger in producing a very detailed chart inasmuch the resulting site dependency easily gets lost leading an inexperienced user to apply the detailed distinctions beyond their geologic validity.

X. The CPTU is an excellent tool for the geotechnical engineer in developing a site profile. Naturally, it cannot serve as the exclusive site investigation tool and soil sampling is still required. However, when the CPTU is used govern the depths from where to recover soil samples for detailed laboratory study, fewer sample levels are needed, reducing the costs of a site investigation while simultaneously increasing the quality of the information because important layer information and layer boundaries are not overlooked.

2.6 Profiling case example

Figure 2.14 shows q_t, f_s, U2, u_0, and f_R diagrams from a CPTU sounding in a sand deposit (in the Fraser River delta outside Vancouver, BC). Borehole samples indicate the soil profile to consist of loose to medium to fine silty sand containing layers or zones of silt, silty clay, and clay. As indicated in the figure, the borehole records agree well with the layering established using the profiling methods of Eslami-Fellenius (1997). The reading spacing is 10 mm. The depth measurements are corrected for the CPT rod inclination (deviation was in the form of a gentle sweep), resulting in an indicated maximum depth of 94 m, whereas the actual maximum depth is 90.5 m (see Section 2.8).

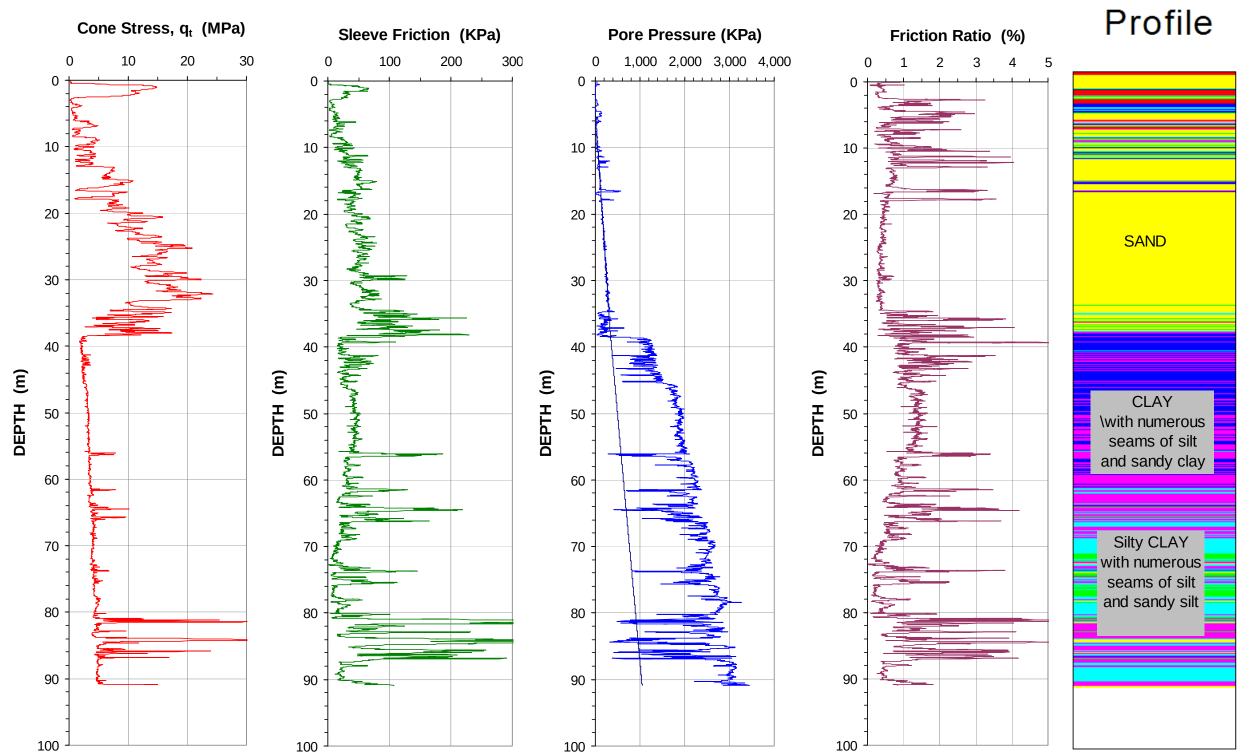

Fig. 2.14 CPTU sounding diagrams with profiling according to the Eslami-Fellenius(1997) method. Data from Amini et al. (2008).

The overall soil profile can be separated on four main zones, as indicated below. The soil descriptions was confirmed from bore hole samples. The colored block diagrams to the right are obtained from soil profiling using the CPTU data directly.

0 m	-	2.6 m	Coarse SAND
2.6 m	-	6.0 m	CLAY, Silty CLAY
6.0 m	-	13.0 m	Medium to fine SAND and Silty SAND (Fine sand portion = 30 % to 80 %)
12.5 m	-	16.0 m	Fine SAND trace silt
16.0 m		34.0 m	Fine to medium SAND
34.0 m		38.0 m	Silty SAND
38.0 m		70.0 m	CLAY with numerous silt seams and sandy clay
70 m		===>	Silty CLAY with seams of silt and sandy silt

Established by the pore pressure dissipation measurements (see Section 2.7), the pore pressure distribution in the clay layer below 38 m depth is artesian; the pore pressure head above ground is about 7 m.

The soil profile determined from CPTU data is usually in agreement with the soil profile determined from the conventional grain size distribution. In normally consolidated sedimentary soils, the CPTU-determined soil profile usually agrees well with grain-size description determined from soil samples. However, in overconsolidated or residual soils, the CPTU soil profile can often deviate from the soil sample description. Every site investigation employing CPTU sounding should include soil sampling. It is not necessary to obtain the soil samples in regular boreholes. Modern CPTU equipment includes the means to push down a plastic sampling tube inside a steel pipe of the same size as the cone rod. A continuous core of soil is recovered from where "disturbed" samples can be selected for detailed study. Figure 2.15 shows sections of four such cores recovered next to a CPTU sounding.

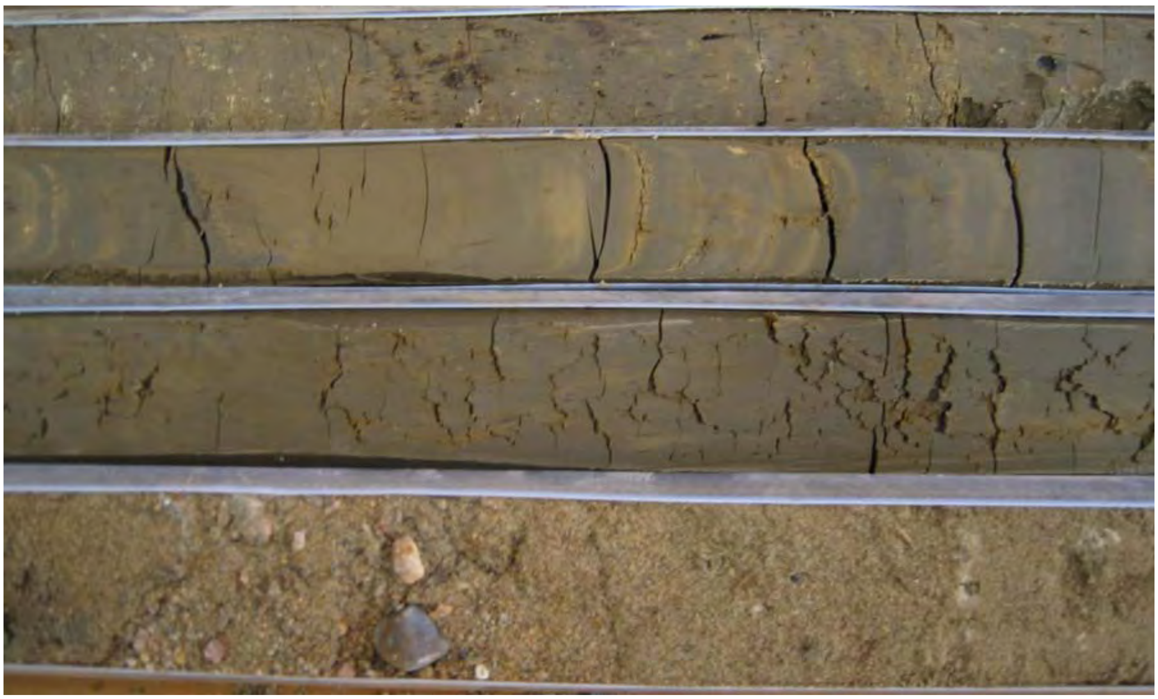

Fig. 2.15 Sections of soil cores , ranging from fill, sandy clay, clay, through sand with pieces of gravel. Sampling by means of CPTU device equipped with separate sampler.

Figure 2.16 (on Page 2-21) shows all cone data for the upper 20 m plotted in a Eslami-Fellenius profiling chart. Figure 2.16A shows the data plotted using axes in the usual logarithmic scales. However, the logarithmic plot only serves the purpose of compressing data so that all can be shown together. The log scale makes small relative changes of small values show up and yet includes similarly relative changes for larger values. However, when, as in the example case, the span between the small and the larger values is limited, the plot can preferably be made using linear scales, as shown in Fig. 2.16B.

Figure 2.17 (on Page 2-22) shows the data in profiling charts according to the Robertson 1986 method in logarithmic and linear scales. The linear plot indicates that the organic soil distinction (Layer 2) is probably not practical and that the separation between Layers 4 and 5 could well be considered as one layer. Figure 2.18 (on Page 2-23) shows the same for Robertson 1990 method. It is clearly evident from Fig. 2.18B that the method is not suitable for linear plotting even for a relatively small range of values of the example.

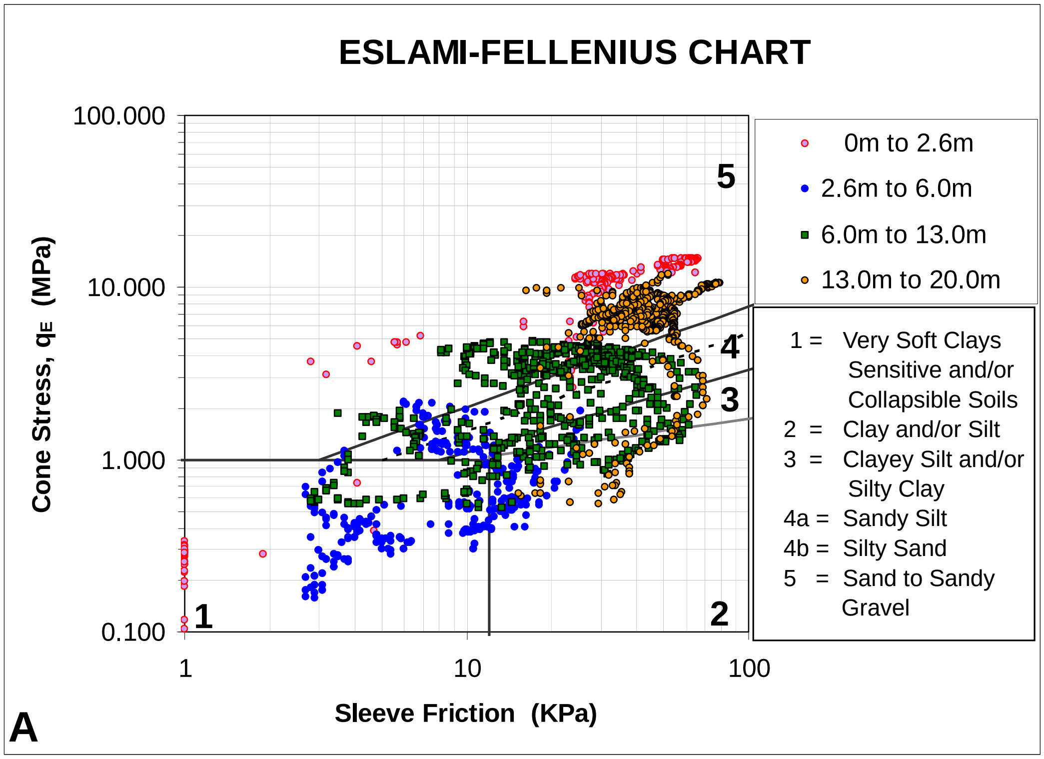

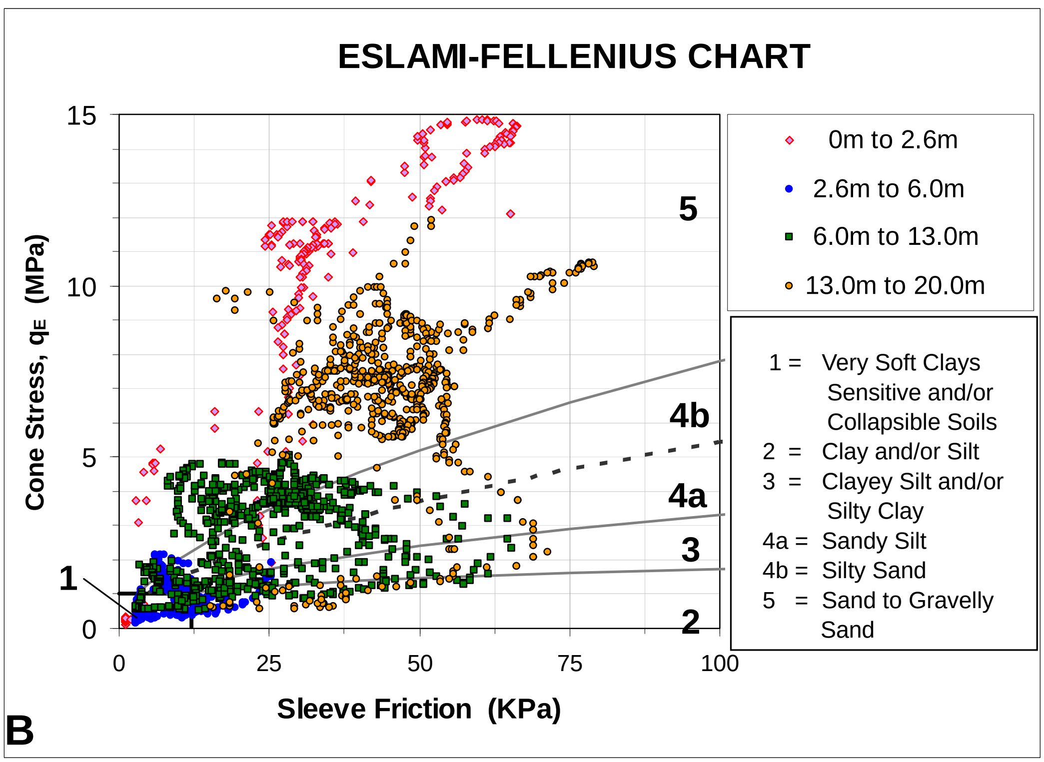

Fig. 2.16 A. Eslami-Fellenius profiling chart with axes in logarithmic scale
B. Eslami-Fellenius profiling chart with axes in linear scale

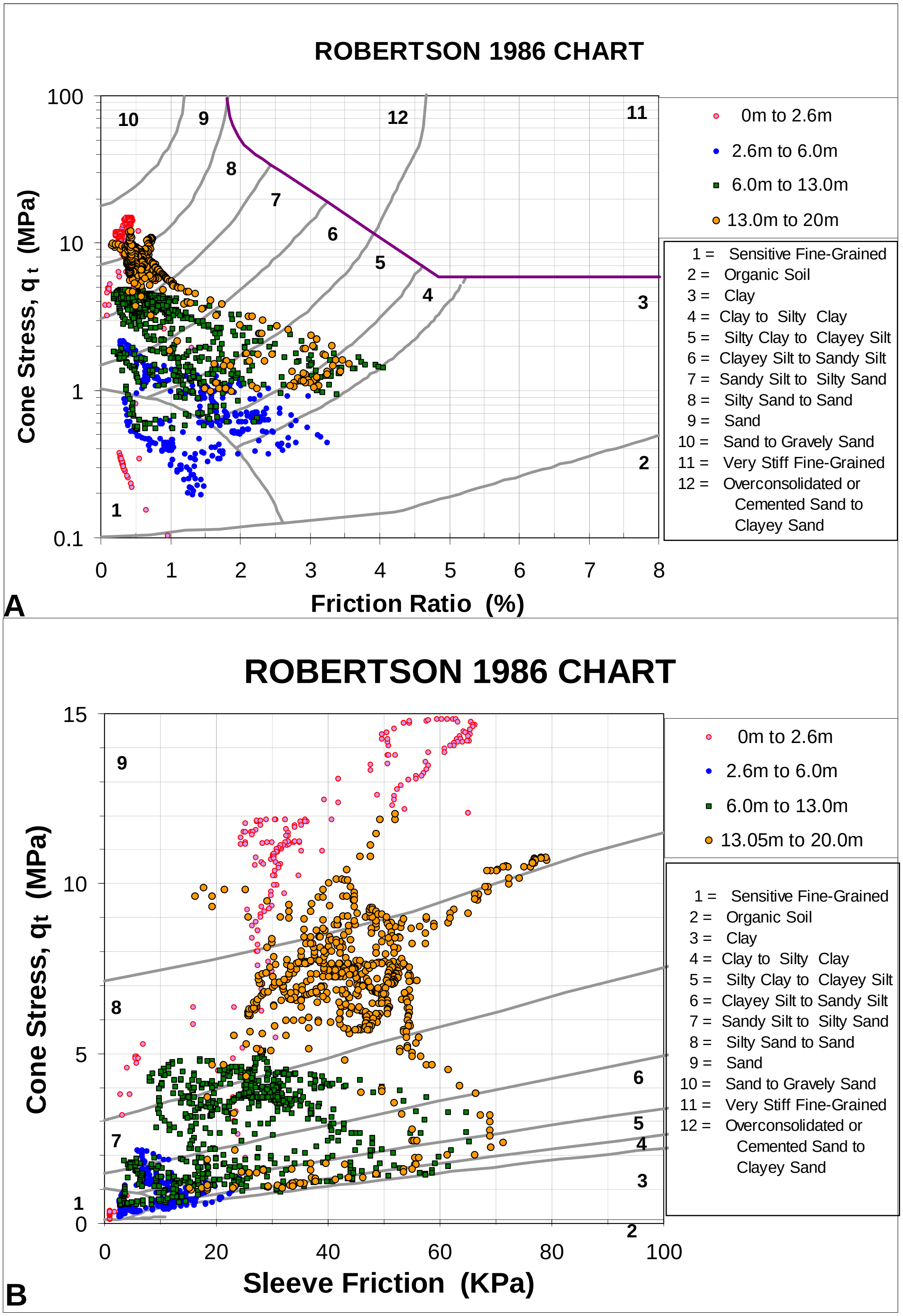

Fig. 2.17 A. Robertson 1986 profiling chart with axes in logarithmic scale
B. Robertson 1986 profiling chart with axes in linear scale

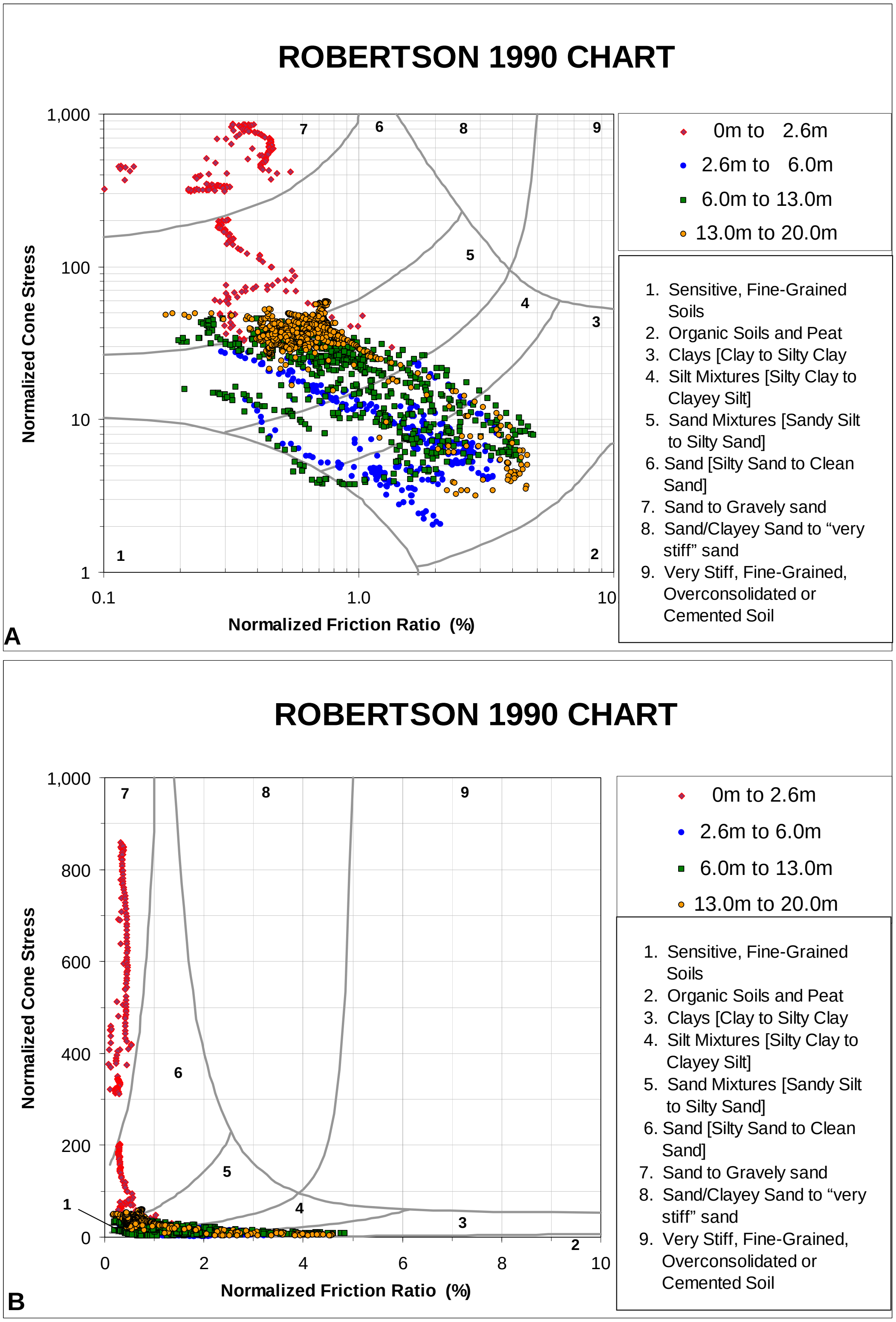

Fig. 2.18 A. Robertson 1990 profiling chart with axes in logarithmic scale
B. Robertson 1990 profiling chart with axes in linear scale

2.7 Dissipation Time Measurement

In fine-grained soils, the time for the dissipation of the generated pore pressure is of interest. Usually in conjunction with adding a rod to the rod assembly, the cone is kept unmoving and the pore pressures (U2) are recorded. The dissipation time to neutral pore pressure is considered a measure of the coefficient of consolidation, c_H. (Mayne et al. 1990, 2001). The pore pressure after full dissipation is a measure of the phreatic height at that depth and can be used as indication of pore pressure gradient in the soil (as was done in the case of the CPTU sounding shown in Fig. 2.14.

2.8 Inclination Measurement

When a cone is pushed into the ground it is started vertically, but, understandably, the cone rod assembly will start to bend in the soil and the cone will deviate from the vertical line through the starting point on the ground. All CPT systems incorporate inclination measurements and the inclination is recorded for each measurements of cone stress, sleeve friction, and pore pressure. Sometimes only a value of the maximum inclination is recorded. This will allow a calculation of the radial and vertical deviation of the cone, but not the direction. Other cones show the inclination in two directions, which measurements then allow for a calculation of the maximum inclination and the location of the cone at each depth. Down to depths of about 30 m, the deviation is usually not significant. Fig. 2.19 shows deviation records that are unmistakably large; the cone moved 12 laterally away from the starting point and the bending cause the depth measurement of 30 m to in reality have been slightly less than 28 m — "the cone is lifting its foot". Inclination measurements are not often reported. Obviously, they should be checked and the cone data corrected for depth deviation, when appropriate.

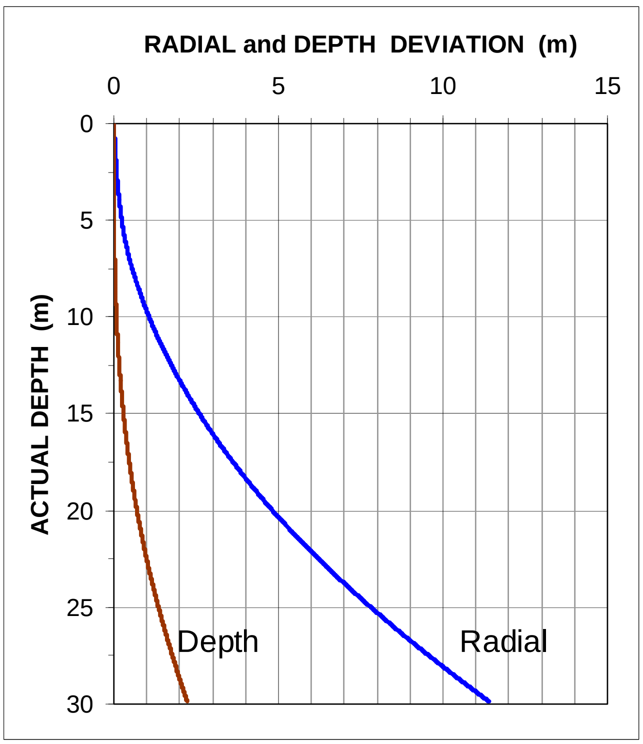

Fig. 2.19 Radial and depth deviation for a 30 m deep cone sounding in Squamish, BC

2.9 Shear -wave Measurement

The seismic CPTU, the SCPTU, incorporates a geophone for measuring the arrival time of a shear wave generated on the ground surface close to the Cone rod. The shear-wave is generated by giving a horizontal impact to a steel plate placed on the ground surface and the time for generating the impact and arrival at the geophone are recorded. The test is normally performed when adding a cone rod to the rod length (that is, the cone is not moving). Impacts are given at intermittent depths and the results are evaluated as the difference in travel time between geophone previous test depth and the current depth, resulting in the shear wave velocity for the soil between the two depths. The shear wave velocity is then used directly in analysis or converted to low-strain dynamic shear modulus (Gmax)

2.10 Additional Use of the CPT

Many geotechnical parameters are diffuse by themselves. Their reliability depends to a large extent on how they are applied, in what geology, for what design problem, and foremost, on what experience the user of the relation has in the application of the parameter. When a parameter is obtained through correlation to the cone penetrometer results, the user's direct experience becomes even more important. **No formula promoting a relation between a geotechnical parameter and the CPT results should be accepted without thorough correlation to independent test results at the site considered**. However, when such correlation, which by necessity is intermittent, has proven a consistent relation at a site, then, it can be used to establish a more detailed distribution of the parameters at a site from the CPTU profile.

2.10.1 Compressibility and Pile Capacity

The CPT can be used to estimate the compressibility parameters of a soil and the ultimate shaft and toe resistances of a pile. Information on these applications is provided in Chapters 3 and 6, respectively.

2.10.2 Undrained Shear Strength

A popular application for CPT results is to estimate values of undrained shear strength and several correlations exist. The popularity exists despite that undrained shear strength can be determined by so many methods, such as in-situ vane, unconfined compression test, triaxial testing, direct shear, simple shear, etc. The method of determining the undrained shear strength often varies with the design problem to be addressed. Eq. 2.7 is typical of the relations which have been proposed for determining the undrained shear strength from CPTU data. (Kulhawy and Mayne 1990).

$$\tau_u = \frac{q_t - \sigma_v}{N_{kt}} \tag{2.7}$$

where τ_u = undrained shear strength
q_t = cone resistance corrected for pore water pressure on shoulder (Eq. 2.1)
σ_v = total overburden stress
N_{kt} = a coefficient; $10 < N_{kt} < 20$

An examples of undrained shear strength values calculated from Eq. 2.7 is presented in Fig. 2.20A along with the cone stress profile. The sounding is from a site in Alberta 185 Km north of Edmonton described by Fellenius (2008). The groundwater table lies at a depth of 1.5 m and the pore pressure is hydrostatically distributed. The soil profile consists of 7.5 m of soft silty clay with a water content of about 35 % through 70 %, a Liquid Limit of about 60 % through 70 %, a Plastic Limit of about 15 through 40 , and a Plasticity Index of about 25. The Janbu modulus number ranges from about 12 through 20. The upper about 7 m of the clay is overconsolidated with an OCR of about 2 through 5.

Triaxial consolidated and undrained tests and direct shear testing on the clay indicated a strain-softening soil having a friction angle ranging from 21° through 25° with a residual (post peak) value of about 21°. A small cohesion intercept was found in the range of 10 KPa through 25 KPa. The clay is a re worked, transported, and re deposited glacial till clay. The clay is interrupted at 5 m depth by an about 0.5 m thick layer of silty sand. At a depth of 7.5 m lies a second 0.5 m thick layer of silty sand. The sand is followed by soft silty sandy gravely ablation clay till that continues to the end of the borehole at a depth of about 25 m. The ranges of water content and indices of the clay till are about the same as those of the upper clay layer. Consolidation tests on samples from the clay till show the Janbu modulus number of the clay to range from 20 through 30. No recompression modulus is available, but the sandy clay till is clearly overconsolidated.

A second example of undrained shear strength values calculated from Eq. 2.7 is presented in Fig. 2.20B. The sounding is from the Langley, BC. Below 5 m depth, the soils consist of lightly to over-consolidated stiff clay to large depth. Some thin sand layers exist between 33 m and 37 m depth.

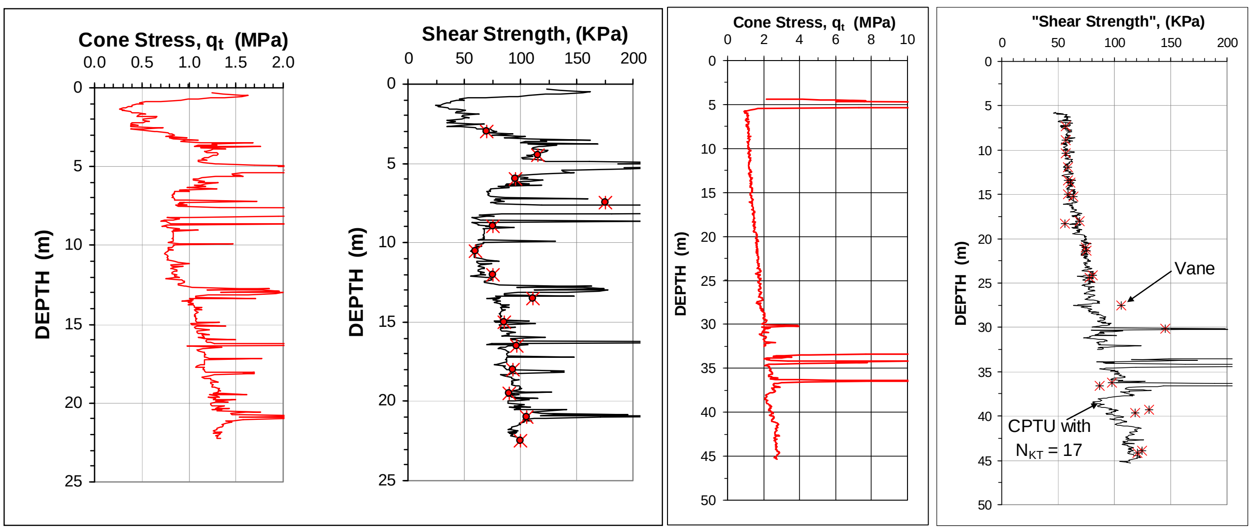

A Data from Paddle River, AB, using N_{kt} = 10 (Fellenius 2008)

B Data from Fraser River, Vancouver, B using N_{kt} = 17 (Amini et al. 2008

Fig. 2.20 Cone stress (q_t) and undrained shear strength profiles fitted to a vane shear profile from tests next to CPTU sounding.

2.10.3 Overconsolidation Ratio, OCR

Correlations between the CPTU test data and the overconsolidation ratio, OCR, have also been proposed. Eq. 2.8 presents one method (Kulhawy and Mayne 1990).

(2.8) $$OCR = C_{OCR} \frac{q_t - \sigma_v}{\sigma'_v}$$

where OCR = overconsolidation ratio
C_{OCR} = a coefficient; $\cong 0.2 < C_{OCR} < \cong 0.3$
q_t = cone resistance corrected for pore water pressure on shoulder (Eq. 2.1)
σ_v = total overburden stress
σ'_v = effective overburden stress

An OCR profile from the Alberta CPTU sounding is shown in Fig. 2.21 fitted to OCR values determined in eight oedometer tests on Shelby sample recovered in a bore hole next to the CPTU sounding. The fit was obtained with an OCR-coefficient of 0.2.

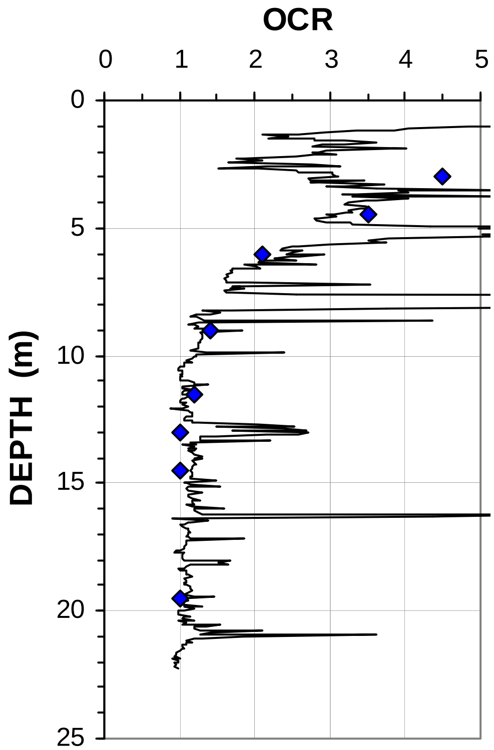

Fig. 2.21 OCR profile fitted to OCR values determined from oedometer tests on Shelby samples. Data from Paddle River site, Alberta (Fellenius 2008).

2.10.4 Earth Stress Coefficient, K_0

Also the earth stress coefficient, K0, can be correlated to CPTU test results. Eq. 2.9 presents one method (Kulhawy and Mayne 1990).

(2.9) $$K_0 = C_K \frac{q_t - \sigma_v}{\sigma'_v}$$

where C_K = a coefficient; $C_K \cong 0.1$
q_t = cone resistance corrected for pore water pressure on shoulder (Eq. 2.1)
σ_v = total overburden stress
σ'_v = effective overburden stress

A K_0-profile from the Alberta CPTU sounding is shown in Fig. 2.22.

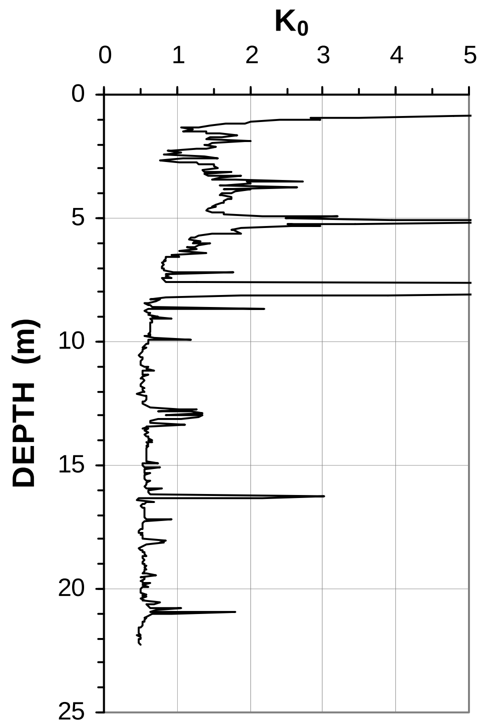

Fig. 2.22 K_0 profile determined from the CPTU sounding.
Data from Paddle River site, Alberta (Fellenius 2006).

2.10.5 Friction Angle

The CPTU results are frequently used to estimate a value for the effective friction angle of sand, typically, using the relation shown in Eq. 2.10 (Robertson and Campanella 1983).

(2.10) $$tg\phi' = C_\phi \lg \frac{q_t}{\sigma'_v} + K_\phi$$

where ϕ' = effective friction angle
C_ϕ = a coefficient; $C_\phi \cong 0.37$ (= 1/2.68)
K_ϕ = a coefficient; $K_\phi \cong 0.1$
q_t = cone resistance corrected for pore water pressure on shoulder (Eq. 2.1)
σ'_v = effective overburden stress

A φ'-profile from the Alberta CPTU sounding is shown in Fig. 2.23. The profile also includes three friction angle values determined in triaxial tests. The basic 0.37 C_φ- and 0.1 K_φ coefficients are used..

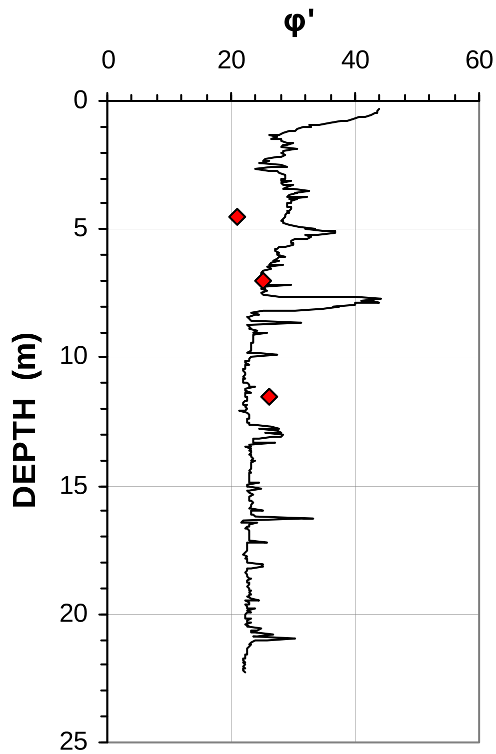

Fig. 2.23 Friction angle, φ', profile determined from the CPTU sounding with three values from triaxial tests. The basic 0.37 C_φ and $K\varphi$ coefficients are used. Data from Paddle River site, Alberta (Fellenius 2006).

2.10.6 Density Index, I_D

Equation 2.11 shows an empirical relation for the Density Index (Kulhawy and Mayne 1990).

$$I_D = \sqrt{\frac{q_{cl}}{305 F_{OCR} F_{AGE}}} = \sqrt{\frac{q_{cl}}{300}} \qquad (2.11)$$

where I_D = density index
q_{cl} = normalized cone resistance (1/√(σ' σ$_r$), where σ_r = 100 KPa)
F_{OCR} = adjustment factor for overconsolidation ratio (OCR) ~ 1
F_{AGE} = adjustment factor for age = ~ 1

Baldi et al. (1986) presented an empirical relation for the Density Index shown in Eq. 2.12.

(2.12) $$I_D = \left(\frac{1}{2.61}\right) \ln\left(\frac{q_c}{181 \sigma'^{0.55}_m}\right)$$

where I_D = density index
q_c = cone resistance
σ_m = mean effective overburden stress = $\sigma'_v(1 + K_0)/3$
σ'_v = effective overburden stress
K_0 = earth stress coefficient

The density index is primarily intended to be applied to sands. Fig. 2.24 shows the results from a CPT sounding in a loose sand at Vilano Beach Florida (McVay et al. 1999).

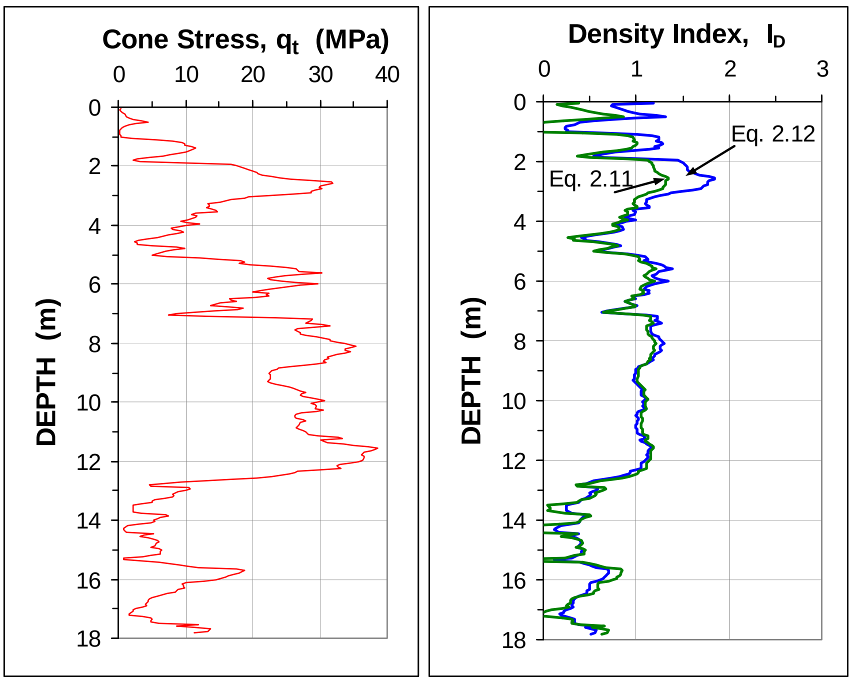

Fig. 2.24 Profiles of cone stress and Density Index, I_D, determined from the CPTU sounding according to Eq. 2.11 and 2.12. No reference values are available from the site. (CPT data from McVay et al. 1999).

2.10.7 Conversion to SPT N-index

Robertson et al. (1983) presented correlations between CPT cone stress values and N-indices from SPTs at 18 sites, as shown in Fig. 2.25A. The conversion ratios are plotted to the mean grain size determined for the SPT samples. The log-scale on the abscissa overemphasizes the data in the fine-grained soils. The data are therefore shown also with the abscissa in linear scale, Fig. 2.25B, which also shows that the scatter in the ratio values is rather large.

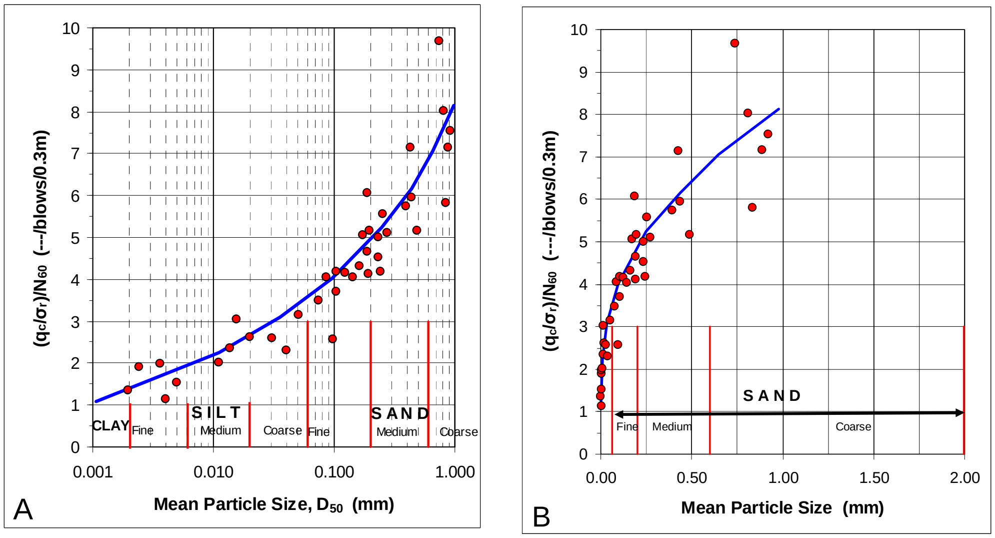

Fig. 2.25 Correlations between CPT cone stress values, q_c (KPa) divided by σ_r (= 100 KPa) and SPT N_{60}-indices from 18 sites. Fig. 2.25A abscissa is in Log-scale and Fig. 2.25B abscissa is in linear scale. Data from Robertson et al. 1983.

The conversion curve shown by Robertson et al. (1983) has seen much use for determining N-indices from CPT soundings in order to apply the so-determined "N"-values to various calculations. Actually, these days, the cone stress is the pore pressure corrected stress, q_t. The conversion results are rather questionable, however. The conversions do not just show a scatter, conversions at other sites are often very different to those shown in Fig. 2.25. For example, Fig. 2.26 shows a plot of the same data supplemented with conversions obtained from N-indices presented by McVay et al. (1999) for the Vilano Beach site, Florida. The mean grain diameter for the Florida site is not known and all data points are plotted at d = 0.65 mm, which is a reasonably representative value for the sand at the site. However, even if the actual mid-range grain size had been known, the plot would still neither have shown any relation to the 1983 curve, nor to any other correlation.

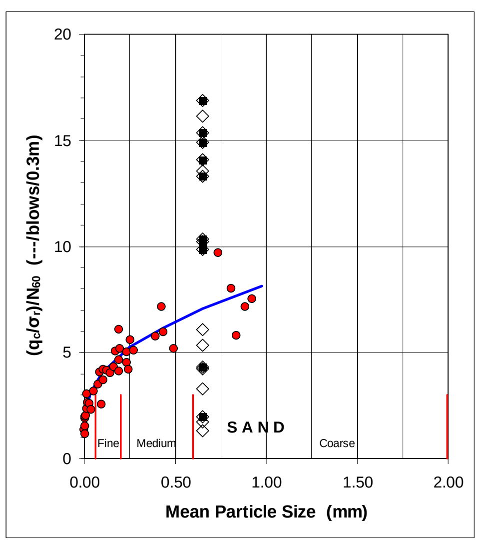

Fig. 2.26 The SPT-CPT correlations of Fig. 2.25 supplemented with correlations from Vilano Beach site, Florida. Data from McVay et al. 1999.

2.10.8 Assessing Earthquake Susceptibility

When an earthquake hits, as the name implies, the soil will "quake in shear"; movements back and forth occur (more rarely, up and down). If the shear movements, as is most commonly the case, make grains move into the voids, the soil volume reduces —the soil contracts—and the effective stress decreases. In a series of repeated shaking—cyclic shear—the pore pressure increases can accumulate, affect a large volume of soil, and cause a complete loss of effective stress, i.e., the soil liquefies. If so, the volume loss in the liquefied zone will cause the foundations placed on the ground above to settle by the amount of the volume decrease. Shear movements of magnitude associated with an earthquake in fine-grained and cohesive soils are considered less susceptible to liquefaction, as the soil grains in such soil cannot as easily be rearranged by the shaking. Moreover, dense coarse-grained soil will not liquefy, because when the grains in such soils are rearranged and move relative each other, they "climb over each other"[1]. In the process, the soil elements affected will increase in volume—dilate, and the pore pressures will decrease rather than increase—the soil does not liquefy. However, loose coarse-grained soil are contractant and the looser the soil, the more prone to liquefaction it is. Figure 2.27 illustrates the sometime drastic consequence of liquefaction.

In the following, principles of the assessment of liquefaction susceptibility are presented. The material is not exhaustive and the reader is strongly recommended to review the references for additional information.

Fig. 2.27 Effect of liquefaction from the 7.4 Magnitude Kocaeli Earthquake of August 17, 1999 in Turkey. Courtesy of Dr. N.J. Gardner, University of Ottawa.

[1] When subjected to a shear movement, initially, also a dense sand will contract, but when the movement gets larger, as in the case of an earthquake shaking, dense sand will dilate.

2.10.8.1 Cyclic Stress Ratio, CSR, and Cyclic Resistance Ratio, CRR

Data from CPTU soundings are often employed to assess susceptibility due to earthquake induced liquefaction. The following summarizes the procedures of Robertson and Wride (1998) and Youd et al. (2001). The analysis starts by determining the driving effect, called **Cyclic Stress Ratio, CSR**, calculated from Eqs. 2.13 through 2.15.

(2.13) $$CSR = 0.65\,(MWF)\,\frac{a_{\max}}{g}\,\frac{\sigma_v}{\sigma'_v}\,r_d$$

(2.14) $$MWF = \frac{(M)^{2.56}}{173}$$

(2.15) $$r_d = 1 - 0.015z$$

where
- CSR = Cyclic Stress Ratio
- MWF = Earthquake Magnitude Weighting Factor, dimensionless; increases with increasing earthquake magnitude, M
- M = earthquake magnitude per Richter scale, dimensionless
- a_{max} = maximum horizontal acceleration at ground surface (m/s^2)
- g = gravity constant (m/s^2), dimensionless
- r_d = stress reduction coefficient for depth, dimensionless
- z = depth below ground surface, (m)

Usually the term a_{max}/g is given as a ratio to the gravity constant, "g", e.g., 0.3g. When M is equal to a magnitude of 7.5, MWF becomes equal to unity. (For, say, magnitudes ranging from 6.0 through 8.0, MWF ranges from 0.57 through 1.19). MWF is the inverse of the Magnitude Scaling Factor, MSF, also commonly used for weighting or scaling earthquake magnitudes. For recommendations regarding choice of MWF or MSF, see Youd et al. (2001).

The depth factor or stress reduction coefficient, r_d, serves to respond to the observation that the incidence of liquefaction reduces with depth. Slightly different relations for the depth factor, r_d, are proposed by different authors, as summarized by Youd et al. (2001) and Moss et al. (2006).

The ability of the soil to resist liquefaction is calculated using a **Cyclic Resistance Ratio, CRR**, determined according to an approach proposed by Robertson and Campanella (1985) further developed by Robertson and Wride (1998), who correlated information for a large number of earthquakes. Figure, 2.28 shows the CSR-values as calculated from Eq. 2.13 and plotted against values of Normalized Cone Stress, q_{c1}, as defined by Eq. 2.17. The plotted data points are from where liquefaction occurred and where it did not occur, and the boundary between the two scenarios is termed the CRR-curve. It is considered applicable to clean sand defined as sand with a fines content smaller than 5 %, which is also the upper boundary for free-draining sand.

(2.16) $$q_{c1} = q_c\,C_{N\,c1}$$

where
- q_{c1} = cone stress normalized for liquefaction calculation (MPa)
- q_c = cone stress. In sand, whether the cone stress is uncorrected q_c, or corrected, q_t, for the pore pressure, $U2$, on the cone shoulder makes very little difference to the normalized cone stress value (MPa).
- C_{Nc1} = normalization factor expressed in Eq. 2.16

$$(2.17) \quad C_{Nc1} = \sqrt{\frac{\sigma_r}{\sigma'_v}}$$

where C_{Nc1} = normalization factor
σ_r = reference stress = 100 KPa (= atmospheric pressure)
σ'_v = effective overburden stress at the depth of the cone stress considered (KPa).

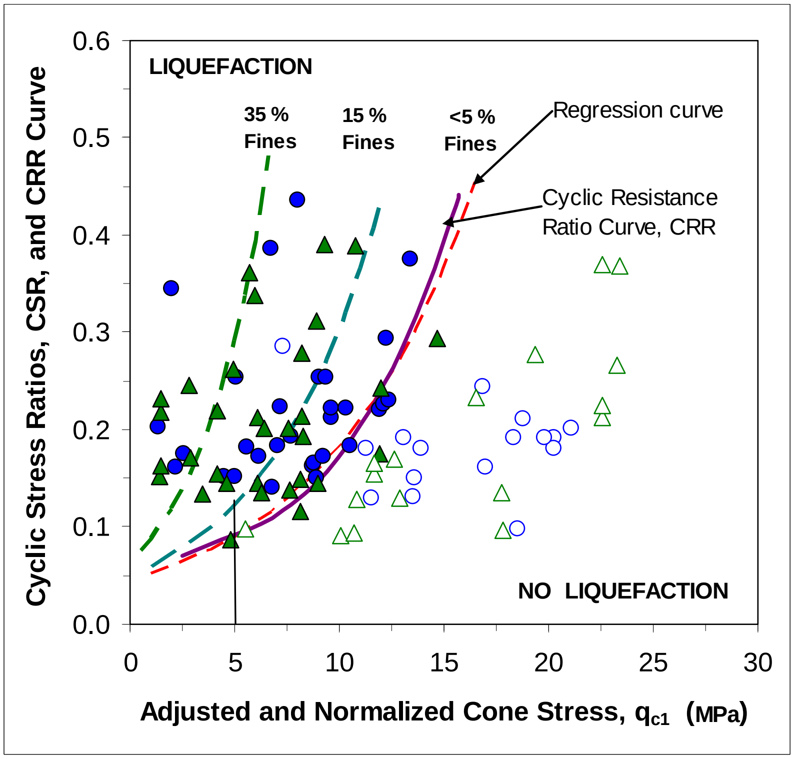

Fig. 2.28 Correlations between CRR-values calculated from actual earthquakes versus q_{c1}-values for cases of liquefaction (solid symbols) and no liquefaction (open symbols), and boundary curve (solid line) according to Robertson and Wride (1998) and Youd et al. (2001). The boundary line is the Cyclic Resistance Ratio Curve, CRR, which is also shown as a linear regression curve (Eq. 2.18) for the boundary values (M=7.5). The two dashed curves show the boundary curves for sand with fines contents of 15 % and 35 %, respectively (copied from Stark and Olsen 1995, Eqs. 2.19a and 2.19b). The original diagram has the cone stress, q_c, divided by atmospheric pressure to make the number non-dimensional.

According to the sources of Fig. 2.28, sand containing fines will be less liquefiable, that is, the boundary line moves to the left for increasing fines contents. Start and Olsen (1995) presented a graph similar to that shown, which included boundary lines for fines contents of 15 % and 35 %. These curves have been added to the graph. However, recent findings have questioned that fines content would reduce seismic susceptibility (Bray and Sancio 2006, 2007; Boulanger and Idriss 2006, 2007; Boardman 2007).

The boundary curve for the Cyclic Resistance Ratio Curve, CRR, applicable to clean sand is determined according to Eqs. 2.18a and 2.18b. The curve can be approximated by means of regression analysis, which gives Eq. 2.19.

(2.18a) $$CRR = 0.833\left(\frac{q_{c1}}{100}\right) + 0.05 \quad for \quad q_{c1} < 50$$

(2.18b) $$CRR = 93\left(\frac{q_{c1}}{100}\right)^3 + 0.08 \quad for \quad 50 < q_{c1} < 160$$

(2.19) $$CRR = 0.045(e^{0.14q_{c1}})$$

where CRR = Cyclic Resistance Ratio
q_{c1} = cone stress normalized for liquefaction calculation; (MPa) (Eq. 2.16)
e = base of the natural logarithm = 2.718

The two curves for fines contents of 15 % and 35 % correspond to Eqs. 2.20a and 2.20b, respectively.

(2.20a) $$CRR = 0.045(e^{0.20q_{c1}})$$

(2.20b) $$CRR = 0.065(e^{0.30q_{c1}})$$

Juang and Jiang (2000) presented the graph shown in Fig. 2.29, similar to that in Fig. 2.28, showing boundary curves for probability of liquefaction, P_L, ranging from 0.1 through 0.9. Mathematical expressions for the curves are given by Eqs. 2.21a through 2.21f. The curve (Eq. 2.21d) for a probability of 0.5 is almost identical to the boundary curve (Eq. 2.18) of Fig. 2.29.

(2.21a) $$CRR_{PL=0.1} = 0.025(e^{0.14q_{c1}})$$

(2.21b) $$CRR_{PL=0.2} = 0.033(e^{0.14q_{c1}})$$

(2.21c) $$CRR_{PL=0.3} = 0.038(e^{0.014q_{c1}})$$

(2.21d) $$CRR_{PL=0.5} = 0.046(e^{0.14q_{c1}})$$

(2.21e) $$CRR_{PL=0.7} = 0.057(e^{0.14q_{c1}})$$

(2.21f) $$CRR_{PL=0.9} = 0.085(e^{0.14q_{c1}})$$

where CRR = Cyclic Resistance Ratio from the CPTU data
P_L = probability of liquefaction
e = base of the natural logarithm = 2.718
q_c = cone stress (KPa)

Moss et al. (2006) presented methodologies for deterministic and probabilistic assessment of seismic soil liquefaction triggering potential based on the cone penetration test. The data base includes observations at 18 earthquake events and studies of the response of sand layers at 182 localities affected by the earthquake. Of these, liquefaction was observed at 138 cases and the sand did not liquefy in 44 cases. Two of the case histories (Kocaeli, Turkey, and Chi-Chi, Taiwan, involving 32 observations) were from quakes occurring after 1998. The Moss et al. (2006) assessment makes use of probabilistic and statistics as well as information in addition to the cone sounding information . For deterministic assessment the approach is similar to the approach by Robertson and Wride (1998) as illustrated in Fig. 2.30.

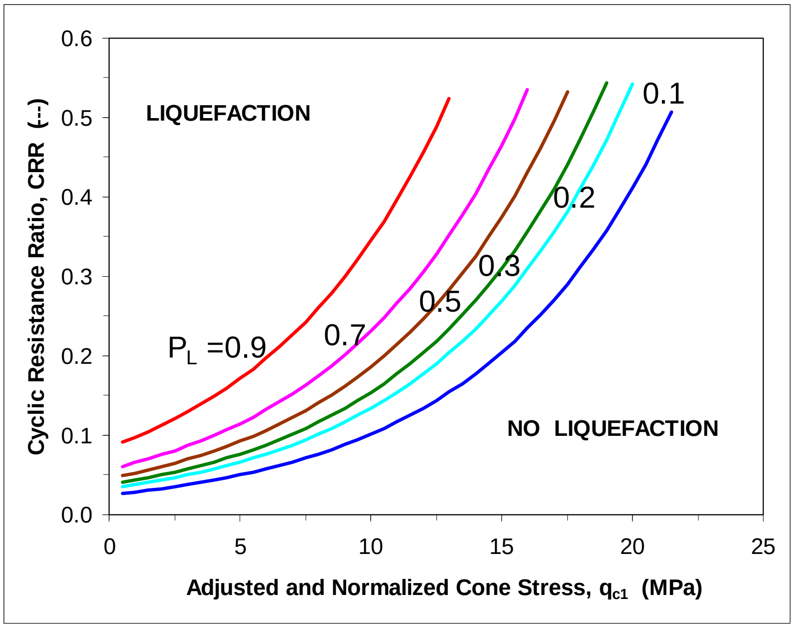

Fig. 2.29 Correlations between CRR-values and q_{c1}-values for different probabilities of liquefaction, P_L. Data from Juang and Jiang (2000).

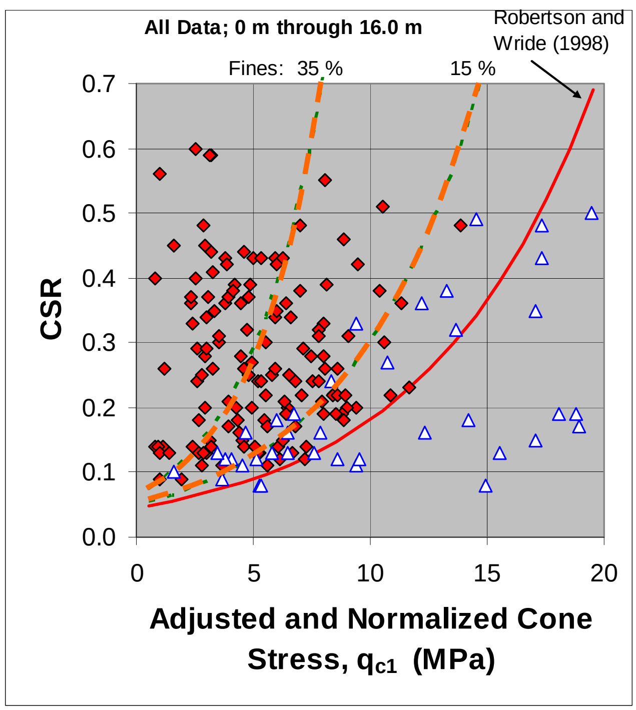

Fig. 2.30 Correlations between CRR-values calculated from actual earthquakes versus q_{c1}-values for cases of liquefaction (solid symbols) and no liquefaction (open symbols), according to Moss et al. (2006) and boundary curve (solid line) according to Robertson and Wride (1998) and Youd et al. (2001). The boundary line is the Cyclic Resistance Ratio Curve, CRR. The two dashed curves show the boundary curves for sand with fines contents of 15 % and 35 %, respectively (copied from Stark and Olsen 1995, Eqs. 2.19a and 2.19b).

Fig. 2.31A and 2.31B present the Moss et al. (2006) data plotted as earthquake acceleration (q_{max}/g) and not-normalized cone stress (the as-measured cone stress). In an actual case, this is the first information available and the figures are useful as aid toward whether or not a detailed liquefaction study is necessary. Fig. 2.31A shows only the data from ground surface to depth of 6.0 m. Fig. 2.32B shows all data in the data base. The dashed curve is the Robertson and Wride CRR curve plotted against the q_c-values as if they were q_{c1}-values. The curve is only included in the figures to serve as reference to Fig. 2.30. Fig. 2.31A demonstrates that for shallow depth (<6 m), and a moderate magnitude earthquake (<0.25g), liquefaction was not observed for as-measured cone stress larger than 5 MPa.

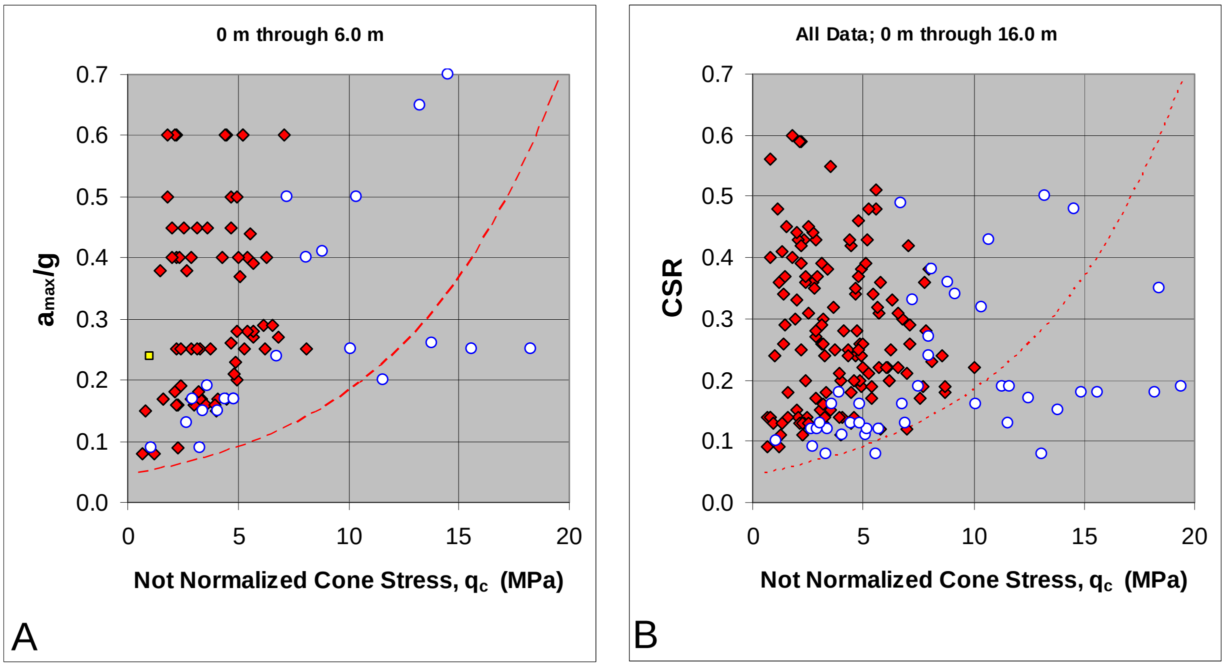

Fig. 2.31 The data points presented as earthquake acceleration (q_{max}/g) versus not-normalized cone stress (the as-measured cone stress).

2.10.8.2 Factor of Safety, F_S, against Liquefaction

The factor of safety (F_S) against liquefaction is the ratio between the resisting condition represented by the CRR-value and the driving condition represented by the CSR-value, according to Eq. 2.22.

$$F_s = \frac{CRR}{CSR} MWF \tag{2.22}$$

where
F_s = factor of safety against liquefaction
CRR = Cyclic Resistance Ratio from the CPTU data
CSR = Cyclic Stress Ratio from the seismic conditions
MWF = Magnitude Weighting Factor

A F_S smaller than unity does not necessarily mean that liquefaction will occur for the considered earthquake magnitude. However, it does indicate the need for a closer look at the risk and susceptibility and a detailed study of the current main references, e.g., Youd et al. (2001) and Moss et al. (2006).

2.10.8.3 Comparison to Susceptibility Determined from SPT N-indices

Evaluation of liquefaction resistance was formerly—and still is in many places—based on the SPT Index. It is generally considered necessary to adjust the N-index to depth, i.e., overburden stress, by means of a coefficient called "normalization factor", C_N, proposed by Seed 1976 for earthquake applications specifically. The N-index is also adjusted to a value for standard condition of energy. The latter is obtained by using transducers for measuring impact stress and acceleration (see Chapter 9) to determine the energy transferred to the SPT rods. As "standard" transferred energy is 60 % of the nominal energy, the measured N-index is proportioned to the actually transferred energy. (Note deviation of the actual transferred energy from 60 % of nominal by more than 25% up or down is not acceptable). The so-adjusted index is expressed in Eqs. 2.23 and 2.24.

(2.23) $$(N_1)_{60} = C_N N_{60}$$

where N_1 = stress-adjusted (depth-adjusted) N-index
C_N = normalization factor expressed in Eq. 2.24.
N_{60} = SPT N-index energy corrected

(2.24) $$C_N = 1 - 1.25 \log\left(\frac{\sigma'_v}{\sigma_r}\right)$$

where σ'_v = effective overburden stress
σ_r = reference stress = 100 KPa

The normalization factors, Eqs. 2.16 and 2.23, are very similar as indicated in Fig. 2.32, where they are plotted together. The assumptions are a soil with a density of 2,000 kg/m^3 and a groundwater table at the ground surface. Below a depth of about 3 m, the factors are almost identical. At a depth of about 10 m, both normalization factors are about equal to unity (effective overburden stress is about equal to the reference stress).

Figure 2.33 shows calculated *CSR*-values versus corresponding $(N_1)_{60}$-values from sites where liquefaction effects did or did not occur for earthquakes with magnitudes of approximately 7.5. The *CRR* curve on this graph was conservatively positioned to separate data points from sites where liquefaction occurred from data points from sites with no liquefaction. Curves were developed for granular soils with fines contents of 5% or less, 15%, and 35% as shown on the plot. The *CRR* curve for fines contents smaller than 5% is the basic penetration criterion for the simplified procedure and is called the "SPT clean sand base curve". The curves are valid only for magnitude 7.5 earthquake, but the values can be adjusted by means of the *MWF* according to Eq. 2.13 (for other suggested relations see Moss et al. 2006).

The boundary *CRR* curve in the original graph is plotted per Eq. 2.25. The dashed curve next to the boundary curve is a regression curve fitting the boundary curve per Eq. 2.26a. Similarly, the two dotted curves showing the boundary curves for fines contents are approximately fitted to Eqs. 2.26b and 2.26c.

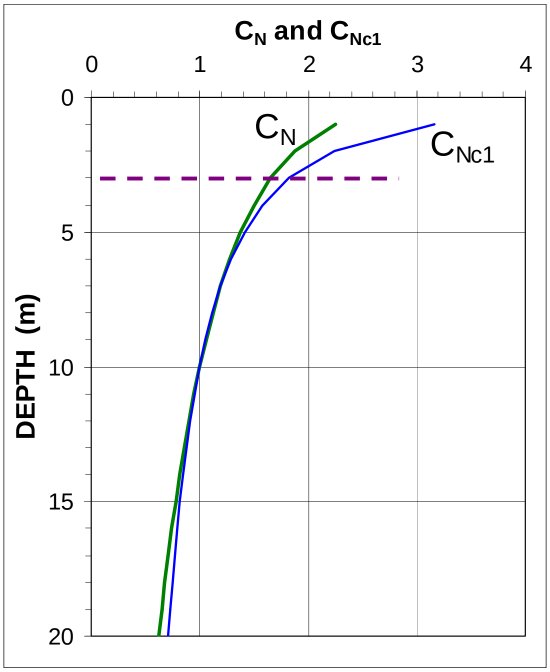

Fig. 2.32 Comparison between the normalization factors for SPT-index and CPT cone stress, q_c.

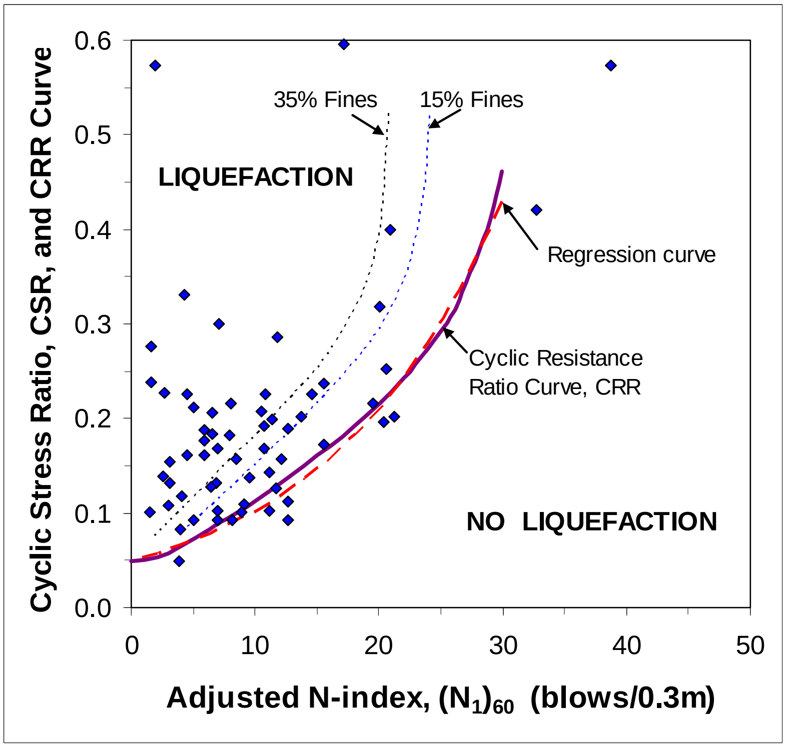

Fig. 2.33 Correlations between *CRR*-values and Adjusted *N*-indices. Data from Youd et al. (2001).

(2.25) $$CRR = \frac{1}{34 - N} + \frac{N}{135} + \frac{50}{(10N + 45)^2} - \frac{1}{200}$$

(2.26a) $$CRR_{FC<5\%} = 0.050\,(e^{0.072\,N_{60}})$$

(2.26b) $$CRR_{FC=015\%} = 0.060\,(e^{0.084\,N_{60}})$$

(2.26c) $$CRR_{FC=035\%} = 0.070\,(e^{0.092\,N_{60}})$$

2.10.8.4 Correlation between the SPT N-index, N_{60}, and the CPT cone stress, q_t.

The adjusted SPT-N indices, $(N_1)_{60}$, can be correlated to the to the adjusted and normalized cone stress, q_{c1}, over the respective values of cyclic stress resistance, *CSR*. For equal *CSR*-values, the relation between the two is approximately linear— the ratio is 0.18, that is, $(N_1)_{60} = 1.8q_{c1}$ (the linear regression coefficient is 0.99). As mentioned, at a depth of 10 m, the normalization factor C_N is approximately equal to unity, i.e., the $(N_1)_{60}$-values is equal to N_{60}, (Eqs. 2.22 and 2.23). Similarly, the factor $\sqrt{(\sigma_r/\sigma'_v)}$ in Eq. 2.15 is equal to unity at this depth. Therefore, the normalized cone stress, q_{c1}, is equal to q_c. So, the ratio at 10 m depth between q_c and $(N)_{60}$ becomes about 2. This means, for example, that at about 10 m depth, a loose sand, as indicated by a cone stress of, say, 3 MPa, correlates to an *N*-index of 6 blows/0.3 m, which does correspond to a loose relative density when judged from the *N*-index. As the normalization factors are very similar, the mentioned 2 ratio is independent of depth (but for above 3 m depth). Referring to Section 2.10.7, the q_c/σ_r-ratio between a q_c equal to 3 MPa and an N_{60} equal to 6 bl./0.3m is 5. To lie on the curve of Fig. 2.25, this value would apply to a "fine sand". The agreement is hardly coincidental, however. Much of the experience behind Fig. 2.28 and its curves (Eqs. 2.15 through 2.18) is transferred from the data behind Fig. 2.31. It is obvious from the discussion in Section 2.8 that correlation between the SPT index and the cone stress is highly variable. It is questionable how relevant and useful a conversion from an SPT Index value to a cone stress would be for an actual site . One would be better served pushing a cone in the first place.

2.10.8.5 Example of determining the liquefaction risk

As an example of calculations of factor of safety against liquefaction, results are presented of cone penetration soundings performed small trial area (12 m by 12 m) at Hong Kong Chek Lap Kok Airport in a sand fill before and after seven days after vibratory densification. The sand fill consisted partly of calcareous material (fragments of shells and clams), and contained about 15 % of fines and occasional layers of silt and silty sand. It was placed by bottom dumping, where the water depth exceeded 4 m, and by spraying, where the water depth was shallower. The final thickness of the sand fill prior to compaction was about 10 m. The groundwater level was located about 1 m below the fill surface. The sand fill was specified to contain less than 10 % of fines. The compaction study of the case is reported by Massarsch and Fellenius (2002).

Figure 2.34 present the results of four CPTU soundings through the as-placed fill before compaction, illustrating that the fill consists mainly of loose sand to a depth of about 4 m below which the sand contain frequent layers of silty sand and an occasional lens of silty clay and even clay. The homogeneity of the fill is demonstrated in the profiling chart shown in Fig. 2.35. The figures include all CPT records (readings were taken every 20 mm) from one CPT sounding. The data points in Zones 4a and 4b indicating silt, sandy silt, and silty sand are all from below 4 m depth. The silty clay and clay lens indicated in the figure at about 6 m depth is 60 mm thick and the profiling chart shows it to be made up of three closely located values, one value indicating clay and two values indicating silty clay.

The site was densified using the Müller Resonance Compaction (MRC) method (Massarsch and Westerberg 1995). By changing the vibration frequency, the system makes use of the vibration amplification, which occurs when the soil deposit is excited at the resonance frequency. Different vibration frequencies are used during the particular phases of the compaction process in order to achieve optimal probe penetration and soil densification, as well as facilitate of probe extraction and to avoid undoing the compaction ("uncompacting" the soil).

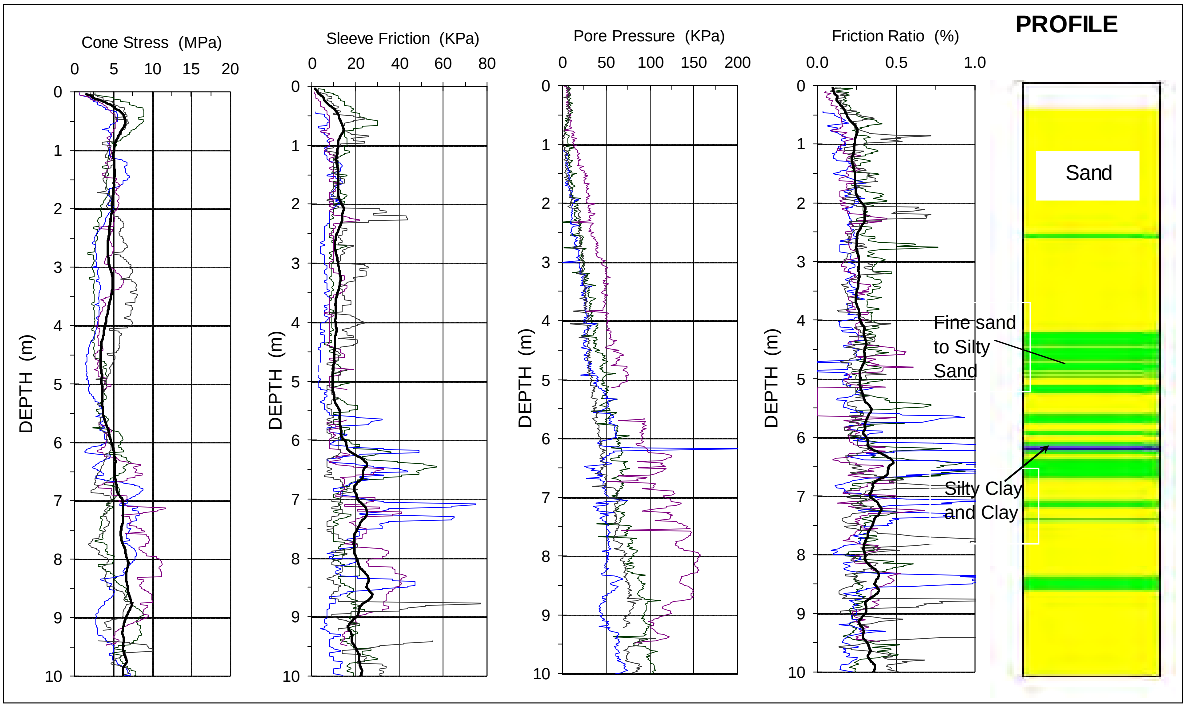

Fig. 2.34 Results of four CPTU initial (before compaction) soundings at Chek Lap Kok Airport. The heavy lines in the cone stress, sleeve friction, and friction ratio diagrams are the geometric averages for each depth of the four soundings.

The results of three cone soundings performed seven days after the vibratory compaction are shown in Fig. 2.36. The diagrams show that the compaction has resulted in increased values of cone stress and sleeve friction, more directly demonstrated in Fig. 2.37, where only the average curves are shown.. The friction ratio is approximately the same, however. The average curves are produced by means of a geometric average running over a distance of 500 mm, that is 25 values. The purpose of the averaging is to reduce the influence of thin layers of soft material that could cause a smaller than actual cone stress and, therefore, indicate a larger than actual susceptibility to liquefaction.

Figure 2.38 shows the data points in an Eslami-Fellenius profiling chart, implying a coarser soil than that shown by the sounding before the compaction (Fig. 2.34). Of course, the soil composition is the same (but for minor variation below about 9 m depth, where the seven-day sounding encountered clay lenses not found in the "before" sounding). The densification has changed the sand from a normally consolidated sand to an overconsolidated sand. As a result, the points plot higher up in the chart implying a coarser soil than found in the "before" sounding.

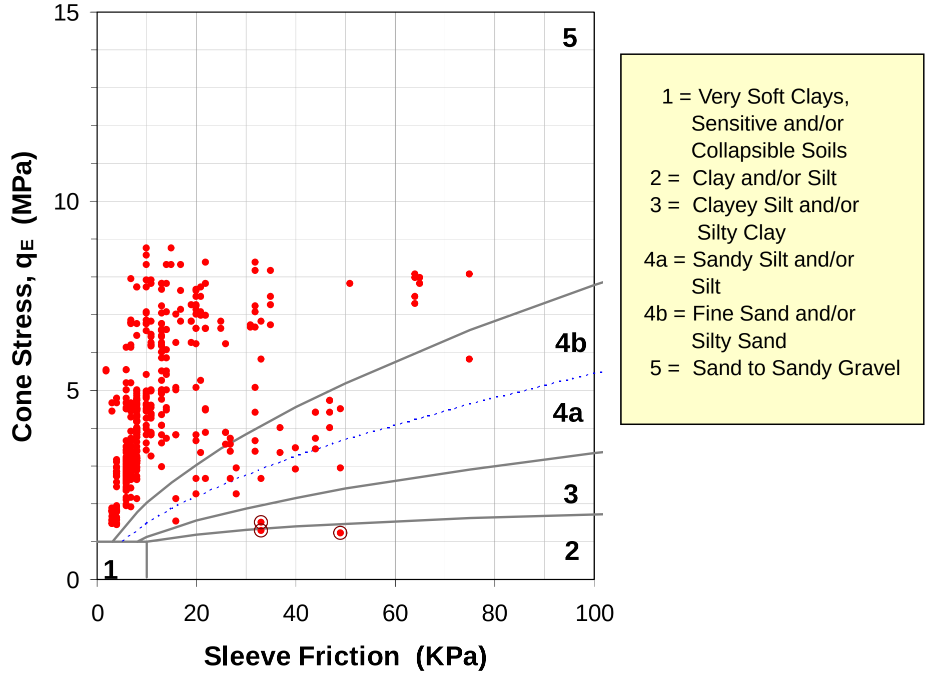

Fig. 2.35 The CPT data from one of the initial cone soundings plotted in an Eslami-Fellenius CPT profiling chart (Eslami and Fellenius 2000). The three separate dots near the boundary between Zones 2 and 3 are from the clay layer at Depth 6.1 m. (Data from Massarsch and Fellenius 2002).

For purpose of demonstrating the seismic analysis described above, the susceptibility for liquefaction at the site is assumed to be affected by an earthquake of magnitude of 7.5 and a seismic acceleration of 30 % of gravity. This assumption determines the site-specific Cyclic Resistance Ratio, *CRR*, according to Eqs. 2.13 through 2.15. The cone stress measurements determine the Cyclic Stress Ratio, *CSR*, from the "before" and "after" soundings, and the factor of safety against liquefaction is the CSR divided by the *CRR* as defined in Eq. 2.20. Figure 2.39 shows the calculated factors of safety for "before" and "after" compaction and demonstrates that the compaction was highly efficient above about 6 m depth and plain efficient in the finer soils below (fine sand and silt are not as suitable for compaction as sand; Massarsch 1991).

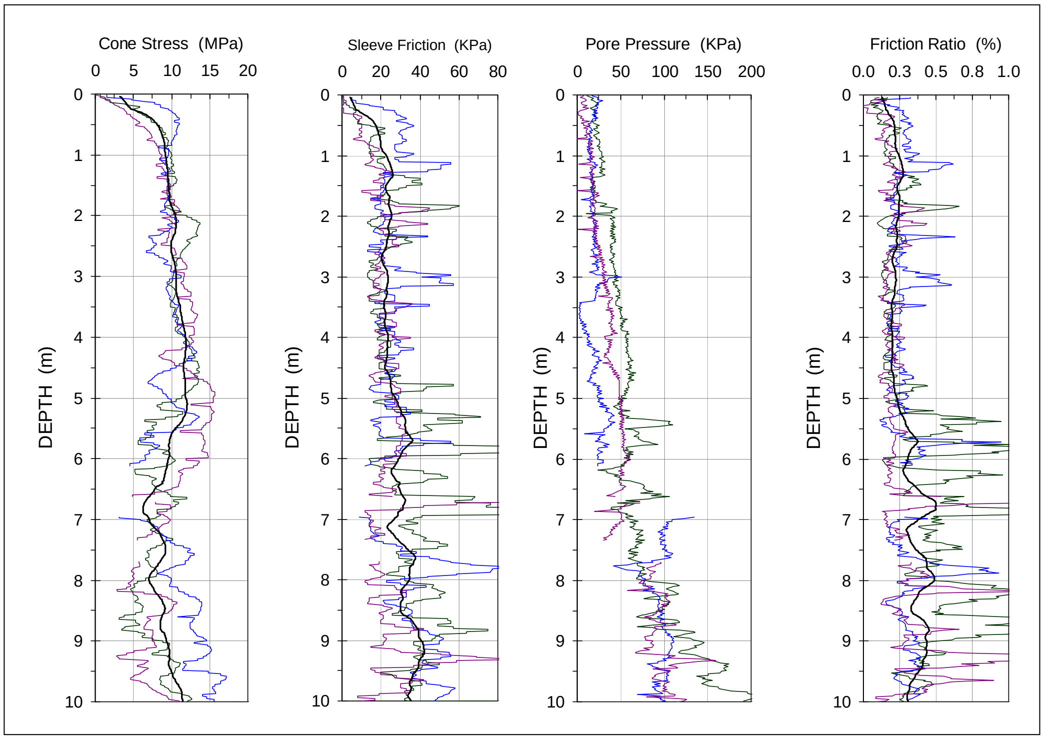

Fig. 2.36 Results of three CPTU soundings at Chek Lap Kok Airport seven days after the vibratory compaction. The heavy lines in the cone stress, sleeve friction, and friction ratio diagrams are the geometric averages for each depth of the four soundings.

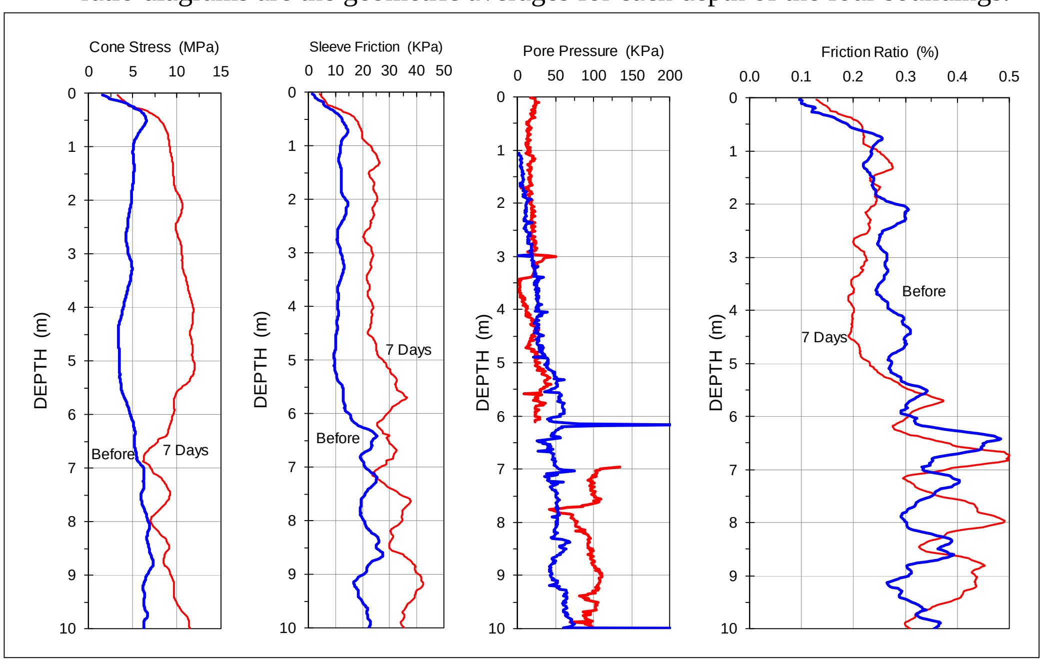

Fig. 2.37 Geometric average values of cone stress, sleeve friction, and friction ratios and measured pore pressures from CPTU soundings at Chek Lap Kok Airport before and seven days after the vibratory compaction.

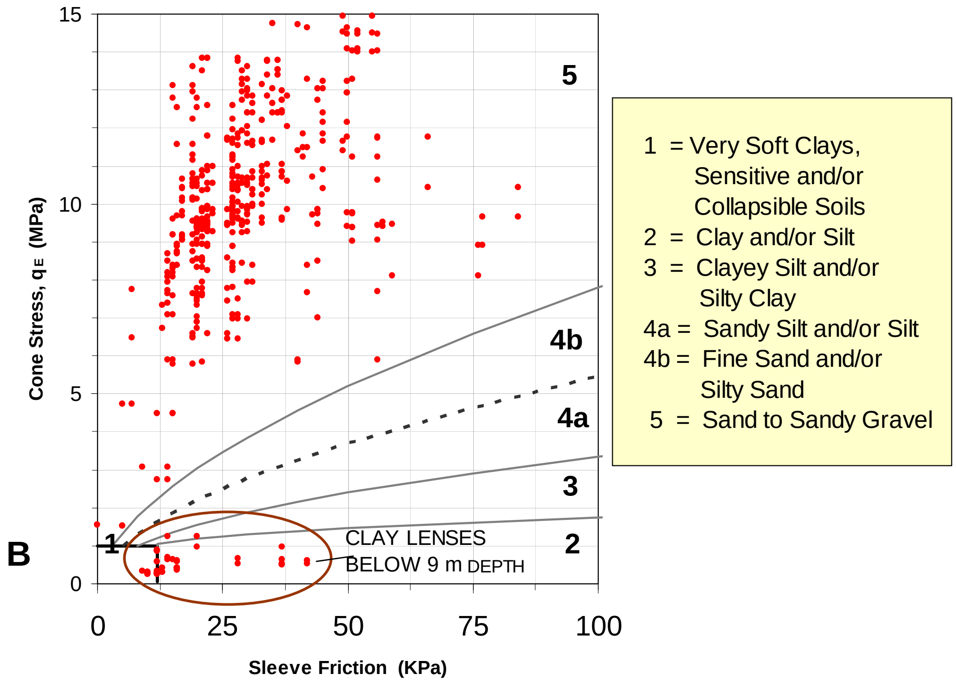

Fig. 2.38 The CPT data from one of the 7-day after cone soundings plotted in an Eslami-Fellenius profiling chart (Eslami and Fellenius 2000).

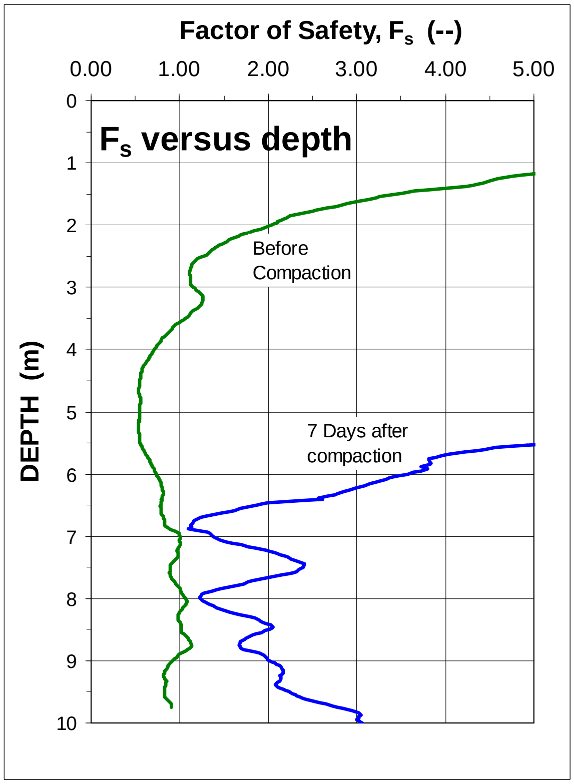

Fig. 2.39 Factor of safety against liquefaction before and after vibratory compaction.

CHAPTER 3

SETTLEMENT CALCULATION

3.1 Introduction

A foundation is a constructed unit that transfers the load from a superstructure to the ground. With regard to vertical loads, most foundations receive a more or less concentrated load from the superstructure and transfer this load to the soil underneath the foundation, distributing the load as a stress over the "footprint" of the foundation. Part of the soil-structure interaction requirement is then the condition that the stress must not give rise to a deformation of the soil manifested in the superstructure in excess of what the superstructure can tolerate.

Deformation is expressed by the terms movement, settlement, and creep. Although all three mean deformation, they are not synonyms—they are related, but not equal. It is important not to confuse the terms.

3.2 Movement, Settlement, and Creep

Movement occurs as a response when a stress is applied to a soil, but the term should be reserved to deformation due to *increase of* ***total*** *stress*. Movement is the result of a transfer of stress to the soil (the movement occurs as necessary to build up the resistance to the load), when the involved, or influenced, soil volume successively increases as the stress increases. For example, when adding load increments to a pile or to a plate in a static loading test (where, erroneously, the term "settlement" instead of properly "movement" is often used). As a term, movement is used when the involved, or influenced, soil volume increases as the load increases.

Settlement is volume reduction of soil volume as a consequence of an *increase in* ***effective*** *stress*, when the involved, or influenced, soil volume stays "the same" as the stress increases. It consists of either one or the sum of "elastic" compression and deformation due to consolidation,. The elastic compression is the compression of the soil grains (soil skeleton) and of any free gas present in the voids. The elastic compression is often called "immediate settlement". It occurs quickly and is normally small (the elastic compression is not associated with expulsion of water). The deformation due to consolidation, on the other hand, is volume change due to the compression of the soil structure associated with an expulsion of water—consolidation. In the process, the imposed stress, initially carried by the pore water, is transferred to the soil structure. Consolidation occurs quickly in coarse-grained soils, but slowly in fine-grained soils. As a term, "settlement" is used when the total stress is constant and the involved, or influenced, soil zone stays the same, while the effective stress increases.

Creep is compression occurring ***without*** *an increase of effective stress*. Creep does not usually involve expulsion of water, but is mainly associated with slow long-term compression of the soil skeleton. Creep is usually small, but may in some soils add significantly to the total deformation of the soil. It is then acceptable to talk in terms of "settlement due to creep" or "creep settlement".

The term "settlement" is also used for the deformation resulting from the ***combined effect*** of load transfer, increase of effective stress, and creep during long-term conditions.

The magnitude of the settlement is a function of the *relative increase of effective stress*: The larger the existing effective stress before a specific additional stress is applied, the smaller the induced settlement. For this reason, most soil materials do not show a linear relation between stress and strain. Cohesive soils, in particular, have a distinct stress-strain non-linearity. The exception being, for example, very dense soils, such as glacial tills, where the stress-strain behavior can be approximated to a linear relation. A special case of non-linearity is stress-increase beyond the preconsolidation stress in an over-consolidated soil, that is, a pre-consolidation stress that is larger than the current effective overburden stress in the soil, resulting in a stress-strain behavior that is much stiffer below the preconsolidation stress than beyond.

The amount of deformation for a given contact stress depends on the distribution of the stress in the affected soil mass in relation to the existing stress (the imposed change of effective stress) and the compressibility of the soil layer. The change of effective stress is the difference between the initial (original) effective stress and the final effective stress. (See Chapter 1 and Table 1.6 for an example of how to calculate the distribution of the effective stresses at a site).

3.3 Linear Elastic Deformation

Linear stress-strain behavior follows Hooke's law ("elastic modulus method") according to Eq. 3.1.

(3.1) $$\varepsilon = \frac{\Delta\sigma'}{E}$$

where ε = induced strain in a soil layer
$\Delta\sigma'$ = imposed change of effective stress in the soil layer
E = elastic modulus of the soil layer

Often, the 'elastic modulus' is called Young's modulus. Strictly speaking, however, Young's modulus is the modulus for when lateral expansion is allowed, which may be the case for soil loaded by a small footing, but not when loading a larger area. In the latter case, the lateral expansion is constrained. The constrained modulus, D, is larger than the E-modulus. The constrained modulus is also called the "oedometer modulus". For ideally elastic soils, the ratio between D and E is shown in Eq. 3.2.

(3.2) $$\frac{D}{E} = \frac{(1-\nu)}{(1+\nu)\,(1-2\nu)}$$

where D = constrained modulus
E Young's modulus
ν = Poisson's ratio

For example, for a soil material with a Poisson's ratio of 0.3, a common value, the constrained modulus is 35 % larger than the Young's modulus. (As an illustration, unrelated to settlement of soils, but not to foundation engineering: the concrete inside a concrete-filled thick-wall pipe pile behaves as a constrained material as opposed to the concrete in a concrete pile. Therefore, when analyzing the deformation under load, the constrained modulus needs to be used for the former and the Young's modulus for the latter).

The deformation of a soil layer, *s*, is the strain, ε, times the thickness, *h*, of the layer. The settlement, *S*, of the foundation is the sum of the deformations of the soil layers below the foundation (Eq. 3.3).

$$S = \Sigma s = \Sigma(\varepsilon h) \tag{3.3}$$

3.4 Non-Linear Elastic Deformation

Stress-strain behavior is non-linear for most soils. The non-linearity cannot be disregarded when analyzing compressible soils, such as silts and clays, that is, the elastic modulus approach is not appropriate for these soils. Non-linear stress-strain behavior of compressible soils is conventionally modeled by Eq. 3.4.

$$\varepsilon = \frac{C_c}{1+e_0} \lg \frac{\sigma'_1}{\sigma'_0} = CR \lg \frac{\sigma'_1}{\sigma'_0} \tag{3.4}$$

where ε = strain induced by increase of effective stress from σ'_0 to σ'_1
C_c = compression index
e_0 = void ratio
σ'_0 = original (or initial) effective stress
σ'_1 = final effective stress
CR = compression ratio = $C_c/(1 + e_0)$; see explanation in the paragraph immediately before Eq. 3.6.

The compression index and the void ratio parameters, C_c and e_0 , are determined by means of oedometer (consolidation) tests in the laboratory.

If the soil is overconsolidated, that is, consolidated to a stress (called preconsolidation stress) which is larger than the existing effective stress, Eq. 3.4 changes to:

$$\varepsilon = \frac{1}{1+e_0} \left(C_{cr} \lg \frac{\sigma'_p}{\sigma'_0} + C_c \lg \frac{\sigma'_1}{\sigma'_p}\right) \tag{3.5}$$

where σ'_p = preconsolidation stress
C_{cr} = re-compression index

Thus, in conventional engineering practice of settlement design, two compression parameters need to be established. Actually, on surprisingly many occasions, geotechnical engineers only report the C_c-parameter, neglecting to include the e_0-value. Worse, when they do report both parameters, they often report the C_c from the oedometer test and the e_0 from a different soil specimen than used for determining the compression index! This is not acceptable, of course. The undesirable challenge of ascertaining what C_c-value goes with what e_0-value is removed by using the Janbu tangent modulus approach instead of the C_c and e_0 approach, applying the Janbu modulus number, m, instead, determined directly from the oedometer test as presented in Section 3.5.

The inconvenience of having to employ two parameters is also avoided by the MIT approach, where the compressibility of the soil is characterized by the ratios $C_c/(1 + e_0)$ and $C_{cr}/(1 + e_0)$ as single parameters (usually called Compression Ratio, CR, and Recompression ratio, RR, respectively). Or, by the Swedish and Finnish practice of applying a strain value, called ε_2, equal to the strain for a doubling of the applied stress. For the latter, Eq. 3.5 becomes:

(3.6) $$\varepsilon = \frac{\varepsilon_{2r}}{\lg 2} \lg \frac{\sigma'_p}{\sigma'_0} \quad + \quad \frac{\varepsilon_2}{\lg 2} \lg \frac{\sigma'_1}{\sigma'_p}$$

where ε_{2r} = "ε_2-compressibility" for reloading
ε_2 = "ε_2-compressibility" for virgin loading

3.5 The Janbu Approach

3.5.1 General

The Janbu approach, proposed by Nilmar Janbu in the early 1960s (1963; 1965; 1967), and referenced by the Canadian Foundation Engineering Manual, CFEM (1985, 1992), combines the basic principles of linear and non-linear stress-strain behavior. The method applies to all soils, clays as well as sand. By the Janbu method, the relation between stress and strain is a function of two non-dimensional parameters which are unique for any soil: a stress exponent, **j**, and a modulus number, **m**. Professor Janbu has presented a comprehensive summary of his method (Janbu 1998).

The Janbu relations are derived from the definition of tangent modulus, $M_t = \partial\sigma/\partial\varepsilon$ by the following expression (Eq. 3.7).

(3.7) $$M_t = \frac{\partial \sigma}{\partial \varepsilon} = m\,\sigma_r \left(\frac{\sigma'}{\sigma_r}\right)^{1-j}$$

where ε = strain induced by increase of effective stress
σ' = effective stress
j = a stress exponent
m = a modulus number
σ'_r = a reference stress, a constant, which is equal to 100 KPa (= 1 tsf = 2 ksf = 1 kg/cm^2 = 1 at)

The Janbu expressions for strain are derived as follows.

3.5.2 Cohesionless Soil — j > 0

For cohesionless soil, the stress exponent is larger than zero, $j > 0$. Integrating Eq. 3.7 results in the following formula:

(3.8) $$\varepsilon = \frac{1}{mj}\left[\left(\frac{\sigma'_1}{\sigma'_r}\right)^j - \left(\frac{\sigma'_0}{\sigma'_r}\right)^j\right]$$

where	ε	=	strain induced by increase of effective stress
	σ'_0	=	original effective stress
	σ'_1	=	final effective stress
	j	=	stress exponent
	m	=	modulus number, which is determined from laboratory and/or field testing
	σ'_r	=	reference stress, a constant, which is equal to 100 KPa (= 1 tsf = 2 ksf = 1 kg/cm^2 = 1 at)

3.5.3 Dense Coarse-Grained Soil — j = 1

The stress-strain behavior (settlement) in dense coarse-grained soils, such as glacial till, can be assumed to be 'elastic', which means that the stress exponent is equal to unity (j = 1). By inserting this value and considering that the reference stress, σ_r, is equal to 100 KPa, Eq. 3.7 becomes:

(**3.9**) $$\varepsilon = \frac{1}{100\,m}\,(\sigma'_1 - \sigma'_0) = \frac{1}{100\,m}\,\Delta\,\sigma'$$

Notice, because the reference stress is inserted with a value in the SI-system of units, Eq. 3.9 presupposes that E is given in the same units, usually in KPa. If the units for E are in tsf or ksf, Eq. 3.9 changes to Eqs. 3.9a or 3.9b, respectively.

(3.9a) $$\varepsilon = \frac{1}{m}\,(\sigma'_1 - \sigma'_0) = \frac{1}{m}\,\Delta\,\sigma'$$

(3.9b) $$\varepsilon = \frac{1}{2\,m}\,(\sigma'_1 - \sigma'_0) = \frac{1}{2\,m}\,\Delta\,\sigma'$$

Comparing Eqs. 3.1 and 3.9 for soils with a stress exponent of unity and considering that the reference stress, σ_r, is equal to 100 KPa, for E in units of KPa, tsf, and ksf, the respective relations between the modulus number and the E-modulus are:

(**3.10**) m = E/100 (3.10a) m = E (3.10b) m = E/2

3.5.4 Sandy or Silty Soil — j = 0.5

Janbu's original concept considered a gradual increase of the stress exponent, j, from zero to unity when going from clay to dense gravel, though this gradual change is considered redundant. Values of "j" other than j = 0 or j = 1, are only used for **sandy or silty** soils, where the stress exponent is often taken as equal to 0.5. By inserting this value and considering that the reference stress (100 KPa), Eq. 3.7 is simplified to Eq. 3.11.

(**3.11**) $$\varepsilon = \frac{1}{5m}\,(\sqrt{\sigma'_1} - \sqrt{\sigma'_0})$$ **units in KPa**

Notice, Eq. 3.11 is <u>not independent</u> of the choice of units and the stress values must be inserted in KPa. That is, a value of 5 MPa is to be inserted as the number 5,000 and a value of 300 Pa as the number 0.3.

In English units and with stress in units of tsf, alternatively, in ksf, Eq. 3.11 becomes

(3.11a) $\varepsilon = \frac{2}{m}(\sqrt{\sigma'_1} - \sqrt{\sigma'_0})$ units in tsf (3.11b) $\varepsilon = \frac{\sqrt{2}}{m}(\sqrt{\sigma'_1} - \sqrt{\sigma'_0})$ units in ksf

Take care, the equations are not independent of units—to repeat, in Eqs. 3.10a and 3.10b, the stress units must be inserted in units of tsf and ksf, respectively.

If the soil is overconsolidated and the final stress exceeds the preconsolidation stress, Eqs. 3.11, 3.11a and 3.11b change to:

(3.12) $$\varepsilon = \frac{1}{5m_r}(\sqrt{\sigma'_p} - \sqrt{\sigma'_0}) + \frac{1}{5m}(\sqrt{\sigma'_1} - \sqrt{\sigma'_p}$$ **units in KPa**

(3.12a) $$\varepsilon = \frac{2}{m_r}(\sqrt{\sigma'_p} - \sqrt{\sigma'_0}) + \frac{2}{m}(\sqrt{\sigma'_1} - \sqrt{\sigma'_p}$$ units in tsf

(3.12b) $$\varepsilon = \frac{\sqrt{2}}{m_r}(\sqrt{\sigma'_p} - \sqrt{\sigma'_0}) + \frac{\sqrt{2}}{m}(\sqrt{\sigma'_1} - \sqrt{\sigma'_p}$$ units in ksf

where σ'_0 = original effective stress (KPa, tsf, and ksf, respectively)
σ'_p = preconsolidation stress (KPa, tsf, and ksf, respectively)
σ'_1 = final effective stress (KPa, tsf, and ksf, respectively)
m = modulus number (dimensionless)
m_r = recompression modulus number (dimensionless)

If the imposed stress does not result in a new (final) stress that exceeds the preconsolidation stress, Eqs. 3.12, 3.12a, and 3.12b become:

(**3.13**) $$\varepsilon = \frac{1}{5m_r}(\sqrt{\sigma'_1} - \sqrt{\sigma'_0})$$ **units in KPa**

(3.13a) $\varepsilon = \frac{2}{m_r}(\sqrt{\sigma'_1} - \sqrt{\sigma'_0})$ units in tsf (3.13b) $\varepsilon = \frac{\sqrt{2}}{m_r}(\sqrt{\sigma'_1} - \sqrt{\sigma'_0})$ units in ksf

In a cohesionless soil, where the stress exponent is 0.5 and where previous experience exists from settlement analysis using the elastic modulus approach (Eqs. 3.1 and 3.3), a direct conversion can be made between E and m, which results in Eq. 3.14.

(**3.14**) $$m = \frac{E}{5(\sqrt{\sigma'_1} + \sqrt{\sigma'_0})} = \frac{E}{10\sqrt{\sigma'}}$$ **units in KPa**

Notice, stress and E-modulus must be input in the same units, normally KPa when the analysis is metric (SI units). When using English units (stress and E-modulus in tsf or ksf), Eqs. 3.14a and 3.14b apply).

(3.14a) $$m = \frac{2E}{(\sqrt{\sigma'_1} + \sqrt{\sigma'_0})} = \frac{E}{\sqrt{\sigma'}}$$ units in tsf

(3.14b) $$m = \frac{\sqrt{2}\ E}{(\sqrt{\sigma'_1} + \sqrt{\sigma'_0})} = \frac{\sqrt{2}\ E}{\sqrt{\sigma'}}$$ units in tsf

3.5.5 Cohesive Soil — j = 0

In cohesive soil, the stress exponent is zero, j = 0. For normally consolidated cohesive soils, the integration of Eq. 3.6 then results in Eq. 3.15 (the formula is independent of the stress units).

(**3.15**) $$\varepsilon = \frac{1}{m} \ln\frac{\sigma'_1}{\sigma'_0}$$

Most natural soils other than very young or organic clays are overconsolidated. Thus, in an overconsolidated, cohesive soil, Eq. 3.16 applies:

(**3.16**) $$\varepsilon = \frac{1}{m_r} \ln\frac{\sigma'_p}{\sigma'_0} + \frac{1}{m} \ln\frac{\sigma'_1}{\sigma'_p}]$$

Notice, the ratio (σ'_p/σ'_0) is equal to the Overconsolidation Ratio, OCR. However, the extent of overconsolidation is often also expressed as a stress difference, or "preconsolidation margin": σ'_p - σ'_0.

By the way, soils can be normally consolidated or overconsolidated, but never 'underconsolidated'. The latter is just a misnomer for soils that are "undergoing consolidation". The actual effective overburden stress in a soil that is consolidating is equal to the actual preconsolidation stress. If piezometer measurements at a site would indicate that the effective overburden stress (remember, effective stress is equal to total stress minus pore pressure) is larger than the preconsolidation stress determined in consolidation testing, then, either or both of the results of the consolidation test or of the determination of effective overburden stress are wrong. Ongoing consolidation means ongoing pore pressure dissipation and non-linear distribution of pore pressure, and, N.B., non-linear distribution of effective stress.

If the applied foundation stress does not result in a new stress that exceeds the preconsolidation stress, Eq. 3.16 becomes:

(3.17) $$\varepsilon = \frac{1}{m_r} \ln\frac{\sigma'_1}{\sigma'_0}$$

3.5.6 Typical values of Modulus Number, m

With knowledge of the original effective stress, the increase of stress, and the type of soil involved (without which knowledge no reliable settlement analysis can ever be made), the only soil parameter required is the modulus number. The modulus numbers to use in a particular case can be determined from conventional laboratory testing, as well as in-situ tests. As a reference, Table 3.1 shows a range of normally conservative modulus numbers, m, which are typical of various soil types (quoted from the

Canadian Foundation Engineering Manual, 1992). Re-compression modulus numbers, m_r, can often, but far from always, be expected to range from 8 to 12 times the numbers for normally consolidated conditions. A smaller range is often an indication of sample disturbance.

TABLE 3.1 Typical and Normally Conservative Modulus Numbers

SOIL TYPE		MODULUS NUMBER	STRESS EXP.
Till, very dense to dense		1,000 — 300	(j=1)
Gravel		400 — 40	– " –
Sand	dense	400 — 250	(j=0.5)
	compact	250 — 150	– " –
	loose	150 — 100	– " –
Silt	dense	200 — 80	(j=0.5)
	compact	80 — 60	– " –
	loose	60 — 40	– " –
Clays			
Silty clay	hard, stiff	60 — 20	(j=0)
and	stiff, firm	20 — 10	– " –
Clayey silt	soft	10 5	– " –
Soft marine clays and organic clays		20 — 5	(j=0)
Peat		5 — 1	(j=0)

The modulus numbers in the table are approximate and mixed soils will be different. For example, a silty sand will be more compressible than a clean sand (Huang et al. 1999). Similarly, a sand containing even a small amount, a few percent is enough, of mica will be substantially more compressible than a sand with no mica (Gilboy 1928).

Designing for settlement of a foundation is a prediction exercise. The quality of the prediction, that is, the agreement between the calculated and the actual settlement value, depends on how accurately the soil profile and stress distributions applied to the analysis represent the site conditions, and how closely the loads, fills, and excavations at the site resemble those actually occurring. The quality depends also on the quality of the soil parameters used as input to the analysis. Soil parameters for cohesive soils depend on the quality of the sampling and laboratory testing. Clay samples tested in the laboratory should be from carefully obtained 'undisturbed' samples. When testing overconsolidated clays, paradoxically, the more disturbed the sample is, the less compressible the clay appears to be. The error which this could cause is to a degree 'compensated for' by the simultaneous apparent reduction in the preconsolidation value. Furthermore, high quality sampling and oedometer tests are costly, which limits the amounts of information procured for a routine project. The designer usually runs the tests on the 'worst' samples and arrives at a 'conservative' prediction. This may be acceptable, but never so when the word 'conservative' is nothing but a disguise for the more appropriate terms of 'erroneous' and 'unrepresentative'. Then, the end results may perhaps not even be on the 'safe side'.

Non-cohesive soils cannot easily be sampled and tested (however, as indicated in Section 3.13, CPT sounding can be used to estimate a compressibility profile for a site). Therefore, settlement analysis of foundations in such soils must rely on empirical relations derived from in-situ tests and experience values. Usually, non-cohesive soils are less compressible than cohesive soils and have a more pronounced overconsolidation. Therefore, testing of compressibility and analysis of settlement is often considered less important for non-cohesive soils. However, considering the current trend toward larger loads and contact stresses, foundation design must prudently address also the settlement expected in non-cohesive soils. Regardless of which methods that are used for predicting the settlement, it is necessary to refer the analysis results back to basics. That is, if the settlement values used for the assessment of the foundation design are not determined from a full analysis, the foundation should be evaluated to indicate what range of compressibility parameters (Janbu modulus numbers) the settlement values represent for the actual soil profile and conditions of effective stress and load. For example, if the design of the superstructure indicates that a settlement of 35 mm is the acceptable limit, the foundation design engineer should back-calculate the modulus numbers that correspond to the limit under the given conditions of soil profile and effective stress. This is a small effort that will provide a worthwhile check on the reasonableness of the results as well as assist in building up a reference data base for future analyses.

Because of sample disturbance and other influences, the fact that most soils are preconsolidated is often overlooked. Some even believe that preconsolidation only applies to clays. Actually, sands are almost always overconsolidated, and significantly so. In sands, however, the values of OCR or preconsolidation margin are difficult to determine by conventional soil investigation methods. Note, the compressibility values (modulus numbers or E-values) employed in an analysis are often experience values obtained from relatively low stress levels applicable to the preconsolidation condition. When a foundation exerting larger stress is considered, the stress level might exceed the preconsolidation stress level and the settlement be governed by the virgin compressibility. If so, the settlements will be larger, much larger, than those based on low-stress level experience values.

3.6 Evaluating oedometer tests by the e-lg p and the strain-stress methods

To repeat, with regard to the options of linearly elastic response to an applied load, the Janbu method with the stress exponent set equal to unity is the same as using an E-modulus. Similarly, the Janbu method with the stress exponent equal to zero, is the same as using the C_c/e_0 method. The Janbu method adds a third option, that of j = 0.5, which is applicable to silty sand and sandy silt, which method is not covered by the conventional methods.

The Janbu method is easy to use. For clays, it provides a single unified parameter, the modulus number. With only one parameter, it easy for the geotechnical engineer to establish a reference data base of values.

Fig. 3.1 presents the results of an oedometer test (consolidation test; data from Bowles, 1988) plotted both in the conventional (North American) manner (Fig. 3.1A) of e versus lg p' and as strain (ε) versus lg p' (Fig. 3.1B). The same test data are used for both diagrams. The compression index, C_c, is determined to 0.38 in the first diagram as the void ratio distance for one log cycle. The modulus number, m, is determined to 12 from the second diagram as the inverse of the strain for a stress change from p to 2.718p, or from Eq. 3.12 (the initial void ratio of the soil sample is 1.01).

The recompression index and recompression modulus number are determined in similar manner. Most geotechnical textbooks include details on how to analyze the results of an oedometer test, for example Holtz and Kovacs (1981), Bowles (1988), and Coduto (1994), including correction for sample disturbance.

Preconsolidation stress is often difficult to determine even from oedometer tests on high quality (undisturbed) samples. Janbu (1998) recommends to obtain it from a plot of the slope of the tangent modulus line, as shown in Fig. 3.2. For the subject example, the preconsolidation stress is clearly noticeable at the applied stress of 200 KPa. Most text books include several conventional methods of determining the preconsolidation stress. Grozic et al. (2003) describe the methods in details and offer an interesting discussion on the processes. See also Tanaka et al. (2002) and references therein.

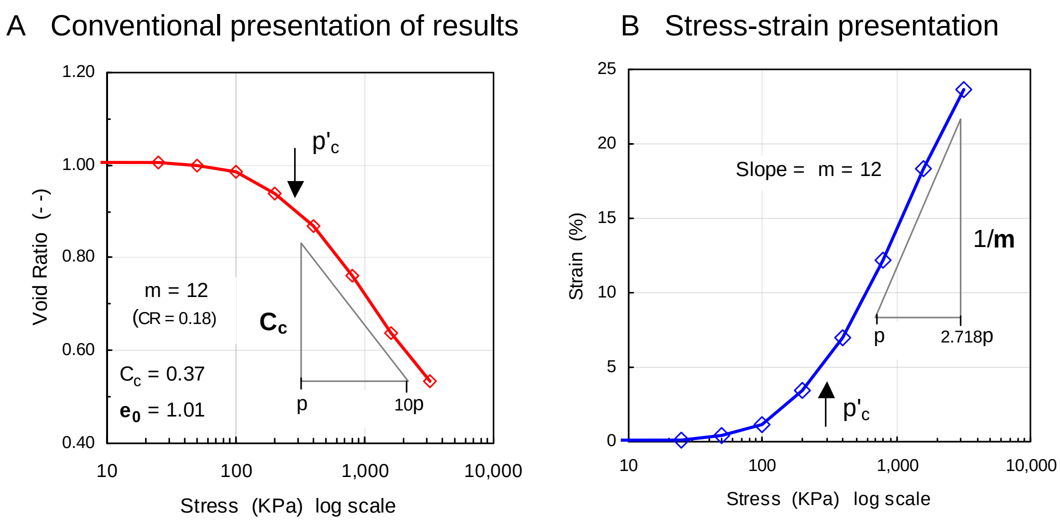

Fig. 3.1 Results from a consolidometer test (data from Bowles, 1988). (The preconsolidation stress is taken directly from the source where it was indicated to have been determined by eye" to 280 KPa).

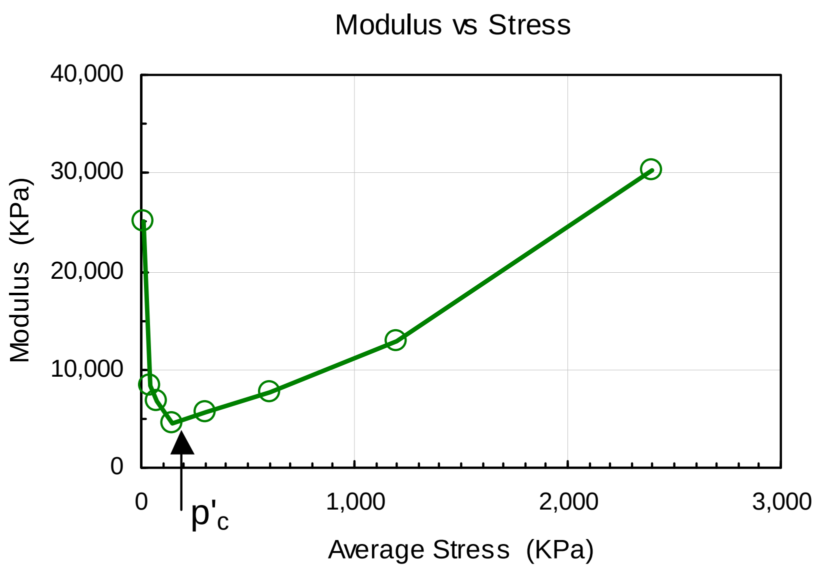

Fig. 3.2 The tangent modulus plot to determine preconsolidation stress according to Janbu (1998)

3.7 The Janbu Method versus Conventional Methods

The Janbu tangent modulus method is not different to—does not contrast or conflict with—the 'conventional' methods. The Janbu method for calculation of settlements and the conventional elastic modulus approach give identical results, as do the Janbu method and the conventional C_c and e_0 method (Eqs. 3.4 and 3.5, and Eqs. 3.13, 3.14, and 3.15). There are simple direct conversions between the modulus numbers and the E-modulus and the C_c-e_0 values. The relation for a linearly elastic soil (“E-modulus soils”) is given in Eq. 3.10 (repeated below).

(**3.10**) m = E/100 **units in KPa**

(3.10a) m = E units in tsf (3.10b) m = E/2 units in ksf

The conversion relation between the conventional C_c and e_0 method and the Janbu modulus method is given in Eq. 3.18.

$$m = \ln 10 \frac{1+e_0}{C_c} = 2.3 \frac{1+e_0}{C_c} \tag{3.18}$$

Similarly, a strict mathematical relation can be determined for the Swedish-Finnish ε_2 approach (Eq. 3.6), as described in Eq. 3.19.

$$m = \ln 10 \frac{\lg 2}{\varepsilon_2} = 2.3 \frac{\lg 2}{\varepsilon_2} = \frac{0.69}{\varepsilon_2} \tag{3.19}$$

The Janbu method of treating the intermediate soils (sandy silt, silty sand, and sand) is “extra” to the C_c-e_0 method and the elastic method (Eqs. 3.12 and 3.13).

It is not possible to express the relative degree of compressibility using the C_c/e_0 approach. That is, a specific C_c-value cannot be referred to as representing a high compressibility or medium compressibility, etc. without also coupling it with the e_0-value and few can correlate to two numbers simultaneously. The following couple of examples will demonstrate the advantage of the Janbu modulus number approach as opposed to the conventional C_c/e_0 approach.

Figure 3.3 shows results from oedometer tests on an overconsolidated Texas Gulf Clay (Beaumont clay), with void ratios ranging from about 0.4 through 1.2 (Endley et al. 1996). Figure 3.3A presents the C_c-values and implies that the compressibility, expressed as increased C_c-value, would be increasing with depth. However, Fig. 3.3B, which shows the C_c/e_0-values converted to Janbu modulus numbers, demonstrates that there is no such trend with depth. The modulus numbers range—from about 10 through almost 40—is quite wide, going from high through low compressibility.

Figure 3.4 presents results from oedometer tests on a normally consolidated to slightly overconsolidated silty clay outside Vancouver, BC with void ratios ranging from about 0.8 through 1.4. The relative range between the smallest and largest C_c-value (a factor of 2) suggests a somewhat wider range of compressibility than the actual, represented by the modulus number where the relative range between the smallest and largest value is a factor of 1.3. The average modulus number is approximately 10, which is the upper boundary of a very compressible soil.

The Janbu method is widely used internationally and by several North American engineering companies and engineers. However, many others are yet reluctant to use the Janbu approach, despite its obvious advantages over the conventional C_c/e_0 method. The approach has been available for more than twenty years in the third second and third editions of the broadly used Canadian Foundation Engineering Manual, CFEM (1985, 1992). (By accident or other, the committee revising the CFEM for the fourth Edition published in 2006 omitted to keep the Janbu approach in the Manual).

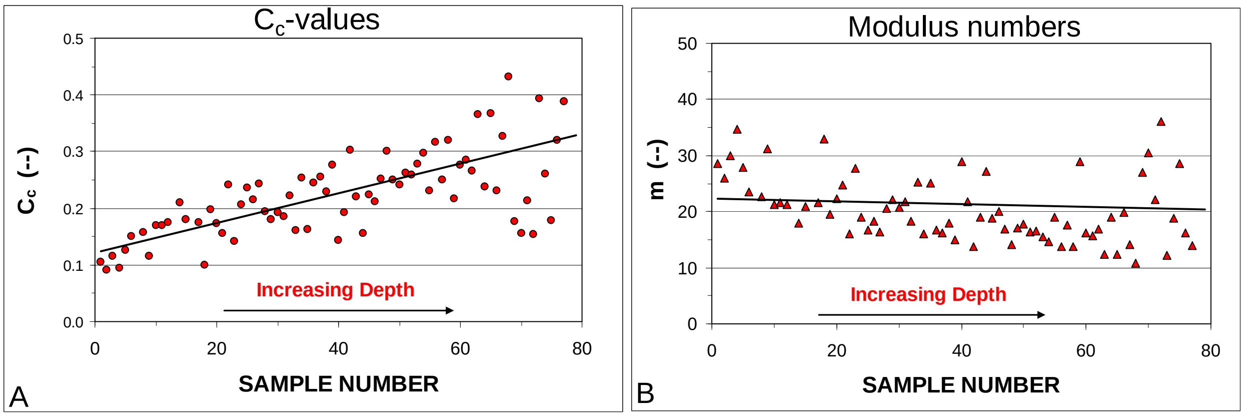

Fig. 3.3 C_c-values and modulus numbers from Beaumont clay. Data from Endley et al. 1996.

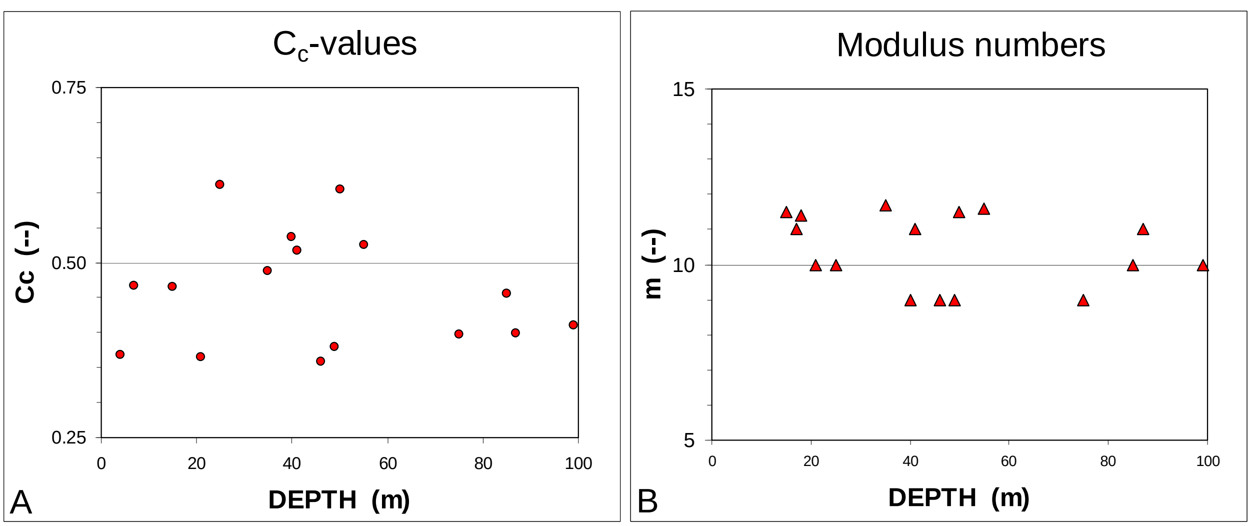

Fig. 3.4 C_c-values and modulus numbers from Fraser River clay, BC.

Those not fully convinced by the previous examples, should reflect on the results shown in Fig. 3.5 and 3.6. Figure 3.5A shows a fairly typical array of C_c-values ranging from abut 0.3 through 0.9, implying a rather randomly varying compressibility. However, when coupled with the associated e_0-values, admittedly judiciously selected, as shown in Fig. 3.5B, the different picture evolves: the compressibility is constant for the C_c-values. Figure 3.6A shows a set of constant c_c-values, that is, they imply a constant compressibility. Similarly, however, when coupled with their associated e_0-values, again admittedly judiciously selected, as shown in Fig. 3.6B, the different picture evolves: the compressibility is highly variable despite the constant C_c-values.

Engineers working in a well-known area where the soils have a range of water contents and void ratios well-known to the engineers, can work very well with C_c-values. However, those encountering foundation problems in different geologies are well advised to start using the modulus number as a measure of and reference to soil compressibility.

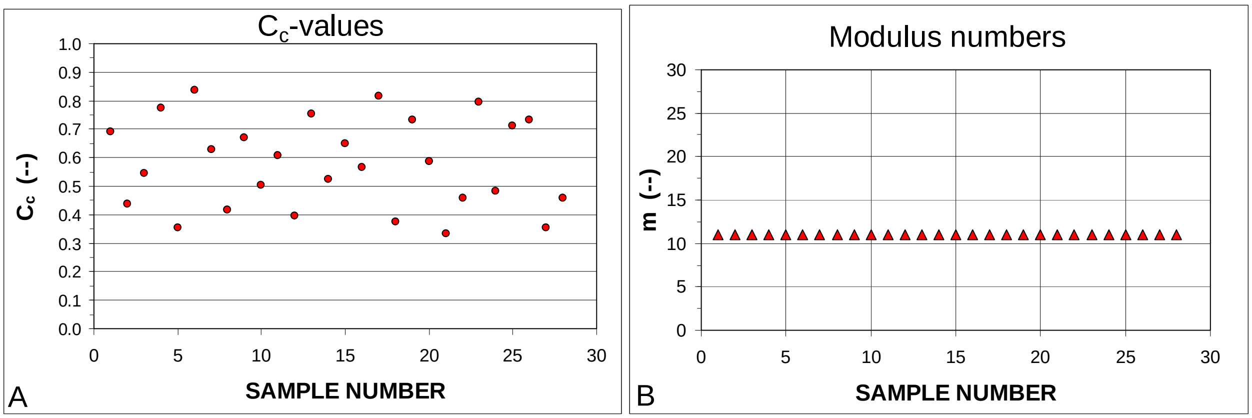

Fig. 3.5 Typical, but "selected" C_c-values, and converted via associated "selected" e_0-values to "m"-values.

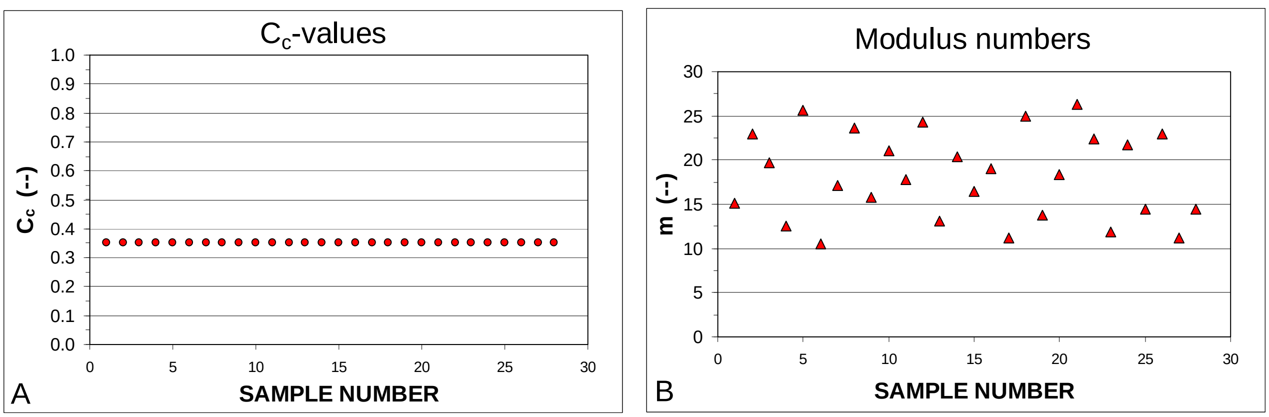

Fig. 3.6 "Selected" constant C_c-values, and converted via associated "selected" e_0-values to "m"-values.

3.8 Time Dependent Settlement

Because soil solids compress very little, settlement is mostly the result of a change of pore volume. Compression of the solids is called ‘initial compression’. It occurs quickly and it is usually considered elastic, that is, the stress-strain response is linear. In contrast, the change of pore volume will not occur before the water occupying the pores is squeezed out by the stress increase. The process is rapid in coarse-grained soils and slow in fine-grained soils. In fine clays, the process can take a longer time than the life expectancy of the building, or of the designing engineer, at least. The process is called consolidation and it usually occurs with an increase of both undrained and drained soil shear strength. By analogy with heat dissipation in solid materials, the Terzaghi consolidation theory indicates simple relations for the time required for the consolidation. The most commonly applied theory builds on the assumption that water is able to drain out of the soil at one surface boundary (upper or lower) and not at all at the opposite boundary (nor horizontally). The consolidation is fast in the beginning, when the driving pore pressures are greater and slows down with time as the pressures reduce. The analysis makes use of the relative amount of consolidation obtained at a certain time, called average degree of consolidation, which is defined in Eq. 3.20.

(3.20) $$U_{AVG} = \frac{S_t}{S_f} = 1 - \frac{u_t}{u_0}$$

where U_{AVG} = ***average*** degree of consolidation
S_t = settlement at Time t
S_f = final settlement at full consolidation
u_t = *average* pore pressure at Time t
u_0 = initial *average* pore pressure (on application of the load at Time $t = 0$)

Notice that the pore pressure varies throughout the soil layer and that Eq. 3.20 assumes an average value through the soil profile. In contrast, the settlement values are not the average, but the accumulated values.

The time for a achieving certain degree consolidation is then, as follows (Eq.3.21).

(3.21) $$t = T_v \frac{H^2}{c_v}$$

where t = time to obtain a certain degree of consolidation
T_v = a dimensionless time coefficient
c_v = coefficient of consolidation
H = length of the longest drainage path

The time coefficient, T_v, is a function of the type of pore pressure distribution. Of course, the shape of the distribution affects the average pore pressure values and a parabolic shape is usually assumed. The coefficient of consolidation is determined in the laboratory oedometer test (some in-situ tests can also provide c_v-values) and it can rarely be obtained more accurately than within a ratio ranging from 2 to 3. The length of the longest drainage path, H, for a soil layer that drains at both surface boundaries is half the layer thickness. If drainage only occurs at one boundary, H is equal to the full layer thickness. Naturally, in layered soils, the value of H is difficult to ascertain.

Approximate values of T_v for different average values of the average degree of consolidation, U_{AVG}, are given in Table 3.3. For more exact values and values to use when the pore pressure distribution is different, see, for example, Holtz and Kovacs (1981), who also present formulae for calculating T_v for intermediate values of U_{AVG}.

TABLE 3.2 Approximate values of T_v for different average values of the degree of consolidation, U_{AVG}

U_{AVG} (%)	25	50	70	80	90	"100"
T_v	0.05	0.20	0.40	0.57	0.85	≈1.00

In saturated soils, water has to be expelled from the soil before the pore volume can reduce. In partially saturated soils, however, consolidation determined from observed settlement initially appears rapid, because gas (air) will readily compress when subjected to an increase of pressure, allowing the pore volume to decrease rapidly. This settlement is often mistaken for the initial compression of the soil—the solids.

Inorganic soils below the groundwater table are usually saturated and contain no gas. In contrast, organic soils will invariably contain gas in the form of small bubbles (as well as gas dissolved in the water, which gas becomes free gas on release of confining pressure when sampling the soil) and these soils will appear to have a large immediate compression (large 'elastic' compression). During the consolidation process, as the pore pressure gradually reduces, the bubbles return to the original size and the consolidation process will appear to be slower than the actual rate.

Generally, the determination — prediction — of the time for a settlement to develop is filled with uncertainty and it is difficult to reliably estimate the amount of settlement occurring within a specific time after the load application. The prediction is not any easier when one has to consider the development during the build-up of the load. For details on the subject, see Ladd (1991).

The rather long consolidation time in clay soils can be shortened considerably by means of vertical drains (see Chapter 4). Vertical drains installed at a spacing ranging from about 1.2 m through 3.0 m have been very successful in accelerating consolidation to develop in weeks or months as opposed to requiring years. In the past, vertical drains consisted of sand drains and installation disturbance in some soils often made the drains cause more problems than they solved. However, the sand drain is now replaced by premanufactured band-shaped drains ("wick drains"), most which do not share the difficulties and adverse behavior of sand drains (some do, however, and quality and performance of wick drains vary from type to type, usually in inverse to the cost of material).

Theoretically, when vertical drains have been installed, the drainage is in the horizontal direction and design formulae have been developed based on radial drainage. However, vertical drains connect horizontal layers of greater permeability, which frequently are interspersed in natural soils (See Section 5.3.5). This must be addressed in the design. The only way to determine the existence and frequency of such horizontal permeable layers, is by continuous Shelby tube sampling or by CPT in-situ sounding. The extruded samples are left to dry in room temperature. After a few days or so, pervious layers or bands of silt and sand will show up as light-colored partitions in the sample. After full drying, the layers will no longer be visible. The CPT in-situ sounding needs to be performed with readings taken every 10 mm (which does not infer any extra costs and, anyway, should be the norm for all CPTU soundings).

3.9 Creep

Settlement will continue after the end of the consolidation due to slow continued compression of the soil skeleton. This type of settlement is called "creep" or "secondary compression" (the consolidation can be called "primary compression"). Creep is a function of a coefficient of secondary compression, C_α, (See Holtz and Kovacs, 1981). One relation for the amount of creep developing over time after the consolidation is completed is shown in Eq. 3.22. Notice that creep is not a function of the applied load itself, but of the time relative to time for completed consolidation for the applied load.

(3.22) $$\varepsilon = \frac{C_\alpha}{1+e_0} \ln \frac{t_\alpha}{t_{100}}$$

where C_α = coefficient of secondary compression
t_α = length of time after end of consolidation considered
t_{100} = time for achieving 100 % primary compression (Eq. 3.21)

In most soils, creep is small in relation to the initial plus consolidation settlement (primary compression) and is, therefore, neglected. However, in organic soils, creep may be substantial.

3.10 Example

Example 3.1. Figure 3.7 presents an example of calculated and measured settlements for a test embankment at the Bangkok International Airport. As shown, initially, most of the settlement is from initial ('elastic") compression, which ceases once full embankment height is reached. The total settlement is then due to consolidation, only. No vertical drains were used, and the consolidation is still continuing at the end of the observation period.

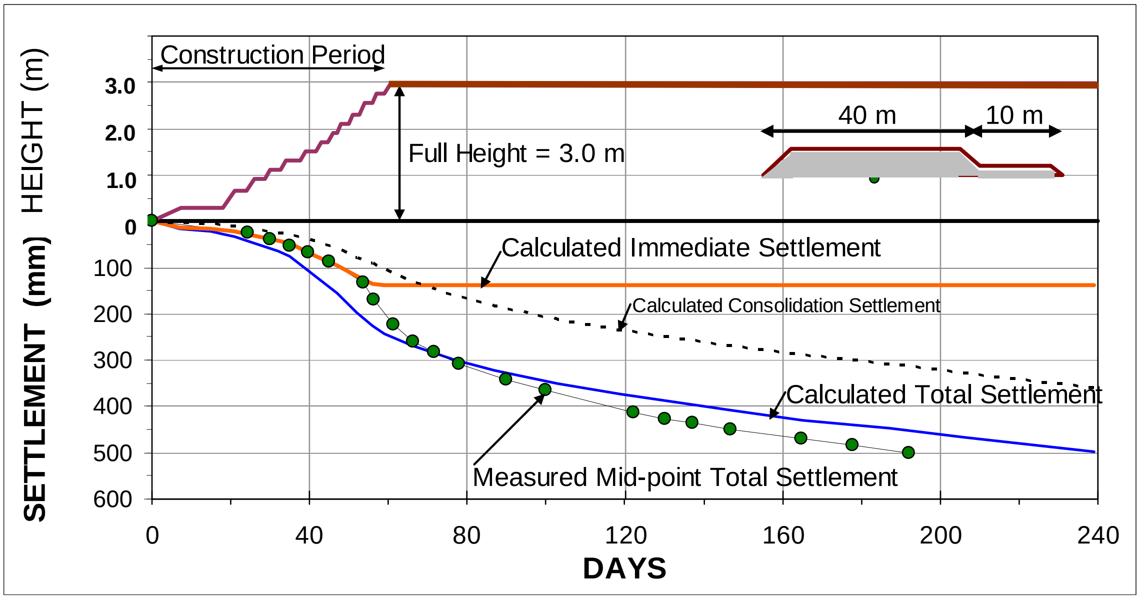

Fig. 3.7 Calculated and measured settlements during 200 days at center line of for a long, 40 m wide, 3.0 m high, stage-constructed embankment on 20 m thick deposit of soft marine clay. Data from Moh and Lin (2006).

3.11 Magnitude of Acceptable Settlement

Settlement analysis is often limited to ascertaining that the expected settlement would not exceed one inch. (Realizing that 25 mm is too precise a value when transferring this limit to the SI-system, some have argued whether “the metric inch” should be 20 mm or 30 mm!). However, in evaluating settlement in a design, the calculations need to provide more than just an upper boundary. The actual settlement value and both total and differential settlements must be evaluated. The Canadian Foundation Engineering Manual (1992) lists allowable displacement criteria in terms of maximum deflection between point supports, maximum slope of continuous structures, and rotation limits for structures. The multitude of limits demonstrate clearly that the acceptable settlement varies with the type and size of structure considered. Moreover, modern structures often have small tolerance for settlement and, therefore, require a more thorough settlement analysis. The advent of the computer and development of sophisticated yet simple to use design software has enabled the structural engineers to be very precise in the analysis of deformations and the effect of deformations on the stress and strain in various parts of a structure. As a not-so-surprising consequence, requests for "settlement-free" foundations have increased. This means that the geotechnical analysis must determine also the magnitude of small values of settlement.

When the geotechnical engineer is vague on the predicted settlement, the structural designer "plays it safe" and increases the size of footings or changes the foundation type, which may increase the costs of the structure. These days, in fact, the geotechnical engineer can no longer just offer an estimated "less than one inch" value, but must provide a more accurate value by performing a thorough analysis considering soil compressibility, soil layering, and load variations. Moreover, the analysis must be put into the full context of the structure, which necessitates a continuous communication between the geotechnical and structural engineers during the design effort. Building codes have started to recognize the complexity of the problem and mandate that the designers collaborate continuously during the design phases as well as during the construction. See, for example, the Canadian Highway Bridge Design Code, CAN/CSA-S6 2006.

3.12 Calculation of Settlement

Calculation of settlement should be performed in the following steps.

1. Determine the soil profile (i.e., the soil layering and pore pressure distribution; Chapter 2) at the initial state for the site and foundation unit(s) so that the initial effective stress (σ'_0) distribution is adequately established (Chapter 1).
2. Determine and compile the soil compressibility parameters (modulus number and stress exponents, or the "conventional" parameters). Do not overlook potential preconsolidation.
3. Determine the stresses imposed by the foundation units(s) and any changes to the initial site conditions (excavations, fills, groundwater table lowering, etc.) and calculate the new (the final) distribution of effective stress, σ'_1.
4. Divide each soil layer in a suitable number of sub layers and calculate the initial and final effective stress representative for each sub layer using the suitable equations given in Chapter 3. (Perform the calculations in either the middle of each sub layer, or at top and bottom of each and take an average of these two; if the sub layers are reasonably thin, the two approaches will give equal result)
5. Calculate for each sub layer the strain caused by the change of effective stress from σ'_0 to σ'_1 (Section 3.5 contains the formulae to use)
6. Calculate the settlement for each sub layer and add up to find the accumulated settlement value (Eq. 3.3)

A settlement analysis must incorporate all relevant facts. Because the person performing the analysis does not know all details of a project, important facts may get overlooked, such as that the site information does not include that the ground has either been excavated or backfilled prior to construction, the adjacent embankment will affect the stresses underneath the foundation that is being analyzed. Often, even though all the relevant facts from the local site are applied, regional conditions must also be included in the analysis. For example, in the Texas Gulf Coast Region, notably in Greater Houston area, past lowering of the groundwater table due water mining in deep wells (starting in the 1920s) and recent ongoing rise of the water table (since ceasing to pump in the mid-1970s) have resulted in a regional subsidence — in places larger than 2 m — and a large downward water gradient, which are now rising. (Negative head larger than 100 m have been measured at depths of 400 m). Figure 3.7 presents observations in three deep wells from 1930 onward.

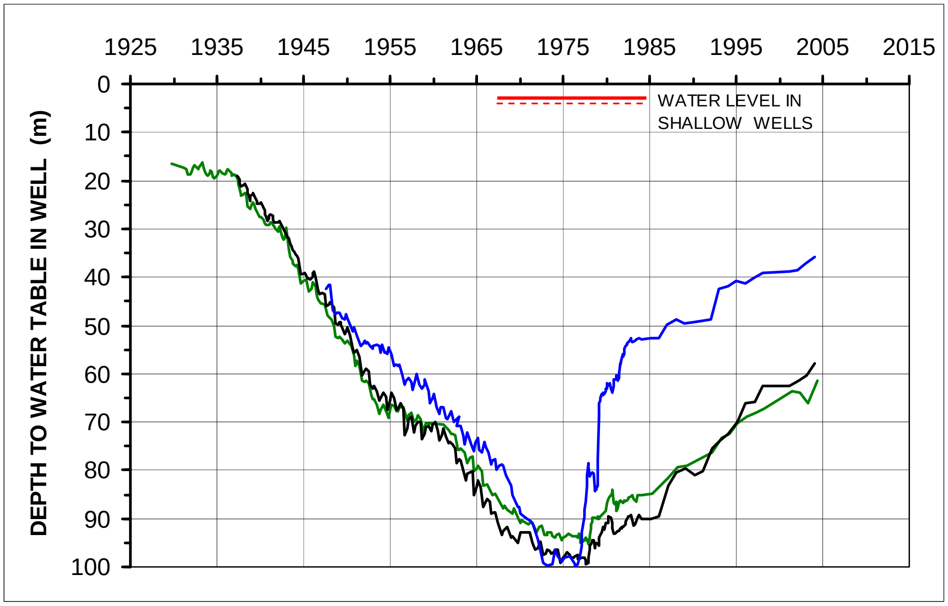

Fig. 3.7 Example of measured depth to water level in 160 m through 350 m deep wells near the San Jacinto Monument. (Data from Barbie et al., 2005, and Fellenius and Ochoa, 2008).

The clay soils in the area are desiccated and overconsolidated from ancient desiccation and from the recent lowering of the pore pressures. The overconsolidation degree is getting larger as the water pressures now are returning to pre-1920 levels. Old and new foundations need to take the changing pore pressure gradient into account. Figure 3.8 shows settlement observations for the San Jacinto Monument (Briaud et al. 2007) and how, after completed construction in 1936, initially, the lowering of the groundwater did not appreciably affect the settlement development, and how, from 1940 onward, the settlement due to the groundwater lowering took over. The heavy blue line with solid dots shows the measured settlement of the Monument. The dashed line marked "Monument only" is the assumed settlement of the monument had there been no groundwater lowering.

The actual pore pressure gradient will differ from site to site. For either back analysis (for future reference) or for design calculations of expected settlement, the regional pore pressure conditions must be carefully established and, therefore, a site investigation must include piezometer geared to establish the pore pressure distribution.

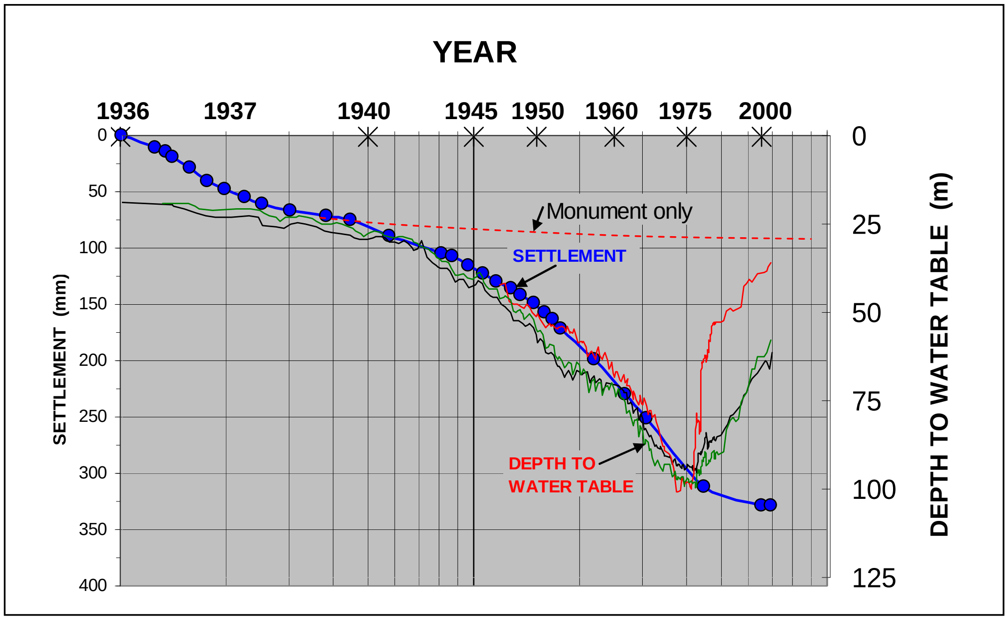

Fig. 3.8 Observed settlement of the San Jacinto Monument plotted together with the observed depths to water in wells near the Monument. (Data from Fellenius and Ochoa, 2008).

3.13 Special Approach -- Block Analysis

When a foundation design analysis indicates a likelihood that ordinary foundations (footings, rafts, or mats) would experience excessive settlement, site improvement techniques are frequently employed. For example, deep vibratory compaction, dynamic consolidation, stone-columns, or lime-cement columns. Common for these techniques is that the compressibility of an upper soil zone (the depth of the treatment) at the site is improved. The result of the treatment is rarely uniform. It usually consists of treatment in vertical zone leaving untreated soil in between. If the overall treated area is larger than the footprint of the foundation, the settlement analysis consists of determining the average (proportional) modulus number of the treated zone as indicated in Eq. 3.23. This average is then applied to calculations for the treated zone replacing the original soil modulus.

(3.23)
$$m_{AVG} = \frac{m_{UNTR} \times A_{UNTR} \quad + \quad m_{TR} \times A_{TR}}{A_{UNTR} \quad + \quad A_{TR}}$$

where m_{AVG} = average modulus number for the treated zone
m_{UNTR} = modulus number for untreated soil
m_{TR} = modulus number for treated soil
A_{UNTR} = area of untreated soil
A_{TR} = area of treated soil

When the size of the footprint is at least about equal to the treated area, the imposed stress is assumed to be transferred undiminished through the treated zone (taken as a block of soil), i.e., *no stress distribution within the treated zone (or out from its side)*. The block will compress for the load and the compression (settlement contribution) is determined using the average modulus and applying elastic stress-strain (stress exponent = unity). At the bottom of the block, the imposed stress is now distributed down into the soil and the resulting strains and settlements are calculated as before.

3.14 Determining the Modulus Number from In-Situ Tests

3.14.1 In-Situ Plate Tests

To supplement results from laboratory tests, the compressibility parameters (modulus number, as well as E-moduli) can be determined by back-calculation using settlement data from structures with a well-defined footprint placed on a well-investigated soil. However, the results are approximate, as no information is obtained on preconsolidation or on settlement for applied stresses different from that stress causing the observed settlement. Moreover, if the soil is layered, the compressibility parameter is a blend (average) of the values in whole soil body affected. Values for a specific soil layer can be determined in in-situ plate tests. Plate tests have the advantage of enabling settlements to be determined from a range of applied load. The plate test is usually performed at the ground surface or at shallow depth. For the latter case, the plate is placed at the bottom of an excavated hole. Use of a screw-plate can extend the depth, but the depth is still limited as screw-plates can rarely be "screwed-in" more than a few metres. Janbu applied 0.3 m diameter screw-plates and evaluated the modulus number assuming that the strain induced by the applied load increments was the measured settlement divided by half the plate diameter. The Canadian Foundation Engineering Manual (1992) presents how the modulus number can be established from the so-determined stress-strain values. It is of course better to actually measure the strain induced by the loading of the plate. This can be done by equipping the test plate with a small centrally placed screw-plate that can be moved down, say, a distance below the main plate. The central plate is not loaded, but its movement due to the load applied to the main test plate is measured. The difference in movement between the main plate and the small central plate divided by the distance is the induced strain. The distance of the central plate below the main plate can be determined from Boussinesq stress distribution calculation, fitting the distance to a depth corresponding to the calculated average strain.

Figure 3.9 presents the results of loading tests in sand on three square footings of 1.0 m, 1.5 m, and 2.5 m, and two footings of 3.0 m diameter. Figure 3.9A shows the load-movement for the individual footings and Fig. 3.9B shows the results as stress versus movement divided with the footing width. Figure 3.9B is important because it shows that the load-movement in sand is independent of scale.

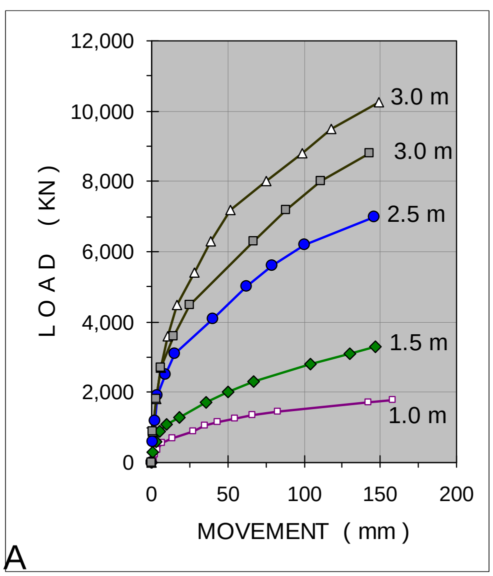

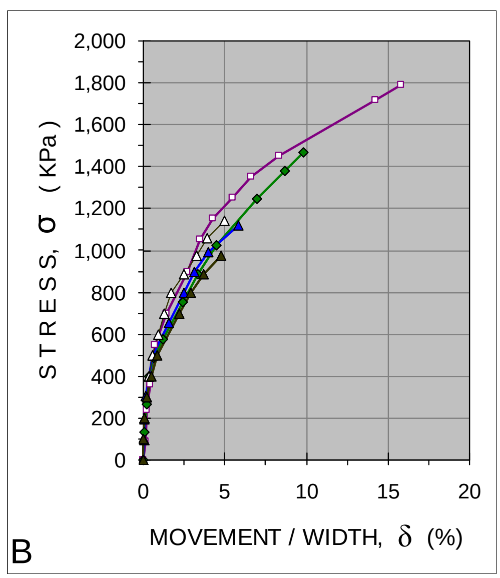

Fig. 3.9 Observed load-movement (A) and stress-normalized movement (B) of five footings tested at Texas A&M University (data from Briaud and Gibbens 1994, 1999).

By dividing each stress values with its relative movement value, the secant modulus is established for each such data pair. Similarly, by dividing for each pair each value of change of stress with the change of relative movement, the tangent modulus is determined. The results are shown in Figs. 3.10A and 3.10B, respectively, and indicate as many modulus values as there are applied values of stress. This is no surprise, the movements of the example tests are affected by immediate deformation, creep during load-holding, increased volume of soil affected from one applied load to the next, and, primarily, by a significant cementation or preconsolidation condition for the example case— most sands are preconsolidated and this sand is no exception.

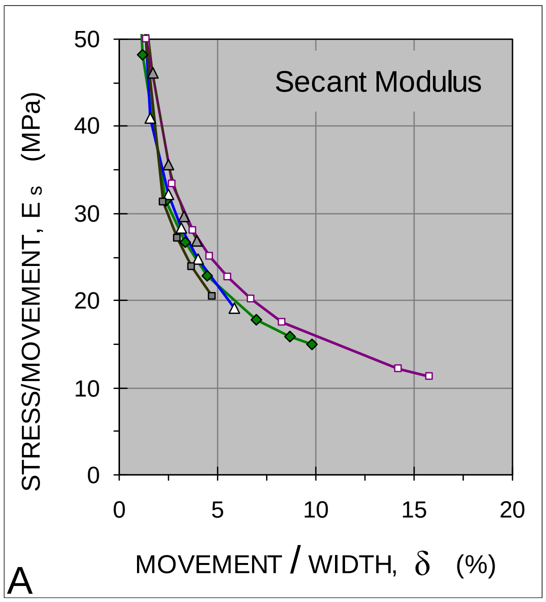

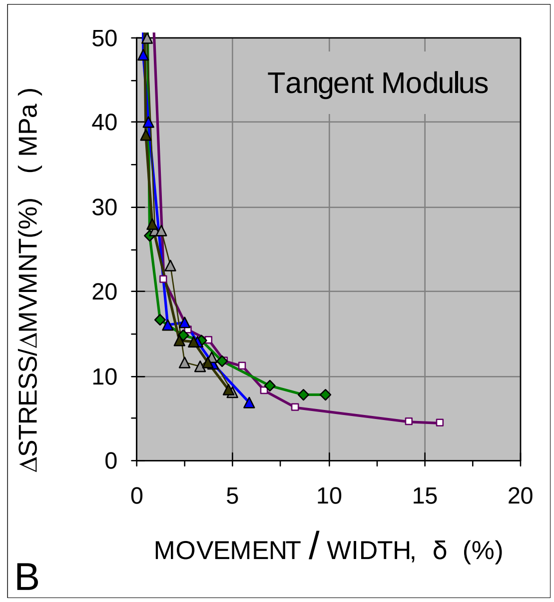

Fig. 3.10 Calculated Secant and tangent modulus curves for the five footing tests shown in Fig. 3.9.

In Fig. 3,10B, the large initial tangent modulus value is influenced by the reloading modulus, while toward the end of the loading tests, the tangent modulus is mostly influenced by the virgin modulus of he sand. The curves can be used to estimate the starting point for a fitting of the test data to a theoretical calculation, employing a common "preconsolidation stress" and fixed values of reloading and virgin modulus numbers. The process involves a rather laborious trial and error series of calculations, assuming either a linear elastic response, j = 1, or Janbu's mid-type response, j = 0.5, Boussinesq distribution, and calculating the settlement at the characteristic point. For the linear elastic assumption (j=1), the calculated values match the observed values when applying a preconsolidation stress of about 500 KPa and modulus numbers, m and m_r, about 60 and 900, respectively. The corresponding E-values are about 6 MPa and 90 MPa, respectively. (For additional reference to this important case history, see Section 6.10).

3.14.2 Determining the E-Modulus from CPT cone-stress values

The static cone penetrometer can be used for determining the modulus number. It has the advantage of providing a continuous profile.

When calculating settlement, the E-modulus of interest is the modulus for an average applied stress limited to a value equal to about 25 % of the estimated ultimate bearing resistance. The modulus is called E_{25}, and it can be related to the average cone stress according to the relationship given in Eq. 3.24.

(3.24) $$E_{25} = \alpha\ q_t$$

where E_{25} = secant modulus for a stress equal to about 25 % of the ultimate stress
α = an empirical coefficient
q_t = cone stress

Test data indicate that the empirical coefficient, α, varies considerably and depends on the soil type and stress conditions as well as on the applied load level. According to the Canadian Foundation Engineering Manual (1985, 1992), when correlated to plate load tests on sand, α varies between 1.5 and 4. Based on a review of results of cone tests in normally consolidated, uncemented sand in calibration chambers, Robertson and Campanella (1986) proposed a range for α between 1.3 and 3.0. This range agrees well with recommendation by Schmertmann (1970) for use of CPT data to analyze settlement of isolated footings on coarse-grained soils. Dahlberg (1975) performed tests in overconsolidated sand and found that α ranged from 2.4 through 4, increasing with increasing value of q_t. The Canadian Foundation Engineering Manual (1992) states that α is a function of soil type and compactness, as listed in the following table.

TABLE 3.3 α from Static Cone Penetration Tests (CFEM 1992)

Soil type	α
Silt and sand	1.5
Compact sand	2.0
Dense sand	3.0
Sand and gravel	4.0

The values of α shown in Table 3.1 apply to a settlement analysis in soils that can be assumed to have a linear (“elastic”) response to a load increase.

3.14.3 CPT Depth and Stress Adjustment*)

The results of cone and sleeve friction measurements as used for compressibility reference are believed affected by the effective overburden stress (Jamiolkowski et al., 1988). Therefore, it is necessary to consider this effect when interpreting CPT results used for settlement analysis. For the depth adjustment of the cone stress, Massarsch (1994) proposed to apply a dimensionless adjustment factor, C_M, to the cone stress according to Eq. 3.25, based on the mean effective stress, σ'_m.

(3.25) $$C_M = \left[\frac{\sigma_r}{\sigma'_m}\right]^{0.5}$$

where C_M = stress adjustment factor ≤ 2.5
σ_r = reference stress = 100 KPa
σ'_m = mean effective stress

The mean effective stress is determined according to Eq. 3.26.

*) The information in Section 3.14.3 is quoted from Massarsch and Fellenius (2002)

(3.26) $$\sigma'_m = \frac{\sigma'_v \left(1 + 2\,K_0\right)}{3}$$

where σ'_m = mean effective stress
σ'_v = vertical effective stress
K_0 = coefficient of horizontal earth stress at rest (effective stress condition)

Near the ground surface, values per Eq. 3.26 increase disproportionally and it is necessary to limit the adjustment factor to a value of 2.5.

The stress-adjusted cone penetration stress, q_{tM}, is

(3.27) $$q_{tM} = q_t C_M = q_t \left(\frac{\sigma_r}{\sigma'_m}\right)^{0.5}$$

where q_t = unadjusted—as measured—cone stress (but corrected for pore pressure on the shoulder)
σ_r = reference stress = 100 KPa
q_{tM} = stress-adjusted cone stress

Determining the mean stress (Eq. 3.26) requires knowledge of the coefficient of earth stress at rest, K_0. In normally consolidated soils, the magnitude of the horizontal earth stress is usually assumed to follow Eq. 3.28 (Jaky, 1948).

(3.28) $$K_0 = 1 - \sin\phi'$$

where K_0 = coefficient of horizontal earth stress (effective stress condition)
ϕ' = effective friction angle

The effective friction angle for normally consolidated sand and silt ranges between 30° and 36°, which range, according to Eq. 3.28, corresponds to the relatively narrow range of a K_0 of about 0.4 through 0.6.

Compaction results in an increase of the earth stress coefficient at rest, K_0. However, in overconsolidated soils, that is, compacted soils, it is more difficult to estimate K_0. Several investigators have proposed empirical relationships between the earth stress coefficient of normally and overconsolidated sands and the overconsolidation ratio, OCR, as given in Eq. 3.29.

(3.29) $$\frac{K_1}{K_0} = OCR^{\beta}$$ which converts to: (3.29a) $$OCR = \left[\frac{K_1}{K_0}\right]^{\frac{1}{\beta}}$$

where K_0 = coefficient of earth stress at rest for normally consolidated sand
K_1 = coefficient of earth stress at rest for overconsolidated sand
β = empirically determined exponent, usually assumed equal to about 0.4

3.14.4 Determination of the Modulus Number, m, from CPT

Massarsch (1994) proposed a semi-empirical relationship shown in Eq. 3.30 between the modulus number and the cone stress adjusted for depth.

(3.30) $$m = a\,\left(\frac{q_{tM}}{\sigma_r}\right)^{0.5}$$

where m = modulus number
a = empirical modulus modifier, which depends on soil type
q_{tM} = stress-adjusted cone stress
σ_r = reference stress = 100 KPa

The modulus modifier, *a*, has been determined from the evaluation of extensive field and laboratory data (Massarsch, 1994) and shown to vary within a relatively narrow range for each soil type. Massarsch et al. (1997) proposed the values for silt, sand, and gravel listed in Table 3.4.

TABLE 3.4 Modulus factor, a, for different soil types, Massarsch et al. (1997)

Soil Type	Modulus Modifier, a
Soft clay	3*)
Firm clay	5*)
Silt, organic soft	7
Silt, loose	12
Silt, compact	15
Silt, dense	20
Sand, silty loose	20
Sand, loose	22
Sand, compact	28
Sand, dense	35
Gravel, loose	35
Gravel, dense	45

*) These values are based on the author's limited calibration to consolidometer tests in normally consolidated lacustrine and marine clays. Clays at other sites may differ considerably from the shown values.

Eqs. 3.25 through 3.30 can be combined in a single equation, Eq. 3.31.

(3.31) $$m = a\left[\left(\frac{q_t}{(\sigma'_r\ \sigma'_v)^{0.5}}\right)\left(\frac{3}{1+2K_0}\right)^{0.5}\right]^{0.5}$$

where m = modulus number
a = empirical modulus modifier, which depends on soil type
q_t = unadjusted—as measured—cone stress (but corrected for pore pressure on the shoulder)
σ_r = reference stress = 100 KPa

For a soil with K_0 ranging from 0.5 through 5.0, the term $[3/(1 + K_0)^{0.5}]$ ranges from 1.2 to 0.8, that is, the term can be approximated to unity and Eq. 3.31 becomes Eq. 3.32. Notice, compaction can increase the earth stress coefficient beyond a value of 5 and Eq. 3.31 is then needed for the evaluation of the results of the compaction effort.

$$m = a\left[\frac{q_t}{(\sigma'_r\,\sigma'_v)^{0.5}}\right]^{0.5} \tag{3.32}$$

CPT readings are taken intermittently at closely spaced distances, normally every 20 mm, preferably every 10 mm. Normally, to be useful for determining the modulus number, the cone stress values, q_t, must be filtered so that the peaks and troughs in the data are removed. The most useful filtering is obtained by a geometric average running over about 0.5 m length.

The values of the Modulus Modifier, a, given in Table 3.4 have been verified in compacted hydraulic fills. They have yet to be verified in naturally deposited soils. Therefore, use of the values should be done with cautionary judgment. At sites where oedometer testing of recovered ‘undisturbed’ samples can be performed, the CPT data from the corresponding layer can, and should be, calibrated to verify the Modulus Modifier for the site.

The effect of filtering and depth-adjusting the q_t values and calculation of the modulus number profile is illustrated in Fig. 3.11 using the CPT soundings of Fig. 2.1.

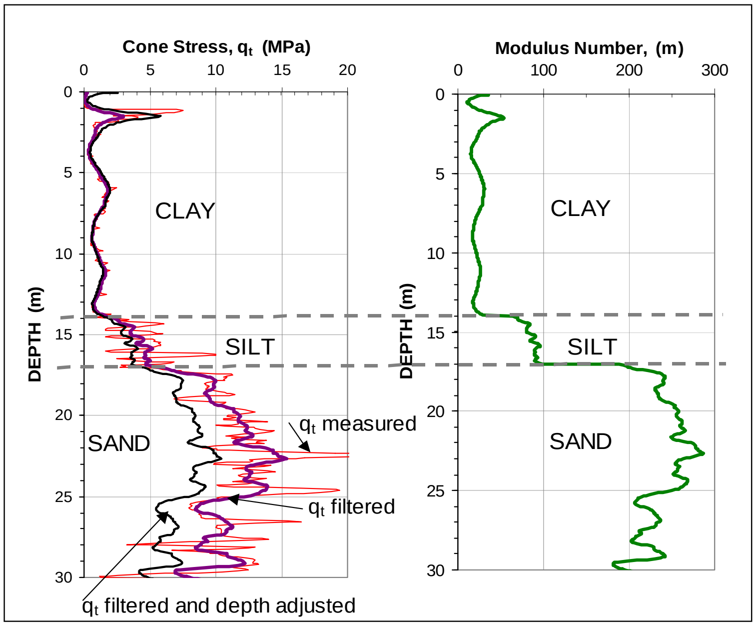

Fig. 3.11 Example of filtered and depth-adjusted q_t-v and profile of the resulting modulus number, m

The CPTU sounding used as example in Chapter 2 to show profiles of various soil parameters has also been used to calculate the compressibility (modulus number) profile for the Alberta site. Fig. 3.12 shows the results. Similar to Fig. 3.3, the figure shows the unfiltered q_t-profile, the filtered qt-profile, and the depth-adjusted values. The second figure shows the calculated modulus number profile and the modulus numbers from oedometer tests to which the CPTU curve is fitted. The third profile shows the modulus modifiers, the "a-exponents", resulting from the fitting of the data.

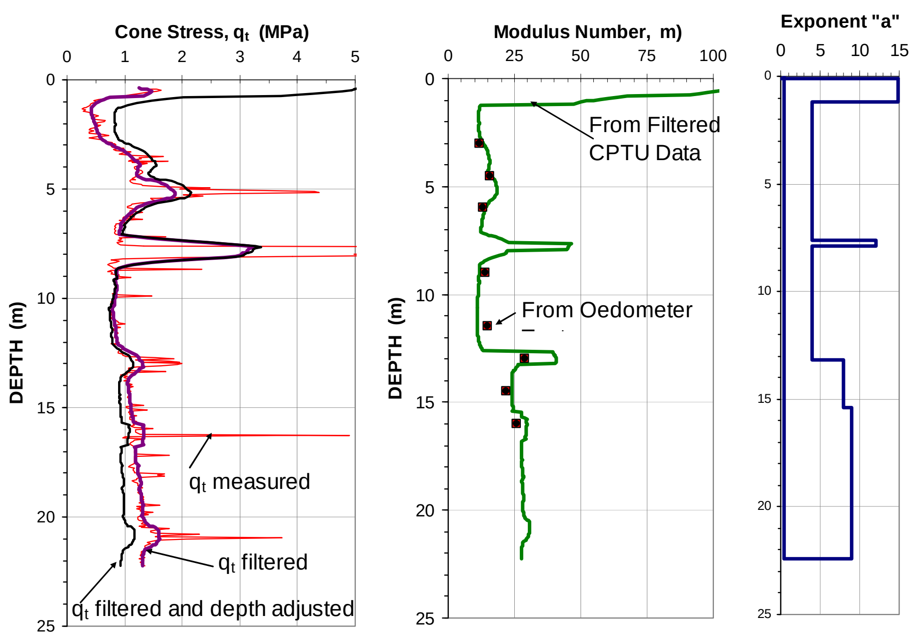

Fig. 3.12 Example of filtered and depth-adjusted q_t values and profile of the resulting modulus number, m, fitted by means of the "*a*-exponent" to values determined in oedometer tests.

CHAPTER 4

VERTICAL DRAINS TO ACCELERATE SETTLEMENT

4.1 Introduction

All materials will undergo volume change when subjected to stress change and soils are no exception. Unlike steel or concrete and other solids, soils are made up of granular materials, grains, and, moreover, the pores between the grains are usually filled with water, often a water and air (gas) mix. This fact makes the response of soil to an increase of stress more complex as opposed to other building materials. The shear strength of soil is more important for foundation design than compressive strength, for example. The central aspect, however, is that in order for a volume change (other than the 'elastic' compression of the grains themselves) to take place, the space between the grains, the pores, must be able to reduce in volume. That is, the water and/or gas must be squeezed out of the soil pores. The process is as follows. An increase of stress results in a small immediate, 'initial' or 'elastic', compression of the soil skeleton. If the pores contain free gas ('bubbles'), the bubbles will compress, some of it may go into solution. This is also an immediate effect, and the corresponding volume change (settlement) cannot be distinguished from the 'initial' compression. In inorganic soils, the 'initial' compression is small compared to the compression due to the reduction of the pore volume. However, the latter cannot take place until the water in the pores is expelled. The driving force is the increase of pore pressure, which at first is about equal to the imposed stress increase. As the water leaves the soil, the pressure reduces, "dissipates", until, finally, all the imposed stress is carried as contact stress between the grains. The process is called "consolidation".

As presented in Section 3.8, the time for consolidation is a function of how easy or difficult is for the water to flow through the soil — the soil hydraulic conductivity ("permeability") is a measure of the "difficulty" — along with the drainage path, that is, the length the water has to flow to leave the zone of increased stress. The time is more or less a linear function of the "permeability" (related to the "coefficient of consolidation"), but is an exponential function (square) of the drainage path. Therefore, if the drainage path can be shortened, the time for the consolidation portion of the settlement, which is the largest portion, can be shortened, "accelerated", substantially. This is achieved by inserting drains into the soil, providing the water with the easy means of travel — "escape" — from the zone of stress increase. The spacing between the drains controls the length of the drainage path. For example, drains installed at a spacing that is a tenth of the thickness of a soil layer that is drained on both sides could, theoretically, shorten the consolidation time to a percentage point or two of the case without drains. An additional benefit is that because the water flows horizontally toward the drains (radially, rather), the flow makes use of the horizontal hydraulic conductivity of the soil, which normally is much larger in the horizontal as opposed to the vertical direction.

The potential benefits of using vertical drains became obvious very soon after Terzaghi in 1926 published his theory of consolidation. Thus, vertical drains have been used in engineering practice for more than 75 years. At first, vertical drains were made of columns of free-draining sand (sand drains) installed by various means (Barron 1948). In about 1945, premanufactured wick drains, termed "wick drains", were invented (Kjellman 1948a, 1948b) and, since about 1970, the technical and economical advantages of the wick drain have all but excluded the use of sand drains. Holtz et al. (1991) have presented a comprehensive account of the history of vertical drains.

4.2 Conventional Approach to Pore Pressure Dissipation and Consolidation of a Drain Project

The basic principles of the behavior of consolidation in the presence of vertical drains is illustrated in Fig. 4.1. The dissipation of the excess pore pressures in the soil body is governed by the water flowing horizontally toward the drain and then up to the groundwater table. (Vertical flow toward draining layers above and below the soil body is usually disregarded). The pore water pressure distribution inside the drain is assumed to be hydrostatic at all time.

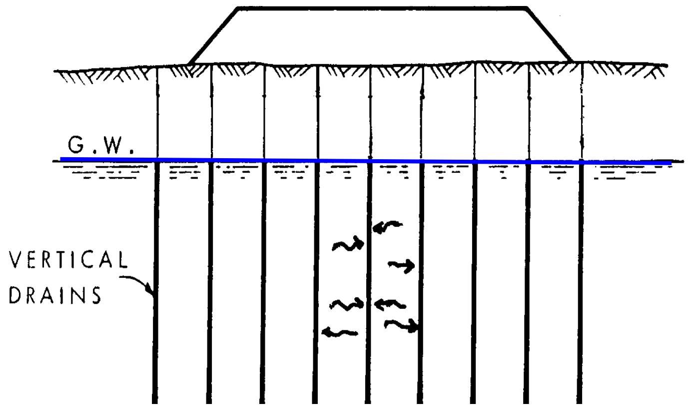

Fig. 4.1 Basic principles of consolidation process in the presence of vertical drains

For the analysis of acceleration of pore pressure dissipation in fine-grained soils (consolidation) and subsequent settlement, Barron (1948) and Kjellman (1948a 1948b) developed a theory based on radial flow toward a circular drain in the center of a cylinder of homogeneous soil with an impervious outer boundary surface (Hansbo 1960; 1979; 1981; 1994). Vertical flow was assumed not to occur. Fig. 4.2 shows a simplified sketch of the principle for consolidation of a soil layer. Fig. 4.2A shows a soil layer sandwiched between free-draining boundaries: the ground surface and a free-draining soil layer below the consolidating layer. The parabolic shape curve indicates the pore pressure distribution at a particular time. The time required for a certain degree of consolidation (in addition to the soil parameters of the case) is primarily a function of the longest drainage path, that is half the thickness of the clay layer, and vertical flow. Fig. 4.2B shows the corresponding picture where vertical drains have been installed. Here, the consolidation time is primarily a function of the spacing of the drains and horizontal flow.

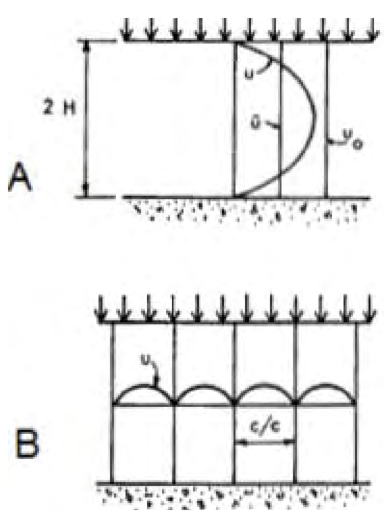

WITHOUT VERTICAL DRAINS

$$t = T_v \cdot \frac{1}{c_v} \cdot H^2$$

$$T_v = -0.1 - \lg (1 - \bar{U})$$

$$\bar{U} = 1 - \frac{\bar{u}}{u_o}$$

Vertical flow between free-draining layers above and below the soil layer

WITH VERTICAL DRAINS

$$t = T_h \cdot \frac{1}{c_h} \cdot D^2$$

$$T_h = \frac{1}{8} \left(\ln \frac{D}{d} - \frac{3}{4} \right) \ln \frac{1}{1 - \bar{U}}$$

Horizontal flow between vertical drains

Fig. 4.2 Principles and formulae for consolidation of a soil layer

The theory is summarized in the Kjellman-Barron formula, Eq. 4.1. The Kjellman-Barron formula is based on the assumption of presence of horizontal (radial) flow only and a homogeneous soil. Relations for average degree of consolidation combining horizontal and vertical flows have been developed by Carillo (1978).

(4.1) $$t = \frac{D^2}{8c_h}[\ln\frac{D}{d} - 0.75]\ln\frac{1}{1-U_h}$$

where
t = time from start of consolidation
D = zone of influence of a drain
d = equivalent diameter of a drain
U_h = average degree of consolidation for horizontal flow
c_h = coefficient of horizontal consolidation

The zone of influence of a drain is defined as the diameter of a cylinder having the same cross section area as the area influenced by the drain. That is, if in a given large area of Size A there are n drains placed at some equal spacing and in some grid pattern, each drain influences the area A/n. Thus, for drains with a center-to-center spacing, c/c, in a square or triangular pattern, the zone of influence, D, is 1.13 c/c or 1.05 c/c, respectively, as illustrated in Fig. 4.3

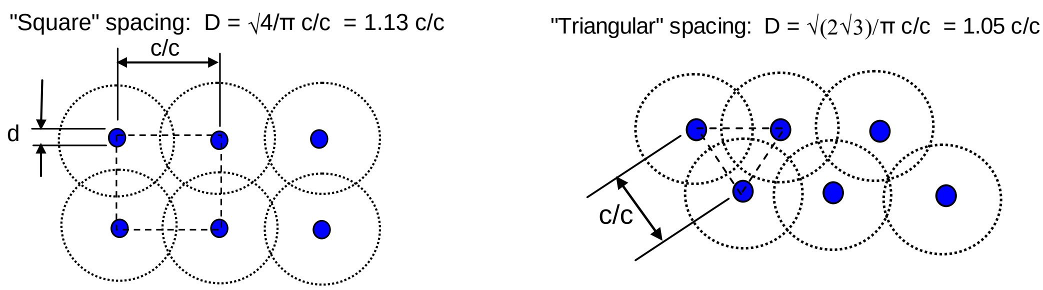

Fig. 4.3 Width of the Zone of influence for square and triangular spacings, c/c, between drains.

In the case of sand drains, the equivalent diameter, d, is often taken as equal to the nominal diameter of the sand drain. In the case of wick drains (Section 4.5), there is no agreement on what to use as the equivalent diameter of the drain. One approach used is simply to equalize the outside surface area of the wick drain with a circular sand drain of the same surface. However, this approach does not recognize the difference between the usually open surface of the premanufactured drain and the rather closed surface of the sand drain, nor the differences between various makes of wick drains.

Strictly speaking, the equivalent diameter of a wick drain should be termed “the equivalent cylinder diameter” to separate it from 'the equivalent sand drain diameter'. Fellenius (1977) suggested that the equivalent cylinder diameter of a sand drain is the nominal diameter of the sand drain multiplied by the porosity of the sand in the drain. The porosity of loose, free-draining sand is normally about 0.4 to 0.5. Thus, the equivalent cylinder diameter of a sand drain is about half of the nominal diameter. However, the consolidation time is not very sensitive to the variations of the value of the equivalent diameter. (In contrast, the consolidation time is very sensitive to the spacing of the drains).

For wick drains of, commonly, 100-mm width, values proposed as the equivalent cylinder diameter have ranged between 30 mm and 80 mm, and full-scale studies have indicated that the performance of such drains have equaled the performance of sand drains of 200 mm to 300 mm in nominal diameter (Hansbo, 1960).

The average degree of consolidation at a certain time, $\overline{U}$, is defined as the ratio between the average increase of effective stress, $\Delta\sigma'$, in the soil over the applied stress causing the consolidation process, i.e., $\Delta\sigma'/q$. In practice, average degree of consolidation is determined from measurements of either pore pressure increase or settlement and, alternatively, defined as 1 minus the ratio between the average pore pressure increase in the soil over the total pore-pressure increase resulting from the applied stress, i.e., $\overline{U} = 1 - u/u_0$, or, the amount of settlement obtained over the final amount of settlement at completed consolidation, $\overline{U} = \Delta S/S_f$. Because pore pressures can be determined at the start of a project, whereas the value of the final settlement is not obtained until after the project is completed, the consolidation ratio is usually based on pore pressure measurements. However, pore pressures and pore-pressure dissipation vary with the distance to the draining layer and, in particular, with the distance to the drains. Seasonal variation is also a factor. Therefore, and in particular because pore-pressure measurements are usually made in only a few points, pore pressure values are very imprecise references to the average degree of consolidation.

As the rate of consolidation may differ at different depths and locations. Therefore, also the average degree of consolidation based on settlement observations is also rather diffuse, unless related to measurements of the compression of a specific layer (difference between settlement at top and bottom of the layer) and as the average of several such layers.

In a homogeneous soil layer, the horizontal coefficient of consolidation, c_h, is usually several times larger than the vertical coefficient, c_v. Dissipation time calculated according to the Barron and Kjellman formula (Eq. 4.1), is inversely proportional to the c_h-value. Note however, that the drain installation will disturb the soil and break down the horizontal pathways nearest the drain (smear zone) and, therefore, the benefit of the undisturbed horizontal coefficient may not be available. For sand drains, in particular displacement-type sand drains, a c_h-value greater than the c_v-value can rarely be mobilized.

The coefficient of consolidation varies widely in natural soils. In **normally consolidated** clays, the c_v-value usually ranges from 1×10^{-8} m^2/s to 30×10^{-8} m^2/s. In silty clays and clayey silts, the c_v-value can range from 5×10^{-8} m^2/s to 50×10^{-8} m^2/s.

The coefficient of consolidation is normally determined from laboratory testing of undisturbed soil samples or, preferably, in-situ by determining the pore-pressure dissipation time in a piezocone (CPTU; see Chapter 2). The actual value to use requires considerable judgment in its selection, and it cannot be determined more closely than within a relative range of three to five times. This means that engineering design of a project requires supporting data for selection of the c_h-value in order to avoid the necessity of employing an excessively conservative approach.

4.3 Practical Aspects Influencing the Design of a Vertical Drain Project

In addition to the theoretical aspects, a design of a vertical drain project is affected by several practical matters, as outlined in this section. (The simplifications of the Kjellman-Barron formula is addressed in Section 4.7.1 as they affect the outcome of a design calculation).

4.3.1 Drainage Blanket on the Ground Surface and Back Pressure

Unless the drains are taken into a free-draining soil layer below the fine-grained layer to be drained, the ground surface must be equipped with a drainage blanket and/or trenches to receive and lead away the water discharged from the drains. Drainage of the "below" layer is rarely assured and, therefore, most projects will include a drainage blanket on the ground surface. Sometimes, the natural ground may provide sufficient drainage to serve as the drainage blanket. Absence of a suitable drainage blanket may result in water ponding in the bowl-shaped depression that develops as the soil settles, creating a back pressure in the drains that impairs the consolidation process. This is illustrated in Fig. 4.4. Ponding due to insufficient horizontal drainage on the ground surface is not acceptable, of course. In a design of a vertical drain project, the expected amount of settlement must be calculated and a drainage scheme designed that ensures a horizontal gradient away from the treated area at all times.

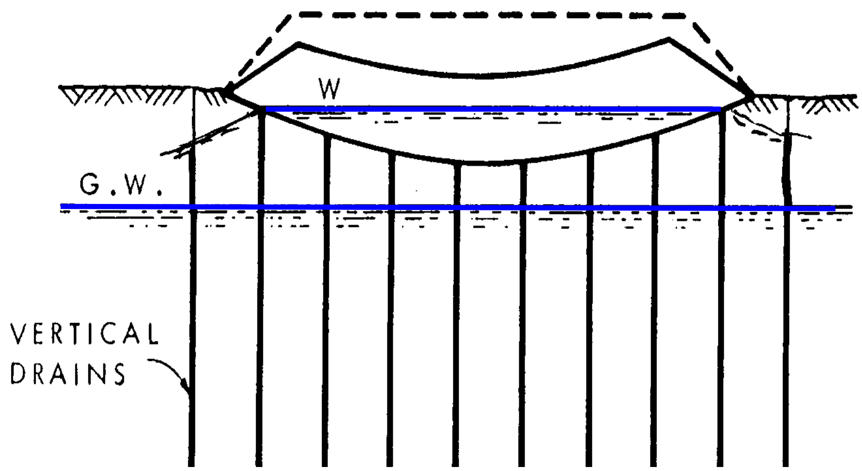

Fig. 4.4 Effect of water ponding below the embankment in the absence of a surface drainage blanket

The build-up of back pressure will temporarily halt or slow down the time development of the consolidation settlement, which, if the process is monitored, is discernible as a flattening out of the time-settlement curve. This may lead to the false conclusion that all of the primary settlement has been obtained. However, eventually, the back pressure will disappear, and the settlement, delayed due to the back pressure, will recur.

It is also important to realize that as the embankment settles, the total vertical stress imposed to the original ground surface over and above the existing vertical stress reduces accordingly, which the loading programme needs to take into consideration. This is particularly important where the groundwater level lies close to the original ground surface.

4.3.2 Effect of Winter Conditions

In areas where Winter conditions prevail, consideration must be given to the risk of the ground frost reducing or preventing the drain discharge at the groundwater table or into the drainage blanket at the ground surface building up a back pressure. The result is similar to that of ponding**:** a slow-down of the settlement, which can be mistaken for the project having reached the end of the primary consolidation. After the Spring thaw, the settlement will recur.

4.3.3 Depth of Installation

The installation depth is governed by several considerations. One is that drains will not accelerate consolidation unless the imposed stress triggering the consolidation brings the effective stress in the soil to a value that is larger than the preconsolidation stress. The imposed stress decreases with depth (as, for example, determined by Boussinesq formulae; Chapter 3) and the in-situ stress increases. From this consideration, the optimum depth of the drains is where the two stresses are equal. However, other considerations may show that a deeper installation is desirable, for example, assuring the discharge of the water into a deeper located pervious soil layer.

4.3.4 Width of Installation

Drains installed underneath an embankment to accelerate consolidation must be distributed across the <u>entire footprint of the embankment and a small distance beyond</u>. A rule-of-thumb is to place the outermost row of the drains at a distance out from the foot of the embankment of about a third to half the height of the embankment. If the drains are installed over a smaller width, not only will differential settlement (bowing) increase during the consolidation period, the consolidation time will become longer.

4.3.5 Effect of Pervious Horizontal Zones, Lenses, Bands, and Layers

The assumption of only homogeneous soil, whether with only radial flow or radial flow combined with vertical flow, used in the derivation of the formulae is not realistic. In fact, most fine-grained clay soils contain horizontal zones of pervious soil consisting of thin lenses, bands, or even layers of coarse-grained soil, such as silty sand or sand. These layers have no influence on the consolidation process where and when no drains are used. However, where vertical drains have been installed, the drainage is to a large extent controlled by the vertical communication between these zones as facilitated by the drains. As illustrated in Fig. 4.5, the consolidation is then by way of slow <u>vertical</u> flow in the fine-grained soil to the lenses, followed by rapid <u>horizontal</u> flow in the lens to the vertical drain, and, then, in the drain to the surface blanket. In effect, the lenses take on the important function of drainage boundaries of the less pervious layers of the soil body sandwiched between the lenses. That is, the mechanism is still very much that of a vertical flow.

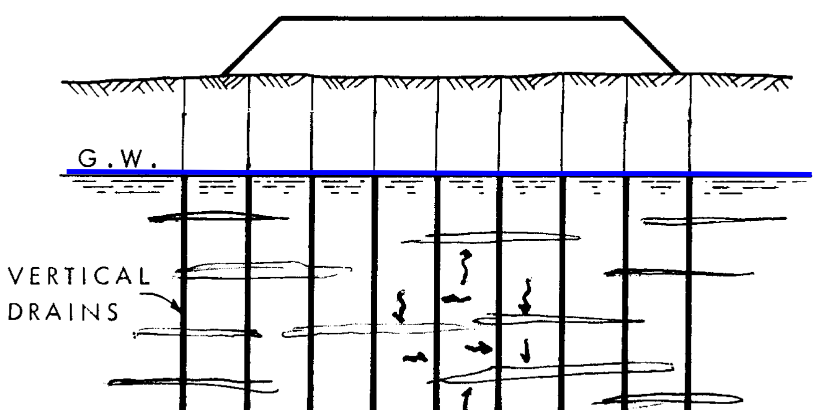

Fig. 4.5 Actual flow in a soil containing pervious lenses, bands, or layers

It is vital for a design of vertical drain project to establish the presence of such lenses, bands, or layers of coarse-grained soil and their vertical spacing. Conventional boreholes and laboratory analysis of recovered samples are rarely fully suitable for this purpose and, usually, once it becomes clear that vertical drains are considered for a project, additional field investigation involving both undisturbed sampling, CPTU tests, and special laboratory testing may become necessary.

4.3.6 Surcharging

The rate of consolidation always slows down significantly toward the end of the consolidation period. The time between about 80 % and 95 % of primary consolidation can require as long time as that from start to 80 %, and the time from 95 % to, say, 98 % can take a very long time. It is not practical to design for a target completion level greater than an average degree of consolidation of 80 %. To reach even that level within a reasonable time requires a surcharge to be placed along with embankment. The surcharge is an extra embankment load (extra height) that is removed when the average degree of consolidation has reached the target level, usually 80 % of the average degree of consolidation for the embankment plus surcharge. The magnitude of the surcharge load should be designed so that after removal, the consolidation of the remaining embankment is completed, resulting in more than a "100 % consolidation" for the embankment without the surcharge. The timing of the removal of the surcharge normally coincides with preparing the embankment for paving of the road bed.

Figure 4.6 shows settlements measured in one point below a test embankment, where wick-drains were installed. The dotted lines indicate the reducing fill height due to the ongoing settlement. On removal of the surcharge (to half height), settlement essentially ceased (a small heave is expected to have occurred, provided full consolidation has had time to develop for the remaining embankment height.

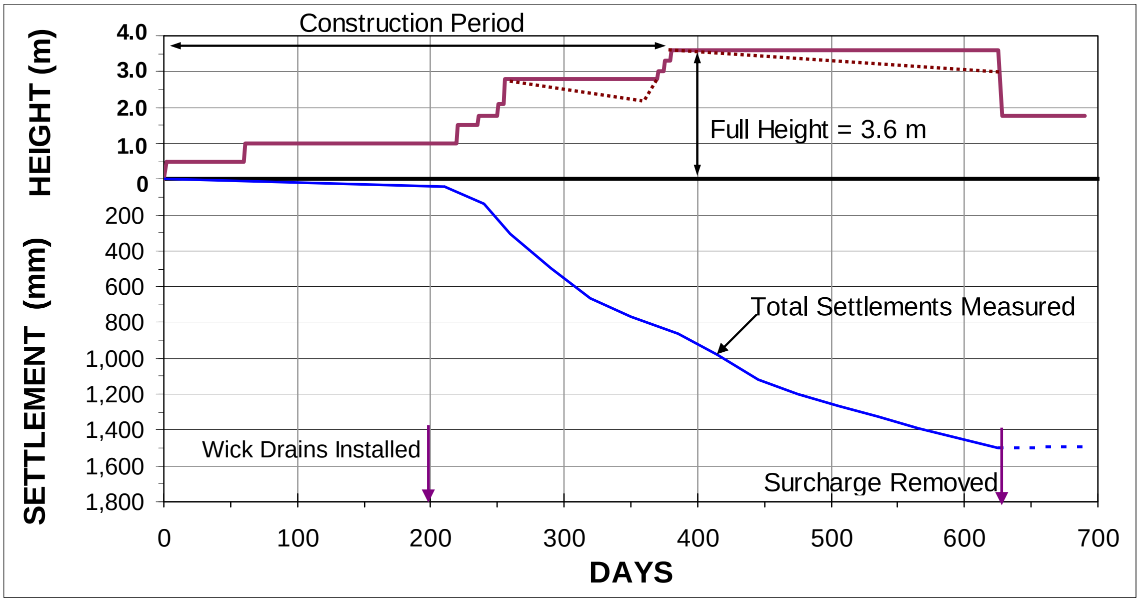

Fig. 4.6 Settlement measured for a stage-constructed test embankment. Data from Moh and Lin (2006).

On completion of the consolidation, the soil supporting the embankment is normally consolidated. This means that future settlement may occur due to small additional loading of the soil from, for example, a moderate raising of the elevation of the road bed or widening the embankment during future maintenance work, or, indeed, even from a load increase due to seasonal variation of the groundwater table (a lowering of the groundwater table will increase the effective stress and initiate — renew — the consolidation). For this reason, it is advisable that the project be designed so as to leave the soil underneath the final structure at a suitable level of preconsolidation stress. This means that the design of a vertical drain project should always incorporate a surcharge (i.e., an extra embankment load to be removed on completion of the consolidation).

4.3.7 Stage Construction

Constructing an embankment to full height in one stage may give rise to concern for the stability of the embankment. Lateral soil spreading will be of concern and not just slope failure. Usually, the instability occurs in the beginning of construction and the risk subsides as the pore pressures reduce due to the consolidation. The stability of the embankment can be ensured during the construction by building in stages—stage construction—and with careful monitoring and evaluation (engineering review) of the consolidation progress. The construction time can be very long, however.

Vertical drains are very effective means to minimize lateral spreading and improve embankment stability. The drains accelerate the consolidation process so that the construction rate is not at all, or only moderately, affected by the stability concern, whereas constructing the embankment without drains would have necessitated stage construction and generally prolonged the construction time and/or necessitated incorporating relief embankments or other resource-demanding methods to offset the concern for stability and lateral movements.

Figure 4.5 shows observed settlements and movements for a stage-constructed 3.6 m high test embankment during the construction of the new Bangkok International Airport, Thailand. Settlement was monitored in center and at embankment edges and horizontal movement was monitored near the sides of embankment. Time from start to end of surcharge placement was nine months. Observation time after end of surcharge placement was eleven months. Compare the maximum lateral movements at the embankment edges, about 180 mm, to the settlements, 1,400 mm. The lateral movements are large. However, without the drains they could easily have twice as large. Note also that the lateral movement is the reason for that the edges of the embankment settle more than the center.

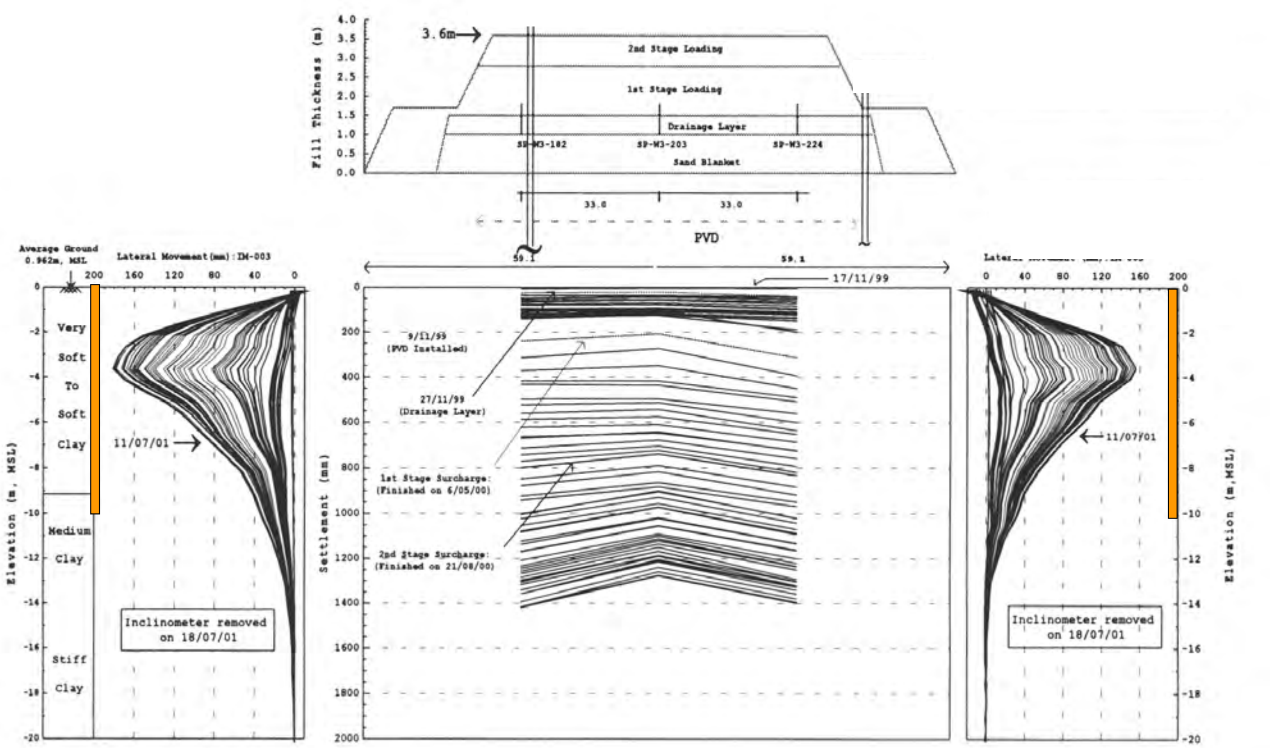

Fig. 4.5 Settlement and lateral movement for a stage-constructed 3.6 m high test embankment. From Moh and Lin (2006).

4.3.8 Loading by Means of Vacuum

Instead of, or in conjunction with, an embankment load, the stress increase driving the consolidation process can be by means of suction, that is, applying a vacuum on the ground surface with vertical drains installed in the ground (Holtz and Wager 1975). Usually, the vacuum method involves placing an impervious membrane (a tarp) on the ground and pumping out the air underneath it. (Chai et al. 2005; 2006). The method involves many practical issues not mentioned here. One alternative application of the method includes connecting each drain to a suction pipe (Cortlever et al. 2006). The theoretical maximum vacuum is equal to the atmospheric pressure (100 KPa), which corresponds to an embankment height of 5 m. However, the actual vacuum possible is no more than about half the theoretical maximum. A difference between applying a stress using the vacuum method is that the stress does not cause outward lateral movement, but a small inward. Also, even in very soft soils, no slope stability concerns exists. Combining the vacuum method with an embankment loading may eliminate the need for stage-construction.

4.3.9 Pore Pressure Gradient and Artesian Flow

Bridges and associated embankments are usually placed near rivers, in valleys, or other low-lying areas. Most of these areas are characterized by a clay layer underlain by pervious soils that function as an aquifer separated from the surficial water table. Commonly, the pore pressure distribution in the lower layers at the site has an upward gradient, it may even be artesian. Drains installed at these sites will not change the pore pressure in the lower soils. However, the drains may change the pore pressure gradient to hydrostatic. This change will offset some of the increase of effective stress due to the embankment and have the beneficial effect of reducing the magnitude of the embankment induced settlement. However, the change of the pore pressure distribution from upward gradient to hydrostatic distribution will act as a back pressure and slow down the consolidation rate. To adjust for this, an extra surcharge may be required. Moreover, arranging for a proper surface drainage of the site will be important as water may be transported up to the ground surface from the lower soil layers for a very long time.

4.3.10 Secondary Compression

Settlement will continue after completion of the consolidation in the form of "*secondary compression*". Secondary compression is not a function of the imposed stress, but of time after completion of the primary consolidation, t_α, time for achieving 100 % primary compression, and of the "*secondary compression index*", C_α,. (See Eq. 3.20 in Chapter 3).

In inorganic soils, secondary compression is normally small in relation to the primary consolidation settlement. However, in organic soils, such as peat and mud, the secondary compression is often appreciable, and secondary compression must be assessed in the design.

4.3.11 Monitoring and Instrumentation

It is imperative to verify that the consolidation proceeds as postulated in the design. Therefore, a vertical drain project must always be combined with an instrumentation programme to monitor the progress of the consolidation in terms of **settlement and pore pressure** development during the entire consolidation period, and often include also lateral movement during the construction. Pore pressures must be monitored also outside the area affected by either the embankment or the drains to serve as independent reference to the measurements.

Instrumentation of a construction site has a poor survival rate. It is very difficult to protect the instrumentation from inadvertent damage. Sometimes, to avoid disturbing the construction work, the monitoring may have to be postponed. Often, a scheduled reading may have to be omitted as it may be too risky for a technician to approach the gage readout unit. Therefore, the monitoring programme should include buried gages and readings by remote sensing. As it is normally not possible for the monitoring programme to control the construction and to ensure that records are taken at important construction milestones, the programme should include automatic data logging set to take readings at frequent intervals. Still, the possibility of damage to the gages cannot be discounted. Therefore, a certain level of redundancy in the layout of instrumentation is necessary.

The monitoring programme must include frequent correlations between the monitoring results and the design to catch any anomalies that can adversely affect the project. To this end, the design should include calculations of expected response at the locations of planned instrumentation. However, a design can never anticipate every event that will arise at a construction project. Therefore, the design should preauthorize provisions for performing analysis of the effect of unexpected events, such as extreme rainfall or drought during the monitoring period, unanticipated construction events involving fill, excavation, or pumping of groundwater, delays of completion of the construction, etc., so that necessary calculations are not delayed because time otherwise required for authorizing the subsequent analyses and adding supplemental instrumentation. Instrumentation design (type, placement depths and locations etc.) is a task for a specialist—the inexperienced must solicit assistance.

4.4 Sand Drains

The sand drain was the first type of vertical drain to be used for accelerating the pore pressure dissipation (during the mid-1930s). The following aspects are specific to the use of sand drains.

Sand drains are usually made by driving or vibrating a pipe into the ground, filling it with sand and withdrawing it. As indicated by Casagrande and Poulos (1969), the installation of full-displacement sand drains (driven drains) in soils that are sensitive to disturbance and displacement may decrease hydraulic conductivity and increase compressibility. As a consequence, the settlement could actually increase due to the construction of the drains.

The sand used in a sand drain must be free draining (not just "clean"), which means that the portion of fine-grained soil in the sand — in the finished sand drain — must not exceed 5 % by weight and preferably be less than 3 %. Constructing sand drains by pouring sand down a jetted water-filled hole will have the effect that silt and clay under suspension in the water will mix with the sand and cause the fines contents to increase to the point that the sand is no longer free-draining. In theory, this can be avoided by washing the hole with water until the water is clear. However, in the process, the hole will widen and the site will become very muddy and, potentially, the mud will render useless the drainage blanket on the ground. Simply put, a free-standing hole that can be washed clear of fines is made in a soil that does not need drains. If the hole is created by washing out the soil, then, before the sand is placed, a pipe must be inserted into which the sand is poured. The pipe is withdrawn after the pipe has been filled with sand. It is advisable to use vibratory equipment to make sure that the sand does not arch inside the pipe.

Sand drains are apt to neck and become disrupted during the installation work, or as a consequence of horizontal movements in the soil. The function of a necked or disrupted drain is severely reduced.

Sand drains have been constructed in the form of sand-filled long bags, hoses, called "sand wicks", which are inserted into a drilled hole

The stated disadvantages notwithstanding, sand drains can be useful where large flows of water are expected, in soils less sensitive to disturbance by the installation, and where the ratio of length to the nominal diameter of the drain is not greater than 50, and the ratio of spacing to nominal diameter is larger than 10.

Since the advent of the prefabricated bandshaped drain, the wick drain, sand drains are rarely used as vertical drains to accelerate consolidation in fine-grained soils.

4.5 Wick Drains

4.5.1 Definition

A wick drain is a prefabricated band-shaped about 100 mm wide and 5 mm to 10 mm thick unit consisting in principle of a channeled (grooved or studded) core wrapped with a filter jacket. Installation is usually by means of a mandrel pushed into the ground (Figs. 4.6, 4.7, and 4.8). The filter jacket serves the purpose of letting water into the drain core while preventing fine soil particles from entering. The channels lead the water up to the a drainage layer on the ground surface, or to the groundwater table, or down to a draining layer below the consolidating soil layer. For details see Holtz et al. (1991).

The Kjellman Cardboard Wick (1942)

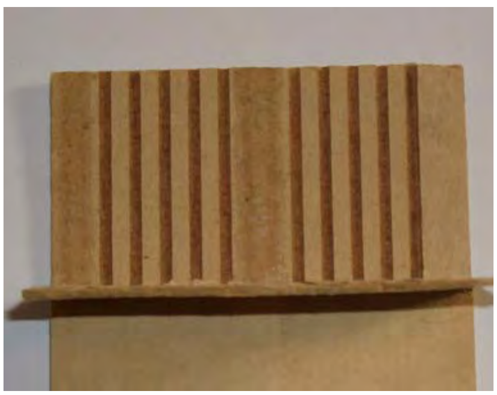

The Geodrain (1976)

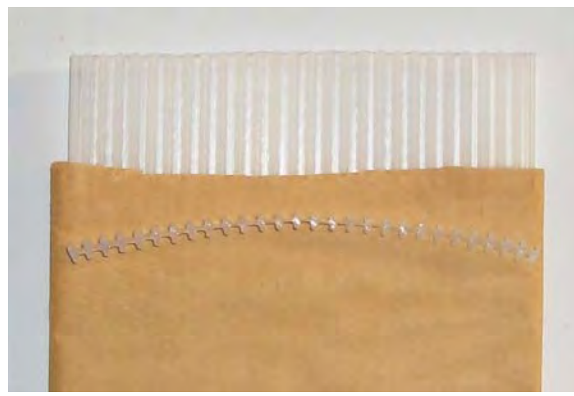

The Alidrain (1978)

The Mebra Drain (1984) (Castleboard Drain, 1979)

Fig. 4.6 Photos of four types of wick drains

Fig. 4.7 View over a site after completed wick drain installation

Fig. 4.8 Installation of wick drains type Alidrain (courtesy of J.C. Brodeur, Burcan Industries Ltd.)

4.5.2 Permeability of the Filter Jacket

There are statements in the literature (e.g., Hansbo, 1979) that the drain filter would not need to be any more pervious to water than the soil is, that is, have a hydraulic conductivity of about 1×10^{-8} m/s. This value is representative to that of a practically impervious membrane and the statement is fundamentally wrong. The filter must be able to accept an inflow of water not only from clay soil, but also from coarser soils, such as silty, fine sand typically found in lenses, or layers in most fine-grained soils—plentiful in most clays. In such soils, the portion reaching the drain through the clay is practically negligible. Moreover, the ***outflow***, i.e., the discharge, of water must also be considered**: what enters the drain must exit the drain** (Fig. 4.9). While the drain receives water over its full length, typically, 5 m through over 20 m, it must be capable of discharging this water through a very short distance of its length (discharge through the end of the drain is a rather special case). Therefore, the hydraulic conductivity of the filter must not be so small as to impede the outflow of water. Generally, the filter must have a hydraulic conductivity (permeability coefficient) no smaller than that of coarse silt or fine sand, approximately 1×10^{-6} m/s. Fig. 4.9 illustrates the effect of water rising in a wick drain with a low-permeability filter.

Fig. 4.9 Water discharging from a drain immediately outside the embankment

If the permeability of the drain filter is such that a head above the ground water table develops inside the drain, a back pressure (Fig. 4.10) develops that will slow down the consolidation process and impair the function of the drain. Examples exist where, due to a too low hydraulic conductivity of the filter jacket, the water has risen more than two metre inside the drain above the groundwater table before a balance was achieved between inflow in the soil below and outflow in the soil above the groundwater table (Fellenius, 1981). The effect is that about one metre of surcharge was wasted to compensate for the two metre rise of the water above the groundwater table. It is the rare occasion that the water can flow out of the drain at the cut-off end of the drain, which usually is well above the groundwater table.

4.5.3 Discharge Capacity

An aspect of importance to a wick drain is the discharge capacity (well resistance) of the drain. Holtz et al. (1991) define the discharge capacity of a drain as the longitudinal flow under a gradient of unity (1.00). However, when this definition is coupled with the, by others, oft-repeated statement that the discharge capacity of most drain wicks is greater than 100 m^3/year, i.e., 20 cm^3/minute (the volume in a small-size glass of water), the inevitable conclusion is that the discharge capacity is not important. The face value of this conclusion is correct, discharge capacity at a gradient of unity is not important. However, discharge capacity at low gradient is very important! The flow in a drain occurs under a very small gradient, about 0.01, not 1.00 Note that the basic premise of the Kjellman-Barron relation that the pore pressure distribution inside the drain is hydrostatic is not quite true—a gradient of zero means no flow! As to the actual discharge, in the extreme, consolidation settlement accelerated by means of drains can amount to about 0.1 m to 0.5 m, for the first month. A drain typically discharges water from a plan area, "footprint", of about 2 m^2. Therefore, the corresponding discharge per drain is approximately 0.2 m^3 to 1 m^3 per month, or 0.005 to 0.02 cm^3/minute . To achieve this flow of water under the more realistic small gradient, adequate discharge capacity and well resistance are important factors to consider.

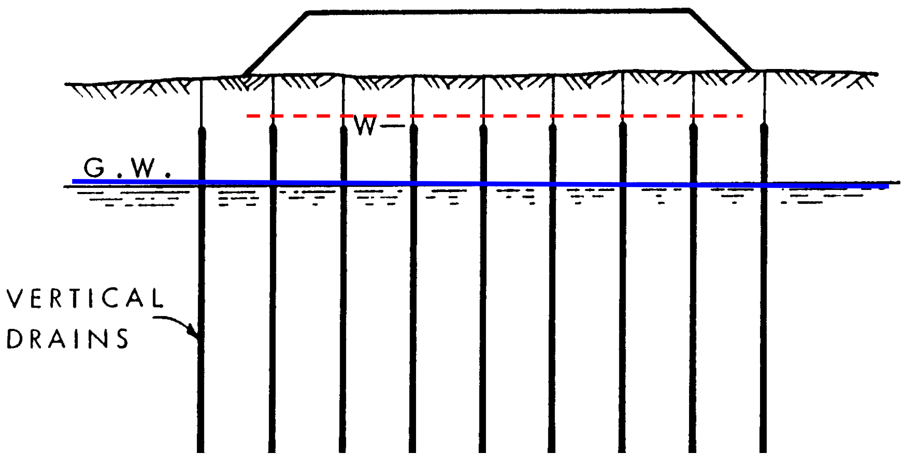

Fig. 4.10 Back pressure in wick drains with filter jacket inadequate for discharge of water

Nevertheless, laboratory tests suggest that most modern prefabricated drains have adequate discharge capacity and little well resistance. That is, water having entered through the filter is not appreciably impeded from flowing up toward the groundwater table through the drain (or down into pervious non-consolidating layers, if the drains have been installed to reach into such layers). ***Nota Bene***, this is conditional on that one can assume that the drains stay straight and have no kinks or folds (microfolds) crimping the drain core. However, this one cannot assume, because, as the soil consolidates, the drains shorten and develop a multitude of kinks and folds, as explained in the following.

4.5.4 Microfolding and Crimping

Settlement is the accumulation of relative compression of the soil which for most cases ranges from about 5 % through 20 % and beyond. A drain cannot buckle out into the soil, nor can it compress elastically, but must accommodate the soil compression in shortening through developing series of folds—microfolds, also called crimping. Microfolds will reduce the discharge capacity, because the grooves or channels block off the flow of the water when folded over. Some drain types are more susceptible to the crimping effect of microfolding than others. Most of the time, the filter jacket will channel the water so as to circumvent a blocked location. Drains where the filter jacket is kept away from the central core by a series of studs, which maintain the open flow area inside the drain, as opposed to longitudinal grooves or channels, can accommodate microfolding without impeding the flow of water.

4.5.5 Handling on Site

The wick drain is often manhandled on the construction site: it is dragged on a truck floor and on the ground, it is left in the sun and in the rain, it gets soaked and is then allowed to freeze, it is stepped on, etc. This puts great demands on strength, in particular wet strength, on the filter and the glue, or weld, used to hold the longitudinal filter seam together. Clay or mud can easily enter and block of the flow in the drain core through a rip or tear in the filter. One such spot in a drain may be enough to considerably impair its function. The filter must have an adequate strength, dry or wet.

4.5.6 Axial Tensile Strength of the Drain Core

A factor also affecting the proper function of a drain and its discharge ability is the tensile strength of the drain core. Wick drains are installed from a roll placed near the ground from where they are pulled up to the top of the installation rig, where they pass over a pulley and go down into an installation mandrel that is forced into the ground. Ever so often, the mandrel tip meets resistance in an interbedded dense layer. This resistance is often overcome very suddenly resulting in an abrupt increase of mandrel installation velocity with the consequence that the drain is yanked down. The filter jacket is usually loose and able to accommodate the sudden pull, but many types of wick drains have thin and weak cores that can easily be torn apart. A drain with a partial or full-width tear of the core will not function well and, as the damage cannot be seen by the field inspection, adequate tensile strength is an important condition to consider in the selection of a drain.

4.5.7 Lateral Compression Strength of the Drain Core

The drain core must be strong enough to resist large, lateral (confining) soil stresses without collapsing as this could close off the longitudinal drainage path. For example, at a depth of 20 m in a clay soil underneath a 10-m high embankment, the effective soil stress can reach 300 KPa, and it is important that the drain can resist this stress without the function of the drain becoming impaired.

4.5.8 Smear Zone

When moving the installation mandrel down and up in a clay, a zone nearest the mandrel is remolded. This zone is called the smear zone. The Kjellman-Barron solution can be refined by incorporating a smear zone into the formula apparatus. It is questionable how important a role smear plays, however. A wick drain has typically a cross sectional area of 5 cm^2. It is sometimes installed using a flattened mandrel having a cross section of about 100 cm^2, or, more commonly, using a circular mandrel having a cross section of 200 cm^2. The installation, therefore, leaves a considerable void in the ground, which, on withdrawing the mandrel, is partially and more or less immediately closed up. In the process, fissures open out from the drain and into the soil. The fissuring and "closing of the void" may be affected by the installation of the next drain, placing of fill on the ground, and/or by the passing of time. The net effect will vary from locality to locality. However, the creation of a void and its closing up, and creation of fissures is far more important than what thickness and parameters to assign to a smear zone. Smear requires careful modeling of the soil hydraulic conductivity and coefficient of consolidation in both horizontal and vertical directions, as well as of all other pertinent soil parameters. To incorporate smear in the Kjellman-Barron radial flow formula is not much more than a fudge concept to fit data to the formula.

4.5.9 Site Investigation

A properly designed and executed subsurface investigation is vital to any geotechnical design. Unfortunately, it is the rare project where the designer has the luxury of knowing the soil in sufficient detail. On many occasions, the paucity of information forces the designer to base the design on "playing it safe". The design of a wick drain project will be very much assisted by having CPTU soundings and continuous tube sampling, as both will aid in determining the presence and extent of lenses, bands, and seams in the soil.

4.5.10 Spacing of Wick Drains

The design of the spacing to use for a wick drain project can be calculated by means of the Kjellman-Barron formula (Eq. 4.1) with input of the coefficient of consolidation and the desired time for the desired degree of consolidation to be achieved with due consideration of the amount of surcharge to use, etc. More sophisticated analysis methods are available. However, the accuracy of the input is frequently such that the spacing can only be determined within a fairly wide range, be the calculation based on the simple or the sophisticated methods. It is often more reliable to consider that the spacing of drains in a homogeneous clay is usually between 1.0 m and 1.6 m, in a silty clay between 1.2 m to 1.8 m, and in a coarser soil between 1.5 m to 2.0 m. The low-range values apply when presence of appreciable seams or lenses have not been found and the upper-range values apply to sites and soils where distinct seams or lenses of silt or sand have been established to exist. It is often meaningful to include an initial test area with a narrow spacing and monitor the pore pressures and settlement for a month or so until most of the consolidation has developed. The observations can then be used to calibrate the site and the design of the rest of the site can then be completed with a wider and more economical spacing.

4.6 Closing remarks

Acceleration of settlement by means of vertical wick drains is an approach with many spin-off benefits. The drains will accelerate the settlement, maybe to the point that, for example in case of a highway, when the road is about to be paved, most of the consolidation settlement has occurred, which minimizes future maintenance costs. If a structure, be it a bridge or a building is to be placed on piles and downdrag (i.e., settlement) is a concern for the piles, a quite common situation, accelerating the settlement with drains so that the settlement occurs before the structure is completed, may alleviate the downdrag problem. If lateral spreading (horizontal movements in the soil) due to fills or embankments imposes lateral movements in the soil that cause the piles to bend, wick drains will reduce the maximum pore pressures and reduce the lateral spreading (Harris et al. 2003).

The analysis of the site conditions aided by the more careful site investigation will have the beneficial effect that the designers will become more aware of what the site entails and be able to improve on the overall geotechnical design for the site and the structures involved.

CHAPTER 5

EARTH PRESSURE — EARTH STRESS

5.1 Introduction

“Earth pressure” is a term for soil stress exerted against the side of a foundation structure—a “wall”. The proper term should really be “earth stress”, because it is directional, whereas “pressure” denotes an omni-directional situation, such as pressure in water. The misnomer is solidly anchored in the profession and to try to correct it is probably futile. Nevertheless, this chapter appliees the term “earth pressure” as opposed to “earth stress”.

Earth stress is stress against a wall from a retained soil body. Loads supported on or in the soil body near the wall will add to the earth stress. The magnitude of the stress against a wall is determined by the physical parameters of the soil, the physical interaction between the soil and the wall, the flexibility of the wall, and the direction and magnitude as well as manner of movement (tilting and/or translation) of the wall. The latter aspect is particularly important. When the wall moves outward, that is, away from the soil—by the soil pushing onto the wall, moving out it or tilting it away, an ‘active’ condition is at hand and the earth stress is said to be “active”. If instead the wall moves toward the soil—by outside forces pushing the wall into the soil— the earth stress is said to be “passive”. In terms of magnitude, the active stress against the wall is much smaller than the passive stress; the relative magnitude can be a factor of ten, and, in terms of amount of movement required for full development of stress, the active stress requires a smaller movement than that required for developing the passive stress. The displacement necessary for full active condition is about 1 % of the wall height; less in dense sand, more in soft clay, and that necessary for full passive condition is about 5 % of the wall height; less in dense sand, more in soft clay. Many text books and manuals include diagrams illustrating the relative displacement necessary to fully develop (reduce the intensity) the active stress and ditto for the passive stress (increase the intensity) for a range of conditions.

In non-cohesive soils, conventionally, the unit stress at a point on the wall is proportional to the overburden stress in the soil immediately outside the wall. The proportionality factor is called “earth stress coefficient” and given the symbol “K” (the word coefficient is spelled “Koefficient” in German, Terzaghi’s first language). The earth stress acting against the wall at a point is a product of the K-coefficient and the overburden stress. In a soil deposited by regular geologic process in horizontal planes, the horizontal stress is about half of the stress in vertical direction, that is, the earth stress coefficient is about 0.5 (notice, the value can vary significantly; see also Section 3.13.3). It is called the “coefficient of earth stress at rest” (“coefficient of earth pressure at rest") and denoted K_0 (pronounced “K-nought”). Once a movement or an unbalanced force is imposed, the ratio changes. If the wall is let to move and the soil follows suit, the earth stress coefficient reduces to a minimum value called “coefficient of active earth stress” and denoted K_a. Conversely, if the wall moves toward the soil, the earth stress coefficient increases to a maximum value called “coefficient of passive earth stress” and denoted K_p.

The earth stress coefficient is a function of many physical parameters, such as the soil strength expressed by the friction angle, the roughness of the wall surface in contact with the soil, the inclination of the wall, and the effective overburden stress. The effective overburden stress is governed by the weight of the soil, the depth of the point below the ground surface, and the pore pressure acting at the point. Despite this complexity, the earth stress coefficient is determined from simple formulae.

5.2 The Earth Stress Coefficient

Fig. 5.1 shows an inclined, rough-surface gravity retaining wall subjected to earth stress from a non-cohesive soil body with an inclined ground surface. The unit active earth stress against the wall acts at an angle of δ formed by a counter-clockwise rotation to a line normal to the wall surface. The unit active earth stress is calculated as K_a times the effective overburden stress and the coefficient, K_a, is given in Eq. 5.1a.

(5.1a) $$K_a = \frac{\sin(\beta - \phi')}{\sin\beta[\sqrt{\sin(\beta+\delta)} + \sqrt{\sin(\delta+\phi')\sin(\phi'-\alpha)/\sin(\beta-\alpha)}]}$$

where
- α = slope of the ground surface measured counter clock-wise from the horizontal
- β = inclination of the wall surface measured counter clock-wise from the base
- ϕ' = effective internal friction angle of the soil
- δ = effective wall friction angle and the rotation of the earth stress measured counter clock-wise from the normal to the wall surface

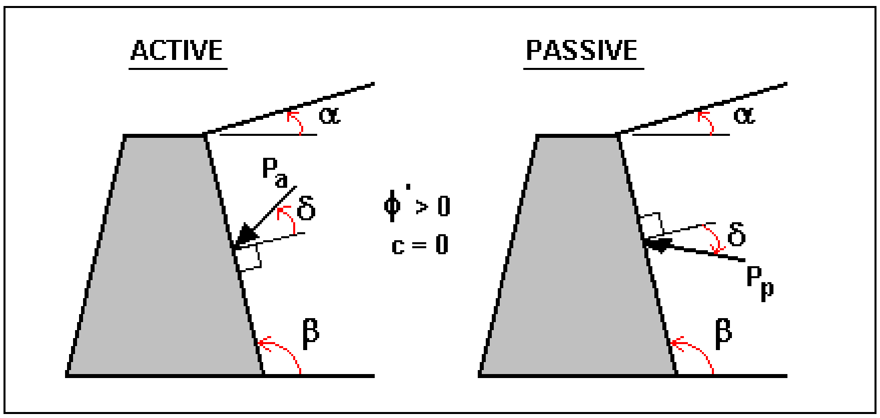

Fig. 5.1 Earth stress against the face of a rough surface gravity wall from a soil body with an inclined ground surface.

Fig. 5.1 shows that for active earth stress, the earth stress has a counter clock-wise rotation, δ, relative the normal to the wall surface and the passive earth stress coefficient, K_a, is given in Eq. 5.1a.

The horizontal component of the active earth stress, K_{ah}, is given in Eq. 5.1b

(5.1b) $$K_{ah} = K_a \sin(\beta + \delta)$$

If the wall is vertical and smooth, that is, $\beta = 90°$ and $\delta = 0°$, then, Eqs. 5.1a and 5.1b both reduce to Eq. 5.1c.

(5.1c) $$K_{ah} = K_a = \frac{1 - \sin\phi'}{1 + \sin\phi'}$$

Fig. 5.1 shows that for passive earth stress, the earth stress has a clock-wise rotation, δ, relative the normal to the wall surface and the passive earth stress coefficient, K_p, is given in Eq. 5.2a.

(5.2a) $$K_p = \frac{\sin(\beta + \phi')}{\sin\beta[\sqrt{\sin(\beta - \delta)} + \sqrt{\sin(\delta + \phi')\sin(\phi' + \alpha)/\sin(\beta - \alpha)}]}$$

The horizontal component of the passive earth stress, K_p, is given in Eq. 5.2b

(5.2b) $$K_{ph} = K_p \sin(\beta - \delta)$$

If the wall is vertical and smooth, that is, β = 90° and δ = 0°, Eqs. 5.2a and 5.2b both reduce to Eq. 5.2c

(5.2c) $$K_{ph} = K_p = \frac{1 + \sin\phi'}{1 - \sin\phi'}$$

Notice that in Fig. 5.1 the wall friction angle (the rotation of the normal force against the wall surface) occurs in different directions for the active and passive cases. The directions indicate the situation for the soil wedge movement relative to the wall—downward in the active case and upward in the passive case. That is, in the active case, the wall moves outward and down; in the passive case, the wall is forced inward and up. For special cases, an outside force may move (slide) the wall in a direction that is opposite to the usual direction (for example, a wall simultaneously retaining soil and supporting a vertical load). The corresponding effect on the earth stress coefficient can be determined by inserting the wall friction angle, δ, with a negative sign in Eqs. 5.1a and 5.2a.

5.3 Active and Passive Earth Stress

The unit active earth stress, p_a, in a soil exhibiting both cohesion and friction is given by Eq. 5.3

(5.3) $$p_a = K_a \sigma'_z - 2c'\sqrt{K_a}$$

where σ'_z = effective overburden stress
c' = effective cohesion intercept

The unit passive earth stress, p_p, in a soil exhibiting both cohesion and friction is given by Eq. 5.4

(5.4) $$p_p = K_p \sigma'_z + 2c'\sqrt{K_p}$$

Usually, if pore water pressure exists in the soil next to a retaining wall, it can be assumed to be hydrostatic and the effective overburden stress be calculated using a buoyant unit weight. However, when this is not the case, the pore pressure gradient must be considered in the determination of the effective stress distribution.

The pressure of the water must be added to the earth stress. Below the water table, therefore, the active and passive earth stress are given by Eqs. 5.5 and 5.6, respectively.

(5.5) $$p_a = K_a \sigma'_z - 2c'\sqrt{K_a} + u$$

(5.6) $$p_p = K_p \sigma'_z + 2c'\sqrt{K_p} + u$$

where u = the pore water pressure

In total stress analysis, which may be applicable to cohesive soils with $\phi = 0$, Eqs. 5.1a and 5.2a reduce to Eq. 5.7a and Eqs. 5.1b and 5.2b reduce to Eq. 5.7b.

(5.7a) $$K_a = K_p = \frac{1}{\sin\beta}$$ and (5.7b) $$K_{ah} = K_{ap} = 1$$

where β = inclination of the wall from Eq. 5.1a

Where $\phi = 0$, and where the undrained shear strength, τ_u, of the soil is used in lieu of effective cohesion, Eqs. 5.5 and 5.6 reduce to Eqs. 5.8a and 5.8b.

(5.8a) $$p_a = \sigma_z - 2\tau_u$$

(5.8b) $$p_p = \sigma_z + 2\tau_u$$

where σ_z = the total overburden stress

Notice, however, that if a crack develops near the wall that can be filled with water, the pressure against the wall will increase. Therefore, the earth stress calculated by Eqs. 5.8a and 5.8b should always be assumed to be at least equal to the water pressure, u, acting against the wall from the water-filled crack (even if the soil away from the wall could be assumed to stay “dry”).

Fig. 5.2 illustrates an inclined, rough-surface wall having on the side to the right (“active side” or “inboard side”) a soil (a backfill, say) with a sloping ground surface. A smaller height soil exists on the other side (the “passive side” or the “outboard side”). The inboard soil is saturated and a water table exists at about mid-height of the wall. The inboard soil is retained by the wall and the soil is therefore in an active state. The soil layer on the outboard side aids the wall in retaining the active side soil and water. It is therefore in a passive state.

The figure includes the angles α, β, and δ, which are parameters used in Eqs. 5.1a and 5.2a. They denote the slope of the ground surface, the slope of the wall surface, and the wall friction angle and rotation of the earth stress acting on the wall surface. (The equations also include the angle ϕ‘, but this angle cannot be shown, because the soil internal friction angle is not a geometric feature).

Fig. 5.2 includes two stress diagrams illustrating the horizontal passive and active earth stress (p_{ph} and p_{ah}) acting against the wall (proportional to the vertical effective stress within the soil layers). The distribution of water pressure, u, against the passive and active side of the wall is also shown in the stress diagram.

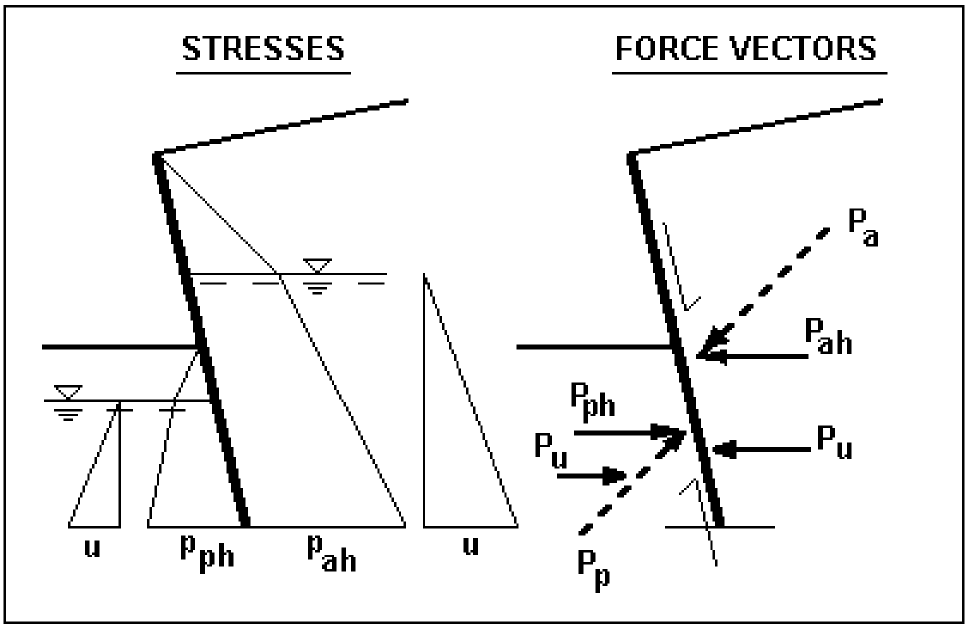

Fig. 5.2 Stresses and force vectors against an inclined wall

The force vectors (P_{ph} and P_{ah}) are the sum of all the horizontal earth stresses and act in the centroids of the stress diagrams. Notice, because of the wall friction, the total earth stress force vectors (P_p and P_a—dashed vectors) are not normal to the wall surface. Notice also that the wall friction vectors acting along the wall surface on the active and passive side point in opposing directions. (The weight of the wall and the forces at the base of the wall are not shown, and neither is the net bending moment).

In developing the forces, movements will have occurred that mobilize the active and passive states (and, also, the contact stresses and sliding resistance at the base of the wall). However, the wall as shown is in equilibrium, that is, the movements have ceased. The movements may well have been sufficiently large to develop active stress (and, probably, also the full sliding resistance, depending on the type of soil present under the base of the wall). However, no more passive resistance has developed than that necessary to halt the movement of the wall. (Remember, the movement necessary for full passive resistance is larger than for full active resistance).

When cohesion dominates in the retained soil, Eq. 5.3 may result in a negative active earth stress near the ground surface. Negative earth stress implies a tension stress onto the wall, which cannot occur. Therefore, when calculating earth stress, the negative values should be disregarded.

5.4 Surcharge, Line, and Strip Loads

A surcharge over the ground surface increases the earth stress on the wall. A uniform surcharge load can be considered quite simply by including its effect when calculating the effective overburden stress. However, other forces on the ground surface, such as strip loads, line loads, and point loads also cause earth stress. Strip loads, which are loads on areas of limited extent (limited size footprint), and line and point loads produce non-uniform contribution to the effective overburden stress and, therefore, their contribution to the earth stress is difficult to determine. Terzaghi (1954) applied Boussinesq stress distribution to calculate the earth stress from line loads and strip loads. This approach has been widely accepted in current codes and manuals (e. g., Canadian Foundation Engineering Manual 1992; NAVFAC DM7 1982). According to Terzaghi (1954), the earth stress against the wall is twice the Boussinesq stress.

Fig. 5.3 illustrates the principles of the stress acting on a wall due to surface loads calculated according to Boussinesq distribution. The so calculated stress is independent of the earth stress coefficient, the soil strength parameters, and, indeed, whether an active or a passive state exists in the soil. The figure shows the Boussinesq distributions for the horizontal stress at a point, z, below the ground surface from a line load, a uniformly loaded strip load, and a strip load with a linearly varying load on the ground surface, are given by Eqs. 5.9a through 5.9.c. For symbols, see Fig. 5.4. Notice, the angles α and β are not the same as those used in Eq. 5.1, α is the angle between the vector to the edge of the strip load, and β is the angle between the wall and the left vector to the strip.

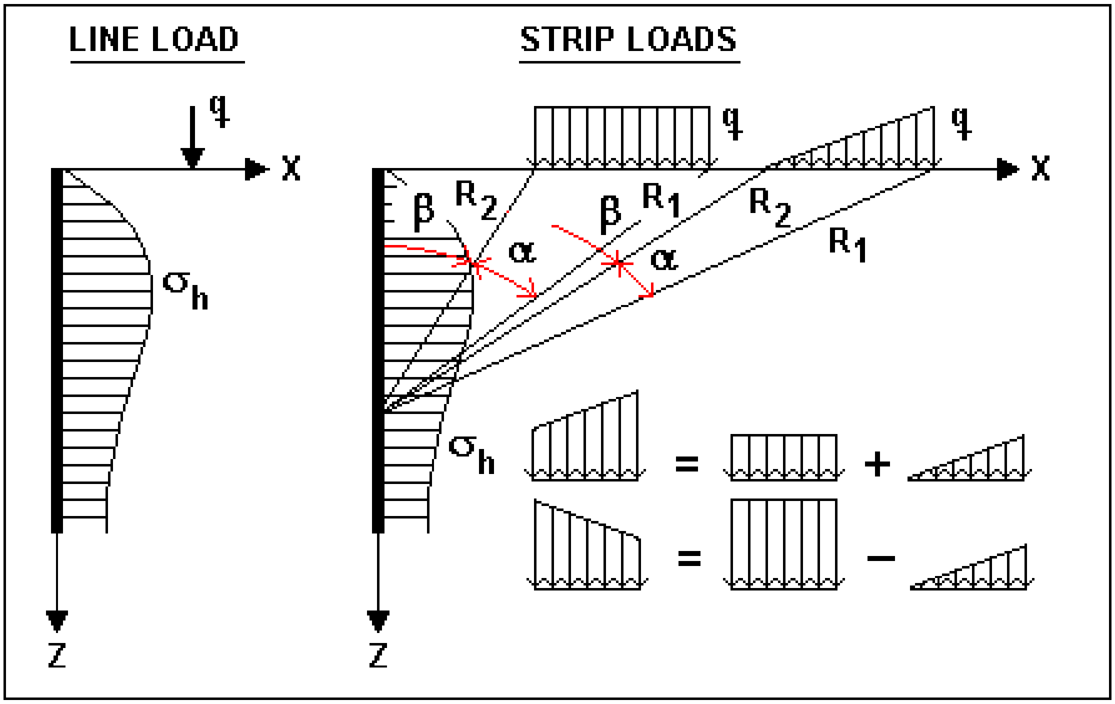

Fig. 5.3 Earth stress on a wall from line and strip loads on the ground surface as determined by Boussinesq distribution.

Stress from a line load, q**:**

(5.9a) $$\sigma_h = \frac{2q}{\pi} \frac{x^2 z}{(x^2 + z^2)^2}$$

Stress from uniform strip load, q**:**

(5.9b) $$\sigma_h = \frac{q}{\pi} [\alpha - \sin\alpha \cos(\alpha + 2\beta)]$$

Stress from a uniform strip load that varies linearly from zero at one side to q at the other side**:**

(5.9c) $$\sigma_h = \frac{q}{\pi} [\frac{x\alpha}{\beta} - \frac{z}{\beta} \ln(\frac{R_1^{\ 2}}{R_2^{\ 2}}) + \frac{\sin 2\beta}{2}]$$

Integration of the equations gives the expression for the horizontal earth stress acting against a wall resulting from the line and strip loads. As mentioned above, the integrated value is doubled to provide the earth stress acting on the wall. A linearly varying (increasing or decreasing) strip load can be determined by combining Eqs. 5.9b and 5.9c.

Terzaghi (1953) presented nomograms for finding the point of application of the resultant of the unit earth stress acting against a vertical wall. By means of applying numerical computer methods, as available in the UniBear program by UniSoft Ltd., the location of the earth stress resultant and its magnitude can be directly located and, moreover, also the solution for inclined walls (for details, see the UniBear Manual).

According to Terzaghi (1952), the earth stress calculated according to Eq. 5.9a is not valid for a line load acting closer to the wall than a distance of 40 % of the wall height. For such line loads, the earth stress should be assumed equal to the earth stress from a line load at a distance of 40 % of the height. The resulting force on the wall is 55 % of the line load and its point of application lies about 60 % of the wall height above the wall base.

For a cantilever wall having a base or a footing, a surface load will, of course, also act against the horizontal surface of the base, as indicated in Fig 5.4. The vertical stress on the base can be determined from Eqs. 5.10a through 5.10c below applying the symbols used in Fig. 5.3 and Eqs. 5.9a through 5.9c.

Vertical stress from a line load, q**:**

(5.10a) $$\sigma_v = \frac{2q}{\pi} \frac{z^3}{(x^2 + z^2)^2}$$

Vertical stress from a uniform strip load, q**:**

(5.10b) $$\sigma_v = \frac{q}{\pi} [\alpha + \sin\alpha \cos(\alpha + 2\beta)]$$

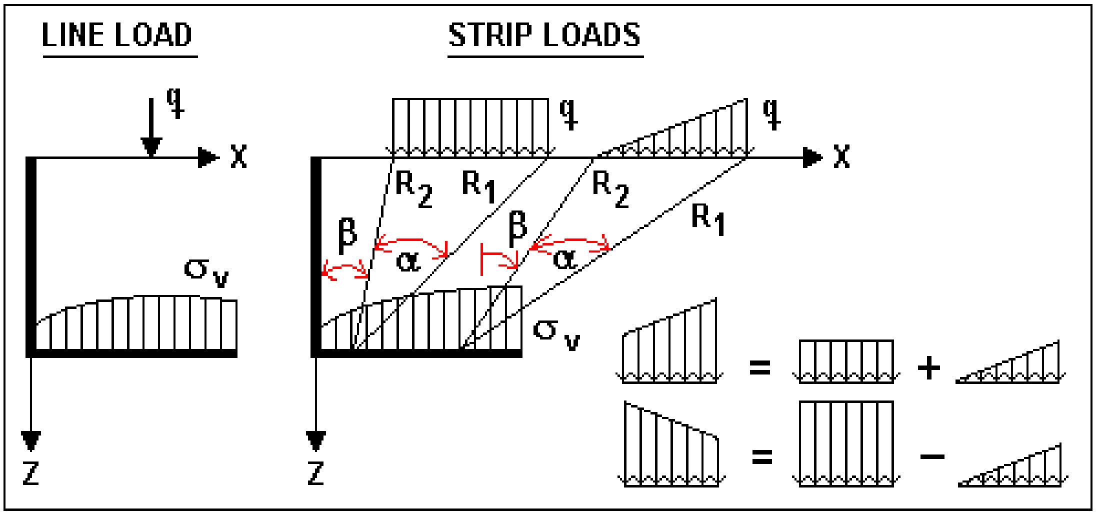

Fig. 5.4 Vertical earth stress on the base of a cantilever wall from line and strip loads on the ground surface as determined by Boussinesq distribution.

Vertical stress from uniform strip load that varies linearly from zero at one side to q at the other side**:**

(5.10c) $$\sigma_v = \frac{q}{\pi}\left[\frac{x\alpha}{\beta} - \frac{\sin 2\beta}{2}\right]$$

Integration of the equations gives the resulting vertical earth stress acting against the base and, also, its location. A linearly varying (increasing or decreasing) strip load can be determined by combining Eqs. 5.10b and 5.10c. Notice, the stress according to Eqs. 5.10a through 5.10c acting on the base can have a stabilizing influence on a footing foundation.

5.5 Factors of Safety and Resistance Factors

In a design for earth stress forces, the factors of safety (resistance factors in a LRFD) appropriate to the structures and types of loads involved should be applied. Note, however, that "safety" against overturning and location of the resultant, should be applied without any factor of safety or resistance factor applied to the loads and earth forces. See also Section 6.6.

CHAPTER 6

BEARING CAPACITY OF SHALLOW FOUNDATIONS

6.1 Introduction

When Society started building structures imposing large concentrated loads onto the soil, occasionally, catastrophic failures occurred. Initially, the understanding of foundation behavior merely progressed from the lessons of one failure to the next. Later, "preemptive" tests were run of model footings in different soils and the test results were extrapolated to the behavior of full-scale foundations by means of theoretical analysis. For example, loading tests on model size footings in clay showed load-movement curves with a distinct peak value—bearing capacity failure—agreeing with a theoretical analysis that the capacity (not the settlement) of a footing in clay is independent of the footing size. In contrast, test on model footings in sand have shown that the capacity (in terms of ultimate or maximum contact stress) increases with the footing size (see Section 6.10). As a result of the tests, calculation of bearing capacity is a part of a conventional footing design.

6.2 The Bearing Capacity Formula

Buisman (1935; 1940) and Terzaghi (1943) compiled observed behaviors into a "bearing capacity formula", as given in Eqs. 6.1a through 6.1d (applicable to a continuous footing).

(6.1a) $$r_u = c'N_c + q'N_q + 0.5B\gamma' N_\gamma$$

where
r_u = ultimate unit resistance of the footing
c' = effective cohesion intercept
B = footing width
q' = overburden effective stress at the foundation level
γ' = average effective unit weight of the soil below the foundation
N_c, N_q, N_γ = non-dimensional bearing capacity factors

When the groundwater table lies above or at the base, the effective unit weight, γ', is the buoyant unit weight of the soil. When it lies below the base and at a distance equal to the width, B, γ' is equal to the total unit weight. When the groundwater table lies within a distance of B, the value of γ' in Eq. 6.1a is equal to the buoyant value plus a portion of the unit weight of water proportioned to the relative distance to the groundwater table.

The bearing capacity factors are a function of the effective friction angle of the soil. The factors were originated by Buisman (1935; 1940) and Terzaghi (1943), later modified by Meyerhof (1951; 1963), Hansen (1961), and others. According to the Canadian Foundation Engineering Manual (1992), the bearing capacity factors, which are somewhat interdependent, are as follows.

(6.1b) $$N_q = e^{\pi \tan\phi}\left(\frac{1+\sin\phi}{1-\sin\phi}\right) \qquad \phi \to 0 \qquad N_q \to 1$$

(6.1c) $$N_c = (N_q - 1)(\cot\phi') \qquad \phi' \to 0 \qquad N_c \to \pi + 2 = 5.14$$

(6.1d) $$N_\gamma = 1.5(N_q - 1)(\tan\phi') \qquad \phi' \to 0 \qquad N_\gamma \to 0$$

where ϕ' = the effective internal friction angle of the soil

Terzaghi and many others refined the original coefficients of the "triple N formula", relying mainly on results of test on model footings. The range of published values for the N_q coefficient is about 50 through about 600 (Coduto 1994). (This wide range of the key parameter should have alerted the profession to that perhaps the pertinence of the formula could be questionable).

Equation 6.1d is not the only one used for determining the N_γ bearing capacity coefficient. Eq. 6.1e is a commonly applied relation that was developed by Vesic (1973; 1975) by means of fitting a curve to a set of values from values in a table produced by Caquot and Kerisel (1953)**:**

(6.1e) $$N_\gamma = 2(N_q + 1)(\tan\phi') \qquad \phi' \to 0 \qquad N_\gamma \to 0$$

Vesic (1975) presented a table listing the factors according to Eq. 6.1e ranging from 0° through 50°, which table is reproduced in the AASHTO Specifications (1992).

There are many other expressions in use for the N_γ bearing capacity factor. For example, the German code DIN 4017 uses $N_\gamma = 2(N_q - 1)(\tan\phi')$ in its expression, that is, a "-" instead of a "+" (Hansbo, 1994). For details, see Tomlinson (1980), Bowles (1988), and Coduto (1994).

Notice, for friction angles larger than about 37°, the bearing capacity factors increase rapidly and Eq. 6.1 loses in relevance.

6.3 The Factor of Safety

In the design of a footing for bearing capacity, the applied load is only allowed to reach a certain portion of the maximum available (ultimate) resistance, as given by Eq. 6.1a. That is, as is the case for all foundation designs, the design must include a margin of safety against failure. In most geotechnical applications, this margin is achieved by applying a factor of safety defined as the available soil strength divided by the mobilized shear resistance. The available strength is either cohesion (c) or friction (tan ϕ), or both combined. (Notice that friction is not the friction angle, ϕ, but its tangent, tan ϕ). In contrast, for bearing capacity problems, the factor of safety is not defined as a ratio between strength and mobilized resistance, but as given by Eq. 6.2.

(6.2) $$F_s = \frac{r_u - q'}{q_{allow}} \qquad \text{or, alternatively} \qquad F_s = \frac{r_u}{q_{allow}}$$

where
F_s = factor of safety
r_u = ultimate unit resistance (unit bearing capacity)
q' = overburden effective stress at the foundation level
q_{allow} = the allowable bearing stress (contact stress)

The factor of safety applied to the bearing capacity formula is usually recommended to be no smaller than 3.0. There is some confusion whether, in calculating the bearing capacity according to Eq. 6.2, the relation (N_q - 1) should be used in lieu of N_q. Moreover, subtracting the overburden stress, q', from r_u is also in some contention. That is, whether or not the factor of safety should apply to a "net" stress. The Canadian Foundation Engineering Manual (1992) omits the q' part, that is, uses the second alternative of Eq. 6.2. The difference has little practical importance, however. In coarse-grained soils, for example, the friction angle, ϕ', normally exceeds a value of 33° and the corresponding N_q-value exceeds 25, that is, when also considering the effect of N_γ , the "error" is no greater than a percentage point or two. In terms of the effect on the friction angle, the difference amounts to about 0.2°, which is too small to have any practical relevance.

More important, as mentioned, the definition of factor of safety given by Eq. 6.2 is very different from the definition when the factor of safety is applied to the shear strength value in the bearing capacity formula. This is because the ultimate resistance determined by the bearing capacity formula includes several aspects other than soil shear strength. Particularly so for foundations on soil having a substantial friction component. Depending on the particulars of each case, a value of 3 to 4 for the factor defined by Eq. 6.2 corresponds, very approximately, to a factor of safety on shear strength in the range of 1.5 through 2.0 (Fellenius, 1994).

In fact, the bearing capacity formula is wrought with much uncertainty and the factor of safety, be it 3 or 4, applied to a bearing capacity formula is really a "*factor of ignorance*" and does not always guarantee an adequate safety against failure. Therefore, in the design of footings, be it in clays or sands, the settlement analysis should be given more weight than the bearing capacity calculation.

The ultimate resistance according to the bearing capacity formula, Eq. 6.1a, assumes a relatively incompressible subsoil. For footings placed on compressible soils, the formula can be adjusted by a rigidity factor as indicated by Vesic (1973; 1975), resulting in a reduction of the calculated ultimate resistance, r_u. Where the soil is compressible enough to warrant such adjustment, settlement analysis, not bearing capacity analysis, should be let to govern the limiting (allowable) stress. Notice, it is equally important to consider stability against sliding and to limit the load eccentricity. Either of the three may prove to govern a design.

6.4 Inclined and Eccentric Loads

Fig. 6.1 shows a cross sections of two strip footings of width, B, subjected to vertical load, Q and Q_v. The load on the left footing is vertical and concentric. The applied contact stress is q per unit length (q = Q/B) and it mobilizes an equally large soil resistance, r.

However, loads on footings are normally eccentric and inclined, as shown for the footing to the right. Loading a footing eccentrically will reduce the bearing capacity of the footing. An off-center load will increase the stress (edge stress) on one side and decrease it on the opposing side. A large edge stress can be the starting point of a bearing failure. The edge stress is taken into account by replacing the full footing width (B) with an effective footing width (B') in the bearing capacity formula (Eq. 6.1a; which assumes a uniform load).

The effective footing width is the width of a smaller footing having the resultant load in its center. That is, the calculated ultimate resistance is decreased because of the reduced width (γ-component in Eq. 6.1) and the applied stress is increased because it is calculated over the effective area as q = Q/(B' L). The approach is approximate and its use is limited to the requirement that the contact stress must not be reduced beyond a zero value at the opposite edge ("no tension at the heel"). This means that the resultant must fall within the middle third of the footing, that is, the eccentricity must not be greater than B/6 (= 16.7 % of the footing width). Fig. 6.2 illustrates the difference in contact stress between a footing loaded within its middle third area as opposed to outside that area.

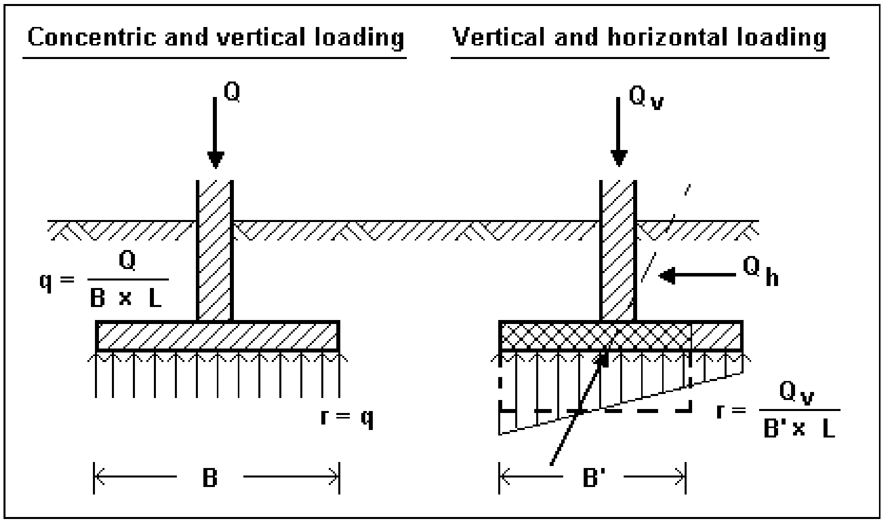

Fig. 6.1 A strip footing a) loaded concentrically and vertically, only, and b) loaded vertically and horizontally

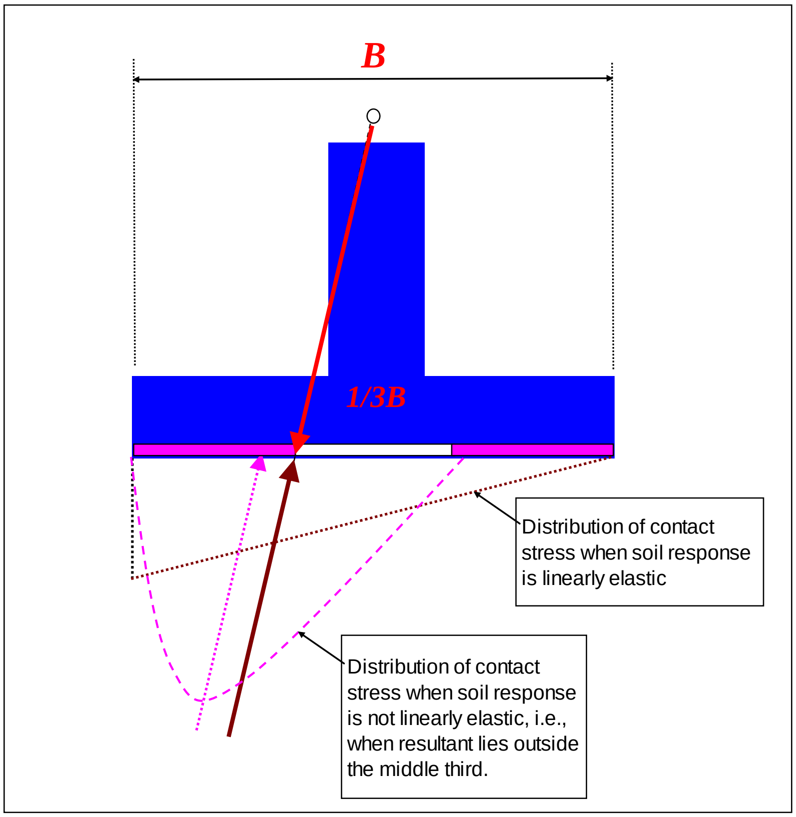

Fig. 6.2 Contact stress distributions when the resultant lies within the middle third and outside.

6.5 Inclination and Shape Factors

Combining a vertical load with a horizontal load, that is, inclining the load, will also reduce the bearing capacity of a footing. The effect of the inclination is expressed by means of reduction factors called Inclination Factors, i. An inclination may have an indirect additional effect due to that the resultant to the load on most occasions acts off center, reducing the effective area of the footing.

Also the shape of the footing influences the capacity, which is expressed by means of reduction factors called Shape Factors, s. The bearing capacity formula is derived under the assumption of an infinitely long strip footing. A footing with finite length, L, will have a contribution of soil resistance from the footing ends. This contribution is what the shape factors adjust for, making the formula with its bearing capacity factors applicable also to rectangularly shaped footings. Notice, Eq. 6.3 does not include Depth Factors. However, many will consider the depth of the footing by including the overburden stress, q'.

Thus, to represent the general case of a footing subjected to both inclined and eccentric load, Eq. 6.1a changes to

(6.3) $$r_u = s_c\, i_c\, c' N_c + s_q\, i_q\, q' N_q + s_\gamma\, i_\gamma\, 0.5 B' \gamma' N_\gamma$$

where factors not defined earlier are

s_c, s_q, s_γ = non-dimensional shape factors
i_c, i_q, i_γ = non-dimensional inclination factors
B' = equivalent or effective footing width

When the load is offset from the center of the footing toward the long side, the L-side, rather than toward the short side, the B-side, the bearing stress is assumed to act over a footing area of B times L'. When the resultant is eccentric in the directions of both the short and long sides of the footing, the effective area according to the Ontario Highway Bridge Design Code (1991) takes the shape of a triangle with the resultant in its centroid. In contrast, the AASHTO Specifications (1992) defines the effective area as a rectangle with sides B' and L'.

As long as the resultant falls within the middle third of the footing width, it can acceptably be assumed that the stress distribution below the footing is approximately linear. However, when the resultant moves beyond the third point, that is, closer to the edge of the footing, not only does the edge stress increase rapidly, the assumption of linearity is no longer valid. The requirement of having the resultant in the middle third is, therefore, very important in the design. In fact, if the resultant lies outside the middle third, the adequacy of the design becomes highly questionable. See also Section 6.6.

The shape factors are

(6.3a) $$s_c = s_q = 1 + \frac{B'}{L'} \frac{N_q}{N_c}$$

(6.3b) $$s_\gamma = 1 - 0.4 \frac{B'}{L'}$$

where B' = equivalent or effective footing width

L' = equivalent or effective footing length

According to the Canadian Foundation Engineering Manual (1992) and the OHBDC (1991), the inclination factors are:

(6.3c) $$i_c = i_q = (1 - \frac{\alpha}{90^\circ})^2$$

(6.3d) $$i_\gamma = (1 - \frac{\alpha}{\phi'})^2$$

where α = the inclination of the resultant (angle to the vertical)
ϕ' = the effective internal friction angle of the soil

As for the case of the bearing capacity factor N_γ, different expressions for the inclination factor i_γ are in use. Hansen (1961) proposed to use

(6.3e) $$i_\gamma = (1 - \frac{P}{Q + B'L'c'\cot\phi'})^2$$

where *P* = the horizontal resultant to the forces
Q = the vertical resultant to the forces
c' = effective cohesion intercept
ϕ' = effective friction angle
B' = equivalent or effective footing width
L' = equivalent or effective footing length

Vesic (1975) proposed to use an expression similar to Eq. 6.3e, but with an exponent "m" instead of the exponent of "2", where m is determined as follows:

(6.3f) $$m = \frac{2 + \frac{L}{B}}{1 + \frac{L}{B}}$$

The AASHTO Specifications (AASHTO 1992) includes a somewhat different definition of the inclination factors, as follows:

(6.3g) $$i_c = i_q - \frac{1 - i_q}{N_c \tan\phi'}$$ for ϕ' > 0

(6.3h) $$i_c = 1 - \frac{n\,P}{B'\,L'\,c'\,N'_c}$$ for ϕ' = 0

(6.3i) $$i_q = 1 - \frac{n\ P}{\theta + B'\ L'\ c'\cot\phi'}$$

(6.3j) $$i_\gamma = 1 - \frac{(n+1)\ P}{\theta + B'\ L'\ c'\cot\phi'}$$

The factor "n" is determined as follows:

(6.3k) $$n = \frac{2 + L'/B'}{1 + L'/B'}\cos^2\theta \quad + \quad \frac{2 + B'/L'}{2 + B'/L'}\sin^2\theta$$

where θ = angle of load eccentricity (angle of the force resultant with the long side of the footing)
B' = equivalent or effective footing width
L' = equivalent or effective footing length

Notice, all the above inclination factors as quoted from the various sources can result in values that are larger than unity. Such a calculation result is an indication of that the particular expression used is not valid.

Many textbooks present a basic formulae multiplied with influence factors for shape and inclination of the resultant. These influence factors are calculated from formulae similar to the ones listed above and are often to be determined from nomograms as opposed to from formulae. They may also include considerations of stress distribution for different shapes (or separate influence factors are added). Such influence factors are from before the advent of the computer, when calculations were time-consuming.

6.6 Overturning

Frequently, one finds in text books and codes that the stability of a footing is expressed as an overturning ratio: "Factor-of-Safety against overturning". This is the ratio between rotating moment around the toe of the footing taken as the quotient between the forces that try to topple (overturn) the footing and the forces that counteract the overturning. Commonly, the recommended "factor-of-safety against overturning" is 1.50. However, while the ratio between the calculated moments may be 1.50, the Factor of Safety, F_s, is not 1.50. For the factor of safety concept to be valid, a value of F_s close to unity must be possible, which is not the case when the resultant moves beyond the third point. For such a situation, the combination of increasing edge stress and progressively developing non-linearity causes the point of rotation to move inward (see Fig. 6.2). At an overturning ratio of about 1.2, failure becomes imminent. Ballerinas dance on toe, real footings do not, and the overturning ratio must not be thought of as being the same as a factor of safety. **Safety against overturning cannot be by a factor of safety. It is best guarded against by keeping the resultant inside the middle third of the footing.**

6.7 Sliding

The calculation of a footing stability must include a check that the safety against horizontal sliding is sufficient. The calculation is simple and consists of determining the ratio between the sum of the horizontal resistance and the sum of all horizontal loads, $\Sigma R_h/\Sigma Q_h$ at the interface between the footing underside and the soil. This ratio is taken as the factor of safety against sliding. Usually, the safety against sliding is considered satisfactory if the factor of safety lies in the range of 1.5 through 1.8. The horizontal resistance is made up of friction ($\Sigma Q_v \tan \varphi'$) and cohesion components ($c'BL$).

6.8 Combined Calculation of a Retaining Wall and Footing

Fig. 6.3 illustrates the general case of earth stress acting on a 'stubby' cantilever wall. The bearing capacity of the footing has to consider loads from sources not shown in the figure, such as the weight of the wall itself and the outside forces acting on the wall and the soil. The earth stress governing the structural design of the wall (P1) is determined from the product of the active earth stress coefficient (K_a) and the effective overburden stress. The calculations must consider the soil internal friction angle (ϕ), inclination of the wall (β), wall friction ($\tan \delta$), as well as sloping of the ground surface (α). When the heel of the footing and/or the ground surface are sloping, the average height (H1) is used in the calculation of the effective overburden stress used for P1, as shown in the figure. Notice, many codes postulates that the backfill soil nearest the wall stem may not relax into full active condition. These codes therefore require a larger earth stress coefficient (closer to K_0) in the calculation of the earth stress acting directly on the stem. The vertical component of the earth stress is often disregarded because including it would necessitate the corresponding reduction of the weight of the soil resting on the base.

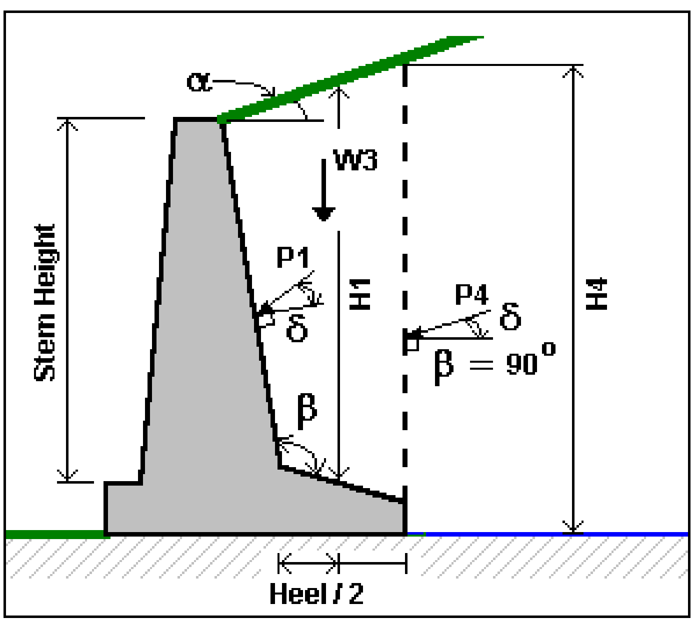

Fig. 6.3 Example of forces acting on a cantilever wall

The geotechnical design for bearing capacity and overturning requires the calculation of the resultant of all loads acting on a free body comprised by the wall and footing and the soil resting on the heel. The earth stress (P4) to include in the calculation of the force resultant the acts against the boundary of the free body, which is a normal rising from the heel, that is, its earth stress coefficient is determined from a β equal to 90°. Notice also that the height of the normal (H4) is used in determining the overburden stress applied in calculating P4.

In contrast to the case for the earth stress against the stem, the earth stress acting on the normal from the heel should be calculated disregarding wall friction in the soil (Tschebotarioff 1978).

In summary, the design for capacity of a footing consists of ensuring that the factors of safety on bearing capacity of a uniformly loaded equivalent footing and on sliding are adequate, and verifying that the edge stress is not excessive.

6.9 Numerical Example

The bearing capacity calculations are illustrated in a numerical example summarized in Fig. 6.4. The example involves a 10.0 m long and 8.0 m high, vertically and horizontally loaded retaining wall (bridge abutment). The wall is assumed to be infinitely thin so that its weight can be neglected in the calculations. It is placed on the surface of a 'natural' coarse-grained soil and a coarse material (backfill) is placed behind the wall. A 1.0 m thick fill is placed in front of the wall and over the toe area. The groundwater table lies close the ground surface at the base of the wall and the ground surface is horizontal.

In any analysis of a foundation case, a free-body diagram is necessary to ensure that all forces are accounted for in the analysis, such as shown in Fig. 6.5. Although the length of the wall is finite, it is normally advantageous to calculate the forces per unit length of the wall (the length, L, then only enters into the calculations when determining the shape factors).

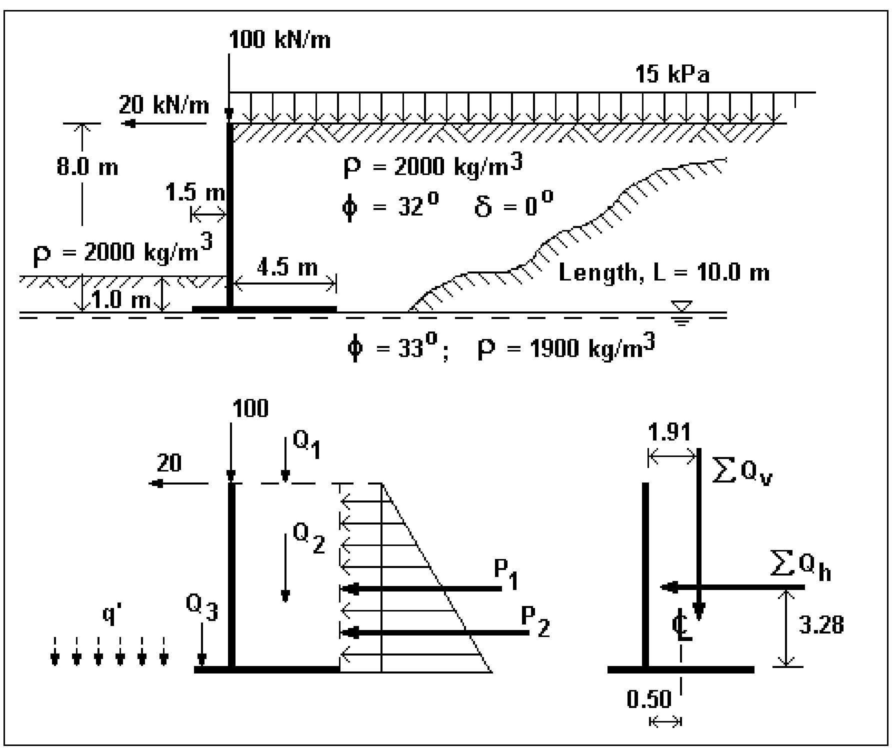

Fig. 6.4 Cantilever wall example (Fellenius, 1995)

The vertical forces denoted Q_1 and Q_2 are loads on the base (heel portion). Q_1 is from the surcharge on the ground surface calculated over a width equal to the length of the heel. Q_2 is the weight of the soil on the heel. The two horizontal forces denoted P_1 and P_2 are the active earth stress forces acting on a fictitious wall rising from the heel, which wall is the boundary of the free body. Because this fictitious wall is soil, it is commonly assumed that wall friction does not occur (Tschebotarioff, 1978).

Because of compaction of the backfill and the inherent stiffness of the stem, the earth stress coefficient to use for earth stress against the stem is larger than active pressure coefficient. This earth stress is of importance for the structural design of the stem and it is quite different from the earth stress to consider in the stability analysis of the wall.

Fig. 6.4 does not include any passive earth stress in front of the wall, because this front wall earth stress is normally neglected in practice. The design assumes that movements are large enough to develop active earth stress behind the wall, but not large enough to develop fully the passive earth stress against the front of the wall. Not just because the passive earth stress is small, but also because in many projects a more or less narrow trench for burying pipes and other conduits is often dug in front of the wall. This, of course, eliminates the passive earth stress, albeit temporarily.

Calculations by applying the above quoted equations from the Canadian Foundation Engineering Manual (CFEM 1985) result in the following.

$\phi' = 32° \implies K_a = 0.307$ $\qquad$ K_p is assumed to be zero

$\phi' = 33° \implies N_q = 26.09$ $\qquad$ $N_c = 38.64$ $\quad N_\gamma = 25.44$

$i_q = i_c = 0.69 \quad i_\gamma = 0.28$ $\qquad$ $s_q = s_c = 1.34 \quad s_\gamma = 0.80$

$e = 0.50$ m $\quad B' = 5.0$ m $\qquad$ $r_u = 603$ KPa $\quad q = 183$ KPa

` $\quad$ F_s-bearing = 3.29 $\quad$ F_s-sliding = 2.35 $\quad$ Overturning ratio = 3.76

The design calculations show that the factors of safety against bearing failure and against sliding are 3.29 and 2.35, respectively. The resultant acts at a point on the base of the footing at a distance of 0.50 m from the center, which is smaller than the limit of 1.00 m. Thus, it appears as if the footing is safe and stable and the edge stress acceptable. However, a calculation result must always be reviewed in a "*what if*" situation. That is, what if for some reason the backfill in front of the wall were to be removed? Well, this seemingly minor change results in a reduction of the calculated factor of safety to 0.90. The possibility that this fill is removed at some time during the life of the structure is real. Therefore, despite that under the given conditions for the design problem, the factor of safety for the footing is adequate, the structure may not be safe.

6.10 Words of Caution

Some words of caution**:** Footing design must emphasize settlement analysis. The bearing capacity formula approach is very approximate and should never be taken as anything beyond a simple estimate for purpose of comparing a footing design to previous designs. When concerns for capacity are at hand, the capacity analysis should include calculation using results from in-situ testing (e.g., piezocone penetrometer). Finite element analysis may serve as a very useful tool provided that a site-specific proven soil model is applied. Critical design calculations should never be let to rely solely on information from simple borehole data and N-values (SPT-test data) applied to bearing capacity formulae.

The bearing capacity formula applies best to the behavior of small model footings in dense sand. When applying load to actual, real-life footings, the formula's relevance is very much in question. Full-scale testing shows that no clear ultimate value can be obtained even at very large deformations. When critical state soil mechanics came about (Roscoe et al. 1958, advancing the concept proposed by Casagrande 1935), the reason for the model tests reaching an ultimate value became clear: model tests affect only the soil to shallow depth, where even the loosest soil behaves as an overconsolidated soil. That is, on loading the model, after some initial volume change, the soil dilates and finally contracts resulting in a stress-deformation curve that implies an ultimate resistance (e.g., Been and Jefferies 1991; Altaee and Fellenius 1994).

Fig. 6.5 presents results from loading tests performed by Ismael (1985) on square footings with sides of 0.25 m, 0.50 m, 0.75 m, and 1.00 m at a site where the soils consisted of fine sand 2.8 m above the groundwater table. The sand was compact as indicated by a N-index equal to 20 blows/0.3 m. The footings were placed at a depth of 1.0 m. The measured stress-movement behavior of the footing is shown in the left diagram. The diagram to the right shows the same data plotted as stress versus relative movement, i. e., the measured movement divided by the footing side. Notice that the curves are gently curving having no break or other indication of failure despite relative movements as large as 10 % to 15 % of the footing side.

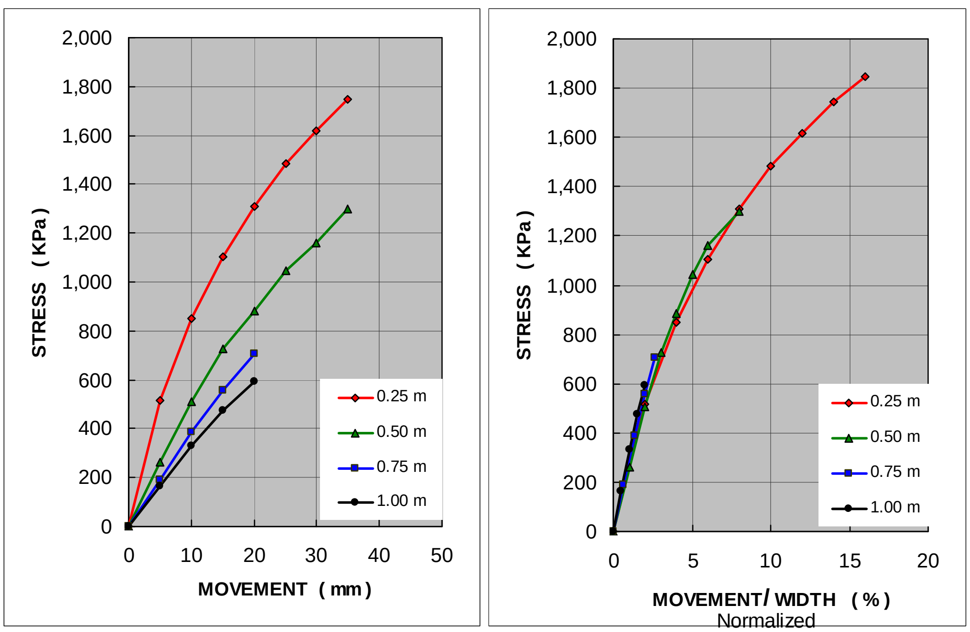

Fig. 6.5 Results of static loading tests on square footings in well graded sand (Data from Ismael, 1985)

Similar static loading tests on square footings placed at a depth of 0.8 m in sand were performed by Briaud and Gibbens (1994) in a slightly preconsolidated, silty fine sand well above the groundwater table. The natural void ratio of the sand was 0.8. The footing sides were 1.0 m, 1.5 m, 2.0 m, and 3.0 m. Two footings were of the size 3.0 m. The results of the test are presented in Fig. 6.6, which, again, shows no indication of failure despite the large relative movements.

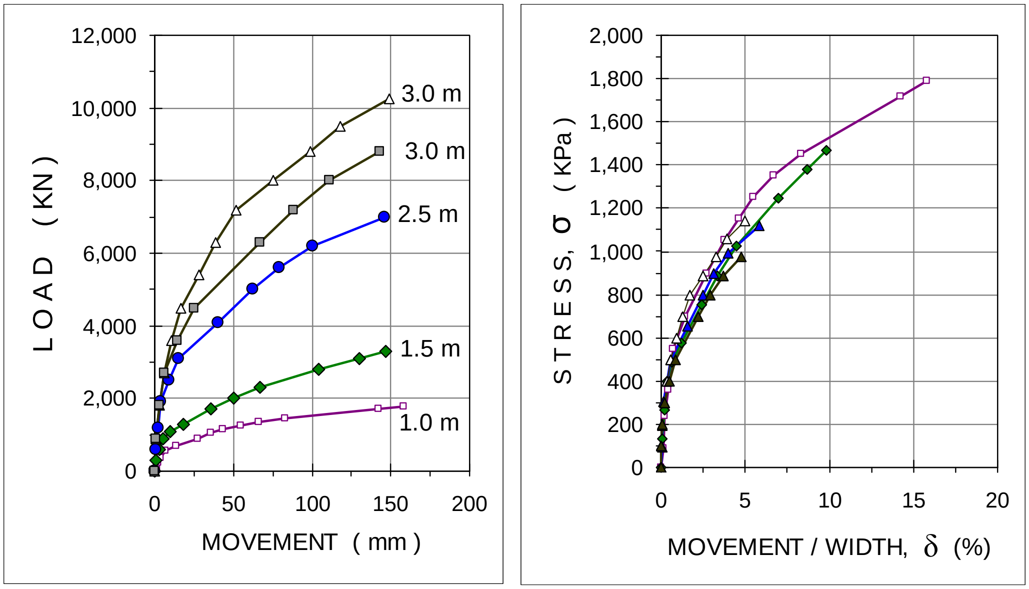

Fig. 6.6 Results of static loading tests on square footings in well graded sand
(Data from Briaud and Gibbens, 1994)

The foregoing two tests and several others available in the literature, show conclusively that bearing failure, i.e., capacity or ultimate resistance, does not exist (but for the exception of when soil pore pressures are generated by the imposed loading). The concept of capacity is a condition associated with shear failure. However, in contrast to a body sliding against a soil (footing sliding on its base or shaft resistance when a pile slides against the soil), the movement of soil body affected by the applied load is governed by deformation characteristics of the soil and the fact that the affected soil body increases for each load applied. That is, the volume of soil involved changes all through the loading, and, while there is an increasing total movement, the deformation in an individual soil element can actually diminish as the loading increases. When the basic concept for a response is wrong, simply, any interpretation of the results based on that concept are also wrong!

The fallacies of the bearing capacity formula notwithstanding, the formula is frequently applied to current foundation designs and most building codes, handbooks, and guidelines recommend its use. Therefore, applying the bearing capacity formula to routine designs is still considered within the accepted standard of care. This notwithstanding the fact that bearing capacity of a footing in a normal soil does not really exist (Fellenius 1999)! Moreover, there is a fundamental difference between the movements recorded in a loading test and the settlement of a footing for a long-term unchanging load. This should be recognized and a footing design, therefore, should be based on deformation analysis, not on capacity.

6.11 Aspects of Structural Design

Once the geometry of the structure and the geotechnical aspects of the design (such as the bearing resistance, settlement, and sliding resistance) are acceptable, the structural engineer has to ensure that the retaining structure itself is able to sustain the forces acting on each of its parts, such as the stem, the toe, and the heel.

The stem is the vertical portion of the structure supporting the horizontal components of all loads. The toe is the portion of the footing located on the "outboard side" of the retaining structure and the heel is the portion of the footing located on the "inboard side" of the retaining structure.

While the overall geometry of the structure is often dictated by the external stability of the retaining wall (active pressure), the structural design (member thickness, reinforcing steel, etc.) is based entirely on the internal stability (backfill stress).

Stem Design

The stem must be designed for shear, compression, and, most important, bending stresses. The shear forces acting on the stem are the summation of all horizontal forces acting above the top of the footing toe. In addition to shear forces, the stem must be capable of resisting compression forces. These forces can include the weight of the stem, the vertical components of the soil pressures acting along the face of the stem (inclined stem and/or wall friction exist), and other vertical forces acting directly on the stem. Bending forces acting on the stem are obtained by multiplying all shear and compression forces by their respective distances to the base of the stem. The design of the stem must consider both the loads applied during the construction stage as well as loads during service conditions. Often in the design of the stem, the effect of the passive forces will be excluded while loads are added that are induced by the compaction of the backfill on the active side of the stem.

For concrete walls, the thickness of the stem and the amount and spacing of reinforcing steel should be sized based on the interaction of the shear, compression, and bending forces.

Toe Design

The footing toe area is designed to resist the upward stresses created by the bearing layer at equilibrium condition. The design assumes that there is no deformation of the footing or the stem following installation of the backfill. It is also assumed that sliding or bearing failure will not occur. According to the Ontario Highway Bridge Design Code (OHBDC 1991), the design of the toe should consider both a uniform and a linear contact stress distribution. The design must include shear and bending forces. For concrete structures, these forces will usually dictate the amount and spacing of the bottom reinforcing steel in the footing.

Heel Design

The footing heel area is designed to resist the downward stresses caused by the fill and forces on the inboard side. The design assumes that the structure will rotate around a point located at the toe of the footing. All loads from the active side, included in the external stability design, must be included also in the bending and shear design of the heel. For concrete structures, the heel design will usually dictate the amount and spacing of upper surface reinforcing steel in the footing.

Drainage

Apart from design cases involving footings and walls designed in water, such as a sea wall, both footing and wall should be provided with drainage (pinholes, french drains, etc.) to ensure that no water can collect under the footing or behind the wall. This is particularly important in areas where freezing conditions can occur or where swelling soils exist under the footing or behind the wall. The commonly occurring tilting and cracking condition of walls along driveways etc. is not due to earth stress from weight of retained soil, but to a neglect of the frost and/or swelling conditions.

6.12 Limit States Design and Load and Resistance Factor Design

Several countries and regions are currently preparing for a forthcoming shift of the foundation design approach from the working stress design, WSD, to a Limit States Design, LSD, or a Load and Resistance

Factor Design, LRFD. New limit states codes have recently been proposed in Canada, USA, and Europe. The Canadian efforts are contained in the Ontario Highway Bridge Design Code (OHBDC 1991), published in 1994 by the Ministry of Transportation and Communication, Ontario, MTO. A further development of this code is under way by the Canadian Standards Association, CSA. The US development is led by the Federal Highway Administration, FHWA, and a report has been published by Barker et al. (1991). The American Association of State Highway and Transportation Officials, AASHTO, has a Specification that applies Limit States Design rules to structural components as well as to the geotechnical design.

The European Community, EC, has a committee working on a limit states foundation code, Eurocode, to be applied to all countries of the European Community.

The working stress approach to geotechnical design consists of establishing the soil strength and determining the allowable shear by dividing the strength with a factor of safety—“global factor of safety approach”. The particular value of the factor of safety to apply depends on the type of foundation problem as guided by experience and ranges from a low of about 1.3 applied to problems of slope stability of embankments to a high of 3 or 4 applied to bearing capacity equations, while a factor of safety value of about 2 is applied to a capacity determined in a loading test. As mentioned, the capacity expressed by the bearing capacity equation does not just depend on soil strength values (cohesion and friction), other aspects are also included in the equation.

Often, the global factor to apply is an empirically determined function of the type of load—dead or live, common or exceptional. Initially, practice was to let those distinctions be taken care of by applying coefficients to the load values. From this basis, starting in Europe some years ago, a full “partial factor of safety approach” has grown, in which each component, load as well as resistance, is assigned its own uncertainty and importance. The design requirement is that the sum of factored loads must not exceed the sum of factored resistances.

The partial factor of safety approach combines load factors, which increase the values of the various loads on a structure and its components, with resistance factors, which reduce the ultimate resistance or strength of the resisting components. This design approach is called Ultimate Limit States, ULS, or Load and Resistance Factor Design, LRFD.

Initially, geotechnical engineers were rather unwilling to consider changing to a ULS design approach as it applies to soils and foundations. However, in 1983, a committee formed by the Ontario Ministry of Transportation, MTO, produced a limit states design code for foundations of bridges and substructures. The 1983 Code very closely adopted the Danish system of partial factors of safety, where all factors are larger than or equal to unity (loads and other ‘undesirable’ effects are multiplied and resistances and other ‘beneficial’ effects, are divided by the respective factors). In the 1983 Canadian version, all factors were multipliers and the resistance factors were smaller than unity. Because the load factors were essentially already determined (the same values as applied to the superstructure were used), the code committee was left with determining what values to assign to the resistance factors. Notice the importance distinction that these resistance factors are applied to the soil strength, only.

Soil strength in classical soil mechanics is governed by cohesion, c, and friction, $\tan\phi$. After some comparison calculations between the final design according to the WSD and ULS approaches, a process known as ‘calibration’, the committee adopted the reductions used in the Danish Code of applying resistance factors to cohesion and friction of 0.5 and 0.8, respectively. However, the calibration calculations showed considerable differences in the design end product between the ‘old’ and the ‘new’. A ‘fudge’ factor was therefore developed called “resistance modification factor” to improve the calibration agreement. The idea was that once a calibration was established, the presumed benefits of the ULS approach as opposed to the WSD approach would let the profession advance the state-of-the-art. Such advancement was apparently not considered to be possible within the 'old' system. Details of the LSD approach used in the MTO 1983 Code are presented in the 2nd edition of the Canadian Foundation Engineering Manual (CFEM 1985).

Very soon after implementation of the 1983 Code, the industry voiced considerable criticism against the new approach, claiming that designs according to the WSD and the ULS agreed poorly in many projects, in particular for more complicated design situations, such as certain high retaining walls and large pile groups. It is the author's impression that many in the industry, to overcome the difficulties, continued to design the most common and simple cases according to the WSD method and, thereafter, resorting to a one-to-one calibration, determined what the ULS values should be in the individual cases! Hardly a situation inspiring confidence in the new code.

The root to the difficulty in establishing a transition from the WSD to the ULS lies in the strict application of fixed values of the strength factors to fit all foundation cases, ignoring the existing practice of adjusting the factor-of-safety to the specific type of foundation problem and method of analysis. It soon became very obvious that the to-all-cases-applicable-one-value-resistance-modification-factor approach is not workable. For the same reason, neither is the partial-factor-of-safety approach (favored in the draft European code).

In 1988, the Ministry decided to revise the Code. A foundation code committee reviewed the experience thus far and came to the conclusion that the partial-factor-of-safety approach with fixed values on cohesion and friction should be abandoned. Of course, the Code could not be returned to the WSD approach, nor would this be desirable. Instead, it was decided to apply resistance factors to the ultimate resistance of a foundation rather than to the soil strength and to differentiate between types of foundations and methods of determining the capacity of the foundation. In 1992, it was decided that the MTO Ontario code should be further developed into a national code on foundations under the auspices of the Canadian Standards Association, CSA, which work resulted in the National Standard of Canada, Canadian Highway Bridge Design Code, CAN/CSA-S6-06.

The 1991 Code specifies numerous loads and load factors, such as permanent (dead), transient (live), and exceptional loads**;** making differences between loads due to weight of building materials, earth stress, earth fill, wind, earthquake, collision, stream flow, etc., with consideration given to the effect of various load combinations, and providing minimum and maximum ranges for the load factors. The factors combine and it is not easy to come up with an estimated average factor**;** the average value for a typical design appears to hover around 1.25 on dead load and 1.40 on live load. The unit weights of the soil backfill material, such as sandy soil, rock fill, and glacial till, are all given with values that assume that they are fully saturated. Because most backfills are drained, this is an assumption on the safe side.

Independently of the MTO, a US Committee working on a contract from the US Federal Highway Administration, FHWA, developed a limit states design manual for bridge foundations (Barker et al., 1991) employing the same approach as that used by the MTO second committee. (Because the Eurocode has stayed with the partial factor-of-safety approach, there exists now a fundamental difference between the Eurocode and the Canadian and US approaches).

The Load and Resistance Factor Design as well as the Ultimate Limit states design for footings have one major thing in common with the Working Stress Design of old. All presume that bearing capacity is a reality and that it can be quantified and therefore be assigned a safety factor (partial factor or resistance factor, as the case may be). This is a fallacy, because, while bearing capacity exists as a concept, it does not exist in reality. What matters to a structure founded on the footing is the movement that the structure can accept and what movement that results from the load applied to the footing. The objective of a design is that the former be larger than the latter. This notwithstanding that in the special case of a footing in clay subjected to rapid loading, bearing capacity failure may occur. Thie latter is a situation where pore pressure dissipation is an issue and it may affect the design of silos and storage tanks. Simple bearing capacity analysis of such cases can then be stated to model the soil response. However, the behavior is complex and a design based on 'simple' bearing capacity calculation is not satisfactory.

Deformation of the structure and its components is determined in an unfactored analysis (all factors are equal to unity) and the resulting values are compared to what reasonably can be accepted without impairing the use of the structure, that is, its serviceability. This design approach is called Serviceability Limit States, SLS. e.g., the Canadian Highway Bridge Design Code, CAN/CSA-S6-06. Indeed, for footings, the serviceability approach, i.e., settlement and movement calculation is the only approach that has a rational base.

6.13 A brief history of the Factor of Safety, F_S

The concept of Factor of safety, F_S, was introduced to geotechnical engineering about 100 years ago. Of old, people designed for expected settlement and tests, and full-scale were very few, and when performed, the test were intended to tell the expected amount of settlement. The concept of capacity was introduced in 1893, when Wellington presented the Engineering News formula that proposed a ratio between the intended load and the pile capacity, that is, the factor of safety, F_S. About Year 1900, Swedish pioneers, Hjalmar Granholm and Ernst Wendel, published results of static loading tests on piles in clay and discussed the ratio between the intended load and the pile capacity, the F_S. At that time, however, the response of other foundations, such as footings, was still considered in terms of expected settlement, and thre was no theoretical calculation of capacity of footings.

In the 1910s, Wolmar Fellenius completed slope stability analysis to incorporate cohesive and friction strengths simultaneously and brought forward the F_S-concept as a ratio between induced rotating moment to the rotating moment that would fail the embankment. Less known is that he also developed a calculation method for bearing capacity of footings based on the same circular/cylindrical rotation analysis applying a factor of safety on the shear strength (W. Fellenius 1926). In 1943, Terzaghi presented his bearing capacity theory and applied a F_S-factor as a ratio between the applied load and the calculated bearing capacity. Since then, everybody uses the F_S-concept and settlement analysis is not common — many assume that, if the factor of safety is good, settlement will not be of concern for the foundation.

Yet, settlement is the governing aspect of a foundation design. Note, in contrast to the case of the old days, we have now know how to do a settlement analysis and do not need to continue relying on a quasi F_S-approach on capacity. Besides, the bearing capacity theory for footings is totally wrong (Section 6.10). And, while we can determine — by some definition — the bearing capacity of a pile, again, it is the settlement of the pile that governs and that settlement is a result more from what occurs around the pile than the load applied to the pile.

With regard to piled foundations, while foundations on single piles or just a few piles need to satisfy a F_S criterion, this is not necessarily so for groups of piles. Piled foundations on groups of piles need primarily to be designed for settlement. On occasions, the piles are not even connected to the foundation structure (Section 7.5) and, therefore, pile capacity and F_S is not an issue, but settlement is. It is time to return to the design principles of old.

CHAPTER 7

STATIC ANALYSIS OF PILE LOAD-TRANSFER

7.1 Introduction

Where designing on shallow foundations would mean unacceptable settlement, or where scour and other environmental risks exist which could impair the structure in the future, deep foundations are used. Deep foundations usually consist of piles, that is, structural units installed by driving or by in-situ construction methods, to competent soils through soft compressible soil layers. Piles can be made of wood, concrete, or steel, or of composite materials, such as concrete-filled steel pipes or an upper concrete section connected to a lower steel or wood section. They can be round, square, hexagonal, octagonal, even triangular in shape, and straight-shafted, step-tapered, or conical. They can be short or long, or slender or stubby. In order to arrive at a reliable design, all the particulars of the pile, including the method of construction, must be considered together with the soil data and desired function of the pile.

Design of a pile foundation for axial load starts with an analysis of how the load is transferred to the soil, often thought limited to determining only the pile capacity, sometimes separating the capacity on components of shaft and toe resistances. However, the load-transfer is also the basis for a settlement analysis, because in contrast to the design of shallow foundations, settlement analysis of piles cannot be separated from a load-transfer analysis. The load-transfer analysis is often called static analysis or capacity analysis. Total-stress analysis using undrained shear strength (so-called α-method) has very limited application, because the load transfer between a pile and the soil is governed by effective stress behavior (i.e., the pile resistance is proportional to the effective overburden stress). Therefore, an effective stress analysis (also called β-method) is the preferred method. Sometimes, the β-method includes an adhesion (effective cohesion intercept) component. The adhesion component is normally not applicable to driven piles, but may be useful for bored piles ("cast-in-situ piles", "drilled-shafts", "caissons", "augercasts", etc. — "t'is a sweet child that has many names"). The total stress and effective stress approaches refer to both shaft and toe resistances, although the equivalent terms, "α- and β-methods", usually refer to shaft resistance, specifically.

7.2 Static Analysis

Shaft Resistance

The general numerical relation for the ultimate unit shaft resistance, r_s, is

(7.1a) $$r_s = c' + \beta\sigma'_z$$

where
c' = effective cohesion intercept
β = Bjerrum-Burland coefficient
σ'_z = effective overburden stress

The adhesion component, c', is normally set to zero for driven piles and Eq. 7.1a then expresses that unit shaft resistance is directly proportional to the effective overburden stress.

The accumulated (total) shaft resistance from Depth 0 through Depth z is

(7.1b) $$R_s = \int A_s r_s dz = \int A_s (c' + \beta \sigma'_z) dz$$

where R_s = total shaft resistance
A_s = circumferential area of the pile at Depth z
(i.e., surface area over a unit length of the pile)

The beta-coefficient varies with soil gradation, mineralogical composition, density, depositional history (genesis), and soil strength. Table 7.1 shows what approximate range of values to expect from basic soil types. The values are derived from pile tests in mechanically weathered, inorganic, alluvially transported and deposited soils. In particular, highly overconsolidated soils, or soils with organics (e.g. “muck”), residual soils, calcareous soils, micaceous soils, and many others may — nay, will — exhibit different ranges of β-coefficients. Fellenius (2008) has compiled β-coefficients from different case histories.

TABLE 7.1
Approximate Ranges of Beta-coefficients

SOIL TYPE	Phi	Beta
Clay	25 - 30	0.15 - 0.35
Silt	28 - 34	0.25 - 0.50
Sand	32 - 40	0.30 - 0.90
Gravel	35 - 45	0.35 - 0.80

The beta-coefficients can deviate significantly from the values shown in Table 7.1. For example, Rollins et al. 2005) performed uplift static loading tests and determined beta-coefficients at ultimate resistance as shown in Fig. 7.1.

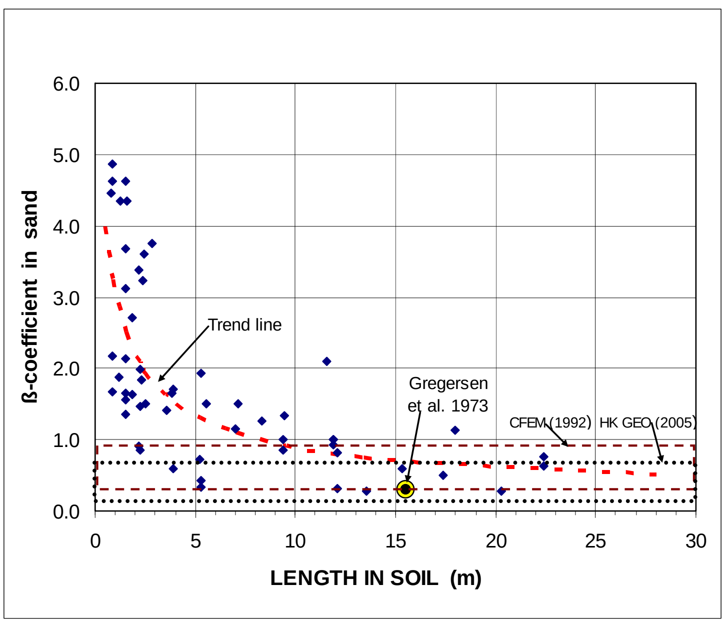

Fig. 7.1. Beta-coefficient versus embedment length for piles in sand. (Data from Rollins et al. 2005) with ranges suggested by CFEM (1993), Gregersen et al 1973, and Hong Kong Geo (2006).

Clausen et al. (2005) proposed beta-coefficients for different types (material) of piles as shown in Fig. 7.2, and, for piles in clay, coefficients versus plasticity index, as shown in Fig. 7.3.

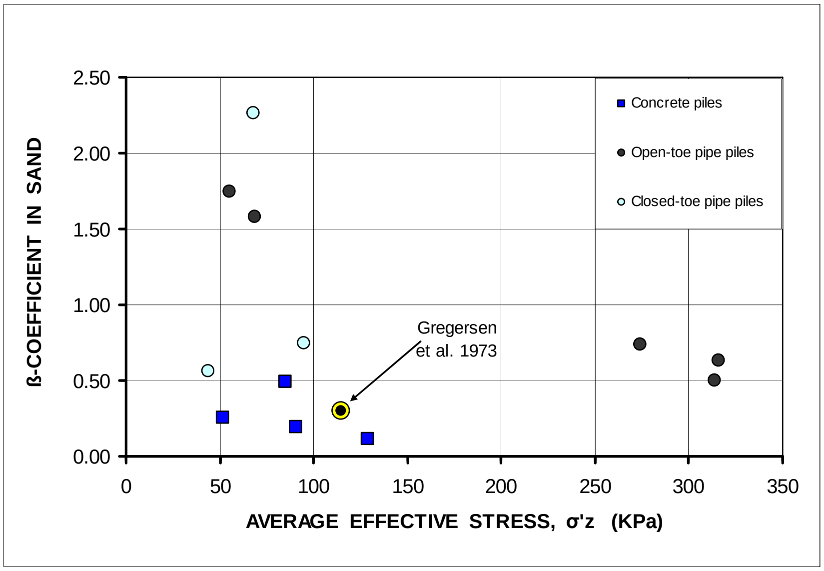

Fig. 7.2 Beta-coefficient versus average effective stress. (Data from Clausen et al. 2005).

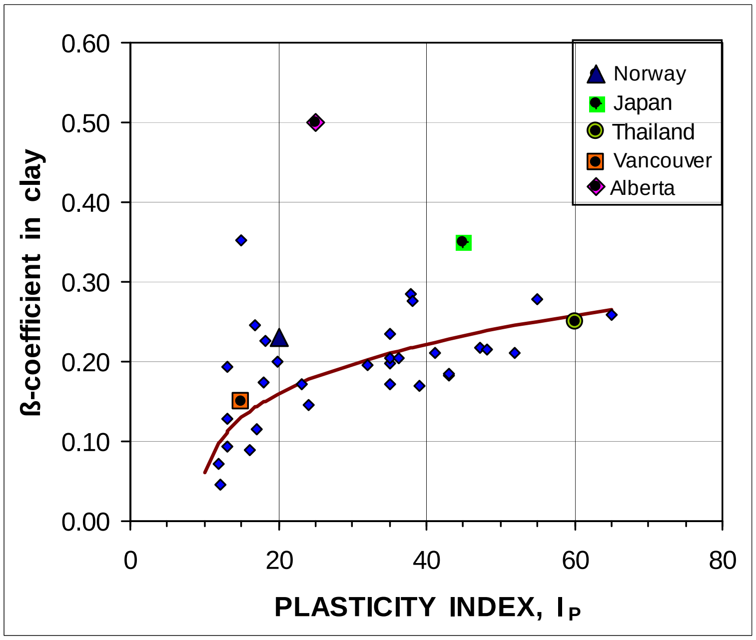

Fig. 7.3 Beta-coefficient for pile sin clay versus plasticity index, I_P. (Data from Clausen et al. 2005 with results from five cases added. Fellenius 2006).

Available analysis results from measurements of distribution of shaft resistance indicate unquestionably that the unit shaft resistance increases more or less linearly with depth. That is, effective stress governs the unit shaft resistance. The actual proportionality coefficient, the ß-coefficient, can obviously vary within rather large ranges and depends on not just grain size distribution, but also on mineral composition, overconsolidation ratio, whether sedimentary or weathered residual soil, etc.

To mobilize the ultimate pile shaft resistance requires very small relative movement between the pile and the soil. In inorganic soils, about 90 % of the shear resistance is usually mobilized at a relative movement of one millimetre and less. In a static loading test, for example, the movement observed for the pile head before any significant toe movement is obtained from compression ('elastic' shortening) of the pile for the imposed load.

The direction of the movement has no effect on the load-movement for the shaft resistance. That is, push or pull, positive or negative, the maximum shear stress is the same. Moreover, the movement necessary for full mobilization of the shaft resistance is independent of the diameter of the pile.

Toe Resistance

Also the ultimate unit toe resistance is considered proportional to the effective stress, i.e., the effective stress at the pile toe. Based on this premise, the unit toe resistance is:

(7.2a) $$r_t = N_t \, \sigma'_{z=D}$$

where
r_t = unit toe resistance
N_t = toe bearing capacity coefficient
D = embedment depth
$\sigma'_{z=D}$ = effective overburden stress at the pile toe

The total toe resistance is

(7.2b) $$R_t = A_t r_t = A_t \, N_t \, \sigma'_{z=D}$$

where
R_t = total toe resistance
A_t = toe area (normally, the cross sectional area of the pile)

Also the toe-coefficient, N_t, varies widely. Table 7.2 shows an approximate range of values for the four basic soil types. These values are typical of those determined in a static loading test to “failure” (see Chapter 7), which usually occurs at a pile head movement of 30 mm to 80 mm. At this pile head movement, the pile toe has normally been pushed down no more than about 10± mm, sometimes not at all and only rarely more.

TABLE 7.2
Approximate Range of N_t-coefficients

SOIL TYPE	Phi	N_t
Clay	25 - 30	3 - 30
Silt	28 - 34	20 - 40
Sand	32 - 40	30 - 150
Gravel	35 - 45	60 - 300

The value of the toe proportionality coefficient is sometimes stated to be of some relation to the conventional bearing capacity coefficient, N_q, but the validity of any such relation is not true. The truth is that neither the N_q-coefficient for a footing (See Chapter 6) nor the N_t-coefficient correctly represent the pile toe behavior for an imposed load. As discussed by Fellenius (1999), the concept of bearing capacity does not apply to a pile toe. Instead, the pile toe load-movement is a function of the stiffness (compressibility) of the soil below the pile toe in combination with the effective overburden stress in a relation called q-z curve (See Section 7.10). Even for piles tested to ultimate resistance (see Chapter 8), the value represented by the N_t-coefficient corresponds to the resistance at a toe movement of, usually, no more than about 5 mm to 12 mm from the start of the test. Indeed, toe resistance does not exhibit an ultimate value but continues to increase with increasing toe movement.

Ultimate Resistance (Capacity)

The capacity of the pile, Q_{ult}, (alternatively written R_{ult}) is the sum of the shaft and toe resistances[1)].

(7.3) $$Q_{ult} = R_s + R_t$$

When the shaft and toe resistances are fully mobilized, the load in pile, Q_z (as in the case of a static loading test brought to 'failure') is

(7.4) $$Q_z = Q_u - \int A_s \beta \sigma'_z \, dz = Q_u - R_s$$

Eq. 7.4 shows the load and resistance distribution curve calculated from Eqs. 7.3 and 7.4. As is obvious from the equation, at the depth z = D, i.e. depth to the pile toe, $Q_z = R_t$.

During service conditions, loads from the structure will be applied to the pile head via a pile cap. The loads are normally permanent (or 'dead' or "sustained") loads, Q_{dead}, and transient (or 'live') loads Q_{live}. Not generally recognized is that even if soil settlements are small, even when too small to be noticeable, the soil will in the majority of cases, move down in relation to the pile and in the process transfer load to the pile by negative skin friction. (An exception is a pile in swelling soils and the exception is limited to the length of pile in the swelling zone, where then 'positive skin friction' develops). Already the small relative movements always occurring between a pile shaft and the soil are sufficient to develop significant negative skin friction (as well as positive skin friction, and positive and negative shaft resistances—the separation of the terms signifies whether the shear is introduced by the soil or by outside forces). Therefore, every pile develops an equilibrium of forces between, on the one side, the sum of dead load applied to the pile head, Q_d, and drag load, Q_n, induced by negative skin friction in the upper part of the pile, and, on the other side, the sum of positive shaft resistance and toe resistance in the lower part of the pile. The point of force equilibrium, called the neutral plane, is the depth where the shear stress along the pile changes over from negative skin friction into positive shaft resistance. This is also where there is no relative displacement between the pile and the soil, that is, the depth to "settlement equilibrium".

The key aspect of the foregoing is that the development of a neutral plane and drag load due to negative skin friction is an always occurring phenomenon in piles and not limited to where large soil settlement

[1)] Notice, the commonly used term "ultimate capacity' is a misnomer: a tautology. The term is a mix of the synonym terms "ultimate resistance" and "capacity". Although one cannot be mistaken of the meaning of "ultimate capacity", the adjective should not be used, because it makes the use of other adjectives seem proper, such as "load capacity", "allowable capacity", "design capacity", "working capacity", "carrying capacity", which are at best awkward and at worst misleading, because what is meant is not clear. Sometimes, even the person modifying "capacity" with these adjectives is unsure of the meaning. The only modifiers to use with the term "capacity" are "long-term capacity" as opposed to "short-term capacity", "axial capacity" as opposed to "lateral capacity", and "bearing capacity" or "geotechnical capacity" as opposed to "structural strength" (the term "structural capacity" is awkward and best avoided).

occurs around the piles. Numerous well-documented case histories testify to the veracity of the underlined statement (Fellenius 2004).

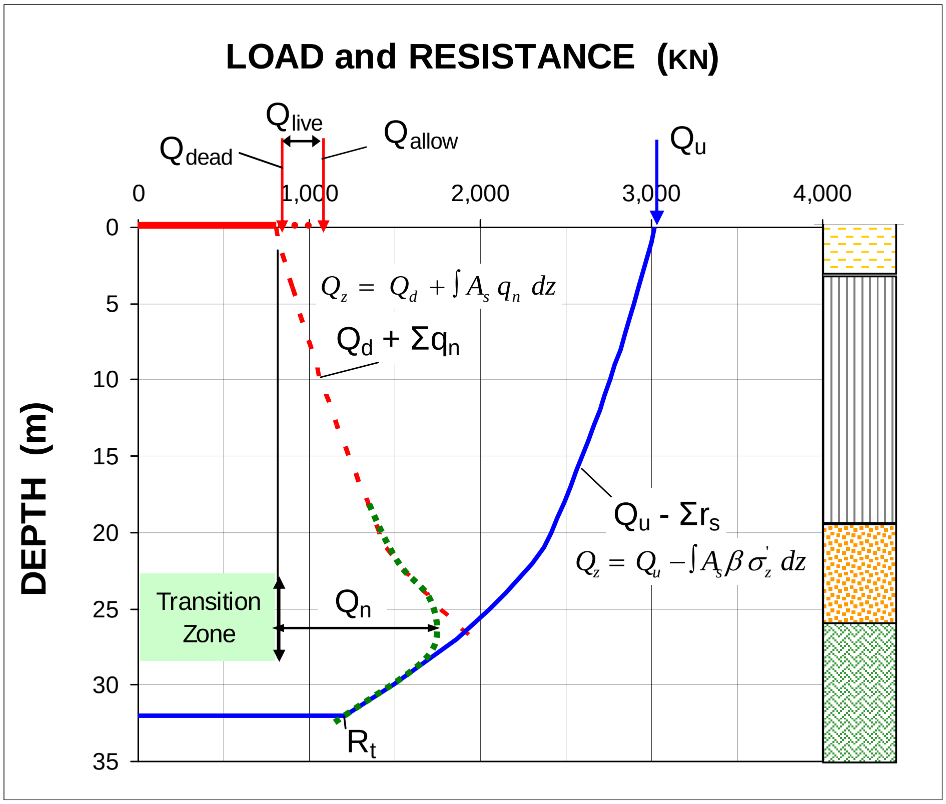

Fig. 7.4 Load-Transfer and Resistance Curves

For piles designed with a normal margin against failure (e.g., Factor-of-Safety on the capacity), the neutral plane lies below the mid-point of a pile. The extreme case is for a pile bearing on bedrock, where the location of the neutral plane is at the pile toe, at the bedrock elevation. For a lightly loaded, dominantly shaft-bearing pile 'floating' in a homogeneous soil with linearly increasing shear resistance, the neutral plane lies at a depth which is about equal to the lower third point of the pile embedment length[2)]. See also comments on “Piled Raft Design”, below.

The larger the toe resistance, the deeper lies the neutral plane. And, the larger the dead load, the shallower the neutral plane.

The load distribution in the pile during long-term conditions down to the neutral plane is given by the following load-transfer relation (below the neutral plane, Q_z follows Eq. 7.4).

(7.5) $$Q_z = Q_d + \int A_s\, q_n\, dz = Q_d - Q_n$$

[2)] This is the basis for the "Terzaghi-Peck" rule of calculating the settlement of a pile group consisting of shaft bearing piles in uniform soil as the settlement for an equivalent raft placed at the lower third point.

where Q_d = dead load on the pile
Q_n = drag load at the neutral plane
A_s = circumferential pile area
q_n = unit negative skin friction; $q_n = r_s = \beta\,\sigma'_z$

The transition between the resistance curve (Eq. 7.4) and the load-transfer curve (Eq. 7.5) is in reality not the sudden kink the equations suggest, but a smooth transition from fully developed negative skin friction to fully developed positive shaft resistance occurring over some length of pile above and below the neutral plane, as shown in Fig. 7.4. The length of the this transition zone varies with the type of soil and the rate or gradient of the relative movement between the pile and the soil at the neutral plane. Its length can be estimated to be the length over which the relative movement between the pile and the soil is smaller than about 2 mm to 5 mm. Thus, the theoretically calculated value of the maximum load in the pile is higher than the real value and it is easy to overestimate the magnitude of the drag load and, therefore, the maximum load in the pile. Notice, also, that the calculations are interactive inasmuch that a change of the value of the dead load applied to a pile will change the location of the neutral plane and the magnitude of the maximum load in the pile.

7.3 Example

The analysis is illustrated in the following example**:** A pile group (twenty-five 355-mm pipe piles) is to be installed at a site where the soil profile consists of an upper layer of silt deposited on soft clay followed by silty sand on glacial till. A 1.5 m thick earth fill will be placed symmetrically over 36 m square area around the pile group. (The soil profile — final condition — is detailed in Chapter 1, Table 1.1). The pile cap is 9.0 m square and placed level with the ground surface. Each pile will be subjected to dead and live loads of 800 KN and 200 KN, respectively.

The design begins with a load-transfer analysis, which is best performed using a range (boundary values) of β and N_t-parameters that provide upper and lower limits of reasonable values. The particular range of values of soil parameters necessary for the calculations has been established in a soils investigation. The parameters are density, compressibility, consolidation coefficient, as well as the parameters (β and N_t) used in the effective stress calculations of load transfer. The analysis includes several steps in approximately the following order.

Determine first the range of installation length (using the range of effective stress parameters) as based on the required at-least capacity, which is stated, say, to be at least equal to the sum of the loads times a Factor-of-Safety, say 3.0, times the total load on the pile**:** 3.0 (800 + 200) = 3,000 KN. Thus, to achieve a capacity of 3,000 KN when applying the lower boundary values of β and N_t, the piles have to be installed to a penetration into the sandy till layer of 5 m, i.e., to a depth of 32 m.

Table 7.3 presents the results of the load-transfer calculations for this embedment depth. The calculations have been made with the UniPile program (Goudreault and Fellenius 2006) and the results are presented in the format of a spread-sheet “hand calculation” to simplify verifying the computer calculations. The precision indicated by that the stress values are given with two decimals is to assist in the verification and does not suggest a corresponding level of accuracy. Moreover, the effect of the 9 m square “hole” in the fill for the pile cap was ignored in the calculation. Were its effect to be included in the calculations, the calculated capacity would reduce by 93 KN or the required embedment length increase by 0.35 m.

TABLE 7.3
CALCULATION OF PILE CAPACITY [Calculations by means of UniPile]

Area, A_s = 1.115 m^2/m	Live Load, Q_l = 200 KN	Shaft Resistance, R_s =	1,817 KN
Area, A_t = 0.099 m^2	Dead Load, Q_d = 800 KN	Toe Resistance, R_t =	1,205 KN
	Total Load = 1,000 KN	Total Resistance, R_u =	3,021 KN
F_S = 3.02	Depth to N. P. = 26.51 m	Load at N. P., Q_{max} =	1,911 KN

DEPTH (m)	TOTAL STRESS (KPa)	PORE PRES. (KPa)	EFFECTIVE STRESS (KPa)	INCR. R_s (KN)	Q_d+Q_n (KN)	Q_U-R_S (KN)
LAYER 1 Sandy Silt			**ρ = 2,000 kg/m³**	**β = 0.40**		
0.00	30.00	0.00	30.00	0.0	800	3021
1.00(GWT)	48.40	0.00	48.40	17.5	817	3004
4.00	104.30	30.00	74.30	82.1	900	2922
LAYER 2 Soft Clay			**ρ = 1,700 kg/m³**	**β = 0.30**		
4.00	104.30	30.00	74.30		900	2922
5.00	120.13	43.53	76.60	25.2	925	2896
6.00	136.04	57.06	78.98	26.0	951	2870
7.00	152.03	70.59	81.44	26.8	978	2844
8.00	168.08	84.12	83.96	27.7	1005	2816
9.00	184.20	97.65	86.55	28.5	1034	2787
10.00	200.37	111.18	89.20	29.4	1063	2758
11.00	216.60	124.71	91.89	30.3	1094	2728
12.00	232.88	138.24	94.64	31.2	1125	2697
13.00	249.19	151.76	97.43	32.1	1157	2664
14.00	265.55	165.29	100.26	33.1	1190	2631
15.00	281.95	178.82	103.12	34.0	1224	2597
16.00	298.38	192.35	106.03	35.0	1259	2562
17.00	314.84	205.88	108.96	36.0	1295	2526
18.00	331.33	219.41	111.92	37.0	1332	2489
19.00	347.85	232.94	114.91	37.9	1370	2451
20.00	364.40	246.47	117.93	39.0	1409	2413
21.00	380.97	260.00	120.97	40.0	1449	2373
LAYER 3 Silty sand			**ρ = 2,100 kg/m³**	**β = 0.50**		
21.00	380.97	260.00	120.97		1449	2373
22.00	401.56	270.00	131.56	70.4	1519	2302
23.00	422.17	280.00	142.17	76.3	1596	2226
24.00	442.80	290.00	152.80	82.2	1678	2144
25.00	463.45	300.00	163.45	88.2	1766	2055
26.00	484.11	310.00	174.11	94.1	1860	1961
27.00	504.80	320.00	184.80	100.1	1960	1861
LAYER 4 Ablation Till			**ρ = 2,200 kg/m³**	**β = 0.55**		
27.00	504.80	320.00	184.80		1960	1861
30.00	569.93	350.00	219.93	372.4	2332	1489
32.00	613.41	370.00	243.41	285.1	2617	1205
						N_t = 50

The calculated load and resistance distributions for the example pile according to Eqs. 7.4 and 7.5 are given in the two rightmost columns in Table 7.3. The values have been plotted in Fig. 7.4 (above) in the form of two curves**:** a resistance curve and a load-transfer curve. The resistance curve starts at the capacity of 3,000 KN (as obtained in a static loading test to failure) and decreases with depth due to the shaft resistance. The value plotted at the pile toe is the toe resistance. The load-transfer curve represents the long-term conditions at a site. As shown in the diagram, it starts at the dead load of 800 KN and increases due to negative skin friction to a maximum at the neutral plane, where the two curves intersect. Note, the shown load-transfer curve represents the **extreme case of a relative movement** between the pile(s) and the soil, a movement that is large enough to fully mobilize the shaft shear, resulting in a transfer zone of a minimal length, as well as including a toe movement that is large enough to mobilize a large toe resistance. That is, the load-transfer curve assumes that the movement of the pile toe into the soil is about equal to that found in a static loading test to "failure".

The piles have reached well into the sand layers, which will not compress much for the increase of effective stress due to the pile loads and the earth fill. Therefore, the settlement of the pile group will be minimal and does not govern the design. Settlement analysis will be discussed in Section 7.15.

7.4 Critical Depth

Many texts suggest the existence of a so-called 'critical depth' below which the shaft and toe resistances would be constant and independent of the increasing effective stress. This concept is a fallacy and based on incorrect interpretation of test data and should not be applied. Fellenius and Altaee (1995) present a discussion on the "Critical Depth" and the reasons for how such an erroneous concept could come about. (Note some authors have borrowed the term when addressing the distribution of unit shaft resistance along very long offshore piles, where the resistance at depth in a homogeneous soil can start to decrease, but that is not the generally understood use of the term).

7.5 Piled Raft and Piled Pad Foundations

Every design of a piled foundation postulates a stable long term situation. "Stable" means that the foundation has reached an equilibrium state with the location of the neutral plane established and when more or less all settlement has developed. For a conventional piled foundation design, i.e., a pile cap cast on the piles, the neutral plane lies well down in the soil. This means that there is no physical contact between the underside of the pile cap and the soil immediately below the pile cap, or, at least, there is no load transfer to the soil from the pile cap (i.e., no contact stress). Therefore, a conventional design for service conditions must not include any benefit from the pile cap transferring loads directly onto the soil through contact stress. A design considering contact stress is not a conventional design, it is a design for a piled raft.

A **piled raft** is a foundation supported on piles that have a factor of safety of unity or smaller, which places the neutral plane at the underside of the pile cap—the raft. Such designs emphasize the settlement behavior of the foundation (discussed below). Note, the neutral plane is the location of the force equilibrium and of the settlement equilibrium. Both are affected by the magnitude of the toe resistance, which is a function of the load-movement response of the pile toe with the movement governed by the soil settlement at the neutral plane, and both are located at the same depth.

The emphasis of the design for a piled raft lies on ensuring that the contact stress is uniformly distributed across the raft. The contact stress is the effect of the load on the raft that is not supported by the piles. This means that contact stress only develops if the piles support less than the full load ($F_s \leq 1.0$)[3].

The piled-raft design intends for the piles to serve both as soil reinforcing (stiffening) elements reducing settlements and as units for receiving unavoidable concentrated loads on the raft. This condition governs the distribution across the raft of the number and spacing of the piles.

The design of a piled raft first decides on the depth of the piles and stiffness of the piles plus soil (governs the average spacing and lower boundary number of piles) necessary for reinforcing the soil so that the settlement of the raft is at or below the acceptable level. This analysis includes all loads to be supported by the raft and embraces a check that the number of piles assumed involved will be assigned an average load larger than the capacity of the average pile, i.e., the average F_s is equal to or smaller than unity. Thereafter, a uniform, lower-bound magnitude, design contact stress is chosen, and the design verifies that the piles do not have an average factor of safety larger than unity for that lower-bound contact stress. Unavoidably, the raft will have concentrations of load, however. Wherever this occurs, the portion of the load that causes a stress larger than the chosen design contact stress is supported on additional piles at number, spacing, and depth governed by the surplus (or "overload") portion. An iterative procedure of these steps may be required. The design of the raft itself needs to include margins for the possibility that the contact stress is larger than estimated and, also, that the pile loads will be larger than estimated. Where the loading conditions include large and unevenly distributed live loads, a piled raft foundation may be less suitable.

A **piled pad** foundation is similar to a piled raft foundation[4)]. However, the piles are not connected to the raft, as a pad of compacted coarse-grained fill is placed around the pile heads and above. The foundation is then a conventional footing cast on the compacted fill above the pile-reinforced soil.

With regard to the soil response to vertical loads of the foundation, the difference between the types is small (though the structural design of the concrete footing and the concrete cap will be different). For both the piled raft and the piled pad foundations, the piles are designed to a factor of safety of unity or smaller. For in particular the piled raft foundation, a factor of safety larger than unity on the pile capacity may result in undesirable stress concentrations. The main difference between the raft and the pad approaches lies with regard to the response of the foundations to horizontal loading and seismic events.

The piles for a piled raft foundation (similarly to the piles for a conventional piled foundation) are connected through the raft and this will minimize the effect of any lateral spreading due to the contact stress. Resistance to horizontal loading by a piled raft foundation is obtained by means of pile response to horizontal load. A piled pad foundation provides little resistance to either lateral spreading or horizontal loads. The potential of lateral soil-spreading under the foundation can be offset by having the pile group area larger than the area (footprint) of the footing on the pad, incorporating horizontal soil reinforcement in the pad, minimizing the lateral spreading by incorporating vertical drains (wick drains, see Chapter 4) to suitable depths, etc. A main advantage for the piled pad foundation is claimed to lie in that the pad can provide a beneficial cushioning effect during a seismic event.

---

[3] Of course, the transition from no contact stress to contact stress is not sudden at a $f_s = 1.0$, but gradual. Some contact stress will exist even in the presence of $F_s = 1.1$, say, and some may not be significant even at a f_s calculated to be smaller than 1.0. Capacity is not a singular value for a pile and, therefore, neither is the factor of safety value.

[4)] The foundation type is also called "column-supported embankment foundation, "inclusion pile foundation", and "disconnected footing concept"; none of which is a good term.

Perhaps the largest difference between the piled raft and piled pad foundation, as opposed to a conventional piled foundation lies in that the former are soil improvement methods to be analyzed from the view of deformation (vertical and horizontal), whereas the conventional foundation also needs to be analyzed from a bearing capacity view with due application of factor-of-safety to the pile capacity.

For settlement response, both foundations can be analyzed as a block (within the pile depths) having a compressibility obtained from proportioning the modulus of the soil and the pile to the respective cross section areas.

A conventional piled foundation is used to support all kinds of structures, whereas piled raft foundations are thought best for supporting structures with large footprint (large floor area), such as buildings as opposed to pile bents, and bridge piers, for example. However, a piled raft or a piled pad can equally well be used to support small footprint structures.

Piled raft foundations have been used since many years. The piled pad foundations may appear to be new, but its principle is also an old technique. In Scandinavia, piles have since long been used to support road embankments without being connected to any structural element. A recent modern application of a piled pad foundation is the foundations for the Rion-Antirion bridge piers (Pecker 2004). Another is the foundations of the piers supporting the Golden Ears Bridge in Vancouver, BC, illustrated in Fig. 7.5 (Sampaco et al. 2008). The piles consist of 350 mm, 36 m long prestressed concrete piles reinforcing the silty clay at the site to reduce settlement. To provide lateral resistance in a seismic event, the footing on the pad is supplied with 900 mm diameter, 5 m long bored piles connected to the footing and pile cap.

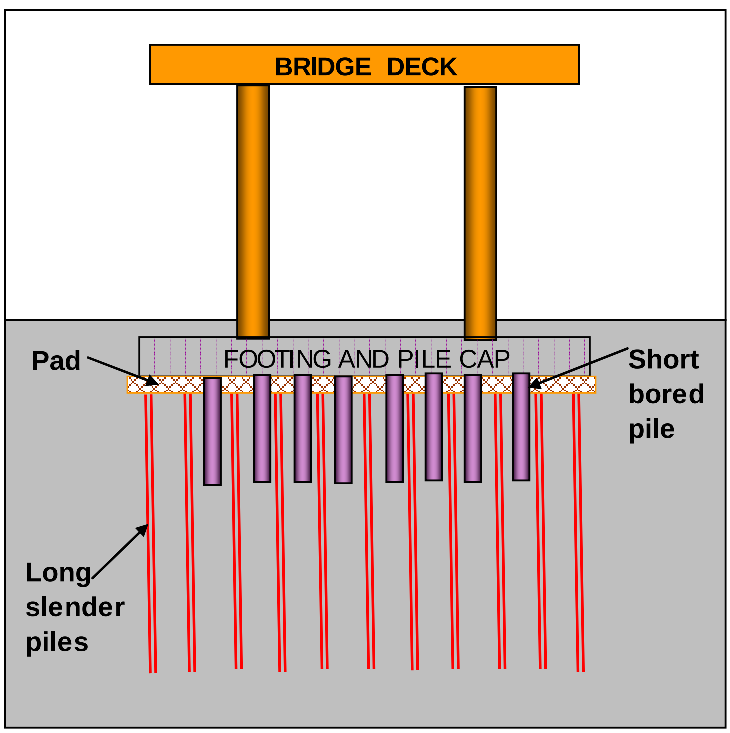

Fig. 7.5 Piled pad foundations for the Golden Ears Bridge piers. (After Sampaco et al. 2008).

7.6 Effect of Installation

Whether a pile is installed by driving or by other means, the installation affects—disturbs—the soil. Before the disturbance from the pile installation has subsided, it is difficult to determine the magnitude of what shaft and toe resistances to expect. For instance, presence of dissipating excess pore pressures causes uncertainty in the magnitude of the effective stress in the soil and the strength gain (set-up) due to reconsolidation is hard to estimate. Such installation effects can take long time to disappear, especially in clays. They can be estimated in an effective stress analysis using suitable assumptions as to the distribution of pore pressure along the pile at any particular time. Usually, to calculate the installation effect, a good estimate can be obtained by imposing excess pore pressures in the fine-grained soil layers—the more, the finer the soil—taking care that the pore pressure must not exceed the total overburden stress. By restoring the pore pressure values to the original conditions, which again will prevail when the induced excess pore pressures have dissipated, the long-term capacity is established. (Fellenius 2008). Notice, in some soils, even sands, the increase of capacity, the set-up, can continue also well after the pore pressures induced during the driving have dissipated (Bullock et al. 2005).

7.7 Residual Load

The dissipation of induced excess pore pressures (called “reconsolidation”) imposes load (residual load) in the pile by negative skin friction in the upper part of the pile, which is resisted by positive shaft resistance in the lower part of the pile and some toe resistance. In driven piles, residual load also results from strain built in during the driving (“locked-in load”). Residual load, as well as capacity, may continue to increase also after the excess pore pressures have dissipated.

The quantitative effect of not recognizing the residual load in the evaluation of results from a static loading test, is that erroneous conclusions will be drawn from the test: the shaft resistance appears larger than the true value, while the toe resistance appears correspondingly smaller. Typically, when the residual load is not recognized, the distribution of load in the pile will be with a decreasing curvature with depth, indicating a shaft resistance that gets smaller with depth, as opposed to the more realistic shape (in a homogeneous soil) of increasing curvature, indicating a progressively increasing shaft resistance.

The existence of residual load, also called “locked-in load”, in piles has been known for a long time. Nordlund (1963) is probably the first to point out its importance for evaluating load distribution from the results of an instrumented static pile loading test. However, it is not easy to demonstrate that test data are influenced by residual load. To quantify their effect is even more difficult. Practice is, regrettably, to consider the residual load to be small and not significant to the analysis and to proceed with an evaluation based on “zeroing” all gages immediately before the start of the test. That is, the problem is 'solved' by declaring it not to exist. This is why the soil mechanics literature includes theories applying “critical depth” and statements that unit shaft resistance would reduce as a function of depth in a homogeneous soil. For more details on this effect and how to analyze the test data to account for residual load, see Altae et al. (1992; 1993), Fellenius et al. (2000), and Fellenius (2002).

Notice, capacity as a term means ultimate resistance, and, in contrast to ultimate shaft resistance, ultimate toe resistance does not exist. As used in the practice, the capacity of a pile determined from a static loading test is the load for which the load movement <u>of the pile head</u> appears to show continued movement for a small increase of applied load, ‘failure’ occurs. This ‘failure’ value is a combination of shaft resistance and toe resistance as indicated in Fig. 7.6, which illustrates how a strain-softening (post-peak) behavior for the shaft resistance combined with an increasing toe resistance, implies a ultimate failure that easily can be assumed to occur also at the pile toe. The toe load-movement curve includes a suggested effect of a residual (locked-in) toe load. Additional discussion on this topic is offered in Chapter 8.

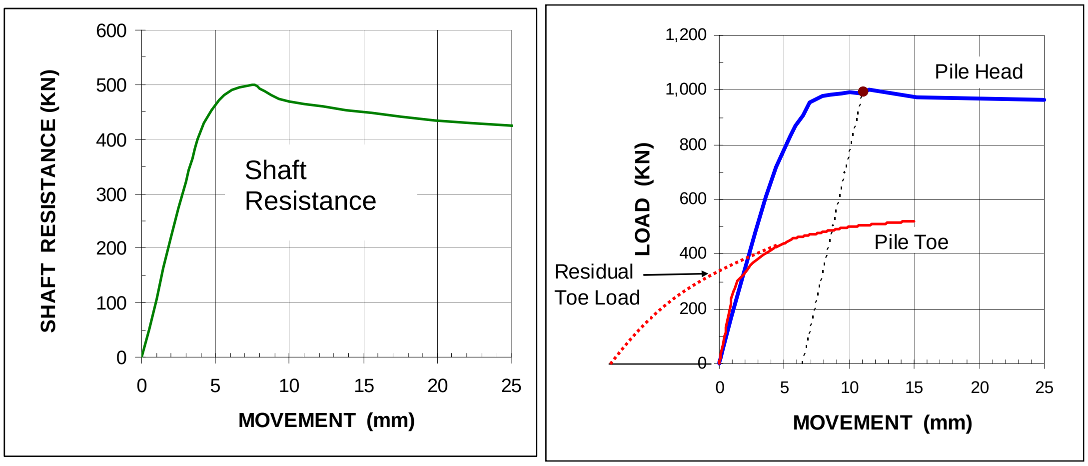

Fig. 7. 6 Load-Movement curves for shaft resistance and for total ("Pile Head") and toe resistances.

7.8 Analysis of Capacity for Tapered Piles

Many piles are not cylindrical or otherwise uniform in shape throughout the length. The most common example is the wood pile, which has a conical shape. Step-tapered piles are also common, consisting of two or more concrete-filled steel tubes (pipes) of different diameters connected to each other, normally, the larger above the smaller. Sometimes, a pile can consist of a steel pipe with a lower conical section, for example, the Monotube pile, and the Steel-Taper-Tube pile which typically have a 25 feet (7.6 m) long conical toe section, tapering the diameter down from 14 inch (355 mm) to 8 inches (203 mm). Composite piles can have an upper solid concrete section and a bottom smaller diameter H-pile extension.

For the step-tapered piles, obviously each 'step' provides an extra resistance point, which needs to be considered in an analysis. (The GRLWEAP wave equation program, for example, can model a pile with one diameter change as having a second pile toe at the location of the 'step'). Similarly, in a static analysis, each such step can be considered as an extra pile toe with a donut-shaped area, A_t, and assigned a corresponding toe resistance per Eq. 7.2b, or toe unit resistance value, r_t, times the donut area. Each such extra toe resistance value is then added to the shaft resistance calculated using the actual pile diameter.

Piles with a continuous taper (conical piles) are less easy to analyze. Nordlund (1963) suggested a taper correction factor to use to increase the unit shaft resistance in sand for conical piles. The correction factor is a function of the taper angle and the soil friction angle. A taper angle of 1° (0.25-inch/foot) in a sand with a 35° friction angle would give a correction factor of about 4. At an angle of 0.5°, the factor would be about 2.

The author prefers to use a more direct calculation method consisting of dividing up the soil layers into sub-layers of some thickness and, at the bottom of each such sub-layer, project the diameter change. This donut-shaped area is then treated as an extra toe similar to the analysis of the step-taper pile. The shaft resistance is calculated using the mean diameter of the pile over the same "stepped" length. The shaft resistance over each such particular length consists of the sum of the shear resistance over the shaft area and the toe resistance of the "donut" area. This method requires that a toe coefficient, N_t, or a unit toe resistance value, r_t, be assigned to each "stepped" length.

The taper does not come into play for negative skin friction. This means that, when determining the drag load, the effect of the taper (the "donut") should be excluded. Below the neutral plane, however, the effect should be included. Therefore, the taper will influence the location of the neutral plane (because the taper increases the positive shaft resistance below the neutral plane).

7.9 Factor-of-Safety

The pile design must distinguish between the design for **bearing capacity** (Eq. 7.3) and design for structural strength. The capacity is determined considering positive shaft resistance developed along the full length of the pile plus full toe resistance. The loads consist of dead and live load, but no drag load **(**because the drag load does not affect the bearing capacity of the pile). Drag load is of structural concern, not geotechnical; see Section 7.18. If design is based on only theoretical analysis, the usual factor of safety is about 3.0. If the analysis is supported by the results of a loading test, static or dynamic, the factor of safety is reduced, depending on reliance on and confidence in the capacity value, and importance and sensitivity of the structure to foundation deformations. Design for bearing capacity includes applying a Factor-of-Safety (Working Stress Design, WSD). Factors-of-safety as low as 1.8 are not extreme. The principle of the approach is also valid in Ultimate Limit States design (ULS) and Load and Resistance Factor Design (LRFD). That is, while the factors are different, the ratio between the factors in the ULS and LRFD are about the same as in the WSD.

Notice that a static analysis must always be performed. If results from static and/or dynamic field tests are available, the static analysis should always be correlated to the field test results.

A static analysis is often considered uncertain enough to warrant a factor-of-safety of 3.0 in determining the safe embedment depth. This depth only too often becomes the installation depth for the contract. Yet, the uncertainty can just as well hit the other way and not only result in that much shorter piles will do, the 'designed' installation depth may be totally unattainable. Blindly imposing a factor-of-safety is not a safe approach. See also the discussion below on factor-of-safety for the example case under the heading Installation Phase, Section 7.14.

7.10 Standard Penetration Test, SPT, Method for Determining Axial Pile Capacity

For many years, the N-index of standard penetration test has been used to calculate capacity of piles. Meyerhof (1976) compiled and rationalized some of the wealth of experience then available and recommended that the capacity be a function of the N-index, as follows:

$$R = R_t + R_s = mN_tA_t + nN_sA_sD \tag{7.6}$$

where
- m = a toe coefficient
- n = a shaft coefficient
- N_t = N-index at the pile toe (taken as a pure number)
- N_s = average N-index along the pile shaft (taken as a pure number)
- A_t = pile toe area
- A_s = unit shaft area; circumferential area
- D = embedment depth

For values inserted into Eq. 7.6 using base SI-units, that is, **R** in newton, **D** in metre, and **A** in m^2, the toe and shaft coefficients, **m** and **n**, become:

m = $400 \cdot 10^3$ for driven piles and $120 \cdot 10^3$ for bored piles (N/m^2)
n = $2 \cdot 10^3$ for driven piles and $1 \cdot 10^3$ for bored piles (N/m^3)

For values inserted into Eq. 7.6 using English units with **R** in ton, **D** in feet, and **A** in ft^2, the toe and shaft coefficients, **m** and **n**, become:

m = 4 for driven piles and 1.2 for bored piles (t/ft^2)
n = 0.02 for driven piles and 0.01 for bored piles (t/ft^3)

The standard penetration test (SPT) is a subjective and highly variable test. The test and the N-index have substantial qualitative value, but should be used only very cautiously for quantitative analysis—that is, the N-index should not be used numerically in formulae, such as Eq. 7.6. The Canadian Foundation Engineering Manual (1992) lists the numerous irrational factors influencing the N-index. However, when the use of the N-index is considered with the sample of the soil obtained and related to a site and area-specific experience, the crude and decried SPT-test does not come out worse than other methods of analyses.

7.11 Cone Penetration Test, CPTU, Method for Determining Axial Pile Capacity

The static cone penetrometer resembles a pile. There is shaft resistance in the form of the sleeve friction measured immediately above the cone, and there is toe resistance in the form of the directly applied and measured cone stress. The piezocone, CPTU, which is a cone penetrometer equipped with a gage measuring the pore pressure at the cone (usually immediately behind the cone; at the cone shoulder, the so-called U2-position), is a considerable advancement on the static cone. By means of the piezocone, the cone information can be related more dependably to soil parameters and a more detailed analysis be performed.

Two main approaches for application of cone data to pile design has evolved: indirect and direct methods.

Indirect CPT methods employ soil parameters, such as friction angle and undrained shear strength estimated from the cone data as based on bearing capacity and/or cavity expansion theories, which introduces significant uncertainties. The indirect methods disregard horizontal stress, apply strip-footing bearing capacity theory, and neglect soil compressibility and strain softening. These methods are not particularly suitable for use in engineering practice and are here not further referenced.

Direct CPT methods more or less equal the cone resistance with the pile unit resistances. Some methods may use the cone sleeve friction in determining unit shaft resistance. Several methods modify the resistance values to consider the difference in diameter between the pile and the cone. The influence of mean effective stress, soil compressibility, and rigidity affect the pile and the cone in equal measure, which eliminates the need to supplement the field data with laboratory testing and to calculate intermediate values, such as K_s and N_q.

Since its first development in the Netherlands, the cone penetrometer test, CPT, has been applied as tool for determining pile capacity. Seven methods are presented in the following. The first six are based on the mechanical or the electric cones. The seventh method is the Eslami-Fellenius method, which is based on the piezocone, CPTU. Of course, the Eslami-Fellenius method can also be applied to CPT results, subject to suitable assumptions made on the distribution of the pore pressure, usually applying the neutral pore pressure, u_0.

1. Schmertmann and Nottingham
2. DeRuiter and Beringen (commonly called the "Dutch Method" or the “European Method”)
3. Bustamante and Gianselli (commonly called the "LCPC Method" or the “French Method”)
4. Meyerhof (method for sand)
5. Tumay and Fakhroo (method limited to piles in soft clay)
6. The ICP method
7. Eslami and Fellenius

Often, CPT and CPTU data include a small amount of randomly distributed extreme values, "peaks and troughs", that may be representative for the response of the cone to the soil characteristics, but not for a pile having a much larger diameter. Keeping the extreme values will have a minor influence on the pile shaft resistance, but it will have a major influence on the pile toe resistance not representative for the pile resistance at the site. Therefore, when calculating pile toe capacity, it is common practice to manually filter and smoothen the data. Either by applying a "minimum path" rule or, more subjectively, by reducing the influence of the peaks and troughs from the records. To establish a representative value of the cone resistance to the pile unit toe resistance, the first five methods determine an arithmetic average of the CPT data averaged over an "influence zone", whereas the sixth method applies geometric mean to achieve the filtering for the toe resistance determination.

7.11.1 Schmertmann and Nottingham

Toe resistance

The **Schmertmann and Nottingham** method is based on a summary of the work on model and full-scale piles presented by Nottingham (1975) and Schmertmann (1978). The unit toe resistance, r_t, is a "minimum path" average obtained from the cone stress values in an influence zone extending from 8b above the pile toe (b is the pile diameter) and 0.7b or 4b, as indicated in Fig. 7.7.

The procedure consists of five steps of filtering the q_c data to “minimum path” values. Step 1 is determining two averages of cone stress within the zone below the pile toe, one for a zone depth of 0.7b and one for 0.4b along the path "a" through "b". The smallest of the two is retained. (The zone height 0.7b applies to where the cone stress increases with depth below the pile toe). Step 2 is determining the smallest cone stress within the zone used for the Step 1. Step 3 consists of determining the average of the two values per Steps 1 and 2. Step 4 is determining the average cone stress in the zone above the pile toe according to the minimum path shown in Fig. 7.7. (Usually, just the average of the cone stress within the zone is good enough). Step 5, finally, is determining the average of the Step 3 and Step 4 values. This value is denoted q_{ca}.

The pile toe resistance is then determined according to Eq. 7.7.

(7.7) $$r_t = C\, q_{ca}$$

where
r_t = pile unit toe resistance; an upper limit of 15 MPa is imposed
C = correlation coefficient governed by the overconsolidation ratio, OCR
q_{ca} = the filtered value obtained in the influence zone per the above procedure

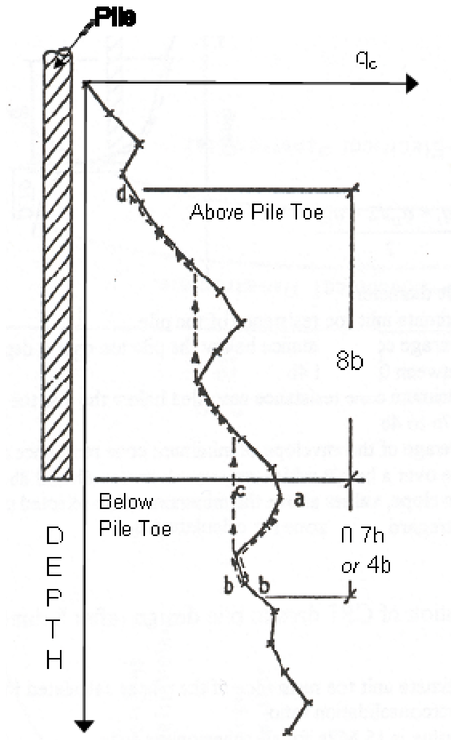

Fig. 7.7 Determining the influence zone for toe resistance (Schmertmann, 1978)

The correlation coefficient, C, ranges from 0.5 through 1.0 depending on overconsolidation ratio, OCR, as the slope between the toe resistance, r_t, and The 'minimum path' average of the cone stress, as indicated in Fig. 7.8. For simplicity, the relations are usually also applied to a pile toe located in clay.

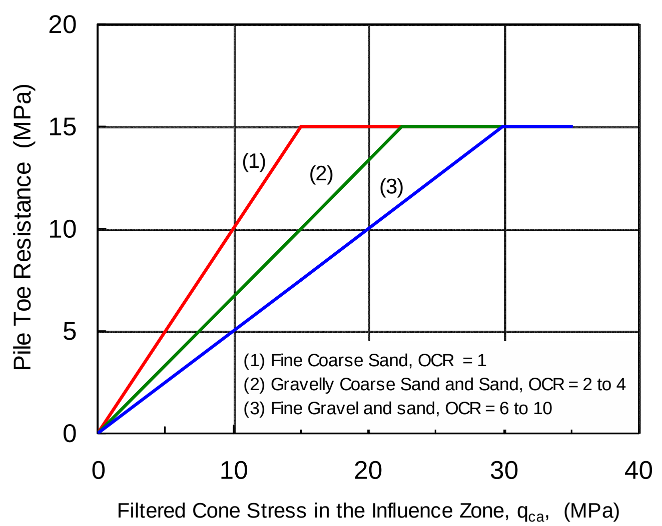

Fig. 7.8 Adjustment of the coefficient to OCR

Unit shaft resistance

The unit shaft resistance, r_s, may be determined from the sleeve friction as expressed by Eq. 7.8.

(7.8) $$r_s = K_f \, f_s$$

where r_s = pile unit shaft resistance; an upper limit of 120 KPa is imposed
K_f = a dimensionless coefficient
f_s = sleeve friction

In sand, K_f is assumed to be a function of the pile embedment ratio, D/b. Within a depth of the first eight pile diameters below the ground surface (D/b = 8), the K_f-coefficient is linearly interpolated from zero at the ground surface to 2.5. Hereunder, the value reduces from 2.5 to 0.891 at an embedment of 20 D/b. Simply applying K_f = 0.9 straight out is usually satisfactory.

In clay, K_f is a function of the sleeve friction and ranges from 0.2 through 1.25 as indicated in Fig. 7.9.

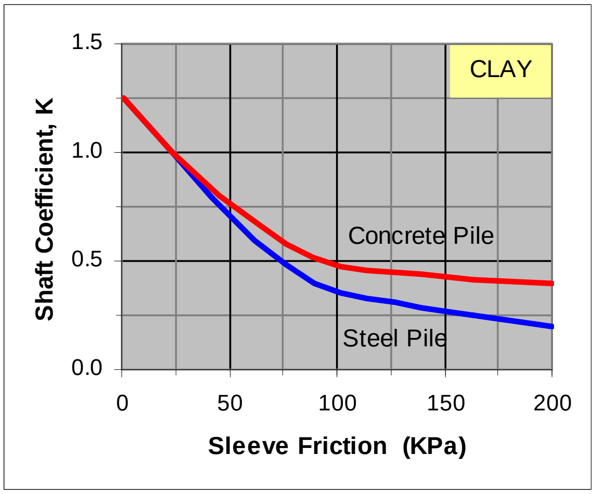

Fig. 7.9 Shaft coefficients for use in Eqs. 7.8

Alternatively, in sand, but not in clay, the shaft resistance may be determined from the cone stress, q_c, according to Eq. 7.9.

(7.9) $$r_s = K_c \, q_c$$

where r_s = unit shaft resistance; an upper limit of 120 KPa is imposed
K_c = a dimensionless coefficient; a function of the pile type.
for open toe, steel piles K_c = 0.8 %
for closed-toe pipe piles K_c = 1.8 %
for concrete piles K_c = 1.2 %
q_c = cone resistance

7.11.2 deRuiter and Beringen

Toe resistance

The Dutch method was presented by deRuiter and Beringen (1979). For unit toe resistance of a pile in sand, the method is the same as the Schmertmann and Nottingham method. In clay, the unit toe resistance is determined from total stress analysis applied according to conventional bearing capacity theory as indicated in Eqs. 7.10 and 7.11.

(7.10) $$r_t = 5\,S_u$$

(7.11) $$S_u = \frac{q_c}{N_k}$$

where r_t = pile unit toe resistance; an upper limit of 15 MPa is imposed
S_u = undrained shear strength
N_k = a dimensionless coefficient, ranging from 15 through 20, usually = 20

Shaft resistance

In **sand**, the unit shaft resistance is the smallest of the sleeve friction, f_s, and $q_c/300$.

In **clay**, the unit shaft resistance may also be determined from the undrained shear strength, S_u, as given in Eq. 7.12.

(7.12) $$r_s = \alpha\,S_u \quad = \quad \alpha\frac{q_c}{N_k} \quad = \quad 0.05\alpha\,q_c$$

where r_s = pile unit shaft resistance
α = adhesion factor equal to 1.0 for normally consolidated clay and 0.5 for overconsolidated clay
S_u = undrained shear strength according to Eq. 7.11

An upper limit of 120 KPa is imposed on the unit shaft resistance.

7.11.3 LCPC

The **LCPC** method, also called the **French** or **Bustamente** method (LCPC = Laboratoire Central des Ponts et Chausees) method is based on experimental work of Bustamante and Gianeselli (1982) for the French Highway Department. For details, see CFEM 1992. The sleeve friction, f_s, is neglected.

Toe resistance

The unit toe resistance, r_t, is determined from the cone resistance within an influence zone of 1.5 b above and 1.5 b below the pile toe, as illustrated in Fig. 7.9. First, the cone resistance within the influence zone is averaged to q_{ca}. Next, an average, q_{caa}, is calculated of the average of the q_{ca}-values that are within a range of 0.7 through 1.3 of q_{ca}. Finally, the toe resistance is obtained from multiplying the equivalent value with a correlation coefficient, C_{LCPC}, according to Eq. 7.13.

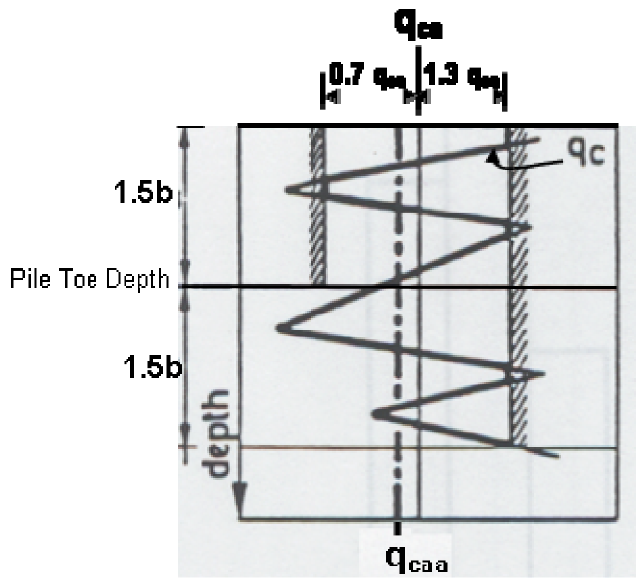

Fig. 7.9 Averaging the cone resistance according to the LCPC method. (Bustamante and Gianselli, 1982) .

(7.13) $$r_t = C_{LCPC}\ q_{caa}$$

where r_t = pile unit toe resistance; an upper limit of 15 MPa is imposed
C_{LCPC} = correlation coefficient
q_{caa} = average of the average cone resistance in the influence zone

As indicated in Table 7.4A, for driven steel piles and driven precast piles, the correlation coefficient, C_{LCPC}, ranges from 0.45 through 0.55 in clay and from 0.40 through 0.50 in sand. For bored piles, the values are about 20 % smaller.

TABLE 7.4A Coefficients of Unit Toe Resistance in the LCPC Method Quoted from the CFEM (1992)

Soil Type	Cone Stress (MPa)	Bored Piles C_{LCPC} (- - -)	Driven Piles C_{LCPC} (- - -)
CLAY	- - $q_c <$ 1	0.04	0.50
	1 $< q_c <$ 5	0.35	0.45
	5 $< q_c$ - - -	0.45	0.55
SAND	- - - $q_c <$ 12	0.40	0.50
	12 $< q_c$ - - -	0.30	0.40

Shaft resistance

The unit shaft resistance, r_s, is determined from Eq. 7.14 with the K_{LCPC}-coefficient ranging from 0.5 % through 3.0 %, as governed by magnitude of the cone resistance, type of soil, and type of pile. Upper limits of the unit shaft resistance are imposed, ranging from 15 KPa through 120 KPa depending on soil type, pile type, and pile installation method.

(7.14) $$r_s = K_{LCPC}\ q_c \leq J$$

where r_s = unit shaft resistance; for imposed limits see Table 7.4B
K_{LCPC} = a dimensionless coefficient; a function of the pile type and cone resistance
J = upper limit value of unit shaft resistance
q_c = cone resistance (note, uncorrected for pore pressure on cone shoulder)

TABLE 7.4B Coefficients and Limits of Unit Shaft Resistance in the LCPC Method Quoted from the CFEM (1992)

Soil Type	Cone Stress (MPa)	Concrete Piles & Bored Piles K_{LCPC} (- - -)	Steel Piles K_{LCPC} (- - -)	Maximum r_S J (KPa)
CLAY	- - $q_c <$ 1	0.011 (1/90)	0.033 (=1/30)	15
	1 $< q_c <$ 5	0.025 (1/40)	0.011 (=1/80)	35
	5 $< q_c$ - - -	0.017 (1/60)	0.008 (=1/120)	35
	(for $q_c > 5$, the unit shaft resistance, r_s, is always larger than 35 KPa)			
SAND	- - - $q_c <$ 5	0.017 (1/60)	0.008 (=1/120)	35
	5 $< q_c <$ 12	0.010 (1/100)	0.005 (=1/200)	80
	12 $< q_c$ - - -	0.007 (1/150)	0.005 (=1/200)	120

The values in the parentheses are the inverse of the K_{LCPC} -coefficient

The limits shown in Table 7.4B are developed in its own practice and geologic setting, and it is questionable if they have any general validity. It is common for users to either remove the limits or to adjust them to new values. Many also apply other values, personally preferred, of the K and J coefficients, as well as the C-coefficient for toe resistance. Therefore, where the LCPC method or a "modified LCPC method" is claimed to be used, the method is often not the method by Bustamante and Gianselli (1982), but simply a method whereby the CPT cone resistance by some correlation is used to calculate pile shaft and toe resistances. Such adjustments do not remove the rather capricious nature of the limits.

The correlation between unit shaft resistance and cone stress, q_c, is represented graphically in Fig. 7.10, with Fig. 7.10A showing the values in “CLAY” and Fig. 7.10B in "SAND”. Note, the LCPC method does not correct the cone stress values for the pore pressure on the cone shoulder.

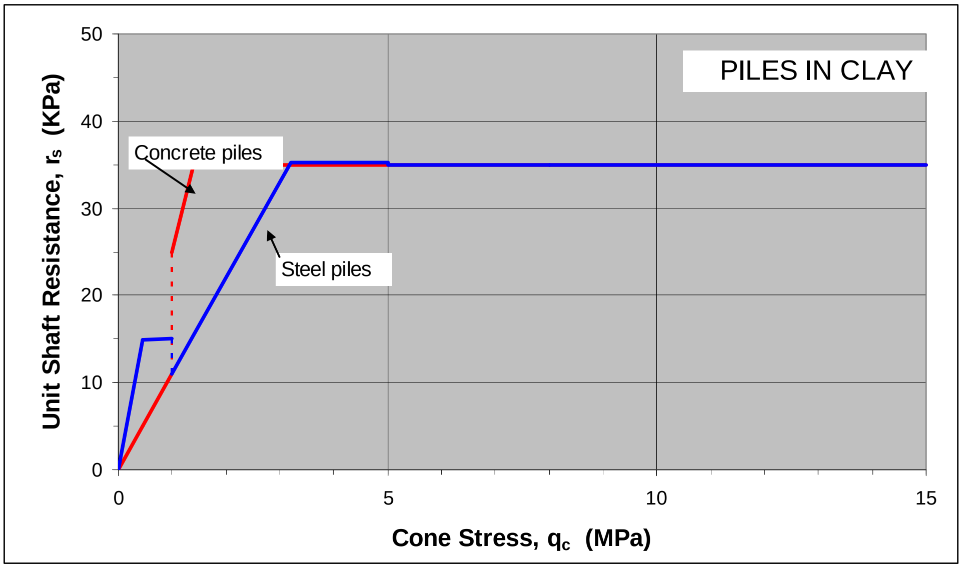

Fig. 7.10A Unit shaft resistance versus cone stress, q_c, for piles in clay according to the LCPC method.

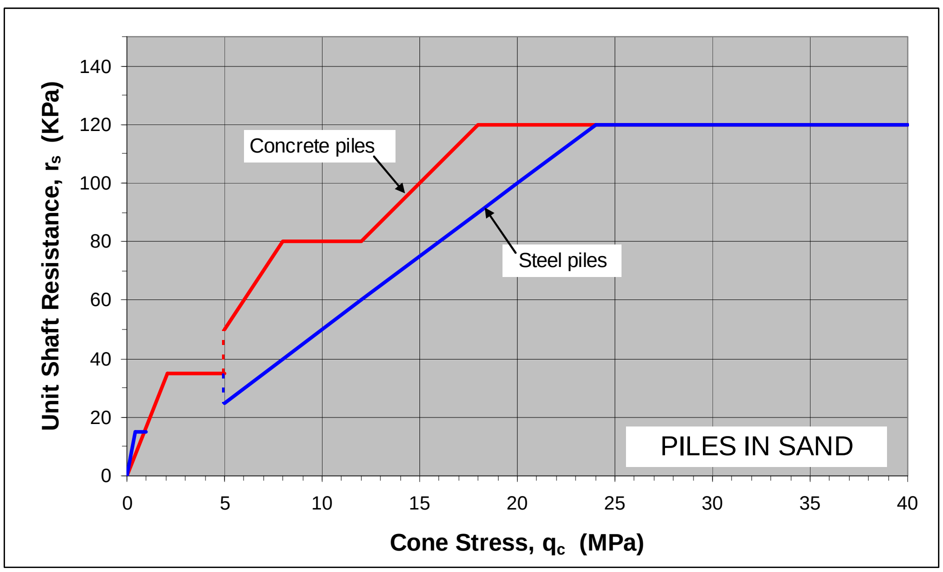

Fig. 7.10B Unit shaft resistance versus cone stress, q_c, for piles in sand according to the LCPC method.

7.11.4 Meyerhof

Toe resistance

The **Meyerhof** method (Meyerhof 1956; 1976; 1983) is intended for calculating the capacity of piles in sand. For unit toe resistance, the influence of scale effect of piles and shallow penetration in dense sand strata is considered by applying two modification factors, C_1 and C_2, to the q_c average. The unit toe resistance for driven piles is given by Eq. 7.13.

(7.13) $$r_t = q_{ca}\, C_1\, C_2$$

where r_t = unit toe resistance; for bored piles, reduce to 70 % of r_t per Eq. 7.13
q_{ca} = arithmetic average of q_c in a zone ranging from "1b" below through "4b" above pile toe
C_1 = $[(b + 0.5)/2b]^n$; modification factor for scale effect when b > 0.5 m, otherwise $C_1 = 1$
C_2 = D/10b; modification for penetration into dense strata when D < 10b, otherwise $C_2 = 1$
n = an exponent equal to
1 for loose sand ($q_c < 5$ MPa)
2 for medium dense sand ($5 < q_c < 12$ MPa)
3 for dense sand ($q_c > 12$ MPa)
b = pile diameter
D = embedment of pile in dense sand strata

Shaft resistance

For driven piles, the unit shaft resistance is either taken as equal to the sleeve friction, f_s, or as 0.5 % of the cone stress, q_c., as indicated in Eqs. 7.14 and 7.15. For bored piles, reduction factors of 70 % and 50 %, respectively, are applied to these calculated values of shaft resistance.

(7.14) $$r_s = K_f\, f_s \qquad K_f = 1.0$$

(7.15) $$r_s = K_c\, q_c \qquad K_c = 0.5$$

where r_s = unit shaft resistance
K_f = sleeve resistance modification coefficient
K_f = cone resistance modification coefficient

7.11.5 Tumay and Fakhroo

Toe resistance

The **Tumay and Fakhroo** method is based on an experimental study in clay soils in Louisiana (Tumay and Fakhroo 1981). The **unit toe resistance** is determined in the same way as in the Schmertmann and Nottingham method, Eq. 7.7.

Shaft resistance

The unit shaft resistance is determined according to Eq. 7.16 with the K_f-coefficient determined according to Eq. 7.17. Note, the K-coefficient is not dimensionless in Eq. 7.17.

(7.16) $$r_s = K_f\, f_s$$

where r_s = pile unit shaft resistance, KPa
K_f = a coefficient
f_s = sleeve friction, **KPa**

(7.17) $$K_f = 0.5 + 9.5e^{-90 f_s}$$

where e = base of natural logarithm = 2.718
f_s = sleeve friction, **MPa**

7.11.6 ICP Method

Jardine at al. (2005) present the Imperial College method of using CPT results to determine pile capacity in sand and clay. As in the other CPT methods, the sleeve friction is not considered and the cone stress is not corrected for the effect of the pore pressure acting on the cone shoulder. The following description is limited to the method for sand, as it is a bit simpler than the method for clay.

Toe resistance in sand

The ICP method applies the cone stress with adjustment to the relative difference between the cone diameter and the pile toe diameter as indicated in Eq. 7.18.

(7.18) $$r_t = q_{ca}[1 - 0.5\,\lg(\frac{b_{pile}}{b_{cone}})]$$

where r_t = pile unit toe resistance
q_{ca} = unit cone resistance filtered according to the LCPC method
b_{pile} = pile toe diameter
b_{cone} = cone diameter; 36 mm for a cone with 10 cm^2 base area

For pile diameters larger than 900 mm, a lower limit of $r_t = 0.3q_c$ applies. Moreover, for piles driven open-toe, a different set of equations apply, which depends on whether or not the pile is plugged.

Shaft resistance in sand

The unit shaft resistance of closed-toe piles driven in sand is determined according to Eq. 7.19

(7.19) $$r_s = K_J\ q_c$$

where K_j is determined according to Eq. 7.20

(7.20) $$K_J = \left\{0.0145 q_c (\frac{\sigma'_z}{\sigma_r})^{0.13} (\frac{b}{h_t})^{0.38} + [2q_c (0.0203 + 0.00125 q_c (\sigma'_z\ \sigma_r)^{-0.5} - 1.216\times10^{-6} (\frac{q_c^2}{\sigma'_z\ \sigma_r})]^{-1} \frac{0.01}{b}\right\} \tan\delta$$

where σ'_z = effective overburden stress
σ'_r = effective radial stress
b = pile diameter
h_f = depth below considered point to pile toe; limited to 8b
δ = interface angle of friction

Eq. 7.20 employs principles of "Coulomb failure criterion", "free-field vertical effective stress (σ'_z) normalized by absolute atmospheric pressure", "local radial effective stress (σ'_r) with dilatant increase", "interface angle of friction at constant volume test" (or estimate from graph), is "uncorrected for overconsolidation", and applies to compression loading. The method has been developed by fitting to results from six field tests listed by Jardine at al. (2005).

7.11.7 Eslami and Fellenius

Toe resistance

In the Eslami and Fellenius CPTU method (Eslami 1996, Eslami and Fellenius 1997), the cone stress is transferred to an apparent "effective" cone stress, q_E, by subtracting the measured pore pressure, *u2*, from the measured total cone stress (corrected for pore pressure acting against the shoulder). The pile **unit toe resistance** is the geometric average of the "effective" cone stress over an influence zone that depends on the soil layering, which reduces — removes — potentially disproportionate influences of odd "peaks and troughs", which the simple arithmetic average used by the CPT methods does not do. When a pile is installed through a weak soil into a dense soil, the average is determined over an **influence zone** extending from 4b below the pile toe through a height of 8b above the pile toe. When a pile is installed through a dense soil into a weak soil, the average above the pile toe is determined over an influence zone height of 2b above the pile toe as opposed to 8b. The relation is given in Eq. 7.21.

(7.21) $$r_t = C_t\ q_{Eg}$$

where
- r_t = pile unit toe resistance
- C_t = toe correlation coefficient (toe adjustment factor)—equal to unity in most cases
- q_{Eg} = geometric average of the cone point resistance over the influence zone after correction for pore pressure on shoulder and adjustment to "effective" stress

The toe correlation coefficient, C_t, also called toe adjustment factor, is a function of the pile size (toe diameter). The larger the pile diameter, the larger the movement required to mobilize the toe resistance. Therefore, the "usable" pile toe resistance diminishes with increasing pile toe diameter. For pile diameters larger than about 0.4 m, the adjustment factor should be determined by the relation given in Eq. 7.22.

(7.22) $$C_t = \frac{1}{3b} \qquad C_t = \frac{12}{b} \qquad C_t = \frac{1}{b}$$

([‘b’ in metre] [‘b’ in inches] [‘b’ in feet]

where b = pile diameter in units of either metre (or inches or feet)

Shaft resistance

Also the pile unit shaft resistance is correlated to the average "effective" cone point stress with a modification according to soil type per the approach detailed below. The C_s correlation coefficient is determined from the soil profiling chart (Chapter 2, Fig. 2.11), which uses both cone stress and sleeve friction. However, because the sleeve friction is a more variable measurement than the cone point stress, the sleeve friction value is not applied directly.

(7.23) $$r_s = C_s\ q_E$$

where
- r_s = pile unit shaft resistance
- C_s = shaft correlation coefficient, which is a function of soil type determined from the Eslami-Fellenius soil profiling and Table 7.5
- q_E = cone point resistance after correction for pore pressure on the cone shoulder and adjustment to apparent "effective" stress; $q_E = q_t - u2$

Fig. 7.11 combines the unit shaft resistance for piles in sand according to the LCPC method, which does not differentiate between different types of sand and the Eslami-Fellenius method which separates the sand (Types 4a, 4b, and 5 in Table 7.5) as determined from the actual cone sounding. The difference between q_c and q_t is disregarded in the figure.

TABLE 7.5 Shaft Correlation Coefficient, C_s

Soil Type	C_s
1. Soft sensitive soils	8.0 %
2. Clay	5.0 %
3. Silty clay, stiff clay and silt	2.5 %
4a. Sandy silt and silt	1.5 %
4b. Fine sand or silty sand	1.0 %
5. Sand to sandy gravel	0.4 %

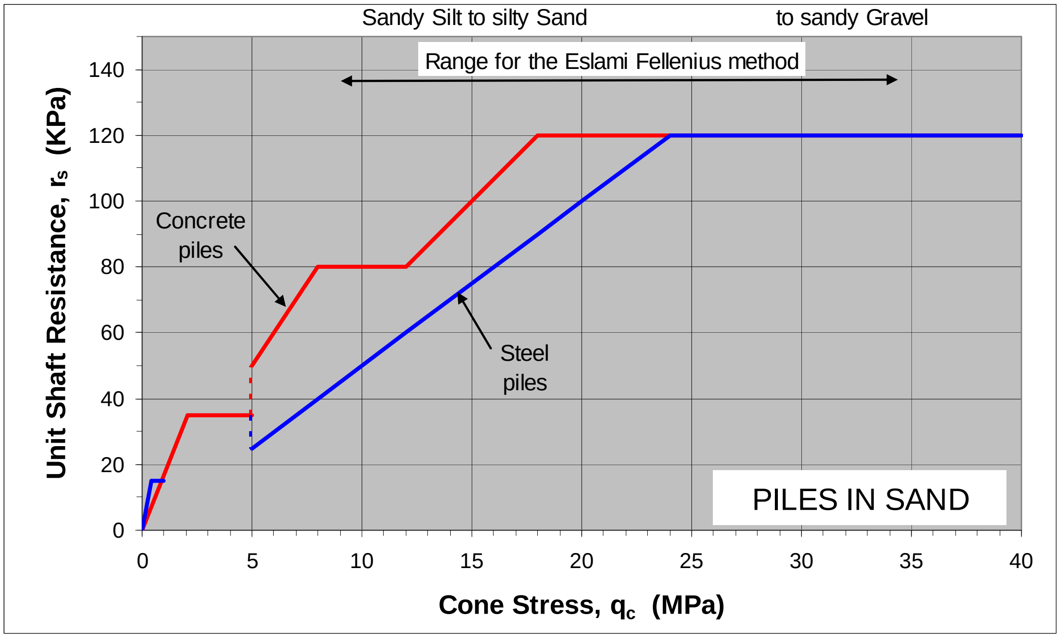

Fig. 7.11 Unit Shaft resistance versus cone stress, q_c, for piles in sand according to the LCPC method (the red and blue lines) and the Eslami-Fellenius method.

Notice, all analysis of pile capacity, whether from laboratory data, SPT-data, CPT-data, or other methods should be correlated back to an effective stress calculation and the corresponding beta-coefficients and N_t-coefficients be determined from the calculation for future reference.

Soil is variable, and digestive judgment of the various analysis results can and must be exercised to filter the data for computation of pile capacity, and site-specific experience is almost always absolutely necessary. The more representative the information is, the less likely the designer is to jump to false conclusions, but one must always reckon with an uncertainty in the prediction.

While the six categories indicate a much larger differentiation than the "clay/sand" division of the CPT-methods, the shaft correlation coefficients values shown in Table 7.4 still present sudden changes when the q_t and f_s values change from plotting above and below a line in the classification chart. It is advisable to always plot the data in the classification chart and apply the same shaft correlation coefficient to soil layers that show data points that are grouped together even if they straddle a boundary line. If results from measured shaft distribution is available, the correlation coefficient should be determined by fitting to the measured shaft resistance.

7.11.8 Comments on the Methods

When using either of the CPT methods (the six first methods), difficulties arise in applying some of the recommendations of the methods. For example:

1. Although the recommendations are specified to soil type (clay and sand; very cursorily characterized), the CPT methods do not include a means for identifying the soil type from the data. Instead, the soil profile governing the coefficients relies on information from conventional boring and sampling, and laboratory testing, which may not be fully relevant to the CPT data.
2. All the CPT methods include random smoothing and filtering of the CPT data to eliminate extreme values. This results in considerable operator-subjective influence of the results.
3. The CPT methods were developed before the advent of the piezocone and, therefore, omit correcting for the pore pressure acting on the cone shoulder (Campanella and Robertson, 1988). The error in the cone stress value is smaller in sand, larger in clay.
4. The CPT methods employ total stress values, whereas effective stress governs the behavior of piles.
5. All of the CPT methods are developed in a specific geographic area with more or less unique geological conditions, that is, each method is based on limited types of piles and soils and may not be relevant outside its related local area.
6. The upper limit of 15 MPa, which is imposed on the unit toe resistance in the Schmertmann and Nottingham, and European methods, is not reasonable in very dense sands where values of pile unit toe resistance higher than 15 MPa frequently occur. Excepting Meyerhof method, all CPT methods impose an upper limit also to the unit shaft resistance. For example, the upper limits (15 KPa, 35 KPa, 80 KPa, and 120 KPa) imposed in the French (LCPC) method quoted in Table 7.4. Values of pile unit shaft resistance higher than the recommended limits occur frequently. Therefore, the limits are arbitrary and their general relevance is questionable.
7. All CPT methods involve a judgment in selecting the coefficient to apply to the average cone resistance used in determining the unit toe resistance.
8. In the Schmertmann and Nottingham and the European methods, the overconsolidation ratio, OCR is used to relate q_c to r_t. However, while the OCR is normally known in clay, it is rarely known for sand.
9. In the European (Dutch) method, considerable uncertainty results when converting cone data to undrained shear strength, S_u, and, then, in using S_u to estimate the pile toe capacity. S_u is not a unique parameter and depends significantly on the type of test used, strain rate, and the orientation of the failure plane. Furthermore, drained soil characteristics govern long-term pile capacity also in cohesive soils. The use of undrained strength characteristics for long-term capacity is therefore not justified. (Nor is it really a direct CPT method).

10. In the French method, the length of the influence zone is very limited, and perhaps too limited. (The influence zone is the zone above and below the pile toe in which the cone resistance is averaged). Particularly if the soil strength decreases below the pile toe, the soil average must include the conditions over a depth larger than 1.5b distance below the pile toe.
11. The French (LCPC) and the ICP methods make no use of sleeve friction, which disregards an important aspect of the CPT results and soil characterization.
12. The various imposed maximum unit shaft shear values appear arbitrary and cannot have general validity.

Obviously, the current methods leave something to be desired with regard to the estimation of pile capacity from cone penetrometer data. The advent of the piezocone has provided the means for an improved method, and the CPTU method (Eslami and Fellenius method) avoids the mentioned difficulties. Note, however, that all methods, the Eslami-Fellenius as well as the CPT methods, are developed from empirical correlations. Before relying on the CPT or CPTU analysis results, the method used must to be calibrated to the site and the specific conditions and its suitability verified.

7.12 The Lambda Method

Vijayvergia and Focht (1972) compiled a large number of results from static loading tests on essentially shaft bearing piles in reasonably uniform soil and found that, for these test results, the mean unit shaft resistance is a function of depth and could be correlated to the sum of the mean overburden effective stress plus twice the mean undrained shear strength within the embedment depth, as shown in Eq. 7.24.

(7.24) $$r_s = \lambda(\sigma'_m + 2c_m)$$

where r_m = mean shaft resistance along the pile
λ = the 'lambda' correlation coefficient
σ_m = mean overburden effective stress
c_m = mean undrained shear strength

The correlation factor is called "lambda" and it is a function of pile embedment depth, reducing with increasing depth, as shown in Table 7.6.

The lambda method is almost exclusively applied to determining the shaft resistance for heavily loaded pipe piles for offshore structures in relatively uniform soils. Again, the method should be correlated back to an effective stress calculation and the corresponding beta-ratios and N_t-coefficients be determined from the calculation for future reference.

TABLE 7.6
Approximate Values of λ

Embedment (Feet)	(m)	λ (-)
0	0	0.50
10	3	0.36
25	7	0.27
50	15	0.22
75	23	0.17
100	30	0.15
200	60	0.12

7.13 Field Testing for Determining Axial Pile Capacity

The static capacity of a pile is most reliable when determined in a full-scale field static loading test (see Chapter 8). However, the test determines the capacity of the specific tested pile(s), only. The capacity of other piles in the group or at the site must still be determined by analysis, albeit one that now can be calibrated by the field testing. As several times emphasized in the foregoing, all capacity values obtained should be referenced to a static analysis using effective stress parameters. Moreover, despite the numerous static loading tests that have been carried out and the many papers that have reported on such tests and their analyses, the understanding of static pile testing in current engineering practice leaves much to be desired. The reason is that engineers have concerned themselves with mainly one question, only "does the pile have a certain least capacity?" finding little of practical value in analyzing the pile-soil interaction and the load-transfer, i.e., determining the distribution of resistance along the pile and the load-movement behavior of the pile, which aspects are of major importance for the safe and economical design of a piled foundation.

The field test can also be in the form of a dynamic test (Chapter 9), that is, during the driving or restriking of the pile, measurements are taken and later analyzed to determine the static resistance of the pile mobilized during a blow from the pile driving hammer. The small uncertainty involved in transferring the dynamic data to static behavior is offset by having results from more than one pile. Of course, also the capacity from the dynamic test should be referenced to a static analysis.

7.14 Installation Phase

Most design analyses pertain to the service condition of the pile and are not quite representative for the installation (construction) phase. However, as implied above (Section 7.6), it is equally important that the design includes an analysis of the conditions during the installation (the construction, the drilling, the driving) of the piles. For instance, when driving a pile, the stress conditions in the soil are different from those during the service condition. The example presented in Section 7.3 considered service conditions. However, when installing the piles (the example piles are driven piles), the earth fill is not yet placed, which means that the effective stress in the soil is smaller than during the service conditions. More important, during the pile driving, large excess pore pressures are induced in the soft clay layer and, probably, also in the silty sand, which further reduces the effective stress. An analysis imposing increased pore pressures in these layers suggests that the capacity is about 2,200 KN at the end-of-the-initial-driving (EOID) using the depth and effective stress parameters indicated in Table 7.3 for the 32-m installation depth. The subsequent dissipation of the pore pressures will result in an about 600 KN soil increase of capacity due to set-up. (The stress increase due to the earth fill will provide the additional about 200 KN toward the 3,000-KN capacity during the service condition). For details on pile dynamics, see Chapter 9.

The design must include the selection of the pile driving hammer, which requires the use of software for wave equation analysis, called WEAP analysis (Goble et al., 1980; GRL, 1993; Hannigan, 1990). This analysis requires input of soil resistance in the form as result of static load-transfer analysis. For the installation (initial driving) conditions, the input is calculated considering the induced pore pressures. For restriking conditions, the analysis should consider the effect of soil set-up.

By means of wave equation analysis, pile penetration resistance (blow-count) at initial driving, in particular the EOID, and restriking (RSTR) can be estimated. However, the analysis also provides information on what driving stresses to expect, indeed, even the length of time and the number of blows necessary to drive the pile. The most commonly used result is the bearing graph, that is, a curve showing the ultimate resistance (capacity) versus the penetration resistance (blow count). As in the case of the static analysis, the parameters to input to a wave equation analysis can vary within upper and lower limits, which results in not one curve but a band of curves within envelopes as shown in Fig. 7.12.

The input parameters consist of the distribution of static resistance, which requires a prior static analysis. Additional input consists of the particular hammer to use with its expected efficiency, etc., the dynamic parameters for the soil, such as damping and quake values, and many other parameters. It should be obvious that no one should expect a single answer to the analysis. Fig. 7.12 shows that at EOID for the subject example, when the predicted capacity is about 2,200 KN, the penetration resistance (PRES) will be about 10 blows/25 mm through about 20 blows/25 mm.

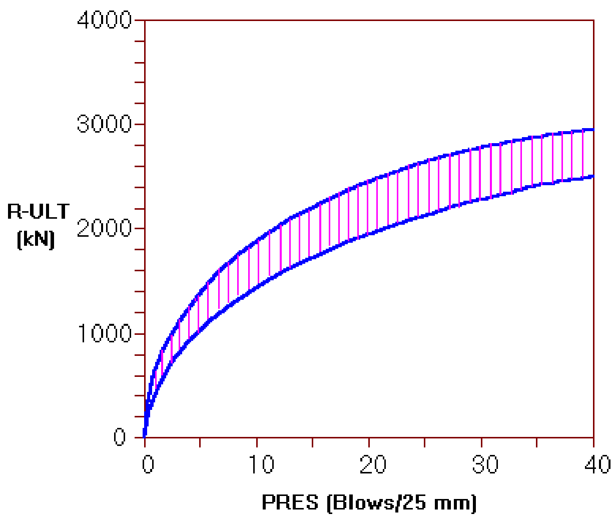

Fig. 7.12 Bearing Graph from WEAP Analysis

Notice that the wave equation analysis postulates observation of the actual penetration resistance when driving the piles, as well as a preceding static analysis. Then, common practice is to combine the analysis with a factor of safety ranging from 2.5 (never smaller) through 3.0.

Fig. 7.12 demonstrates that the hammer selected for the driving cannot drive the pile against the 3,000 KN capacity expected after full set-up. That is, restriking cannot prove out the capacity. This is a common occurrence. Bringing in a larger hammer, may be a costly proposition. It may also be quite unnecessary. If the soil profile is well known, the static analysis correlated to the soil profile and to careful observation during the entire installation driving for a few piles, sufficient information is usually obtained to support a satisfactory analysis of the pile capacity and load-transfer. That is, the capacity after set-up is inferred and sufficient for the required factor of safety.

When conditions are less consistent, when savings may result, and when safety otherwise suggests it to be good practice, the pile capacity is tested directly. Conventionally, this is made by means of a static loading test. Since about 1975, also dynamic tests are often performed (Chapter 9). Static tests are costly and time-consuming, and are, therefore, usually limited to one or a few piles. In contrast, dynamic tests can be obtained quickly and economically, and be performed on several piles, thus providing assurance in numbers. For larger projects, static and dynamic tests are often combined. More recently, new testing methods have been proposed that apply a long-duration impulse to the pile and use the measured response for determining the pile capacity (Chapter 8).

7.15 Structural Strength

Design for structural strength includes consideration of the conditions at the pile head and at the neutral plane. At the pile head, the loads consist of dead and live load (combined with bending and lateral loads at the pile head), but no drag load. At the neutral plane, the loads consist of dead load and drag load, but no live load. (Live load and drag load cannot occur at the same time and must, therefore, not be combined in the analysis).

Most limitations of allowable axial load or factored resistance for piles originate in considerations of the conditions at the pile head, or pile cap, rather, and driving conditions. At the pile cap, the axial load is combined with bending and shear forces. In the driving of a pile, the achievable capacity is not determined by the axial strength of the pile but by the combination of the hammer ability and the pile impedance, EA/c. It does not make sense to apply the same limits to the portion of structural strength to the condition at the neutral pane as at the pile cap. Moreover, it should be recognized that, for axial structural strength of the pile, the design considers a material that is significantly better known and which strength varies less than the soil strength. Therefore, the restrictions on the axial force (the safety factor) should be smaller than those applied to soil strength.

The author recommends that for straight and undamaged piles, the allowable maximum load at the neutral plane be limited to 70 % of the pile axial strength. For composite piles, such as concrete-filled pipe piles, one cannot calculate the allowable stress by adding the "safe" values for the various materials, but must design according to strain compatibility in recognition of that all parts of the pile cross section deforms at the same strain. The author recommends that the allowable load be limited to a value that induces a maximum compression strain of 1 millistrain into the pile with no material becoming stressed beyond 70 % of its strength. See Section 7.17 for a discussion on the location of the neutral plane and the magnitude of the drag load.

7.16 Settlement

The third aspect in the design is the calculation of settlement. Concerns for settlement pertains more to pile groups than to single piles. It must be recognized that a pile group is made up of a number of individual piles which have different embedment lengths and which have mobilized toe resistance to different degrees. The piles in the group have two things in common, however: They are connected to the same pile cap and, therefore, all pile heads move equally, and the piles must all have developed a neutral plane at the same depth somewhere down in the soil (long-term condition, of course). For the neutral plane to be the same (common) for the piles in the group, with the mentioned variation of length, etc., the dead load applied to the pile head from the cap differs between the piles. A pile with a longer embedment below the neutral plane, or one having mobilized a larger toe resistance as opposed to other piles, will carry a greater portion of the dead load on the group. On the other hand, a pile with a smaller toe resistance than the other piles in the group will carry a smaller portion of the dead load. If a pile is damaged at the toe, it is possible that the pile exerts a negative — pulling — force at the cap and thus increases the total load on the piles. For the long-term conditions, the pile stiffness matters little and the load distribution is mainly a function of the resistance below the neutral plane. The approach can be used to discuss the variation of load within a group of piles rigidly connected at the pile head (cap) and will provide a healthy view on the reliability of the results from refined "elastic half sphere" calculation of load distribution in a pile group consisting of piles with different embedment length installed in layered soils.

An obvious result of the development of the neutral plane is that <u>no portion of the dead load is transferred to the soil via the pile cap</u>. Unless, of course, the neutral plane lies right at the pile cap and the entire pile group is at the ultimate resistance. (See the comments on Design of Piled Rafts and Piled Pads, Section 7.5, above).

Above the neutral plane, the soil moves down relative to the pile and below the neutral plane, the pile moves down relative to the soil. Therefore, at the neutral plane, the relative movement between the pile and the soil is zero, or, in other words, whatever the settlement of the soil that occurs at the neutral plane is equal to the settlement of the pile (the pile group) at the neutral plane. Between the pile head and the neutral plane, the settlement is due to deformation of the pile and the magnitude of this 'elastic' shortening is usually small. Therefore, settlement of the pile and the pile group is governed by the settlement of the soil at and below the neutral plane. The soil below the neutral plane is influenced by the stress increase from the permanent load on the pile group and other causes of load, such as the fill. The settlement due to the stress increase caused by the dead load on the piles is usually small to be negligible. It can easily be calculated, however. A simple method of calculation is to exchange the pile group for an equivalent footing with a footprint area equal to the area of the pile cap placed at the depth of the neutral plane. The load on the pile group load is then distributed as a stress on this footing calculating the settlement for this footing stress in combination with all other stress changes at the site, such as the earth fill, potential groundwater table changes, adjacent excavations, etc. Notice that the portion of the soil between the neutral plane and the pile toe depth is 'reinforced' with the piles and, therefore, not very compressible, which must be taken into account.

A fast way to determine the settlement of a pile group is to first calculate the settlement from all stress changes but the pile loads, taking note of the settlement value at the neutral plane **and** at the pile toe. The calculation is then repeated with now also the pile loads (dead load only, live loads do not cause settlement) acting on an equivalent footing placed at the neutral plane, taking note of the settlement at the pile toe. The difference between the first and second calculated <u>settlement at the pile toe</u> level is then added to the first settlement value for <u>the neutral plane location</u> and this value can then be taken as the settlement of the pile group at the neutral plane location. The settlement of the pile group is then this value plus the 'elastic' shortening of the pile above the neutral plane (usually a negligible value). The calculation will also provide an insight in the expected pile toe movement, which governs the pile toe load assigned in the calculation of the neutral plane — the force equilibrium.

7.17 The Location of the Neutral Plane and the Magnitude of the Drag Load

The rules for the static analysis presented in this chapter include merely the most basics of the topic. They are derived from many well-documented case histories from around the world. Some of which are summarized by Fellenius (1998, 2006). One major reference is a case history presented by Endo et al.

(1969) from which work Fig. 7.13 is quoted. The figure shows two diagrams which clearly demonstrates the interdependence of the load-transfer and the movement and settlement behavior.

The left diagram in Fig. 7.13 shows the load distribution measured during almost three years after the installation of a telltale-instrumented steel pile. The loads in the pile increase due to negative skin friction to a maximum drag load value at the neutral plane (NP) and reduce from there due to positive shaft resistance. Note that the shear forces increase with depth and that the negative skin friction in the upper portion of the pile does not increase with the settlement. The paper also presents measurements of pore pressure development showing that they did not change much during the last few years of observation in the upper portion of the soil, which means that the effective stress did not change appreciably during that time in that zone. At depth, however, the pore pressures dissipated with time, and, consequently, the effective stress increased, and, the negative skin friction and positive shaft resistance increased accordingly. Clearly, the shear forces are proportional to the effective overburden stress and its development with time and they are independent of the magnitude of the settlement.

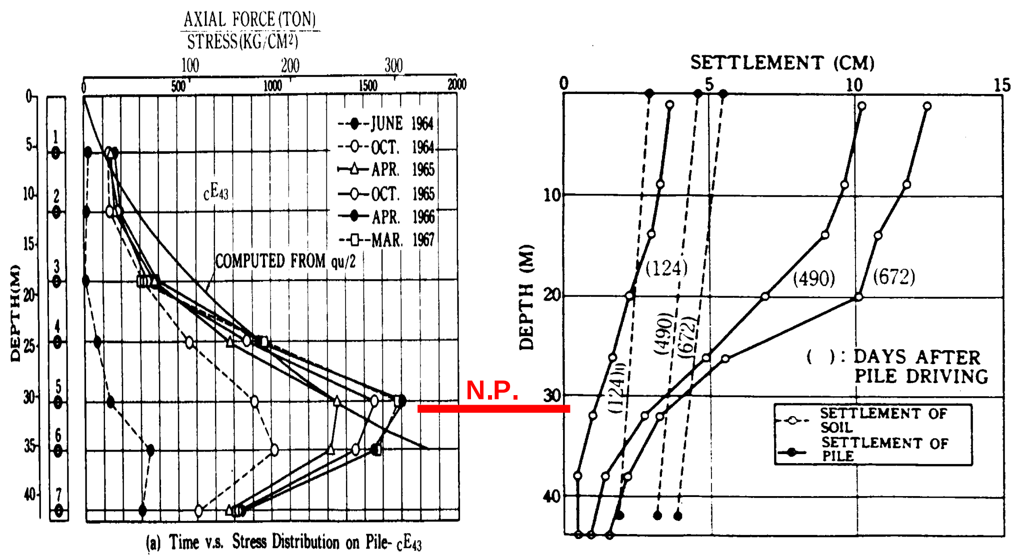

Fig. 7.13 Combination of two diagrams taken from Endo et al. (1969)

The diagram to the right in Fig. 7.13 shows the measured settlement of the soil and the pile over the same time period. Note that the series of settlement curves of the pile and the soil are equal (intersect) at the neutral plane.

Fig. 7.14 presents the principle of determining the interaction between load-transfer and settlement, as well as the associated magnitude of the drag load. The left diagram in Fig. 7.14 shows load-and-resistance curves with distribution of ultimate resistance and two long-term load distributions (marked "1" and "2"), which both start from the dead load applied to the pile. (The dashed extension of the bar at the level of the ground surface indicates the live load also applied to the pile at times, but live load has no influence on a long-term load distributions).

Case 1 and Case 2 are identical with regard to the distributions of ultimate resistance. That is, the two cases would have shown the same load-movement diagram in a static loading test. However, Case 1 is associated with small long-term settlement of the soil. The settlement diagram to the right side diagram shows that while the relative movement between the soil and the pile is sufficient to fully mobilize negative skin friction along the upper portion of the pile and positive shaft resistance in the lower portion, a transition zone exists in between. The length of the transition zone is governed by the distance for which the relative movement between the pile and the soil is very small, smaller than the few millimetre necessary to fully mobilize the shear forces. At a site where the total settlement is small, this minimal relative movement does not materialize nearest the neutral plane and the length of the transition zone can be significant.

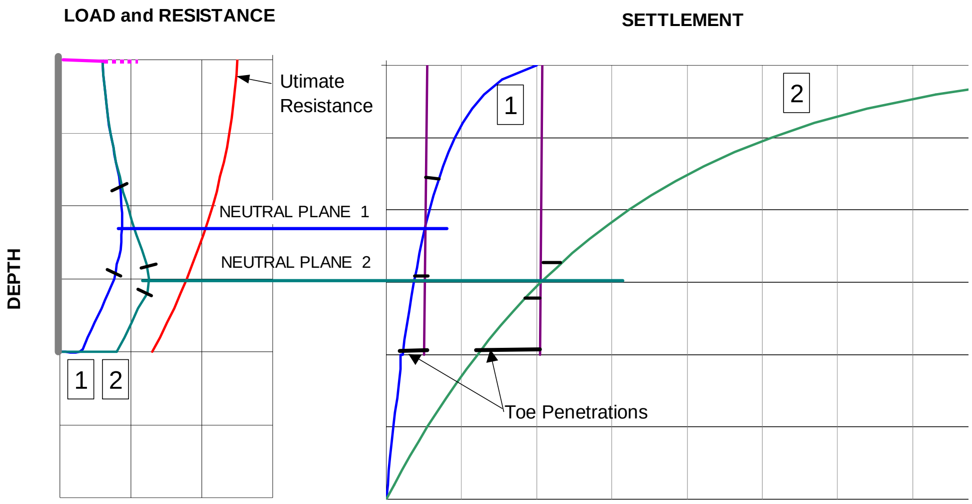

Fig. 7.14 Combination of load-and-resistance diagram and settlement diagram

Fig. 7.14 demonstrates a second important principle. The toe resistance shown in the load diagram is small compared to the ultimate value indicated by the resistance diagram. This is because the toe resistance requires a relatively large movement to become fully mobilized. The toe movement is illustrated as the “toe penetration” in the settlement diagram. The penetration shown for Case 1 is the one that results in the toe resistance shown in the resistance diagram.

Case 2 presents a case where the soil settlement is no longer small. The effect of the larger settlement is that the toe penetration is larger. As a result, the mobilized toe resistance is larger and the point of equilibrium, the neutral plane, has moved down. Moreover, the transition zone is shorter. The maximum load, that is, the sum of the dead load and the drag load, is therefore larger. If the settlement were to become even larger, the toe penetration would increase, the neutral plane would move further down, transition zone would become even shorter, and the drag load would become larger.

For a given resistance distribution, Fig. 7.14 illustrates that the magnitude of the relative settlement between the pile and the soil is one of the factors governing the magnitude of the drag load and the location of the neutral plane. If a pile is installed well into a non-settling layer with a neutral plane that is in that layer or at its upper boundary, then, the toe resistance will be small (in relation to its ultimate value), and the transition zone will be long. The drag load will be correspondingly small (as opposed to a drag load calculated using maximum values of shaft shear and toe resistance and minimal length of the transition zone).

Many use the terms “drag load” and “downdrag” as interchangeable terms, or even in combination: “downdrag load”**!** However, although related, the terms are not synonyms. “Drag load” is the integration of the negative skin friction. Its maximum value occurs at the neutral plane. “Downdrag” refers to the settlement caused by the soil hanging on the pile and dragging it down. The two terms can be said to be the inverse of each other. Where drag load is at its maximum, e.g., for a pile on bedrock, the downdrag is minimal. On the other hand, when the downdrag is large, the drag load is small. Provided the pile strength is not exceeded by the sum of the dead load and the drag load, drag load is beneficial as it merely prestresses the pile, minimizes the 'elastic' compression of the pile due to live loads, etc. In contrast, downdrag is usually undesirable. At a site where the soils are expected to settle, the problem to watch for is the downdrag, not the drag load.

The settlement caused by the load carried by a small group of piles is invariably small. For a group consisting of at least four or five each of rows and columns of piles, the pile loads may affect a large enough volume so that settlement due to the load may become of concern for pile bearing in compressible soil, Normally, however, it is the settlement (i.e. the downdrag) caused by factors outside the pile group that will be of concern. Such factors are embankments or other fills adjacent to the piles and lowering of groundwater table.

Very long piles installed in soils where the settlement is large over most of the length of the piles can be subjected to drag loads that raise concerns for the structural strength of the piles. This is rarely the case for pile of normal size, larger than 0.3 m, before the length exceeds about 40 m.

Figure 7.15 presents the results of a static loading test (O-cell test; see Chapter 8) on a long bored pile and calculations of two alternative distributions of long-term settlement, S_I and S_{II}, at the site. The indicated toe load-movement (Fig. 7.15C) is determined in the O-cell test. The dead load for the pile is 4,000 KN. That is, negative skin friction will develop, and the load in the pile will increase from the dead load value at the pile head down the pile to a maximum at the neutral plane force equilibrium. For Case I, the large soil settlement alternative, the neutral plane will develop at a depth of about 10.2 m. Below the neutral plane, the shaft shear against the pile acts in the positive direction, and, as shown in Fig. 7.15A, the force at the pile toe is equal to the maximum O-cell test load (the example assumptions of supported load and settlement distribution were intentionally selected to give this result). As the measured O-cell load movement diagram (Fig. 7.15C) shows, the movement of the pile toe is then 55 mm. Figure 7.15B illustrates that for this toe movement, and considering the shortening of the pile and the shown interaction between forces and movement, the pile head will settle slightly more than 60 mm. If on the other hand the soil settlement is "small" (Case II), then, the neutral plane is located higher up and the pile toe force is reduced to about 2,300 KN, which only requires a toe movement of 16 mm. By the construction shown in Fig. 7.15B, the pile head will then settle only about 20 mm. (For additional details, see Section 8.15, Figs. 8.27 and 8.28).

7.18 The Unified Design Method for Capacity, Drag Load, Settlement, and Downdrag

Considering the lessons of the quoted case histories, the author (Fellenius 1984, 2004) proposed basing the design of piled foundations on the load-transfer and settlement distributions called "the Unified Pile Design. Section 8.16 provides an example of a project designed per the Unified Design Method.

In summary, the unified design of piled foundations consists of the following steps.

1. Compile all soil data and perform a static analysis of the load-transfer.

2. Verify that the ultimate pile resistance (**capacity**) is at least equal to the factor of safety times the sum of the dead and the live load (the drag load must not be included in this calculation).

3. Verify that the maximum load in the pile, which is the sum of the dead load and the drag load is adequately smaller than the **structural strength** of the pile by an appropriate factor of safety (usually 1.5) or that the strain resulting from the is limited to 1 millistrain (again, do not include the

live load in this calculation). Note, the maximum load is a function of the location of the neutral plane, the degree of mobilization of the toe resistance, the length of the transition zone (the transfer from negative skin friction to positive shaft resistance above and below the neutral plane).

4. Calculate the expected **settlement** profile including all aspects that can result in a change of effective stress at or near the pile(s). Note, settlement due to the pile-supported loads (dead) is mostly determined by load-transfer movements and further settlement applies mostly to relatively large pile group. Verify that the settlement does not exceed the maximum value permitted by the structural design with due consideration of permissible differential settlement. Note that the location of the neutral plane and the pile settlement is a function of the net pile toe movement. It is determined, as illustrated in Fig. 7.15, using known (or test determined, or assumed) distributions of load (dead) and shaft resistance and known (or test determined, or assumed) pile toe load-movement response (q z function) a match is determined between pile toe load and pile toe movement, which controls the location of he neutral plane.

5. Perform wave equation analysis to select the pile driving hammer and to decide on the driving and termination criteria (for driven piles).

6. Observe carefully the pile driving (construction) and verify that the work proceeds as anticipated. Document the observations (that is, keep a complete and carefully prepared log!).

7. When the factor of safety needs to be 2.5 or smaller, verify pile capacity by means of static or dynamic testing.

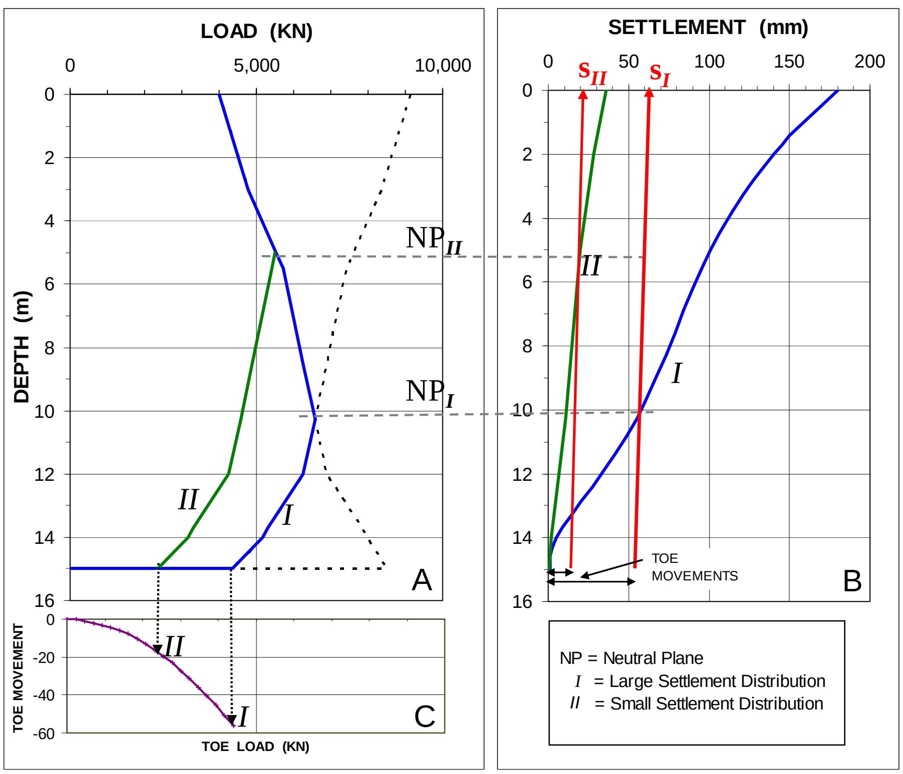

Fig. 7.15 Example of a pile with load and resistance curves determined from a static loading test (O-cell test) and subjected to two alternative distributions of settlement (I and II).

The analysis of the load-transfer curve are illustrated in Fig. 7.16. The diagrams assume that above the neutral plane, the unit negative skin friction, q_n, and positive shaft resistance, r_s, are equal, an assumption on the safe side. Notice, a key factor in the analysis is the estimate of the pile toe resistance. In order to show how the allowable load is determined, Fig. 7.16 assumes that the toe resistance is fully mobilized. This presumes that the settlement is very large (note that no transition zone is shown). If the pile toe resistance is not fully mobilized, the neutral plane lies higher than when the toe resistance is fully mobilized and the length of the transition zone is longer. Of course, this will not affect the allowable load. Further, if the pile toe is located in a non-settling soil and the pile toe resistance is not fully mobilized, the pile settlement will be negligible.

Reducing the dead load on the pile has very little effect on the maximum load in the pile, as illustrated in Fig. 7.16 (left diagram). The diagram to the right is a schematic illustration of the settlement in the soil and the downdrag for the pile. The soil curve is drawn assuming that the soil does settle below the pile toe. The pile cap settlement is the soil settlement at the neutral plane plus the 'elastic' compression of the pile for the load in the pile. Notice, a good deal of this load and associated compression has occurred before the structure is built on the pile foundation.

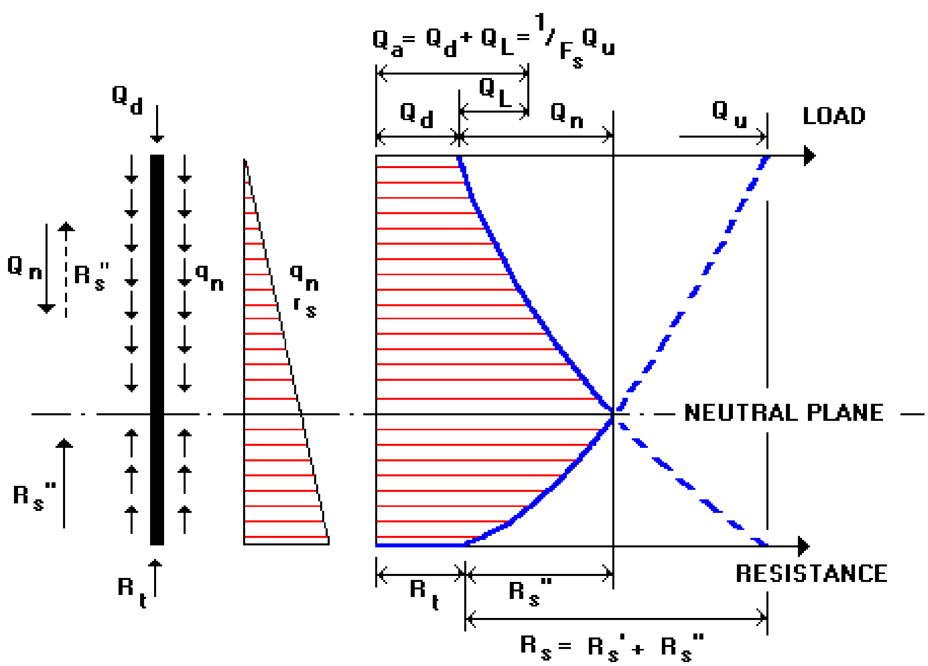

Fig. 7.16 Construing the Neutral Plane and Determining the Allowable Load

Of the design points mentioned above, it is Point 4, the calculation of expected settlement that causes the greatest quandary for design engineers. Settlement of a piled foundation is caused by two factors, A and B, as follows.

A. Load placed on a pile causes downward movements of the pile head due to:

1. 'Elastic' compression of the pile.
2. Load transfer due the movement response of the soil at the pile toe. Along the shaft, movement occurs in the soil, of course, but that is irrelevant. The only soil movement due to

the applied load other than pile shortening affecting the movement at the pile head is that occurring at the pile toe due to load transfer.

3. Settlement below the pile toe due to the increase of stress in the soil. This is only of importance for large pile groups, and where the soil layers below the piles are compressible.

B. Additional settlement can be caused by downdrag, that is, the settlement in the soil due to factors such as fills, lowering of the groundwater table, loads placed on adjacent footings and unsupported floors, etc.

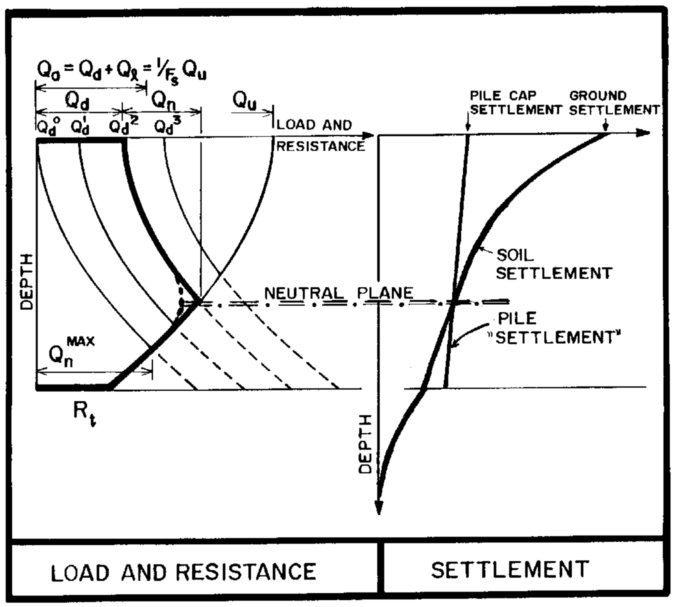

Fig. 7.17 Load-Transfer and Resistance Curves and Settlement Distribution

A drag load will only directly cause movement due to Point A1, the 'elastic' compression. While it could be argued that Point A2 also is at play, because the stiffness of the soil at the pile toe is an important factor here, it is the downdrag that affects (a) the pile toe movement, (b) the pile toe load, and (c) the location of the neutral plane in an interactive — "unified" — process.

The drag load cannot cause settlement due to Point A3, because there has been no stress change in the soil below the pile toe. (Note, the unloading of the soil due to negative skin friction does not result in a heave of those soil layers).

While the principle of the interdependence of the load-transfer and the movement and settlement behavior has general validity, the actual magnitude of the loads and movements varies with the local geology and soil composition. Every design analysis should be referenced to case histories representative for the condition of the specific design, establishing the appropriate boundaries of the soil β and N_t parameters and soil compressibility.

7.19 Piles in swelling soil

Piles in swelling soil are not subjected to negative skin friction, but to positive skin friction. The analysis of the distributions of shaft shear and load in the pile installed in swelling soil follows the same principles as for piles in settling soil, only the directions and signs are reversed. Figures 7.17A and 7.17B illustrate the response of a pile installed through a swelling soil and some distance into a non-swelling soil. The pile is assumed to have a dead load of Q_d at the pile head. The dashed and solid lines in Fig. 7.17A show the distribution of shaft shear in both negative and positive directions. The dashed and solid red line to the left in Fig. 7.17B show the tension load in the pile caused by the swelling soil. The blue line to the right starting at the applied load (Q_d) is the load distribution in the pile reducing with depth due to the swelling tension. The intersection between the two curves is where the neutral plane is located and it is further indicated in Fig. 7.17A by the change between dashed and solid lines indicating the change-over from positive shaft shear (positive skin friction) to negative shaft shear (negative shaft resistance).

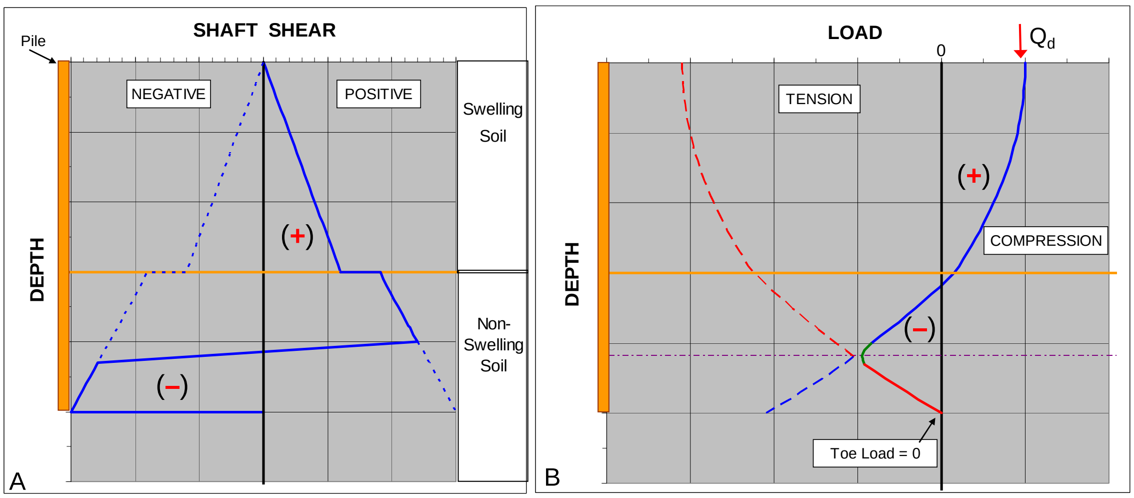

Fig. 7.17 Distributions of unit shaft shear and load for a pile in swelling soil

As a special conditions, Fig. 7.18 shows the load distribution for a pile installed through swelling soil layer and into a settling soil. The pile is subjected to an uplift load. The distribution shows that although the pile is in tension throughout its length, it can still show a net settlement, as the neutral plane lies in the settling soil.

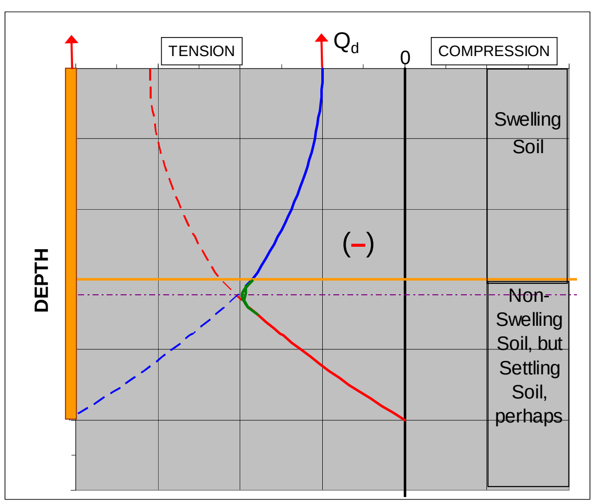

Fig. 7.18 Load distribution for a pile in swelling soil underlain by a settling soil

7.20 Group effect

The analysis of the capacity and resistance distribution detailed in the foregoing deals with analysis of a single pile or small groups of piles, where interaction between the piles does not occur or is negligible. However, for larger groups, the group effect is substantial. For example, neither the shaft resistance (positive or negative direction) nor the negative skin friction, can be larger than the effective (buoyant) weight of the soil between the piles in the group. As an illustrative example, Fig. 7.19 shows a single pile and three groups of piles each pile having a circular 318 mm diameter (the circumference is 1.00 m) and installed at a c/c of 3.14 m, that is, each pile in the groups has a 1.0 m^2 foot print. The foot print of the three pile groups are 6 m by 6 m square, 4 m by 4 m square, and 1 m by 2 m rectangular for 36-pile, 4-pile, and the 2-pile groups, respectively. The piles are installed through a consolidating/settling soil layer of given thickness, *h*, and some distance into a non-settling/bearing layer below. The groundwater table lies at the ground surface and the pore pressure distribution is hydrostatic (disregarding the ongoing consolidation). The dead load from the structure supported on the piles is 1,000 KN and all piles have the same stiffness response to load and the same capacity.

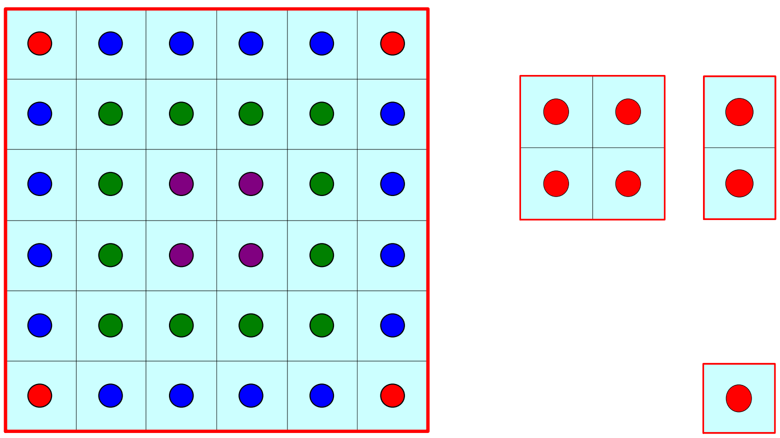

Fig. 7.19 Configuration of the pile groups

The settlement tolerance for the structure supported on the piles and the settlement and potential downdrag in the consolidating layer are such that the neutral plane must not be located higher up than at the boundary between the consolidating layer and the non-settling bearing layer, that is, the neutral plane is at depth *h*. Assuming further that the soil density is 2,000 kg/m^3 and the beta-coefficient, *ß*, is 0.25, then, the drag load on the single pile at depth *h* is $1.25h^2$ KN (= $\Sigma ß\ \sigma'_z$ = 0.25γ' h^2/2). The drag load on a single pile where the consolidating layer is 40 m thick is therefore 2,000 KN.

The drag load on each of the piles making up the 2-pile group and the 4-pile group can be assumed to be equal to that of the single pile. However, the inner ("Center") piles in the 36-pile group are shielded by the outer piles, so the drag load developing on at least for the four innermost piles cannot be larger than that corresponding to the weight of the soil in between the piles. And, each such pile will have a maximum drag load of 10 KN/m in the consolidating layer, that is, a drag load of *10h* KN and 400 KN for *h* = 40 m.

For the innermost piles, the negative skin friction in the upper 4 m is smaller than the weight of the soil, but below 4 m depth, the weight of the soil governs the maximum drag load on the pile. At 8 m depth, the drag load is the same for the inner and the outer pile. Fig. 7.20 shows the distribution of unit negative skin friction and drag load for the two conditions: innermost pile in the center of the group and a single pile.

As indicated, the outer piles will experience a larger amount of drag load as opposed to the inner piles. An approximate pile group effect with regard to the drag load can be assumed to be that the 16 piles making up the inner piles will only have a drag load equal to their share of the weight of the soil, while the outer row of piles along the side of the group will have three "sides" where the maximum negative skin friction is governed by the soil weight and an outward side where the negative skin friction is the full soil strength ($ß\ \sigma'_z$). Similarly, the four corner piles will have two sides governed by the soil weight and two sides governed by the soil strength. By this approach, the maximum drag loads for the side and corner piles at 40 m depth are 800 KN and 1,200 KN, respectively.

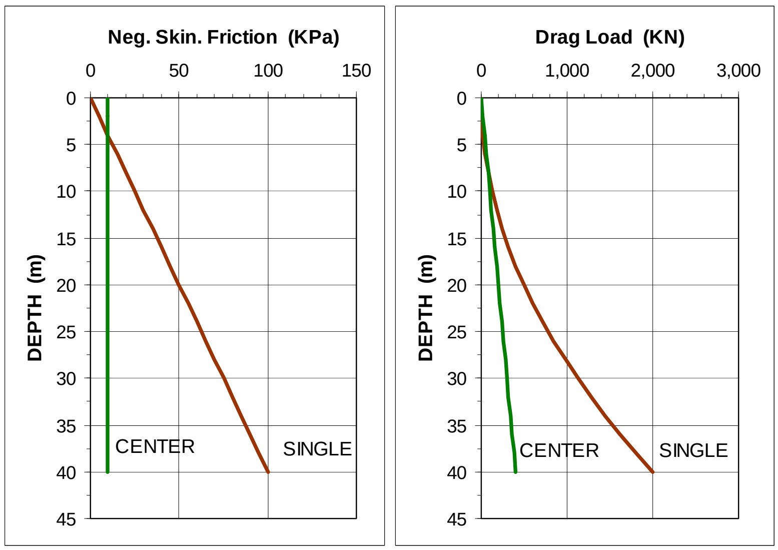

Fig. 7.20 Distributions of unit negative skin friction and of accumulated drag load

The piles in a group connected to a common rigid pile cap must have the same neutral plane location. Therefore, the dead load applied to the pile head must be different for the two conditions, as illustrated in Fig. 7.21.

An alternative approximation could be that all 20 outer row piles have the same drag load as a single pile and the 16 center piles have only a drag load equal to each pile's share of the weight of the soil between the piles. Then, the difference between the piles in ability to support the structure becomes even larger. This is illustrated in Fig. 7.22. Note, were the consolidating layer just a few metre thicker, then, the outer piles would hang in the pile cap, be in tension and actually add load to the inner piles.

Qualitatively, the pile responses show that for a pile group connected by a rigid pile cap, for long-term conditions, the outer rows of piles may not receive much load from the structure, and the pile cap, therefore, needs to be designed considering that the loads will be directed toward the center piles.

The calculations are only hypothetical. In a real pile group, the piles have different length and, in particular, they differ in pile toe response. Figure 7.23 shows the effect on three piles in a pile group, where one pile has been installed to a much larger toe resistance than the neighboring piles and one pile has been damaged during the installation and lost all toe resistance. The condition that all piles must have the same neutral plane location, in comparison to the average pile in the group, i.e., the design pile, results in that the first pile will receive a greater share of the load from the structure while the second pile will actually hang in the pile cap, transferring extra load to the other piles in the group.

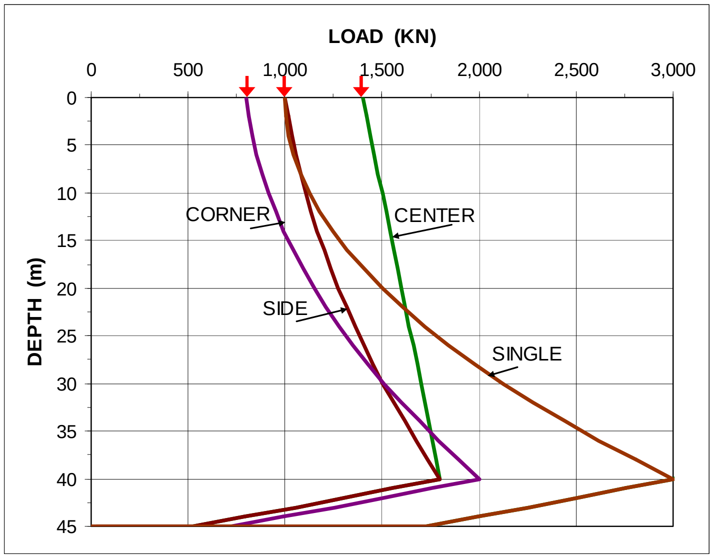

Fig. 7.21 Load distribution in the pile group piles ("Center", "Side", and "Corner") and single pile ("Single), assuming the Center piles fully shielded, and the Center and Corner piles partially shielded from the negative skin friction effect.

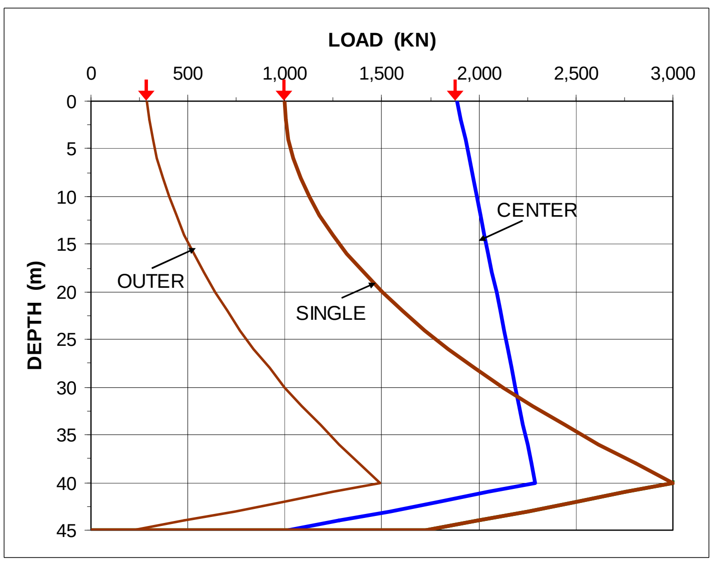

Fig. 7.22 Load distribution in the pile group piles ("Outer" and "Corner") and single pile ("Single), assuming the Center piles fully shielded, and the Outer piles not shielded from the negative skin friction effect.

An important observation is evident. Similarly to that the negative skin friction acting along the inner piles is limited by the weight of the soil, the positive shaft resistance acting along the inner piles is smaller than the soil strength. Therefore, the shaft resistance available to the pile group is not the number of piles times the shaft resistance for a single pile. Instead, the response of the pile group to a load is that of a block of reinforced soil rather than a number of individual piles. The shaft resistance acting (positive in the short-term condition) on the outside of the block (perimeter of the pile group) is small and the response is governed by the effect of the load acting at the pile toe level. Were the load applied to the group to increase, the downward movement of the block would increase as determined by the conditions of the soil below the pile toe level. In the process, the distribution of load between the piles will change to the outer piles receiving the larger load (because positive shaft resistance occurring for the short term response makes their outer piles' response stiffer than the inner piles). For whatever load increase, once the resulting movement has ceased, the negative skin friction will return and the load distribution at the pile cap will again become that of Figs. 7.22 or 7.23.

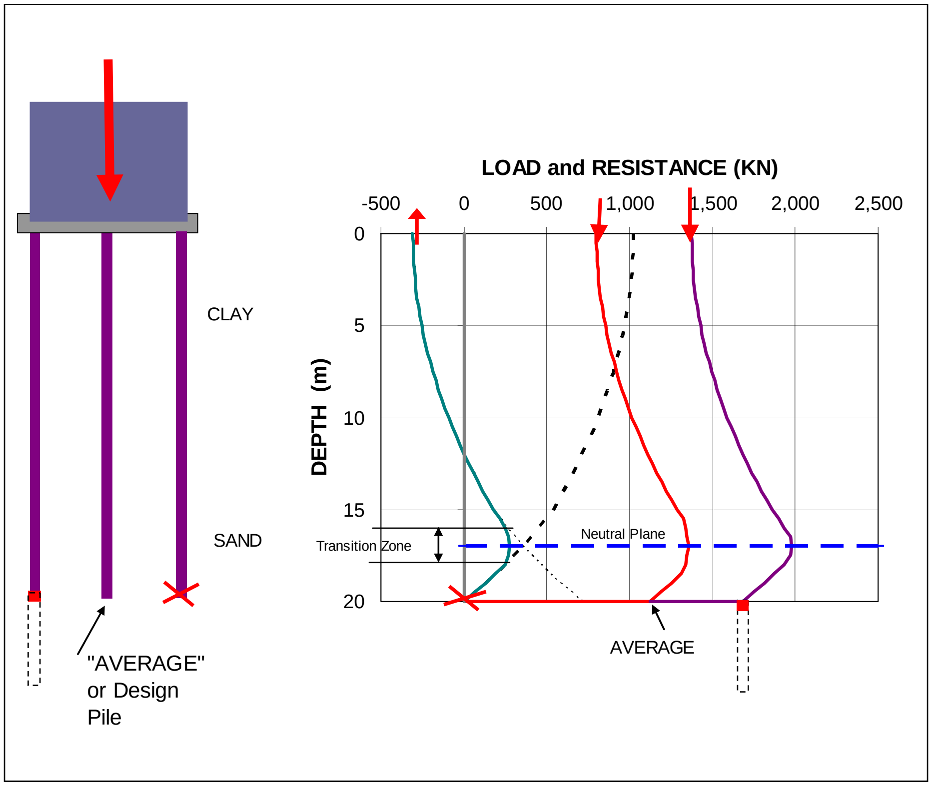

Fig. 7.23 Effect of different toe resistance on the ability of a pile to support the load from the structure.

For design of a pile group, some consider capacity of the group as the sum of the single piles times a reduction factor, a "group efficiency factor". However, the response of a group, such as the example case, is by load-movement and settlement. Estimating group capacity, or group efficiency, is not meaningful. It cannot be emphasized enough that pile design is design for settlement. Design of piles to sound bedrock is easy, the structural strength of the pile governs. Design of piles bearing in competent, low-compressibility soil is similarly easy—the load-movement response at the pile toe will govern (along with pile structural strength; the neutral plane will be at the pile toe or slightly above). Where the soils at the pile toe are less competent, the design of a single pile or small pile groups (along with acceptable settlement value) and, therefore, the neutral plane will be higher up in the soil, the settlement at the neutral plane will govern. For a large pile group, large being a group where inner rows are shielded by outer rows, the design is governed by the settlement at the pile toe elevation. The simplest analysis is then to calculate the settlement for an equivalent footing at the pile toe elevation.

Note, pile design requires that the site investigation is geared to determine the compressibility characteristic in the deeper sol layers, so a settlement analysis can be made. A design based on "*the capacity is with a factor of safety of two or better, so we will have no settlement*" is an inadequate approach as many have learnt to their peril. Note, the settlement is only partially caused by the load on the piles. Unless the pile group is very large (see example in Section 7.21), the bothersome settlement is caused by other factors than the pile loads, such as, fills, groundwater table lowering, neighboring structures, etc.

7.21 An example of settlement of a large pile group

A large pile group consists of s number of individual piles, of course. However, the design of a large pile group is not a summation of so many single piles. As indicated in Section 7.20, considering usual spacing between piles, the shaft resistance per pile is small or non-existing. The design is simply best taking the foundation as a pile-reinforced block of soil with a proportioned stiffness and then to calculate the settlement of the soil below this block. Capacity is not an issue, which will be illustrated in the following.

Measurements of settlement of a large pile group piled foundation for a grain terminal in Ghent are presented by Goossens and VanImpe (1991). A series of circular silos are placed on a 1.2 m thick concrete raft with length of 84 m and width of 34 m. The soil profile at the site is indicated by the cone stress diagram (q_c) shown in Fig. 7.24A. The soils consist of clayey sand to 15 m depth followed by a 5 m thick clay layer and a 3 m thick sand layer underlain by clay. A very dense sand layer is found at 38 m depth.

The stress applied over the raft footprint from the fully loaded silos is about 300 KPa, which was distributed on 41 rows and 17 columns of piles, total 697 piles, as shown in Fig. 7.24B. The piles consisted of 520 mm diameter expanded base piles (Franki piles) with a 680 mm expanded base placed at a depth of 13.4 m. The pile center-to-center spacing, c/c, is 2.00 m. The results of two static loading tests, Fig. 7.24C, were used to decide on an allowable load of 1,500 KN/pile. However, the actual load is indicated to be closer to 1,300 KN/pile. The results of the two static loading tests show that at the load of 1,300 KN, the pile head moved a mere 3 mm.

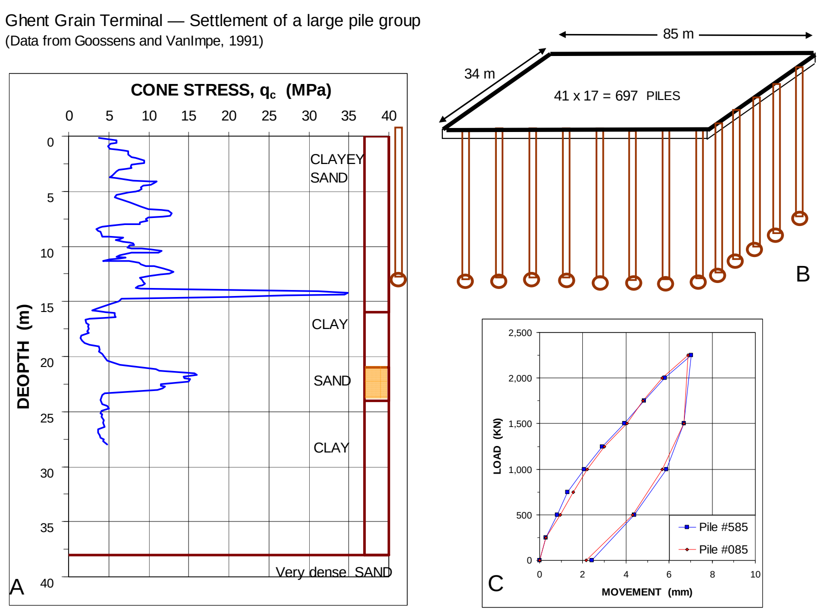

Fig. 7.24 Soil profile (A), pile group (B), and load-movement in two static loading tests

The settlement of the raft was measured at five benchmarks located along the side of the raft as indicated in Fig. 7.25. The monitoring of the settlement started when the raft was cast and continued for 10.5 years as the silo was getting full load. Benchmark BM 4 (the benchmark nearest a lightly loaded tower building at one gable side of the raft) was only monitored for the first 1,245 days. Fig. 7.25 also shows the settlements measured on seven occasions up to 3,880 days after start. The diagram indicates that the settlements at the center and corner of the long side of the building was about 180 mm and 110 mm. The 70-mm differential settlement corresponds to a slope of about 0.2 %, or 1 in 500.

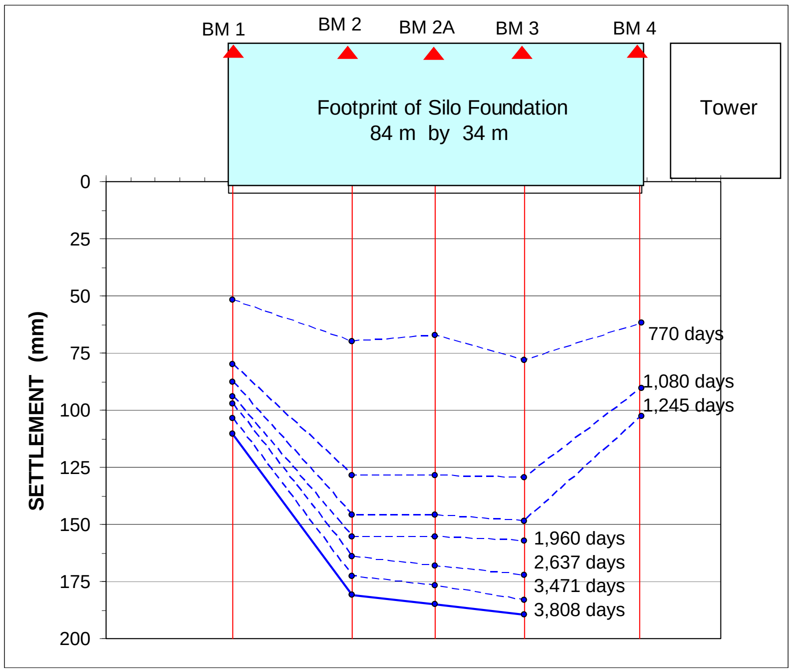

Fig. 7.25 Soil settlement monitored at five benchmarks along the side of the raft.

The observed settlements at the middle of the raft side can be used to calibrate the soil compressibility. One can assume that the compressibility of the upper clayey sand within the piled zone derives its stiffness from a combined soil and concrete, which makes its compressibility very small, indeed. Then, carrying out a settlement calculation matched to the 180-mm value for an equivalent raft placed at the pile toe depth returns a 110-mm value for the settlement at the raft corner (BM 1), that is, a value in approximate agreement with the measured value. The same load and stress input results in 290 mm settlement calculated for the center of the raft.

The case history shows clearly, as also pointed out by Goossens and VanImpe (1991), that the load-movement of the static loading test bears little relation to the settlement of the raft. As indicated, the raft settlement is best calculated as the settlement of an equivalent raft placed at the pile toe depth.

Moreover, the bearing capacity of the individual pile is not governing the response of the raft to the applied load. It is obvious that the pile spacing could have been widened to, say, 3.00 m from the 2.00 m value used without resulting in any larger settlement or inadequate response of the foundation. This change would have resulted in a halving of the number of piles and considerable savings of costs and construction time.

Indeed, the foundation could have been turned into a piled pad foundation (See Section 7.5) by not connecting the piles to the raft. The densification of the upper 13.4 m zone would have been the same and the settlement below the piles would have been unchanged. The case history demonstrates conclusively that the design of a large pile group is not the same as the design of single piles or small pile groups.

7.22 A few related comments

7.22.1 Pile Spacing

Determining the size of the pile cap is a part of the design. The size is decided by the pile diameter, of course, and the number of piles in the pile group. The decisive parameter, however, is the spacing between the piles. Pile caps are not cheap, therefore, piles are often placed close together at center-to-center spacings of only 2.5 to 3 pile diameters. A c/c spacing of 2.5 diameters can be considered O.K. for short toe-bearing piles, but it is too close for long shaft-bearing piles. The longer the pile, the larger the risk for physical interference between the piles during the installation, be the piles driven or bored. Therefore, the criterion for minimum pile spacing must be a function of the pile length. A suggestion is given in Eq. 7.25.

(7.25) $$c/c = 2.5b + 0.02D$$

where
- c/c = minimum center-to-center pile spacing
- b = pile diameter (face to face for non circular pile section)
- D = pile embedment length

The pile spacing for a group of long piles can become large and result in expensive pile caps. For example, Eq. 7.25 requires a spacing of 1.75 m (3.5 diameter) for a group of nine 0.5 m diameter, 50 m long piles. However, the spacing at the pile head can be appreciably reduced, if the outer row(s) of piles are inclined outward by a small amount, say, 1(vertical):10(horizontal) or even 1(vertical):20(horizontal).

7.22.2 Design of Piles for Horizontal Loading

Because foundation loads act in many different directions, depending on the load combination, piles are rarely loaded in true axial direction only. Therefore, a more or less significant lateral component of the total pile load always acts in combination with an axial load. The imposed lateral component is resisted by the bending stiffness of the pile and the shear resistance mobilized in the soil surrounding the pile.

An imposed horizontal load can also be carried by means of inclined piles, if the horizontal component of the axial pile load is at least equal to and acting in the opposite direction to the imposed horizontal load. Obviously, this approach has its limits as the inclination cannot be impractically large. It should, preferably, not be greater than 4(vertical) to 1(horizontal). Also, only one load combination can provide the optimal lateral resistance.

In general, it is not correct to resist lateral loads by means of combining the soil resistance for the piles (inclined as well as vertical) with the lateral component of the vertical load for the inclined piles. The reason is that resisting an imposed lateral load by means of soil shear requires the pile to move against the soil. The pile will rotate due to such movement and an inclined pile will then either push up against or pull down from the pile cap, which will substantially change the axial load in the pile.

Buried pile caps and foundation walls can often contribute considerable to the lateral resistance (Mokwa and Duncan 2001). The compaction and stiffness response of the backfill and natural soil then becomes an important issue.

In design of vertical piles installed in a homogeneous soil and subjected to horizontal loads, an approximate and usually conservative approach is to assume that each pile can sustain a horizontal load equal to the passive earth pressure acting on an equivalent wall with depth of 6b and width 3b, where b is the pile diameter, or face-to-face distance (Canadian Foundation Engineering Manual, 1985, 1992).

Similarly, the lateral resistance of a pile group may be approximated by the soil resistance on the group calculated as the passive earth pressure over an equivalent wall with depth equal to 6b and width equal to:

(7.26) $$L_e = L + 2B$$

where L_e = Equivalent width

L = the width of the pile group in the plan <u>perpendicular</u> to the direction of the imposed loads

B = the width of the equivalent area of the group in a plane <u>parallel</u> to the direction of the imposed loads

The lateral resistance calculated according to Eq. 7.26 must not exceed the sum of the lateral resistance of the individual piles in the group. That is, for a group of **n** piles, the equivalent width of the group, $\mathbf{L_e}$, must be smaller than **n** times the equivalent width of the individual pile, **6b**. For an imposed load not parallel to a side of the group, calculate for two cases, applying the components of the imposed load that are parallel to the sides.

The very simplified approach expressed above does not give any indication of movement. Nor does it differentiate between piles with fixed heads and those with heads free to rotate, that is, no consideration is given to the influence of pile bending stiffness. Because the governing design aspect with regard to lateral behavior of piles is lateral displacement, and the lateral capacity or ultimate resistance is of secondary importance, the usefulness of the simplified approach is very limited in engineering practice.

The analysis of lateral behavior of piles must consider two aspects: First, the pile response**:** the bending stiffness of the pile, how the head is connected (free head, or fully or partially fixed head) and, second, the soil response: the input in the analysis must include the soil resistance as a function of the magnitude of lateral movement.

The first aspect is modeled by treating the pile as a beam on an "elastic" foundation, which is done by solving a fourth-degree differential equation with input of axial load on the pile, material properties of the pile, and the soil resistance as a nonlinear function of the pile displacement.

The derivation of lateral stress may make use of a simple concept called "coefficient of subgrade reaction" having the dimension of force per volume (Terzaghi, 1955). The coefficient is a function of the soil density or strength, the depth below the ground surface, and the diameter (side) of the pile. In cohesionless soils, the following relation is used:

(7.27) $$k_s = n_h \frac{z}{b}$$

where k_s = coefficient of horizontal subgrade reaction
n_h = coefficient related to soil density
z = depth
b = pile diameter

The intensity of the lateral stress, p_z, mobilized on the pile at Depth z follows a "p-y" curve as shown in Eq. 7.28.

(7.28) $$p_z = k_s\, y_z\, b$$

where y_z = the horizontal displacement of the pile at Depth z

Combining Eqs. 7.27 and 7.28**:**

(7.29) $$p_z = n_h\, y_z\, z$$

The relation governing the behavior of a laterally loaded pile is then as follows**:**

(7.30) $$Q_h = EI\,\frac{d^4y}{dx^4} + Q_v\,\frac{d^2y}{dx^2} - p_z$$

where Q_h = lateral load on the pile
EI = bending stiffness (flexural rigidity) (Note, for concrete piles, the bending stiffness reduces with bending moment)
Q_v = axial load on the pile

Design charts have been developed that, for an input of imposed load, basic pile data, and soil coefficients, provide values of displacement and bending moment. See, for instance, the Canadian Foundation Engineering Manual (1985, 1992). The software LPile of Ensoft Inc. is a most useful program for analysis lateral response of piles and its manual provides a solid background to the topic.

The design charts cannot consider all the many variations possible in an actual case. For instance, the p-y curve can be a smooth rising curve, can have an ideal elastic-plastic shape, or can be decaying after a peak value. As an analysis without simplifying shortcuts is very tedious and time-consuming, resort to charts has been necessary in the past. However, with the advent of the personal computer, special software has been developed, which makes the calculations easy and fast. In fact, as in the case of pile driving analysis and wave equation programs, engineering design today has no need for computational simplifications. Exact solutions can be obtained as easily as approximate ones. Several proprietary and public-domain programs are available for analysis of laterally loaded piles.

One must not be led to believe that, because an analysis is theoretically correct, the results also predict to the true behavior of the pile or pile group. The results must be correlated to pertinent experience, and, lacking this, to a full-scale test at the site. If the experience is limited and funds are lacking for a full-scale correlation test, then, a prudent choice is necessary of input data, as well as of margins and factors of safety.

Designing and analyzing a lateral test is much more complex than for the case of axial behavior of piles. In service, a laterally loaded pile almost always has a fixed-head condition. However, a fixed-head test is more difficult and costly to perform as opposed to a free-head test. A lateral test without inclusion of measurement of lateral deflection down the pile (bending) is of limited value. While an axial test should not include unloading cycles, a lateral test should be a cyclic test and include a large number of cycles at different load levels. The laterally tested pile is much more sensitive to the influence of neighboring piles than is the axially tested pile. Finally, the analysis of the test results is very complex and requires the use of a computer and appropriate software.

7.22.3 Seismic Design of Lateral Pile Behavior

A seismic wave appears to a pile foundation as a soil movement forcing the piles to move with the soil. The movement is resisted by the pile cap, bending and shear are induced in the piles, and a horizontal force develops in the foundation, starting it to move in the direction of the wave. A half period later, the soil swings back, but the pile cap is still moving in the first direction, and, therefore, the forces increase. This situation is not the same as one originated by a static force.

Seismic lateral pile design consists of determining the probable amplitude and frequency of the seismic wave as well as the natural frequency of the foundation and structure supported by the piles. The first requirement is, as in all seismic design, that the natural frequency of the foundation and structure must not be the same as that of the seismic wave (a phenomenon called "resonance"). Then, the probable maximum displacement, bending, and shear induced at the pile cap are estimated. Finally, the pile connection and the pile cap are designed to resist the induced forces.

In the past, seismic design consisted of assigning a horizontal force equal to a quasi-static load as a percentage of the gravity load from the supported structure, e.g., 10 %, proceeding to do a static design. Often this approach resulted in installing some of the piles as inclined piles to resist the load by the horizontal component of the axial force in the inclined piles. This is not just very arbitrary, it is also wrong. The earthquake does not produce a load, but a movement, a horizontal displacement. The force is simply the result of that movement and its magnitude is a function of the flexural stiffness of the pile and its connection to the pile cap. The stiffer and stronger the stiffness, the larger the horizontal load. Moreover, while a vertical pile in the group will move sideways and the force mainly be a shear force at the connection of the piles to the pile cap, the inclined pile will rotate and to the extent the movement is parallel to the inclination plane and in the direction of the inclination, the pile will try to rise. As the pile cap prevents the rise, the pile will have to compress, causing the axial force to increase. As a result of the increased load, the pile could be pushed down. Moreover, the pile will take a larger share of the total load on the group. The pile inclined in the other direction will have to become longer to stay in the pile cap and its load will reduce — the pile could be pulled up or, in the extreme, be torn apart. Then when the seismic action swings back, the roles of the two inclined piles will reverse. After a few cycles of seismic action, the inclined piles will have punched through the pile cap, developed cracks, become disconnected from the pile cap, lose bearing capacity — essentially, the foundation could be left with only the vertical piles to carry the structure, which might be too much for them. If this worst scenario would not occur, at least the foundation will be impaired and the structure suffer differential movements. Inclined piles are not suitable for resisting seismic forces. If a piled foundation is expected to have to resist horizontal forces, it is normally better to do this by means other than inclined piles.

An analysis of seismic horizontal loads on vertical piles can be made by static analysis. However, one should realize that the so-determined horizontal force on the pile and its connection to the pile cap is not a force casing a movement, but one resulting from an induced movement — the seismic displacement.

7.22.4 Pile Testing

A pile design should consider the need and/or value of a pile test. A "routine static loading test" involving only loading the pile head to twice the allowable load and recording the pile head movement is essentially only justified if performed for proof testing reasons. It is rarely worth the money and effort, especially if the loading procedure involves just a few (eight or so) load increments of different duration and/or an unloading sequence or two before the maximum load. The only information attainable from such a test is that the pile capacity was not reached. If it was reached, its exact value is difficult to determine and the test gives no information on the load-transfer and portion of shaft and toe resistance.

In contrast, a static loading test performed building up the applied load by a good number of equal load increments with constant duration, no unloading, to a maximum load at least equal to twice the allowable load and on an instrumented pile (designed to determine the load-transfer) will be very advantageous for most projects. If performed during the design phase, the results can provide significant benefits to a project. When embarking on the design of a piling project, the designer should take into account that a properly designed and executed pile test can save money and time as well as improve safety. The O-cell test will meet all objectives of a properly designed test. A dynamic test with proper analysis (CAPWAP) will also provide valuable information on load-transfer, pile hammer behavior, and involve testing of several piles.

For detailed information on pile testing and analysis of pile tests, see Chapter 8.

7.22.5 Pile Jetting

Where dense soil of limitations of the pile driving hammer hampers the installation of a pile, or just to speed up the driving, jetting is often resorted to. The water jet serves to cut the soil ahead of the pile toe. For hollow piles, pipe piles and cylinder piles, the spoils are let to flow up inside the pile. When the flow is along the outside of the pile, the effect is a reduction of the shaft resistance, sometimes to the point of the pile sinking into the void created by the jet. The objective of the jetting may range from the cutting of the dense soil ahead of the pile toe or just to obtain the lubricating flow along the pile shaft. When the objective is to cut the soil, a small diameter jet nozzle is needed to obtain a large velocity jet. When the objective is to obtain a "lubricating" flow, the jet nozzle is larger to provide for the needed flow of water. It is necessary to watch for the water flowing up along the pile does not become so large that the soil near the surface can erode resulting a crater that makes the pile loose lateral support. It is also necessary to ensure that the jetting cutting is symmetrical so that the pile will not drift to the side. For this reason, outside placement of jetting pipes is risky as opposed to inside jet placement, say, in a center hole cast in a concrete pile.

Water pumps for jetting are large-volume, large-pressure pumps that provide small flow at large pressure and large flow at small pressure. The pumps are usually rated for 200 gal/min to 400 gal/min, i.e., 0.01 m^3/s to 0.02 m^3/s to account for the significant energy loss occurring in the pipes and nozzle during jetting. The flow is simply measured by a flow meter. However, to measure the pump pressure is difficult. The flow rate (volume/time) at the pump and out through the jet nozzle and at any point in the system is the same. However, the pressure at the jet nozzle is significantly smaller than the pump pressure due to energy losses. The governing pressure value is the pressure at the jet nozzle, of course. It can quite easily be determined from simple relations represented by Eq. 7.31 (Toricelli's relation) and Eq. 7.32 (Bernoulli's relation) combined into Eq. 7.33. The relations are used to design the jet nozzle as appropriate for the requirements of volume (flow) and jetting pressure in the specific case.

(7.31) $$Q = \mu A v$$

where Q = flow rate (m^3/s)
μ = jetting coefficient ≈0.8
A = cross sectional area of nozzle
v = velocity (m/s)

(7.32) $$\frac{v^2}{2g} = \frac{p}{\gamma}$$ which converts to: Eq. 7.32a $$v^2 = \frac{2p}{\rho}$$

where v = velocity (m/s)
g = gravity constant (m/s^2)
p = pressure difference between inside jet pipe at nozzle and in soil outside
γ = unit weight of water (KN/m^3)
ρ = unit density of water (kg/m^3)

(7.33) $$A = \frac{Q\sqrt{\rho}}{\mu\sqrt{2p}}$$

where A = cross sectional area of nozzle
Q = flow rate (m^3/s)
μ = jetting coefficient ≈0.8
ρ = unit density of water (kg/m^3); ≈1,000 kg/m^3
p = pressure; difference between inside jet pipe at nozzle and in soil outside

When inserting the values (0.8 and 1,000) for μ and ρ into Eq. 7.33a, produces Eq. 7.34.

(7.34) $$A = 28\frac{Q}{\sqrt{p}}$$

For example, to obtain a cutting jet with a flow of 1 L/s (0.001 m^3/s; 16 us gallons/minute) combined with a jet pressure of 1.4 KPa (~200 psi), the cross sectional area of the jet nozzle need to be 7 cm^2. That is, the diameter of the nozzle needs to be 30 mm (1.2 inch).

During jetting and after end of jetting, a pile will have very small toe resistance. Driving of the pile must proceed with caution to make sure that damaging tensile reflections do not occur in the pile.

The shaft resistance in the jetted zone is not just reduced during the jetting, the shaft resistance will also be smaller after the jetting as opposed to the conditions without jetting. Driving the pile after finished jetting will not improve the reduced shaft resistance.

7.22.6 Bitumen Coating

When the drag load (plus dead load) is expected to be larger than the pile structural strength can accept, or the soil settlement at the neutral plane (settlement equilibrium) is larger than the structure can tolerate, the drag load (the negative skin friction) can be reduced by means of applying a coat of bitumen (asphalt) to the pile surface. Resort to such reduction of shaft shear is messy, costly, and time-consuming. In most cases, it is also not necessary, when the long-term conditions for the piles and the piled foundation are properly analyzed. Moreover, other solutions may show to be more efficient and useful. However, bitumen coating is efficient in reducing negative skin friction and the drag load, as well as in lowering the neutral plane. Note, a bitumen coat will equally well reduce the positive shaft resistance and, hence, lower the pile capacity. The coat can be quite thin, a layer of 1 mm to 2 mm will reduce the negative skin friction to values of 25 % through 10 % of the value for the uncoated pile. The primary concern lies with making sure that the bitumen is not scraped off or spalls off in driving the pile. The bitumen is usually heated and brushed on to the pile. In a cold climate, the coat can spall off, i.e., loosen and fall off in sheets "sailing" down from the piles, which risks for severe damage to people down below. In a hot climate, the coat may flow off the pile before the pile is driven. A dusty pile surface — be it a concrete pile or steel pile — may have to be primed by "painting" the surface with very thin layer of heated, hard bitumen before applying the shear layer. Fig. 7.26 illustrate brushing the shear layer onto a primed surface of a concrete pile. Figure 7.27 shows the coated pile when driven through a protective casing. Note that the bitumen has flowed and formed a belly under the pile after the coating was applied.

Fig. 7.26 View of work under way to apply a bitumen coat to a concrete pile.

Fig. 7.26 View of a bitumen-coated pile driven through a protective casing. The left side of the pile was the pile underside in storage.

A functional bitumen coat on a pile to reduce shaft resistance can be obtained from a regular bitumen supplier. The same bitumen as used for road payment can be used. Be careful about roofing bitumen as often some fibers have been added to make it flow less. Note also, that driving through coarse soil will scrape off the bitumen coat—even a "thick one"—and preboring, or driving through a pre-installed casing, or another means to protect the bitumen, may be necessary. Moreover, in hot weather, it may be necessary to employ a two-layer bitumen coat to ensure that the bitumen will not flow off between coating the pile and driving it. The inner coat is the about 1 mm to 2 mm "slip coat" and an outer coat of about the same thickness of very stiff bitumen is then apply to cover the inner coat to keep it in place.

The range of bitumen to use depends a bit on the climate of the site location. The ground temperature is about equal to the average annual temperature of the site. Therefore, a harder bitumen is recommended for use in tropical climate than in a cold climate. For most sites, a bitumen of penetration 80/100 (ASTM D946) is suitable (Fellenius 1975).

7.22.7 Pile Buckling

Buckling of piles is are often thought to be a design condition, and in very soft, organic soils, buckling could be an issue. However, even the softest inorganic soil is able to confine a pile and prevent buckling. The corollary to the fact that the soil support is always sufficient to prevent a pile from moving toward or into it, is that when the soils moves, the pile has no option other than to move right along. Therefore, piles in slopes and near excavations, where the soil moves, will move with the soil. Fig. 7.28 is a 1979 photo from Port of Seattle and shows how 24-inch prestressed piles supporting a dock broke when a hydraulic fill of very soft silt flowed against the piles.

Fig. 7.28 View of the consequence of a hydraulic fill of fine silt flowing against 24-inch piles

7.22.8 Plugging of open-two pipe piles and in-between flanges of H-piles

Plugging of the inside of a pipe pile driven open-toe is a common occurrence. The question often raised is how the presence of a plug should be considered in a design analysis. First, there is the question if the soil inside the pipe is really a plug, or just a soil column over which the pipe slides. If it is a column, clearly, as the pile moves against the column, shaft resistance develops along the interface between the pipe inside and the column. However, while the "outside" shaft resistance can be, and should be, calculated using the overburden effective stress, the "inside" shaft resistance is harder to determine. The push on the column from the shaft resistance mobilized along the upper portion of the column will be the source of an increase of stress from the column that, through the "Poisson's Ratio effect", will increase the lateral stress against the inside further down the column. If electing to use total stress analysis, one avoids that problem, but not the problem of determining the magnitude of the inside shaft resistance. The general view appears to be that the inside shear force is smaller than the outside. The issue of set-up is also different and unknown.

If a plug has formed, the issue is easier, as a definite plug that moves down with the pile, will simply cause the pile to act as a closed-toe pile. The soil mass inside will be of importance for the driving, but not for the static shaft resistance and the plug will provide the pile with a larger toe resistance than had instead a column formed. For design, it is a matter of whether to trust this toe resistance to be available in the long-term, of course. In case of an open-toe pipe driven through soft or loose soil and into a competent dense soil therein forming a base, the so-obtained toe resistance can be trusted in most conditions.

Plugging can also occur in-between the flanges of an H-pile. If an H-pile has developed a "column", then the shaft resistance can be calculated on the total circumference, the "H", If a plug, the shaft resistance should be calculated on the "square". The similar approach applies to the toe of the H-pile, but a bit more cautiously. Analyzing an H-pile is harder than analyzing an open-toe pipe pile, because the plug/column can occur along different length of the pile, Indeed, also at different times during the short interval of the driving impact.

The issue of plug/column is not a major one for land-piles or short marine piles. However, it is a major issue for offshore piles used for support of offshore platforms. However, such foundations are not part of this brief text.

7.22.9 Sweeping and bending of piles

Practically all piles, particularly when driven, are more or less out of design alignment, and a perfectly straight pile is a theoretical concept, seldom achieved in practice. It should be recognized that the deviation from alignment of a deep foundation unit has little influence on its geotechnical capacity. Assigning a specific tolerance value of deviation, say, a percentage of inclination change only applies to the pile at the pile cap or cut-off location (as does a specific deviation of location).

When long piles are driven into any type of soil, or shorter piles driven through soils containing obstructions, the piles can bend, dogleg, and even break, without this being recognized by usual inspection means after the driving. Pipe piles, and cylinder concrete piles, that are closed at the toe provide the possibility of inspection of the curvature and integrity given by the open pipe. A closed-toe pile that was filled with soil during the driving can be cleaned out to provide access to the inside of the pile. It is normally not possible to inspect a precast concrete pile or an H-pile for bending. However, by casting a center tube in the precast concrete pile and a small diameter pipe to the flanges of the H-pile before it is driven, access is provided for inspection down the pile after driving.

The location of a pile and its curvature can be determined from lowering an inclinometer down the pile, if access is provided by the open pipe or through a center pipe. Fig. 7.29 show an example of deviations between the pile head and pile toe locations for a group of 60 m (200 ft) long, vertically driven prestressed piles in soft soil (Keehi Interchange, Hawaii. The piles were made from two segments spliced with a mechanical splice. The main cause of the deviations was found to be that the piles were cast with the pile segment ends not being square with the pile. When this was corrected, the piles drove with only small deviations).

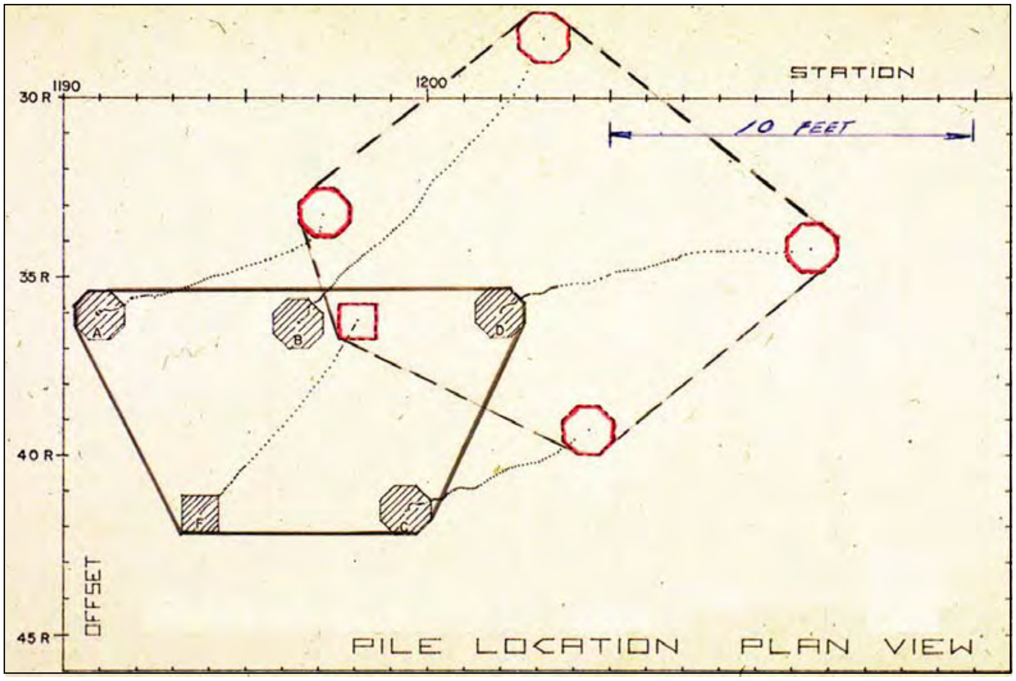

Fig. 7.29 Example of deviations determined by inclinometer measurements in 60 m long prestressed piles. Principle of the curvature probe

For a pipe pile, inspection down the open pile is often only carried out by lowering a flashlight into the pipe, or center tube, to check that the pile is sound, which it is considered to be if the flash light can reach the bottom of the pile while still being seen from above. However, dust and water can obstruct the light, and if the light disappears because the pile is bent, there is no possibility to determine from this fact whether the pile is just gently sweeping, which is of little concern, or whether the pile is severely bent, or doglegged. In such a case, a specially designed, but simple, curvature probe can be used to vindicate undamaged piles, and to provide data for aid in judging and evaluating a suspect pile.

The curvature probe consists of a stiff, straight pipe of dimensions so chosen that it, theoretically, will 'jam' inside the pipe, or center tube, at a predetermined limiting bending radius expressed in Eq. 7.35 (Fellenius 1972).

(7.35) $$R = \frac{L^2}{8t} = \frac{L^2}{8(D_1 - D_2)}$$

Where
- R = Bending radius
- L = Probe length
- t = Annulus D_1 - D_2
- D_1 = Inside diameter of the pile or center tube
- D_2 = Outside diameter of the curvature probe

The principle of the use of the curvature probe are illustrated in Fig. 7.30.

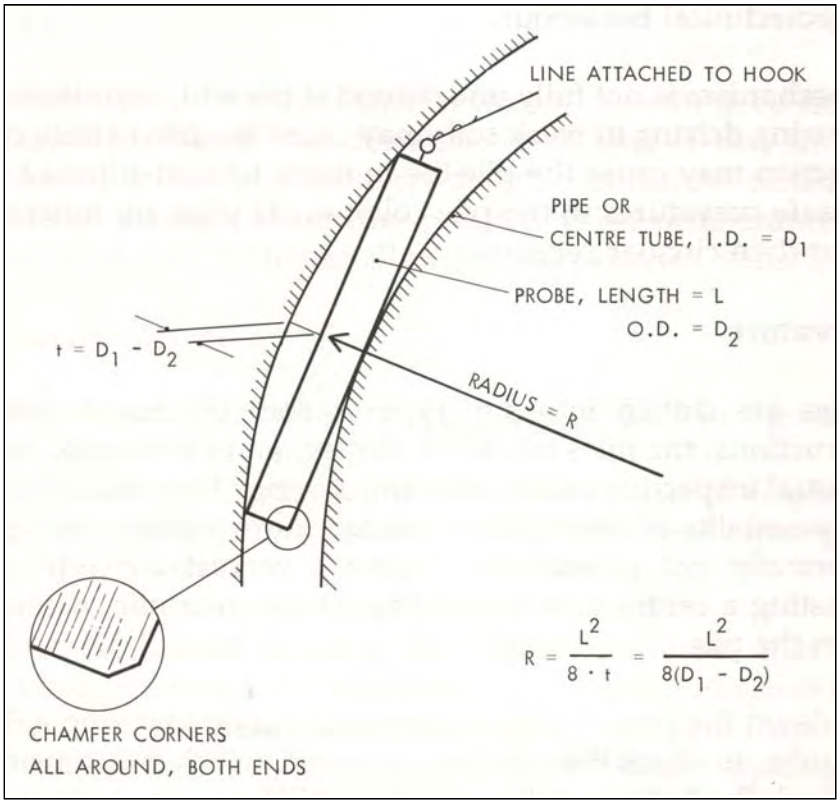

Fig. 7.30 Principle of the curvature probe

For obvious reasons, both the probe and the center tube should be made from standard pipe sizes. The probe must be stiff, that is, be a heavy-wall pipe. The length of a probe for use in steel pipe piles can be determined from selecting a probe with diameter (outside) that is about 80 % of the inside diameter of the pipe.

The passage of the curvature probe down the pile is affected by numerous imprecisions, such as any ovality of the shape of the pipe, diameter tolerances of pipe, unavoidable 'snaking' of the center tube cast in a concrete pile, offsets when splicing pile, etc. However, the curvature is not intended to be an exact instrument for determining bending. (If exact measurement is desired, lower an inclinometer down the pile). Instead, the curvature probe is a refinement of the slow, crude, and imprecise inspection by eye and flashlight. Its main purpose is to vindicate piles, which otherwise may have to be rejected. Consequently, in deciding the limiting bending radius, one should not base the design on calculations of the bending moment (M) and fiber stress (the radius determined from the relation: M = EI/R). Such calculations imply a non-existent exact relation and will suggest that the limiting radii be about 400 m, and more. Probes designed according to such strict values are impractical and cause more difficulties than they solve. Practice has shown that the most suitable probes are those designed for limiting radii of 200 m and 100 m, the 100-m probe being used only if the 200-m probe 'jams'. Any 'jamming' (inability of the probe to reach the bottom of the pile) would then be evaluated, considering location of the 'stop', pile driving records, results from probing neighboring piles, intended use of the pile, etc.

A center pipe for placement in a precast concrete pile usually consists of small diameter, 1.5-inch (40 mm) steel tubing cast concentrically in the pile. Sometimes, for purpose of special testing, such as telltale instrumentation in combination with inclinometer measurements, larger diameter center pipes are used. Up to 6 inches (150 mm) pipes have been used in practice in 16-inch (400 mm) piles. For cost reasons, the larger center pipes often consist of PVC-pipes. (When center pipes larger than 6 inches are used, the pile is more to be considered a hollow pile, or a hollow-core cylinder pile, with a certain wall thickness). The PVC-pipes are cheaper than steel pipes, but they are more apt to snake laterally, to float in the fresh concrete, and to be dislocated by the vibrator.

A suitable size of center tube in precast concrete piles is 1.5 inch schedule 40 (inside diameter 40.9 mm), with a corresponding size of pipe for the curvature probe of 1.0 inch schedule 80 (33.4 mm outside diameter).

It is important that the splicing of the center pipes in the casting form is made without lips or burrs on the inside, obstructing the pipe. The splicing of the tubes must be made square and with outside couplings to ensure that no inside lips or edges are obstructing the passage of the probe. Steel center tubes are preferred, as they are stiffer and heavier. When using PVC-pipes, it must be considered that the PVC exhibits an appreciable thermal expansion and contraction from the heat generated during the curing of the concrete. Conical connections (splicing) must therefore not be used. Naturally, all PVC-couplings must be almost water tight to prevent the cement solution from entering the tubes.

In mechanically spliced piles, the center pipe is taken through the splices by means of a special standard arrangement, which supports the center pipe through the splicing plates and ensures that it is truly perpendicular to the plates. The splicing plates must be equipped with o-ring seals. Otherwise, due to the very large pore pressures generated and the remolding of the soil nearest the pile surface during the pile driving, soil would enter the center pipe and costly cleaning work would be required after the driving. That the seal is properly designed and arranged is essential. For instance, the author has observed that the center pipe in 200 ft (60 m) long spliced pile filled completely with clay due to a faulty o-ring in one of the splices.

To ensure a straight center tube, it must be supported in the casting form and tied to the longitudinal reinforcement. A center tube is considered straight in the casting form before pouring the concrete, if the maximum deviation of the tube, as measured over a distance of 4 metre is 5 mm. This deviation tolerance corresponds to a calculated bending radius of 400 m. The limit is quite liberal. Practice has shown that there is no difficulty in having the tubes cast within tolerances in the piles.

Piles with center tubes are usually also equipped with pile shoes. Where that is the case, it is necessary to supply the base plate of the shoes with a receiving pipe to center the tube in the pile, and to ensure positively that the tube at the toe of the pile (the zone of particular importance in the inspection) is straight.

If splices are used in the pile, a similar centering of the tube is necessary to enable the probe to pass through the splices without encountering difficulties due to offset of centers, 'knees', etc.

It is advisable to check that the tubes are straight and unobstructed after casting by pushing the probe into and through the center tube, while the pile lies on the ground in the casting yard (the probe has to be attached to the end of a standard pipe of small diameter, or pulled through by a line blown ahead through the tube). Fig. 7.31 shows such a test in progress on an about 30 m (100 ft) long prestressed concrete pile segment. Bending is induced in the pile segment to verify the practicality of the bending radius assigned to the curvature probe.

Adding center pipes to precast concrete piles increases in-place cost per unit length of the pile by about 10 percent. However, properly handled, the total costs are reduced. The tremendous assurance gained by adding center pipes to the pile and carrying out a qualified inspection through these, will in almost every case justify an increase of the design load and reduction in the number of piles for the project. I have experienced projects, where, if the center pipes in the piles had not been used, a reduction of the recommended safe allowable load would have been necessary, whereas having the center pipes resulted in a recommendation to use increased allowable loads.

Fig. 7.31 Verifying the Principle of the curvature probe

Center pipes have additional advantageous uses. For instance, providing a center pipe in a pile selected for a static loading test lends itself very obviously, and very cheaply, to accommodate a telltale rod to the bottom of the pipe. This rod is then used to record the pile toe movements during the loading test.

Center pipes provide the possibility of jetting a pile through dense soil layers in order to reduce driving time, increase penetration, and/or reduce bending.

Standard arrangements are available for pile shoes and driving plates, which will allow the jetting through the soil, when required. The practical advantage is that standard pile segments are used. Therefore, if jetting is found to advisable at a site, this can be resorted to without much cost increase or delay, provided the piles are already equipped with center pipes.

Again, with a slight change of pile shoe, the center pipe can be used to insert a drill rod through the pile and to drill beyond the pile toe for grouting a soil or rock anchor into the ground, when in need of an increased tensile capacity. Or in the case of a pile driven to sloping bedrock, when the pile-toe support even when using rock shoes is doubtful, a steel rod can be dropped through the center pipe and beyond the pile toe into a drilled hole and grouted to provide the desired fixity of the pile end.

CHAPTER 8

ANALYSIS OF RESULTS FROM THE STATIC LOADING TEST

8.1 Introduction

For piled foundation projects, it is usually necessary to confirm capacity and to verify that the behavior of the piles agrees with the assumptions of the design. The most common such effort is by means of a static loading test and, normally, determining the capacity is the primary purpose of the test. The capacity is the total ultimate soil resistance of the pile determined from the measured load-movement behavior. It can, crudely, be defined as the load for which rapid movement occurs under sustained or slight increase of the applied load — the pile plunges. This definition is inadequate, however, because large movements are required for a pile to plunge and the ultimate load reached is often governed less by the capacity of the pile-soil system and more of the man-pump system. On most occasions, a distinct plunging ultimate load is not obtained in the test and, therefore, the pile capacity or ultimate load must be determined by some definition based on the load-movement data recorded in the test.

An old definition of capacity, usually credited to Terzaghi, is been the load for which the pile head movement exceeds a certain value, usually 10 % of the diameter of the pile, or the load at a given pile head movement, often 1.5 inch. Such definitions do not consider the elastic shortening of the pile, which can be substantial for long piles, while it is negligible for short piles. In reality, a movement limit relates only to a movement allowed by the superstructure to be supported by the pile, and it does not relate to the capacity as a soil response to the loads applied to the pile in a static loading test. Notwithstanding this remark, a movement limit is an important pile design requirement, perhaps even the most important one, but it does not define capacity in the geotechnical sense of the word.

Sometimes, the pile capacity is defined as the load at the intersection of two straight lines, approximating an initial pseudo-elastic portion of the load-movement curve and a final pseudo-plastic portion. This definition results in interpreted capacity values, which depend greatly on judgment and, above all, on the scale of the graph. Change the scales and the perceived capacity value changes also. A loading test interpretation is influenced by many occurrences, but the draughting manner should not be one of these.

Without a proper definition, interpretation becomes a meaningless venture. To be useful, a definition of pile capacity from the load-movement curve must be based on some mathematical rule and generate a repeatable value that is independent of scale relations and the judgment call or eye-balling ability of the individual interpreter. Furthermore, it has to consider shape of the load-movement curve, or, if not, it must consider the length of the pile (which the shape of the curve indirectly does).

Fellenius (1975, 1980) presented nine different definitions of pile capacity evaluated from load-movement records of a static loading test. Five of these have particular interest, namely, the Davisson Offset Limit, the Hansen Ultimate Load, the Chin-Kondner Extrapolation, the Decourt Extrapolation and the DeBeer Yield Limit. A sixth limit is the Maximum Curvature Point. All are detailed in the following.

There is more to a static loading test than analysis of the data obtained. As a minimum requirement, the test should be performed in accordance with the ASTM guidelines (D 1143 and D 3689) for axial loading (compression and tension, respectively), keeping in mind that the guidelines refer to routine testing. Tests for special purposes may well need stricter performance rules.

8.2 Davisson Offset Limit

The Offset Limit Method proposed by Davisson (1972) is presented in Fig. 8.1, showing the load-movement results of a static loading test performed on a 12-inch precast concrete pile. The Davisson limit load is defined as the load corresponding to the movement which exceeds the elastic compression of the pile by a value of 0.15 inch (4 mm) plus a factor equal to the diameter of the pile divided by 120 (Eqs. 8.1a and 8.1b). For the 12-inch diameter example pile, the offset value is 0.25 inch (6 mm) and the Load Limit is 375 kips.

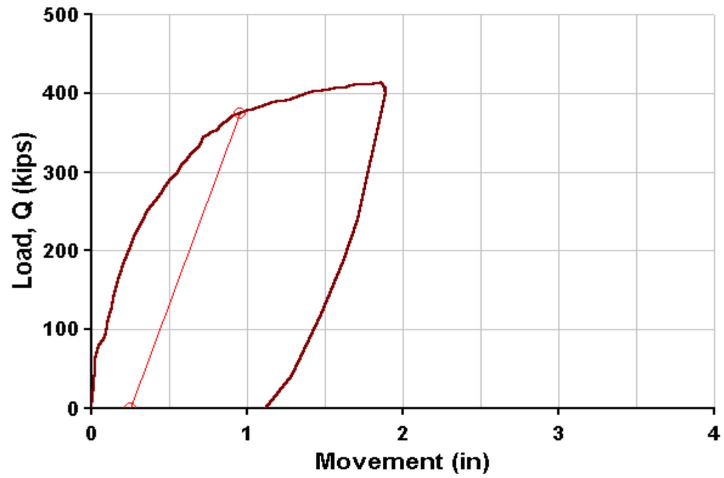

Fig. 8.1 The Offset Limit Method

(Eq. 8.1a) OFFSET (inches) = 0.15 + b/120

(Eq. 8.1b) OFFSET (SI-units—mm) = 4 + b/120

where b = pile diameter (inch or mm, respectively)

Notice that the Offset Limit Load is not necessarily the ultimate load. The method is based on the assumption that capacity is reached at a certain small toe movement and tries to estimate that movement by compensating for the stiffness (length and diameter) of the pile. It was developed by correlating subjectively-considered pile-capacity values for a large number of pile loading tests to one single criterion. It is primarily intended for test results from driven piles tested according to quick methods and it has gained a widespread use in phase with the increasing popularity of wave equation analysis of driven piles and dynamic measurements.

8.3 Hansen Ultimate Load

Hansen (1963) proposed a definition for pile capacity as the load that gives four times the movement of the pile head as obtained for 80 % of that load. This '80%- criterion' can be estimated directly from the load-movement curve, but it is more accurately determined in a plot of the square root of each movement value divided by its load value and plotted against the movement. Fig. 8.2 shows the construction for the same example as used above. (The method of testing this pile is the constant-rate-of-penetration method, which is why so many points were obtained).

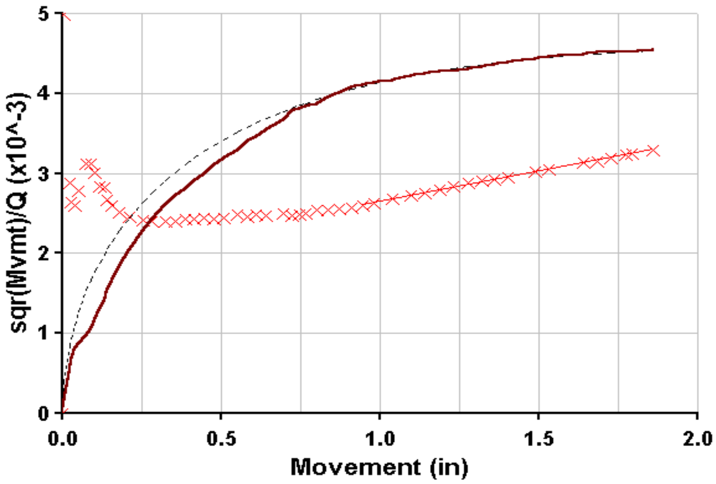

Fig. 8.2 Hansen's Plot for the 80 percent criterion

Normally, the 80%-criterion agrees well with the intuitively perceived “plunging failure” of the pile. The following simple relations can be derived for computing the capacity or ultimate resistance, Q_u, according to the Hansen 80%-criterion:

(Eq. 8.2) $$Q_u = \frac{1}{2\sqrt{C_1 C_2}}$$

(Eq. 8.3) $$\delta_u = \frac{C_2}{C_1}$$

Where Q_u = capacity or ultimate load
δ_u = movement at the ultimate load
C_1 = slope of the straight line
C_2 = y-intercept of the straight line

For the example shown in Fig. 8.2, Eq. 8.2 indicates that the Hansen Ultimate Load is 418 kips, a value slightly smaller than the 440-kip maximum test load applied to the pile head.

The 80-% criterion determines the load-movement curve for which the Hansen plot is a straight line throughout. The equation for this ‘ideal’ curve is shown as a dashed line in Fig. 8.2 and the Eq. 8.4 gives the relation for the curve.

(Eq. 8.4) $$Q = \frac{\sqrt{\delta}}{C_1\delta + C_2}$$

Where Q = applied load
δ = movement

When using the Hansen 80%-criterion, it is important to check that the point 0.80 Q_u/0.25 δ_u indeed lies on or near the measured load-movement curve. The relevance of evaluation can be reviewed by superimposing the load-movement curve according to Eq. 8.4 on the observed load-movement curve. The two curves should preferably be in close proximity between the load equal to about 80 % of the Hansen ultimate load and the ultimate load itself.

8.4 Chin-Kondner Extrapolation

Fig. 8.3 gives a method proposed by Chin (1970; 1971) for piles (in applying the general work by Kondner, 1963). To apply the Chin-Kondner method, divide each movement with its corresponding load and plot the resulting value against the movement. As shown, after some initial variation, the plotted values fall on straight line. The inverse slope of this line is the Chin-Kondner Extrapolation of the ultimate load.

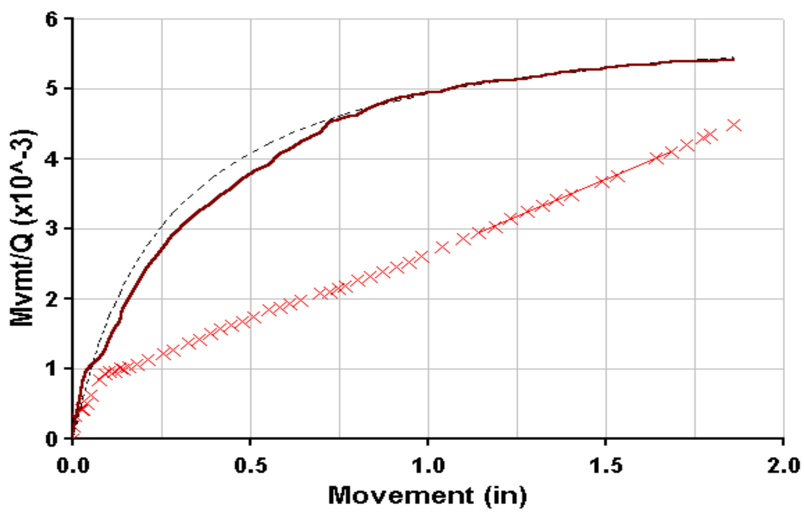

Fig. 8.3 Chin-Kondner Extrapolation Method

(Eq. 8.5) $$Q_u = \frac{1}{C_1}$$

Where Q_u = capacity or ultimate load
C_1 = slope of the straight line

The inverse slope of the straight line indicates a Chin-Kondner Extrapolation Limit of 475 kips, a value exceeding the 440-kip maximum test load applied to the pile head. Although some indeed use the Chin-Kondner Extrapolation Limit as the pile capacity established in the test (with an appropriately large factor of safety), this approach is not advisable. One should not extrapolate the results when determining the allowable load by dividing the extrapolated capacity value with a factor of safety; The maximum test load is also the maximum capacity value to use (see elaboration below).

The criterion determines the load-movement curve for which the Chin-Kondner plot is a straight line throughout. The equation for this 'ideal' curve is shown as a dashed line in Fig. 8.3 and the Eq. 8.6 gives the relation for the curve.

(Eq. 8.6) $$Q = \frac{\delta}{C_1\delta + C_2}$$

Where
C_1 = slope of the straight line
C_2 = y-intercept of the straight line
Q = applied load
δ = movement

The Chin-Kondner Extrapolation load is approached asymptotically. Therefore, the value is always an extrapolation. The Chin method is often termed the "hyperbolic fit" (of data to theory) and, indeed, it is commonly used to extrapolate a trend to a final value. However, it is a sound engineering rule <u>never to interpret the results from a static loading test as to an ultimate load larger than the maximum load applied to the pile in the test</u>. For this reason, an allowable load cannot, must not, be determined by dividing the Chin-Kondner limit load with a factor of safety. This does not mean that the Chin-Kondner extrapolation would be useless. For example, if during the progress of a static loading test, a weakness in the pile would develop in the pile, the Chin-Kondner line would show a kink. Therefore, there is considerable merit in plotting the readings per the Chin-Kondner method as the test progresses. Moreover, the Chin-Kondner limit load is of interest when judging the results of a static loading test, particularly in conjunction with the values determined according to the other two methods mentioned.

Generally speaking, two points will determine a line and third point on the same line confirms the line. However, it is very easy to arrive at a false Chin value if applied too early in the test. Normally, the correct straight line does not start to materialize until the test load has passed the Davisson Offset Limit. As an approximate rule, the Chin-Kondner Extrapolation load is about 20 % to 40 % greater than the Davisson limit. When this is not a case, it is advisable to take a closer look at all the test data.

The Chin method is applicable on both quick and slow tests, provided constant time increments are used. The ASTM "standard method" is therefore usually not applicable. Also, the number of monitored values are too few in the "standard test"; the interesting development could well appear between the seventh and eighth load increments and be lost.

8.5 Decourt Extrapolation

Decourt (1999) proposed a method, which construction is similar to those used in Chin-Kondner and Hansen methods. To apply the method, divide each load with its corresponding movement and plot the resulting value against the applied load. The results are shown in the left of the two diagrams of Fig. 8.4, a curve that tends to a line for which the extrapolation intersects with the abscissa. A linear regression over the apparent line (last five points in the example case) determines the line. The Decourt extrapolation load limit is the value of load at the intersection, 474 kips in this case. As shown in the right diagram of Fig. 8.4, similarly to the Chin-Kondner and Hansen methods, an 'ideal' curve can be calculated and compared to the actual load-movement curve of the test.

The Decourt extrapolation load limit is equal to the ratio between the y-intercept and the slope of the line as given in Eq. 8.6A. The equation of the 'ideal' curve is given in Eq. 8.6B.

(Eq. 8.6A) $$Q_u = \frac{C_2}{C_1}$$ (Eq. 8.6B) $$Q = \frac{C_2\delta}{1 - C_1\delta}$$

Where Q_u = capacity or ultimate load
Q = applied load
δ = movement
C_1 = slope of the straight line
C_2 = y-intercept of the straight line

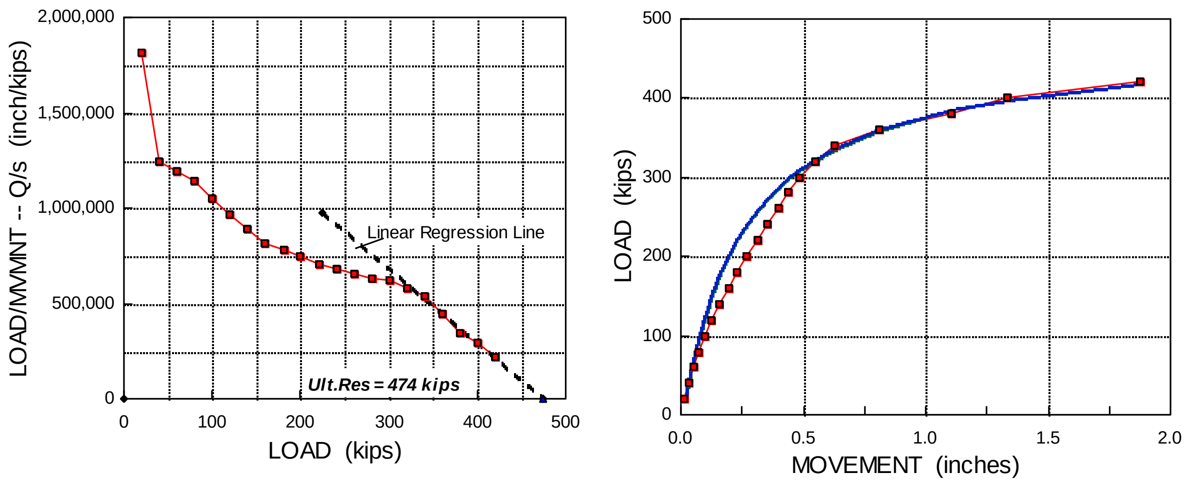

Fig. 8.4 Decourt Extrapolation Method

Results from using the Decourt method are very similar to those of the Chin-Kondner method. The Decourt method has the advantage that a plot prepared while the static loading test is in progress will allow the User to 'eyeball' the projected capacity once a straight line plot starts to develop.

8.6 De Beer Yield Load

If a trend is difficult to discern when analyzing data, a well known trick is to plot the data to logarithmic scale rather than to linear scale. Then, provided the data spread is an order of magnitude or two, all relations become linear showing, i.e., they show a clear trend. (Determining the slope and location of the line and using this for some 'mathematical truths' is not advisable; such "truths" rarely serve other purpose than that of fooling oneself).

DeBeer (1968) and DeBeer and Walays (1972) made use of the logarithmic linearity by plotting the load-movement data in a double-logarithmic diagram. If the load-movement log-log plots show different slopes of a line connecting the data before and after the ultimate load is reached (provided the number of points allow the linear trend to develop), two line approximations will appear and these lines will intersect, which intersection DeBeer called the yield load.

Fig. 8.5 shows that the intersection occurs at a load of 360 kips for the example test.

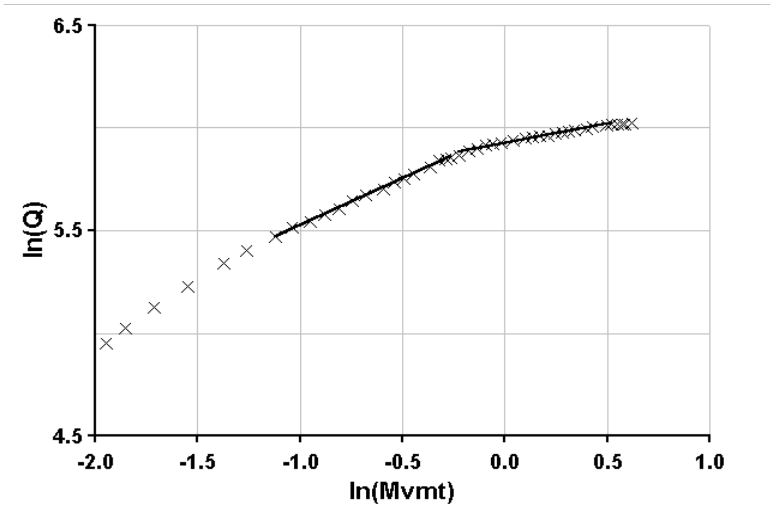

Fig. 8.5 DeBeer's double-logarithmic plot of load-movement data

8.7 The Creep Method

For loading tests using the method of constant increment of load applied at constant intervals of time, Housel (1956) proposed that the movement of the pile head during the later part of each load duration be plotted against the applied total load. These "creep" movements would plot along two straight lines, which intersection is termed the "creep load". For examples of the Creep Method, see Stoll (1961). The example used in the foregoing, being taken from a CRP-test, is not applicable to the Creep Method. To illustrate the creep method, data are taken from a test where the quick maintained-load method was used with increments applied every ten minutes. The "creep" measured between the six-minute and ten-minute readings is plotted in Fig. 8.6. The intersection between the two trends indicates a Creep Limit of 550 kips. For reference to the test, the small diagram beside Fig. 8.6 shows the load-movement diagram of the test and the offset Limit Load.

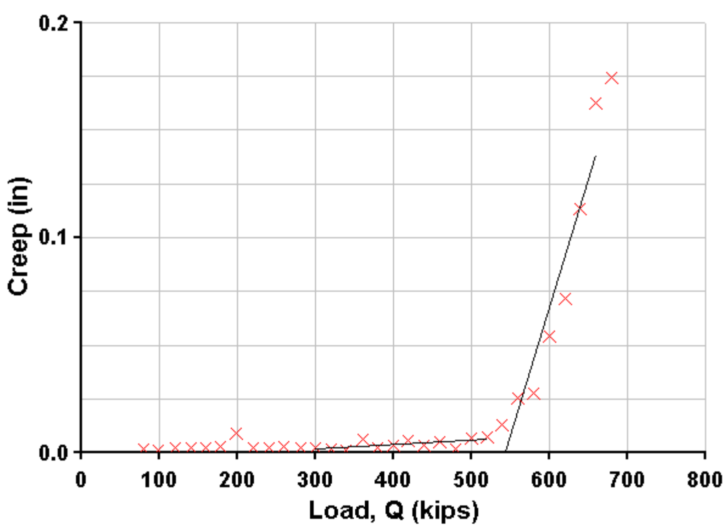

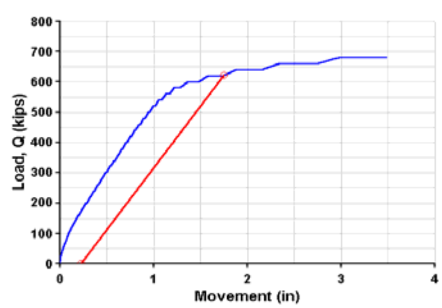

Fig. 8.6 Plot for determining the creep limit

8.8 Load at Maximum Curvature

When applying increments of load to the pile head, the movement increases progressively with the increasing load until the ultimate resistance is reached, say, as a state of continued movement for no increase of load — plastic deformation. Of course, plastic deformation develops progressively and the load applied to the pile head when the plastic deformation has developed sufficiently to become the dominate feature is called the yield load. At loads smaller than the yield load, the curvature of the exponential load-movement curve increases progressively. Beyond the yield load, the curve becomes more of a straight line. The yield load is, therefore, the point of maximum curvature of the load-movement curve. Provided that the increments are reasonably small so that the load-movement curve is built from a number of closely spaced points, the location of maximum curvature can usually be "eye-balled" to determine the yield limit load.

Shen and Niu (1991) proposed to determine the curvature by its mathematical definition and to plot the curvature of the load-movement curve against the applied load, as shown in Fig. 8.7. Their mathematical treatment is quoted below. (Shen and Niu state that the third derivative is the curvature, which is not quite correct. Moreover, there is no merit in studying the third derivative instead of the curvature of the load-movement curve). Initially, this plot shows a constant value or a small gradual increase until a peak is obtained followed by troughs and peaks. The first peak is defined as the yield load. Shen and Niu define the first peak to occur as the Yield Load and claim that the second peak occurs at the ultimate load.

First, the slope, K, of the load-movement curve is determined:

(Eq. 8.7) $$K = \frac{\Delta\delta}{\Delta Q} = \frac{\delta_i - \delta_{i-1}}{Q_i - Q_{i-1}}$$

Then, the change of slope for a change of load

(Eq. 8.8) $$\Delta K = \frac{\Delta K}{\Delta Q} = \frac{K_{i+1} - K_i}{Q_{i+1} - Q_i}$$

and, again

(Eq. 8.9) $$\Delta^2 K = \frac{\Delta^2 K}{\Delta Q^2} = \frac{\Delta K_{i+1} - \Delta K_i}{\Delta Q_{i+1} - \Delta Q_i}$$

and the third derivative is

(Eq. 8.10) $$\Delta^3 K = \frac{\Delta^3 K}{\Delta Q^3} = \frac{\Delta^2 K_{i+1} - \Delta^2 K_i}{\Delta Q_{i+1}^2 - \Delta Q_i^2}$$

Strictly, the curvature, ρ is

(Eq. 8.11) $$\rho = \frac{\Delta^2 K}{(1 + K^2)^{3/2}}$$

The primary condition for the Shen-Niu yield load method to be useful is that all load increments are equal and accurately determined. Even a small variation in magnitude of the load increments or irregular movement values will result in a hodgepodge of peaks to appear in the curvature graph, or, even, in a false yield load. It is then more practical to eyeball the point of maximum curvature from the load-movement curve.

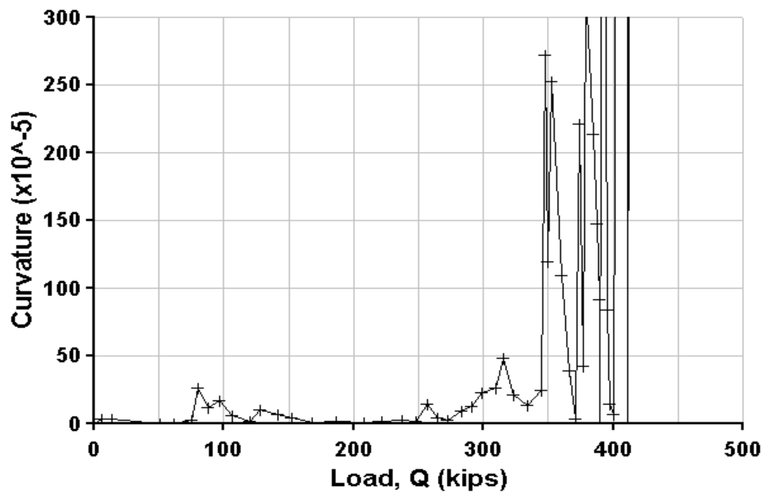

Fig. 8.7 Plot for determining the load-movement curve maximum curvature.

8.9 Factor of Safety

To determine the allowable load on a pile, pile capacity is normally divided by a factor of safety. The factor of safety is not a singular value applicable at all times. The value to use depends on the desired freedom from unacceptable consequence of a failure, as well as on the level of knowledge and control of the aspects influencing the variation of capacity at the site. Not least important are, one, the method used to determine or define the ultimate load from the test results and, two, how representative the test is for the site. For pile foundations, practice has developed toward using a range of factors, as follows. See also the discussion on Factor-of-Safety presented in Chapter 6, Section 10.

In a testing programme performed early in the design work and testing piles which are not necessarily the same type, size, or length as those which will be used for the final project, the safety factor applied should be at least 2.5. In the case of testing during a final design phase, when the loading test occurs under conditions well representative for the project, the safety factor could be reduced to 2.2. When a test is performed for purpose of verifying the final design, testing a pile that is installed by the actual piling contractor and intended for the actual project, the factor commonly applied is 2.0. Well into the project, when testing is carried out for purpose of proof testing and conditions are favorable, the factor may be further reduced and become 1.8. Reduction of the safety factor may also be warranted when limited variability is confirmed by means of combining the design with detailed site investigation and control procedures of high quality. One must also consider the number of tests performed and the scatter of results between tests. Not to forget the assurance gained by means of incorporating dynamic methods for controlling hammer performance and for capacity determination alongside the static procedures.

However, the value of the factor of safety to apply depends, as mentioned, on the method used to determine the capacity. A conservative method, such as the Davisson Offset Limit Load, warrants the use of a smaller factor as opposed to when applying a method such as the Hansen 80%-criterion. It is good practice to apply more than one method for defining the capacity and to apply to each method its own factor of safety letting the smallest allowable load govern the design. That is, the different analysis methods defines lower and upper boundaries of the ultimate resistance. Moreover, the lower boundary does not have to be the Offset Limit. It can be defined as the load on the pile when the load-moment curve starts to fit (becomes close to) the "ideal" Hansen, Chin-Kondner, or Decourt load-movement curves.

In **factored design** (LRFD—Load and Resistance Factor Design or ULS—Ulitimate Limit States Design), a "resistance factor" is applied to the capacity and a "load factor" is applied to the load. Considering both that factored design must always be coupled with a serviceability limit state design (ULS—Serviceablity Limit States Design, or unfactored design), the pile capacity should be determined by a method closer to the plunging limit load, that is, the Hansen 80 %-criterion is preferred over the Offset Limit Load. Note, that the serviceability state addresses settlement and the load-transfer distribution determined in an instrumented static loading test is tremendously valuable when assessing settlement of a piled foundation.

8.10 Choice of Criterion

It is difficult to make a rational choice of the best capacity criterion to use, because the preferred criterion depends heavily on one's past experience and conception of what constitutes the ultimate resistance of a pile. One of the main reasons for having a strict criterion is, after all, to enable compatible reference cases to be established.

The Davisson Offset Limit is very sensitive to errors in the measurements of load and movement and requires well maintained equipment and accurate measurements. No static loading test should rely on the jack pressure for determining the applied load. A load-cell must be used at all times (Fellenius, 1984). In a sense, the Offset Limit is a modification of the "gross movement" criterion of the past (which used to be 1.5 inch movement at the maximum load). Moreover, the Offset-Limit method is an empirical method that does not really consider the shape of the load-movement curve and the actual transfer of the applied load to the soil. However, it is easy to apply and has gained a wide acceptance, because it has the merit of allowing the engineer, when proof testing a pile for a certain allowable load, to determine <u>in advance</u> the maximum allowable movement for this load with consideration of the length and size of the pile. Thus, as proposed by Fellenius (1975), contract specifications can be drawn up including an acceptance criterion for piles proof tested according to quick testing methods. The specifications can simply call for a test to at least twice the design load, as usual, and declare that at a test load equal to a factor, F, times the design load, the movement shall be smaller than the elastic column compression of the pile, plus 0.15 inch (4 mm), plus a value equal to the diameter divided by 120. The factor F is a safety factor and should be chosen according to circumstances in each case. The usual range is 1.8 through 2.0.

The Hansen 80%-criterion usually gives a Q_u-value, which is close to what one subjectively accepts as the true ultimate resistance determined from the results of the static loading test. The value is smaller than the Chin-Kondner or Decourt value. Note, however, that the Hansen method is more sensitive to inaccuracies of the test data than is the Chin-Kondner or Decourt methods.

The Chin-Kondner and Decourt Extrapolation methods allow continuous check on the test, if a plot is made as the test proceeds, and an extrapolating prediction of the maximum load that will be applied during the test. Sudden kinks or slope changes in the Chin line indicate that something is amiss with either the pile or with the test arrangement (Chin, 1978).

The Hansen's 80%-criterion, Chin-Kondner, and Decourt methods allow the later part of the load-movement curve to be plotted according to a mathematical relation, and, which is often very tempting, they make possible an "exact" extrapolation of the curve. That is, it is easy to fool oneself and believe that the extrapolated part of the curve is as true as the measured. As mentioned earlier, whatever one's preferred mathematical criterion, the pile capacity value intended for use in design of a pile foundation must not be higher than the maximum load applied to the pile in the test.

8.11 Loading Test Simulation

The resistance of a pile to the load applied in a static loading test is a function of the relative movement between the pile and the soil. When calculating the capacity of a pile, the movement necessary to mobilize the ultimate resistance of the pile is not considered. However, a resistance is always coupled to a movement. In fact, to perform a static loading test, instead of applying a series of load increments, one can just as well apply a series of predetermined increments of movement and record the subsequent increases of load. For example, this is actually how the constant-rate-of-penetration test is performed. Usually, however, a test is performed by adding predetermined increments of load to a pile head and recording the subsequent pile head movement.

In a static loading test, the resistance in the upper regions of the soil profile is engaged (mobilized) first. That is, the shaft resistance is engaged progressively from the pile head and down the pile. The first increment of load only engages a short upper portion of the pile. The length is determined by the length necessary to reach an equilibrium between the applied load and the shaft resistance (mobilized as the pile head is moved down). The movement is the ‘elastic’ shortening (compression) of the length of pile active in the transfer of the load from the pile to the soil. The pile toe does not receive any load until all the soil along the pile shaft has become engaged. Up till that time, the movement of the pile head is the accumulated ‘elastic’ shortening of the pile. This is due that the moment necessary for mobilizing shaft resistance is very much smaller than the movement necessary for mobilizing the toe resistance. If the soil has a strain-softening behavior, the shaft resistance may be reducing once the pile toe is engaged.

While the shaft resistance normally has a clear maximum value, the toe resistance continues to increase with increasing movement. Figure 8.8 shows a few typical shapes of resistance versus movement curves.

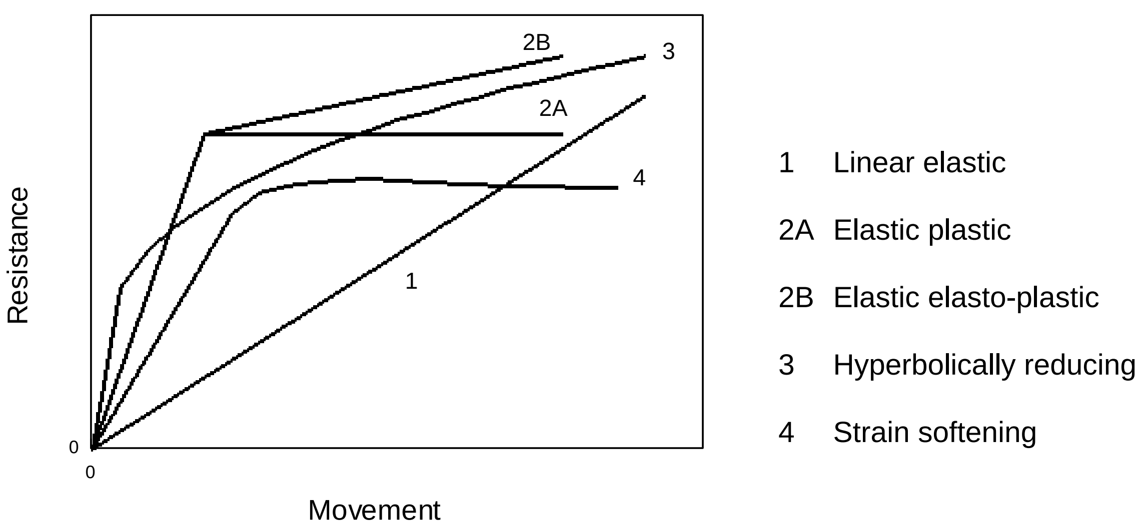

Fig. 8.8 Typical resistance versus movement curves

Resistance versus movement curves (load-movement curves) for shaft and toe resistances are called t-z and q-z curves, respectively. Such curves can be defined by the ratio of two resistances as a function of movement ratio and an exponent. The equation is as follows:

(Eq. 8.12)
$$\frac{R_1}{R_2} = \left(\frac{\delta_1}{\delta_2}\right)^e$$

where
R_1 = Load 1
R_2 = Load 2
δ_1 = movement mobilized at R_1
δ_2 = movement mobilized at R_2
e = an exponent usually ranging from a small value through unity

The general shape of a t-z curve is governed by the exponent as illustrated in Fig 8.9. The resistance is given in percent of the ultimate resistance and the movement is given in percent of the movement necessary to mobilize the ultimate resistance. Notice, a custom t-z curve can be computed for a mobilized resistance that is larger than the ultimate.

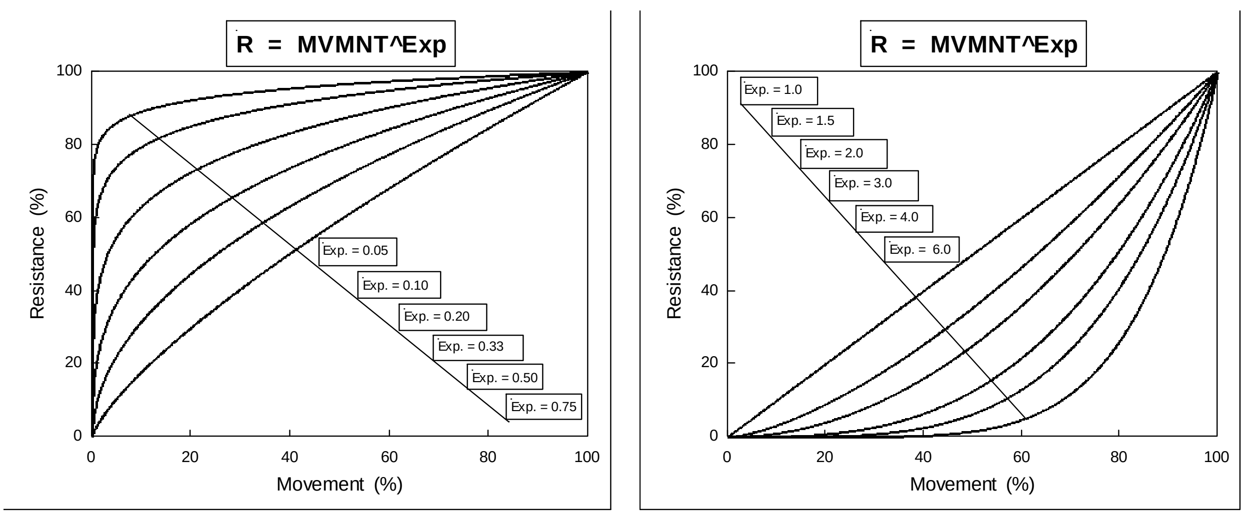

Fig. 8.9 Shape of t-z and q-z curves for a range of exponents

The shapes of the t-z curves for shaft resistance and q-z curves for toe resistance follow the same relation (Eq. 8.12), but their exponents are very different. A curve with the exponent of 0.05 to 0.1 is typical for a shaft resistance, and the toe resistance behavior is closer to the curves for exponents between 0.4 and 1.0. A resistance curve, shaft or toe, conforming to an exponent larger than 1.0 would be extraordinary. For toe resistance, it could be used to model a pile with a gap, or some softened zone, below the pile toe that has to be closed or densified before the soil resistance can be fully engaged.

Fig. 8.10 shows a load-movement diagram computed by the UniPile program. The diagram presents the applied test load versus the movements of the pile head, pile compression, and pile toe. It also includes the pile mobilized toe resistance versus the pile toe movement.

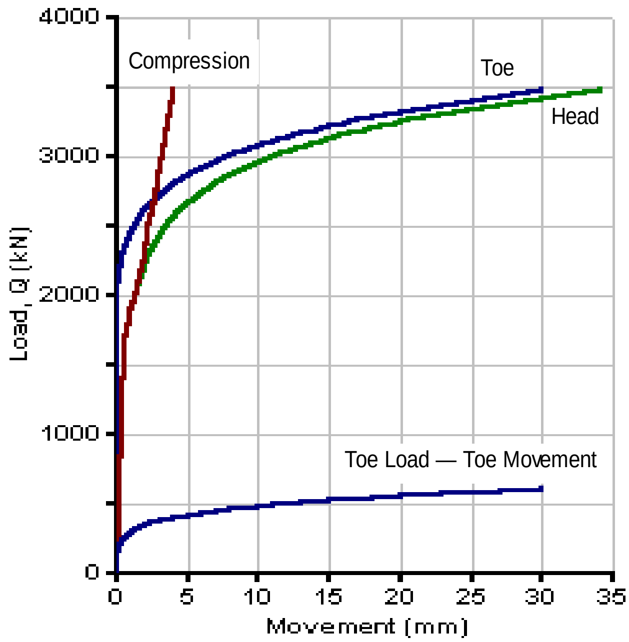

Fig. 8.10 Results from a simulation of a static loading test

The t-z and q-z curves for the shown example are chosen to indicate that the ultimate shaft resistance will occur at a small relative movement between the pile shaft and the soil (set to be the same for all soil layers). The ultimate toe resistance is set to occur at a movement of 25 mm (the value is larger than normally found in a static loading test). At this toe movement, the load-movement curve for the pile head will indicate the capacity calculated by UniPile (the beta-coefficient times the effective overburden stress). However, the program allows continuing to simulate the test curves also beyond the 25-mm movement. The computed load, therefore, goes beyond the calculated capacity (3,410 KN). The steep initial rise of the load-movement curve shown for the pile toe in Fig 8.10 is typical of a pile subjected to residual load prestressing the soil at and below the pile toe.

8.12 Determining Toe Movement

The simplest instrumentation consists of a single telltale to the pile toe to record the pile toe movement, which is a low-cost addition to a static test that greatly enhances is value. It is futile to try to use the telltale as measurement of strain (i.e., load) in the pile. Such strain is pile shortening (tell-tales should always be installed to measure pile shortening) determined from two telltales with a length difference of about 5 m, divided by the length and cross sectional area and the value is rather inaccurate. However, a tell-tale to the pile toe is still a valuable addition to a static loading test. Fig 8.11 presents the results of a static loading test performed on a 20 m long pile instrumented with a telltale to the pile toe for measuring the pile toe movement. The pile toe load was not measured. The load-movement diagram for the pile head shows that the pile clearly has reached the ultimate load. In fact, the pile “plunged”. Judging by the curve showing the applied load versus the pile toe movement, it would appear that also the pile toe reached an ultimate resistance — in other words, attained its bearing capacity. However, this is not the case as will be discussed in the following.

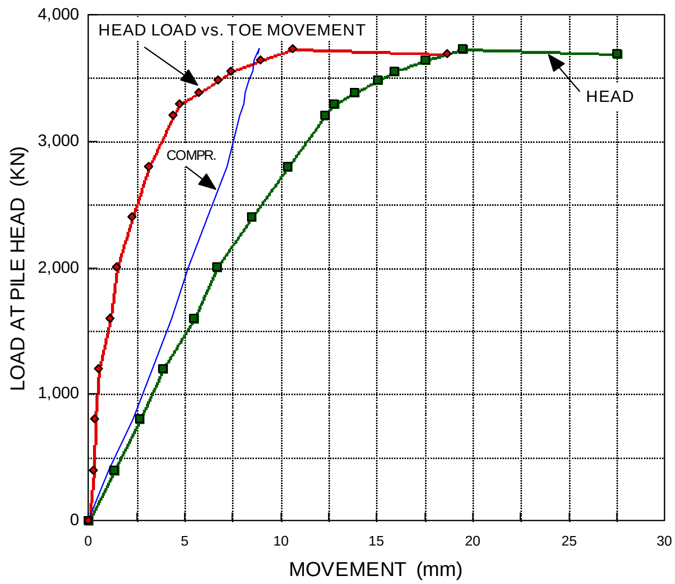

Fig. 8.11 Load-movement diagram of a static loading test on a 20 m long, 450 mm diameter closed-toe pipe pile in compact sand with telltale measurements of toe movement (Fellenius 1999)

Most of the shaft resistance was probably mobilized at a toe movement of about 2 mm to 3 mm, that is, at an applied load of about 2,500 KN. At an applied load beyond about 3,300 KN, where the movements start to increase progressively, the shaft resistance probably started to deteriorate (strain softening). Thus, approximately between pile toe movements of about 3 mm to about 10 mm, the shaft resistance can be assumed to be fully mobilized and approximately constant. An adjacent test indicates that the ultimate shaft resistance was about 2,000 KN. When subtracting the 2,000 KN from the total load over this range of toe movement, the toe load can be estimated. This is shown in Fig. 8.12, which also shows an extrapolation of the toe load-movement curve beyond the 100-mm movement, which implies a strain softening behavior of the pile shaft resistance. Extrapolating the toe curve toward the ordinate indicates the existence of a residual load in the pile prior to the start of the static loading test.

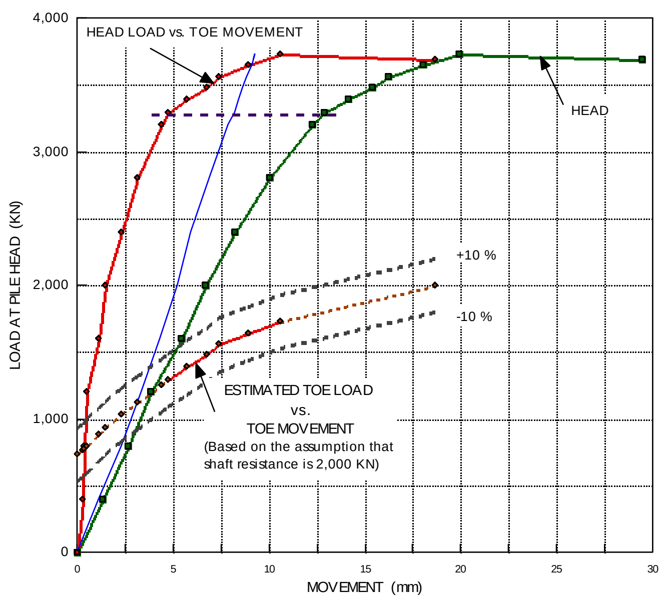

Fig. 8.12 The data shown in Fig. 8.11 with the results of analysis of the load-movement of the pile toe [Reference is made of the results from a static loading test on an adjacent pile instrumented with strain gages indicating a shaft resistance of 2,000 KN] (Fellenius 1999)

A back calculation of the toe movement curve and a simulation of the observed pile load-movement behavior can quite easily be performed by means of so-called t-z curves to represent the soil response along the pile shaft and at the pile toe, as presented in Section 8.10. In this case, the shaft curve would reference the shaft resistance at a movement of about 3 mm and with an exponent of about 0.15. The toe curve would reference a toe movement of 10 mm and apply an exponent of 0.5. The latter indicates a toe load-movement behavior that does not show an ultimate value.

8.13 Effect of Residual load

The load-movement consists of three components: the load-movement of the shaft resistance, the compression of the pile, and the load-movement of the pile toe. The combined load-movement response to a load applied to a pile head therefore reflects the relative magnitude of the three. Moreover, only the shaft resistance exhibits an ultimate resistance. The compression of the pile is really a more or less linear response to the applied load and does not have an ultimate value (disregarding a structural failure when the load reaches the strength of the pile material). However, the load-movement of the pile toe is also a more or less linear response to the load that has no failure value. Therefore, the concept of an ultimate load, a failure load or capacity is really a fallacy and a design based on the ultimate load is a quasi concept, and of uncertain relevance for the assessment of a pile.

The statement is illustrated in Fig. 8.13, which presents the results from a typical test on a 15 m long, 300 mm diameter, driven concrete pile. Fig. 8.13B shows the probable "virgin" toe load-movement superimposed on the diagram. The diagrams include the load-movement of the pile toe, measured, say, by a strain gage or a load cell at the pile toe and a toe telltale. The load-movement is shown both as the applied load and as actual toe resistance versus the measured toe movement. For the test shown, the Offset Limit Load occurs at a toe movement of about 5 mm. The test was continued until plunging failure appeared in the load-movement curve for the pile head at an about 22-mm movement of the pile head. The maximum toe movement was 15 mm. The maximum applied load at the pile head, the shaft resistance, and the load at the pile toe were 1,100 KN, 600 KN, and 500 KN, respectively. The round dot indicates the Offset Limit load; at an applied load of 1,050 KN. Fig. 8.13B shows the probable "virgin" toe load-movement superimposed on the diagram.

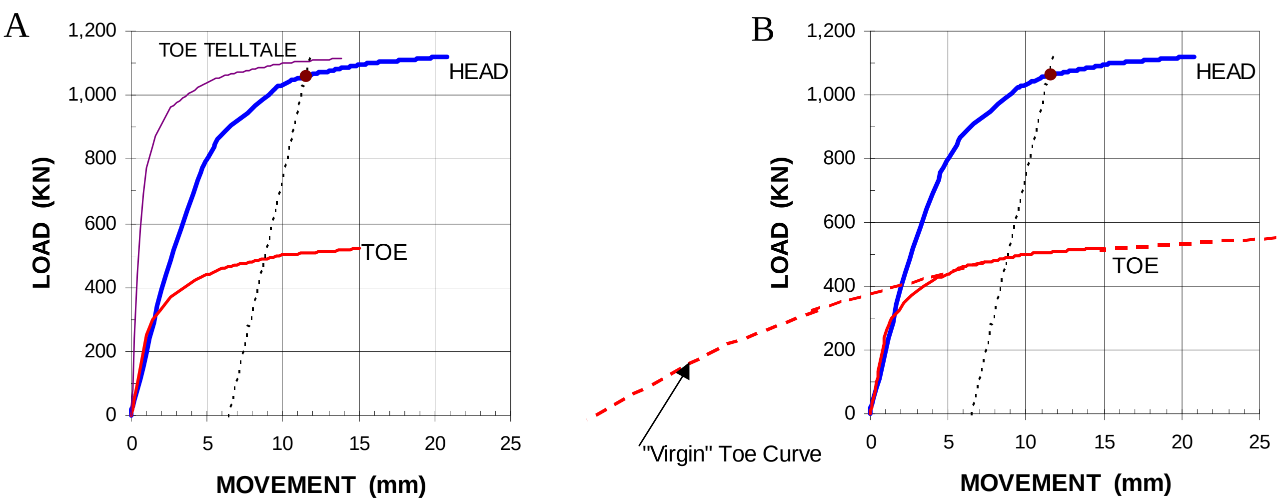

Fig. 8.13 **A**. Typical results of a static loading test **B**. Fig. A with a superimposed "Virgin" toe curve

(Toe movement is determined by means of a telltale)

Knowing the pile toe load-movement response is an obvious enhancement of the test results. However, residual load will always develop in a pile, a driven pile in particular. Therefore, at the start of the static loading test, the pile toe is already subjected to load and the toe load-movement curve displays an initial steep reloading portion. Depending on the magnitude of the residual load, the measured toe response can vary considerably. For examples and discussion, see Fellenius (1999).

The analyses behind Fig. 8.13, assume very simple shaft and toe soil responses. The pile toe load-movement is indicated in the figures. The load-movement of the shaft resistance assumed in establishing the load-movement diagram of Fig. 8.13 is shown in Fig. 8.14A. A bit more complex, but more realistic diagram over shaft resistance versus relative movement between the pile shaft and the soil is presented in Fig. 8.14B. The latter diagram shows a soil response where the shear resistance drops off to about 80 % of the peak value , after having reached a peak value, demonstrating a strain-softening response. The test results for this shaft resistance are shown in Fig. 8.15.

As shown in Fig. 8.15, because of the effect of the strain softening, the Offset Limit Load is now smaller than that shown in Fig. 8.13B.

Were any of the other methods of determining the “Failure Load” used as reference instead of the Offset Limit Load, the results would be similar.

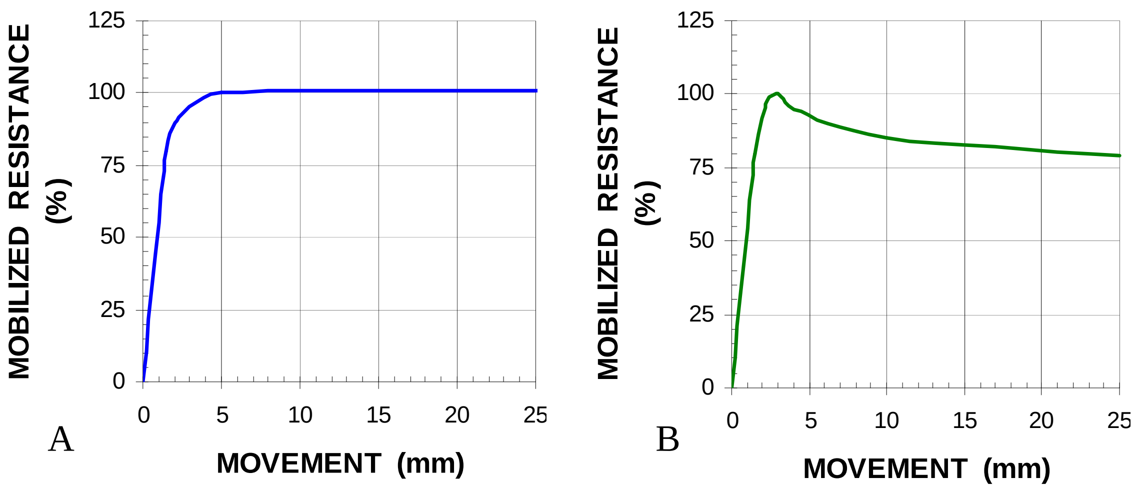

Fig. 8.14 Percent shaft resistance as a function of the relative movement between pile shaft and soil **A**. For an ideally elastic-plastic behavior and, **B**, for a strain-softening soil.

The result of a static loading test does not provide the simple answers one at first may think. First, there is a considerable variation in the methods of “Failure Load” interpretation used in the industry. Then, the effect of residual load and varying degree of strain-softening will appreciably affect the interpretation. Indeed, a static test that measures only the applied load and the pile head movement is a very crude test. For small and non-complex projects, such level of sophistication, or lack thereof, is acceptable if the uncertainty is covered by a judiciously large factor of safety. For larger projects, however, this approach is costly. For these, the test pile should be instrumented and the test data evaluated carefully to work out the various influencing factors. For projects involving many piles, several test piles may be desirable, though this could be prohibitively costly. If so, combining an instrumented static loading test with dynamic testing, which can be performed on many piles at a relatively small cost, can extend the application of the more detailed results of the instrumented static test.

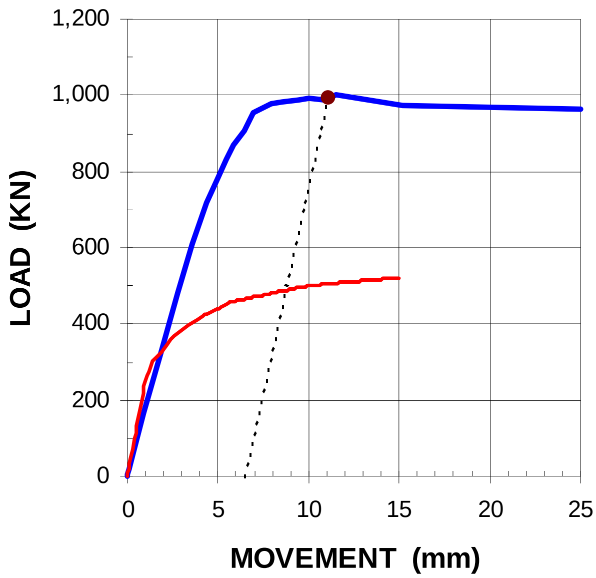

Fig. 8.15 The effect of strain-softening shaft resistance.
The lower curve indicates the load-movement of the pile toe.

The potential presence of residual load and its varying magnitude makes methods of interpretation based on initial and final slopes of the load-movement curve somewhat illogical.

Design of piles should be less based on the capacity value and more emphasize the settlement of the pile under sustained load. It will then be easier and more logical to incorporate aspects such as downdrag and drag load into the design.

8.14 Instrumented Tests

More and more, our profession is realizing that a conventional static loading test on a pile provides limited information. While the load-movement measured at the pile head does establish the capacity of the pile (per the user's preferred definition), it gives no quantitative information on the load-transfer mechanism (magnitude of the toe resistance and the distribution of shaft resistance). Yet, this information is what the designer often needs in order to complete a safe and economical design. Therefore, more and more frequently, the conventional test arrangement is expanded to include instrumentation to obtain the required information.

The oldest and simplest, but not always the cheapest, method of instrumenting a test pile is to place one or several telltales to measure the shortening of the pile during the test. The measurements are used to determine the average load in the pile. Two telltales placed with tips at different depths in the pile provide three values of average load: each gives an average load over its length and the third value is the shortening over the distance between the telltale tips (as the difference between the two full-length values). Similarly, three telltales provide six values. The most important telltale is the one that has its tip placed at the pile toe, because it provides the pile toe movement (by subtracting the shortening of the pile from the pile head movement). If the telltale dial gage is arranged to measure shortening directly and the length considered is at least 5 m, the commonly used 0.001 inch dial-gage reading gradation usually results in an acceptably accurate value of strain over the telltale length.

When using a telltale value for determining average load, the shortening must be measured directly and not be determined as the difference between movement of telltale tip and pile head movement. This is because extraneous small movements of the reference beam always occur and they result in large errors of the shortening values If you don't measure shortening directly, forget about using the data to estimate average load.

Load Distribution. The main use of the average load in a pile calculated from a telltale, or the average loads if several telltales are placed in the pile, is to produce a load distribution diagram for the pile. The distribution diagram is determined by drawing a line from the plotted value of load applied to the pile head through plots of each value of average load calculated for that applied load. Case history papers reporting load distribution resulting from the analysis of telltale-instrumented pile loading tests invariably plot the average loads at the mid-point of each telltale length considered. But, is that really correct?

Although several telltales are usually placed in the pile, even with only one telltale in the pile (provided it goes to the pile toe) we can determine a load distribution line or curve for each load applied to the pile head. As the toe telltale supplies the pile toe movement for each such distribution, the data establish the load-movement curve of the pile toe, which is much more useful than the load-movement curve for the pile head.

If the average load is determined in a pile that has no shaft resistance—it acts as a free-standing column—the load distribution is a vertical line down from the applied load; the applied load goes undiminished down to the pile toe. In a pile, however, the load reduces with depth due to shaft resistance. Assuming that the unit shaft resistance is constant along the pile, then, the load distribution is a straight line from the applied load to the pile toe, as shown in Fig. 8.16 (in order to make the figure more clear, it is assumed that the pile has no toe resistance).

The straight-line load distribution line crosses a vertical line drawn through the average load at mid height of the pile, the mid height of the telltale length, rather. Clearly, a straight-line distribution must have equal areas, A1 and A2, between load-distribution line and the vertical through the average load over the telltale length. This "equal-area-condition" means that, for the case of constant unit shaft resistance, the average load should be plotted at mid height of the telltale length. Actually, a load-distribution of any shape must satisfy an "equal-area-condition". However, this does not mean that the average load must always be plotted at mid height.

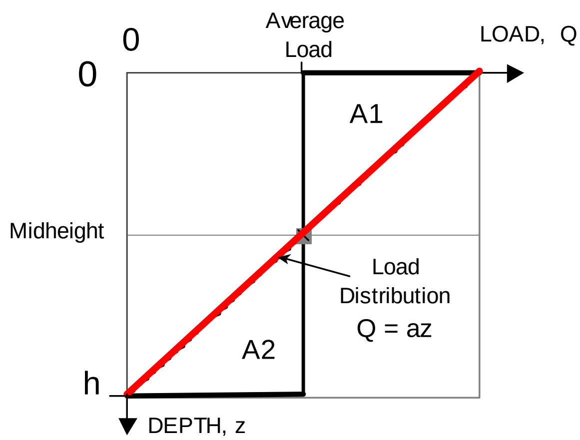

Fig. 8.16 Load distribution for constant unit shaft resistance

Let us assume a more realistic distribution of the unit shaft resistance, for example, linearly increasing with depth, such as a unit shaft resistance proportional to the effective overburden stress. Fig. 8.17 shows two diagrams, one with unit shaft resistance (az) versus depth and one with load distribution versus depth (z). The shaft resistance is a line proportional to the effective overburden stress and the load distribution curve is the result of the integration of the unit shaft resistance. Fig. 8.17 also shows a vertical line through the average load and two areas, A1 and A2. For A1 and A2 to be equal, obviously, the average load must be plotted below the mid height of the telltale length. The exact location can easily be found, as follows.

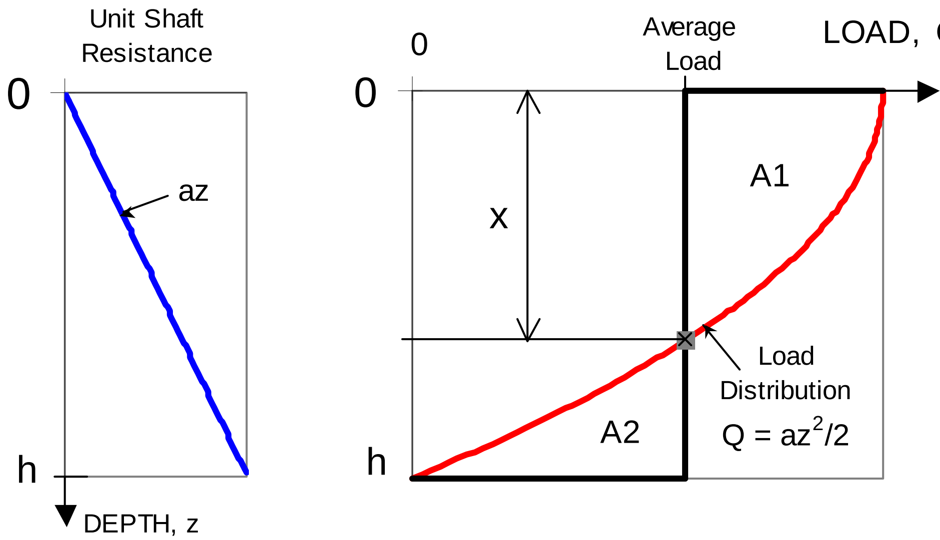

Fig. 8.17 Linearly increasing unit shaft resistance and the resulting load distribution

If we assume that

h	=	height (length) of pile considered (distance from the pile head to the telltale tip, or distance between two telltale tips)
x	=	height of area A1
z	=	depth
az	=	unit shaft resistance (proportional to effective overburden stress)

we can determine the area of Area A1 as indicated in Eq. 8.13.

(Eq. 8.13) $$A1 = \frac{ax^3}{3}$$

Similarly, we can determine that Area A2 is

(Eq. 8.14) $$A2 = \frac{a(h^3 - 3x^2h + 2x^3)}{6}$$

The "equal-area-condition" of A1 equal to A2 gives

(Eq. 8.15) $$X = \frac{h}{\sqrt{3}} = 0.58h$$

When the shaft resistance is not constant but proportional to the effective stress, as shown above, plotting the value of average load at mid height of the telltale length, h, is then not correct. The value should be plotted at a distance down equal to 0.58h. This is not trite matter. The incorrect representation of the average load implies more shaft resistance in the upper portion of a pile and less in the lower portion. The error has contributed to the "critical depth" fallacy.

The possibility, and often also the probability, of the data having been incorrectly plotted and analyzed is a good thing to keep in mind when consulting old case histories. When producing results to go into new case histories, use vibrating wire strain gages rather than telltales for determining load—and limit the telltale instrumentation to one telltale at the toe for determining the pile toe movement.

8.15 The Osterberg Test

It is difficult to determine the magnitude of the portion of the applied test load that reaches the pile toe. Even when a load cell or similar instrumentation is placed at the pile toe and a telltale is used to measure the pile toe movement, the data from a conventional "head-down" test the interpretation is complex, because neither amount if shaft resistance reducing the load reaching the pile toe nor the "zero load" at the toe, better termed "the starting load at the toe", are known. (The "residual load", acts at the pile toe already before the start of the static loading test).

In the mid-90s, a testing method was developed that eliminated these difficulties, called the bi-directional test or the Osterberg Cell or O-cell test, which is a great new tool for use by the geotechnical engineer (Osterberg 1998) The O-cell method incorporates one or more sacrificial hydraulic jack-like device(s) placed at or near the toe (base) of the pile (be it a driven, augercast, drilled-shaft pile or a barrette) to be tested. When hydraulic pressure is applied to the cell, the O-cell expands, pushing the shaft upward and the toe downward. The upward movement of the O-cell top plate is the movement of the shaft at the O-cell location and it is measured by means of telltales extending from the O-cell top plate to the ground surface. In addition, the separation of the top and bottom O-cell plates is measured by displacement transducers placed between the plates. The downward movement of the O-cell base plate is obtained as the difference between the upward movement of the top plate and the cell plate separation. It is important to realize that the upward and downward load-movements are not equal. The upward load-movement is governed by the shear resistance characteristics of the soil along the shaft, whereas the downward load-movement is governed by the compressibility of the soil below the pile toe. The fact that in a conventional "head-down" test the shaft moves downward, while in the O-cell test it moves upward, is of no consequence for the determination of the shaft resistance. Shaft resistance in either upward or downward (positive and negative) directions are equal.

At the start of the test, the pressure in the O-cell is zero and the self-weight of the pile at the location of the O-cell is carried structurally by the O-cell assembly and interior contact. The test consists of applying load increments to the pile by means of incrementally increasing pressure in the O-cell and recording the resulting plate separation and telltale movements. The first pressure increments transfer the pile "self-weight" from the cell assembly and the interior contact to the O-cell fluid. The O-cell load determined from the hydraulic pressure reading at completed transfer, when the "gap" in the O-cell top and bottom plates start to separate. The "self-weight" consists of the buoyant weight of the pile plus any residual load in the pile at the location of the O-cell.

When the full “self-weight” of the pile has been transferred to pressure in the O-cell , a further increase of pressure expands the O-cell, that is, the top plate moves upward and the bottom plate moves downward. The assembly is built with an internal bond between the plates, a construction feature, which breaks along with the interior contact of the concrete outside the O-cell(s) when the separation starts.

The O-cell load versus the *upward* movement is the load-movement curve of the pile shaft. The O-cell load versus the *downward* movement is the load-movement curve of the O-cell bottom plate. This separation of the load-movement behavior of the shaft and base is not obtainable from a conventional static loading test. Of course, the “self-weight” must be subtracted to obtain the true upward load-movement of the pile shaft. The self-weight should be included in the load-movement for the downward movement, however. If the O-cell is located near the pile toe, the shaft resistance below the O-cell can be disregarded and the measured O-cell plate downward movement is approximately equal to the pile toe movement.

An additional O-cell can be placed anywhere along the pile shaft to determine separately shaft resistance along an upper and a lower length of the shaft. Then, however, the test results and the distribution of the shaft resistance are affected by tension built into the soil at the location of the O-cell. Including this effect in the evaluation and analyses is not a routine task.

Fig. 8.18 presents typical results of an O-cell test (a 2.8 m by 0.8 m, 24 m deep barrette in Manila, Philippines; Fellenius et al. 1999). The soils at the site are silty sandy volcanic tuff. The diagram shows both the downward movement of the barrette base (toe) and the upward movement of the barrette shaft. The load indicated for the toe includes the buoyant weight of the barrette, whereas this load has been subtracted from the shaft loads before plotting the data. While the barrette shaft obviously has reached a ultimate resistance state, no such state or failure mode is evident for the barrette toe.

At the start of the test, the barrette is influenced by residual load. The solid line added to the beginning of the toe movement indicates an approximate extension of the toe movement to the zero conditions. The residual load is about 2,500 KN and the soil at the toe are precompressed by a toe movement of about 10 mm. The maximum toe movement is 65 mm. The relative movement is 2 % or 8 % depending on which cross section length one prefers to use as reference to the pile diameter.

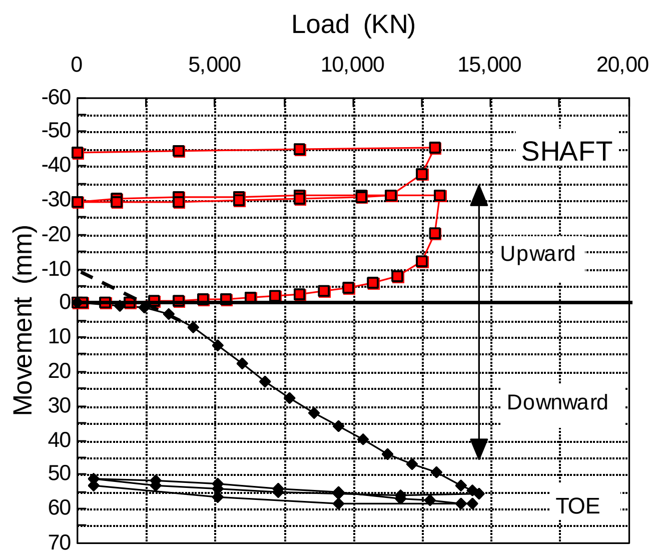

Fig. 8.18 Illustration of main O-cell results. An O-Cell Test on a 2.8 m x 0.8 m, 24 m deep Barrette at Belle Bay Plaza, Manila, Philippines. (Fellenius et al., 1999).

Fig. 8.19 presents the results of an O-cell test on a 2.5 m circular shape pile, 85.5 m into a clayey silty soil in Vietnam. The steep rise over the first 25 mm movement as opposed to the behavior thereafter appears to suggest that a failure value could be determined, say, by the intersection of two lines representing the initial and final trend of the curves. However, this would be an error. Also this pile (as all piles, really) is prestressed by the surrounding soils to a significant residual load. As shown in the diagram, an approximate extension of the curve intersects the abscissa at a movement of about -50 mm.

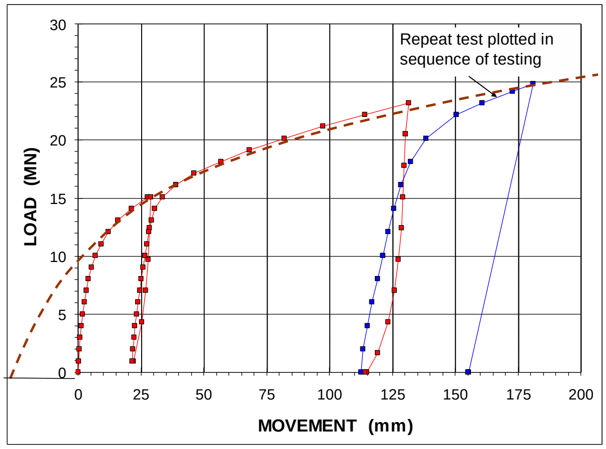

Fig. 8.19 Downward load-movement results from an O-Cell Test on a 2.5 m diameter, 85.5 m long, bored pile at My Thuan Bridge, Vietnam (Fellenius 2002)

The apparent residual load is about 10 MN and amounts to about one third of the ultimate shaft resistance (determined in the O-cell test). Compare also the two unloading and reloading cycles. The reloading curve shows that the residual load increased for each such cycle. The maximum toe movement is 180 mm. The relative movement is 7 % (or 9 %, if the precompression movement is included). No failure is evident from the test records.

A further example of what the O-cell test can provide is shown in Fig. 8.20, which presents the results of repeated O-cell tests on a 457 mm square shape prestressed pile with an embedment of 10.7 m in a compact sand in East Florida (Vilano East), performed at 8 hours, 4 days, and 16 days after the driving The dashed lines show the sudden reduction of load in the pile on reaching the ultimate resistance. The repeated testing showed that the shaft resistance increased with time even though the pore pressures dissipated within minutes after the impact from the pile driving hammer. Bullock et al. (2005) have included the details of the tests results in a study of the increase of capacity with time.

Fig. 8.21 shows a CPT sounding from the site close to the test pile indicating a compact to dense sand to a depth of 12 m, that is, one metre below the pile toe depth. From 12 m on, the soil consists of loose sand.

The Florida test is interesting also for what it shows with regard to the residual load in the pile. As shown in Fig. 8.22, after the unloading to zero load in the O-cell, the lower plate (the pile toe) was almost 3 mm higher up than before the start of the test, which is an indication that the test released some of the residual load (the locked-in load) at the pile toe. This is confirmed by the fact that, after unloading, the pile was 0.08 mm longer than it had been before the start of Test 1. It may not seem much. However, the pile was very stiff in relation to the applied loads. The pile compression at the maximum test load was only 0.14 mm.

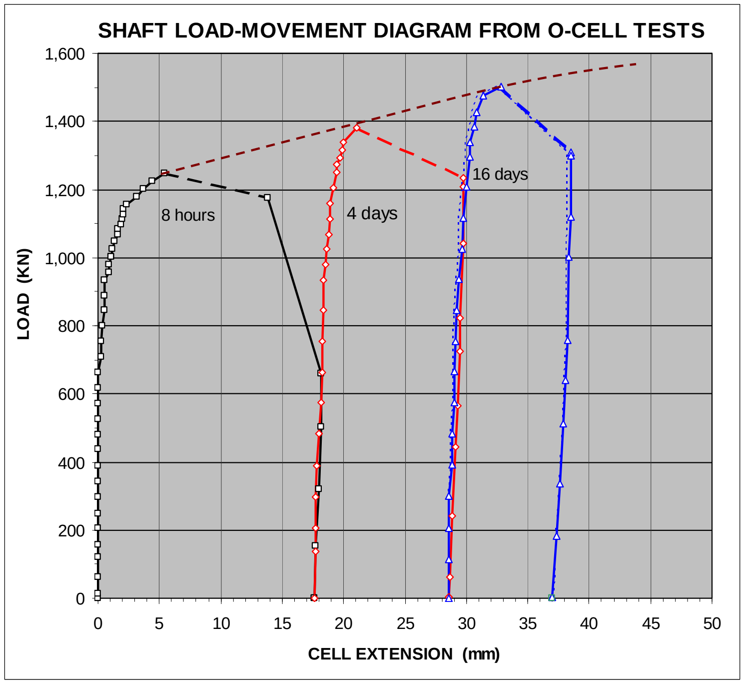

Fig. 8.20 Load-movement curves for the pile shaft. (Data from McVay et al. 1999).

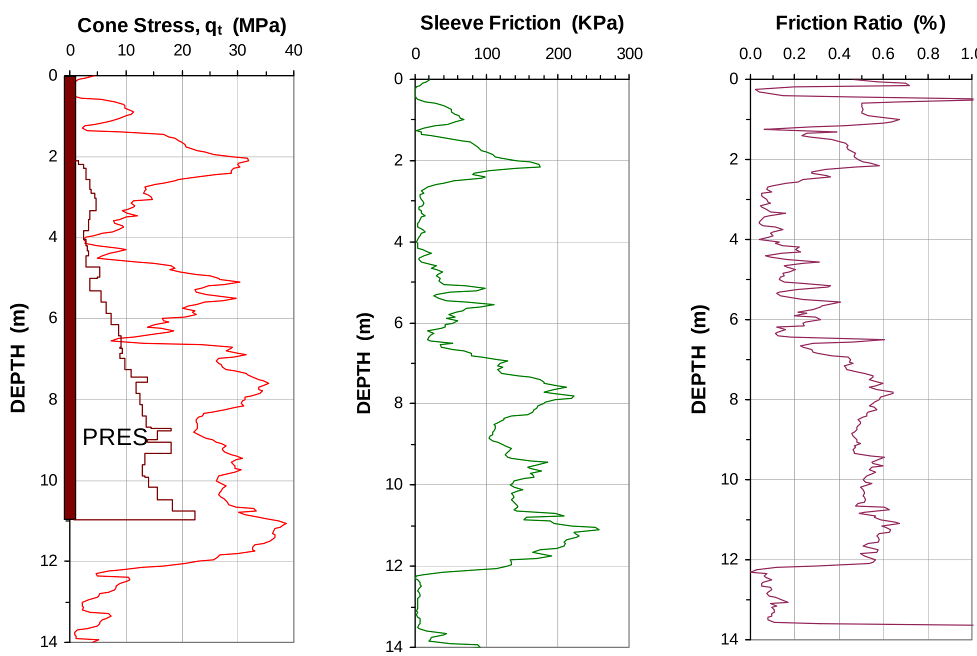

Fig. 8.21 Results of a CPT sounding at the Florida site.

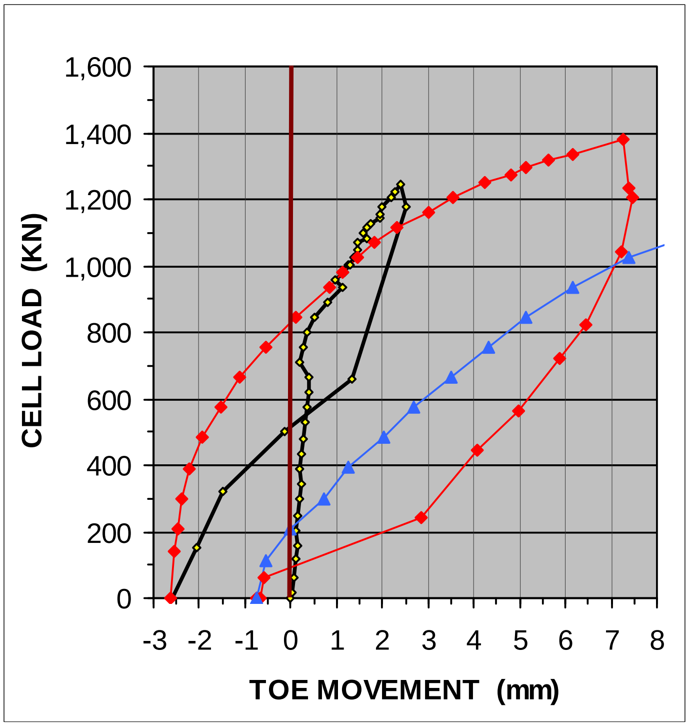

Fig. 8.22 Load-movement curves for the pile toe during the first two load cycles. (Data from McVay et al. 1999).

Moreover, as indicated in the CPT diagram, the pile toe was about 1 m, i.e., 2 pile diameters, above the boundary between the compact to dense soil. The vicinity of the less competent soil did not affect the pile toe response during first two cycles of load. However, as indicated in Fig. 8.23, the third cycle indicates a softer load-movement response, and in the fourth cycle the response became quite soft. The repeated cycles obviously created a lateral tension at the boundary between the dense and the loose sand that progressed upward for each load cycle, loosening the dense sand below the pile toe.

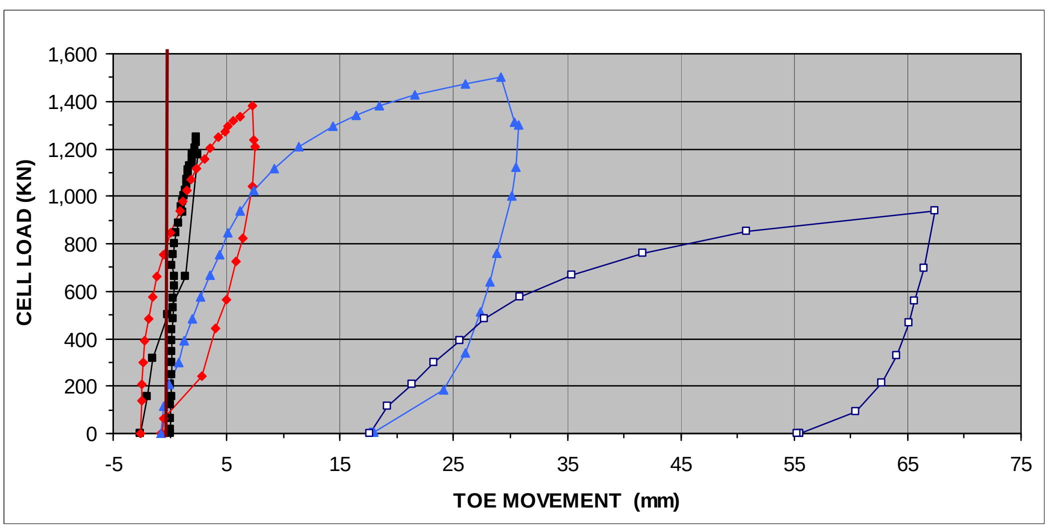

Fig. 8.23 Load-movement curves for the pile toe during all four load cycles. (Data from McVay et al. 1999).

An additional example of results from an O-cell test are shown n Fig. 8.24. The test was carried out on a 900-mm diameter, 16 m long drilled shaft in clayey silt saprolite and socketed a short distance into weathered bedrock in Guaynabo, Puerto Rico. The test was concluded when the pile toe (bottom O-plate) had moved 55 mm downward. As made clear by the upward movement of the shaft is small and almost linear, the shaft resistance was not fully mobilized in the test. Similarly to the footing tests presented in Figs. 6.5 and 6.6 (Section 6.10), the O cell test pile toe load movement follows a slightly curved line and no ultimate resistance is discernable despite the maximum movement of 6 % of the pile diameter.

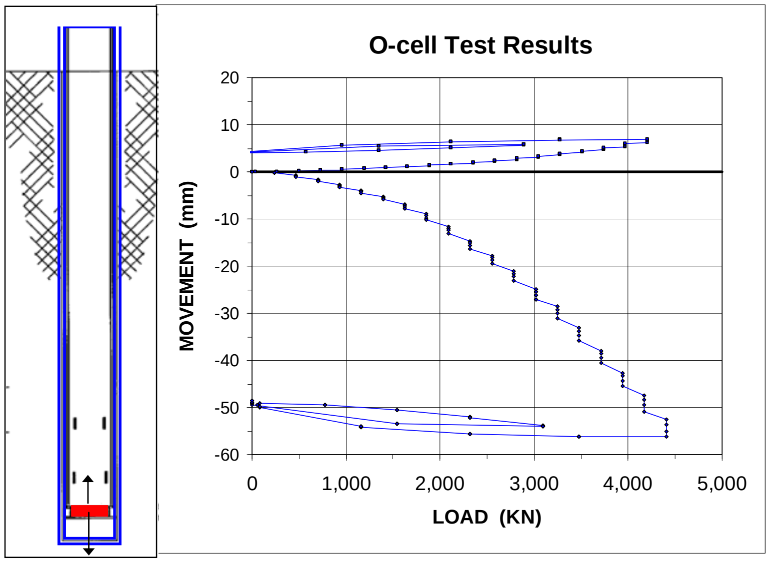

Fig. 8.24 Results of an O-cell test on a 900 mm diameter, 16 m deep bored pile with an O-cell placed near the pile toe. (Data courtesy of GMTS Corp., San Juan, Puerto Rico, and Loadtest Inc., Gainesville, Florida).

Also the load-movement of the pile toe can be approximated to a q-z curve (Eq. 8.12). Indeed, so can the load-movement of the shaft, which is then called "t-z curve". Figure 8.25 illustrates the results of the analysis of the measured data, where the shaft resistance is determined assuming, conservatively, that the shaft was about to start developing ultimate resistance along the full length of the shaft. This is achieved by input of the test data to Eq. 8.12 and an exponent of 0.20. Similarly, the toe movement is simulated with the test data with an exponent of 0.55. The so-determined relations can be combined in a simple analysis incorporating the stiffness of the pile to establish the equivalent head-down load-movement curve, as demonstrated in Fig. 8.25[1]. An interesting exercise, of course, but the head-movement curve does not add much insight to the assessment of the pile foundation. Apply a larger load and the pile moves down some more. The conventional capacity thinking is of little relevance in contrast to the key result of an O-cell test, which is the distribution of resistance along the pile. The distribution is the central part of determining the settlement of the pile or, rather, the structure founded on the piled foundation. In contrast to a head-down test, the O-cell test can be used not just for a capacity analysis, but also for the far more important settlement analysis of the piled foundation.

[1] Routinely, reports of results of O-cell test include an equivalent head-down load-movement curve which is plotted from loads at measured equal movement (upward movement shifted to downward) with an approximation of the curve beyond where one of the components (upward or downward direction values) has reached its maximum value. The so-determined curve is adjusted to reflect that, in a head-down test, the pile axial 'elastic' shortening is larger than that measured in an O-cell test because in a head-down test the loads at the pile toe are conveyed through the shaft, compressing it.

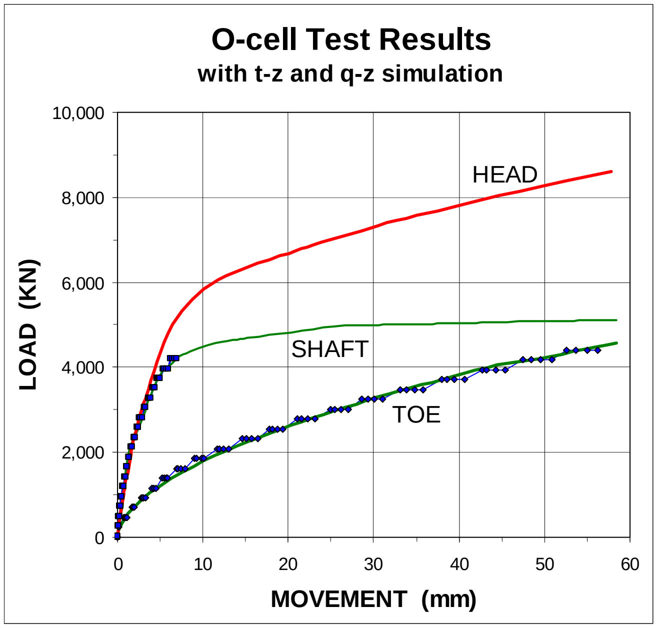

Fig. 8.25 The test data fitted to q-z and t-z relations that then are used to determine the load-movement curve of the equivalent head-down static loading test.

Figure. 8.26 shows the results of an Osterberg-cell test on a strain-gage instrumented test pile in Panama. The array of load distribution curves are the direct measurements from the test. 'Flipping' over the curve measured at the maximum load to the right (the red curve), provides the load distribution of an equivalent head-down test. By means of an effective stress analysis, the fitting of the calculated curve to the measured curve "calibrates" of the test results to the basic soil parameters. Such analysis should always be performed by the project engineers responsible for applying the test results to the foundation design.

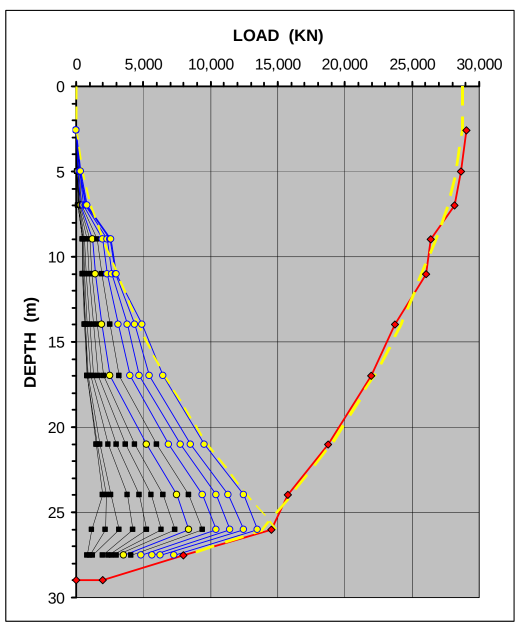

Fig. 8.26 Results from a strain-gage instrumented 2.0 m diameter, 30 m deep bored pile in Panama. The red dots are measured values (vibrating wire gages) and the yellow line is the effective stress fit.

When, as often is the case, a project involves settlement concerns, the O-cell determined load-distribution allows a detailed analysis of the movement response of the pile for the applied load from the supported structure coupled with the effect of the settlement in the surrounding soil. Figure 8.27 shows how the results of the O-cell test on the example presented in Figs. 8.24 and 8.25 are used to analyze potential long-term load-distribution for the pile, when supporting a dead load of 4,000 KN in settling soil. (The example case is also addressed in Section 7.17, Fig. 7.15). Fig. 8.27A and Fig. 8.27B show the load distribution and pile toe load-movement for two scenarios of settlement, I and II, as shown in Fig. 8.27C. Curves marked "I" apply to the case of small settlement in the surrounding soils, which will result in a shallow location of the neutral plane, NP_I, and a small pile toe movement. If on the other hand the settlement is large, as indicated in Case II, the neutral plane lies deeper, NP_{II}, and the pile toe movement is larger. As illustrated, the magnitude of the settlement in the soil surrounding the pile will govern not just the settlement of the pile head, S_I and S_{II}, and of the supported structure, but it will also determine the maximum load in the pile and the pile toe movement. Load and settlement for a pile are interconnected — "unified".

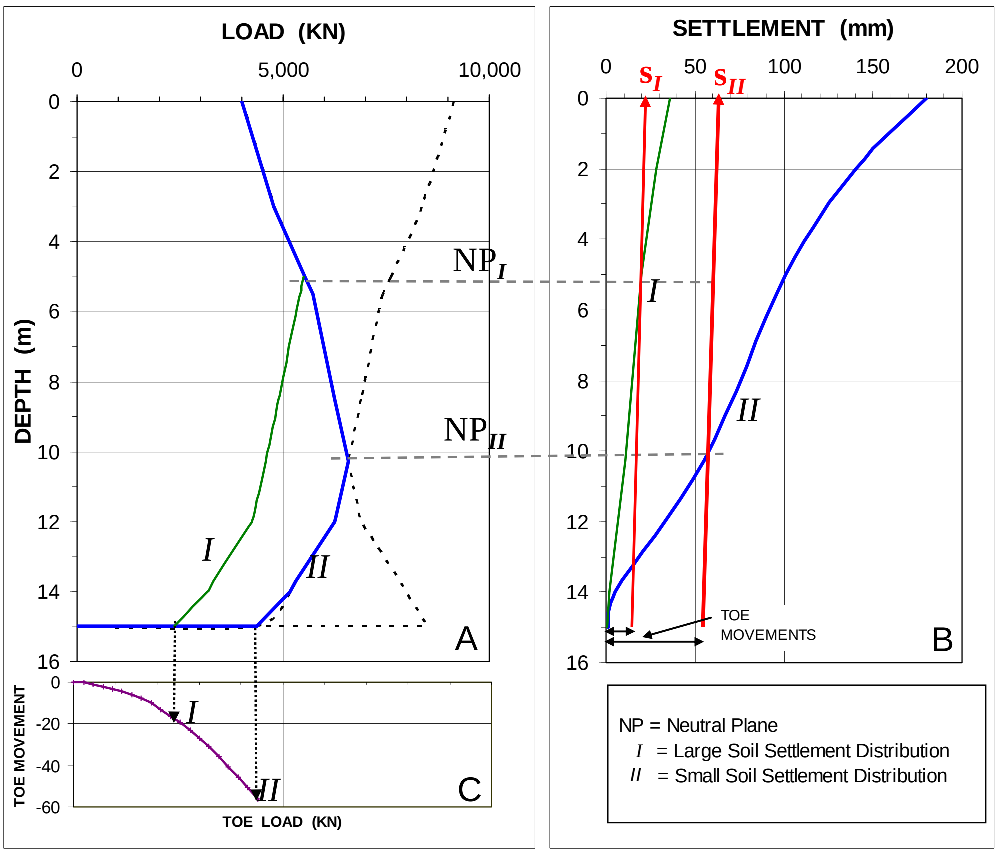

Fig. 8.27 Example of the mutual dependence of soil and pile settlement to load distribution

The illustration in Fig. 8.27 is complex and could be hard to understand. The same O-cell case is simplified and used in Fig. 8.28 to show the typical approach to combine load distribution and settlement in a design. The graphs show the load distribution (Graph A), the settlement distribution (Graph B), and the load movement relation for the pile toe. The latter is obtained directly from the O-cell test, but can also be calculated in a q-z analysis. At the start of the pile construction, settlement is not an issue.

However, settlement occurring from after that point in time and onward will be an issue for the piled foundation. The load distribution at that point is indicated in Graph A as the "Initial Load Distribution". Graph B shows the distribution of long-term settlement developing in the surrounding soil from that initial point in time (Note the pile toe is in bedrock, so no settlement occurs below the pile toe). That settlement will cause downdrag and the pile toe will be forced to move a distance into the soil/bedrock. The movement causes a load at the pile toe to develop to the magnitude indicated in the load-movement diagram (Graph C). That toe load will add to the existing load a the pile toe. The load distribution curves shown in (Graph A) consist of one curve coming down from the applied dead load and increasing with the shaft shear acting downward (negative skin friction) and a second curve rising from the final toe load with the load increasing by the shaft shear as positive shaft resistance. The intersection of the two curves is the neutral plane.

Figure 8.28 shows the end results after a series of iterations— trial and error calculations— to match an assumed toe load due to downdrag letting the iterations determine the neutral plane location, which in turn determines a toe movement. That toe movement should show a toe load equal to the assumed toe load. Initially it will not do so, but by adjusting the starting value and trying again, eventually it will. When the match is achieved, the settlement at the pile head (of the pile cap) is determined as indicated in Graph C.

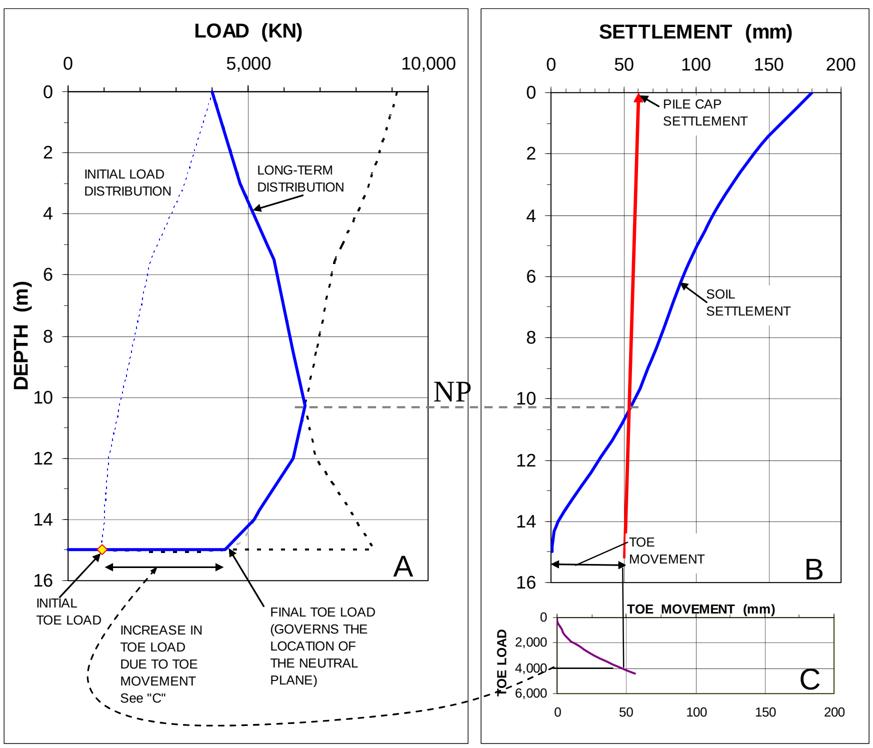

Fig. 8.28 Results of a typical trial -and-error approach to match toe load, neutral plane location, and pile toe movement due to downdrag.

Combining the O-cell test with a conventional head-down test and performing the O-cell test first will provide a test where both the response of the shaft and toe to load will be determined. If the "weakest" part is the pile toe, the head-down test will establish the shaft response. If the shaft is the "weakest" part, the add-on resistance provided by the head-down arrangement will enable the O-cell to determine the toe response. The combination is obtained at low-cost because the head-down load will be small. It is highly recommended.

8.16 A Case History Example of Final Analysis Results from and O-cell Test

Figure 8.29 presents an additioal example of compilation of results of O-cell tests on 25 m long bored piles constructed through sand and silty clay to bearing in a glacial till which project was designed according to the Unified Design Method described in Section 7.18 (Fellenius and Ochoa 2009). The short-term distribution of shaft resistance (thin-line blue curve) determined from the tests is shown in the left diagrams. The distribution is plotted from the values of dead-load applied by the structure supported on the piled foundation. The distribution is matched to an effective stress analysis of resistance (thin red line), which is rising from a toe load of 1,000 KN. In the long-term, effective stress will increase due to a fill placed over the site, which will increase the shaft resistance along the pile. In addition, the fill will cause soil settlement, which distribution is shown to the right. The settlement will cause negative skin friction to develop. Consequently, the long-term load distribution will increase downward from the applied dead load to a maximum at the location where there is no relative movement between the pile and the soil—the neutral plane. The location of the neutral plane is determined by the requirement that the enforced toe movement generates the load at the pile toe that together with the shaft resistance distribution gives a location of the force-equilibrium neutral plane that is equal to the settlement-equilibrium neutral plane. The diagrams demonstrate that an increasign or reducing settletment will change the locatin of theneutral plane and, therfore, the penetration of the pile toe, which will change the value of the pile toe load, which will change the location of the force equlibrium, etc. Forces, settlement and movemtns are interrealted and the design cannot simply be based on a facor of safery approach, but must consider all aspects.

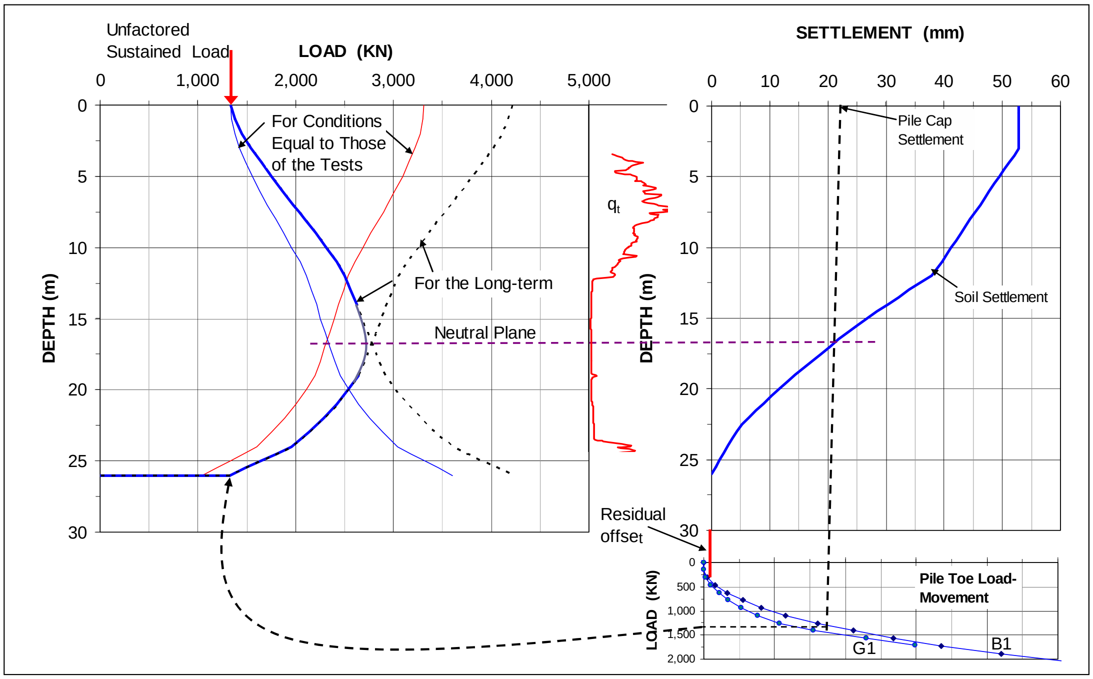

Fig. 8.29 Compilation of test and analysis data: Load distribution in the O-cell static loading test and during long-tem conditions, Load distribution of soil settlement, and Load-movement relation for the pile toe determined in the O-cell test. The soil profile is indicated in a CPT cone resistance diagram. (Fellenius and Ochoa 2009).

Note (1) that the factor of safety is about 2.5, indicating an adequate safety against the pile capacity, (2) the drag load is about equal to the dead load, but it is only of concern for the pile structural strength, which is adequate for the maximum load (dead load plus drag load), and (3) the settlement of the piled foundation is estimated to be smaller than about 25 mm, the criterion for the project.

The live loads affecting the foundations of the project were insignificant. To complete the illustration of the design method, Fig. 8.30 shows the effect on the load distribution of adding an 800-KN live load to the dead load. As shown, the live load only affects the axial load in the pile near the pile head. No change in maximum load in the pile occurs and the settlement is not changed (disregarding the small deformation from 'elastic' compression).

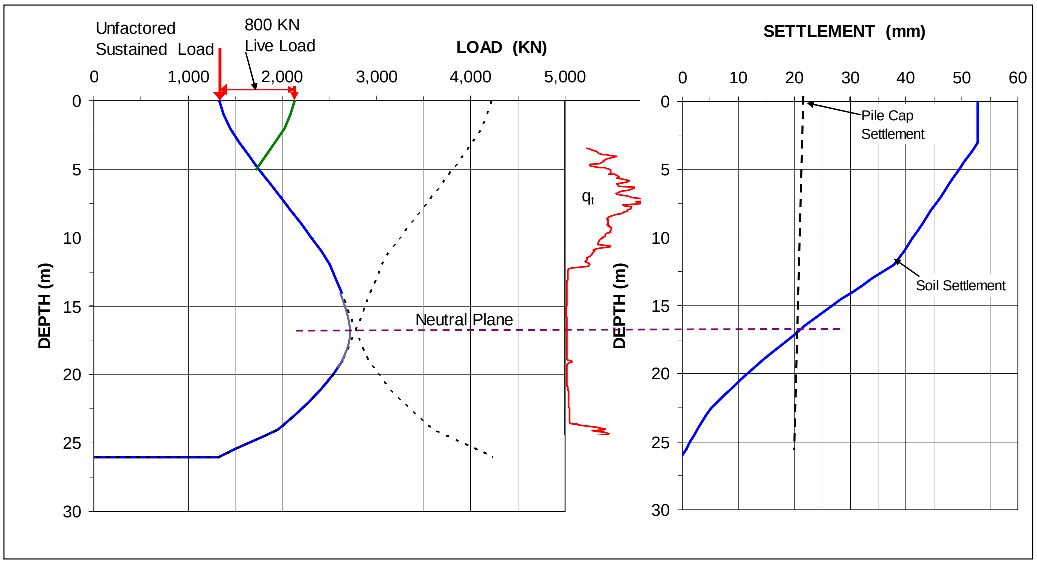

Fig. 8.30 The effect of adding a live load to the pile head.

To empahsize the effect of a live load, Fig. 8.31 shows the conditions when the loads would be from live load, only. The settlement distribution is the same as before, however, the load districbution curve (before applying the live load) is governed by the absence of load at the pile head and the subsequent lowering of the force equilibrium (because of the changed pile toe force and pile toe penetration). Again, when the the live load (assumed as 2,000 KN)0 is applied, it causes no change in maximum load or of pile settlement.

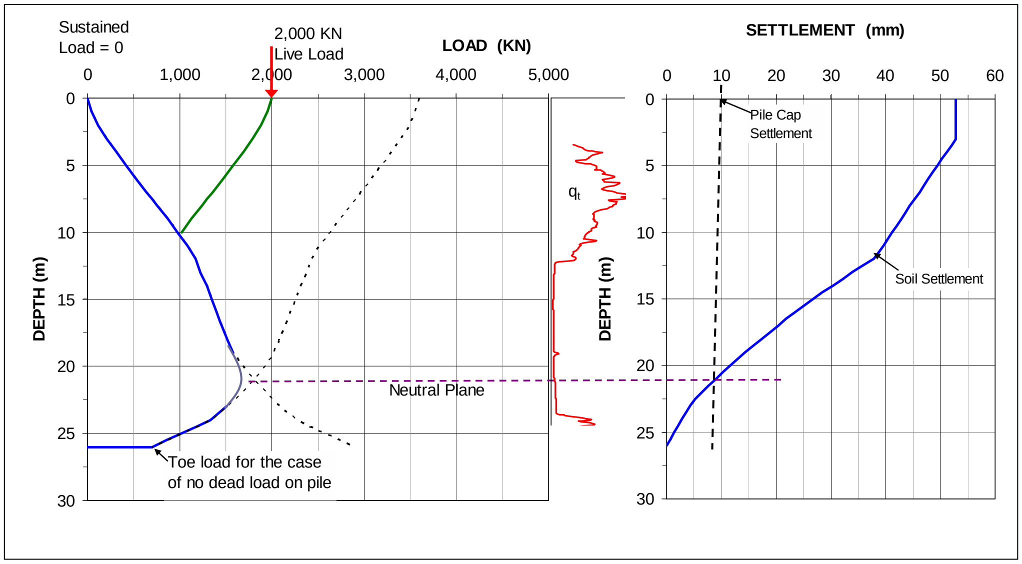

Fig. 8.31 The effect of adding a live load to a pile having zero dead load.

8.17 Procedure for Determining Residual Load in an Instrumented Pile

In contrast to the O-Cell test, the results of conventional "head-down" static loading tests on instrumented piles do not provide the residual load directly. Pile instrumentation consists of strain gages, i.e., the measurement is strain, not load. The load in the pile at the gage location is determined from the change of strain, induced by a load applied to the pile head, by multiplying it with the pile material modulus and cross sectional area. The change of strain is the strain reading minus the "zero reading" of the gage. In a driven pile, the zero reading is ideally taken immediately before the driving of the pile. However, the "zero" value of strain in a pile can change due to the driving—particularly for a steel pile. Moreover, even if the gages are insensitive to temperature change, the pile material is not and the cooler environment in the ground will have some effect on the "zero level" of strain in the pile. The concrete in a concreted pipe pile or a precast pile is affected by aging and time-dependent changes. In case of a prestressed pile, some change of the zero strain introduced by the release of the strands continues for days after the release. For a bored pile, the value of "zero strain" is not that clearly defined in the first place—is the "zero" before concreting or immediately after, or, perhaps, at a specific time later? In fact, the zero reading of a gage is not one value but several, and all need to be considered (and included in an engineering report of the test results). For example, in case of a driven prestressed concrete pile, the first zero reading is the factory zero reading. Second is the reading taken immediately before placing the gages in the casting forms. Third is the reading after the release of the strands and removal of the piles from the form. Fourth is the reading before placing the pile in the leads to start driving. Fifth is the reading immediately after completion of driving. Sixth is the reading immediately before starting the test. The principle is that a gage readings should be taken immediately before (and after) every event of the piling work and not just during the actual loading test. A similar sequence of readings applies to other pile types.

Note, if we place only one gage at a cross section, we cannot separate the influence of bending. Therefore, we need at least one pair of gages with the gages placed at opposite ends of a diameter at equal distance from the center (neutral axis) of the pile cross section. If we need better accuracy, and/or redundancy, we need to place two pairs ("Diamond or square orientation"). Three gages placed in a "Triangular orientation" is the worst approach.

Strains may develop that have no connection to the average strain across a pile, that is, they are not caused by a change of load in the pile. An example of this is the elongation of a reinforcing bar (with strain gage attached) due to the temperature rise at the outset of the grouting of a pile, as shown in Fig. 8.32. Part of the contraction during the subsequent cooling is prevented by the grout and soil leaving the bar (and the gage) with a permanent elongation, i.e., an apparent tension load. Residual load will eliminate or to some extent offset this false tension, causing the data to suggest—erroneously—that no locked-in load exists in the pile at the start of the static loading test. Moreover, the analysis of strain changes and residual load in precast concrete piles and bored piles must also consider the effect of swelling of the concrete in absorbing water from the soil.

However, even if the only available or reliable zero reading is the reading immediately before the start of the test", the strain-gage data can still be used to determine the residual load and the true distributions in a pile. That is, provide that the soil profile is reasonably homogeneous. The method of analysis will be demonstrated using data from CAPWAP analysis of dynamic measurements taken in restriking a pile. The pile is a 250 mm diameter square precast concrete pile driven 19 m into a sand deposit. (As described in Chapter 9, CAPWAP analysis makes use of strain and acceleration measured for an impact with a pile driving hammer. The analysis delivers amongst other results the static resistance mobilized by the impact. In the calculation, the pile is simulated as a series of many short elements and the results are presented element per element, as had measurements been made at many equally spaced locations along the pile).

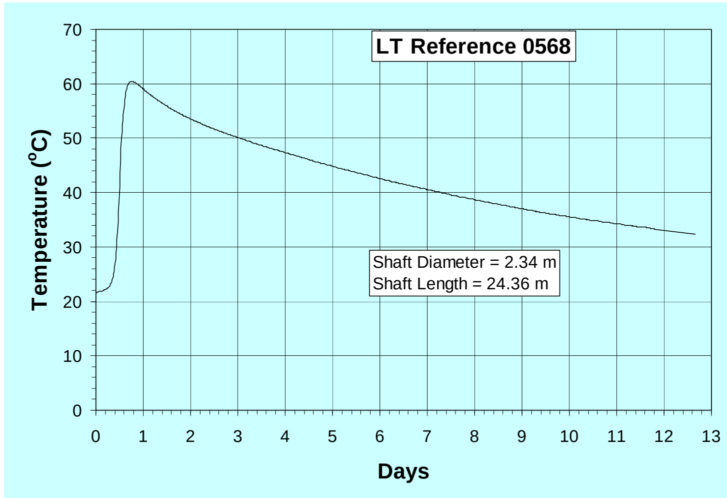

Fig. 8.32 Temperature in a pile after grouting and during the first two weeks of curing of the grout. Data courtesy of Loadtest Inc.

Although the CAPWAP program allows an adjustment for locked-in load due to the immediately preceding impact, if the pile is subjected to residual load, the CAPWAP analysis cannot determine these but presents a resistance distribution that is affected by these loads in a manner similar to that of a resistance distribution measured by strain gages in static loading test on an instrumented pile.

Fig. 8.33A presents a CPT q_t-diagram from a sounding close to the test pile. The sand is loose to compact. Fig. 8.33B presents the CAPWAP determined resistance distribution from the first blow of restrike on the pile 216 days after the initial driving. The CAPWAP determined ultimate resistance is 1,770 KN. The total shaft resistance is 1,360 KN and the toe resistance is 410 KN. The CAPWAP distribution has an "S-shape indicting that the unit shaft resistance increases with depth to a depth of about 13 m. However, below this depth, the distribution curve indicates that the unit shaft resistance is progressively becoming smaller with depth. From a depth of about 15 m, the unit shaft resistance is very small. This distribution is not consistent with the soil profile established by the CPT sounding. In fact, the resistance distribution is consistent with a pile subjected to residual load. Because the soil is relatively homogeneous, the data can be used to determine the distribution of residual load as well as the resistance distribution unaffected by the residual load, the "true" ultimate resistance.

As mentioned, residual load is the consequence of negative skin friction acting in the upper part of the pile. The analysis procedure presented in the following is based on the assumption that the negative skin friction is fully mobilized and equal to the positive shaft resistance mobilized by the impact ("applied test load"). The assumption of fully mobilized negative skin is not always valid or not valid for the full length of the pile. Where the residual load is built up from fully mobilized negative skin friction, the "true" shaft resistance (positive or negative direction of shear) is half of that determined directly from the test data. Fig. 8.34 shows the Fig. 8.30 processed test data. In Fig. 8.34A, a curve has been added that shows half the CAPWAP determined shaft resistance: Starting at the ground surface and to a depth of 13 m, the curvature increases progressively. To this depth, the curve represents the distribution of the residual load (Fig. 8.34B) and, also, of the true shaft resistance. The progressive increase indicates proportionally to the effective overburden stress. A back-calculation of the resistance shows that the beta-coefficient (the proportionality factor in the effective stress analysis) is about 0.6.

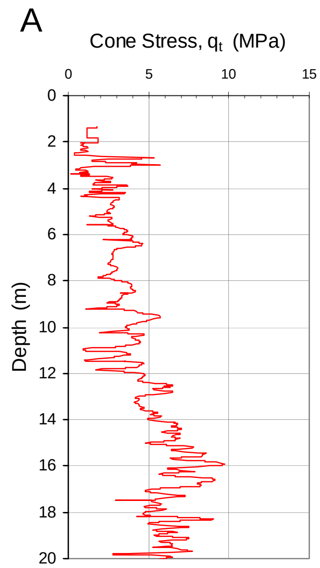

Fig. 8.33A CPT profile

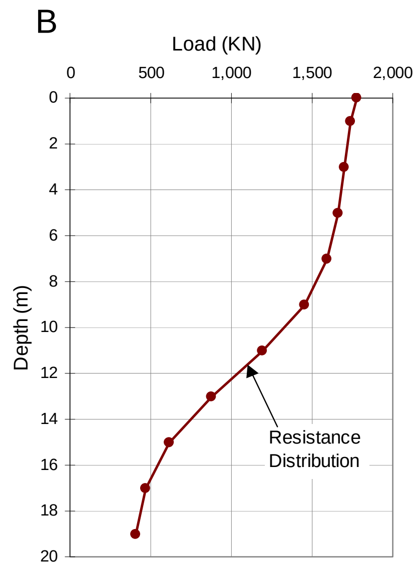

Fig. 8.33B CAPWAP determined load-distribution

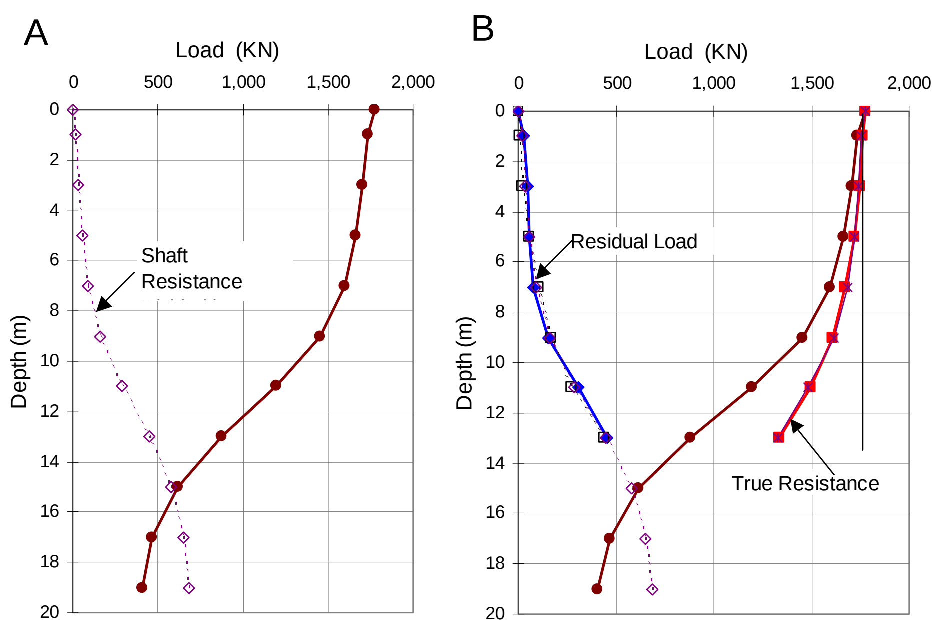

Fig. 8.34 Procedure for determining the distribution of residual load and "true" resistance

To the depth of 13 m, the "true" resistance distribution in the test can be determined by starting from the maximum test load (the CAPWAP capacity) and reducing the load by positive shaft resistance taken as equal to the half the CAPWAP determined shaft resistance (or calculating it using the back-calculated beta-coefficient). Below the 13-m depth, however, the "half-curve" bends off. The depth is where the transition from negative skin friction to positive toe resistance starts and the assumption of fully mobilized negative skin friction is no longer valid. To extend the residual load distribution curve beyond the 13 m depth, one has to resort to the assumption that the beta-coefficient found in the upper soil layers applies also below 13 m depth and calculate the continuation of the true resistance distribution. The continuation of the distribution of the residual load is then obtained as the difference between the true resistance and the CAPWAP determined distribution. The results of this calculation are presented in Fig. 8.35.

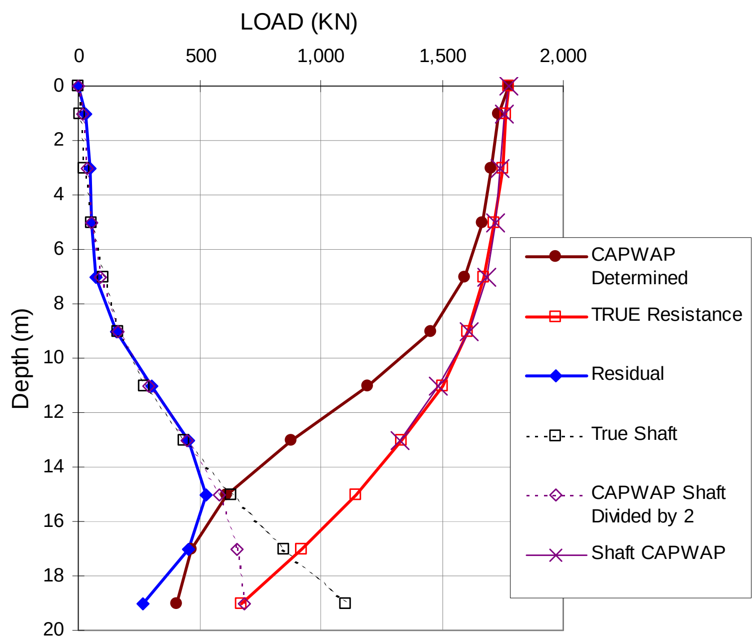

Fig. 8.35 Final Results: Measured Load, Residual Load, and True Resistance

The objective of the analysis procedure is to obtain a more representative distribution of resistance for the test pile. The CAPWAP determined resistance distribution (or as it could have been, the distribution that would have been obtained from a static loading test on a strain-gage instrumented pile), misrepresents the condition unless the distribution is corrected for residual load. The corrected shaft and toe resistances are 1,100 KN and 670 KN as opposed the direct values of 1,360 KN and 410 KN.

The full benefit of the O-cell test is sometimes—indeed, very often—best achieved by combining the O-cell test with a conventional head-down test. For the case where the shaft resistance is expected to be larger than the toe resistance, the O-cell is the engaged first to move the pile toe down and establish the pile-toe load-movement relation, using the shaft resistance as a reaction to pushing down the pile toe. The O-cell opening constitutes opening a "gap" above the pile toe. The head-down test is then performed with the O-cell "draining", i.e., providing zero resistance to the pile toe, which establishes the shaft resistance relation. Together, the two tests have thus determined the full capacity of the pile. For the case where the shaft resistance is expected to be smaller than the toe resistance, the O-cell is again the engaged first, to establish the pile shaft resistance. Then, the reaction at the pile head is used to provide the extra resistance to the pile shaft to enable the O-cell to fully engage the pile toe. Again, together the two tests have thus determined the full capacity of the pile.

It is important to include a sufficient number of strain-gage levels in the test pile with a good deal of redundancy to ensure the means of full analysis of the results. More details and examples of the analysis method are provided by Fellenius (2002).

8.18 Modulus of 'Elasticity' of the Instrumented Pile

Aspects to consider. In arranging for instrumentation of a pile, several aspects must be considered. The gages must be placed in the correct location in the pile cross section to eliminate influence of bending moment. If the gages are installed in a concrete pile, a key point is how to ensure that the gages survive the installation—a gage finds the visit from a vibrator a most traumatic experience, for example. We need the assistance of specialists for this work. The survival of gages and cables during the installation of the pile is no less important and this requires the knowledge and interested participation and collaboration of the piling contractor, or, more precisely, his field crew.

Once the gages have survived the pile manufacture and installation—or most of the gages, a certain redundancy is advised—the test can proceed and all should be well. That is, provided we have ensured the participation of a specialist having experience in arranging the data acquisition system and the recording of the readings. Then, however, the geotechnical engineer often relaxes in the false security of having all these knowledgeable friends to rely on. He fails to realize that the reason for why the friends do not interfere with the testing programme and testing method is not that they trust the geotechnical engineer's superior knowledge, but because advising on the programme and method is not their mandate.

The information obtained from a static loading test on an instrumented pile can easily be distorted by unloading events, uneven load-level durations, and/or uneven magnitude of load increments. Therefore, a static test for determining load transfer should be carried through in one continuous direction of movement and load without disruptions or unloading. Hold all load levels an equal length of time —an extended load holding will adversely affect the interpretation of the results and provide nothing worthwhile in return.

So, once all the thoughts, know-how, planning, and hands-on have gone into the testing and the test data are secured, the rest is straightforward, is it not? No, this is where the fun starts. Now comes how to turn strain into load, a detail that is surprisingly often overlooked in the data reduction and evaluation of the test results.

Converting to load using the elastic modulus. Strain gages are usually vibrating wire gages. The gages provide values of strain, not load, which difference many think is trivial. Load is just strain multiplied by the cross sectional area of the pile and the elastic modulus, right?

The measured strain data are transferred to load by use of the Young's modulus of the pile material and of the pile cross sectional area. For steel piles, this is normally no problem (cross sectional changes, guide pipes, etc. can throw a "monkey-wrench" into a the best laid plans, however.). In case of precast piles, prestressed concrete piles, and concreted pipe piles, the modulus is a combined modulus of the steel and concrete, normally proportional to area and modulus, as shown in Eq. 8.16.

(8.16) $$E_{comb} = \frac{E_s A_s + E_c A_c}{A_s + A_c}$$

where
E_{comb} = combined modulus
E_s = modulus for steel
A_s = area of steel
E_c = modulus for concrete
A_c = area of concrete

The steel modulus is known quite accurately. It is a constant value (about 29.5 x 10^6 ksi or 205 GPa). In contrast, not only can the concrete modulus have many values, the concrete modulus is also a function of the applied stress or strain. Common relations for its calculation, such as the relation between the modulus and the cylinder strength, are not reliable enough. A steel pile is only an all-steel pile in driving—during the test it is often a concrete-filled steel pipe. The modulus to use in determining the load is the combined value of the steel and concrete moduli. By the way, in calculating the concrete modulus in a concrete-filled steel pipe, would you choose the unconfined or the confined modulus?

Usually, the modulus reduces with increasing stress or strain. This means that when load is applied to a pile or a column, the load-movement follows a curve, not a straight line. Fellenius (1989) presented a method (explained below) for determining the strain-dependency from test data based on the assumption that the curved line is a second degree function. Then, the change of stress divided by the strain and plotted against the strain should show a straight, but sloping line for the column. For the pile, the equivalent plot will only show the straight line when all shaft resistance is mobilized and the applied increment of load goes unreduced to the pile toe.

Well, the question of what modulus value to use is simple, one would think. Just place a gage level near the pile head where the load in the pile is the same as the load applied to the pile head, and let the data calibrate themselves, as it were, to find <u>the concrete modulus</u>. However, in contrast to the elastic modulus of steel, the elastic modulus of concrete is not a constant, but a function of the imposed load, or better stated, of the imposed strain. Over the large stress range imposed during a static loading test, the difference between the initial and the final moduli for the pile material can be substantial. This is because the load-movement relationship (stress-strain, rather) of the tested pile, taken as a free-standing column, is not a straight line. Approximating the curve to a straight line may introduce significant error in the load evaluation from the strain measurement. However, the stress-strain curve can with sufficient accuracy be assumed to follow a second-degree line: $y = ax^2 + bx + c$, where y is stress and x is strain (Fellenius, 1989). The trick is to determine the constants a and b (the constant c is zero).

The approach builds on the fact that the stress, y, can be taken as equal to <u>the secant modulus</u> multiplied by the strain. This is achieved by way of first determining the tangent modulus, and then using it to determine the secant modulus. The following presents the mathematics of the method.

Mathematics of the Tangent Modulus Method. For a pile taken as a free-standing column (case of no shaft resistance), the tangent modulus of the composite material is a straight line sloping from a larger tangent modulus to a smaller. Every measured strain value can be converted to stress via its corresponding strain-dependent secant modulus.

The equation for the tangent modulus M_t, is:

(8.17) $$M_t = \left(\frac{d\sigma}{d\varepsilon}\right) = a\varepsilon + b$$

which can be integrated to:

(8.18) $$\sigma = \left(\frac{a}{2}\right)\varepsilon^2 + b\varepsilon$$

Eq. 8.19 shows an alternative way of calculating the stress

(8.19) $\sigma = E_s\,\varepsilon$

Therefore,

(8.20) $\sigma = E_s\,\varepsilon = 0.5a\,\varepsilon^2 + b\,\varepsilon$ and $E_s = 0.5a\,\varepsilon + b$

where
M = tangent modulus of composite pile material
E_s = secant modulus of composite pile material
σ = stress (load divided by cross section area)
$d\sigma$ = $(\sigma_{n+1} - \sigma_1)$ = change of stress from one load increment to the next
a = slope of the tangent modulus line
ε = measured strain
$d\varepsilon$ = $(\varepsilon_{n+1} - \varepsilon_1)$ = change of strain from one load increment to the next
b = y-intercept of the tangent modulus line (i.e., initial tangent modulus)

With knowledge of the strain-dependent, composite, secant modulus relation, the measured strain values are converted to the stress in the pile at the gage location. The load at the gage is then obtained by multiplying the stress by the pile cross sectional area.

Procedure. When data reduction is completed, the evaluation of the test data starts by plotting the measured tangent modulus versus strain for each load increment (the values of change of load or stress divided by change of strain are plotted versus the measured strain). For a gage located near the pile head (in particular, if above the ground surface, the modulus calculated for each increment is unaffected by shaft resistance and the calculated tangent modulus is the actual modulus. For gages located further down the pile, the first load increments are substantially reduced by shaft resistance along the pile above the gage location and a linear relation will not develop until the shaft resistance is fully mobilize at and above the gage location. Initially, therefore, the tangent modulus values calculated from the full load increment divided by the measured strain will be large. However, as the shaft resistance is being mobilized down the pile, the strain increments become larger and the calculated modulus values become smaller. When all shaft resistance above a gage location is mobilized, the calculated modulus values for the subsequent increases in load at that gage location are the computed tangent modulus values of the pile cross section at the gage location.

For a gage located down the pile, shaft resistance above the gage will make the tangent modulus line plot above the modulus line for an equivalent free-standing column—giving the line a translation to the left. The larger the shaft resistance, the higher the line. However, the slope of the line is unaffected by the amount of shaft resistance above the gage location. The lowering of the line is not normally significant. For a pile affected by residual load, strains will exist in the pile before the start of the test. Such strains will result in a lowering of the line—a translation to the right—offsetting the shaft resistance effect.

It is a good rule, therefore, always to determine the tangent modulus line by placing one or two gage levels near the pile head where the strain is unaffected by shaft resistance. An additional reason for having a reference gage level located at or above the ground surface is that such a placement will also eliminate any influence from strain-softening of the shaft resistance If the shaft resistance exhibits strain-softening, the calculated modulus values will become smaller and infer a steeper slope than the true slope of the modulus line. If the softening is not gradual, but suddenly reducing to a more or less constant post-peak value, a kink or a spike will appear in the diagram.

Example

To illustrate the approach, the results of a static loading test on a 20 m long Monotube pile will be used. The pile is a thin-wall steel pipe pile, tapered over the lowest 8.6 m length. (For complete information on the test, see Fellenius et al., 2000).

The soil consisted of compact sand. Vibrating wire strain gages were placed at seven levels, with Gage Level 1 at the ground surface. Gage Levels 2 through 5 were placed at depths of about 2, 4, 9, and 12 m. Gage Level 6 was placed in the middle of the tapered portion of the pile, and Gage Level 7 was placed at the pile toe.

Fig. 8.36 shows curves of applied load and measured strain for the seven gages levels in the pile. Because the load-strain curves of Gage Levels 1, 2, and 3 are very similar, it is obvious that not much shaft resistance developed above the Gage Level 3.

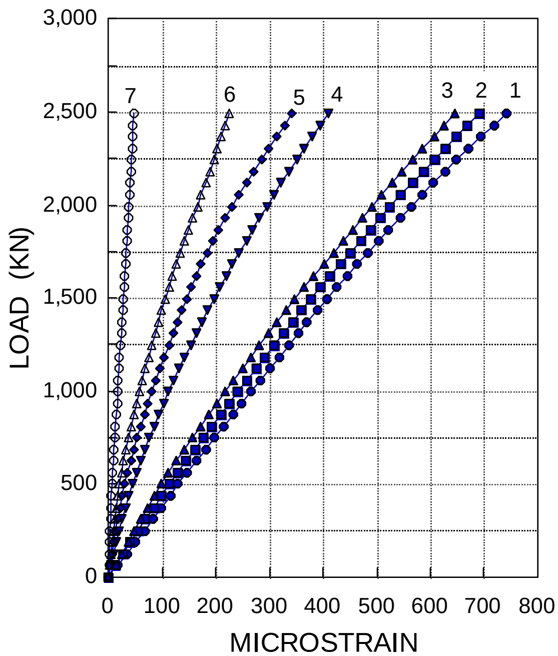

Fig. 8.36 Strain measured at Gage Levels 1 through 7

Fig. 8.37 shows that tangent modulus values for the five gages placed in the straight upper length of the pile, Gages Levels 1 through 5. The values converge to a straight line represented by the “Best Fit Line”.

Linear regression of the slope of the tangent-modulus line indicates that the initial tangent modulus is 44.8 GPa (the constant “B” in Eqs. 1 through 4). The slope of the line (coefficient “A” in Eqs. 1 through 4) is -0.021 GPa per microstrain ($\mu\,\varepsilon$). The resulting secant moduli are 40.5 GPa, 36.3 GPa, 32.0 GPa, and 27.7 GPa at strain values of 200 $\mu\,\varepsilon$, 400 $\mu\,\varepsilon$, 600 $\mu\,\varepsilon$, and 800 $\mu\,\varepsilon$, respectively.

The pile cross sectional area as well as the proportion of concrete and steel change in the tapered length of the pile. The load-strain relation must be corrected for the changes before the loads can be calculated from the measured strains. This is simple to do when realizing that the tangent modulus relation (the “Best Fit Line”) is composed of the area-weighted steel and concrete moduli. Conventional calculation using the known steel modulus provides the value of the concrete tangent modulus. The so-determined concrete modulus is then used as input to a calculation of the combined modulus for the composite cross sections at the locations of Gage Levels 6 and 7, respectively, in the tapered pile portion.

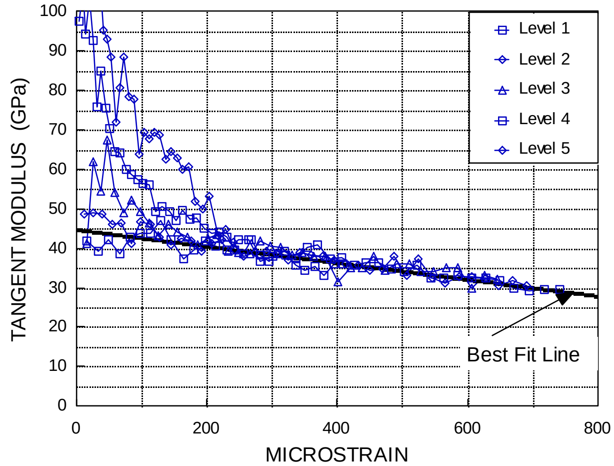

Fig. 8.37 Tangent Modulus Diagram

Fig 8.38 presents the strain gage readings converted to load, and plotted against depth to show the load distribution in the pile as evaluated from the measurements of strain used with Eq. 4. The figure presents the distribution of the loads actually applied to the pile in the test. Note, however, that the strain values measured in the static loading test do not include the strain in the pile that existed before the start of the test due to residual load. Where residual loads exist, the values of applied load must be adjusted for the residual loads before the true load distribution is established.

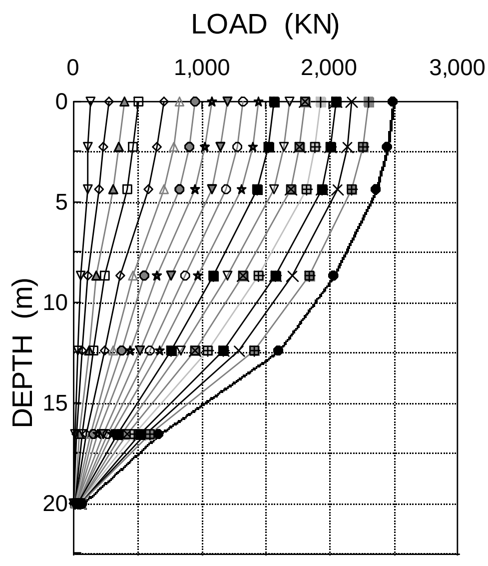

Fig. 8.38 Load distribution for each load applied to the pile head

When determining the load distribution in an instrumented pile subjected to a static loading test, one usually assumes that the loads are linearly proportional to the measured strains and multiplies the strains with a constant—the elastic modulus. However, only the modulus of steel is constant. The modulus of a concrete can vary within a wide range and is also a function of the imposed load. Over the large stress range imposed during a static loading test, the difference between the initial and the final tangent moduli for the pile material can be substantial. While the secant modulus follows a curved line in the load range, in contrast, the tangent modulus of the composite material is a straight line. The line can be determined and used to establish the expression for the secant elastic modulus curve. Every measured strain value can therefore be converted to stress and load via its corresponding strain-dependent secant modulus.

For a gage located near the pile head (in particular, if above the ground surface, the tangent modulus calculated for each increment is unaffected by shaft resistance and it is the true modulus (the load increment divided by the measured strain). For gages located further down the pile, the first load increments are substantially reduced by shaft resistance along the pile above the gage location. Initially, therefore, the tangent modulus values will be large. However, as the shaft resistance is being mobilized down the pile, the strain increments become larger and the calculated modulus values become smaller. When all shaft resistance above a gage level is mobilized, the calculated modulus values for the subsequent increases in load at that gage location are the tangent modulus values of the pile cross section.

By the way. The example of determining the measured values of load presented in the foregoing is only the starting point of the analysis. Next comes assessing whether or not the pile is subjected to residual load. Fig. 8.39 presents the final result after adjustment to residual load according to the procedure given in Section 8.16.

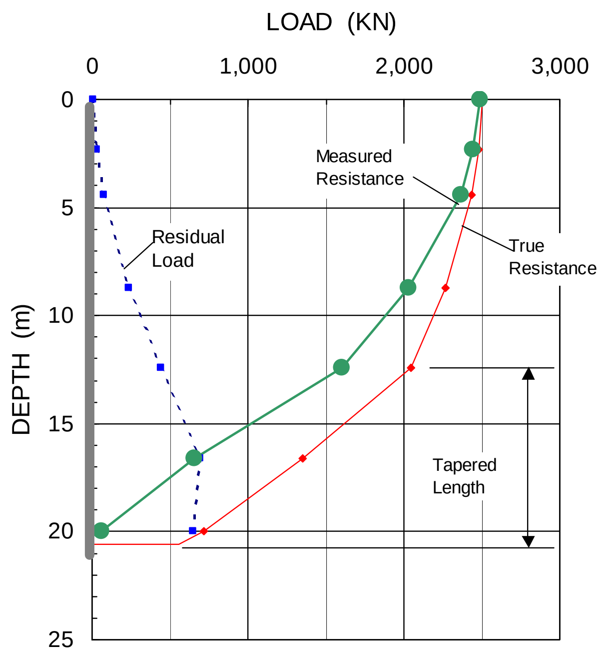

Fig. 8.39 The example case with Measured Load, Residual Load, and True Resistance

8.18 Concluding Comments

Be the test a simple proof test or an elaborate instrumented test, a careful analysis of the recorded data is necessary. Continuing the test until the ultimate resistance is reached and combining full-scale field tests with analysis using basic soil mechanics principles of effective stress and load-transfer mechanism will optimize the information for the pile. Moreover, such analysis is necessary for any meaningful transfer of the test result to other piles for the same project as well as for gaining insight of general validity. Notice, forgetting that piles are subjected to residual loads throws the most elaborate instrumentation and analysis scheme to the wind.

As indicated in the foregoing, the concept of ultimate resistance (capacity) does not apply to the pile toe. When accounting for residual load in an analysis, a pile toe does not develop a capacity failure, but shows only a line curving due to moderately larger movement for each applied load increment. For most piles used in current practice, the failure load inferred from the pile head load-movement curve occurs at a pile toe movement (additional to that introduced by the residual load) in the range of 5 mm through 15 mm, about 10 mm on average. In a test performed for reasons beyond simple proof testing, as a minimum, a toe telltale should be included in the test and the analysis of the test results include establishing the q-z (t-z) curve for the pile toe and the residual load. The data and analysis will enable the estimation of the long-term pile toe movement and pile toe load, which information is necessary for locating the neutral plane, determining the maximum load in the pile, and verifying the long-term settlement of the pile group.

A project can normally only afford one static loading test. For driven piles, the pile driving can become a part of a dynamic test by means of the Pile Driving Analyzer and the analysis of measured strain and acceleration in the Analyzer and by means of CAPWAP and WEAP analysis. The dynamic test has the advantage of low cost and the possibility of testing several piles at the site to identify variations and ranges of capacity. It also determines the adequacy of the pile driving equipment and enables the engineers to put the capacity values into context with the installation procedures. A CAPWAP analysis also produces the distribution of shaft resistance along the pile and determines the pile toe resistance. Notice, however, also the dynamic test includes the residual load, which results in the analysis exaggerating the shaft resistance and underestimating the toe resistance correspondingly. By testing and analyzing records from initial driving and from restrike after some time (letting set-up develop along with increased residual load), as well as testing a slightly shorter pile not driven to full toe resistance, engineering analysis will assist the analyses at very moderate extra cost. If is often more advantageous to perform an Osterberg O-Cell test rather than a conventional head-down test, because the O-Cell test will provide separation of the shaft and toe resistances, the pile-toe load-movement behavior, and the residual load in the pile (at the location of the O-Cell).

When applying the results of a static loading test to a pile group design, it quickly becomes obvious that the deciding total capacity and the factor of safety is not always governing the design of a piled foundation. Do not let the effort toward deciding on the pile capacity and factor of safety overshadow the fact that in the end it is the pile settlement that governs. The serviceability of a design is the key aspect.

To assess the settlement issue, the analysis of the loading test should produce information on the load distribution along a pile, the location of the neutral plane, and the anticipated settlement of the soils around the piles. When the results of even a routine test performed with no instrumentation are combined with a well established soil profile and a static analysis (Chapter 6), reasonably representative load and resistance distributions can sometimes be derived from the data. The final design may then be with a factor of safety that is smaller than the originally assigned values, as well as, in some cases, larger. The more important the project, the more information that becomes available, and the more detailed and representative the analysis of the pile behavior — for which a static test is only a part of the overall design effort — the more weight the settlement analysis gets and the less the factor of safety governs the design.

Finally, the analysis of the results of a static loading test is never better than the test allows. The so-called "standard test procedure" of loading up the pile in eight increments waiting for "zero movement" to occur at each load level and then keeping the maximum load on the pile for 24 hours is the worst possible test. Indeed, if the pile capacity is larger than twice the allowable load (the usual maximum load applied in a routine pile loading test), the results of the test according to this method are very well able to prove this. However, a test by this method gives no information on what the margin might be, and, therefore, no information on any savings of efforts, such as relaxing of pile depths, pile construction method and pile driving termination criteria, etc. On the other hand, if the pile capacity is inadequate so that the pile fails before the maximum load, the "standard test procedure" provides very little information to use for determining the actual pile capacity (it probably occurred somewhere when adding the last increment, or when trying to do so). Nothing is so bad, however, that it cannot be made worse. Some "engineers", some codes, even, incorporate at one or two load levels an unloading and reloading of the pile and/or extra load-holding period, ensuring that the test results are practically useless for informed engineering decisions.

Frankly, the "standard test procedure" is only good for when the pile is good and not when it isn't, and it is therefore a rather useless method.

The method that provides the best data for analysis of capacity and load-transfer is a test performed by measn of a large number of small increments applied at constant short time intervals. For example, the test should aim for a minimum of 25 increments to twice the design load, each increment applied exactly at every 10 minutes. If the pile has not reached capacity and if the reaction system allows it, a few more increments can be applied, greatly enhancing the value of the test at no cost. After the maximum load has been on the pile for the 10-minute increment duration, the pile should be unloaded in about six or eight steps with each held constant for no more than 2 minutes. After unloading and a ten-minute pause to check that records are fine, the pile should be loaded in about six steps to within four increments below the prior maximum load and the original load application procedure repeated. Such a test is completed with the course of a normal working day.

Notice, once a test is started with a certain increment magnitude and duration, do not change this at any time during the test. It is a common mistake to half the increments when the movement of the pile start to increase. Don't. Start out with small enough increments, instead. And, notice, the response of the pile to small loads applied in the early part of the test is quite important for the analysis of the overall test results.

For some special cases, cyclic testing may provide useful information. However, the cyclic loading should not be combined with the test for load-transfer and capacity, but must be performed separately and after completion of the regular test. Notice, a simple unloading and reloading makes no cyclic test. A useful cyclic test requires many cycles and the sequence should be designed to fit the actual conditions of interest.

In spite of their obvious deficiencies and unreliability, pile driving formulas still enjoy great popularity among practicing engineers, because the use of these formulas reduces the design of pile foundations to a very simple procedure. The price one pays for this artificial simplification is very high. Karl Terzaghi 1943. Theoretical Soil Mechanics. John Wiley & Sons, New York.

CHAPTER 9

PILE DYNAMICS

9.1 Introduction

The development of the wave equation analysis from the pre-computer era of the fifties (Smith 1960) to the advent of a computer version in the mid-seventies was a quantum leap in foundation engineering. For the first time, a design could consider the entire pile driving system, such as wave propagation characteristics, velocity dependent aspects (damping), soil deformation characteristics, soil resistance (total as well as its distribution of resistance along the pile shaft and between the pile shaft and the pile toe), hammer behavior, and hammer cushion and pile cushion parameters.

The full power of the wave equation analysis is first realized when combined with dynamic monitoring of the pile during driving. The dynamic monitoring consists in principle of recording and analyzing the strain and acceleration induced in the pile by the hammer impact. It was developed in the USA by Drs. G.G. Goble and F. Rausche, and co-workers at Case Western University in the late 1960’s and early 1970's. It has since evolved further and, as of the early 1980’s, it was accepted all over the world as a viable tool in geotechnical engineering practice.

Pile driving consists of forcing a pile to penetrate into the ground by means of a series of short duration impacts. The impact force has to be greater than the static soil resistance, because a portion of the force is needed to overcome the dynamic resistance to the pile penetration (the dynamic resistance is a function of the velocity of the pile). Mass of the ram (hammer), ram impact velocity, specifics of the pile helmet and of cushioning element such as hammer and pile cushions, as well as cross section of the ram, and cross section and length of the pile are all important factors to consider in an analysis of a specific pile driving situation. Of course, also the soil parameters, such as strength, shaft resistance including its distribution along the pile, toe resistance, and dynamic soil parameters, must be included in the analysis. It is obvious that for an analysis to be relevant requires that information used as input to the analysis correctly represents the conditions at the site. It a complex undertaking. Just because a computer program allows input of many parameters does not mean that the analysis results are true to the situation analyzed.

The soil resistance acting against a driven pile is based on the same mechanics as the resistance developed from a static load on the pile. That is, the resistance is governed by the principle of effective stress. Therefore, to estimate in the design stage how a pile will behave during driving at a specific site requires reliable information on the soil conditions including the location of the groundwater table and the pore pressure distribution. For method and details of the static analysis procedures, refer to Chapter 7.

The design of piles for support of a structure is directed toward the site conditions prevailing during the life of the structure. However, the conditions during the pile installation can differ substantially from those of the service situation—invariably and considerably. The installation may be represented by the initial driving conditions, while the service situation may be represented by the restrike conditions.

Questions of importance at the outset of the pile driving are the site conditions, including soil profile and details such as the following**:** will the piles be driven in an excavation or from the existing ground surface, is there a fill on the ground near the piles, and where is the groundwater table and what is the pore pressure distribution? Additional important questions are**:** will the soils be remolded by the driving and develop excess pore pressures? Is there a risk for the opposite, that is, dilating conditions, which may impart a false resistance? Could the soils become densified during the continued pile installation and cause the conditions to change as the pile driving progresses? To properly analyze the pile driving conditions and select the pile driving hammer requires the answers to questions such as these.

In restriking, the pore pressure distribution, and, therefore, the resistance distribution is very different to that developing during the initial driving. For this reason, a pile construction project normally involves restriking of piles for verification of capacity. Usually, the restrike observation indicates that a set-up has occurred. (Notice, it is not possible to quantify the amount of soil set-up unless the hammer is able to move the pile). On occasions, the restrike will show that relaxation, i.e., diminishing capacity, the opposite to soil set-up, may have occurred, instead.

As is the case for so much in engineering design and analysis, the last few decades have produced immense gains in the understanding of "how things are and how they behave". Thus, the complexity of pile driving in combination with the complexity of the transfer of the loads from the structure to a pile can now be addressed by rational analysis. In the past, analysis of pile driving was simply a matter of applying a so-called pile driving formula to combine "blow count" and capacity. Several hundred such formulae exist. They are all fundamentally flawed and lack proper empirical support. Their continued use is strongly discouraged.[1)]

9. 2. Principles of Hammer Function and Performance

Rather simplistically expressed, a pile can be installed by means of a static force, i.e. a load, which forces the pile into the soil <u>until it will not advance further</u>. Such installation techniques exist and the piles are called "jacked piles", see for example Yan et al. (2006). The jacked load is then about equal to the static capacity of the pile. However, for most piles and conditions, the magnitude of the static load needs to be so large as to make it impractical to use a static load to install a pile other than under special conditions.

---

1 In the past, when an engineer applied a "proven" formula — "proven" by the engineer through years of well-thought-through experience from the actual pile type and geology of the experience — the use of a dynamic formula could be defended. It did not matter what formula the engineer preferred to use, as it was the engineer's ability that controlled. That solid experience is vital is of course true also when applying modern methods. The engineers of today, however, can lessen the learning pain and save much trouble and costs by relating their experience to the modern methods. Sadly, despite all the advances, dynamic formulae are still in use. For example, some Transportation Authorities and their engineers even include nomograms of the Hiley formula in the contract specifications, refusing to take notice of the advances in technology and practice! Well, each generation has its share of die-hards. A couple of centuries or so ago, they, or their counterpart of the days, claimed that the Earth was round, that ships made of iron could not float, that the future could be predicted by looking at the color of the innards of a freshly killed bird, etc., rejecting all evidence to the contrary. Let's make it absolutely clear, basing a pile design today on a dynamic formula shows unacceptable ignorance and demonstrates incompetence. Note, however, that the use of the most sophisticated computer program does not provide any better results unless coupled with experience and good judgment.

In driving a pile, one is faced with the question of what portion of the applied dynamic force is effective in overcoming the capacity (that is, the "useful" static soil resistance) and what portion is used up to overcome the resistance to the pile movement, or, rather, its velocity of penetration. This velocity dependent resistance is called damping. In principle, a pile is driven by placing a small weight some distance over the pile head and releasing it to fall. In falling, the weight picks up velocity, and, on impacting the pile head, it slows down before bouncing off the pile head. The weight's change of velocity, that is, this deceleration, creates a force between the hammer and the pile during the short duration of the contact. Even a relatively light weight impacting at a certain significant velocity can give rise to a considerable force in the pile, which then causes the pile to penetrate a short distance into the soil, overcoming static resistance, inertia of the masses involved, as well as overcoming resistance due to the velocity of penetration. Accumulation of impacts and consequential individual penetrations make up the pile installation.

The impact duration is so short, typically 0.05 seconds, that although the peak penetration velocity lies in the range of several metre/second, the net penetration for a blow is often no more than about a millimetre or two. (Considering 'elastic' response of pile and soil, the gross penetration per blow can be about 20 times larger). In contrast to forcing the pile down using a static force, when driving a pile, the damping force is often considerable. For this reason, the driving force must be much larger than the desired pile capacity.[2)]

The ratio between the mass of the impacting weight and the mass of the pile (or, rather, its cross section and total mass) and its velocity on impact will govern the magnitude of the impact force (impact stress) and the duration of the impact event. A light weight impacting at high velocity can create a large local stress, but the duration may be very short. A low velocity impact from a heavy weight may have a long duration, but the force may not be enough to overcome the soil resistance. The impact velocity of a ram and the duration of a blow are, in a sense, measures of force and energy, respectively.

The force generated during the impact is not constant. It first builds up very rapidly to a peak and, then, decays at a lesser rate. The peak force can be very large, but be of such short duration that it results in no pile penetration. Yet, it could be larger than the strength of the pile material, which, of course, would result in damage to the pile head. By inserting a cushioning pad between the pile head and the impacting weight (the hammer or ram), this peak force is reduced and the impact duration is lengthened, thus both keeping the maximum force below damaging values and making it work longer, i.e., increasing the penetration per blow.

The effect of a hammer impact is a complex combination of factors, such as the velocity at impact of the hammer, the weight of the hammer (impacting mass) and the weight of the pile, the cross section of the hammer and the cross section of the pile, the various cushions in the system between the hammer and the pile, and the condition of the impact surfaces (for example, a damage to the pile head would have a subsequent cushioning effect on the impact, undesirable as it reduces the ability of the hammer to drive the pile), the weight of the supporting system involved (for example, the weight of the pile driving helmet), and last, but not least, the soil resistance, how much of the resistance is toe resistance and how much is shaft resistance, as well as the distribution of the shaft resistance. All these must be considered when selecting a hammer for a specific situation to achieve the desired results, that is, a pile installed the pile to a certain depth and/or capacity, quickly and without damage.

---

2 This seemingly obvious statement is far from always true. The allowable load relates to the pile capacity after the disturbance from the pile driving has dissipated. In the process, the pile will often gain capacity due to set-up (see Chapter 7).

Old rules-of-thumb, e.g., that the pile weight to ram weight ratio should be 'at least 2 for an air/steam hammer' and 'at least 4 for a diesel hammer' are still frequently quoted. These rules, however, only address one of the multitude of influencing aspects. They are also very inaccurate and have no general validity.

The hammer energy, or rather, the hammer "**rated energy**" is frequently used to indicate the size of a hammer and its suitability for driving a certain pile. The rated energy is the weight of the ram times its travel length and it is, thus, the same as the "positional" energy of the hammer. The rated or positional energy is a rather diffuse term to use, because it has little reference to the energy actually delivered to the pile and, therefore, it says very little about the hammer performance. By an old rule-of-thumb, for example, for steel piles, the rated energy of a hammer was referenced to the cross section of the pile as 6 MJ/m^2. This rule has little merit and leads often to an incorrect choice of hammer. (In English units, the rule was 3 ft-kips per square inch of steel).

A more useful reference for pile driving energy is the "**transferred energy**", which is energy actually transferred to a pile and, therefore, useful for the driving. It can be determined from measurements of acceleration and strain near the pile head during actual pile driving obtained by means of the Pile Driving Analyzer (see Section 9.7). The transferred energy value is determined after losses of energy have occurred (such as losses before the ram impacts the pile, impact losses, losses in the helmet, and between helmet and pile head).

Although, no single definition for hammer selection includes all aspects of the pile driving, energy is one of the more important aspects. Energy is addressed in more than one term, as explained in the following.

For example, the term "**hammer efficiency**". Hammer efficiency is defined as the ratio between the kinetic energy of the ram at impact to the ideal kinetic energy, which is a function of the ram velocity. A 100 % efficiency corresponds to ideal kinetic energy**:** the velocity the ram would be the same as the ram would have had in free fall in vacuum with no losses. Notice, the hammer efficiency does not consider the influence of cushioning and losses in the helmet, the helmet components, and the pile head.

The term "**energy ratio**" is also commonly used to characterize a hammer function. The energy ratio is the ratio between the transferred energy and the rated energy. This value is highly variable as evidenced in the frequency chart shown in Fig. 9.1. The measurements shown in the diagram were from properly functioning hammer and the variations are representative for variation that can occur in the field.

Obviously, energy alone is not a sufficient measure of the characteristic of an impact. Knowledge of the magnitude of the impact force is also required and it is actually the more important parameter. However, as the frequency chart presented in Fig. 9.2 demonstrates, field measurements indicate that also the impact stress varies considerably.

The reasons for the variations of energy and stress are only partly due to a variation of hammer size, hammer cushion characteristics, and hammer performance. The variations are also due to factors such as pile size (diameter and cross sectional area), pile length, and soil characteristics. As will be explained below, these factors can be taken into account in a wave equation analysis.

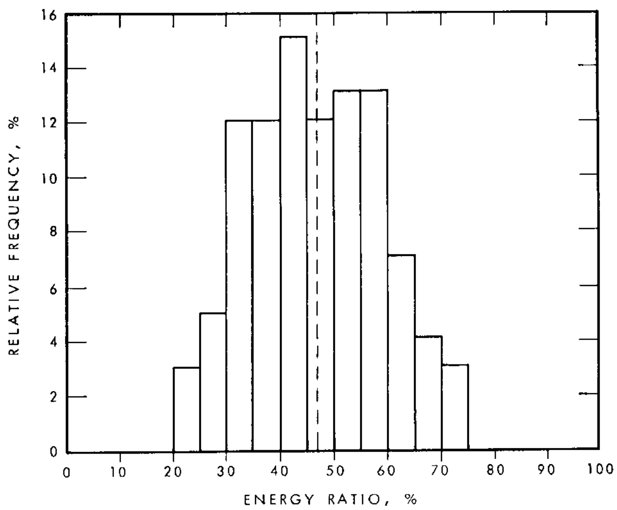

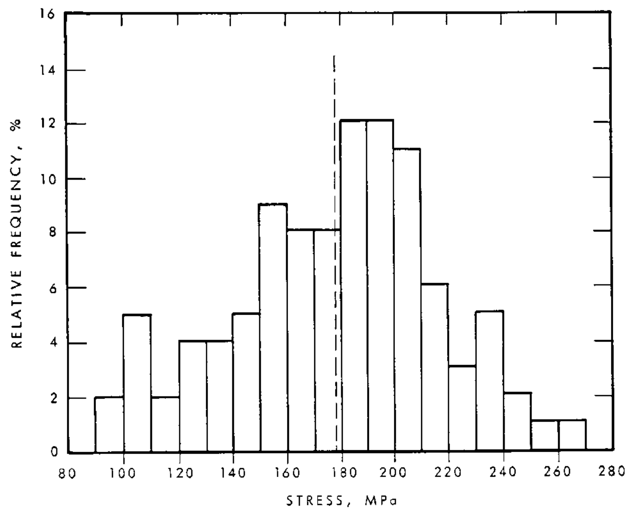

Fig. 9.1 Energy ratio Fig. 9.2 Impact stress
From measurements on 226 steel piles (Fellenius et al. 1978)

9.3. Hammer Types

The oldest pile driving hammer is the conventional "**drop hammer**". Its essential function was described already by Caesar 2,000 years ago in an account of a Roman campaign against some Germanic tribe (building a bridge, no less). The drop hammer is still commonly used. As technology advanced, hammers that operate on steam power came into use around the turn of the century. Today, steam power is replaced by air power from compressors and the common term is now "**air/steam hammer**". Hammers operating on diesel power, "**diesel hammers**", were developed during the 1930's. Electric power is used to operate "**vibratory hammers**", which function on a principle very different to that of impact hammers. Commonly used hammers are described below.

9.3.1 Drop Hammers

The conventional drop hammer consists chiefly of a weight that is hoisted to a distance above the pile head by means of a cable going up to a pulley on top of the leads and down to be wound up on a rotating drum in the pile driver machine. When released, the weight falls by gravity pulling the cable along and spinning the drum where the excess cable length is stored. The presence of the cable influences the efficiency of the hammer.[3)] The influence depends on total cable length (i.e., mass) as well as the length of cable on the drum, the length between the drum and the top of the leads, and the length of cable between the leads and the drop weight. This means, that the efficiency of the hammer operating near the top of the leads differs from when it operates near the ground. The amount of friction between the ram weight and the guides in the leads also influences the hammer operation and its efficiency. Whether the pile is vertical or inclined is another factor affecting the frictional losses during the "fall" and, therefore, the hammer efficiency. In addition, to minimize the bouncing and rattling of the weight, the operator usually tries to catch the hammer on the bounce, engaging the reversal of the drum before the impact. In the process, the cable is often tightened just before the impact, which results in a slowing down of the falling ram weight just before the impact, significantly reducing the efficiency of the impact.

---

3 Note, as indicated above, hammer efficiency is a defined ratio of kinetic energy and the term must not be used loosely to imply something unspecified but essentially good and desirable about the hammer.

9.3.2 Air/Steam Hammers

The air/steam hammer operates on compressed air from a compressor or steam from a boiler, which is fed to the hammer through a hose. Fig. 9.3 illustrates the working principle of the single-acting air/steam hammer. (The figure is schematic and does not show assembly details such as slide bar, striker plate helmet items, etc.). At the start of the upstroke, a valve opens letting the air (or steam) into a cylinder and a piston, which hoists the ram. The air pressure and the volume of air getting into the cylinder controls the upward velocity of the ram. After a certain length of travel (the upward stroke), the ram passes an exhaust port and the exhaust valve opens (by a slide bar activating a cam), which vents the pressure in the cylinder and allows the ram to fall by gravity to impact the hammer cushion and helmet anvil. At the end of the downward stroke, another cam is activated which opens the inlet valve starting the cycle anew. The positional, nominal, or rated energy of the hammer is the stroke times the weight of the ram with its parts such as piston rod, keys, and slide bar.

As in the case of the drop hammer, the efficiency of the impact is reduced by friction acting against the downward moving ram. However, two very important aspects specific to the air/steam hammer can be of greater importance for the hammer efficiency. First, the inlet valve is always activated shortly before the impact, creating a small pre-admission of the air. If, however, the release cam is so placed that the valve opens too soon, the air that then is forced into the cylinder will slow the fall of the weight and reduce the hammer efficiency. The design of modern air/steam hammers is such as to trap some air in above the ram piston, which cushions the upward impact of the piston and gives the downward travel an initial “push”. The purpose of the “push” is also to compensate for the pre-admission at impact. For more details, see the hammer guidelines published by Deep Foundations Institute (DFI 1979).

When the air pressure of the compressor (or boiler) is high, it can accelerate the upward movement of the ram to a significant velocity at the opening of the exhaust port. If so, the inertia of the weight will make it overshoot and travel an additional distance before starting to fall (or increase the “push” pressure in the “trap”), which will add to the ram travel and seemingly increase the efficiency.

For the double-acting air/steam hammer, air (steam) is also introduced above the piston to accelerate the down stroke, as illustrated in Fig. 9.4. The effect of this is to increase the impact rate, that is, the number of blows per minute. A single-acting hammer may perform at a rate of about 60 blows/minute, and a double acting may perform at twice this rate. The rated energy of the double-acting hammer is more difficult to determine. It is normally determined as the ram stroke times the sum of the weights and the area of the piston head multiplied by the downward acting air pressure. The actual efficiency is quite variable between hammers, even between hammers of the same model and type.

A double-acting air/steam hammer is closed to its environment and can be operated submerged.

9.3.3 Diesel Hammers

A diesel hammer consists in principle of a single cylinder engine. A diesel hammer is smaller and lighter than an air/steam hammer of similar capability. Fig. 9.5 illustrates the working principle of a liquid injection **single-acting open-end diesel hammer**. The hammer is started by raising the ram with a lifting mechanism. At the upper end of its travel, the lifting mechanism releases the ram to descend under the action of gravity. When the lower end of the ram passes the exhaust ports, a certain volume of air is trapped, compressed, and, therefore, heated. Some time before impact, a certain amount of fuel is squirted into the cylinder onto the impact block. When the ram end impacts the impact block, the fuel splatters into the heated compressed air, and the combustion is initiated. There is a small combustion delay due to the time required for the fuel to mix with the hot air and to ignite. More volatile fuels have a shorter combustion delay as opposed to heavier fuels. This means, for example, that if Winter fuel would be used in the Summer, pre-ignition may result. Pre-ignition is combustion occurring before impact and can be caused by the wrong fuel type or an overheated hammer. Pre-ignition is usually undesirable.

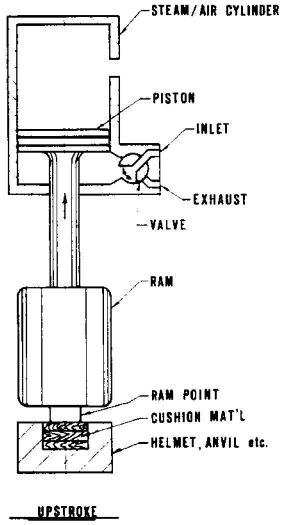

Fig. 9.3 The single-acting air/steam hammer (DFI 1979)

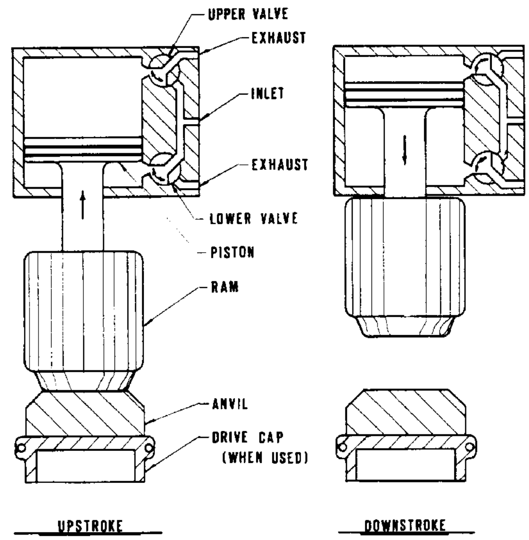

Fig. 9.4 The double-acting air/steam hammer (DFI 1979)

The rebound of the pile and the combustion pressure push the ram upward. When the exhaust ports are cleared, some of the combustion products are exhausted leaving in the cylinder a volume of burned gases at ambient pressures. As the ram continues to travel upward, fresh air, drawn in through the exhaust ports, mixes with the remaining burned gases.

The ram will rise to a height (stroke) that depends on the reaction of the pile and soil combination to the impact and to the energy provided by the combustion. It then descends under the action of gravity to start a new cycle. The nominal or rated energy of the hammer is the potential energy of the weight of the ram times its travel length. It has been claimed that the energy released in the combustion should be added to the potential energy. That approach, however, neglects the loss of energy due to the compression of the air in the combustion chamber.

Fig. 9.5 Working principle of the liquid injection, open-end diesel hammer (GRL 1993)

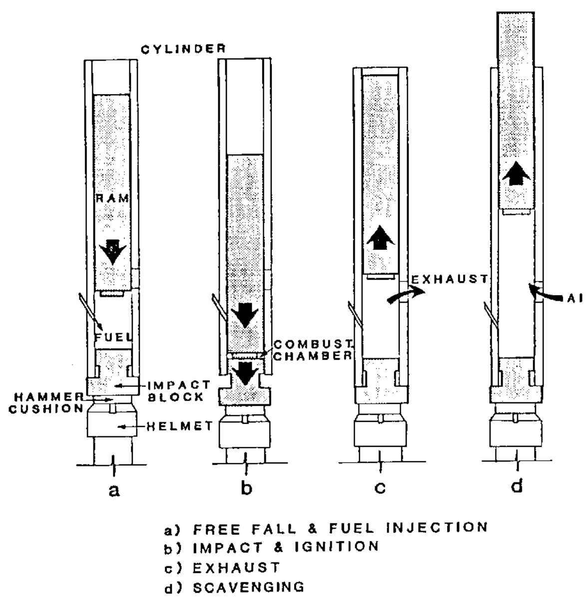

The sequence of the combustion in the diesel hammer is illustrated in Fig. 9.6 showing the pressure in the chamber from the time the exhaust port closes, during the precompression, at impact, and for the combustion duration, and until the exhaust port opens. The diagram illustrates how the pressure in the combustion chamber changes from the atmospheric pressure just before the exhaust port closes, during the compression of the air and the combustion process until the port again opens as triggered by the ram upstroke. During the sequence, the volume of the combustion chamber changes approximately in reverse proportion to the pressure. Different hammers follow different combustion paths and the effect on the pile of the combustion, therefore, differs between different hammers.

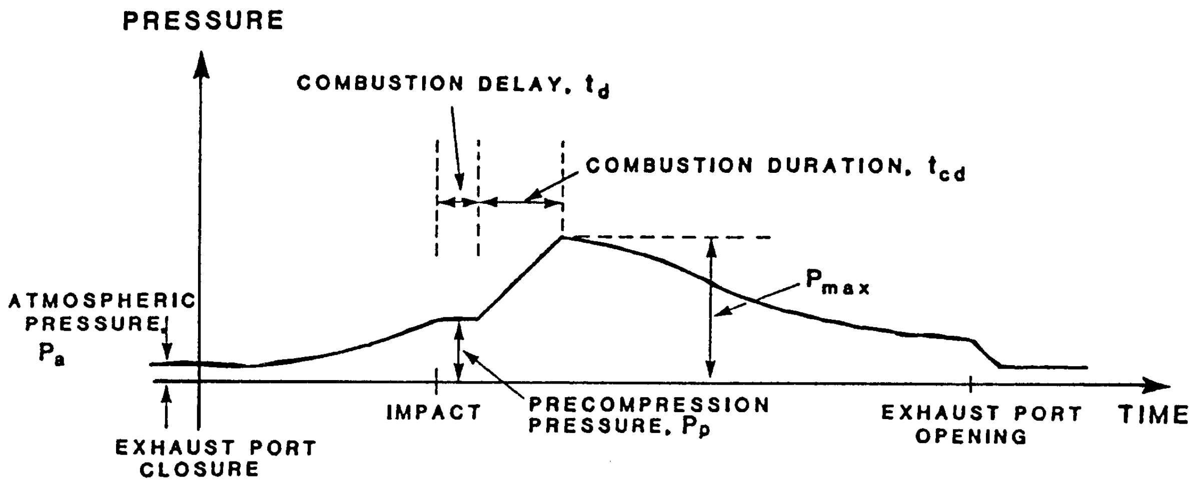

Fig. 9.6 Pressure in combustion chamber versus time for the liquid injection diesel hammer (GRL 1993)

The pressure in the chamber can be reduced if the cylinder or impact block rings allow pressure to leak off resulting in poor compression and inadequate ram rise, that is, reduced efficiency. Other reasons for low ram rise is excessive friction between the ram and the cylinder wall, which may be due to inadequate lubrication or worn parts, or a poorly functioning fuel pump injecting too little fuel into the combustion chamber.

The reason for a low hammer rise lies usually not in a poorly functioning hammer. More common causes are "soft or spongy soils" or long flexible piles, which do not allow the combustion pressure to build up. The hammer rise (ram travel) of a single-acting diesel hammer is a function of the blow-rate, as shown in Eq. 9.1 (derived from the basic relations Acceleration = g; Velocity = gt; Distance = $gt^2/2$ and recognizing that for each impact, the hammer travels the height-of-fall twice).

(9.1) $$H = \frac{g}{8\,f^2}$$

where H = hammer stroke (m)
g = gravity constant (m/s^2)
f = frequency (blows/second)

In practice, however, the hammer blow rate is considered in blows per minute, BPM, and the expression for the hammer rise in metre is shown by Eq. 9.2 (English units—rise in feet—are given in Eq. 9.2a). The hammer rise (ft) as a function of the blow rate (blows/min) expressed by Eq. 9.2a is shown in Fig. 9.7.

(9.2) $$H = \frac{14{,}400}{BPM^2}$$

(9.2a) $$H = \frac{4{,}400}{BPM^2}$$

(Effect of friction in ram cylinder is not included)

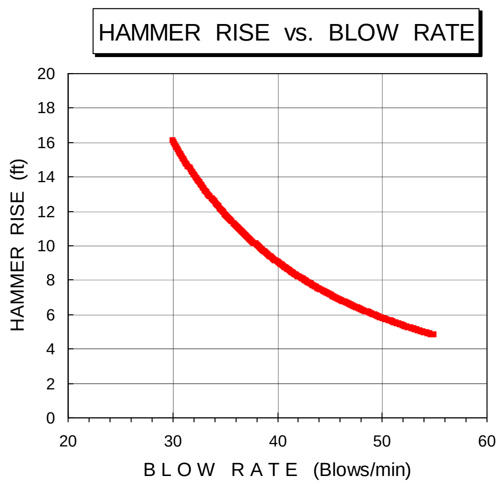

Fig. 9.7 Hammer rise (ft) as a function of blow-rate (BPM) (single-acting diesel hammer)

Eqs. 9.2 and 9.2a provide a simple means of determining the hammer rise in the field. The ram travel value so determined is more accurate than sighting against a bar to physically see the hammer rise against a marked stripe.

For some types of hammers, which are called **atomized injection hammers**, the fuel is injected at high pressure when the ram has descended to within a small distance of the impact block. The high pressure injection mixes the fuel with the hot compressed air, and combustion starts almost instantaneously. Injection then lasts until some time after impact, at which time the ram has traveled a certain distance up from the impact block. The times from the start of injection to impact and then to the end of combustion depend on the velocity of the ram. The higher the ram velocity, the shorter the time periods between ignition, impact, and end of combustion.

Similar to the drop hammer and air/steam hammer, on and during impact of a diesel hammer ram, the impact block, hammer cushion, and pile head move rapidly downward leaving cylinder with no support. Thus, it starts to descend by gravity and when it encounters the rebounding pile head, a secondary impact to the pile results called "**assembly drop**".

Closed-end diesel hammers are very similar to open end diesel hammers, except for the addition of a bounce chamber at the top of the cylinder. The bounce chamber has ports which, when open, allow the pressure inside the chamber to equalize with atmospheric pressure. As the ram moves toward the cylinder top, it passes these ports and closes them. Once these ports are closed, the pressure in the bounce chamber increases rapidly, stops the ram, and prevents a metal to metal impact between ram and cylinder top. This pressure can increase only until it is in balance with the weight and inertial force of the cylinder itself. If the ram still has an upward velocity, uplift of the entire cylinder will result in noisy rattling and vibrations of the system, so-called “racking”. Racking of the hammer cannot be tolerated as it can lead both to an unstable driving condition and to the destruction of the hammer. For this reason, the fuel amount, and hence maximum combustion chamber pressure, has to be reduced so that there is only a very slight "lift-off" or none at all.

9.3.4 Direct-Drive Hammers

A recent modification of the atomized injection hammer is to replace the hammer cushion with a striker plate and to exchange the pile helmet for a lighter “direct drive housing”. This change, and other structural changes made necessary by the modification, improves the alignment between the hammer and the pile and reduces energy loss in the drive system. These modified hammers are called ”direct drive hammers” and measurements have indicated the normally beneficial results that both impact force and transferred energy have increased due to the modification.

9.3.5 Vibratory Hammers

The vibratory hammer is a mechanical sine wave oscillator with two weights rotating eccentrically in opposite directions so that their centripetal actions combine in the vertical direction (pile axis direction), but cancel out in the horizontal. The effect of the vibrations is an oscillating vertical force classified as to frequency and amplitude.

Vibratory hammers work by eliminating soil resistance acting on the pile. The vibrations generate pore pressures which reduce the effective stress in the soil and, therefore, the soil shear strength. The process is more effective along the pile shaft as opposed to the pile toe and works best in loose to compact silty sandy soils which do not dilate and where the pore pressure induced by the cyclic loading can accumulate (draining off is not immediate). The pile penetrates by force of its own weight plus that of the hammer weight plus the vertical force (a function of the amplitude of the pulse) exerted by the hammer. Two types of drivers exist**:** drivers working at high frequency, and drivers working at a low frequency in resonance with the natural frequency of the soil. For details, see Massarsch (2004, 2005).

Because the fundamental effect of the vibratory hammer is to reduce or remove soil resistance, the capacity cannot be estimated from observations of pile penetration combined with hammer data, such as amplitude and frequency. This is because the static resistance (‘capacity’) of the pile during the driving is much smaller than the resistance (capacity) of the pile after the driving and only the resistance during the driving can be estimated from observations during the driving. The resistance removed by the vibrations is usually the larger portion and it is not known from any observation.

Several case histories have indicated that vibratorily driven piles have smaller shaft resistance as opposed to impact driven piles. This is of importance for tension piles. Note, however, that the difference between the two types of installation may be less in regard to cyclically loaded piles, for example, in the case of an earthquake, where the advantage of the impact driven pile may disappear.

9.4 Basic Concepts

When a hammer impacts on a pile head, the force, or stress, transferred to the pile builds progressively to a peak value and then decays to zero. The entire event is over within a few hundreds of a second. During this time, the transfer initiates a compression strain wave that propagates down the pile at the speed of sound (which speed is a function of the pile material—steel, concrete, or wood). At the pile toe, the wave is reflected back toward to the pile head. If the pile toe is located in dense soil, the reflected wave is in compression. If the pile toe is located in soft soil, the reflection is in tension. Hard driving on concrete piles in soft soil can cause the tension forces to become so large that the pile may be torn apart, for example[4)].

That pile driving must be analyzed by means of the theory of wave propagation in long rods has been known since the 1930's. The basics of the mathematical approach was presented by E.A. Smith in the late 1950's. When the computer came into common use in the early 1970's, wave equation analysis of pile driving was developed at the Texas A&M University, College Station, and at the Case Western Reserve University, Cleveland. Computer software for wave equation analysis has been available to the profession since 1976.

During the past two decades, a continuous development has taken place in the ease of use and, more important, the accuracy and representativeness of the wave equation analysis. Several generations of programs are in use as developed by different groups. The most versatile and generally accepted program is the GRLWEAP (GRL 1993; 2002). For drop hammers, analysis by early program versions, or other programs, e. g., the TTI program, can in some cases provide acceptable results. For analysis of diesel hammer driven piles and piles in unusual soils, program versions from before 1990 are not useful.

Axial wave propagation occurs in a uniform, homogeneous rod—a pile—is governed by Eq. 9.3.

(9.3) $$\sigma = \frac{E}{c}v \qquad \text{derived from the “Wave Equation”:} \quad \rho\frac{\partial^2 u}{\partial t^2} = E\frac{\partial^2 u}{\partial x^2}$$

where
σ = stress
E = Young's modulus
c = wave propagation velocity $c = \sqrt{\frac{E}{\rho}}$
v = particle velocity

The wave equation analysis starts the pile driving simulation by letting the hammer ram impact the pile at a certain velocity, which is imparted to the pile head over a large number of small time increments. The

---

4) What driving tension to accept or permit in precast concrete piles is often mismanaged, be the piles ordinary reinforced or prestressed. Most standards and codes indicate the limit tension to be a percentage of the steel yield plus a portion of the concrete tension strength. For prestressed pile the limit for the steel reinforcement (the strands) is often set to the net prestress value for the pile (leading some to believe that ordinary precast piles, having no net prestress, cannot accept driving tension!). However, the acceptable driving tension occurs where the pile has a crack and only the reinforcement is left to resist the tension and hold the pile together. Therefore, no contribution can be counted on from the concrete tension strength—it may be a factor everywhere else in the pile, but not in that crack. The allowable driving tension is simply the steel yield divided by a factor of safety, usually about 1.5, which is applicable to ordinary reinforced as well as prestressed pile alike. Incidentally, the net prestress is usually about ≈70 % of the strand yield point, that is about $^1/_{1.5}$, which makes the net prestress a good value for what tension value to accept, though the fact of the prestressing is not the point in this context.

analysis calculates the response of the pile and the soil. The hammer and the pile are simulated as a series of short infinitely stiff elements connected by weightless elastic springs. Below the ground surface, each pile element is affected by the soil resistance defined as having elastic and plastic response to movement an damping (viscous) response to velocity. Thus, a 20 metre long pile driven at an embedment depth of 15 metre may be simulated as consisting of 20 pile elements and 15 soil elements. The time increments for the computation are set approximately equal to the time for the strain wave to travel the length of half a pile element. Considering that the speed of travel in a pile is in the range of about 3,000 m/s through 5,000+ m/s, each time increment is a fraction of a millisecond and the analysis of the full event involves more than a thousand calculations. During the first few increments, the momentum and kinetic energy of the ram is imparted to the pile accelerating the helmet, cushions, and pile head. As the calculation progresses, more and more pile elements become engaged. The computer keeps track of the development and can output how the pile elements move relative to each other and to the original position, as well as the velocities of each element and the forces and stresses developing in the pile.

The **damping** or viscous response of the soil is a linear function of the velocity of the pile element penetration (considering both downward and upward direction of pile movement). The damping response to the velocity of the pile is a crucial aspect of the wave equation simulation, because only by knowing the damping can the static resistance be separated from the total resistance to the driving. Parametric studies have indicated that in most cases, a linear function of velocity will result in acceptable agreement with actual behavior. Sometimes, an additional damping called radial damping is considered, which is dissipation of energy radially away from the pile as the strain wave travels down the pile.

The material constant, **impedance, Z**, is very important for the wave propagation. It is a function of pile modulus, cross section, and wave propagation velocity in the pile as given in Eq. 9.4.

(9.4) $$Z = \frac{EA}{c}$$

where Z = pile impedance
E = Young’s modulus of the pile material
A = pile cross section area
c = wave propagation velocity (= speed of sound in the pile)

Combining Eqs. 9.3 and 9.4 yields Eq. 9.5 and shows that the force is equal to impedance times velocity. Or, in other words, force and velocity in a pile are proportional to impedance. This fact is a key aspect of the study of force and velocity measurements obtained by means of the Pile Driving Analyzer (see Section 9.7).

(9.5) $$\sigma\, A = F = Z\, v$$

where σ = axial stress in the pile
A = pile cross section area
F = force in the pile
Z = pile impedance
v -= pile particle velocity

Eqs. 9.4 and 9.5 can be used to calculate the axial impact force in a pile during driving, as based on measurement of the pile particle velocity (also called "physical velocity"). Immediately before impact, the particle velocity of the hammer is v_0, while the particle velocity of the pile head is zero. When the hammer strikes the pile, a compression wave will be generated simultaneously in the pile and in the hammer. The hammer starts to slows down, by a velocity change denoted v_H, while the pile head starts to accelerate, gaining a velocity of v_P. (The pile head velocity before impact is zero, the velocity change at the pile head is the pile head velocity). Since the force between the hammer and the pile must be equal, applying Eq. 9.3 yields the relationship expressed in Eq. 9.6.

$$(9.6) \qquad Z_H v_H = Z_P v_P$$

where
Z_H = impedance of impact hammer
Z_P = impedance of pile
v_H = particle velocity of wave reflected up the hammer
v_P = particle velocity of pile

At the contact surface, the velocity of the hammer — decreasing — and the velocity of the pile head — increasing — are equal, as expressed in Eq. 9.7. Note, the change of hammer particle velocity is directed upward, while the velocity direction of the pile head is downward (gravity hammer is assumed).

$$(9.7) \qquad v_0 - v_H = v_P$$

where
v_0 = particle velocity of the hammer immediately before impact
v_H = particle velocity of wave reflected up the hammer
v_P = particle velocity of pile

Combining Eqs. 9.6 and 9.7 and rearranging the terms, yields Eq. 9.8.

$$(9.8) \qquad v_P = \frac{v_0}{1 + \dfrac{Z_P}{Z_H}}$$

where
v_P = particle velocity of pile
v_0 = particle velocity of the hammer immediately before impact
Z_H = impedance of hammer
Z_P = impedance of pile

Inserting $Z_H = Z_P$, into Eq. 9.8 yields Eq. 9.9, which shows that when the impedances of the hammer and the piles are equal, the particle velocity of the pile, v_P, in the pile behind the wave front will be half the hammer impact velocity, v_0 (the velocity immediately before touching the pile head).

$$(9.9) \qquad v_P = 0.5\, v_0$$

where
v_P = particle velocity of pile
v_0 = particle velocity of the hammer immediately before impact

Combining Eqs. 9.3, 9.5, and 9.9, yields Eq. 9.10 which expresses the magnitude of the impact force, F_i, at the pile head for equal impedance of hammer and pile.

(9.10) $$F_i = 0.5 v_0 Z_P$$

where F_i = force in pile
Z_P = impedance of pile
v_0 = particle velocity of the hammer immediately before impact

The **duration of the impact**, t_0, that is, the time for when the pile and the hammer are in contact, is the time it takes for the strain wave to travel the length of the hammer, L_H, twice, i.e., from the top of the hammer to the bottom and back up to the top as expressed in Eq. 9.11a. Then, if the impedances of the hammer and the pile are equal, during the same time interval, the wave travels the length, L_W, as expressed in Eq. 9.11b. — Note, equal impedances do not mean that the wave velocities in hammer and pile are equal — Combining Eqs. 9.11a and 9.11b provides the **length of the stress wave** (or strain wave) in the pile as expressed by Eq. 9.11c.

(9.11a) $$t_0 = \frac{2L_H}{c_H}$$ (9.11b) $$t_0 = \frac{2L_W}{c_P}$$ (9.11c) $$L_W = 2L_H \frac{c_P}{c_H}$$

where t_0 = duration of impact (i.e., duration of contact between hammer and pile head)
L_H = length of hammer
L_W = length of the compression wave in pile
c_H = velocity compression wave in hammer
c_P = velocity of compression wave in pile

When a hammer impacts a pile, the force generated in the pile slows down the motion of the hammer and a stress wave ("particle velocity wave") is generated that propagates down the pile. After quickly reaching a peak velocity (and force) — immediately if the pile head is infinitely rigid — the pile head starts moving slower, i.e., the generated particle velocity becomes smaller, and the impact force decays exponentially according to Eq. 9.12a, which expresses the **pile head force**. Combining Eqs. 9.3, 9.5, and 9.12a yields to show that, together with the impact velocity, the ratio between the ram impedance and the pile impedance governs the force a hammer develops in a pile. (For hammer and pile of same material, e.g., steel, the ratio is equal to the ratio of the cross sectional areas). A ram must always have an impedance larger than that of the pile or the hammer will do little else than bounce on the pile head.

(9.12a) $$F = F_i\, e^{-\frac{Z_P}{M_H}t}$$ (9.12b) $$F = F_i e^{-\frac{M_P}{M_H}\frac{L_E}{c_P}}$$

where F = force at pile head and F_i = force at impact
M_H = mass of hammer element and M_P = mass of pile element
e = base of the natural logarithm (= 2.718)
Z_P = impedance of the pile cross section
L_E = length of pile element
t = time

If the pile is of non-uniform cross section, every change of impedance change will result in reflections. If the impedance of the upper pile portion is smaller than that of the lower, the pile will not drive well. When the reverse is the case, that is, the impedance of the upper pile portion is larger than that of the lower, a tension wave will reflect from the cross section change. For example, in marine projects, sometimes a concrete pile is extended by an H-pile, a "stinger". The impedances of the concrete segment and the steel H-pile segment should, ideally, be equal. However, the H-pile size (weight) is usually such that the impedance of the H-pile is smaller than that of the concrete pile. Therefore, a tensile wave will reflect from the cross section change (for a discussion, see Section 8, below). If the impedance change is too large, the reflected tension can damage the concrete portion of the pile, and if the change is substantial, such as in the case of an impedance ratio close to 2 or greater, the tension may exceed the tensile strength of the concrete pile. (A case history of the use of stinger piles is described in Section 9.11, Case 4). As an important practical rule, the impedance of the lower section must never be smaller than half of the upper section. That it at all can work, is due to that the concrete pile end (i.e., where the two segments are joined) is not normally a free end, but is in contact with soil, which reduces the suddenness of the impedance change. However, this problem is compounded by that the purpose of the stinger is usually to achieve a better seating into dense competent soil. As the stinger is in contact with this soil, a strong compression wave may be reflected from the stinger toe and result in an increasing incident wave, which will result in that the tensile reflection from where the section are joined — where the impedance change occurred. If the concrete end is located in soft soil, damage may result.

When a pile has to be driven below the ground surface or below a water surface, a **follower** is often used. The same impedance aspects that governed the driving response of a pile governs also that of a follower. Ideally, a follower should have the same impedance as the pile. Usually, though, it designed for a somewhat larger impedance, because it must never ever have a smaller impedance than the pile, or the achievable capacity of the pile may reduce considerably as compared to the pile driven without a follower. Indeed, a too small follower may be doing little more than chipping away on the pile head.

A parameter of substantial importance for the drivability of the pile is the so-called **quake**, which is the movement between the pile and the soil required to mobilize full plastic resistance (see Fig. 9.8). In other words, the quake is the zone of pile movement relative to the soil where elastic resistance governs the load transfer.

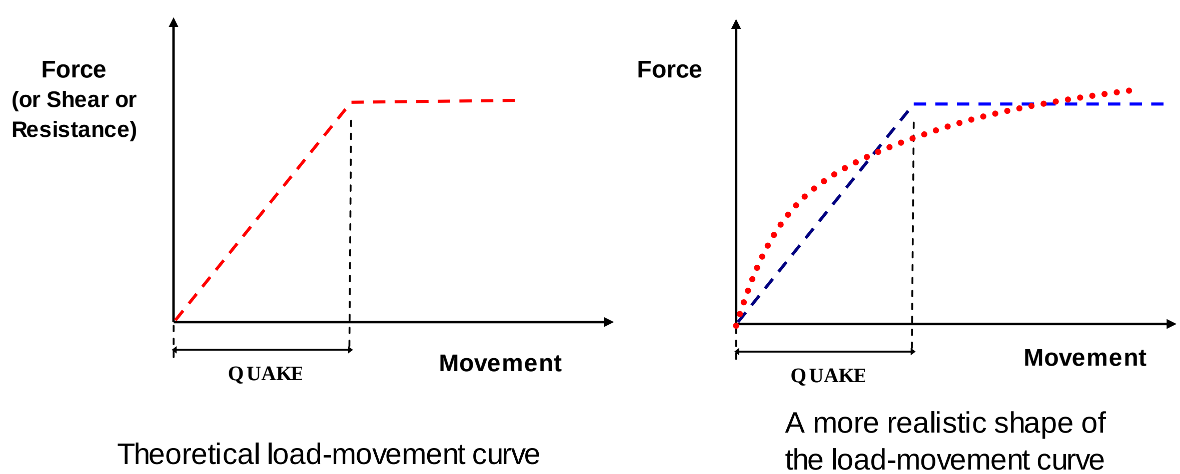

Fig. 9.8 Development of soil resistance to pile movement (q-z curves).

Along the pile shaft, the quake is usually small, about 2 mm to 3 mm or less. The value depends on the soil type and is independent of the size of the pile (diameter). In contrast, at the pile toe, the quake is a function of the pile diameter and, usually, about 1 % of the diameter. However, the range of values can be large; values of about 10 % of the diameter have been observed. The larger the quake, the more energy is required to move the pile and the less is available for overcoming the soil static resistance. For example, measurements and analyses have indicated that a hammer driving a pile into a soil where the quake was about 3 mm (0.1 inch) could achieve a final capacity of 3,000 KN (600 kips), but if the quake is 10 mm (0.4 inch), it could not even drive the pile beyond a capacity of 1,500 KN (300 kips) (Authier and Fellenius 1980).

Aspects which sometimes can be important to include in an analysis are the effect of a soil adhering to the pile, particularly as a **plug** inside an open-end pipe pile or between the flanges of an H-pile. The plug will impart a toe resistance (Fellenius 2002). Similarly, the resistance from a soil column inside a pipe pile that has <u>not</u> plugged will add to the shaft resistance along the outside of the pile.

The **stiffness, k,** of the pile is an additional important parameter to consider in the analysis. The stiffness of an element is defined in Eq. 9.13. The stiffness of the pile is usually well known. The stiffness of details such as the hammer and pile cushions is often more difficult to determine. Cushion stiffness is particularly important for evaluating driving stresses. For example, a new pile cushion intended for driving a concrete pile can start out at a thickness of 150 mm of wood with a modulus of 300 MPa. Typically, after some hundred blows, the thickness has reduced to half and the modulus has increased five times. Consequently, the cushion stiffness has increased ten times.

(9.13) $$k = \frac{E\,A}{L}$$

where
k = stiffness
E = Young's modulus of the pile material
A = pile cross sectional area
L = element length

A parameter related to the stiffness is the **coefficient of restitution**, **e**, which indicates the difference expressed in Eq. 9.14 between stiffness in loading (increasing stress) as opposed to in unloading (decreasing stress). A coefficient of restitution equal to unity only applies to ideal materials, although steel and concrete are normally assigned a value of unity. Cushion material have coefficients ranging from 0.5 through 0.8. For information on how to determine the coefficient of restitution see GRL (1993; 2002).

(9.14) $$e = \sqrt{\frac{k_1}{k_2}}$$

where
e = coefficient of restitution
k_1 = stiffness for increasing stress
k_2 = stiffness for decreasing stress

When the initial compression wave with the force $F_i(t)$ reaches the pile toe, the toe starts to move. The **pile toe force** is expressed by Eq. 9.15.

(9.15) $$F_P(t) = F_i(t) + F_r(t)$$

where $F_P(t)$ = force in pile at toe at Time t
$F_i(t)$ = force of initial wave at pile toe
$F_r(t)$ = force of reflected wave at pile toe

If the material below the pile is infinitely rigid, $F_r = F_i$, and Eq. 9.15 shows that $F_P = 2F_i$. If so, the strain wave will be reflected undiminished back up the pile and the stress at the pile toe will theoretically double. When the soil at the pile toe is less than infinitely rigid, the reflected wave at the pile toe, $F_r(t)$, is smaller, of course. The magnitude is governed by the stiffness of the soil. If the force in the pile represented by the downward propagating compression wave rises more slowly than the soil resistance increases due to the imposed toe movement, the reflected wave is in compression indicating a toe resistance. If the force in the compression wave rises faster than the soil resistance increases due to the imposed toe movement, the reflected wave is in tension. However, the force sent down and out into the soil from the pile toe will be a compression wave for both cases.

In this context and to illustrate the limitation of the dynamic formulae, the driving of two piles will be considered. Both piles are driven with the same potential ("positional") energy. First, assume that the on pile is driven with a hammer having a mass of 4,000 kg and is used at a height-of-fall of 1 m, representing a positional energy of 40 KJ. The impact velocity, v_0, is independent of the mass of the hammer and a function of gravity and height-of-fall, ($v = \sqrt{2gh}$). Thus, the free-fall impact velocity is 4.3 m/s. If instead a 2,000 kg hammer is used at a height-of-fall of 2 m, the positional energy is the same, but the free-fall impact velocity is 6.3 m/s and the force generated in the pile overcoming the soil resistance will be larger. The stress in the pile at impact can be calculated from Eq. 9.16, as derived from Eqs. 9.3 - 9.5.

(9.16) $$\sigma_P = \frac{E_P}{c_P} v_P$$

where σ_P = stress in the pile
E_P = pile elastic modulus
c_P = velocity of compression wave in the pile
v_P = particle velocity in the pile

The impact stress in piles composed of steel, concrete, or wood can be calculated from the material parameters given in Table 9.1. In the case of a concrete pile and assuming equal potential energy, but at heights-of-fall of 1 m and 2 m, the calculated stresses in the pile are 44 MPa and 63 MPa, respectively. In case of a pile cross section of, say, 300 mm and area about 0.09 m^2, the values correspond to theoretical impact forces are 4,000 KN and 5,600 KN. Allowing for losses down the pile due to reflections and damping, the maximum soil forces the impact wave could be expected to mobilize are about a third or a half of the theoretical impact force, i.e., about 2,000 to 3,000 KN for the "heavy" and "light" hammers, respectively. Moreover, because the lighter hammer generates a shorter stress-wave, its large stress may decay faster than the smaller stress generated by the heavier hammer and, therefore, the lighter hammer may be unable to drive a long a pile as the heavier hammer can. Where in the soil a resistance occur is also a factor. For example, a pile essentially subjected to toe resistance will benefit from a high stress level, as generated by the higher impact, whereas a pile driven against shaft resistance drives better when the stress-wave is longer and less apt to dampen out along the pile. A number of influencing factor are left out, but the comparison is an illustration of why the dynamic formulae, which are based on positional energy relations, are inadvisable for use in calculating pile bearing capacity.

Table 9.1 Typical Values

Material	Density, ρ (kg/m^3)	Modulus, E (GPa)	Wave velocity, c (m/s)
Steel	7,850	210	5,120
Concrete	2,450	40	4,000
Wood fresh or wet	1,000	16	3,300

The **maximum stress** in a pile that can be accepted and propagated is related to the maximum dynamic force that can be mobilized in the pile. The peak stress developed in an impact is expressed in Eq. 9.17, as developed from Eq. 9.16.

(9.17) $$\sigma_P = \frac{E_P}{c_P}\sqrt{2gh}$$

where
σ_P = stress in the pile
E_P = pile elastic modulus
c_P = velocity of stress wave in pile
g = gravity constant
h = critical height-of-fall

Transforming Eq. 9.17 into Eq. 9.18 yields an expression for a height that causes a stress equal to the strength of the pile material.

(9.18) $$h_{cr} = \frac{\sigma^2_{P,\max}}{2\,g\,\rho\,E_P}$$

where
h_{cr} = critical height-of-fall
$\sigma_{P,\,max}$ = maximum stress in the pile ≤ strength of the pile material
E_P = pile elastic modulus
g = gravity constant
ρ = density of pile material

For a concrete pile with cylinder strength ranging between 30 MPa and 60 MPa and the material parameters listed in Table 9.1, the critical height-of-fall ranges between 0.5 m and 2.0 m (disregarding losses, usually assumed to amount to an approximately 20 % reduction of impact velocity). In the case of a steel pile with a material yield strength of 300 MPa, the critical height-of-fall becomes 2.8 m. (Note, no factor of safety is included and it is not recommended to specify the calculated limits of height-of-fall for a specific pile driving project).

The above brief discussion demonstrates that stress wave propagation during pile driving is affected by several factors, such as hammer weight, hammer impact velocity, and pile impedance. It is therefore not surprising that a single parameter, driving energy, cannot describe the pile driving operation correctly.

The total soil resistance R_{tot} during pile driving is composed of a movement-dependent (static) component, R_{stat}, and a velocity-dependent (dynamic) component, R_{dyn}, as expressed in Eq. 9.19.

(9.19) $$R_{tot} = R_{stat} + R_{dyn}$$

where R_{tot} = total pile capacity
R_{stat} = static pile capacity
R_{dyn} = dynamic pile capacity

The soil resistances can be modeled as a spring with a certain stiffness and a slider representing the static resistance plus a dashpot representing dynamic resistance—damping — as illustrated in Fig. 9.9. (Note that the figure illustrates also when the pile has slowed down and reversed its direction). For small movements, the static resistance is essentially a linear function of the movement of the pile relative the soil. The damping is a function of the velocity of the pile. Smith (1960) assumed that the damping force is proportional to the static soil resistance times pile velocity by a damping factor, J_s, with the dimension of inverse velocity. Goble et al. (1980) assumed that the damping force is proportional to the pile impedance times pile velocity by a dimensionless damping factor, J_c, called viscous damping factor, as expressed in Eq. 9.20.

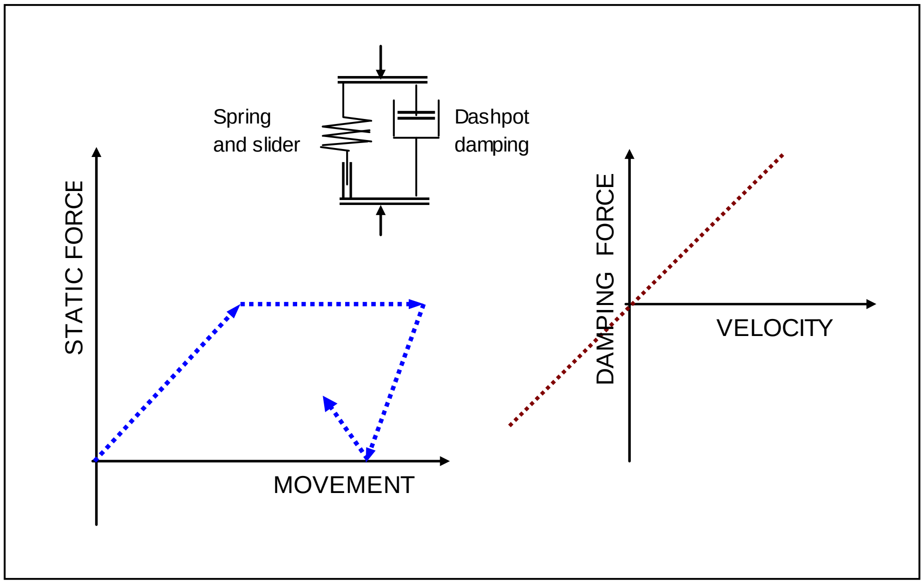

Fig. 9.9 Model and principles of soil resistance — elastic and plastic and damping

(9.20) $$R_{dyn} = J_c Z_P v_P$$

where R_{dyn} = dynamic pile resistance
J_c = a viscous damping factor
Z_P = impedance of pile
v_P = particle velocity of pile

Typical and usually representative ranges of viscous damping factor are given in Table 9.2.

Table 9.2. Damping factors for different soils (Rausche et al. 1985).

Soil Type	J_c
Clay	0.60 – 1.10
Silty clay and clayey silt	0.40 – 0.70
Silt	0.20 – 0. 45
Silty sand and sandy silt	0.15 – 0.30
Sand	0.05 – 0.20

It is generally assumed that J_c depends only on the dynamic soil properties. However, as shown by Massarsch and Fellenius (2008) and Fellenius and Massarsch (2008), in practice, measurements on different size and different material piles in the same soil do show different values of J_c. Iwanowski and Bodare (1988) derived the damping factor analytically, employing the model of a vibrating circular plate in an infinite elastic body to show that the damping factor depends not just on the soil type but also on the ratio between the impedance of the soil at the pile toe and the impedance of the pile. They arrived at the relationship expressed in Eq. 9.21, which is applicable to the conditions at the pile toe.

(9.21) $$J_c = 2\,\frac{\rho_t\, c_s\, A_t}{\rho_p\, c_p\, A_c} = 2\,\frac{Z_s}{Z_P}\,\frac{A_t}{A_c}$$

where J_c = dimensionless damping factor
ρ_t = soil total (bulk) density of the soil
ρ_P = density of the pile material
c_s = shear wave velocity in the soil
c_p = compression wave velocity in the pile
A_t = pile area at pile toe in contact with soil
A_c = pile cross-sectional area
Z_s = impedance of the soil (determined from P-wave velocity)
Z_P = impedance of the pile at the pile toe

Eq. 9.21 shows that the damping factor, J_c depends on the ratio of the soil impedance to the pile impedance and of the ration of pile cross section area and pile toe area. The latter aspect is particularly important in the case of closed-toe or "plugged" pipe piles. Table 9.3 compiles J_c damping values calculated according to Eq. 9.21 for pile with an average soil density of ρ_t = 1,800 kg/m^3 and material parameters taken from Table 9.1. For the steel piles, a ratio between the pile toe area and the pile cross sectional area of 10 was assumed. Table 9.3 shows the results for soil compression wave velocities ranging from 250 m/s to 1,500 m/s. Where the actual soil compression wave velocity can be determined, for example, from cross-hole tests, or seismic CPT soundings, Eq. 9.21 indicates a means for employing the soil compression wave velocity to estimate J_c -factors for the piles of different sizes, geometries, and materials to be driven at a site.

Table 9.3. Values of viscous damping factor, J_c, for different pile materials

Material	Compression wave velocity at pile toe, c_p (m/s)					
	250	500	750	1,000	1,250	1,500
Steel	0.02	0.04	0.07	0.09	0.11	0.13
Concrete	0.09	0.18	0.28	<u>0.37</u>	0.46	0.55
Wood	0.27	0.55	0.82	1.09	1.36	1.64

9.5 Wave Equation Analysis of Pile Driving

The GRLWEAP program includes files that contain all basic information on hammers available in the industry. To perform an analysis of a pile driven with a specific hammer, the hammer is selected by its file number. Of course, when the analysis is for piles driven with drop hammers, or with special hammers that are not included in the software files, the particular data must be entered separately.

The GRLWEAP can perform a drivability analysis with output consisting of estimated penetration resistance (driving log), maximum compression and tension stresses induced during the driving, and many other factors of importance when selecting a pile driving hammer. The program also contains numerous other non-routine useful options. For additional information, see Hannigan (1990).

The most common routine output from a wave equation analysis consists of a bearing graph (ultimate resistance curve plotted versus the penetration resistance—often simply called ”blow-count”[5]) and diagrams showing impact stress and transferred energy as a function of penetration resistance. Fig. 9.10 presents a Bearing Graph showing the relation between the static soil resistance (pile capacity; R-ULT) versus the pile penetration resistance (PRES) at initial driving as the number of blows required for 25 mm penetration of the pile into the soil. The relation is shown as a band rather than as one curve, because natural variations in the soil, hammer performance, cushion characteristics, etc. make it impossible to expect a specific combination of hammer, pile, and soil at a specific site to give the response represented by a single curve. The WEAP analysis results should therefore normally be shown in a band with upper and lower boundaries of expected behavior. The band shown may appear narrow, but as is illustrated in the following, the band may not be narrow enough.

---

5 Penetration resistance is number of blows per a unit of penetration, e. g., 25 mm, 0.3 m, or 1.0 m. Blow count is the actual number of blows counted for a specific penetration, or the inverse of this: a penetration for a specific number of blows. For example, on termination of the driving, an 11 mm penetration may be determined for 8 blows. That is, the blow count is 8 blows/11 mm, but the penetration resistance is 18 blows/25 mm. Sometimes the distinction is made clear by using the term “ equivalent penetration resistance”. Note, the “pile **driving** resistance” refers to force. But it is an ambiguous term that is best not used.

The Bearing Graph is produced from assumed pile capacity values. For this reason, the WEAP analysis alone cannot be used for determining the capacity of a pile without being coupled to observed penetration resistance (and reliable static analysis). WEAP analysis is a design tool for predicting expected pile driving behavior (and for judging suitability of a hammer, etc.), not for determining capacity. For the case illustrated in Fig. 9.10, the desired capacity (at End-of-Initial-Driving, EOID) ranges from 1,900 KN through 2,150 KN. The Bearing Graph indicates that the expected PRES values for this case range from 4 bl./25 mm through 16 bl./25 mm. Obviously, the WEAP analysis ***alone*** is not a very exact tool to use. It must be coupled with a good deal of experience and judgment, and field observations.

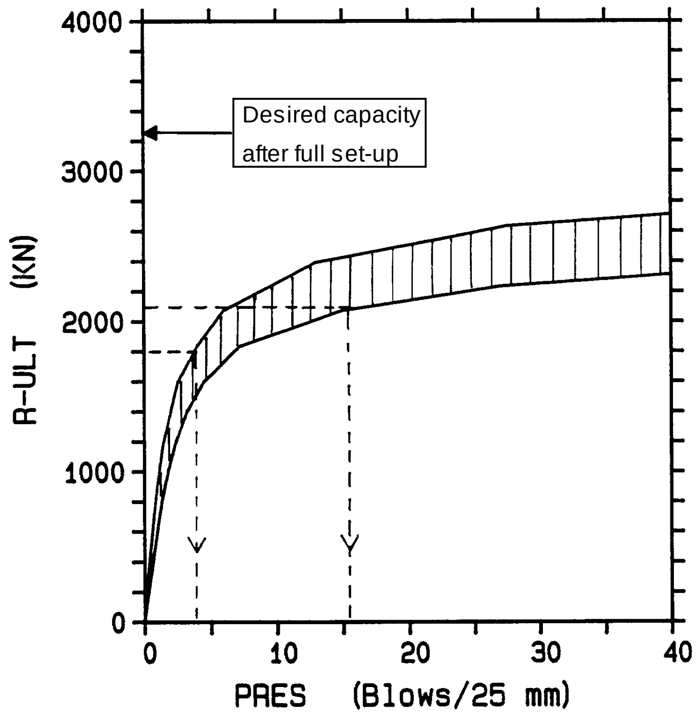

Fig. 9.10 WEAP Bearing Graph

The desired long-term capacity of the pile is 3,150 KN. However, the Bearing Graph shows that, for the particular case and when considering a reasonable penetration resistance (PRES), the hammer cannot drive the pile against a resistance (i.e., to a capacity) greater than about 2,500 KN. Or, in other words, the WEAP analysis shows that the hammer cannot drive the pile to a capacity of 3,150 KN. Is the hammer no good? The answer lies in that the Bearing Graph in Fig. 9.10 pertains, as mentioned, to the capacity of a pile at initial driving. With time after the initial driving, the soil gains strength and the pile capacity increases due to soil set-up. Of course, if the designer considers and takes advantage of the set-up, the hammer does not have to drive the pile to the desired final capacity at the end-of-initial-driving, only to a capacity that when set-up is added the capacity becomes equal to the desired final value. For the case illustrated, the set-up was expected to range from about 1,000 KN through 1,200 KN and as the analysis shows the hammer capable of driving the piles to a capacity of about 2,000 KN at a reasonable PRES value, the hammer was accepted.

Generally, if initial driving is to a capacity near the upper limit of the ability of the hammer, the magnitude of the set-up cannot be proven by restriking the pile with the same hammer. For the case illustrated, the hammer is too light to mobilize the expected at least capacity of 3,150 KN, and the restriking would be meaningless and only show a small penetration per blow, i.e., a high PRES value.

9.6 Hammer Selection by Means of Wave Equation Analysis

The procedure of hammer selection for a given pile starts with a compilation of available experience from previous similar projects in the vicinity of the site and a list of hammers available amongst contractors who can be assumed interested in the project. This effort can be more or less elaborate, depending on the project at hand. Next comes performing a wave equation analysis of the pile driving at the site, as suggested below. Notice, there are many potential error sources. It is important to verify that assumed and actual field conditions are in agreement.

Before start of construction

- Compile the information on the soils at the project site and the pile data. The <u>soil</u> data consist of thickness and horizontal extent of the soil layers and information on the location of the groundwater table and the pore pressure distribution. The <u>pile</u> data consist of the pile geometry and material parameters, supplemented with the estimated pile embedment depth and desired final bearing capacity.

- Calculate the static capacity of the pile at final conditions as well as during initial driving. For conditions during the initial driving, establish the extent of remolding and development of excess pore pressure along the pile. Establish also the capacity and resistance distribution at restrike conditions after the soil has reconsolidated and "set-up", and all excess pore pressures have dissipated.

- Establish a short list of hammers to be considered for the project. Sometimes, the hammer choice is obvious, sometimes, a range of hammers needs to be considered.

- For each hammer considered, perform a wave equation analysis to obtain a Bearing Graph for the end-of-initial-driving and restrike conditions with input of the static soil resistances and pile data as established earlier. For input of hammer data and soil damping and quake data, use the default values available in the program. This analysis is to serve a reference to the upper boundary conditions—the program default values are optimistic. Many soils exhibit damping and quake values that are higher than the default values. Furthermore, the hammer efficiency used as default in the program is for a well-functioning hammer and the actual hammer to be used for the project may be worn, in need of maintenance service, etc. Hence, its efficiency value is usually smaller than the default value. Repeat, therefore, the analysis with best estimate of actual hammer efficiency and dynamic soil parameters. This analysis will establish the more representative Bearing Graph for the case.

- A third Bearing Graph analysis with a pessimistic, or conservative, input of values is always advisable. It will establish the low boundary conditions at the site and together with the previous two analyses form a band that indicates the expected behavior.

- When a suitable hammer has been identified, perform a Drivability Analysis to verify that the pile can be driven to the depth and capacity desired. Also this analysis should be made with a range of input values to establish the upper and lower boundaries of the piling conditions at the site.

- Determine from the results of the analysis what hammer model and size and hammer performance to specify for the project. Hammers should not be specified as to rated energy, but to the what they will develop in the pile under the conditions prevailing at the site. That is, the specifications need to give required values of impact stress and transferred energy for the hammer, pile, and soil system. Suggested phrasings are given in Chapter 11.

During construction

- For most projects, at the start of the pile driving, dynamic monitoring with the Pile Driving Analyzer (PDA; Section 9.7) should be performed. The PDA measurements combined with CAPWAP analyses (Section 9.10) will serve to show whether or not the hammer is performing as per the specifications. The measurements will also serve to confirm the relevance of the theoretical calculations (static and dynamic analyses) and, when appropriate, indicate the need for amendments. Although the primary purpose is to verify the pile capacity, other PDA deliverables are hammer performance, transferred energy, pile stresses, soil set-up, etc.

- It is important that the conditions assumed in the analyses are related to the actual conditions. Check actual pile size, length, and material and verify that cushions and helmets as to size, material type, and condition. Then, ascertain that the hammer runs according to the manufacturer's specifications as to blow rate (blows/minute) and that the correct fuel is used. Request records from recent hammer maintenance.

- Depending on size of project, degree of difficulty, and other factors, additional PDA monitoring and analysis may be necessary during the construction work. If questions or difficulties arise during the continued work, new measurements and analysis will provide answers when correlated to the initial measurement results.

9.7 Aspects to consider when reviewing results of wave equation analysis

- Check the pile stresses to verify that a safe pile installation is possible.

- If the desired capacity requires excessive penetration resistance (PRES values greater than 800 blows/metre — 200 blows/foot), re-analyze with a more powerful hammer (pertinent to piles bearing in dense soil; piles driven to bedrock can be considered for larger PRES values if these can be expected to be met after a limited number of blows).

- If the penetration resistance is acceptable but compressive stresses are unacceptably high, re-analyze with either a reduced stroke (if hammer is adjustable) or an increased cushion thickness.

- If (for concrete piles) the penetration resistance is low but tension stresses are too high, either increase the cushion thickness or decrease the stroke or, possibly, use a hammer with a heavier ram, and then re-analyze.

- If both penetration resistance and compressive stresses are excessive, consider the use of not just a different hammer, but also a different pile.

9.8 High-Strain Dynamic Testing of Piles Using the Pile Driving Analyzer, PDA

Dynamic monitoring consists in principle of attaching gages to the pile shortly below the pile head, measuring force and acceleration induced in the pile by the hammer impact (see Fig. 9.11). The dynamic measurements are collected by a data acquisition unit called the Pile Driving Analyzer, PDA. A detailed guide for the performance of the PDA testing is given in ASTM Designation D4945-89.

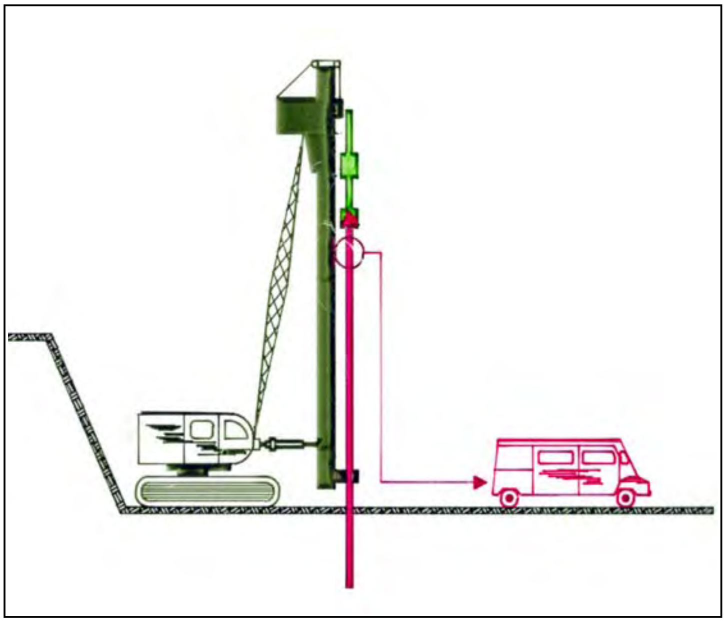

Fig. 9.11 Typical arrangement of dynamic monitoring with the Pile Driving Analyzer (PDA). The two pairs of PDA gages, the accelerometer and the strain-gage, are usually attached shortly below the pile head.

9.8.1 Wave Traces

The PDA data are usually presented in the form of PDA "wave traces", which show the measured force and velocity developments drawn against time as illustrated in Fig. 9.12. The time indicated as 0 L/c, is when the peak impact force occurs, and Time 2 L/c is when the peak force has traveled down to the pile toe, been reflected there, and again appears at the gages at the pile head. The wave has traveled a distance of 2 L at a wave speed of c (ranges from about 3,500 m/s in concrete through about 5,100 m/s in steel – 12,500 ft/s and 16,700 ft/s, respectively).

The most important measurements is the value of peak force, which is called the impact force. When divided by the pile cross sectional area at the gage location, the impact stress is obtained. Fig. 9.12 above shows impact stress measured for a large number of pile PDA records and illustrates how very variable the impact can be.

Notice that Fig. 9.12 shows the force and velocity traces as initially overlapping. This is no coincidence. Force and velocity introduced by an impact are proportional by the impedance, Z (see Eq. 9.4, above). The most fundamental aspect of the wave traces lies in how they react to reflections from the soil, when the traces are no longer identical. When the stress wave on its way down the pile encounters a soil resistance, say at a distance “A“ below the gage location, a reflected wave is sent back up the pile. This wave reaches the gages at Time 2A/c. At that time, force is still being transferred from the hammer to the pile and the gages are still recording the force and velocity in the pile. The reflected stress-wave superimposes the downward wave and the gages are now measuring the combination of the waves. The reflected force will be a compression wave and this compression will add to the measured force, that is, the force wave will rise. At the same time, the pile will slow down because of the resistance in the soil, that is, the measured velocity wave will dip. The consequence is a separation of the traces. The larger this separation, the greater the soil resistance. Soil resistance encountered by the pile toe has usually the most pronounced effect. It is evidenced by a sharp increase of the force wave and a decrease of the velocity wave, usually even a negative velocity—the pile rebounds.[6)]

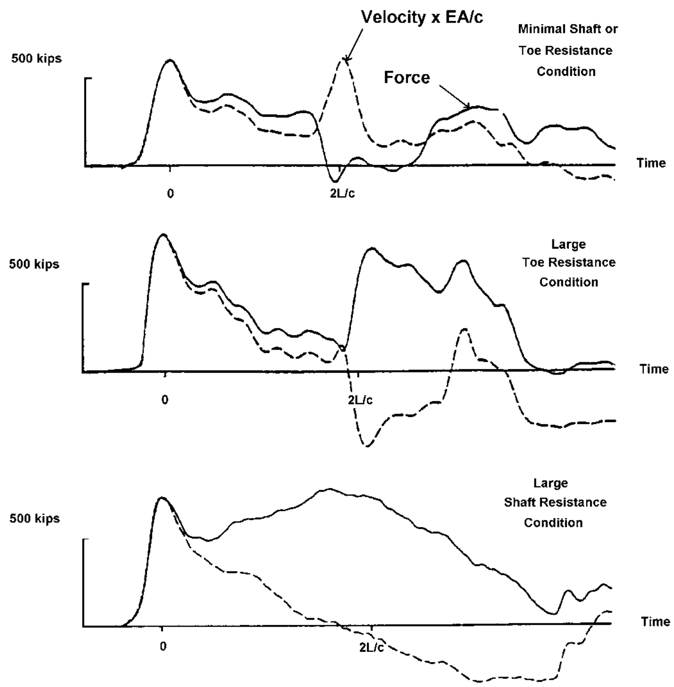

Fig. 9.12 Force and Velocity Wave Traces recorded during initial driving and restriking (Hannigan 1990)

For a pile of length "L" below the gages, reflection from the pile toe will arrive to the gage location at Time 2L/c. This is why the wave traces are always presented in the "L/c scale". The full length of the pile 'in time' is 2L/c and the time of the arrival of a reflection in relation to the 2L/c length is also a direct indication of where in the pile the resistance was encountered.

A resistance along the pile shaft will, as indicated, reflect a compression wave. So will a definite toe resistance as illustrated in the middle wave traces diagram of Fig. 9.12, where the compression trace increases and the velocity traces decreases. Again, the larger the toe resistance, the larger the separation of the two traces. Indeed, the compression stress in the pile at the pile head at Time 2L/c may turn out to be larger than the impacting wave at Time 0L/c. This is because the toe reflection overlaps the incident wave which is still being transferred to the pile head from the hammer. In those cases, the maximum compression stress occurs at the pile toe not at the pile head.

---

6 When dynamic measurements first started to be made in the 1950s, force could be measured by either an accelerometer or a strain gage. At the time, strain gages were prone to malfunction due to moisture and were more laborious to attach, as opposed to accelerometers. The latter were also more accurate, and could be (should be) attached at a single point. However, they were more prone to damage. Depending on preference, either gage type was used. It was not until Dr. Goble and co-workers attached both gage types to the test pile at the same time that the tremendous benefit became apparent of comparing the force determined from measured strain to the force determined from measured and integrated acceleration. The purpose of attaching both gages was that it was hypothesized that the pile capacity would be equal to the force (from the strain gage) when the pile velocity (from the integrated acceleration) was zero and no damping would exist. However, when the velocity at the pile head is zero, the velocity down the pile will not be zero, so the approach did not work and it was abandoned.

A drop hammer does not bounce off the pile head on its impacting the pile head, only when the compression wave originating at the pile toe reaches the ram (if the pile toe is in contact with dense and competent soil). In case of a diesel hammer, its ram lifts off the anvil as a result of the combustion. However, a strong compression wave reflected from the pile toe will increase the upward velocity of the ram and it will reach higher than before. For the next blow, the fall be longer and, therefore, the impact velocity will be higher resulting in a stronger impact wave, which will generate a stronger reflected compression wave, which will send the ram even higher, and . . . If the operator is not quick in reducing the fuel setting, either the diesel hammer or the pile or both can become damaged.

If the soil at the pile toe is soft and unable to offer much resistance to the pile, the reflected wave will be a tensile wave. When the tensile wave reaches the gage location, the gages will record a reduction in the compression wave and an increase in the tensile wave. If the tensile wave is large (very little or no resistance at the pile toe, the pile head may loose contact with the pile driving helmet (temporarily, of course) which will be evidenced by the force trace dropping to the zero line and the velocity trace showing a pronounced peak. The magnitude of the tensile force is directly proportional to the impact wave. A large increase in the velocity trace at Time 2L/c is a visual warning for excessive tension in the pile. This is of particular importance for concrete piles, which piles have limited tension strength.

Whether a tension or a compression wave will be reflected from the pile toe is not just a function of the strength of the soil at the pile toe. Strength is the ultimate resistance after a movement has occurred. In brief, if the force in the pile at the pile toe rises faster than the increase of resistance due to the pile toe penetration, a tension wave is reflected. If, instead, the soil resistance increases at the faster rate, then, a compression wave results. Ordinarily, the quake is small, about 1 % of the pile diameter or 2 mm to 4 mm, and the acceleration of the pile toe is such that the pile toe resistance is mobilized faster than the rise of the force in the pile. However, some soils, for example some silty glacial tills and highly organic soils, demonstrate large quake values, e. g., 20 mm to 50 mm. Yet, these soils may have considerable strength once the pile toe has moved the distance of the quake. When driving piles in such soils, the pile toe will at first experience little resistance. When the pile toe movement is larger that the quake, the pile toe works against the full soil resistance. Dynamic measurements from piles driven in such soils, will show a tensile reflection at 2L/c followed by a compression reflection. The sharper the rise of the impact wave, the clearer the picture. If the conditions are such that the peak of the impact wave has reached the pile toe before the pile toe has moved the distance of the quake, the full toe resistance will not be mobilized and the penetration resistance becomes large without this being ‘reflected” by a corresponding pile capacity. Simply expressed, a large quake will zap the efficacy of the driving (Fellenius and Authier 1980).

The visual message contained in the force and velocity records will provide the experienced PDA operator with much qualitative information on where in the soil the resistance originates—shaft bearing versus toe bearing, or combination of both—consistency in the response of the soil as well as in the behavior of the hammer, ands many other aspects useful the assessment of a pile foundation. For example, it may be difficult to tell whether an earlier-than-expected-stopping-up of a pile is due to a malfunctioning hammer producing too small force or little energy, or if it is due to fuel preignition. The PDA measurements of hammer transferred energy and impact force will serve as indisputable fact to determine whether or not a hammer is functioning as expected.

Included with routine display of PDA traces are Wave-Down and Wave-Up traces. The Wave-Down trace is produced by displaying the average of the velocity and force traces, thus eliminating the influence of the reflected wave and, as the name implies, obtaining a trace showing what the hammer is sending down into the pile. Similarly, half the difference between the two traces displays the reflected wave called Wave-Up, which is the soil response to the impact. Fig. 9.13 shows an example of a routine display of the wave traces (see below for explanation of the Movement and Energy traces).

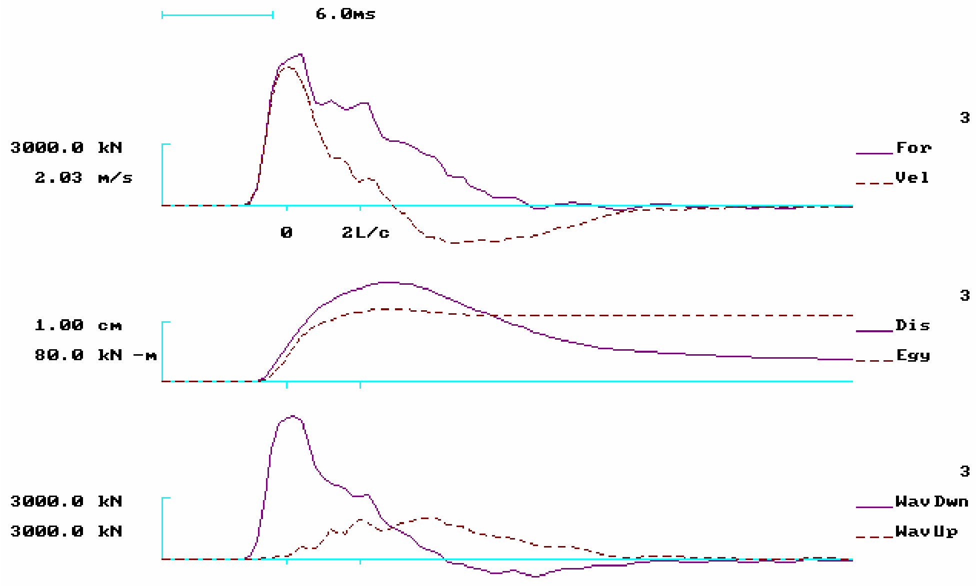

Fig. 9.13 Routine Display of PDA Wave Traces
Force and Velocity, Movement ("Dis.") and Transferred Energy ("Egy."), and Wave Down and Wave Up

Comparing wave traces from different blows will often provided important information. For example, the discussion above referring to the strong compression wave reflecting from the pile toe is illustrated in Fig. 9.14 by two blows recorded from the initial driving of a steel pile through soft and loose silty soil to contact with a very dense glacial till. The pile toe was brought to contact with the glacial till between Blow 55 and Blow 65. The increased toe resistance resulted in a small increase of the impact force (from a stress of about 150 MPa to 170 MPa), which values are well within acceptable levels. However, for Blow 65 at Time 2L/c, which is when the toe reflection reaches the pile head, a stress of 280 MPa was measured. This stress is very close to the steel yield for the pile material (reported to be 300 MPa. No surprise then that several of the pile were subsequently found to have considerable toe damage). Compounding the problem is the very small shaft resistance and a larger than usual toe quake. This is also obvious from the wave traces by the small separation of the traces and the “blip” immediately before Time 2L/c.

9.8.2 Transferred Energy

The energy transferred from the hammer to the pile can be determined from PDA data as the integral of force times velocity times impedance. Its maximum value, called EMX, is usually referred to as the Transferred Energy. In assessing a hammer based on the transferred energy, it should be recognized that the values should be obtained during moderate penetration resistance and from when the maximum value does not occur much earlier than Time 2L/c. Neither should a hammer be assessed by energy values determined from very easy driving. The consistency of the values of transferred energy is sometimes more important than the actual number.

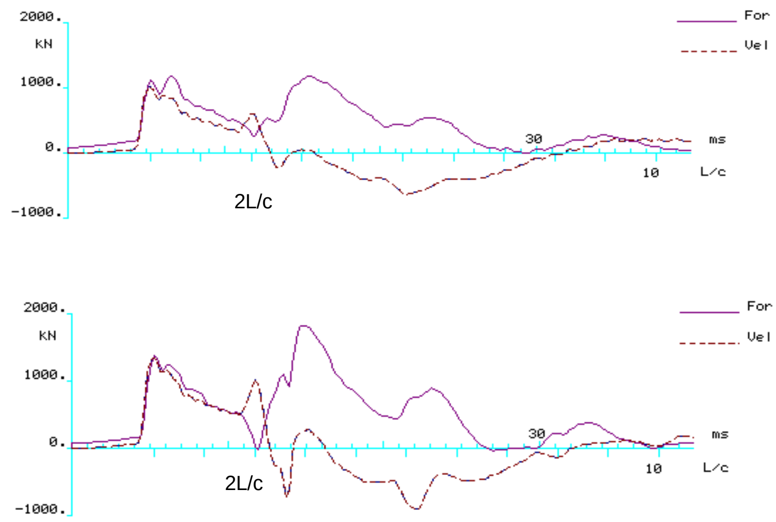

Fig. 9.14 Two Force and Velocity Wave Traces compared

9.8.3 Movement

A double integration of the acceleration produces a pile movement (displacement) trace, displaying the maximum and net penetration of the pile. An example is shown in the middle graph of Fig. 9.13, above.

9.9. Pile Integrity

9.9.1 Integrity determined from high-strain testing

In a free-standing, uniform rod, no reflections will appear before Time 2L/c. For a pile, no sudden changes of shaft resistance normally occur along the pile. Therefore, the separation of the force and velocity traces caused by the shaft resistance is normally relatively gradual before Time 2L/c. However, a sudden impedance reduction, for example, the intentional change of an H-Pile stinger at the end of a concrete section, will result in an increase of the velocity trace and a decrease of the force wave, a “blip” in the records. The magnitude of the “blip” is a sign of the magnitude of the impedance change. A partially broken length of a concrete pile is also an impedance change and will show up as a blip. The location along the time scale will indicate the location of the crack. A crack may be harder to distinguish, unless it is across a substantial part of the cross section. Rausche and Goble (1979) developed how the “blip” can be analyzed to produce a quantified value, called “beta” for the extent of the damage in the pile. The beta value corresponds approximately to the ratio of the reduced cross sectional area to the original undamaged cross sectional area. Beta values close to unity do not necessarily indicate a damage pile. However, a beta value smaller than 0.7 would in most cases indicate a damaged pile. Beta-values between 0.7 and 0.9 may indicate a change in the pile integrity, or impedance, but do not necessarily indicate damage.

9.9.2 Integrity determined from low-strain testing

The purpose of performing low-strain testing is to assess the structural integrity of driven or cast-in-place concrete piles, drilled-shafts, and wood piles, and to determine the length of different types piles including sheet piles where length records are missing or in doubt. A detailed guide for the performance of low-strain integrity testing is given in ASTM Designation D 5882-96.

The work consists of field measurements followed by data processing and interpretation. The measurements consists of hitting the pile with a hand-held hammer and recording the resulting signal with a sensitive accelerometer connected to a special field data collector (PIT Collector). The collector can display the signal (a velocity trace integrated from the measured acceleration) , process the data, and send the trace to a printer or transfer all the data to a computer. Special computer programs are used for data processing and analysis.

Fig. 9.15 shows schematically the principle of low-strain testing—collecting the pulse echo of signals generated by impacting the pile head with a hand-held hammer. The "motion sensor" transmits signals to a unit called the PIT Collector. The PIT Collector is equipped with a processor, and display and storage units. The stored processed data will be transferred to a PC for further processing and interpretation.

The measurements are evaluated on site for preliminary assessment of the pile integrity. Questionable piles, if any, are identified and subjected to detailed analysis. The detailed analysis assists in identifying magnitude and location of structural concerns along the pile.

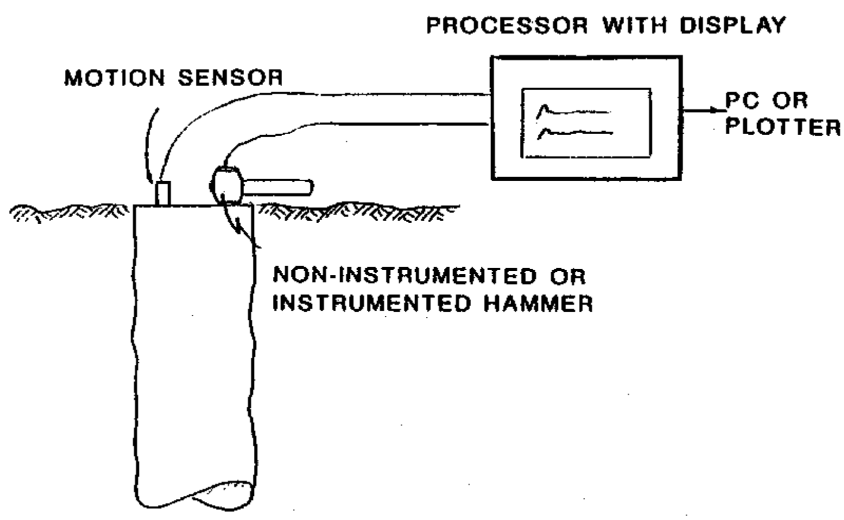

Fig. 9.15 Schematics of low-strain testing arrangement

9.10 Case Method Estimate of Capacity

The data recorded by the PDA are displayed in real time (blow by blow) in the form of wave traces. Routinely, they are also treated analytically and values of stress, energy, etc., are displayed to the operator. The values include an estimate of pile capacity called the Case Method Estimate, CMES. The CMES method uses force and velocity measured at Times 0 L/c and 2 L/c to calculate the total (static and dynamic) resistance, RTL, as shown in Eq. 9.22.

(9.22) $$RTL = \frac{F_{(t1)} + F_{(t1+2L/c)}}{2} + \frac{M\,c}{2L}(V_{(t1)} + V_{(t1+2L/c)})$$

where: RTL = Total resistance

$F_{(t1)}$ = Force measured at the time of maximum pile head velocity
$F_{(t1 + 2L/c)}$ = Force measured at the return of the stress wave from the pile toe
M = Pile mass
c = Wave speed in the pile
L = Length of pile below gage location
$V_{(t1)}$ = Pile velocity measured at the time of maximum pile head velocity
$V_{(t1 + 2L/c)}$ = Pile velocity measured at the return of the stress wave from the pile toe

The total resistance is greater than the static bearing capacity and the difference is the damping force. Damping force is proportional to pile toe velocity and calculated as indicated in Eq. 9.23. (When velocity is zero just at the time when the pile starts to rebound ("unloads"), the total resistance (RTL) is a function of static resistance only. Initially in the development of the method of analysis of dynamic measurements, it was thought that the pile static capacity could be determined from this concept. However, the pile velocity is not zero all along the pile, so the approach was shown to be inapplicable (Goble et al. 1980). It was revived for the "long duration impulse testing method as indicated in Section 9.13).

(9.23) $$R_d = J \frac{M\,c}{L} V_{(toe)} = J\,(F_{(t1)} + \frac{M\,c}{L} V_{(t1)} - RTL)$$

where R_d = Damping force
J = Case damping factor
M = Pile mass
V_{toe} = Pile toe velocity
c = Wave speed in the pile
L = Length of pile below gage location
$F_{(t1)}$ = Force measured at the time of maximum pile head velocity
$V_{(t1)}$ = Pile velocity measured at the time of maximum pile head velocity
RTL = Total resistance

The PDA includes several CMES methods, some of which are damping-dependent and some are damping-independent. The damping-dependent methods evaluate the CMES value by subtracting the damping force, R_d, from the CMES value of total dynamic capacity (RTL). As shown in Eq. 9.23, the damping force is proportional to the measured pile physical velocity, V_{toe}.

The Case Damping factor ranges from zero to unity with the smaller values usually considered to represent damping in coarse-grained soil and the higher in fine-grained soils. The factor is only supposedly a soil parameter, however. Different piles driven at the same site may have different J-factors and a change of hammer may require a reassessment of the J-factor to apply (Fellenius et al. 1989). Therefore, what J-factor to apply to a certain combination of hammer, pile, and soil pile is far from a simple task, but one that requires calibration to actual static capacity and experience. A factor determined for EOID conditions may show to be off considerably for the restrike (RSTR) condition, for example. It is always advisable to calibrate the CMES method capacity to the results of a CAPWAP analysis (Section 9.10).

The most common damping-dependent CMES methods are called RSP, RMX, and RSU. There is also a damping-independent method called RAU.

The **RSP** value is the CMES RTL value calculated from the force and velocity measurements recorded at Times 0 L/c and 2 L/c and applying a Case Damping factor, J, ranging from zero to unity. Typically, a CMES value indicated as RS6 is determined for a J = 0.6.

The **RMX** value is the maximum RSP value occurring in a 30 ms interval after Time 0 L/c, while keeping the 2 L/c distance constant. In case of hard driven piles, the RMX value is often more consistent than the RSP value. For details, see Hannigan (1990). Typically, a CMES value indicated as RX6 is determined for a J = 0.6. The RMX method is the most commonly applied method. Routinely, the output of RMX values will list the capacities for a range of J-factors, implying an upper and lower boundary of capacity.

The **RSU** value may be applied to long shaft bearing piles where most of the movement is in the form of elastic response of the pile to the imposed forces. Often , for such piles, the velocity trace has a tendency to become negative (pile is rebounding) well before Time 2 L/c. This is associated with the length of the stress wave. As the wave progresses down the long pile and the peak of the wave passes, the force in the pile reduces. In response to the reduced force, the pile elongates. The soil resistance, which initially acts in the positive direction, becomes negative along the upper rebounding portion of the pile, working in the opposite direction to the static resistance mobilized along the lower portion of the pile (which still is moving downward). In the RSU method, the shaft resistance along the unloading length of the pile is determined, and then, half this value is added to the RSP value computed for the blow. For long shaft nearing piles, the RSU value, may provide the more representative capacity value. However, the RSU is very sensitive to the Case damping factor and should be used with caution.

The damping-independent **RAU** method consists of the RSP method applied to the results at the time when the toe velocity is zero (the Case J-factor is irrelevant for the results). The RAU method is intended for toe-bearing piles and, for such piles, it may sometimes show more consistent results than the RMX method. It also should be applied with considerable caution.

Although the CMES capacity is derived from wave theory, the values depend so much on choosing the proper J-factor and method, and, indeed, the representative blow record, that their use requires a good deal of experience and engineering judgment. This is not meant as a denigration of the CMES method, of course. There is much experience available and the methods have the advantage of being produced in real time blow for blow. When considered together with the measurements of impact force and transferred energy with due consideration to the soil conditions, and with calibration of a representative record to a signal-matching analysis (CAPWAP; see below), an experienced engineer can usually produce reliable estimates of capacity for every pile tested.

The estimate of capacity makes use of the wave reflected from the soil. If is often overlooked that the soil can never send back up to the gages any more than the hammer has sent down in the first place. Simply, the analysis of the record postulates that the full soil resistance is indeed mobilized. If the hammer is not able to move the pile, the full resistance of the pile is not mobilized. The PDA will then not be able to accurately determine the pile capacity, but will deliver a “lower-bound” value. When the capacity is not fully mobilized, the capacity value is more subjected to operator judgment and, on occasions, the operator may actually overestimate the capacity and produce analysis results of dubious relevance.

Moreover, the capacity determined is the capacity at the time of the testing. If the pile is tested before set-up has developed, the capacity will be smaller than the one determined in a static loading test some time later. A test at RSTR (if the pile moves for the blow) is more representative for the long-term performance of a pile under load than is the test at EOID. (Provided now that the pile has been let to rest during the period between the initial driving and the restrike: no intermediate restriking and no other pile driven in the immediate vicinity).

A restrike will sometimes break down the bond between the pile and the soil and although in time the bond will be recovered this process is often slower than the rate of recovery (set-up) starting from the EOID condition. This is because a restrike does not introduce the any lateral displacement of the soil, while the initial driving introduces a considerable lateral displacement of the soil even in the case of so-called low-displacement piles such as H-piles.

Restriking is usually performed by giving the pile a certain small number of blows or the number necessary to for achieving a certain penetration. The pile capacity reduces with the number of blows given, because the restrike driving disturbs the bond between the pile and the soil and increases pore pressure around the pile. Therefore, the analysis for capacity is normally performed on one of the very first restrike blows, as analysis for one of the later blows would produce a smaller capacity. Normally, the disturbance effect disappears within a few hours or days. However, a static test immediately following the completion of the restrike event may show a smaller capacity value than that determined in the analysis of the PDA data from an early restrike blow. Moreover, a static test is less traumatic for a pile than a dynamic restrike test. For this reason, when comparing dynamic and static test results on a pile, it is preferable to perform the static loading test first.

Performing the static test first is not a trivial recommendation, because when restriking the pile after a set-up period, it would normally have an adequate stick-up to accommodate the monitoring gages. Because a static test is normally performed with a minimum stick-up above ground (the pile is cut off before the test), attaching the gages after a static test may not be straight-forward and require hand excavation around the pile to provide access for placing the gages.

9.11. CAPWAP determined pile capacity

The two traces, force and velocity, are mutually independent records. By taking one trace, say the velocity, as an input to a wave equation computer program called CAPWAP, a force-trace can be calculated. The shape of this calculated force trace depends on the actual hammer input given to the pile as represented by the measured velocity trace <u>and</u> on the distribution of static resistance and dynamic soil parameters used as input in the analysis. Because the latter are assumed values, at first the calculated force-trace will appear very different from the measured force-trace. However, by adjusting the latter data, the calculated and measured force traces can be made to agree better and the match quality is improved. Ultimately, after a few iteration runs on the computer, the calculated force-trace is made to agree well with the measured trace. An agreement, ‘a good signal match’, means that the soil data (such as quake, damping, and ultimate shaft and toe resistance values) are close to those of the soil into which the pile was driven. In other words, the CAPWAP signal match has determined the static capacity of the pile and its distribution along the pile (as the sum of the resistances assigned to the analysis). Fig. 9.16 presents an example of the results of a CAPWAP signal matching along with the wave traces and PDA data and is an example of a routine report sheet summarizing the data from one blow. When several piles have been tested, it is of value to compile all the PDA and CAPWAP results in a table, separating the basic measured values from the analyzed (computed) values.

The CAPWAP determined capacity is usually close to the capacity determined in a static loading test. This does not mean that it is identical to the value obtained from a static test. After all, the capacity of a test pile as evaluated from a static loading test can vary by 20 percent with the definition of failure load applied. Also, only very few static loading tests can be performed with an accuracy of 5 percent on load values. Moreover, the error in the load measurement in the static loading test is usually about 10 percent of the value, sometimes even greater.

EMAX	Energy ratio	Impact force	Max. force	Impact stress	CSX	CSB	PRES	CMES RX4	RX5	RX6	RAU
(kJ)	(%)	(KN)	(KN)	(MPa)	(MPa)	(MPa)	(bl/25mm)	(KN)	(KN)	(KN)	(KN)
18.7	32.8	2,980	2,980	178	178	131	17	2,126	1,859	1,591	2,413

EMAX: Maximum transferred energy CSX: Maximum compr. stress, gage level CSB: Maximum compr. stress, toe
RXJ: CMES, RMX with a J-factor = J RAU: CMES damping independent PRES: Penetration resistance
Energy Ratio is ratio (%) between transferred and rated energy

CAPWAP Table

Mobilized Static Resistance (KN)			Max. Stress (MPa)		Smith Damping (s/m)		Quake (mm)	
Total	Shaft	Toe	Compression	Tension	Shaft	Toe	Shaft	Toe
2,124	2,093	31	183	9	0.114	0.61	1.00	2.50

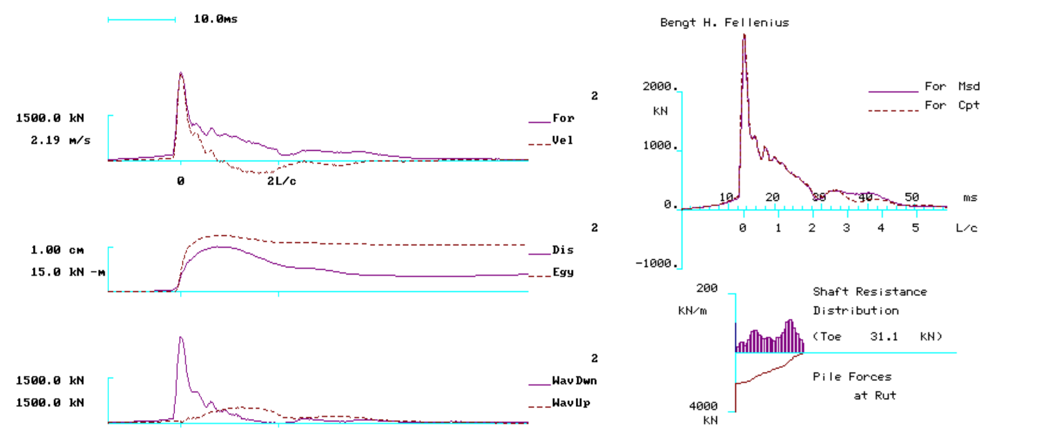

Fig. 9.16 Example of a routine PDA and CAPWAP summary sheet: Table and graph

A CAPWAP analysis performed on measurements taken when a pile penetrates at about 5 blows to 12 blows per inch will provide values of capacity, which are reliable and representative for the static behavior of the pile at the time of the driving. Provided that the static test is equally well performed (not always the case), the two values of static capacity are normally within about 15 percent of each other. For all practical engineering purposes, this can be taken as complete agreement between the results considering that two different methods of testing are used.

In practice, engineers employing dynamic testing and CAPWAP analysis limit the analysis to the last impact given to the test pile at initial driving and the first (if possible) of the impacts given in restriking the test pile. They treat the dynamic tests as so much of a lesser cost static test. However, this is losing the full benefit of the dynamic test. Often at the end of initial driving, the full resistance is not mobilized (the pile is being driving at the maximum ability of the hammer to advanced the pile) and the CAPWAP-determined distribution may not be determined at the optimum use of the method. Therefore, also records of a blow from before the end of initial driving, say, from a foot above termination, should be subjected to a CAPWAP analysis and the results compared and discussed. Similarly, at restrike, also a record from the end of restrike, say the fifth or tenth blow should be analyzed. The latter analysis will often show a larger toe resistance than the analysis for very first restrike record (because the restriking has reduced the set-up and the shaft resistance being smaller allows more force and energy to reach the pile toe. Of course, an extra couple of CAPWAP analyses cost money—but so what, it is cheap money for the value obtained.

A CAPWAP analysis uses as input the speed of wave propagation, c, in the pile. Eqs. 9.11 through 9.17 show the importance and interdependence of the material density, impedance, and elastic modulus. The proper selection of the input parameters will govern the correct location of the soil and pile response (reflections) and of particular importance is the use of a correct wave speed for determining the elastic modulus. For a concrete pile, minute cracks—hairline fissures—can develop and together they could have the effect of slowing down the wave and require a smaller modulus to be input for the correct analysis results. The elastic modulus is usually determined from the time for the wave to reach the pile toe and be reflected up to the gage location at the pile head, Time 2L/c. Also the evaluation of the impact force makes use of the elastic modulus. However, where hair line fissures have slowed down the wave speed and indicated a reduced modulus, no such reduction occurs at the gage location. In such cases, using the E-modulus input from the "2L/c" time is not correct and a unreduced modulus applies.

9.12. Results of a PDA Test

The cost of one conventional static test equals the costs of ten to twenty dynamic tests and analyses, sometimes more. Therefore, the savings realized by the use of dynamic testing can be considerable, even when several dynamic tests are performed to replace one static loading test. Moreover, pile capacity can vary considerably from one pile to the next and the single pile chosen for a static loading test may not be fully representative for the other piles at the site. The low cost of the dynamic test means that for relatively little money, when using dynamic testing, the capacity of several piles can be determined. Consequently, because, establishing the capacity of several piles gives a greater confidence in the adequacy of the pile foundation as opposed to determining it for only one pile, a greater assurance is obtained.

The CAPWAP results include a set of parameters to use as input to a wave equation analysis, which allows the wave equation can be used with confidence to simulate the continued pile driving at the site, even when changes are made to pile lengths, hammer, and pile size, etc.

The limitations mentioned above for when the full resistance is not mobilized apply also to the CAPWAP analysis, although the risk for overestimation of the capacity is smaller.

The distribution of the capacity on shaft and the toe resistances is determined with less accuracy as opposed to the total capacity. The reason lies in that a pile is always to a smaller or larger degree subjected to residual load and the residual load cannot be fully considered in the CAPWAP analysis. The effect of residual load present in a test pile is an overestimation of the resistance along the upper length of the pile (shaft resistance) and an underestimation along the lower length (toe resistance). It has no effect on the total capacity, of course. (It is not always appreciated that the sensitivity of the analysis results to residual load is equally great for the results of a static loading test).

A pile test will unavoidably change—disturb—the pile response to load. A dynamic test more so than a static test. It is not irrelevant, therefore, when comparing static and dynamic tests, for the best compatibility, the static loading test should "go first", as indicated in Fellenius (2008). This is not a trivial recommendation, because a dynamic test requires a stick-up of the pile head above ground, whereas a static loading test is preferably performed with a minimum stick-up.

Some preliminary results of the PDA testing will be available immediately after the test, indeed, even as the pile is being driven. For example, the transferred energy, the impact and maximum stresses in the pile, and a preliminary estimate of capacity according to the CMES method. The following is reported following processing in the office.

- Selected representative blow records including a graphic display of traces showing Force and Velocity, Transferred Energy and Pile Head Movement, and Wave Up and Wave Down.
- Blow data processed presented in tables showing a series of measured data for assessment of the pile driving hammer and pile.
- CAPWAP results showing for each analyzed blow the results in a CAPWAP diagram and the quantified results in tables.
- Complete pile driving diagram encompassing all dynamic data (Fig 9.17)

Figs. 9.17 and 9.18 show examples of the measurements presented in a PDA diagram. The PDA diagram can be used to study how transferred energy, forces and stresses, hammer stroke, and penetration resistance vary with depth. When the PDA monitoring is performed not just for to serve as a simple routine test but to finalize a design, establish criteria for contract specifications, etc., then, a PDA diagram is of great value and assistance to the engineer’s assessment of the piling.

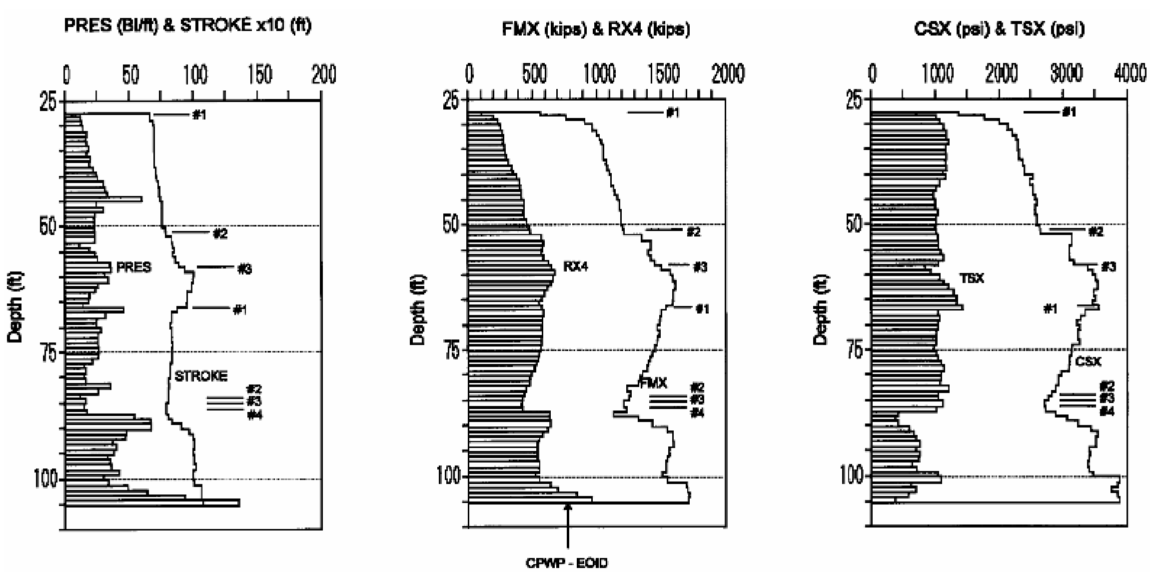

Fig. 9.17 Example of PDA Diagrams from the driving of a concrete pile
(Labels #1 through #4 indicate hammer fuel setting)

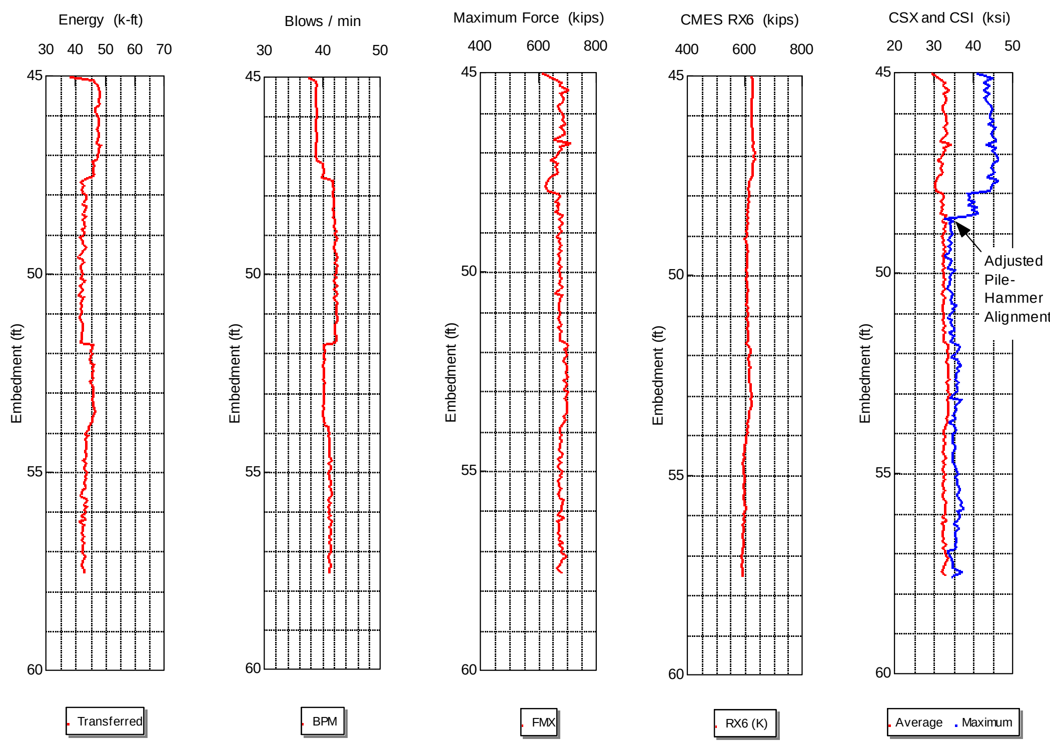

Fig. 9.18 Example of PDA Diagrams from the driving of a steel pile

The foregoing should make it quite clear that relying on a dynamic formula, that is, on essentially only the "blow-count" to determine capacity is a dangerous approach. Salem et al. 2008, present a case history where the blow count was considerably misleading, as was established in dynamic testing and CAPWAP analysis.

9.13. Long Duration Impulse Testing Method—The Statnamic and Fundex Methods

In the conventional dynamic test, the imparted stress-wave has a steep rise and an intensity that changes along the pile length. That is, when the impact peak reaches the pile toe and the entire pile is engaged by the blow, force from the pile hammer transmitted to the pile varies and is superimposed by numerous reflections. The force in the pile varies considerable between the pile head and the pile toe. The steep rise of the stress-wave and the reflections are indeed the condition for the analysis. When the impact is "soft" and the rise, therefore, is less steep, it becomes difficult to determine in the analysis just from where the reflections originate and how large they are. However, in the 1990s, an alternative dynamic method of testing was developed, called Statnamic, here denoted "***long duration impulse method***" consisting of giving the pile just this soft-rising, almost constant force. The method is usually called “rapid loading test” and consists of impacting the pile in a way where the rise of force is much softer than in the pile driving impact, and the impulse (a better word than "impact") was of a much longer duration. The long duration impulse usually makes the pile move as a rigid body, that is, the pile velocity at the pile head is the same as the velocity at the pile toe. This aspect made possible an analysis method, called the "***unloading point method***" for determining the pile capacity (Middendorp et al. 1992).

The long duration impulse method is a dynamic method. However, the transfer of the force to the piles, the impulse, can take 100 to 200 milliseconds, i.e., five to twenty times longer time than the time for a pile driving impact. The stress-wave velocity in the pile is the same, however. This means that the sharp changes of force experienced in the pile driving are absent and that the pile moves more or less as a rigid body. Although the ram travel is long, the peak force is reduced by that the impact velocity has been reduced. As a large ram mass is used, a large energy is still transferred to the pile. The key to the long duration impulse method lies in this slowing down of the transfer of the force from the impacting hammer to the pile. In method employed by a Dutch company, Fundex, this is achieved by letting the ram impact a series of plate springs which compression requires the hammer to move much more than required in case of the ordinary hammer and pile cushions, and thus reduce the kinetic energy in the transfer to the pile. The Statnamic method, developed by Berminghammer in Canada, achieves the effect in the pile in a radically different way, using a propellant to send a weight up in the air above the pile, in the process creating a downward force on the pile according to Newton's third law.

The measurements consist of force, movement, acceleration, and time. The most important display of the results consists of a load-movement curve, as illustrated in Fig. 9.19.

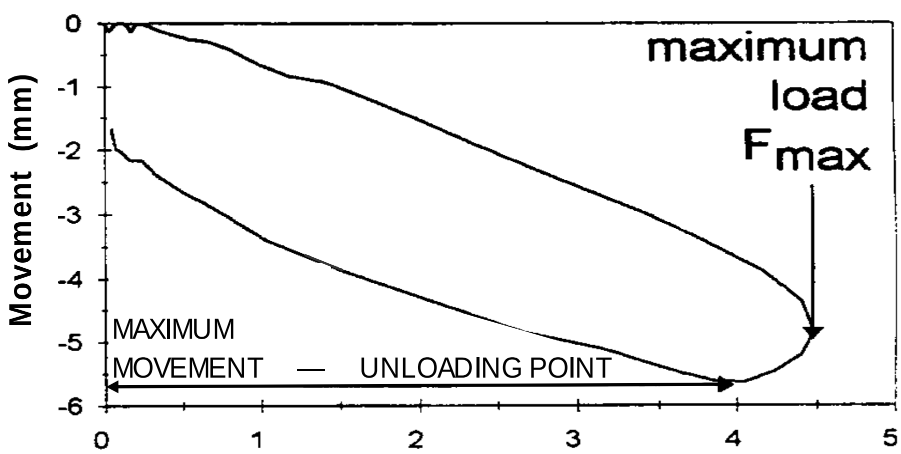

Fig. 9.19 Load-movement curve from Statnamic test (Bermingham et al. 1993)

Load, movement, velocity, and acceleration versus time are important records of the test. An example of these records are presented in Fig. 9.20 (same test as in Fig. 9.19). The maximum movement (about 4 mm in the example case) is where the pile direction changes from downward to upward, i.e., the pile rebounds, is called the "Unloading Point", "P-point" for short. The maximum load applied to the pile by the ram impulse (about 4.5 KN in the example case) occurs a short while (about 3 ms in the example case) before the pile reaches the maximum movement. Most important to realize is that the pile velocity is zero at the unloading point, while the acceleration (upward) is at its maximum. Shortly before and after the maximum force imposed, the velocity of the pile head and the pile toe are considered to be essentially equal, that is, no wave action occurs in the pile. This is assumed true beyond the point of maximum movement of the pile.

In the pile-driving dynamic test, the methods of analysis of the force and velocity measured in a dynamic test includes a separation of the damping portion (the velocity dependent portion) of the dynamic resistance. Inertia forces are considered negligible. In contrast, in the long duration impulse method, the velocity of the pile is zero at the unloading point, which means that damping is not present. However, the acceleration is large at this point and, therefore, inertia is a significant portion of the measured force.

The equilibrium between the measured force and the other forces acting on the pile at any time is described by the following equation (Middendorp et al. 1992).

Eq. 9.24 $$F = ma + cv + ku$$

where
F = measured force (downward)
m = mass of pile
a = acceleration (upward)
c = damping factor
v = velocity
k = modulus
u = movement

The two unknowns in Eq. 9.24 are the damping factor, c, and the modulus, k. The other values are either known or measured. As mentioned, at the unloading point, the velocity is zero along the full length of the pile. This becomes less true as the pile length increases, but for piles shorter than about 40 m, observations and research have shown the statement to be valid (Middendorp et al. 1995; Nishimura et al. 1998).

At the time of zero velocity, the damping component of Eq. 9.24 is zero, because the velocity is zero. This determines the static resistance at the unloading point, because the force and acceleration are measured quantities and the mass is known. Thus, the static resistance acting on the pile at the unloading point is obtained according to Eq. 9.25 as the value of measured force plus the inertia (note acceleration is upward—negative).

Eq. 9.25 $$R_P = (F_P - ma_P)$$

where
R_P = static resistance at the UPM-point
F_P = force measured force at the UPM-point
m = mass of pile
a_P = acceleration measured at the UPM-Point

In the range between the maximum measured force and the unloading point, the load is decreasing (the pile decelerates; acceleration is negative) while the movement is still increasing, and the pile has a velocity (downward and reducing toward zero at the unloading point, which means that damping is present). These quantities are measured. Moreover, it is assumed that at the maximum force, the pile has mobilized the ultimate shaft resistance and that the continued soil response is plastic until the unloading point is reached. That is, the static resistance is known and equal to the value determined by Eq. 9.25. This is the primary assumption of the Unloading Point Method for determining the pile capacity using the UPM (Middendorp et al. 1992).

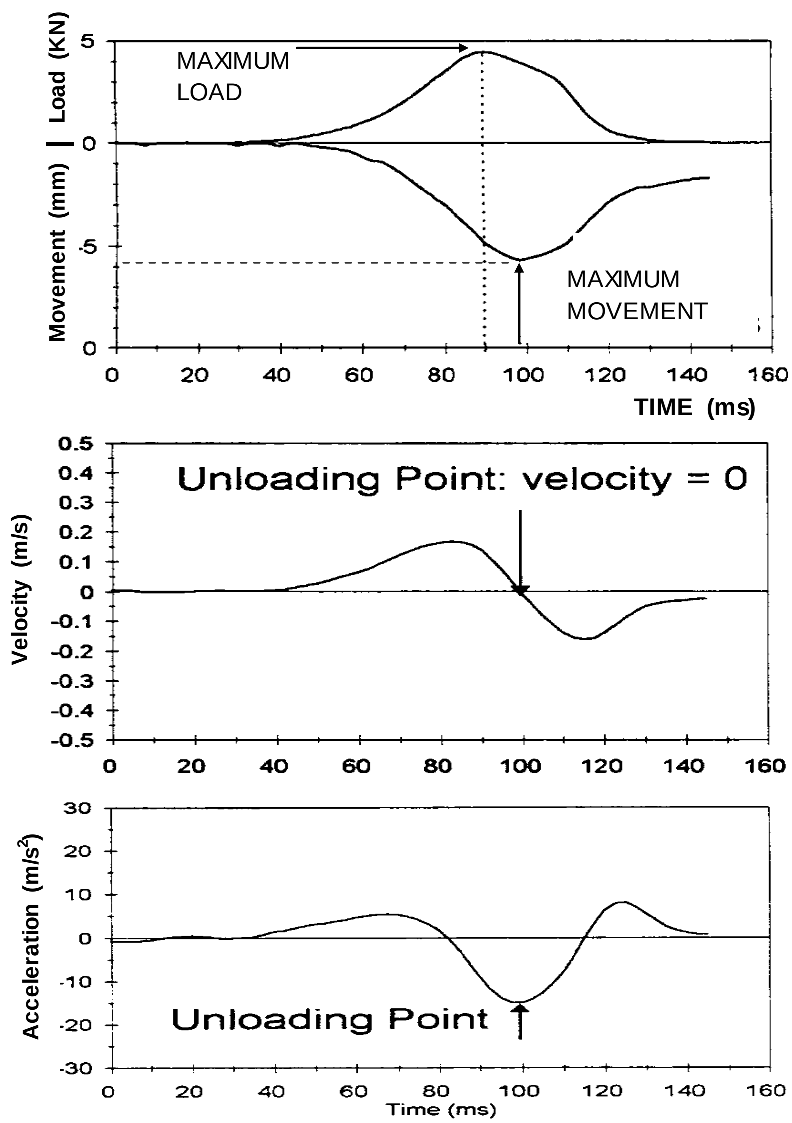

Fig. 9.20 Load, movement, velocity, and acceleration versus time from Statnamic test (Bermingham et al. 1993)

Eq. 9.24 can be rearranged to Eq. 9.26 indicating the solution for the damping factor.

9.26 $$c = \frac{F - ma - R_P}{v}$$

where
c = damping factor
F = measured force (downward)
m = mass of pile
a = acceleration (upward)
R_P = static resistance at the UPM-point
v = velocity

The value of the damping factor, c, in Eq. 9.26 is calculated for each instant in time between the maximum measured force and the unloading point. For the Statnamic test, the number of data points depends on the magnitude of movement of the pile after the maximum Statnamic force is reached. Typically, the number of data points collected in this range is 50 to 200. The c values are averaged and taken to represent the damping factor acting on the pile throughout the test. The measured force and acceleration plus the pile mass then determine the static load-movement curve according to Eq. 9.27.

9.27 $$R_P = F - ma - c_{avg}\,v$$

where
R_P = static resistance at the UPM-point
F = measured force (downward)
m = mass of pile
a = acceleration (upward)
c_{avg} = average damping factor between the maximum force and the P-point
v = velocity

Fig. 9.21 illustrates the results of the analysis for a 9 m long, 910 mm diameter bored pile in clay (Justason and Fellenius 2001).

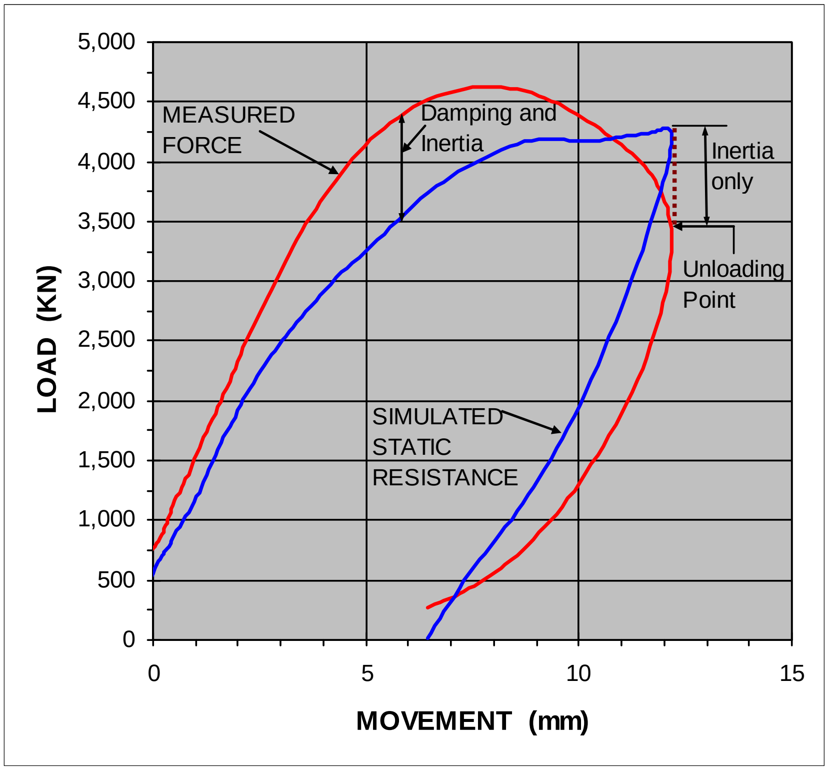

Fig. 9.21 Example of measured force-movement curve and simulated static load-movement curve
Data from Justason and Fellenius (2001)

Lately, several papers have been published showing case histories where the capacity determined in a Statnamic test according to the Unloading Point Method (UPM) to considerably overestimate the capacity determined on the same pile in a static loading test. (e.g., Middendorp et al. 2008; Brown et al. 2006; Brown and Hyde 2008). In clay, the overestimation has been as large as close to a factor of two. The referenced papers hypothesize that the capacity overestimation is a result of the velocity of the pile and associated dynamic effects, notwithstanding that the UPM capacity is determined at zero velocity—non-dynamic condition—, and recommend that a correction factor be applied to the UPM-determined capacity. Such correction factors can never be general factors associated with the method, and it appears necessary to calibrate the Long Duration Impulse Testing Methods to a static loading test before relying on a UPM-determined capacity value for a specific site and project.

9.14. Vibration Caused by Pile Driving

During driving, energy is transmitted from the pile hammer to the pile, and, as the pile penetrates into the soil, both static and velocity-dependent (dynamic) dynamic resistances are generated. The dynamic soil resistance gives rise to ground vibrations which are transmitted through the soil, potentially, causing settlement in some soils, or adversely affecting nearby installations or structures on or in the ground. In this context, the process is more complex than realized by many, but the theoretical format is quite simple, as will be shown below. Massarsch and Fellenius (2008) provide an account of the interactive nature of the pile impedance and the soil impedance which can be used to assess the vibration effect of pile driving, as follows. The fact that the damping factor is a function of the ratio between the pile impedance and the soil impedance for P-waves is verified by a reanalysis of vibration measurements reported by Heckman and Hagerty (1978), who measured the intensity of ground vibrations at different distances away from piles being driven. The piles were of different type, size, and material. Heckman and Hagerty (1978) determined a k factor, expressed in Eq. 9.28, which is a measure of ground vibration intensity (usually the vertical vibration velocity).

9.28 $$v = k\frac{\sqrt{W}}{r}$$

where v = vibration velocity (m/s)
W = energy input at source (J)
k = an empirical vibration factor ($m^2/s\sqrt{J}$)
r = distance from pile (m)

The vibration velocity in Eq. 9.28 is not defined in terms of direction of measurement (vertical, horizontal, or resultant of components). Moreover, the empirical factor, k, is not dimensionless, which has caused some confusion in the literature. Figure 9.22 presents the k-factor values of Heckman and Hagerty (1978) as a function of pile impedance and measurements of pile impedance.

The measurements were taken at different horizontal distances away from piles of different types and sizes driven with hammers of different rated energies. Unfortunately, the paper by Heckman and Hagerty (1978) is somewhat short on details regarding the driving method, ground conditions, and vibration measurements and, therefore, the data also include effects of ground vibration attenuation and, possibly, also effects of vibration amplification in soil layers. Yet, as shown in Fig. 2, a strong correlation exists between the pile impedance and the k-factor, as the ground vibrations increased markedly when the impedance of the pile decreased. In fact, ground vibrations can be ten times larger in the case of a pile with low impedance, as opposed to vibrations generated at the same distance from the driving of a pile with high impedance (Massarsch 1992; Massarsch and Fellenius 2008; Fellenius and Massarsch 2008).

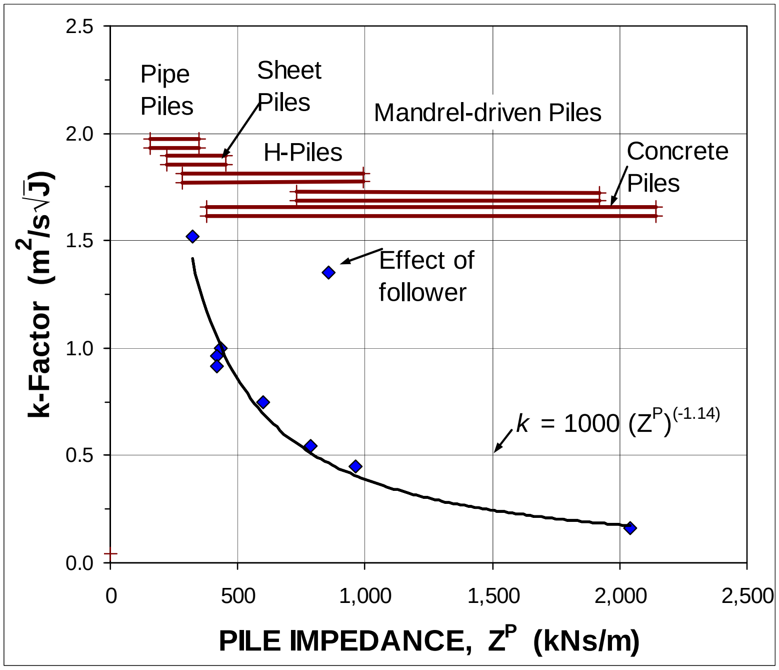

Fig. 9.22 Influence of pile impedance on the vibration factor, k (Eq. 9.28).
(Data from Heckman and Hagerty 1978).

Massarsch and Fellenius (2008) defined "vibration transmission efficacy" as the ratio of the dynamic portion of the driving resistance to the impact force in the pile as shown in Eq. 9.29.

9.29 $$E_T = \frac{R_T}{F_i}$$

where E_T = vibration transmission efficacy at the pile toe
R_T = dynamic resistance at the pile toe
F_i = impact force

The vibration transmission efficacy is equal to J_c and proportional to the ratio between the pile and the soil impedances, which expresses the dynamic stress emitted from the pile toe.

9.30 $$E_T = J_c = 2\frac{Z_P}{Z^P}$$

where J_c = dimensionless damping factor
Z^P = pile impedance
Z_P = soil impedance (from P-wave velocity)

Equation 9.30 indicates that the vibration transmission efficacy and the dynamic resistance (the velocity-dependent resistance) are inversely proportional to the pile impedance. The Heckman and Hagerty (1978) data prove the linearity, when the data are replotted versus the inverse of the pile impedance as shown in Fig. 9.23.

The correlation shown in Fig. 9.23 is surprisingly good, considering that the measurements were taken in different soil conditions. The data provided by Heckman and Hagerty (1978) indicate that ground vibrations in the reported cases mainly originated from the pile toe. Indeed, the data confirm that the energy transmission efficacy correctly reflects the vibration emission from the pile to the surrounding soil layers.

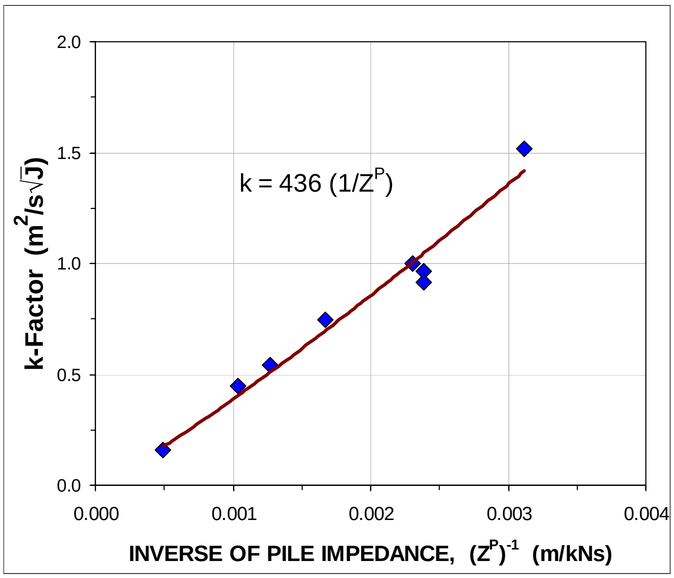

Fig. 9.23 Relationship between k-factor and inverse of pile impedance. Data from Fig. 9.22 replotted.

CHAPTER 10

PILING TERMINOLOGY

10.1 Introduction and Basic Definitions

There is an abominable proliferation of terms, definitions, symbols, and units used in papers and engineering reports written by the geotechnical community. Not only do the terms vary between authors, many authors use several different words for the same thing, sometimes even in the same paper or report, which makes the material difficult to read and conveys an impression of poor professional quality. More important, poor use of terminology in an engineering report could cause errors in the design and construction process and be the root of a construction dispute, which, ultimately, the report writer may have to defend in a litigation. Throughout this book, the author has strived to a consistent use of terminology as summarized in this chapter.

Fig. 10.1 illustrates the main definitions and preferred piling terms.

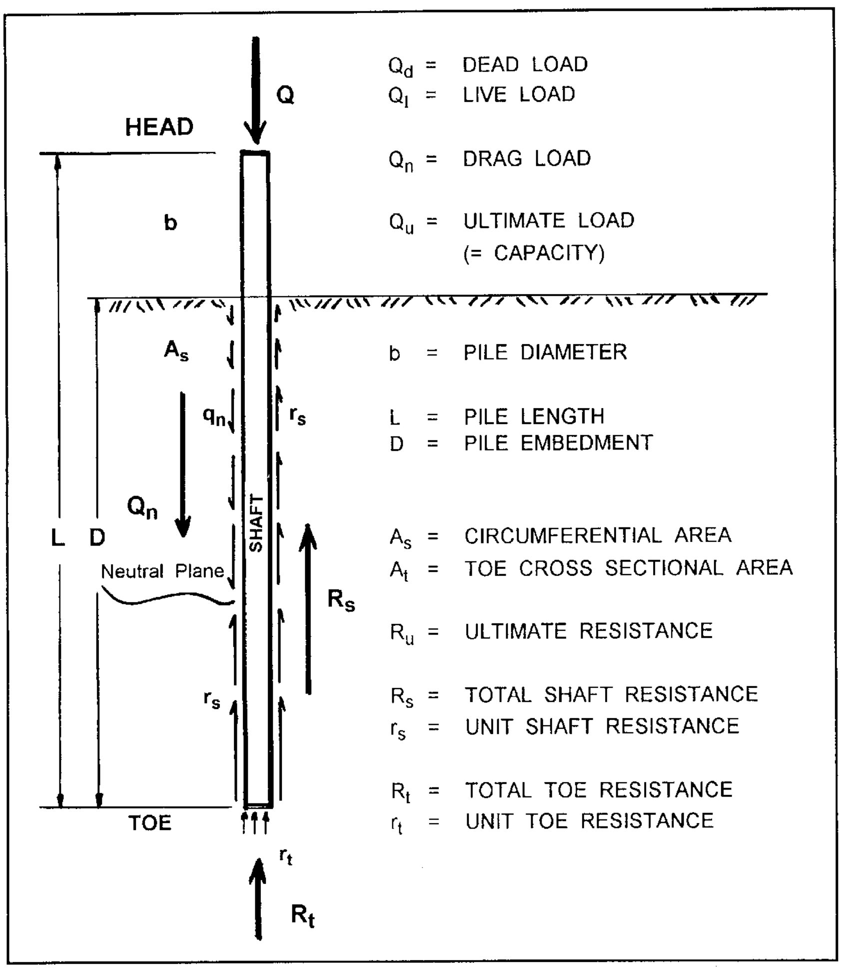

Fig. 10.1.Definitions and Preferred Terms

Upper End of a Pile

One of the most abused terms is the name for the upper and lower ends of a pile. Terms in common use are, for the upper end, “top”, “butt”, and “head”, and for the lower end, “end”, “tip”, “base”, “point”, “bottom”, and “toe”.

The term “top” is not good, because, in case of wood piles, the top of the tree is not normally the 'top' of the pile, which can and has caused confusion. Also, what is meant by the word “top force”? Is it the force at the 'top of the pile' or the maximum (peak) force measured somewhere in the pile? “Butt” is essentially a wood-pile term. “**Head**” is the preferred term. For instance, “the forces were measured at the pile head”.

Lower End of a Pile

With regard to the term for the lower end of a pile, the word “tip” is easily confused with “top”, should the latter term be used—the terms are but a typo apart. A case-in-point is provided by the 3rd edition (1992) of the Canadian Foundation Engineering Manual, Page 289, 2nd paragraph. More important, “tip” implies a uttermost end, usually a pointed end, and piles are usually blunt-ended.

The term “end” is not good for two reasons**:** the pile has two ends, not just one, and, more important, “end” has a connotation of time. Thus, “end resistance” implies a “final resistance”.

“Base” is not a bad term. However, it is used mainly for shallow footings, piers, and drilled-shafts. “Point” is often used for a separate rock-point, that is, a pile shoe with a hardened tip (see!) or point. Then, before driving, there is the point of the pile and on the ground next to the pile lies the separate rock-point, making a sum of two points. After driving, only one, the pile point, remains. Where did the other one go? And what is meant by “at a point in the pile”? Any point or just the one at the lower end?

The preferred term is “**toe**”, as it cannot be confused with any other term and it can, and is, easily be combined with other terms, such as “toe resistance”, “toe damping”, “toe quake”, etc.

Other than for a human connotation, the word “bottom” should be reserved for use as reference to the inside of a pile, for instance, when inspecting down a pipe pile, "the bottom of the hole", and such.

The Pile Shaft

Commonly used for the part of the pile in between the head and toe of the pile are the terms “side”, “skin”, “surface”, and “shaft”. The terms “skin” and “shaft” are about as frequent. “Side” is mostly reserved for stubby piers. “Surface”, although is used, the term is not in frequent use. The preferred term is “**shaft**” because “skin” is restricted to indicate an outer surface and, therefore, if using “skin”, a second term would be necessary when referring to the actual shaft of the pile.

Other Preferred Piling Terms

A word often causing confusion is “capacity”, especially when it is combined with other words. “Capacity” of a unit, as in “lateral capacity”, “axial capacity”, “bearing capacity”, “uplift capacity”, “shaft capacity” and “toe capacity”, is the **ultimate resistance** of the unit. The term “ultimate capacity” is a tautology to avoid, although it cannot be misunderstood. However, the meaningless and utterly confusing combination terms, such as “load capacity”, “design capacity”, "allowable capacity", “carrying capacity”, “load carrying capacity”, even “failure capacity”, which can be found in many papers, should not be used. (I have experienced a court case where the single cause of the $300,000 dispute turned out to originate from the designer’s use of the term “load capacity” to mean capacity, while the field people believed the designer's term to mean "allowable load". As a factor of safety of 2 was applied, the field people drove—attempted to drive—the piles to twice the capacity necessary with predictable results. Use "**capacity**" as a stand-alone term and as a synonym to "**ultimate resistance**".

Incidentally, the term "ultimate load" can be used as a substitute for "capacity" or "ultimate resistance", but it should be reserved for the capacity evaluated from the results of a static loading test.

As to the term "resistance", it can stand alone, or be modified to "ultimate resistance", "mobilized resistance", "shaft resistance", "toe resistance", "static resistance", "initial shaft resistance", "unit toe resistance", etc.

Obviously, combinations such as "skin friction and toe resistance" and "bearing of the pile toe" constitute poor language. They can be replaced with, for instance, "shaft and toe resistances", and "toe resistance" or "toe bearing", respectively. "Shaft bearing" is not commonly used, but it is an acceptable term.

Resistance develops when the pile forces the soil**:** "positive shaft resistance", when loading the pile in compression, and "negative shaft resistance", when loading in tension. The term "skin friction" by itself should not be used, but it may be combined with the 'directional' words "negative" and "positive"**:** "Negative skin friction" is caused by settling soil and "positive skin friction" by swelling soil.

The terms "load test" and "loading test" are often thought to mean the same thing. However, the situation referred to is a test performed by loading a pile, not a test for finding out what load that is applied to a pile. Therefore, "**loading test**" is the semantically correct and the preferred term. Arguing for the term "loading test" as opposed to "load test" may suggest that I am a bit of a fusspot. I may call this favorite desserts of mine "iced cream", but most say "ice cream". In contrast, "iced tea" is the customary term for the thirst-quencher, and the semantically correct, and normally used term for cream-deprived milk is "skimmed milk", not "skim milk". By any name, though, the calories are as many and a rose would smell as sweet. On the other hand, laymen, call them lawyers, judges, or first year students, do subconsciously pick up on the true meaning of "load" as opposed to "loading" and are unnecessarily confused. So, why not use the term "loading test"?

While the terms "static loading test" "static testing" are good terms, do not use the term "dynamic load testing" or worse**:** "dynamic load test". Often a capacity determination is not even meant by these terms. Use "**dynamic testing**" and, when appropriate, "capacity determined by dynamic testing".

When presenting the results of a loading test, many authors write "load-settlement curve" and "settlement" of the pile. The terms should be "**load-movemen**t curve" and "**movement**". The term "settlement" must be reserved to refer to what occurs over long time under a more or less <u>constant</u> load smaller than the ultimate resistance of the pile. The term "displacement" should not be used as synonym for "movement", but preferably be reserved for where soil actually has been displaced, e.g., moved aside. The term "deflection" instead of "movement" is normally used for lateral deflection, but "displacement" is also used for this situation. "Compression", of course, is not a term to use instead of "movement" as it means "shortening".

In fact, as mentioned in Chapter 3, not just in piling terminology, but as a general rule, the terms "movement", "settlement", and "creep" all mean deformation. However, they are not synonyms and it is important not to confuse them.

When there is a perfectly good common term understandable by a layman, one should not use professional jargon. For example, for an inclined pile, the terms “raker pile” and “batter pile” are often used. But “a raker” is not normally a pile, but an inclined support of a retaining wall. As to the term “batter”, I have experienced the difficulty of explaining a situation to a judge whose prior contact with the word “batter” was with regard to “battered wives” and "battered children" and who thought, no, was convinced, that “to batter a pile” was to drive it abusively! The preferred term is “**inclined**”.

The word “set” means penetration for one blow, sometimes penetration for a series of blows. Sometimes, “set” is thought to mean “termination criterion” and applied as blows/inch! The term “set” is avoidable jargon and should not be used. (See my expanded comment in Chapter 11).

The word “refusal” is another example of confusing jargon. It is really an absolute word. It is often used in combinations, such as “practical refusal” meaning the penetration resistance for when the pile cannot <u>reasonably</u> be driven deeper. However, “refusal” used in a combination such as “refusal criterion” means “the criterion for (practical) refusal”, whereas the author might have meant “**termination criterion**”, that is, the criterion for when to terminate the driving of the pile. Avoid the term “refusal” and use “penetration resistance” and “termination criterion”, instead. (See my expanded comment in Chapter 11).

Terms such as “penetration resistance”, “blow-count”, and “driving resistance”, are usually taken to mean the same thing, but they do not. “**Penetration resistance**” is the preferred term for the effort required to advance a pile and, when quantified, it is either the number of blows required for the pile to penetrate a certain distance, or the distance penetrated for a certain number of blows.

“**Blow-count**” is a casual term and should be used only when an actual count of blows is considered. For instance, if blows are counted by the foot, one cannot state that “the blow-count is so and so many inches per blow”, not even say that it is in blows/inch, unless inserting words such as: “which corresponds to a penetration resistance of. . .” Obviously, the term “equivalent blow-count” is a no-good term. In contrast, when the actual <u>blow-count</u> is 0.6 inch for 9 blows, the "<u>equivalent penetration resistance</u>" is 15 blows/inch.

“Driving resistance” is an ambiguous term, as it can be used to also refer to the resistance in terms of force and, therefore, it should be avoided.

Often, the terms “allowable load” and “service load” are taken to be equal. However, “allowable load” is the load obtained by dividing the capacity with a factor of safety. “Service load” or "working load" is the load actually applied to the pile. In most designs, it is smaller than the “allowable load”, and usually equal to "unfactored load", a concept used in the LRFD approach . The term “design load” can be ambiguous — if using it, make sure to supply a clear definition.

The term for describing the effect of resistance increase with time after driving is “**set-up”** (soil set-up). Do not use the term “**freeze**” (soil freeze), as this term has a different meaning for persons working in cold regions of the world.

The term "moisture content" is sometimes used in the same sense as "**water content**". Most people, even geotechnical engineers, will consider that calling a soil "moist", "damp", or "wet" signifies different conditions of the soils (though undefined). It follows that laymen, read lawyers and judges, will believe and expect that "moisture content" is something different to "water content", perhaps thinking that the former indicates a less than saturated soil. However, there is no difference, It is only that saying "moisture" instead of "water" implies a greater degree of sophistication of the User, and, because the term is not immediately understood by the layman, its use sends the message that the User is in the "know", a specialist of some stature. Think of it as equivalent to saying "wetness content" or worse "wetness quotient". Now, you'd be appearing as the real expert, eh? Don't fall into that trap. Use the term "water content" and remember, we should strive to use simple terms that laymen can understand.

Avoid the term “timber pile”, use “wood pile” in conformity with the terms “steel pile” and “concrete pile”.

Do not use the term “reliability” unless presenting an analysis based on probabilistic principles.

Unlike many other languages, English provides the means to express the important fact that soil forces have direction whereas forces in water do not. That is, the term "stress" indicates direction and "pressure" does not. It is fundamentally wrong to state that a certain load on a footing results in a certain "pressure". The term to use is "stress", soil does not have pressure and it is important to apply that distinction. Logically, therefore, the old terms" earth pressure" and "earth pressure coefficient" should be "earth stress" and "earth stress coefficient". To make the point, the author uses "earth stress" throughout this text notwithstanding that it probably vain to think that for the profession would abandon using the so strongly established "pressure" term.

One of the silliest mistakes—unfortunately, also a very common one—is to use the word "predict" to mean "calculate" or "compute". One does not "predict" the response of a pile from, say, test data, one "calculates" or "computes". "Prediction" is an absolute term, and it must only be used for a calculation that is truly a prediction of an expected behavior.

10.2 Brief Compilation of Some Definitions and Terms

Bored pile - A pile that is constructed by methods other than driving, commonly called **drilled shaft**.

Caisson - A large, deep foundation unit other than a driven or bored pile. A caisson is sunk into the ground to carry a structural unit.

Capacity - The maximum or ultimate soil resistance mobilized by a foundation unit.

Capacity, **bearing -** The maximum or ultimate soil resistance mobilized by a foundation unit subjected to downward loading.

Capacity, **geotechnical -** See **capacity, bearing.**

Capacity, **lateral -** The maximum or ultimate soil resistance mobilized by a foundation unit subjected to horizontal loading.

Capacity, structural - The maximum or ultimate strength of the foundation unit (a poor term to use).

Capacity, **tension -** The maximum or ultimate soil resistance mobilized by a foundation unit subjected to tension (upward) loading.

Consolidation - The dissipation of excess pore pressure in the soil.

Cushion, hammer - The material placed in a pile driving helmet to cushion the impact (formerly called “capblock”).

Cushion, pile - The material placed on a **pile head** to cushion the impact.

Downdrag - The downward **settlement** of a deep foundation unit due settlement at the **neutral plane** "dragging" the pile along; expressed in units of movement (mm or inch).

Drag load - The load transferred to a deep foundation unit from **negative skin friction**.

Drilled shaft - A bored pile.

Dynamic method of analysis - The determination of **capacity**, **impact force**, **transferred energy**, etc. of a driven **pile** using analysis of measured **stress-waves** induced by the driving of the pile.

Dynamic monitoring - The recording of strain and acceleration induced in a pile during driving and presentation of the data in terms of stress and **transferred energy** in the pile as well as of estimates of **capacity**.

Factor of safety - The ratio of maximum available resistance or of the **capacity** to the allowable stress or load.

Foundation unit, **deep -** A unit that provides support for a structure by transferring load or stress to the soil at depth considerably larger than the width of the unit. A **pile** is the most common type of deep foundation unit.

Foundations - A system or arrangement of structural members through which the loads are transferred to supporting soil or rock.

Groundwater table - The upper surface of the zone of saturation in the ground.

Impact force - The peak force delivered by a pile driving hammer to the **pile head** as measured by means of **dynamic monitoring** (the peak force must not be influenced by soil resistance reflections).

Load, **allowable -** The maximum load that may be safely applied to a **foundation unit** under expected loading and soil conditions and determined as the **capacity** divided by the **factor of safety**.

Load, **applied** or **load, service -** The load actually applied to a foundation unit.

Neutral plane - The location where equilibrium exists between the sum of downward acting permanent load applied to the pile and **drag load** due to **negative skin friction** and the sum of upward acting **positive shaft resistance** and mobilized **toe resistance**. The neutral plane is also (always) where the relative movement between the pile and the soil is zero, i.e., the location of "settlement equilibrium".

Pile - A slender **deep foundation unit**, made of wood, steel, or concrete, or combinations thereof, which is either premanufactured and placed by driving, jacking, jetting, or screwing, or cast-in-situ in a hole formed by driving, excavating, or boring. A pile can be a non-displacement, a low-displacement, or displacement type.

Pile head - The uppermost end of a **pile**.

Pile impedance - Z = EA/c, a material property of a pile cross section determined as the product of the Young's modulus (E) and area (A) of the cross section divided by the **wave speed** (c).

Pile point - A special type of **pile shoe**.

Pile shaft - The portion of the pile between the **pile head** and the **pile toe**.

Pile shoe - A separate reinforcement attached to the **pile toe** of a pile to facilitate driving, to protect the lower end of the pile, and/or to improve the toe resistance of the pile.

Pile toe - The lowermost end of a **pile**. (Use of terms such as pile tip, **pile point**, or pile end in the same sense as pile toe is discouraged).

Pore pressure - Pressure in the water and gas present in the voids between the soil grains minus the atmospheric pressure.

Pore pressure, **artesian - Pore pressure** in a confined body of water having a level of **hydrostatic pressure** (head) higher than the distance to the ground surface.

Pore pressure, **hydrostatic - Pore pressure** distribution as in a free-standing column of water (no gradient).

Pore pressure elevation, **phreatic -** The elevation of a **groundwater table** corresponding to a **hydrostatic pore pressure** equal to the actual **pore pressure**.

Pore pressure gradient - Non-hydrostatic pore pressure. The gradeint can be upward or dwonward. At downward gradient, effective stress increases more than it would in a hydrostatic condition.

Pressure - Omnidirectional force per unit area. (Compare **stress**).

Settlement - The downward movement of a foundation unit or soil layer due to rapidly or slowly occurring compression of the soils located below the foundation unit or soil layer, when the compression is caused by an increase of effective stress due to an applied load or lowering of pore pressure.

Shaft resistance, **negative -** Soil resistance acting downward along the pile shaft because of an applied uplift load.

Shaft resistance, **positive -** Soil resistance acting upward along the pile shaft because of an applied compressive load.

Skin friction, **negative -** Soil resistance acting downward along the pile shaft as a result of movement of the soil along the pile and inducing compression in the pile.

Skin friction, **positive -** Soil resistance acting upward along the pile shaft caused by swelling of the soil and inducing tension in the pile.

Stress - Unidirectional force per unit area. (Compare **pressure**).

Stress, **effective -** The total stress in a particular direction minus the **pore pressure**.

Toe resistance - soil resistance acting against the **pile toe**.

Transferred energy - The energy transferred to the pile head and determined as the integral over time of the product of force, velocity**,** and **pile impedance**.

Wave speed - The speed of strain propagation in a **pile**.

Wave trace - A graphic representation against time of a force or velocity measurement.

10.3 Units

In the SI-system, all parameters such as length, volume, mass, force, etc. are to be inserted in a formula with the value given in its base unit. If a parameter value is given in a unit using a multiple of the base unit, e.g., 50 MN — 50 meganewton, the multiple is considered as an abbreviated number and inserted with the value, i.e., "mega" means million and the value is inserted into the formula as $50 \cdot 10^6$. Notice that the base units of hydraulic conductivity (permeability), k, and consolidation coefficient, c_v, are m/s and m^2/s, not cm/s or cm^2/s, and not m/year or m^2/hour, respectively.

When indicating length and distance in the SI-system, use the unit metre (m) and multiples millimetre (mm) or kilometre (Km). Avoid using the unit centimetre (cm).

For area, square centimeter (cm^2) can be used when it is alone. However, never in combined terms (for example, when indicating stress). The unit for stress is multiple of newton/square metre or pascal (N/m^2 or Pa). Combination units, such as N/mm^2 and MN/cm^2 violate the principle of the international system (SI) and can be the cause of errors of calculation. That is, prefixes, such as "M" and "m", must only be used in the numerator and never in the denominator. Notice also that the units "atmosphere" and "bar" (**at** = 100 KPa; **bar** = 98.1 KPa) are aberrations to avoid.

When writing out SI-units, do not capitalize the unit. Write "67 newton, 15 pascal, 511 metre, and 96 kilogramme. Moreover, while the kilogramme is written kg—it is really a single unit (base unit) although this is belied by its symbol being composed of two letters. For true multiple units, such as kilonewton and kilometre, the "kilo" is a prefix meaning 1,000. When abbreviating the prefix of these, it is acceptable, indeed preferable, to capitalize the prefix letter**:** "KPa", "KN", etc., instead of writing "kPa", "kN", but be consistent. Notice, "kg" should be considered as a single symbol; it always requires lower case "k"[1)].

If your text uses SI-units and the original work quoted from a paper used English, make sure to apply a soft conversion and avoid writing "30.48 metre", when the original measure was "100 feet", or maybe even "about 100 feet". Similarly, "about one inch" is "about 20 mm" or "about 30 mm", while a values of "2.27 inches" converts to "57.7 mm".

Notice, the abbreviated unit for "second" is "s", not "sec"! — a very common and unnecessary mistake. The units "newton", "pascal", "joule" etc. do not take plural ending. It is logical and acceptable to omit the plural ending for all other units in the SI-system.

The terms "specific weight" and "specific gravity" were canceled as technical terms long ago, but they are still found in many professional papers. "Specific weight" was used to signify the weight of material for a unit volume. However, the proper terms are "**solid density**" and "**unit weight**" (the units are mass/volume and force/volume, respectively). The term "specific gravity" was used to mean the ratio of the density of the material over the density of water (dimensionless). The internationally assigned term for this ratio is "relative density", which term, unfortunately, conflicts with the geotechnical meaning of the term "relative density" as a classification of soil density with respect to its maximum and minimum density. For the latter, however, the internationally assigned term is "**density index**".

Soils can be "moist", "wet", "damp", and "saturated", and the measurement is given in percent of dry weight. (Note, the term for the amount of water in a soil sample is "water content", not "moisture content").

---

1) It is a pity that in developing the SI-system from the old metric systems, the cgs-system and MKSA-system, the unit for mass, the kilogramme, was not given a single symbol letter, e.g., "R" for "ram or ramirez". Surely there must have been a Herr Doctor Ram or Señor Ramirez somewhere who could have been so honored. Then, the old unit "kg" would be "R", and a tonne would be superfluous as a term as it would be replaced by "KR". The author disagrees that applying the convention of capitalizing the multiplying prefix also to "kilo" would conflict with the term "Kelvin" as a measure of temperature from the absolute value of -273 °C.

10.4 Spelling Rules and Special Aspects on Style

A design will invariably result in a written presentation of results and recommendations for a project. Even the best and most elaborate design resulting from a high standard engineering work can be totally shamed by poor report writing style. In the following a few suggestions are made on how to avoid some of the more frequent gaffes in report writing 3 and, for that matter, in writing up the work in a manuscript for professional dissemination.

Use either English or U.S. spelling: for example, English spelling includes the letter "u" in words such as "behaviour", "colour", "favour", "harbour", "labour", "rumour", "neighbouring", "remould", "gauge" and doubles the consonant in words such as "modelling", "travelling", "controlled", "labelling", "omitted", "focussing", and "referring", "preferred", and "occurring", (but "offered" and "offering", because the stress is on the first syllable). American spelling omits the “u” and does not double the consonant in these words. (“occurring” and “occurred”, however, are written the same way by both conventions).

Write "z" instead of "s" in "analyze", "analyzing, and in "analyzer", and in "organize", "organizing", and "organizer", as well as in "capitalize", "horizontal", "idealize", "rationalize", "realize", "specialize", and "summarize".

Use the spelling "to advise" and "to practise" and "the advice" and "the practice" (verb versus noun), and omit "e" before "able" in "arguable", "drivability", "desirable", "lovable", etc. However, the "e" is retained in "serviceability" and "noticeable" (to separate the consonant “c” from the vowel “a”). Notice also the spelling of words such as "mileage". Similarly, use “i before e unless after c”, e.g., “receive”, or when the wovels "ei" sound like “a”, as in neighbor or weigh, or weight.

A simple and useful distinction of meanings can be made by writing "metre" for distance and "meter" when referring to a measuring device. Similarly, the spelling "programme" as in "testing programme" keeps the meaning apart from "program" as in a "computer program".

When using the verbs "centre" (English) or "center" (U.S.), use the correct tense forms: "centred" and "centered", respectively.

Do not use loose contractions such as "don't" or "can't". Write "do not" and "cannot". Also, write "it is", not "it's" or "its". Besides, "its" is a possessive pronoun not to be written "it's".

Capitalize all months, days, and seasons.

Do not overuse nouns as adjectives. Four nouns in a row is an abomination. For instance, "the concrete pile toe capacity", which reads much better if changed to "the toe capacity of the concrete pile". In general emphasizing adjectives “much”, “very”, etc. are redundant, and “extremely”, “absolutely” have no place in a thesis. If something is larger than something else, better than to say “much larger”, quantify it and let the reader judge from the numbers.

Avoid "there are " constructions; write "two critical points are shown. . . ", not "there are two critical points shown...".

Avoid "of the"-phrases. Thus, write "the page length should be 100 mm" rather than "the length of the page should be 100 mm".

The first time a noun, e.g. "test", "measurement", "borehole", etc., is mentioned, avoid using definite article (i.e., "the"). Often, the text flows better is an indefinite article is used, i.e., "a", or no article.

Use plain English and common words rather than fancy ones, and be concise (on account of that sesquipedality does not result in perspicacity). Use short sentences and avoid lengthy or awkward constructions. If a sentence comes out to use more than three lines, it is usually better to split it into two.

Think of the literal meaning of words and expressions and avoid 'ear-sores' such as "up to a depth of …".

It adds to clarity to separate sentences by making two space bar depressions after each end-of-sentence period.

Take care (proof read) not to leave a number alone at line end with its units at the next line, e.g., "16 MPa". Use a non-break space command between numerals and units for getting "16 MPa" to always be on the same line. Similarly, use the non break command to prevent a number from starting a line, i.e. the word immediately before the number should stay with the number.

When writing "Fig. 5", "Author B. C.", "i. e.", "e. g.", and other words using an abbreviation period, the automatic justification of the lines may result in too wide a space after the period, e. g., Fig.   5", "e.   g., and Author B.   C.". To avoid this, always follow such a period with a no-break-space command, or do not use a space. For names shown as only the a first letter followed by a period, the space after the period between a series of such letters can be omitted.

Numerical values consisting of four or more digits can be difficult to read. Then, to improve clarity, separate each set of three digits with a comma, e.g., 7,312,940. (This is North American practice. European practice of separating the digits with a space for every digits is less clear and can lead to mistakes in understanding).

Work on the interpunctuation and, in particular, the use of the comma. Commas are important for the understanding of the text and must not be neglected. Always place a comma before a conjunction introducing an independent clause. For example: “always remember, commas enhance the reader’s understanding of the message”. Also, ponder why the following two sentences have different meanings: “Also the professor may need assistance with regard to commas.” “Also, the professor may need assistance with regard to commas.” (Either meaning may require a bit of diplomacy in rendering the assistance). Finally, consider the life and death importance of whether Caesar's order about your execution or liberation reads "Execute, not liberate" or "Execute not, liberate".

Use always the convention of the "serial comma". Thus, write "red, white, and blue" with a comma separating each item in the series (of three or more items). That is, place a comma before the “and”, as well as before the “or” in a series of alternatives.

When the subject is the same for both sentence clauses and the connective is "but", a comma should be used after the word preceding “but”. Note, when the subject is the same for both clauses and the connective is "and", the comma should be omitted.

Notice that there is often a difference between similar words. For example, "alternate" and "alternative", where "alternate" refers to every second in a series, and "alternative" is one of two possibilities. "Alternate", but not "alternative" can sometimes mean "substitute". The word "substitute" is then preferred. Do not confuse the meaning of the words "objective" and "object"—a common mistake.

You may want to indicate that a particular observation or item is more important than others, starting the sentence making this point as "*More important, the measurements show that ...*". Do not write "importantly". The adverb of important, "importantly", is a synonym to "pompously". Similarly, when presenting items in order of importance, but you prefer not to use a bulleted or numbered list, do not write, "Firstly", "Secondly", "Thirdly", etc. Remove the "-ly" and write "First", "Second", "Third", etc.

Many times, the words “precision” and “accuracy” are improperly used. An example of “precision” is the reading precision of a gage, that is, the number of decimals given in the gage reading. “Accuracy” considers errors in the gage and in a combination of measurements and calculations. The following is a common error: “the accuracy of the prediction of capacity was 3 percent”. The text actually means to refer to an “agreement” between values. Besides, accuracy in prediction of pile capacity can never be as good as 3 percent!

Notice that a verbal message can be spoken or written, heard, or read. If you want to say that the message is spoken as opposed to written, say "oral". A non-verbal message is not necessarily non-spoken, but one not conveyed by words, for example, by grunts and gestures.

The word "anybody" means "anyone". "Any body" means "any corpse". Similarly, "any one" means "any single person".

The word "data" is a plural word and takes plural verbs. So are and do the words "criteria", "formulae", "media", "memoranda", "phenomena", as well as "strata". Therefore, the appertained verb must be in plural form. The corresponding singular words are "datum", "criterion", "formula", "medium", "memorandum", "phenomenon", and "stratum".

Words such as "usage", "finalized", etc. may look refined, but are examples of convoluted style. Use the simple versions: "use", or "final or finished", etc. Note, “utilization” refers to the manner or “using”, and “utilize” is not a refined synonym to the word “use”.

The words "order of magnitude" imply a relation of ten! Usually, the intended meaning is better expressed by plain "magnitude" or "size".

Puristically, "in-situ" should be written in italics, but hyphenating it provides sufficient distinction. Do not write "insitu", or "in situ".

The word "less" is overused. Whenever possible, replace it by its various equivalents, such as "fewer", "smaller", "lighter", "lower", "poorer", etc.

Do not use the ampersand symbol, "&", write "and".

Prefixes such as "pre-" are often unnecessary. For example, the word "predominant" can often be written "dominant" (and preferably be replaced by words such as "governing", "principal", "leading", etc.).

Limit each paragraph to a single message. Short paragraphs focus the reader's attention and assist understanding.

CHAPTER 11

SPECIFICATIONS AND DISPUTE AVOIDANCE

11.1 Introduction and examples

Surprises costing money and causing delays occur frequently during the construction of foundation projects, and in particular for piling projects. The contract specifications often fail to spell out the responsibilities for such events and this omission invariably results in disputed claims that sometimes only can be resolved by litigation. Much of this can be avoided by careful wording of the specifications, expressing all quality requirements in quantifiable terms, and, in anticipating difficulties, setting out beforehand who is responsible.

When the unexpected occurs at a site and costs escalate and delays develop, the Contractor feels justified to submit a claim that the Owner may see little reason to accept. When the parties turn to the technical specifications for the rules of the contract, these often fuel the dispute instead of mitigating it, because the specifications are vague, unclear, unbalanced, and containing weasel clauses that help nobody in resolving the conflict. Rarely are specifications prepared for that deviations from the expected can occur.

Indeed, surprises occur frequently during the construction of foundation projects, and in particular in the case of piling projects. The surprises take many forms, but one aspect is shared between them: they invariably result in difficulties at the site and, more often than not, in disputes between the parties involved.

For example, the soil conditions sometimes turn out to differ substantially from what the contract documents indicate. On other occasions, the piles do not go down as easily as anticipated by the Owner's design engineers and/or by the Contractor's estimator. Or, they may go down more easily and become much longer than anticipated. Or, a proof test shows that the pile capacity is inadequate. Or, the piles do not meet a distinct "refusal" and, consequently, the stringent termination criterion in the specifications results in a very prolonged driving causing delays and excessive wear on the Contractor’s equipment.

Quite often, the Contractor's equipment fails to do the job. Perhaps, the equipment required by the specifications is “misdirected”. Perhaps, the Contractor is inexperienced and cannot perform well, or the equipment is poorly maintained and difficult to use. Whether or not the Contractor honestly believes that the subsequent delays, the inadequate capacity, the breakage, etc. are not his fault, he will submit a claim for compensation. Often, when the claim is disputed by the Owner, the Contractor nevertheless is awarded compensation by the court, because the contract specifications do not normally contain any specific or lucid requirement for the quality of the Contractor’s equipment.

Or, the Contractor's leads are not straight and the helmet occasionally jams in the leads. However, are the leads out of the ordinary*after all, they are the same as used on the previous job—and, besides, although they are not straight can they really be called bent, or crooked?

Or, on looking down a pipe pile, the bottom of the pipe cannot be seen. Well, is then the pile bent and is it bent in excess?

Or, when the use of a water jet is required to aid the pile penetration, the pile does not advance or advances too quickly and drifts to the side or a crater opens up in the soil next to the side of the pile. The pump pressure and water flow are usually detailed in the specifications, but the size and length of the hose and the size of the nozzle are rarely indicated. Yet, these details are vital to the performance of the jetting system, indeed, they govern the pressure and flow.

Frequently, sentences are used such as "in the Engineer's opinion", but with no specific reference to what the opinion would be based on. Such general "come-into-my-parlor" clauses do not hold much water in court, but they are the root of much controversy.

Be careful of the meaning of the terms used. For example, ‘allowable load capacity’ is a totally confusing set of words. A few years ago, I worked on a litigation case where the Engineer used the words ‘allowable load capacity’ to indicate the required working load of the piles. Unfortunately, the Contractor interpreted the words to refer to the capacity to which he had to drive the piles.

A similar confusion appeared on a more recent project (nothing really changes in this regard), where the engineer deliberately reduced the pile lengths to about half the usual length in order to avoid driving into a boulder layer existing at depth at the site. He also, appropriately, reduced the desired capacity and pile working load (50 tons), requiring a “capacity” of only 100 tons on piles normally accepted and installed to a 200 ton capacity, which is what the specs required. However, someone—it was never determined who—thought that plain ‘capacity’ sounded too casual and changed it to ‘load capacity’. At the outset of the pile driving, the contractor asked what loads he was to drive to and was told that the loads were 100 tons. So, naturally, he drove to a capacity of twice the load, which meant that the piles had to be longer and, as the designer had expected, the piles were driven into the boulder layers. The results was much breakage, problems, delays, and costs. The claim for extra was $300,000.

Indeed, jargon terms can be very dear. Incidentally, of all terms, “capacity” is most often misused. It simply means “ultimate resistance” and it does not require an adjective (other than “axial” as opposed to “lateral”, for example). I recently saw a DOT specs text—spell-checked—requiring the Contractor to achieve an “intimate capacity”. I say, that is a daring term in these politically correct times!

On the topic of using jargon: The word “set” is not a synonym for “blow-count” (the blows per a certain penetration length). “Set” is the penetration for one blow or, possibly for a series of blows. Its origin is an abbreviation of “settlement’ meaning the penetration for one blow. I have one example of what “set” can cause: specifications stated that the Contractor was to drive the piles (concrete piles of limited strength concrete) “*to a very small set and the Contractor was cautioned not to overdrive the piles*”. Of course, the Contractor took care not to damage the piles by driving them too hard, which is what “overdriving” means. In fact, the driving turned out to be very easy and several of the piles drove much deeper than the plans and drawings indicated. Unfortunately, in writing the sentence I just quoted, the spec-writer meant to warn the Contractor that the penetration per blow was expected to be very small and that the piles, therefore, could easily drive too deep. Talk about diametrically opposed interpretations. And predictable surprises. In this case, the Engineers insisted that their intended interpretation was the right one and a costly claim and litigation ensued (which the Contractor won). The word “set” is frequently misconstrued to be a synonym for “termination criterion”, which, incidentally, is not the same as “blow count”. As the industry has such a vague understanding of the proper meaning of the term “set”, avoid using it in any context.

The jargon confusion does not get any better by shifting from “set” to “refusal”. Although most people have a qualitative understanding of what is addressed, one person’s refusal is another person’s promise. “Refusal” is an absolute term. It implies that one just cannot drive the piles deeper having exhausts all means to do so. A Contractor claiming this, is not believed. Then, specifications suggesting “a refusal of

6 blows/foot sounds not only silly, but implies a spec writer with a poor command of language. "Termination criterion" is a neutral term that states exactly what is meant. Use it!

What about "battered"? It is a term that separates the men from the boys, or people experienced in — or at least exposed to — piling from people who are not. The latter group includes lawyers, judges, and people serving as jury members in jury trials. I was once assisting a contractor who had to go to court to recover costs. This contractor had quite an uphill battle once the judge realized that he had battered his piles. The judge had experience of battered housewives and children, but he had no knowledge and little appreciation of that the term would have a discrete meaning for piling people. When the matter was made clear to him, he was quite annoyed by that a group of professionals would use a jargon term that had a perfectly suitable every-day English term available, i.e., "inclined". I agreed then and I agree now. Please, stop using "batter". My cry in the wilderness; It is getting worse instead of better. recently read a journal paper where the term was used to characterize a leaning structure!

Most specifications only identify a required pile driving hammer by the manufacturer's rated energy. However, the rated energy says very little of what performance to expect from the hammer. The performance of hammers varies widely and depend on pile size, choice of helmet and cushions, soil behavior, hammer age and past use, hammer fuel, etc. Whether or not a hammer is "performing to specs" is one of the most common causes of discord at a site. The reason is that most specifications are very poor in defining the hammer.

In bidding, a Contractor undertakes to complete a design according to drawings and documents. Amongst these are the Technical Specifications, which purport to describe the requirements for the project in regard to codes, stresses, loads, and materials. Usually, however, only little is stated about the construction. Yet, in the case of a piling project, the conditions during the construction are very different to those during the service of the foundation, and the latter conditions depend very much on the former. When the project is similar to previous projects and the Contractor is experienced and knowledgeable, the technical specifications can be short and essentially only spell out what the end product should be. Such specifications are Performance Specifications. However, these are very difficult to write and can easily become very unbalanced, detailing some aspects and only cursorily mentioning others of equal importance. A specs text, be it for Performance Specifications or for Compliance Specifications (another name is Detailed Specifications), must spell out what is optional to the Contractor and what the Contractor must comply with. Even if the intent is that the specifications be Performance Specifications, and even if they so state, most specifications are actually written as Compliance Specifications. Government specifications are almost always Compliance Specifications.

When surprises arise and the Contractor as a consequence is slowed down, has to make changes to procedures and equipment, and generally loses time and money, then, disputes as to the interpretation of the specifications easily develop. Therefore, the writer of Specifications must strive to avoid loose statements when referring to quality and, instead, endeavor to quantify every aspect of importance. Do not just say that a pile must be straight, but define the limit for when it becomes bent! Do not just say that the pile shall have a certain capacity, but indicate how the capacity will be defined! Do not forget to give the maximum allowable driving stresses and how they will be measured, if measured! In short, take care not to include undefined or unquantified requirements. One of the most non-constructive situation is when the Engineer says that a pile is damaged, or bent, or too short, etc. and the Contractor says "no it ain't". The Engineer answers "it is, too!", and before long whatever communication that existed is gone, the lawyers arrive, and everybody is a looser (well, perhaps not the lawyers).

You may enjoy the following direct quotes from contract specifications submitted by Government agencies.

1. Piles shall be driven to reach the design bearing pressures.
2. The minimum allowable pile penetration under any circumstance shall be 17 feet.
3. The Contracting Officer will determine what procedure should be followed if driving refusal occurs.
4. The hammer shall have a capacity equal to the weight of the pile and the character of the subsurface material to be encountered.
5. The hammer energy in foot-pounds shall be three times the weight of the pile in pounds.
6. Inefficient diesel, air, or steam hammers shall not be used.
7. Each pile shall be driven until the bearing power is equal to the design piles pressure.
8. All piles incorrectly driven as to be unsuitable as determined by the Contracting Officer shall be pulled and no payment will be made for furnishing, driving, or pulling such piles.
9. All piles determined to be unsuitable by the Contracting Officer shall be replaced by and at the expense of the Contractor.
10. The driving shall continue, using hammer falls of 150 mm to 200 mm in a series of 20 blows, until penetration of the pile has stopped. The height of the fall shall then be doubled and the pile again driven to refusal. This procedure shall be continued until the design load of the pile has been achieved.
11. The pile design load is defined as 1.5 times the working load. The design load will be deemed to have been achieved when the pile exhibits zero residual (=net?) set under 10 successive blows of the hammer, where each blow has a sufficient energy to cause elastic deformation of the pile at the ground level equal to the static shortening of the pile at design load, as calculated by Hooke’s Law.

Or have these requirements imposed on you?

A. The hammer shall have a capacity equal to the weight of the pile and the character of the subsurface material to be encountered.

B. Cut off portions of pile which are battered, split, warped, buckled, damaged, or imperfect.

C. Piles shall be driven with a single-acting, partial double-acting, or double acting diesel, air, or steam hammer developing a driving energy of not less than 32,530 newton meters per blow with a minimum ram weight of 3,175 kilograms for an air or steam hammer and 454 kilograms for a diesel hammer.

D. Where unwatering is required, the Contractor shall effect a dewatering scheme.

E. The founding elevation shall be established by driving to a set (sic!) determined in accordance with the dynamic formula specified or by the application of the wave equation analysis procedure that verifies the pile resistance. When new conditions such as change in hammer size, change in pile size or change in soil material may occur, new sets shall be determined.

F. Hammer performance shall be verified to ensure that the actual potential energy is not less than 90 % of the stated potential energy. (b)When the hammer performance is requested to be verified, all costs associated with this work will be included in the contract price when the energy delivered is less than 90 % of the stated potential energy specified in the submission.

When the energy is greater than 90 % of the stated potential energy stated in the required submission, the costs will be paid as extra work.

I promise you that the above quotes are real and not made up by me for the occasion. I am sure that many of you have similar and worse examples to show. However, when you stop smiling, you should ponder what depths of ignorance and incompetence the nine quotes represent. And the consequence to Society of our industry having to function with such players in charge of the purse strings.

The following specs requirements I have not actually seen, but I would not be surprised if I were to find them or something similar to them one of these days:

- If the work is doed without no extra expense to the Contractor, then the work will be tookdown and doed over again until the Contractor's expense is satisfactory to the Engineers.
- If something is drawned wrong, it shall be discovered, corrected, and doed right with no extra expense to the Owner.
- The bid of any contractor walking around on the site with a smile on his face will be subjected to review.

11.2 A few special pointers

Instead of specifying a pile driving hammer by its rated energy, specifications should specify a hammer by the energy transferred to the pile and the impact force delivered to the pile, which are well defined quantities. In the design phase, energy and force values are to be obtained by means of a wave equation analysis. The wave equation analysis will "marry" the hammer to the pile and soil and to the particular drivability conditions and desired capacity. Naturally, the Contractor has the right to expect that the values specified are correct.

More often than not, the analysis will show that theoretical analysis alone is not able to sufficiently accurately determine the hammer requirements. This is then not an argument against performing the analysis or for not specifying the values. It is an argument addressing the inadequacy of omitting hammer details or just giving a rated energy, which puts the risk onto the Contractor. It is also an argument demonstrating the Owner's obligation to find out ahead of time, or at the outset of a project, what the correct hammer values are. For example, by means of taking dynamic measurements with the Pile Driving Analyzer (PDA). PDA measurements are since many years routinely used to finalize a pile design in connection with test driving or during the Contractor's installation of index piles.

When the potential use of the Pile Driving Analyzer (PDA) is included in the technical specifications, then, if during the course of the piling work, reasons arise to question the hammer performance, the PDA can quickly and with a minimum of fuss be brought to the site and the hammer can be accepted or rejected as based on the agreement of the measurements with the specified values. Opinion may differ with regard to the adequacy of the specified values, but such differences are technical in nature and easily resolved without involving the lawyers.

Dynamic measurements may interfere with the Contractor's work, therefore, the general section of the specifications should contain a clause that outlines how the measurements are performed and what the responsibilities are for the parties involved, as well as how the work is going to be paid.

Dynamic measurements are also commonly carried out to determine pile capacity and integrity. Notice, the PDA measurements need analysis to be useful. Also, the data must be combined with conventional records of the pile installation.

Further, what is bent by bending and doglegging of a pile must be defined by a specific bending radius defining straightness, and out-of-location need to be defined by means of specific tolerances. For example, before driving piles must not be bent more than a specific arc of curvature over a certain distance. After driving the bending radius must not be smaller than a certain value. For pipe piles, this is readily determined by means of an inspection probe designed to jam in the pipe at this radius (Detailed in the Canadian Foundation Engineering Manual 1985, 1992). A pipe pile for which the bottom cannot be seen, but into which the probe reaches the bottom, is then by definition straight and acceptable.

The need for well written and well thought-through specifications is illustrated by the following summary of four cases of project disputes that went to litigation.

1. Overdriving of a group of steel piles. Several steel piles were to be driven into a dense sand to a predetermined embedment depth of 85 feet. Already at a depth of about 30 ft, penetration resistance values began to exceed 200 blows/foot. The 'Engineer' insisted that the Contractor drive the piles to the specified depth despite that driving required an excess of 1,000 blows/foot! A "post mortem" review of the records makes it quite clear that although the heads of the about 90 feet long piles were beaten into the specified 5-ft stick-up above the ground surface, the pile toes probably never went past a depth of 60 feet. The Contractor had planned for a two-week project in early Fall. In reality, it took almost three months. As the project was located north of the 60th parallel, one can perhaps realize that the subsequent claim for $6,000,000 was justified. Incidentally, the Contractor could not get out of his obligation to drive the piles. His bond saw to that. However, he won the full amount of his claim from the Owner. The Owner later sued the Engineer for negligence and won. The Engineers went bankrupt.

2. Complete breakdown of communications between Contractor and Engineer. A Contractor got permission to use a heavy diesel hammer at an energy setting lower than the maximum which, according to the hammer manufacturer's notes would be equal to the rated energy for a smaller hammer given in the specifications for the project. At the outset of the piling, it became obvious that the piles drove very slowly at that setting, requiring more than 1,000 blows before the specified termination criterion (minimum depth) was reached. Static testing showed that the capacity was insufficient. The specifications included provision for jetting and the Engineer required this for all piles. Yet, it was clear that the pile could be driven down to the depths and capacities quickly and without jetting if the hammer was set to work at the maximum energy setting. Of course, this meant that the hammer energy was to be set at a values higher than that given in the specifications. The Engineers were willing to accept this change. However, the Contractor required extra payment for the deviation from the contract to do this, which the Engineer did not want to grant. One thing led to another. The Contractor continued to drive at reduced hammer setting and diligently worked to adhere to the smallest detail of the specification wordings. The Engineer refused to budge and required jetting and recorded everything the Contractor did to ensure that, as the Contractor now wanted to follow the specs to the letter, he was not to deviate from any of the details. Incidentally, the specifications called for outside jetting (rather than interior jetting) in silty soil, which resulted in drifting, bending, and breaking of piles. The final suit involved claims for compensation of more than $10,000,000. The Contractor won about 40 % of the claim.

3. Specification for a near-shore piling project required piles to be driven flush with the sea bottom by means of a follower and stated that the follower should have 'sufficient impedance', but did not explained what this was and nobody checked the impedance of the follower. The Contractor drove the piles with a follower consisting of a steel pipe filled with wood chips. As the driving proceeded, the wood chips deteriorated and it became harder and harder to drive the piles. This was thought to be caused by densification of the sand at the site and the Contractor stated that the soil report failed

to show that densifiable soils existed at the site and claimed compensation for changed soil conditions. The contract required that dynamic measurements be performed at the project, and they were. However, the results of the PDA measurements were not looked at by anyone! Eventually they were, of course, and it became obvious to all that the root of the problem was with the inadequate follower. Well, better late than never, but the delay certainly cost the parties a bundle of money.

4. Long prestressed piles were required to support a new dock for a port extension. The soil profile consisted of an about 35 m to 40 m very soft soil deposit with some dense sand layers of varying thickness and depth, followed by very dense gravel and sand with boulders. The depth to the bearing soil layer required piles of such length that they became heavier than the available equipment could handle. The piles problem was solved by building the piles as composite piles, the upper about 30 m long solid concrete section and a lower about 15 m long H pile section. The penetration into the dense soil was expected to vary because of the presence of the boulders. During driving through the soft soils, care was taken not to drive too hard as this would have induced damaging tension in the pile. However, when the pile toe reached the dense soil and the penetration resistance increased, the hammer was set to hit harder to build up capacity and to advance the H pile end into the bearing layer. Several piles broke already at moderate blow-count and others a few feet further into the very dense bearing layer during hard termination driving. Expressed reasons for the breakage ranged from poor quality of the piles through sudden barge movements and inadequate equipment and/or use of wrong pile cushions. Not until the case was before the courts was it established that the H pile extension was so light that the impact wave on reaching the end of the concrete section, which was in the very soft soil, a large portion of the wave was reflected as a tension wave. Because the pile toe was in the dense soil, when the remainder of the wave reached the pile toe, a strong compression wave was reflected. The low blow-count and good toe response made the hammer ram rise high and provide a strong impact to the pile. The tension from the end of the concrete section being proportional to the impact force, therefore, reached damaging levels. A study compiling driving logs showed that the breakage correlated well with the presence of soft soil at the bottom end of the concrete section. Dynamic measurements had been conducted for determining capacity early in the project. The ‘post mortem’ study of the records established that when the bottom end of the concrete section was in soft soil, tension reflections occurred that exceeded safe levels.

It is not possible to give too many details on projects that went to dispute, because space limitation precludes giving an adequately impartial background to the cases. An account giving some of the details could easily appear slanted toward one or the other of the various players, who may then be justified in feeling slighted. Therefore, only the above cursorily information is presented in these notes.

Lucid, comprehensive, and equitable specifications are necessary for successful projects. However, even when the specs are good, if the communication lines break down, the project may still end up keeping our fellow professionals in the legal field living well. However, it is my experience that rarely are the initial ‘surprises’ and difficulties such that the parties really need to go the full way of the courts. Instead of posturing and jockeying for legal position, if the parties show a bit of good intent and willingness to understand each other and make some effort toward finding out what really is happening and why so, litigation can often be avoided. When people keep talking to each other, an understanding can usually develop that the specs are unclear or special technical difficulties have indeed arisen, and that some common sense ‘horse trading’ may settle the money issues. Going to court should be a last resort.

CHAPTER 12

EXAMPLES

12.1 Introduction

This chapter offers a few examples to the analysis methods. A couple of these have been taken from the example section of the manuals of UniPhase, UniSettle, UniBear, and UniPile. A few have been prepared specially for this text. They can all be solved by hand or by the applicable UniSoft program.

12.2 Stress Calculations

Example 12.2.1. The soil profile at a site consists of a 4.0 m thick upper layer of medium sand with a saturated total density of 2,000 kg/m^3, which is followed by 8.0 m of clay (density 1,700 kg/m^3). Below the clay, a sand layer (density 2,050 kg/m^3) has been found overlying glacial till (density 2,100 kg/m^3) at a depth of 20.0 m deposited on bedrock at depth of 23.0 m. The bedrock is pervious. Two piezometers installed at depths of 18.0 m and 23.0 m, respectively, indicate phreatic pressure heights of 11.0 m and 25.0 m, respectively. There is a perched groundwater table in the upper sand layer at a depth of 1.5 m. The water content of the non-saturated sand above the perched groundwater table is 12.6 percent.

Determine the dsitribuiton of effective overburden stress and the pore pressure in the soil. (Assume stationary conditions—no consolidation occurs).

The first step in the solution is to arrange a soil profile that lists all pertinent values, that is, the thickness and soil density of each layer, as well as the depth to the groundwater table and the pore pressures determined from the piezometer readings. The density of the non-saturated sand above the perched groundwater table is not given directly. However, knowing that the total density is 2,000 kg/m^3, and assuming that the solid density is 2,670 kg/m^3, UniPhase will quickly provide the dry density value—1,600 kg/m^3. Keeping the dry density value intact, UniPhase determines that the total density for a water content of 12.6 % is 1,800 kg/m^3. Hand calculations using the formulae in Chapter 1.2 will provide the same answer, of course.

Five soil layers will describe the profile. The key to determining the distribution of effective stress in the soil is realizing that the pore pressure distribution is affected by the existence of three aquifers. First, the perched water in the upper sand, second, the aquifer in the lower sand, and, third the artesian aquifer in the bedrock below the till. The clay and glacial till layers are impervious in relation to the lower sand layer, which is actually draining both layers resulting in a downward gradient in the clay and an upward in the till. In the sand layers, because of the higher hydraulic conductivity (permeability), the pore pressure distribution is hydrostatic (a gradient of unity). Because of the stationary conditions, the pore pressure distribution, although not hydrostatic, is linear in the clay and the till. Therefore, the information given determines the pore pressures at all layer boundaries and a linear interpolation within each layer makes the pore pressure known throughout the profile. The total stress, of course, is equally well known. Finally, the effective stresses are simply determined by subtracting the pore pressure from the total stress.

A stress calculation done by means of UniSettle, UniPile, or any custom-made spreadsheet program, provides the total and effective stresses and pore pressures at top and bottom of each layer. The calculation results are shown in the following table as “Initial Conditions”. For comparison, the “Final Conditions show the stresses if a hydrostatic distribution of pore pressures is assumed throughout the soil profile. The existence of pore pressure gradients in the soil and more than one aquifer is a common occurrence. Considering the considerable influence pore pressure gradients can have as opposed to hydrostatic conditions, it is not possible to explain why so many in the industry so rarely bother about measuring pore pressures other than as the height of water in the borehole, assuming, inanely, hydrostatic conditions throughout the site!

Example 12.2.1. Results of Analysis by UniSettle

	Depth (m)	Initial Conditions Total Stress (kPa)	Initial Conditions Pore Stress (kPa)	Initial Conditions **Eff. Stress** (kPa)	Final Conditions Total Stress (kPa)	Final Conditions Pore Stress (kPa)	Final Conditions **Eff. Stress** (kPa)
	Layer 1	Non-sat Sand	1800. kg/m^3				
	0.00	0.0	0.0	**0.0**	0.0	0.0	**0.0**
	1.50	27.0	0.0	**27.0**	27.0	0.0	**27.0**
	Layer 2	Sand	2000. kg/m^3				
GWT	1.50	27.0	0.0	**27.0**	27.0	0.0	**27.0**
	4.00	77.0	25.0	**52.0**	77.0	25.0	**52.0**
	Layer 3	Clay	1700. kg/m^3				
	4.00	77.0	25.0	**52.0**	77.0	25.0	**52.0**
	12.00	213.0	50.0	**163.0**	213.0	105.0	**108.0**
	Layer 4	Sand	2050. kg/m^3				
	12.00	213.0	50.0	**163.0**	213.0	105.0	**108.0**
	20.00	377.0	130.0	**247.0**	377.0	185.0	**192.0**
	Layer 5	Till	2100. kg/m^3				
	20.00	377.0	130.0	**247.0**	377.0	185.0	**192.0**
	23.00	440.0	250.0	**190.0**	440.0	215.0	**225.0**

--------------------------End of data--------------------------

Example 12.2.2. A laboratory has carried out consolidation tests on a postglacial inorganic clay and reports the results as initial and final water contents ($w_{initial}$ and w_{final}) being 57.0 % and 50.0 %, respectively, an initial void ratio, e_0, of 1.44, S = 100 %, and a total density, ρ_{total}, of 1,650 kg/m^3. Do the values make sense?

Phase system calculations show that the values of $w_{initial}$ of 57 % and the e_0 of 1.44 combine only if the solid density of the material is 2,620 kg/m^3, and the $w_{initial}$ of 57 % and a void ratio of 1.44 combine only if the total density of 2,520 kg/m^3. In reality, the solid density is more likely equal to 2,700 kg/m^3. Then, a water content of 57 % corresponds to e_0 = 1.54 and ρ_{total} = 1,670 kg/m^3.

Are the errors significant? Well, the final water content of 50 % corresponds to a final void ratio of either 1.31 (ρ_s = 2,620 kg/m^3) or 1.35 (ρ_s = 2,700 kg/m^3). Adjusting the void ratio versus stress curve from the consolidation test, accordingly, changes the C_C-value from 0.80 to 1.25. This implies a significant error. However, the modulus number is equal to 7 (indicating a very compressible soil) whether based on the originally reported values or on the values adjusted to the proper value of solid density. In this case, the error in e_0 compensates for the error in C_c.

The example is taken from a soil report produced by a reputable geotechnical engineering firm. Agreed, the errors are not significant. But they are nevertheless errors, and, while it never came about, it would have been a very uncomfortable experience for the responsible engineer under cross examination on the stand to try sound believable to the judge and jury in proclaiming that the errors 'don't matter'.

Example 12.2.3. Errors in the basic soil parameters are not unusual in geotechnical reports. For example, a laboratory report in my files produced by another company that deals with a sample of about the same type of clay as in Example 12.2.2 lists under the heading of "Determination of Density and Water Content" values of the weights of saturated and dry soil and dish etc., and, finally, the value of the water content as 50.8 % and also, although without showing calculations, the solid, total, and dry density values of 2,600 kg/m^3, ***1,782 kg/m^3 and 1,184 kg/m^3***, respectively. The two latter values match for calculations using an input of S = 100 % and a solid density of 2,960 kg/m^3. With the slightly more plausible value of solid density of 2,600 kg/m^3, the total, and dry density values are ***1,690 kg/m^3 and 1,120 kg/m^3***, respectively. Notice that the ratio of the dry density over the total density is 0.66, the same value as the ratio 100% over (100% + 50.8%), implying accurate values. Yet, the value reported by the geotechnical laboratory for the total density is 5 % too large. Significant? Well, perhaps not very much, but it is a bad start of a foundation design.

Example 12.2.4. In illustrating Boussinesq stress distribution, Holtz and Kovacs (1981) borrowed (and converted to SI-units) an example by Newmark (1942): An L-shaped area is loaded by a uniform stress of 250 KPa. (The area is shown below with the dimensions indicated by x and y coordinates). The assignment is to calculate the stress induced at a point located 80 metre below Point O (coordinates x = 2 m; y = 12 m), a point well outside the loaded area. The plan view below shows the loaded area placed on the Newmark's influence diagram with Point O at the center of the diagram. A hand calculation documented by Holtz and Kovacs (1081), gives the results that the stress at Point O is 40 KPa.

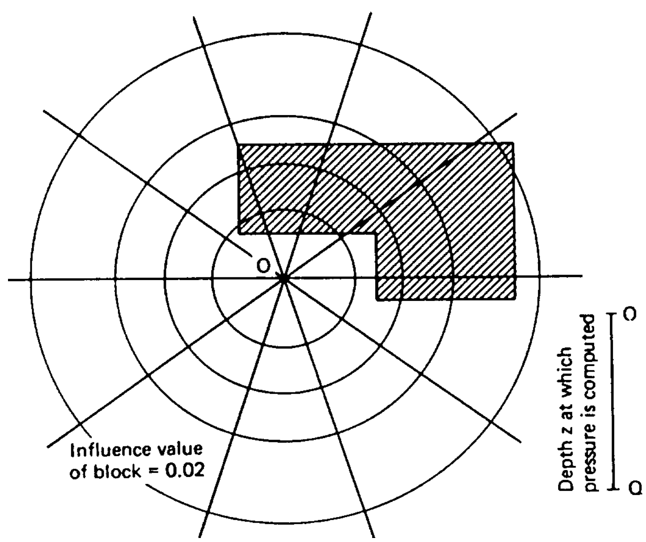

The following figure shows a plan view produced by UniSettle with Point O at coordinates 2;12.

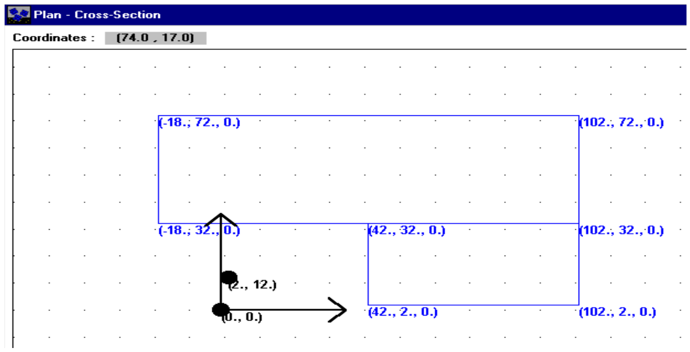

UniSettle shows that the hand calculation is correct, the calculated value of the stress is 40.6 KPa. The full results of the UniSettle calculations are presented in the table and diagram given below; in this case, the stresses at every 5 metre depth from 0 m to 200 m underneath Point O. (The table is limited to show values for 75 m, 80 m, and 85 m).

Stress Analysis - Boussinesq, (2. , 12.)

Depth (m)	Initial Conditions Total Stress (kPa)	Initial Conditions Pore Stress (kPa)	Initial Conditions Eff. Stress (kPa)	Final Conditions Total Stress (kPa)	Final Conditions Pore Stress (kPa)	Final Conditions Eff. Stress (kPa)
75.00	0.0	0.0	0.0	41.8	0.0	41.8
80.00	0.0	0.0	0.0	40.6	0.0	40.6
85.00	0.0	0.0	0.0	39.2	0.0	39.2

The diagram presented below shows the vertical stress distribution underneath Point O according to Boussinesq as calculated by UniSettle. Notice, because Point O lies outside the footprint of the loaded area, the 2:1-method does not apply.

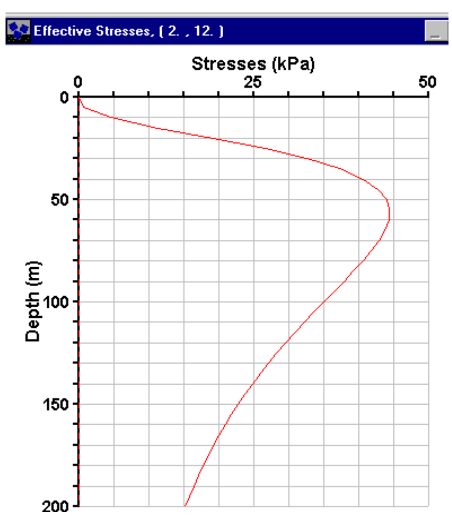

12.3 Settlement Calculations

Example 12.3.1. Example 12.3.1 is taken from a classic geotechnical text: Norwegian Geotechnical Institute, Publication No. 16, Example 7, (Janbu et al., 1956)**:** Calculation of settlement for a structure with a footprint of 10 m by 10 m founded at a depth of 2.0 m on 22 m of normally consolidated clay deposited on bedrock, as shown below. The stress distribution is by Boussinesq below the center of the structure. The groundwater table lies at a depth of 0.5 m and the distribution of pore water pressure is hydrostatic. The clay is built up of four slightly different layers with the parameters indicated in the figure.

As a somewhat cheeky comment, a calculation by means of the UniPhase program shows that the void ratio values of about 1.22 indicated in the figure are not compatible with the 1,900 kg/m^3 value indicated for the total saturated density unless the solid density of the clay particles is about 3,000 kg/m^3, about ten percent higher than the probable value. The void ratio values combined with the more realistic value of solid density of 2,670 kg/m^3 require a saturated density of about 1,750 kg/m^3. The 1,900 kg/m^3 value indicated in the figure has been retained in the following, however. (The Reader will have to excuse that also the Norwegian language has been retained; one does not tinker with the classics)!

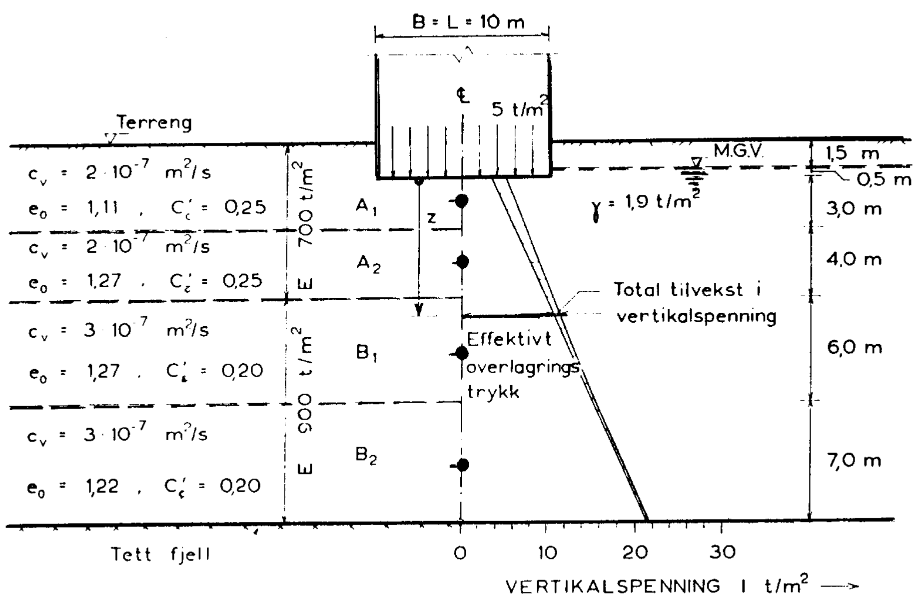

Beregning av spenninger og konsolideringssetning.

LAG	Dybde z i m	Effektivt overlagringstrykk p_0 i t/m²	Tilleggs-spenning Δp i t m²	$\log \frac{p_0 + \Delta p}{p_0}$	$\frac{C'}{1+e_0} \Delta H$ (cm)	Setn. pr. lag $\Delta\delta_c$ (cm)
—	0	1,5 · 1.9 + 0,5 · 0,9 = 3,30	5.0 – 3,3 = 1,70	—	—	—
A_1	1,5	3,30 + 1,5 · 0,9 = 4,65	0,98 · 1,70 = 1,66	0.133	35,5	4,7
A_2	5,0	4,65 + 3,5 · 0,9 = 7,8~~5~~0	0,70 · 1,70 = 1,19	0,061	44,0	2,7
B_1	10,0	7,80 + 5,0 · 0,9 = 12,30	0,34 · 1,70 = 0,58	0,020	53,0	1,1
B_2	16,5	12,30 + 6,5 · 0,9 = 18,15	0,15 · 1,70 = 0,26	0,006	63,0	0,4

Konsolideringssetning: $\underline{\delta_c} = \Sigma \Delta\delta_c = \underline{8,9 \text{ cm}}$

The original units in "old metric" shown in the figure have been converted to “new metric”, i. e. SI units, and the net input of 17 KPa for the stress imposed by the structure (final conditions) has been replaced by an input stress of 50 KPa plus input of final excavation to the 2.0 m depth (reduction by 33 KPa). Because the excavation has the same footprint as the structure, no effect on the stresses is caused by separating input of load from input of excavation as opposed to first reducing the imposed stress by the excavation equivalent.

Moreover, the soil layers are indicated as normally consolidated with compressibility parameters given in the figure in the format of conventional C_c-e_0 parameters. The NGI 16 publication was published in 1956, seven years before the advent of the Janbu tangent modulus approach. The modulus numbers for layers A1, A2, B1, and B2 are (by ***soft*** conversion from the C_c-e_0 parameters) 19.4, 20.9, 26.1, and 25.5.

As given in the figure, settlement calculations result in 89 mm of settlement. Assigning, say, 0.5 m thick sub layers, and repeating the calculations reveals that no appreciable gain is achieved from using many sub layers**:** the settlement value is essentially the same, 92 mm, and the "improved accuracy" is only 3 mm.

The foundation for the structure is probably quite rigid. Therefore, the settlement calculated below the characteristic point (x = 3.7 m; y = 3.7 m) is more representative than below the center**:** In no time at all, UniSettle can calculate the settlement for the characteristic point, obtaining a value of 70 mm, about 25 % smaller than the value calculated for a point under the center of the structure (taken to be flexible).

Or, consider that the structure most likely is not a solid monolith, but a building with a basement. It is then very unlikely that the groundwater table stays at a depth of 1.5 m also inside the structure; most probably, the groundwater table is lowered at least to a depth of 2.0 m. After an adjustment of the elevation of the final groundwater table to 2.0 m and the unloading due to the basement, a re-calculation with UniSettle returns a settlement of 130 mm, much larger than that given by the original calculation.

Well, perhaps the drainage only takes effect down to the bottom of Layer A2 (second layer in the figure) and the pore pressures are unchanged below this depth. UniSettle now calculates a settlement of 109 mm (below the center of the structure).

Obviously, the calculated settlement values can vary widely depending on what case alternative that is considered. After studying various alternatives, perhaps the most realistic and appropriate case should include the draining of the groundwater table in the upper layer and the settlement be calculated below the characteristic point, which calculation is also quickly and easily made. Before becoming too smug about the advances made possible by means of UniSettle and a computer, however, we should consider that this latest calculation returns the settlement of 88 mm, a value essentially equal to that given by NGI 16.

The NGI 16 presentation includes a calculation of the immediate settlement, a value of 33 mm is indicated to be added to the consolidation settlement of 89 mm for the example. Whether or not to include a calculation of immediate settlement in a case similar to the subject one can be argued. As can the method to use for its calculation**:** applying an elastic modulus, or adjusting the compressibility parameters; NGI 16 uses the elastic modulus approach with an E-value of 7,500 KPa.

Example 12.3.2. Example 12.3.2. is also taken from a textbook**:** Example 4.4 in Chapter 4 of Perloff and Baron (1976), which presents a 40 feet wide circular water tank on a ring foundation, with fill placed outside the tank and with the tank bottom flexible and resting on the ground, as illustrated below. The assignment is to calculate Boussinesq stress at Points A and B at a depth of 20 feet. The input file shows the input of the stress from the surcharge and the tank as three overlapping areas. The stresses at the 20 ft depth calculated for A and B are 1.3 ksf and 0.8 ksf, respectively.

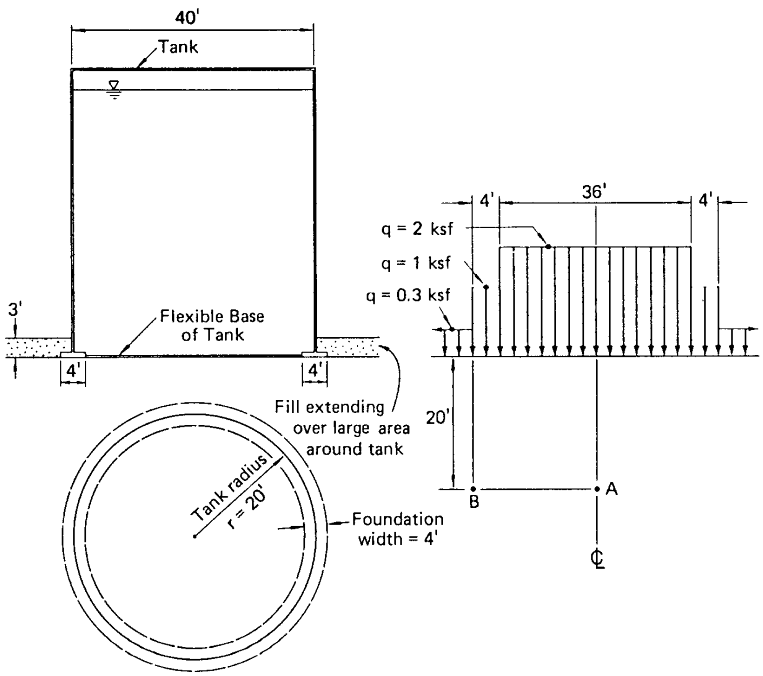

The example is interesting because it pertains to a realistic case and tempts to several what-if studies. So, what if the base of the tank would not flexible, but stiff so that all the tank loads go to the ring foundation (no surcharge is placed under the tank)? What then about the stresses at A and B? And, what about settlements? Make up a soil profile with suitable values of density and modulus numbers, etc. and try it out.

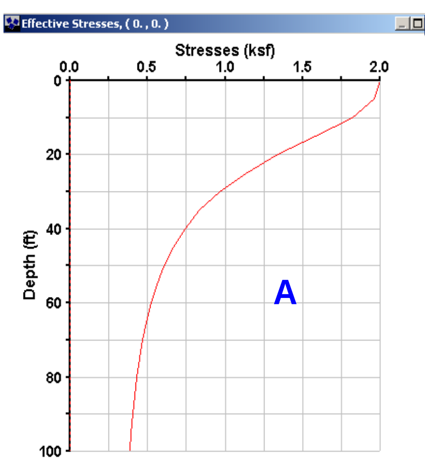

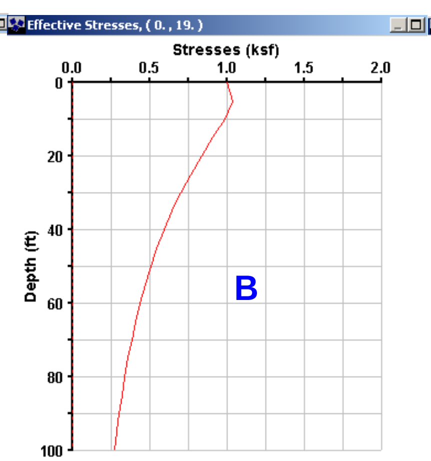

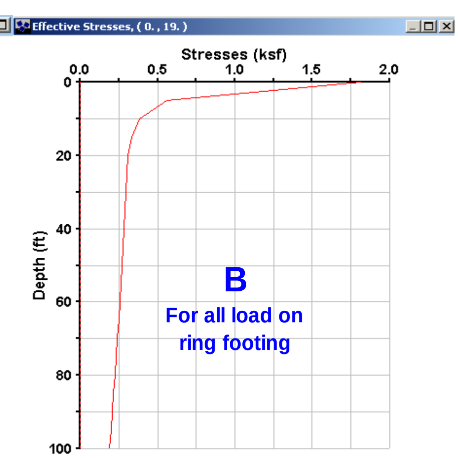

Well, the calculated settlement may actually not change much, but will the ring footing be stable?

12.4 Earth Stress and Bearing Capacity of Retaining Walls

Example 12.4.1. Taylor's unsurpassed textbook "Fundamentals of Soils" (Taylor, 1948) contains several illustrative examples on earth stress and bearing capacity of retaining walls. The first example quoted is a simple question of the difference in the earth stress coefficient when considering as opposed to disregarding that the ground surface behind a wall is sloping 20° (1H:0.364V). The problem assumes Rankine earth stress (that is, wall friction angle is zero). Taylor writes: "*Determine the percentage error introduced by assuming a level fill when the slope angle actually equals 20 degrees. Assume a friction angle of 35 degrees and a vertical wall.*" A computation using UniBear shows that the earth stress coefficient, K_a, is 0.27 for the level backfill and 0.34 for the sloping backfill. The error in disregarding the slope is a 20 % underestimation of the magnitude of the earth stress.

Example 12.4.2. Taylor (1948) includes an example asking for the difference in earth stress coefficient between a wall leaning away from the soil as opposed to leaning toward the soil. The leaning (inclination) is 2 inches per foot, the soil density is 100 pcf, the friction angle is 35 degrees, the ground surface is level, and there is no wall friction. Computation shows that the K_a-coefficient is 0.33 for an inclination away from the backfill soil and 0.18 for leaning toward the backfill. The K_a-coefficient for a vertical wall is 0.25. Obviously, the inclination of the wall should not be disregarded in a design analysis.

Example 12.4.3. Taylor (1948) also deals with a 25 feet high concrete gravity wall (density 150 pcf) with a 4-foot width at the top. The inside face of the wall is vertical and the wall retains soil with a 35-degree friction angle and a density of 100 pcf. The wall friction angle is 30 degrees and the cohesion intercept is zero. Taylor asks for the required width of the wall if the resultant has to be located exactly in the third point of the base considering the case of (1) no wall friction and (2) wall friction included. He also asks for the base stresses and the safety against sliding. Taylor's text uses the Terzaghi original approach to the bearing capacity coefficients. A diagram in the book indicates that the N_q, N_c, and N_γ coefficients are about 22, 37, and 21 for $\phi = 30°$. According to the expressions by Meyerhof, the coefficients are 33, 36, and 44, respectively, and according to the expressions by Caquot and Kerisel, they are 33, 36, and 48, respectively. For the Caquot and Kerisel coefficients, for example, UniBear computes a necessary base width of 9.5 feet for the case of no wall friction on the condition that the resultant lies in the third point. The factor of safety on sliding is 2.09, which is adequate. However, the factor of safety for bearing is a mere 1.11, which is not adequate. Kind of a sly example, is it not?

The disregard of wall friction is not realistic, which perhaps is what Taylor intended to demonstrate. Nota bene, Taylor did not 'correct' for inclined load. When the wall friction is included, the numbers change considerably and even allow a reduction of the wall base width to 5 feet with adequate factors of safety for both sliding and bearing. As the wall has no footing, including wall friction is appropriate.

Example 12.4.4. The following cantilever wall example is quoted from The Civil Engineering Handbook (Chen and McCarron, 1995): The wall is 7.6 m high and wall retains a sand soil with a $\phi' = 35°$ and a density of 1,900 kg/m^3. The wall friction is indicated as equal to the soil friction. The ground surface slopes upward and the slope is stated both as 24° and as 1 m over a distance of 2.8 m, that is, an angle of 19.7°. Both values are used in the calculations in the book. The applicable allowable bearing stress is stated to be 360 KPa. The location of the groundwater table is not mentioned in the book. It is therefore assumed to be well below the footing. A 0.6 m surcharge on the ground surface of soil with the same density as the backfill is included.

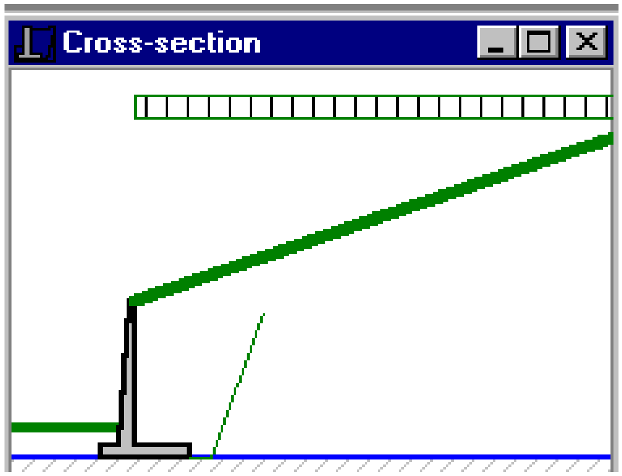

The calculations in the book estimate K_a from the 24-degree slope combined with a nomogram based on logarithmic spiral calculations to be 0.38, as opposed to 0.33 according to the usual Coulomb relation.

The calculations by Chen and McCarron (1995) are made with some effort-saving minor simplifications and the book gives the total gravity force as 614 KN/m and the horizontal and vertical (wall friction component) earth stress forces as 301 KN/m and 211 KN/m. Computations using UniBear result in 669 KN/m, 315 KN/m, and 220 KN/m, respectively. A good agreement. The small difference lies in that UniBear allows including also the outside surcharge on the footing toe in the calculation of the gravity forces.

The book adds the gravity vertical force and the earth stress vertical forces to a total vertical force of 25 KN, and uses this value to calculate the sliding resistance to 825 times tan 35° = 578 KN/m. UniBear calculates 890 KN/m and 670 KN/m, which are about the same values. The book gives an eccentricity of 0.25 m, UniBear 0.30 m. The book gives a sliding ratio of 1.9, UniBear 2.1. The differences are slight and the values would appear to indicate a safe situation.

However, it is principally incorrect to calculate the earth stress using full wall friction on a cantilever wall. A UniBear calculation applying a zero wall friction results in an eccentricity of 1.4 m and a sliding ratio of 1.3. Neither is acceptably safe.

A further difference is that the textbook determines a maximum <u>edge</u> stress of 245 KPa for the full base width without considering the eccentricity and compares this to the allowable bearing, 360 KPa (the 360 KPa-value must be including a factor of safety). In contrast, UniBear determines the <u>average</u> stress over the equivalent footing and compares this to the allowable stress (WSD design). The particulars of the bearing soil were not given. With the assumption that the soil under the base is the same as the backfill, that the groundwater table lies at the base, and that the Meyerhof coefficients apply, the computations result in a bearing resistances of 580 KPa and a factor of safety of only 1.4.

Example 12.4.5. Example 12.4.5 is quoted from a soil mechanics textbook (Craig 1992). The example consists of a simple gravity wall as illustrated below and the text asks for the sliding resistance and the maximum and minimum stresses underneath the footing. The densities of the wall and of the backfill are 2,350 kg/m^3 and 1,800 kg/m^3, respectively. The soil has friction only and ϕ' and δ' are equal to 38° and 25°, respectively. The wall slope angle, β, is 100° and the ground slope angle, α, is 20°.

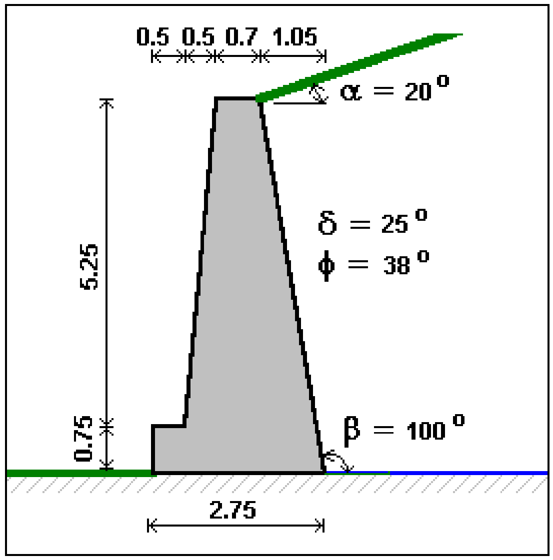

The textbook indicates that the earth stress coefficient is 0.39, which is calculated assuming that the earth stress acts on the wall with full wall friction present. The calculated horizontal and vertical components of the earth stress are 103 KN/m and 72 KN/m, respectively. The weight of the structure is 221 KN/m and the resultant is located 0.98 m from the toe. The eccentricity is 0.40 m or about 15 % of the footing width. That is, the resultant lies within the middle third. The calculated sliding ratio is 1.33, which is somewhat low.

If the calculations are made for the earth stress acting against a normal rising from the heel of the footing and, therefore, with zero wall friction, an earth stress coefficient results of 0.29 and the horizontal component of the earth stress is 108 KN/m, which is close to the textbook's calculated value. The earth stress has no vertical component, but the weight of the backfill wedge on the wall (61 KN/m) is included in the analysis. It is about equal to the vertical component of the earth stress (72 KN/m) calculated by the textbook, so the new vertical force is essentially unchanged. The sliding ratio is 1.22, slightly smaller than before. A six-of-one-and-half-a-dozen-of-another case, is it? However, the resultant is not in the same location and the new eccentricity is 0.54 m or about 20 % of the footing width. That is, the resultant lies outside the middle third of the footing and this is not a safe situation. The UniBear approach is recommended for actual design situations.

The maximum and minimum stresses, q_{max} and q_{min} can be calculated from the following expression with input of the footing width, B, and eccentricity, e. For q_{max} use the plus sign and for q_{min} use the minus sign.

$$q_m = \frac{Q_v}{B}(1 \pm \frac{6e}{B})$$

Notice, the expression builds on that the stress distribution can be assumed to be linear. However, once the resultant lies outside the middle third, this is not a valid assumption.

Example 12.4.6. Example 12.4.6 demonstrates the influence of a line load. The case is taken from a text book by Bowles (1992) and presents a cantilever wall with a sloping ground surface and a 70-KN line load on the ground surface. The footing thickness and width are 1.0 m and 3.05 respectively (no information is given on the density of the wall, regular concrete density is assumed). The stem thickness is 0.73 m at the footing, 0.30 m at the top, and the stem height is 6.1 m. The ground surface slopes 5H:1V. The soil density is 1,745 kg/m^3, and the soil and wall friction angles are equal and 35°. The textbook requests the active earth stress and its point of application. The textbook gives the answer to the problem as "an earth stress of 164 KN/m acting 58.6° from the horizontal" (probably intending to say ”vertical”).

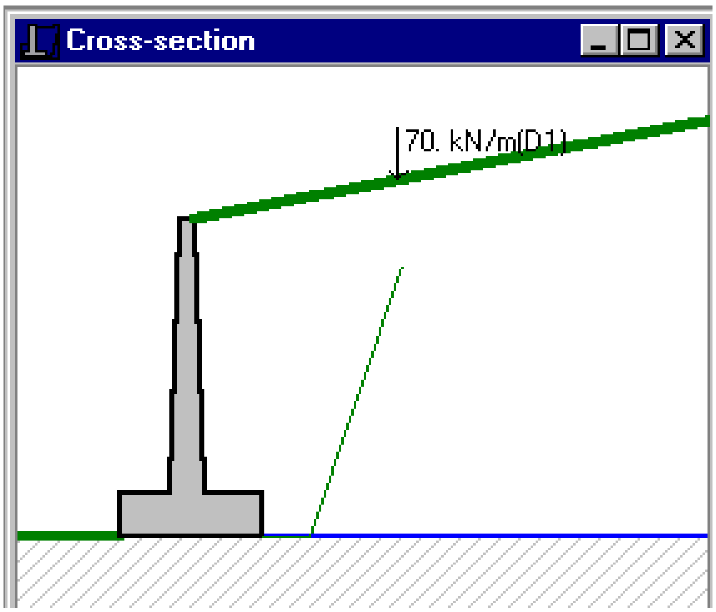

UniBear calculates a horizontal component of the backfill earth stress of 147 KN/m and the total horizontal pressure from the line load of 31 KN/m, together 178 KN/m, not quite the value given in the textbook. However, these values are obtained using a wall friction of zero degrees, which as mentioned is recommended for cantilever walls. A calculation with the wall friction equal to the soil friction, 35°, results in horizontal and the vertical earth stress components of 112.5 KN/m and 78.75 KN/m, respectively. The sum of the horizontal components of the line load and earth stress is equal to 143.6 KN/m. The resultant to this load and the vertical earth stress is 164 KN, the same as given in the textbook. The angle between this load and the normal to the footing, the "vertical", is 61°, very similar to that given in the textbook.

Notice, that UniBear also calculated the vertical component of the line load that acts on the heel. For the subject example, it is 5 KN/m. Before UniBear, it was rather cumbersome to include this component and it was usually omitted. For reference to old analysis cases involving surface loads, some may desire to exclude the effect of this vertical component. This can be easily done by imposing a vertical line load on the footing that is equal on magnitude to the vertical component of the surface line load and which acts at the same distance from the toe but in the opposite direction.

12.5 Pile Capacity and Load-Transfer

Example 12.5.1 In 1968, Hunter and Davisson presented an paper on analysis of load transfer for piles driven in sand. The paper was the first to show that residual loads in a pile will greatly affect the load transfer data evaluated from load measurements in a static loading test (as had been postulated by Nordlund, 1963).

The tests were performed in a homogeneous deposit of “medium dense medium to fine sand” with SPT N-indices ranging from 20 through 40 (mean value of 27) and a bulk saturated density of the sand of 124 pcf. The groundwater table was at a depth of 3 ft (hydrostatic pore pressure distribution can be assumed). Laboratory tests indicated the internal friction angle to be in the range of 31 degrees through 35 degrees. The friction angle for a steel surface sliding on the sand was determined to 25 degrees.

Static loading tests in push (compression test) followed by pull (tension test) were performed on six piles instrumented with strain gages and/or telltales. The piles were all installed an embedment depth of 53 feet and had a 2-foot stick-up above ground. The detailed test data are not included in the paper, only the total load and the evaluated toe loads (in both push and pull).

Pile #	Type	Shaft area (ft^2/ft)	Toe area (ft^2)	Installation manner
1	Pipe 12.75”	3.96	0.98	Driven; Vulcan 140C
2	Pipe 16.0”	5.32	1.59	Driven; Vulcan 140C
3	Pipe 20.0”	5.83	2.27	Driven; Vulcan 140C
7	14HP73	4.70	1.38	Driven; Vulcan 80C
10	Pipe 16.0”	5.32	1.59	Vibrated
16	Pipe 16.0”	4.93	1.49	Jetted first 40 ft, then driven: Vulcan 140C

The areas include the areas of guide pipes and instrumentation channels. The shaft area of the H-pile is given as the area of a square with a side equal to the side of the pile.

The paper does not include the load-movement curves from the static loading tests, only the evaluated ultimate resistances. The following table summarizes the ultimate resistances (pile capacities) and the toe resistances evaluated from the tests.

Pile	Push Test		Pull Test			'Adjusted'	
	R_{ult}	R_s	R_t	R_s	'R_t'	R_s	R_t
#	(kips)	(kips)	(kips)	(kips)	(kips)	(kips)	(kips)
1	344	248	96	184	-74	174	170
2	502	352	150	232	-90	262	240
3	516	292	224	240	-96	196	320
7	440	310	130	150	-50	260	180
10	456	290	166	220	+4	296	160
16	330	230	100	146	-70	150	180

The test data indicate that the piles were subjected to negative toe resistance during the pull test, which, of course, is not possible. (It would mean that there was someone down there holding on and pulling the other way). The negative toe resistance observed is due to residual load induced in the pile caused by the pile installation and the preceding push test. Hunter and Davisson (1969) adjusted the data for the push test by increasing the toe load by a value equal to the apparent toe load of the pull test and decreasing the shaft resistance correspondingly, linearly to the pile head. The so adjusted values are shown in the two rightmost columns above.

The paper reports the effective stress parameters in a beta-analysis matched to the data. These data have been compiled in the table below and used as input to the UniPile program[1)] together with the soil and pile data as given above. The results of the UniPile computations are included in the table. For Pile #16, the soil is split on jetted portion and not jetted using different β-coefficients (0.24 and 0.50) in addition to the 0.35 value given in the paper. The beta-value for the H-pile, 0.65, is a mean of the 0.51 on the steel surface and 0.80 in the sand-to-sand shear (as used in the paper).

Pile	Input Values			UniPile Analysis			β from
	N_t	K_s	β	R_{ult}	R_t	R_s	pull test
#	(--)	(--)	(--)	(kips)	(kips)	(kips)	(--)
1	53	1.07	0.50	342	169	171	0.54
2	46	1.22	0.57	501	239	262	0.50
3	43	0.83	0.39	515	319	197	0.48
7	40	1.10	0.65	444	180	264	0.38
10	31	1.27	0.59	432	161	271	0.48
16	37	0.75	0.35	329	180	149	
			0.24 & 0.50	330	180	150	0.22 & 0.50

1) For information on the program, visit <www.unisoftltd.com>

The analysis of an H-pile is always difficult. Did it or did it not plug? Should one use the square or the H? And should this choice be the same or different for the shaft and the toe? It is obvious that H-pile behaved differently in the push and the pull. Therefore, it is not possible to draw assured conclusions from a comparison between the push and the pull results. In contrast, the results of the tests on the pipe piles are quite conclusive. The paper concludes that there is a difference in shaft resistance in push and pull. The compilations presented in the tables do not support this conclusion, however. A review of the data suggest that the beta-coefficient determining the shaft resistance lies in the range of 0.48 through 0.52 for the piles and that the shaft resistance is about the same in push and pull. An analysis using $\beta = 0.50$ and $N_t = 45$ gives results, which for piles all but the H-pile gives results that are close to the reported values. This approach also reduces the difference between the impact driven and vibratory driven piles. However, the purpose of this account is not to discuss the merits of details given in the paper, but to use the data to demonstrate the load-transfer analysis. The significance of the paper is the clear demonstration that the influence of residual loads must be included in the evaluation of pile test data.

The amount and distribution of residual load in a pile can be calculated by the same effective stress approach as used for matching the test data. A computation of Pile 1 with a utilization degree of 45 % of the toe bearing coefficient, N_t, results in a computed “false toe resistance” of 93 kips and “false shaft resistance” of 348 kips, which is close to what the authors reported in the paper. The diagram below presents the load-transfer curves for the true load distribution curves: the Resistance curve, the Residual load curve, and the False Resistance curve as determined using the UniPile program.

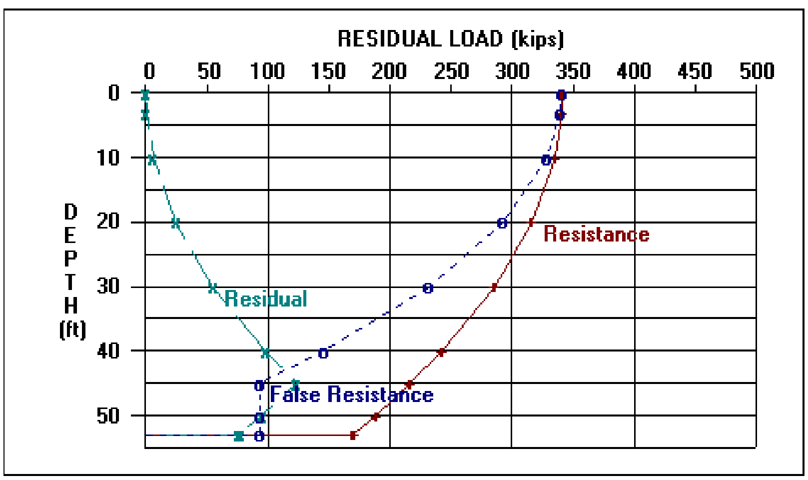

Example 12.5.2 Altaee et al., 1992 presented results and analysis of an instrumented 285 mm square precast concrete pile installed to an embedment of 11.0 m into a sand deposit. Three sequences of push (compression) testing were performed, each close to the ultimate resistance of the pile followed by a pull (tension) test. The instrumentation registered the loads in the pile during the static push testing, but did not provide accurate data during the pull test. During the push test, the groundwater table was at a depth of 6.2 m. During the pull test, it was at 5.0 m. The maximum load applied at the pile head was 1,000 KN, which value was very close the capacity of the pile. The pull test ultimate resistance was 580 KN.

The paper reports both the soil parameters and the magnitude of the residual loads affecting the test data. The effective stress parameters are as follows.

Layer --	Depth (m)	Total Density (kg/m^3)	ß --	N_t --
Silt-Sand	0.0 - 3.0	1,600	0.40	--
Dry Sand	3.0 - 5.0	1,800	0.50	--
Moist Sand	5.0 - 6.5	1,900	0.65	--
Sat. Sand	6.5 - 11.0	2,000	0.65	30

The data have been used as input to a UniPile computation returning a capacity value of 1,034 KN, which is acceptably close to the measured load of 1,000 KN. The table below shows the computed results. The first column shows the computed resistance distribution (at ultimate resistance). The second column shows the results of a residual load computation with 50 % utilization of N_t (as matched to the data reported in the paper). The column headed "False Resistance" is obtained as the difference between the first two. A comparison with the recorded test data, shown in the far right column, indicates clearly that the data recorded during the test are affected by residual load. The small differences in agreement can easily be removed by inputting the soil parameters having the precision of an additional decimal.

DEPTH (m)	RES.DISTR. (KN)	RES.LOAD (KN)	FALSE RES. (KN)	**TEST** (KN)
0	1,034	0	1,034	1,000
4.5	948	85	863	848
6.0	856	177	679	646
7.5	732	302	430	431
9.0	591	(402)	~300	309
10.0	487	299		
10.5	433	245	188	191
11.0	376	188		

The computations assume that the change between increasing residual load (negative skin friction zone) to decreasing (positive shaft resistance zone) is abrupt (appearing as a 'kink' in the curve). In reality, however, the shift between the relative movement from negative and to positive directions occurs in a transition zone. For the tested pile, the analysis shows that this zone extends from about 1.0 m above the neutral plane (Depth 9.7 m) to about 1.0 m below the neutral plane. Therefore, the computed residual load at the Depth 9.0 m is overestimated, which is why it is given in parenthesis in the table. Instead, the residual load between 8.0 m and 12.5 m is approximately constant and about 300 KN. The about 2.0 m length of the transition zone corresponds to about 7 pile diameters in this case history.

The computed shaft resistance in the push test is 657 KN. Repeating the computation for "Final Conditions", that is, with the groundwater at 5.0 m, the shaft resistance is 609 KN, again acceptably close the tested pull capacity (580 KN). Besides, the analysis of the test data indicates that a small degradation of the shaft resistance occurred during the push testing. Considering the degradation, the shaft resistances in push and pull are essentially of equal magnitude. (Notice, UniPile can perform calculation of the residual loads in an uplift test if the soil strength parameters are input as negative values). The load-transfer curves are shown in the following diagram. The vertical line of the Residual Load curve between Depths 7.5 and 12.0 is the mentioned transition zone with essentially constant residual load.

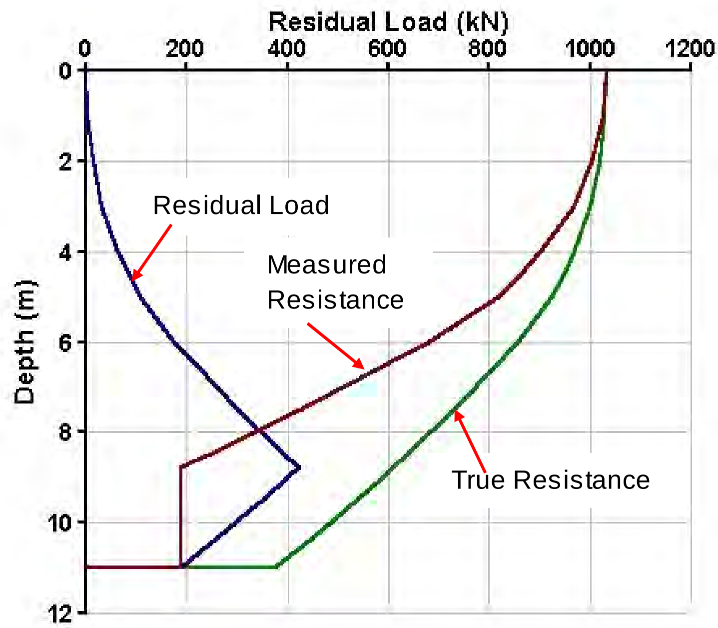

Example 12.5.3. The following example is a case history also obtained from the real world. However, in the dual interest of limiting the presentation and protecting the guilty, the case has been distorted beyond recognition. A small measure of poetic license has also been exercised. (The example has been used in a graduate foundation course (the auhtor used to give at University of Ottawa), where the students not only study foundation analysis and design but also practice presenting the results in an engineering report. The solution to the assignment is to be in the format of a consulting engineering letter report).

Letter to Engineering Design and Perfection Inc. from Mr. So-So Trusting, P. Eng., of Municipal Waterworks in Anylittletown

Dear Sir: This letter will confirm our telephone conversation of this morning requesting your professional services for analysis of the subject piling project with regard to a review of integrity and proper installation procedure of the New Waterworks foundation piles.

The soil conditions at the site are described in the attached Summary of Borehole Records. These data were obtained before the site was excavated to a depth of 4.0 m. The piles are to support a uniformly loaded floor slab and consist of 305 mm (12 inch), square, prestressed concrete piles. The piles have been installed by driving to the predetermined depth below the original ground surface of 12.0 m (39 ft). The total number of piles is 700 and they have been placed at a spacing, center-to-center, of 2.0 m (6.5 ft) across the site.

An indicator pile-testing programme was carried out before the start of the construction. The testing programme included one static loading test of an instrumented test pile. Plunging failure of the test pile occurred at an applied load of 2,550 KN (287 tons) and the measured ultimate shaft resistance acting on the pile was 50 KN (6 tons) in the upper sand layer and 400 KN (45 tons) in the lower sand layer. The measured ultimate toe resistance was 2,100 KN (236 tons).

Relying on the results of the indicator test programme, our structural engineer, Mr. Just A. Textbookman, designed the piles for an allowable load of 1,000 KN incorporating a safety factor of 2.5 against the pile capacity taken as 2,500 KN (the 50-KN resistance in the upper sand layer was deducted because this layer was to be removed across the entire site after the pile driving).

The contractor installed the piles six weeks ago to the mentioned predetermined depth and before the site was excavated. The penetration resistance at termination of the driving was found to be about 130 blows/foot, the same value as found for the indicator piles.

After the completion of the pile driving and removal of the upper 4.0 m sand layer, our site inspector, Mr. Young But, requested the Contractor to restrike two piles. For both these piles, the blow count was a mere 4 blows for a penetration of 2 inches, i. e., equivalent to a penetration resistance of 24 blows/foot! A subsequent static loading test on one of the restruck piles reached failure in plunging when the load was being increased from 1,250 KN to 1,500 KN. We find it hard to believe that relaxation developed at the site reducing the pile capacity (and, therefore, also the penetration resistance) and we suspect that the piles have been broken by the contractor during the excavation work. As soon as we have completed the change-order negotiations with the contractor, we will restrike additional piles to verify the pile integrity. Meanwhile, we will appreciate your review of the records and your recommendations on how best to proceed.

Sincerely yours,

Mr. So-So Trusting, P. Eng.

SUMMARY OF BOREHOLE RECORDS

The soil consists of an upper layer of loose silty backfill of sand with a density of 1,700 kg/m^3 (112 pcf) to a depth of 4 m (13 ft) and placed over a wide area. The sand is followed by a thick deposit of compact to dense clean sand with a density of 2,000 kg/m^3 (125 pcf) changing to very dense sand at about 12.0 m (31 ft), probably ablation till. The groundwater table is encountered at a depth of 5.0 m (15 ft).

Comments Hidden in Mr. Trusting's letter is an omission which would cost the engineers in an ensuing litigation. The results of the two static tests were not analyzed! An effective stress analysis can easily be carried out on the records of the indicator pile test to show that the measured values of shaft resistance in the upper and lower sand layers correspond to beta ratios of 0.30 and 0.35, respectively and that the toe coefficient is 143 (the actual accuracy does not correspond to the precision of the numbers).

Had Mr. Trusting performed such an analysis, he would have realized that excavating the upper sand layer not only removed the small contribution to the shaft resistance in this layer, it also reduced the effective stress in the entire soil profile with a corresponding reduction of both shaft and toe resistance. In fact, applying the mentioned beta ratio and toe coefficient, the shaft and toe resistance values calculated after the excavation are 170 KN (19 tons) and 1200 KN (135 tons), respectively, to a total capacity of 1,366 KN (154 tons), a reduction to about half the original value. No wonder that the penetration resistance plummeted in restriking the piles! (Notice that the reduction of toe resistance is not strictly proportional to the change of effective overburden stress. Had the load-movement curve from the static loading test been analyzed to provide settlement parameters, a load-movement curve could have been determined for the post-excavation conditions. This would have resulted in an evaluated toe resistance being slightly larger toe resistance than the value mentioned above).

Obviously, there was no relaxation, no problem with the pile integrity, and the contractor had not damaged the piles when excavating the site. In the real case behind the story, the engineers came out of the litigation rather red-faced, but they had learnt the importance of not to exclude basic soil mechanics from their analyses and reports.

BEFORE EXCAVATION **AFTER EXCAVATION**

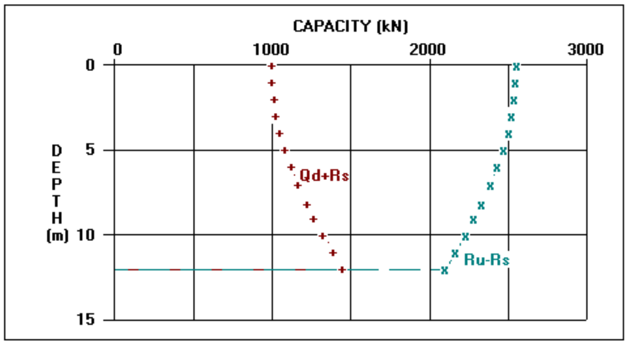

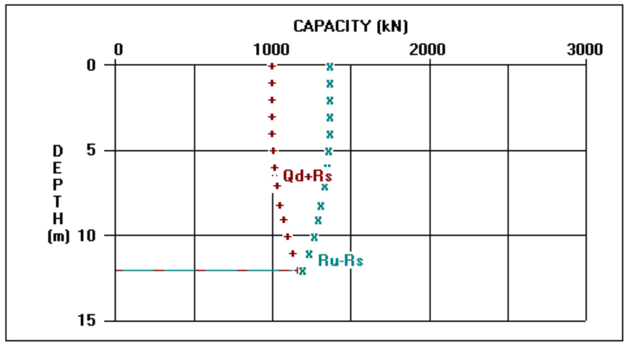

Example 12.5.4. The following problem deals with scour and it also originates in the real world. A couple of bridge piers are founded on groups of 18 inch (450 mm) pipe piles driven closed-toe through an upper 26 ft (8 m) thick layer of silty sand and 36 ft (11 m) into a thick deposit of compact sand. The dry-season groundwater table lies 6.5 ft (2 m) below the ground surface. During the construction work, a static loading test established the pile capacity to be 380 tons (3,400 KN), which corresponds to beta-coefficients of 0.35 and 0.50 in the silty sand and compact sand, respectively, and a toe bearing capacity coefficient of 60. The design load was 1,600 KN (180 tons), which indicates a factor of safety of 2.11—slightly more than adequate.

The static test had been performed during the dry season and a review was triggered when the question was raised whether the capacity would change during the wet season, when the groundwater table was expected to rise above the ground surface (bottom of the river). And, what would the effect be of scour? In the review, it was discovered that the upper 3 m (10 ft) of the soil could be lost to scour. However, in the design of the bridge, this had been thought to be inconsequential to the pile capacity.

A static analysis will answer the question about the effect on the pile capacity after scour. The distribution of pore water pressure is hydrostatic at the site and, in the Spring, when the groundwater table will rise to the ground surface (and go above), the effective overburden stress reduces. As a consequence of the change of the groundwater table, both pile shaft resistance and toe resistance reduce correspondingly and the new total resistance is 670 kips (3,000 KN). That is, the factor of safety is not 2.11 any more, but the somewhat smaller value of 1.86—not quite adequate.

When the effect of scour is considered, the situation worsens. The scour can be estimated to remove the soil over a wide area around the piers, which will further reduce the effective overburden stress. The capacity now becomes 275 tons (2,460 KN) and the factor of safety is only 1.51. The two diagrams below show the resistance distribution curves for the condition of the static loading tests and for when the full effect of scour has occurred. (The load distribution curve, $Q_d + R_s$, is not shown).

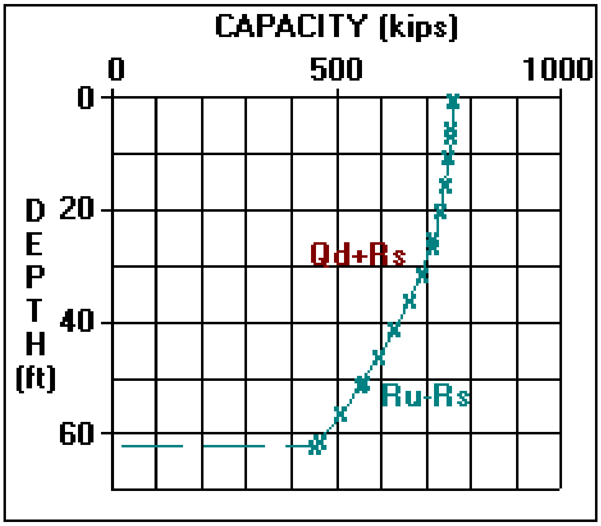

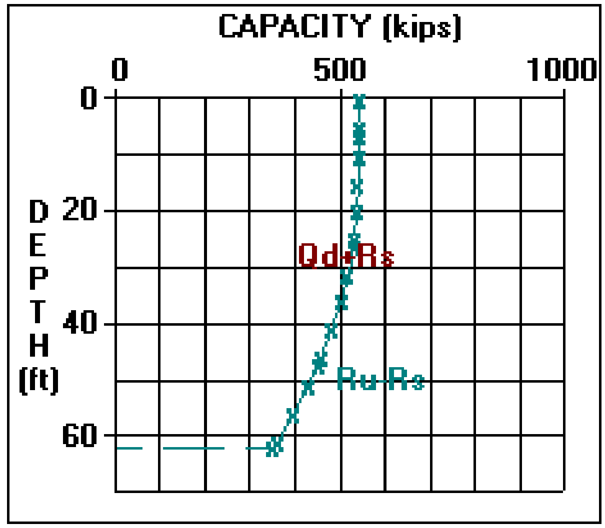

Missing the consequence of reduced effective stress is not that uncommon. The TRUSTING case history in the foregoing is an additional example. Fortunately, in the subject scour case, the consequence was no so traumatic. Of course, the review results created some excitement. And had the site conditions been different, for example, had there been an intermediate layer of settling soil, there would have been cause for some real concern. As it were, the load at the toe of the piles was considered to be smaller than the original ultimate toe resistance, and therefore, the reduced toe capacity due to reduced effective overburden stress would result in only small and acceptable pile toe penetration, that is, the settlement concerns could be laid to rest. In this case, therefore, it was decided to not carry out any remedial measures, but to keep a watchful eye on the scour conditions during the wet seasons to come. Well, a happy ending, but perhaps the solution was more political than technical.

12.6 Analysis of Pile Loading Tests

Example 12.6.1 Example 12.6.1 is from the testing of a 40 ft long H-pile. The pile description and the load-movement test data are as follows:

Head diameter, b	= 12.0 inches	Length, L	= 40.0 ft
Shaft area, A_s	= 4 ft^2/ft	Embedment, D	= 38.0 ft
Section area, A_{sz}	= 0.208 ft^2	Stick-up	= 2.0 ft
Toe diameter, b	= 12.0 inches	Toe area, A_t	= 1.0 ft^2
Modulus, E	= 29,000 ksi	EA/L	= 1,810 kips/inch

Row No.	Jack Load (kips)	Movement Average (inches)
1	0	0.000
2	60	0.007
3	120	0.019
4	180	0.036
5	240	0.061
6	300	0.093
7	360	0.149
8	420	0.230
9	480	0.399
10	540	0.926

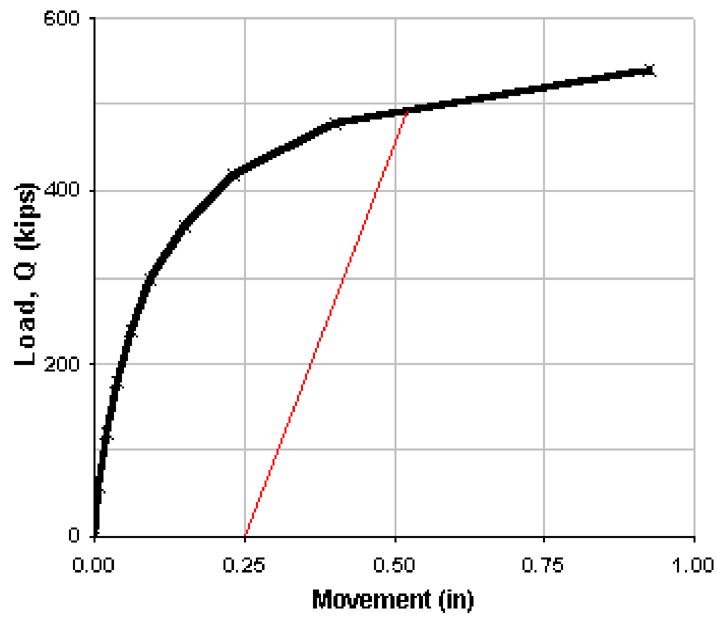

The load-movement diagram indicates that the pile capacity cannot be eyeballed from the load-movement diagram (change the scales of the abscissa and ordinate and the eyeballed value will change too). The offset limit construction is indicated in the load-movement diagram. The BrinchHansen, Chin-Kondner, and Decourt constructions are not shown, although these methods also work well for the case. However, neither the DeBeer nor the Curvature methods work very well for this case.

Example 12.6.2 is from the testing of a hexagonal 12-inch diameter, 112 ft long precast concrete pile. As evidenced from the load-movement diagram shown below, the pile experienced a very sudden failure (soil failure was established) at the applied load of 480 kips. This loading test is an example of when the various interpretation methods are superfluous. Remember, the methods are intended for use when an obvious capacity value is not discernible in the test.

Head diameter, b	= 12.0 inches	Length, L	= 112 feet	Modulus, E	= 7,350 ksi
Shaft area, A_s	= 3.464 ft^2/ft	Embedment, D	= 110 feet	EA/L	= 682 kips/inch
Section area, A_{sz}	= 0.866 ft^2	Toe diameter, b	= 12.0 inches	Toe area, A_t	= 0.866 ft^2
Stick-up	= 2 feet				

Row No.	Jack Load (kips)	Movement Average (inches)
1	0.0	0.000
2	30.0	0.017
3	39.6	0.036
4	88.8	0.061
5	119.2	0.091
6	149.8	0.124
7	177.8	0.166
8	211.0	0.209
9	238.0	0.253
10	271.0	0.305
11	298.2	0.355
12	330.4	0.414
13	357.6	0.473
14	390.2	0.540
15	420.8	0.630
16	450.4	0.694
17	481.0	0.804
18	509.0	0.912
19	500.0	1.314
20	492.4	1.787
21	489.8	2.046
22	480.4	2.472

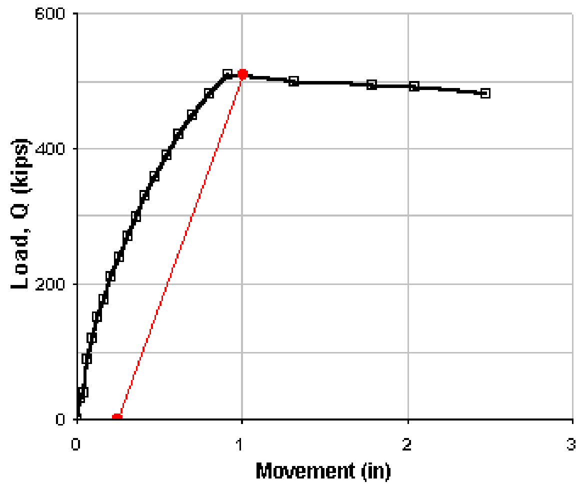

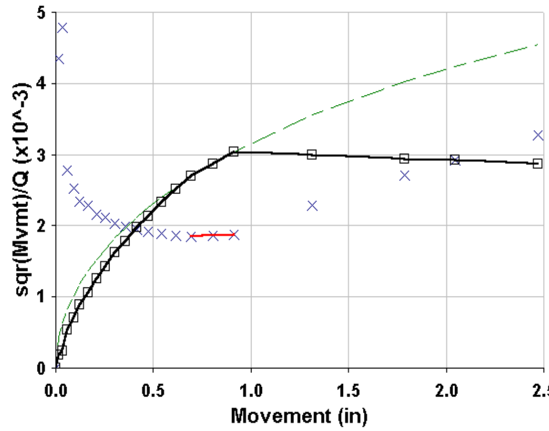

The test was aiming for a maximum load of 600 kips to prove out an allowable load of 260 kips with a factor of safety of 2.5. The 2nd diagram shows the Brinch Hansen construction and an extrapolation of the load-movement curve. Suppose the test had been halted at a maximum load at or slightly below the 480-kip maximum load. It would then have been easy to state from looking at the curve that the pile capacity is “clearly” much greater than 480 kip and show that “probably” the allowable load is safe as designed. This test demonstrates the importance of not extrapolating to a capacity higher than the capacity established in the test.

CHAPTER 13

PROBLEMS

13.1 Introduction

The following offers problems to solve and practice the principles presented in the preceding chapters. The common aspect of the problems is that they require a careful assessment of the soil profile and, in particular, the pore pressure distribution. They can all be solved by hand, although the computer and the UniSoft programs will make the effort easier.

13.2 Stress Distribution

Problem 13.2.1. At a construction site, the soil consists of an upper 6 metre thick compact sand layer, which at elevation +109.5 is deposited on layer of soft, overconsolidated clay. Below the clay, lies a 5 metre thick very dense, sandy coarse silt layer, which at elevation +97.5 is underlain by very dense glacial till followed by bedrock at elevation +91.5.

Borehole observations have revealed a perched groundwater table at elevation +113.5, and measurements in standpipe piezometer show the existence of an artesian water pressure in the silt layer with a phreatic elevation of +119.5. The piezometric head measured at the interface between the pervious bedrock and the glacial till is 15.0 metre.

Laboratory studies have shown index values and physical parameters of the soil to be as follows.

Parameter	Unit	Sand	Clay	Sandy Silt	Glacial till
ρ	kg/m^3	1,900	1,600	2,100	2,350
φ'	°	33	22	38	43
k	m/s	$1 \cdot 10^{-3}$	$1 \cdot 10^{-9}$	$1 \cdot 10^{-4}$	$1 \cdot 10^{-8}$
τ_u	KPa	--	24	--	--
c'	KPa	0	0	0	0
w_L	--	--	0.75	--	--
w_n	%	____	____	____	____
c_v	m^2/s	--	$20 \cdot 10^{-8}$	--	--
m	--	250	20	600	1,000
m_r	--	1,200	160	4,000	20,000
j	--	0.5	0	0.5	1

A. Calculate and tabulate the total stresses, the pore pressures, the effective stresses in the soil layers and **draw** (to scale) the corresponding pressure diagrams.

B. Calculate the water content, w_n, in the four soil layers assuming that the degree of saturation is 100 % and that the solid density of the soil material is 2,670 kg/m^3.

C. Assume that the pore pressure in the lower sandy silt layer was let to rise. (Now, how would Mother Nature be able to do this)? How high (= to what elevation) could the phreatic elevation in the sand layer rise before an unstable situation would be at hand?

The table may seem to contain redundant information. This is true if considering only parameters useful to calculate stresses. However, the "redundant" parameters are helpful when considering which soil layers have hydrostatic pore pressure distribution and which have a pore pressure gradient. (Notice, as the conditions are stationary, all pore pressure distributions are linear).

Problem 13.2.2. A three metre deep excavation will be made in a homogeneous clay soil with a unit weight of 16 KN/m^3. Originally, the groundwater elevation is located at the ground surface and the pore pressure is hydrostatically distributed. As a consequence of the excavation, the groundwater table will be lowered to the bottom of the excavation and, in time, again be hydrostatically distributed over the general site area. There are three alternative ways of performing the excavation, as follows:

A. First, excavate under water (add water to the hole as the excavation proceeds) and, then, pump out the water when the excavation is completed (1A and 1B).

B. First, lower the water table to the bottom of the excavation (assume that it will be hydrostatically distributed in the soil below) and, then, excavate the soil (2A and 2B).

Calculate and tabulate the soil stresses for the original conditions and for the construction phases, Phases 1A and 1B, and 2A, and 2B at depths 0 m, 3 m, 5 m, and 7 m. Compare the calculated effective stresses of the construction phases with each other, in particular the end results Phases 1B and 2B. Comment on the difference.

Problem 13.2.3. The soil profile at a site consists of a 3 metre thick upper layer of medium sand (density 1,800 kg/m^3) followed by 6 metre of clay (density 1,600 kg/m^3) and 4 metre of sand (density 2,000 kg/m^3) overlain dense glacial till (density 2,250 kg/m^3). Pervious bedrock is encountered at a depth of 16 metre. A perched water table exists at a depth of 1.0 metre. Two piezometers are installed to depths of 7 metre and 16 metre, respectively, and the pore pressure readings indicate phreatic pressure heights of 10 metre and 11 metre, respectively. It can be assumed that the soil above the perched water table is saturated by capillary action. The area is surcharged by a widespread load of 10 KPa.

Draw-to scale and neatly separate diagrams over effective overburden stress and pore pressures.

Problem 13.2.4. The soil profile at a site consists of a 4.0 m thick upper layer of medium sand (density 1,800 kg/m^3), which is followed by 8.0 m of clay (density 1,700 kg/m^3). Below the clay, a sand layer (density 2,000 kg/m^3) has been found overlying glacial till (density 2,100 kg/m^3) at a depth of 20.0 m deposited on bedrock at depth of 23.0 m. The bedrock is pervious. Two piezometers installed at depths of 18.0 m and 23.0 m, respectively, indicate phreatic pressure heights of 11.0 m and 19.0 m, respectively. There is a perched groundwater table in the upper sand layer at a depth of 1.5 m. The non-saturated but wet density of the sand above the perched groundwater table is 1,600 kg/m^3.

Draw-to scale and neatly-one diagram showing effective overburden stress and one separate diagram showing the pore pressure in the soil.

Problem 13.2.5. The soil profile at a very level site consists of a 1 m thick upper layer of coarse sand (density 1,900 kg/m^3) deposited on 5 m of soft clay (density 1,600 kg/m^3). Below the clay, silty sand (density 1,800 kg/m^3) is found. A piezometer installed at a depth of 8 m indicates a phreatic pressure height of 9 m. There is a seasonally occurring perched water table in the upper sand layer.

A very wide excavation will be carried out at the site to a depth of 4 m. Any water in the upper sand layer will be eliminated by means of pumping. The water pressure in the lower silty layer is difficult and costly to control. Therefore, it is decided not to try to lower it. Can the excavation be carried out to the planned depth? Your answer must be a "yes" or "no" and followed by a detailed rational supported by calculations.

Problem 13.2.6. The soil at a site consist of an upper 11 metre thick layer of soft, normally consolidated, compressible clay ($c_v = 2 \cdot 10^{-8}$ m^2/s, and unit weight = 16 KN/m^3) deposited on a 4 metre thick layer of overconsolidated, silty clay (cv = $10 \cdot 10^{-8}$ m^2/s, unit weight = 18 KN/m^3, and a constant overconsolidation value of 20 KPa) which is followed by a thick layer of dense, pervious sand and gravel with a unit weight of 20 KN/m^3.

The groundwater table is located at a depth of 1.0 metre. The phreatic water elevation at the bottom of the soft clay layer is located 1.0 metre above the ground surface. At depth 16.0 metre, the pore water pressure is equal to 190 KPa.

In constructing an industrial building (area 20 by 30 metre) at the site, the area underneath the building is excavated to a depth of 1.0 metre. Thereafter, a 1.2 metre thick, compacted backfill (unit weight = 20 KN/m^3) is placed over a vast area surrounding the building area. The building itself subjects the soil to a contact pressure of 80 KPa.

As a preparation for a settlement analysis, calculate and **draw** the effective stress distribution in the soil below the midpoint of the building. Notice, a settlement analysis requires knowledge of both the original effective stress and the final effective stress. Also, there is no need to carry the calculation deeper into the soil than where the change of effective stress ceases to result in settlement. Settlement in "dense sand and gravel" is negligible compared to settlement in clay and silt.

Problem 13.2.7. In sequence, a lake bottom profile consists of a 6 m thick layer of clayey mud (density = 1,700 kg/m^3), a 2 m thick layer of coarse sand (density = 2,000 kg/m^3), and a 3 m thick layer of glacial clay till (density = 2,200 kg/m^3) on pervious bedrock. The water depth in the lake is 3.0 m. Piezometer observations have discovered artesian pressure conditions in the sand layer: at a depth of 7.0 m below the lake bottom the phreatic height is 12 m. Other piezometers have shown a phreatic height of 10 m in the interface between the till and the bedrock.

A circular embankment with a radius of 9 m and a height of 1.5 m (assume vertical sides) will be placed on the lake bottom. The fill material is coarse sand and it will be placed to a density of 2,100 kg/m^3.

Calculate and **draw** (in a combined diagram) the final effective stress and pore pressure profile from the embankment surface to the bedrock. Assume 2:1 distribution of the fill load.

Problem 13.2.8. A structure will be built in a lake where the water depth is 1.5 m and the lake bottom soils consist of an upper 1.5 m thick layer of pervious "muck" followed by 2.5 m layer of overconsolidated clayey silt deposited on a layer of overconsolidated coarse sand. Fractured bedrock is encountered at a depth of 16.0 m below the lake bottom. A soils investigation has established that the soil densities are 1,500 kg/m^3, 1,850 kg/m^3, and 2,100 kg/m^3, respectively. Piezometers in the sand have shown an artesian head corresponding to a level of 2.0 m above the lake surface. The modulus numbers (m and m_r) in the silt and sand are 35 and 80, and 120 and 280, respectively. The stress exponents (silt and sand) are 0 and 0.5, respectively. The OCR in the silt is 2.5. The sand is preconsolidated to a constant preconsolidation stress-difference of 40 KPa.

The structure will be placed on a series of widely spaced footings, each loaded by 1,500 KN dead load (which load includes the weight of the footing material; no live load exists). The footings are 3.0 m by 4.0 m in area and constructed immediately on the silt surface. Before constructing the footings, the muck is dredged out over an area of 6.0 m by 8.0 m, which area will not be back-filled.

Calculate the original and final (after full consolidation) effective stresses and the preconsolidation stresses in the soil underneath the mid-point of the footing.

13.3 Settlement Analysis

Problem 13.3.1. The soil at a site consists of an upper, 2 metre thick layer of sand having a density of 1,900 kg/m^3 and a modulus number of 300. The sand layer is deposited on a very thick layer of clay having a density of 1,600 kg/m^3 and a modulus number of 40. The groundwater table is located at the ground surface and is hydrostatically distributed.

A 3 metre wide, square footing supporting a permanent load of 900 KN is to be located at a depth of either 0.5 metre or 1.5 metre. Which foundation depth will result in the largest settlement? (During the construction, the groundwater table is temporarily lowered to prevent flooding. It is let to return afterward. Also, consider that backfill will be placed around the footing. You may assume that the footing is either very thin or that it is made of "concrete" having the density of soil).

Problem 13.3.2. The soil at a site consists of 2 metre thick layer of organic clay and silt with a density of 1,900 kg/m^3 underlain by a layer of sand with a density of 2,000 kg/m^3 deposited at the depth of 5 metre on a 4 metre thick layer of silty clay with a density of 1,800 kg/m^3 followed by fractured bedrock. The groundwater table is located at a depth of 3.0 metre. The pressure head at the bedrock interface is 10 metre. The modulus number, m, of the clay and silt layer is 15. The sand layer can be considered overconsolidated by a constant value of 40 KPa and to have virgin modulus numbers, m, and reloading modulus numbers, m_r, of 120 and 250, respectively. Also the silty clay layer is overconsolidated, having an OCR-value of 2.0. Its virgin modulus and reloading modulus numbers are 30 and 140, respectively.

At the site, a building being 10 metre by 15 metre in plan area will be founded on a raft placed on top of the sand layer (after first excavating the soil). The load applied to the soil at the foundation level from the building is 12 MN. Around the building, a fill having a density of 1600 kg/m^3, will be placed to a height of 1.25 metre over an area of 50 by 50 metre and concentric with the building. Simultaneously with the construction of the building, the pore pressure at the bedrock interface will lowered to a phreatic height of 6 metre.

Determine the settlement of the sand and the silty clay layers assuming that all construction activities take place simultaneously and very quickly. You must calculate the settlement based on the stress change for each metre of depth. What would the settlement be if the fill had been placed well in advance of the construction of the building?

Problem 13.3.3. A 2.0 m deep lake with a surface elevation at +110.0 m will be used for an industrial development. The lake bottom consists of a 4 m thick layer of soft clayey silt mud followed by a 3-m layer of loose sand deposited on a 1 m thick layer of very dense glacial till. The pore pressures at the site are hydrostatically distributed. The soil densities are 1,600 kg/m^3, 1,900 kg/m^3, and 2,300 kg/m^3, respectively. The clay is slightly overconsolidated with an OCR of 1.2 and has virgin and reloading modulus numbers of 20 and 80. The sand OCR is 3.0 and the modulus numbers are 200 and 500. For the till, m = 1,000. To reclaim the area, the pore pressure in the sand layer will be reduced to a phreatic elevation of +107.0 m and a sand and gravel fill (density = 2,000 kg/m^3) will be dumped in the lake over a wide area and to a height of 2.5 m above Elevation +108.0. Although the lake, the fill rather, will be drained, it is expected that a perched groundwater table will always exist at Elevation +109.0.

Calculate the elevation of the surface of the fill when the soil layers have consolidated.

Problem 13.3.4. Is or are anyone of the following four soil profile descriptions in error? If so, which and why? Comment on all four descriptions and include an effective stress diagram for each of A through D.

A. A 10 m thick clay layer is deposited on a pervious sand layer, the groundwater table lies at the ground surface, the clay is overconsolidated, and the pore water pressure is hydrostatically distributed.

B. A 10 m thick clay layer is deposited on a pervious sand layer, the groundwater table lies at the ground surface, the clay is normally consolidated, and the pore water pressure is artesian.

C. A 10 m thick clay layer is deposited on a pervious sand layer, the groundwater table lies at the ground surface, the clay is undergoing consolidation, and the pore water pressure is linearly distributed.

D. A 10 m thick clay layer is deposited on a pervious sand layer, the groundwater table lies at the ground surface, the clay is preconsolidated, and the pore water pressure has a downward gradient.

Problem 13.3.5. Go back to stress-distribution Problem 13.2.8 and calculate the settlement of the footing assuming that all construction takes place at the same instant.

13.4 Earth Stress and Bearing Capacity of Shallow Foundations

Problem 13.4.1. An anchor-wall (used as dead-man for a retaining wall) consists of a 4 m wide and 3 m high wall (with an insignificant thickness) and is founded at a depth of 4 m in a non-cohesive soil having an effective friction angle of 32° and no cohesion intercept. The soil density is 1,900 kg/m^3 above the groundwater table and 2,100 kg/m^3 below. At times, the groundwater table will rise as high as to a depth of 2.0 m.

Calculate the ultimate resistance of the anchor wall to a horizontal pull and determine the allowable pulling load using a factor of safety of 2.5.

Problem 13.4.2. A trench in a deep soil deposit is excavated between two sheetpile rows installed to adequate depth and with horizontal support going across the trench. As the Engineer responsible for the design of the wall, you have calculated the earth stress acting against the sheetpile walls considering fully developed wall resistance, effective cohesion, and internal effective friction angle of the soil. You have also considered the weight of a wide body, heavy crawler rig traveling parallel and close to the trench by incorporating two line-loads of appropriate magnitude and location in your calculation. Your calculated factor of safety is low, but as you will be in charge of the inspection of the work and physically present at the site at all times, you feel that a low factor of safety is acceptable.

When visiting the site one day during the construction work, you notice that one track of the crawling rig travels on top of one of the sheetpile walls instead of on the ground next to the wall, as you had thought it would be. The load of the crawler track causes a slight, but noticeable downward movement of the so loaded sheetpile row.

Quickly, what are your immediate two decisions, if any? Then, explain, using text and clear sketches including force polygons, the qualitative effect—as to advantage or disadvantage—that the location of the crawler track has on the earth stress acting against the sheetpile wall.

Problem 13.4.3. As a part of a renewal project, a municipality is about to shore up a lake front property and, at the same time, reclaim some land for recreational use. To this end, a 6.0 m high L-shaped retaining wall will be built directly on top of the lake bottom and some distance away from the shore. Inside the wall, hydraulic sand fill will be placed with a horizontal surface level with the top of the wall. The wall is very pervious. The water depth in the lake is kept to 2.0 m. The lake bottom and the hydraulic fill soil parameters are density 1,900 kg/m^3 and 1,000 kg/m^3, and effective friction angle 37° and 35°, respectively, and zero effective cohesion intercept.

Calculate the earth stress against the retaining wall.

Problem 13.4.4. The soil at a site consists of a thick layer of sand with a unit weight of 18 KN/m^3 above the groundwater table and 20 KN/m^3 below the groundwater table. The effective friction angle of the sand is 34° above the groundwater table and 36° below. At this site, a column is founded on a footing having a 3 m by 4 m plan area and its base at a depth of 2.1 m, which is also the depth to the groundwater table. Acting at the ground surface and at the center of the column, the column is loaded by a vertical load of 2,100 KN and a 300 KN horizontal load parallel to the short side of the footing. There is no horizontal load parallel to the long side. Neither is there any surcharge on the ground surface.

Calculate the factor of safety against bearing failure. In the calculations, assume that the column and footing have zero thickness and that the natural soil has been used to backfill around the footing to a density equal to that of the undisturbed soil.

Considering that the bearing capacity formula is a rather dubious model of the soil response to a load, verify the appropriateness of the footing load by calculating the footing settlement using assumed soil parameters typical for the sand.

Problem 13.4.5. A 3.0 m wide strip footing ("strip" = infinitely long) is subjected to a vertical load of 360 KN/linear-metre. Earth stress and wind cause horizontal loads and a recent check on the foundation conditions has revealed that, while the factors of safety concerning bearing capacity and sliding modes are more than adequate, the magnitude of the edge stress is right at the allowable limit. How large is the edge stress?

Problem 13.4.6 A footing for a continuous wall supports a load of 2,000 KN per metre at a site where the soil has a density of 1,900 kg/m^3, an effective cohesion intercept of 25 KPa, and an effective friction angle of 33°. The footing is placed at a depth of 1.0 m which also is the depth to the groundwater table.

Determine the required width of the wall base (footing) to the nearest larger 0.5 m using a Global Factor of Safety of 3.0 and compare this width with the one required by the OHBDC in a ultimate limit states, ULS, design).

13.5 Deep Foundations

Problem 13.5.1. A group of 16 precast concrete piles, circular in shape with a diameter of 400 mm and concrete strength of 50 MPa, will be installed in a square configuration to an anticipated embedment depth of 15.0 m at a site where the soil consists of a 10 m thick upper layer of overconsolidated clay deposited on a thick layer of dense sand. The preconsolidation pressure of the clay is 25 KPa above the existing effective stress. There is a groundwater table at the ground surface. The phreatic elevation in the sand layer lies 2.0 m above the ground surface. With time, it is expected to be lowered by 1.0 m.

The clay parameters are**:** density 1,600 kg/m^3, angle of effective friction 29 degrees, and the modulus numbers are 25 and 250, respectively. The sand parameters are**:** density 2,000 kg/m^3, angle of effective friction 38 degrees, and modulus number 250. The MK_s-ratio in the clay and in the sand are 0.6 and 1.0, respectively. The toe bearing capacity coefficient is 2.0 times the N_q coefficient. ($\beta = MK_s \tan\phi'$).

The piles will be placed at a minimum center-to-center spacing of 2.5 times the pile diameter plus 2.0 % of the anticipated embedment length. The structurally allowable stress at the pile cap is 0.3 times the cylinder strength. It is the intent to apply to the pile group a dead load of 16 times the allowable dead load, 16 times 600 KN, and it can be assumed that this load is evenly distributed between the piles via a stiff pile cap cast directly on the ground.

An 1.0 m thick backfill will be placed around the pile cap to a very large width. The fill consists of granular material and its density is 2,000 kg/m^3.

A. What is the allowable live load per pile for a global factor of safety of 2.5?

B. What is the factored total resistance of a single pile in the group according to the OHBDC?

C. Find the location of the neutral plane in a diagram drawn neatly and to scale and determine the future maximum load in the pile.

D. Are the loads structurally acceptable?

E. Estimate the settlement of the pile group assuming that the shortening of the piles can be neglected.

Problem 13.5.2. An elevated road is to be built across a lake bay, where the water surface is at Elevation +10.0 and the water depth is 2.0 m. The lake bottom consists of a 12 m thick layer of compressible, normally consolidated silty clay deposited on a 40 m thick layer of sand on bedrock. The pore water pressure in the clay is hydrostatically distributed.

The causeway will be supported on a series of pile bents. Each bent will consist of a group of eight, 0.3 m square piles installed to Elevation -22.0 m in three equal rows at an equal spacing of 5 diameters (no pile in the center of the group). In both the clay and the sand layer, and for both positive and negative resistance, the value of MK_s is 0.6. The clay and the sand layers have unit weights of 16 KN/m^3 and 20 KN/m^3, and friction angles of 29° and 37°, respectively. The effective cohesion intercept is zero for both layers. The modulus numbers and stress exponents are 50 and 280, and 0 and 0.5, respectively. The N_t-coefficient is 60. (Lead: calculate $\beta = MK_s \tan\phi'$).

To provide lateral restraint for the piles, as well as establish a working platform above water, a sand fill is placed at the location of each bent. Thus, the sand fill will be permanent feature of each pile bent. The sand fill is 4.0 m thick and covers a 10 by 10 m square area. The sand fill has a saturated unit weight of 20 KN/m^3. Assume that the total unit weight of the sand fill is the same above as below the lake surface and that the shaft resistance in the fill can be neglected.

A. Calculate and plot the distribution of the ultimate soil resistance along a single pile assuming that positive shaft resistance acts along the entire length of the pile and that all excess pore pressure induced by the pile driving and the placement of the sand fill have dissipated.

B. Determine the allowable live load (for a single pile) acting simultaneously with a dead load of 900 KN and using a global factor of safety of 3.0.

C. Calculate the consolidation settlement for the pile group. Then, draw the settlement distribution in the sand. (Assume that the sand fill has vertical sides).

Problem 13.5.3. Typically, a single pile in a specific large (many piles) pile group has a capacity of 200 tons, is assigned a toe resistance of 110 tons, and the allowable dead load is 80 tons. There is no live load acting on the pile group. The soil is homogeneous and large settlement is expected throughout the soil profile. The piles consist of pipes driven open-toe (open-ended) into the soil and connected by means of a stiff pile cap. In driving, the inside of the pipe fills up with soil that afterward is drilled and cleaned out—of course, taking care not to disturb the soil at and below the pile toe. The pipe is then filled with concrete and the short column strength of the concreted pipe is 300 tons. By mistake, when cleaning one pile, the work was continued below the pile toe leaving a void right at the pile toe that was not discovered in time. The concreting did not close the void. The pile shaft was not affected, however, and the pile itself is structurally good. As the geotechnical engineer for the project, you must now analyze the misshapen pile and recommend an adjusted allowable load for this pile. Give your recommendation and justify it with a sketch and succinct explanations.

Problem 13.5.4. The Bearing Graph representative for the system (hammer, helmet cushion) used for driving a particular pile into a very homogeneous non-cohesive soil of a certain density at a site is given by the following data points**:** [600 KN/1; 1,000/2; 1,400/4; 1,600/6; 1,700/8; and 1,900/20 blows/inch**—** that is, ultimate resistance/penetration resistance]. The groundwater table at the site lies at the ground surface and the pore pressure distribution is hydrostatic. The pile is driven open-toe and can be assumed to have no toe resistance (no plug is formed). At the end-of-initial-driving, the penetration resistance is 3 blows/inch and, in restriking the pile a few days after the initial driving, the penetration resistance is 12 blows/inch. This difference is entirely due to pore pressures which were developed and present during initial driving, but which had dissipated at restriking. On assuming that the soil density is either 2,000 kg/m^3 or 1,800 kg/m^3 (i. e., two cases to analyze), determine the average excess pore pressure present during the initial driving in relation to (= in % of) the pore pressure acting during the restriking.

Notice, you will need to avail yourself of a carefully **drawn** bearing graph using adequately scaled axes.

Problem 13.5.5. Piles are being driven for a structure at a site where the soils consist of fine sand to large depth. The density of the sand is 2,000 kg/m^3 and the groundwater table lies at a depth of 3.0 m. The piles are closed-toe pipe piles with a diameter (O. D.) of 12.75 inch. The strength parameters of the soil (the beta and toe bearing coefficients) are assumed to range from 0.35 through 0.50 and 20 through 80, respectively. A test pile is installed to an embedment depth of 15.0 m.

A. Determine the range of bearing capacity to expect for the 15-m test pile (i. e., its minimum and maximum capacities).

B. A static loading test is now performed on the test pile and the pile capacity is shown to be 1,400 KN. Assume that the <u>beta coefficients</u> are of the same range as first assumed (i. e., 0.35 through 0.50) and determine the capacity range for a new pile driven to an embedment depth of 18 m.

Problem 13.5.6. The soil profile at a site consist of a 2.0 m thick layer of silt (ρ = 1,700 kg/m^3) followed by a thick deposit of sand (ρ = 2,050 kg/m^3). The groundwater table is located at a depth of 0.5 m and the pore pressures are hydrostatically distributed.

At the site, an industrial building is considered which will include a series of columns (widely apart), each transferring a permanent (dead) vertical load of 1,000 KN to the soil. The groundwater table will be lowered to a new stable level at a depth of 1.5 m below the ground surface.

A foundation alternative for the columns is to install 0.25 m diameter square piles to a depth of 10.0 m joined by a cap at the ground surface. The beta-parameters of the silt and sand are 0.35 and 0.55, respectively, and the bearing capacity coefficient of the sand is 50.

Calculate using effective stress analysis how many piles that will be needed at each column if the Factor-of-Safety is to be at least 2.5.

CHAPTER 14

REFERENCES

AASHTO Specifications, 1992. Standard specifications for highway bridges, 15th Edition. American Association of State Highway Officials, Washington.

Altaee, A., Evgin, E., and Fellenius, B.H., 1992. Axial load transfer for piles in sand. I: Tests on an instrumented precast pile. Canadian Geotechnical Journal, 29(1) 11-20.

Altaee, A., Evgin, E., and Fellenius, B.H., 1993. Load transfer for piles in sand and the critical depth. Canadian Geotechnical Journal, 30(2) 465-463.

Altaee, A. and Fellenius, B.H., 1994. Physical modeling in sand. Canadian Geotechnical Journal, 31(3) 420-431.

Amini, A, Fellenius, B.H., Sabbagh, M., Naesgaard, E., and Buehler, M., 2008. Pile loading tests at Golden Ears Bridge. 61st Canadian Geotechnical Conference, Edmonton, September 21-24, 2008, Preprint, 8 p.

Athanasopoulos, G.A., 2007. Discusssion on Liquefaction susceptibility criteria for silt and clays. ASCE J. Geotechnical and Geoenvironmental Engineering, (134)7 1025-1027.

Athanasopoulos, G.A., 2007. Discusssion on Assessment of the liquefaction susceptibility of fine-grained soils. ASCE J. Geotechnical and Geoenvironmental Engineering, (134)7 1028-1030.

Authier, J. and Fellenius, B.H., 1980. Quake values determined from dynamic measurements. Proceedings of the First International Seminar on Application of Stress-Wave Theory to Piles, H. Bredenberg Editor, A. A. Balkema, Rotterdam, pp. 197 - 216.

Baldi, G., Bellotti, R., Ghiona, R., Jamiolkowski, M., and Pasqualini, E., 1986. Interpretation of CPTs and CPTUs. 2nd Part: Drained penetration of sands. Proceedings of the Fourth International Geotechnical Seminar on Field Instrumentation and In-situ Measurements, Singapore November 25-27, 1986, 143-156.

Baligh, M. , Vivatrat, V., Wissa, A., Martin R., and Morrison, M., 1981. The piezocone penetrometer. Proceedings of Symposium on Cone Penetration Testing and Experience, ASCE National Convention, St. Louis, October 26 - 30, pp. 247 - 263.

Barbie, D.L, Reece, B.D., and Eames, D.R., 2005. Water Resources Data--Texas, Water Year 2004, Volume 6, Ground-Water Data". U.S. Geological Survey, Texas Water Science Center, Water-Data Report TX-04-6, 754 p.

Barker, R.M., Duncan, J.M., Rojiani, K.B., Ooi, P.S. K, Tan, C.K., and Kim, S.G., 1991. Manual for the design of bridge foundations. National Cooperative Highway Research Programme, Report 343, Transportation Research Board, Washington, D. C., 308 p.

Barron R.A., 1948. Consolidation of fine-grained soils by drain wells. ASCE Transactions, Vol. 113 718-742.

Bean K., Jefferies M.G., and Hachey, J. 1991. The critical state of sand, Geotechnique 41(3) 365 381.

Begemann, H.K.S., 1953. Improved method of determining resistance to adhesion by sounding through a loose sleeve placed behind the cone. Proceedings of the 3rd International Conference on Soil Mechanics and Foundation Engineering, ICSMFE, August 16 - 27, Zurich, Vol. 1, pp. 213 - 217.

Begemann, H.K.S., 1963. The use of the static penetrometer in Holland. New Zealand Engineering, 18(2) 41.

Begemann, H.K.S., 1965. The friction jacket cone as an aid in determining the soil profile. Proceedings of the 6th International Conference on Soil Mechanics and Foundation Engineering, ICSMFE, Montreal, September 8 - 15, Vol. 2, pp. 17 - 20.

Bjerrum L. and Johannessen, I.J. 1965. Measurements of the compression of a steel pile to rock due to settlement of the surrounding clay. Univ. of Toronto Press. Proceedings 6th International Conference on Soil Mechanics and Foundation Engineering, Montreal, September 8 - 15, Vol. 2, pp. 261 - 264.

Boardman, T.B., 2007. Discusssion on Assessment of the liquefaction susceptibility of fine-grained soils. ASCE J. Geotechnical and Geoenvironmental Engineering, (134)7 1030-1031.

Bowles, J.E., 1988. Foundation analysis and design, Fourth Edition. McGraw-Hill Book Company, New York, 1004 p.

Boussinesq, J., 1885. Application des potentiels a l'etude de l'equilibre et due mouvement des solids elastiques. Gauthiers-Villars, Paris, (as referenced by Holtz and Kovacs, 1981).

Briaud J-L and Gibbens R.M., 1994. Predicted and measured behavior of five spread footings on sand. Proceedings of a Symposium sponsored by the Federal Highway Administration at the 1994 ASCE Conference Settlement '94. College Station, Texas, June 16 - 18, pp. 192- 128.

Briaud, J.-L., and Gibbens, R. M., 1999. Behavior of five large spread footings in sand. ASCE J. Geotechnical and Geoenvironmental Engineering 125(9) 787 796.

Briaud, J-L, Nicks J, Rhee, K., and Stieben, G., 2006. San Jacinto Monument case history. ASCE J. Geotechnical and Geoenvironmental Engineering, (133)11 1337-1351.

Bray, J.D. and Sancio, R.B., 2006. Assessment of the liquefaction susceptibility of fine-grained soils. ASCE J. Geotechnical and Geoenvironmental Engineering, (132)11 1165-1187.

Bray, J.D. and Sancio, R.B., 2007. Closure to Discusssion on Assessment of the liquefaction susceptibility of fine-grained soils. ASCE, J. Geotechnical and Geoenvironmental Engineering, (134)7 1031-1034.

Brown, M.J., Hyde, A.F.L., and Anderson, W.F. (2006). Analysis of a rapid load test on an instrumented bored pile in clay, Geotechnique, 56(9), 627-638.

Brown, M.J. and Hyde, A.F.L. (2008). Rate effects from pile shaft resistance measurements'', Can. Geot. J., 45(3) 425-431.

Boulanger, R.W. and Idriss, I.M., 2006. Liquefaction susceptibility criteria for silt and clays. ASCE J. Geotechnical and Geoenvironmental Engineering, (132)9 1413-1426.

Boulanger, R.W. and Idriss, I.M., 2007. Closure to Discusssion on Liquefaction susceptibility criteria for silt and clays. ASCE J. Geotechnical and Geoenvironmental Engineering, (134)7 1027-1028.

Bozozuk, M., Fellenius, B.H. and Samson, L., 1978. Soil disturbance from pile driving in sensitive clay. Canadian Geotechnical Journal, 15(3) 346-361.

Buisman, A.S.K., 1935. De weerstand van paalpunten in zand. De Ingenieur, No. 50, pp. 25 - 28 and 31 - 35. (As referenced by Vesic, 1973).

Buisman, A.S.K., 1940. Grondmechanica. Walman, Delft, 281 p. (As referenced by Vesic, 1973, and Tschebotarioff, 1951).

Bullock, P., Schmertmann, J., McVay, M.C., and Townsend, F.C., 2005. Side shear set-up. Test piles driven in Florida. ASCE Journal of Geotechnical and Geoenvironmental Engineering, 131(3) 292-310.

Campanella, RG.., Gillespie, D., and Robertson, P.K., 1982. Pore pressures during cone penetration testing, Proceedings of the 2nd European Symposium on Penetration Testing, ESOPT-2, Amsterdam, May 24 - 27, Vol. 2, pp. 507 - 512.

Campanella, R.G., and Robertson, P.K., 1988. Current status of the piezocone test. Proceedings of First International Symposium on Penetration Testing, ISOPT-1, Orlando, March 22 - 24, Vol. 1, pp. 93 - 116.

Campanella, R.G., Robertson, P.K., Davies, M.P., and Sy, A., 1989. Use of in-situ tests in pile design. Proceedings 12th International Conference on Soil Mechanics and Foundation Engineering, ICSMFE, Rio de Janeiro, Brazil, Vol. 1, pp. 199 - 203.

Canadian Foundation Engineering Manual, CFEM, 1985. Second Edition. Canadian Geotechnical Society, BiTech Publishers, Vancouver, 456 p.

Canadian Foundation Engineering Manual, CFEM, 1992. Third Edition. Canadian Geotechnical Society, BiTech Publishers, Vancouver, 512 p.

Canadian Foundation Engineering Manual, CFEM, 2006. Fourth Edition. Canadian Geotechnical Society, BiTech Publishers, Vancouver, 488 p.

Canadian Highway Bridge Design Code, CAN/CSA-S6 2006. Code and Commentary, Tenth edition. Canadian Standards Association, Toronto, Ontario, 800 pages.

Caquot, A. and Kerisel J., (1953) Sur le terme de surface dans le calcul des fondations en mileu pulverent. Proceedings Third International Conference on Soil Mechanics and Foundation Engineering, Zurich, Vol. 1, pp. 336-337.

Carillo, N., 1942. Simple two- and three-dimensional cases in the theory of consolidation of soils. Journal of Mathematics and Physics, Vol. 121, pp. 1 - 5.

Casagrande, A., 1935. Characteristics of cohesionless soil affecting the stability of slopes and earth fills. Journal of the Boston Society of Soil Mechanics. Vol. 23, pp. 13-32.

Casagrande, L. and Poulos, S., 1969. On the effectiveness of sand drains. Canadian Geotechnical Journal, 6(3) 287-326.

Chai, J.C., Carter, J.P., and Hayashi, S., 2005. Ground deformation induced by vacuum consolidation. ASCE Journal for Geotechnical and Geoenvironmental Engineering, 131(12) 1552-1561.

Chai, J.C., Carter, J.P., and Hayashi, S., 2006. Vacuum consolidation and its combination with embankment loading. Canadian Geotechnical Journal 43(10) 985-996.

Chang, Y.C.E., Broms, B., and Peck, R.B., 1973. Relationship between settlement of soft clays and excess pore pressure due to imposed loads. Proc. 8th International Conference on Soil Mechanics and Foundation Engineering, ICSMFE, Moscow, Vol. 1.1, pp. 93 - 96.

Chin, F.K. 1970. Estimation of the ultimate load of piles not carried to failure. Proceedings of the 2nd Southeast Asian Conference on Soil Engineering, pp. 81-90.

Chin, F.K., 1971. Discussion on pile test. Arkansas River project. ASCE Journal for Soil Mechanics and Foundation Engineering, 97(SM6) 930-932.

Chin, F.K., 1978. Diagnosis of pile condition. Lecture at 6th Southeast Asian Conference on Soil Engineering, Bangkok, 1977, Geological Engineering, Vol. 9, pp. 85 - 104.

Clausen, C.J.F., Aas, P.M., and Karlsrud, K., 2005. Bearing capacity of driven piles in sand, the NGI approach. Proceedings of International Symposium on Frontiers in Offshore Geotechnics, Perth Sept. 2005, A.A. Balkema Publishers, pp. 677 - 681.

Clausen, C.J.F., Aas, P.M., and Karlsrud, K., 2005. Bearing capacity of driven piles in sand, the NGI approach. Proceedings of Proceedings of International Symposium. on Frontiers in Offshore Geotechnics, Perth, September 2005, A.A. Balkema Publishers, pp. 574 - 580.

Coduto, D.P., 1994. Foundation design – Principles and practices. Prentice Hall 796 p.

Cortlever, N.G., Visser, G.T, and deZwart, T.P., 2006. Geotechnical History of the development of the Suvarnabhumi International Airport. Special Issue of the Journal of South-East Asian Geotechnical Society, December 2006, 37(3) 189-194.

Dahlberg, R. Settlement Characteristics of Preconsolidated Natural Sands. Swedish Council for Building Research, Document D1:1975, 315 p.

Davisson, M. T., 1972. High capacity piles. Proceedings of Lecture Series on Innovations in Foundation Construction, ASCE Illinois Section, Chicago, March 22, pp. 81 - 112.

DeBeer, E.E., 1968. Proefondervindlijke bijdrage tot de studie van het grensdraag vermogen van zand onder funderingen op staal. Tijdshift der Openbar Verken van Belgie, No. 6, 1967 and No. 4, 5, and 6, 1968.

DeBeer, E.E. and Walays, M., 1972. Franki piles with overexpanded bases. La Technique des Travaux, Liege, Belgium, No. 333.

Deep Foundations Institute, DFI, 1979. A pile inspector’s guide to hammers, Sparta, New Jersey, 41 p.

DeRuiter, J. and Beringen F.L., 1979. Pile foundations for large North Sea structures. Marine Geotechnology, 3(3) 267-314.

Douglas, B.J., and Olsen, R.S., 1981. Soil classification using electric cone penetrometer. ASCE Proceedings of Conference on Cone Penetration Testing and Experience, St. Louis, October 26 - 30, pp. 209 - 227.

Endley, S.N., Yeung, A.T., and Vennalaganti, K.M, 1996. A study of consolidation characteristics of Gulf Coast clays. Proceedings of Texas Section of ASCE, Fall Meeting, San Antonio, Texas, September 18-21, 152-160.

Endo M., Minou, A., Kawasaki T, and Shibata, T,1969. Negative skin friction acting on steel piles in clay. Proc. 8th International Conference on Soil Mechanics and Foundation Engineering, Mexico City, August 25 - 29, Vol. 2, pp. 85- 92.

Erwig, H., 1988. The Fugro guide for estimating soil type from CPT data. Proceedings of Seminar on Penetration Testing in the UK, Thomas Telford, London, pp. 261 - 263.

Eslami, A., and Fellenius, B.H., 1995. Toe bearing capacity of piles from cone penetration test (CPT) data. Proceedings of the International Symposium on Cone Penetration Testing, CPT 95, Linköping, Sweden, October 4 - 5, Swedish Geotechnical Institute, SGI, Report 3:95, Vol. 2, pp. 453 - 460.

Eslami, A., and Fellenius, B.H., 1996. Pile shaft capacity determined by piezocone (CPTu) data. Proceedings of 49th Canadian Geotechnical Conference, September 21 - 25, St. John's, Newfoundland, Vol. 2, pp. 859 - 867.

Eslami, A., 1996. Bearing capacity of piles from cone penetrometer test data. Ph. D. Thesis, University of Ottawa, Department of Civil Engineering, 516 p.

Eslami, A. and Fellenius, B.H., 1997. Pile capacity by direct CPT and CPTu methods applied to 102 case histories. Canadian Geotechnical Journal, 34(6) 886–904.

Eurocode, 1990. Eurocode, Chapter 7, Pile Foundations (preliminary draft), 25 p.

Fellenius, B.H., 1972. Bending of piles determined by inclinometer measurements. Canadian Geotechnical Journal 9(1) 25-32.

Fellenius B.H., 1975. Reduction of negative skin friction with bitumen slip layers. Discussion. ASCE 101(GT4) 412-414.

Fellenius B.H., 1975. Test loading of piles. Methods, interpretation and new proof testing procedure. ASCE 101(GT9) 855-869.

Fellenius B.H., 1977. The equivalent sand drain diameter of the bandshaped drain. Discussion. Proc. 9th International Conference on Soil Mechanics and Foundation Engineering, ICSMFE, Tokyo, Vol. 3, p. 395.

Fellenius B.H., 1979. Downdrag on bitumen coated piles. Discussion. ASCE 105(GT10) 1262-1265.

Fellenius, B.H., 1981. Consolidation of clay by band-shaped premanufactured drains. Discussion. Ground Engineering, London, 14(8) 39-40.

Fellenius, B.H., 1984. Ignorance is bliss — And that is why we sleep so well. Geotechnical News, 2(4) 14-15.

Fellenius, B.H., 1984. Negative skin friction and settlement of piles. Proceedings of the Second International Seminar, Pile Foundations, Nanyang Technological Institute, Singapore, 18 p.

Fellenius, B.H., 1988. Unified design of piles and pile groups. Transportation Research Board, Washington, TRB Record 1169, pp. 75-82.

Fellenius, B.H., 1989. Tangent modulus of piles determined from strain data. The ASCE Geotechnical Engineering Division, 1989 Foundation Congress, Edited by F. H. Kulhawy, Vol. 1, pp. 500 - 510.

Fellenius, B.H., 1994. Limit states design for deep foundations. FHWA International Conference on Design and Construction of Deep Foundations, Orlando, December 1994, Vol. II, pp. 415 - 426.

Fellenius, B.H., 1995. Foundations. Chapter 22 in Civil Engineering Handbook, Edited by W. F. Chen. CRC Press, New York, pp. 817 - 853.

Fellenius, B.H., 1996. Reflections on pile dynamics. Proceedings of the 5th International Conference on the Application of Stress-Wave Theory to Piles, September 10 through 13, Orlando, Florida, Edited by M.C. McVay, F. Townsend, and M. Hussein, Keynote Paper, pp. 1 - 15.

Fellenius, B.H., 1998. Recent advances in the design of piles for axial loads, dragloads, downdrag, and settlement. Procs. of a Seminar by ASCE and Port of New York and New Jersey, April 1998, 19 p.

Fellenius, B.H., 1999. Bearing capacity of footings and piles—A delusion? Proceedings of the Deep Foundation Institute Annual Meeting, October 14 though 16, Dearborn 17 p.

Fellenius, B.H., 2000. The O-Cell — A brief introduction to an innovative engineering tool. Väg- och Vattenbyggaren 47(4) 11-14.

Fellenius, B.H., 2002a. Determining the resistance distribution in piles. Part 1: Notes on shift of no-load reading and residual load. Part 2: Method for Determining the Residual Load. Geotechnical News Magazine. Geotechnical News Magazine, (20) 2 35-38, and (20)3 25-29.

Fellenius, B.H., 2002b. Pile Dynamics in Geotechnical Practice — Six Case Histories. ASCE International Deep Foundation Congress, An International Perspective on Theory, Design, Construction, and Performance, Geotechnical Special Publication No. 116, Edited by M.W. O'Neill, and F.C. Townsend, Orlando Florida February 14 - 16, 2002, Vol. 1, pp. 619 - 631.

Fellenius, B.H., 2004. Unified design of piled foundations with emphasis on settlement analysis. "Honoring George G. Goble — Current Practice and Future Trends in Deep Foundations"

GeoInstitute Geo-TRANS Conference, Los Angeles, July 27-30, 2004, Edited by J.A. DiMaggio and M.H. Hussein. ASCE Geotechnical Special Publication, GSP 125, pp. 253-275.

Fellenius, B.H., 2008. Effective stress analysis and set-up for shaft capacity of piles in clay. "Honoring John Schmertmann — "From Research to practice in Geotechnical Engineering", ASCE Geotechnical Special Publication, Edited by J.E. Laier, D.K. Crapps, and M.H. Hussein, GSP180, pp. 384-406.

Fellenius B.H., Samson, L., Thompson, D. E. and Trow, W., 1978. Dynamic Behavior of foundation piles and driving equipment. Terratech Ltd. and the Trow Group Ltd., Final Report, Department of Supply and Services, Canada, Contract No. 1ST77.00045, Vol. I and II, 580 p.

Fellenius, B.H., Riker, R. E., O'Brien, A. J. and Tracy, G. R., 1989. Dynamic and static testing in a soil exhibiting setup. ASCE Journal of Geotechnical Engineering, 115(7) 984-1001.

Fellenius, B.H. and Altaee, A., 1994. The critical depth—How it came into being and why it does not exist. Proceedings of the Institution of Civil Engineers, Geotechnical Engineering Journal, London, 113(2) 107 111.

Fellenius, B.H. and Altaee, A., 1996. The critical depth – How it came into being and why it does not exist. Reply to Discussion. Proceedings of the Institution of Civil Engineers, Geotechnical Engineering Journal, London, 119(4) 244-245.

Fellenius, B.H., Altaee, A., Kulesza, R, and Hayes, J, 1999. O-cell Testing and FE analysis of a 28 m Deep Barrette in Manila, Philippines. ASCE Journal of Geotechnical and Environmental Engineering, 125(7) 566-575.

Fellenius, B.H., Brusey, W. G., and Pepe, F., 2000. Soil set-up, variable concrete modulus, and residual load for tapered instrumented piles in sand. ASCE Specialty Conference on Performance Confirmation of Constructed Geotechnical Facilities, University of Massachusetts, Amherst, April 9 - 12, 2000, Special Geotechnical Publications, GSP94, pp. 98 - 114.

Fellenius, B.H. and Eslami, A., 2000. Soil profile interpreted from CPTu data. Proceedings of Year 2000 Geotechnics Conference, Southeast Asian Geotechnical Society, Asian Institute of Technology, Bangkok, Thailand, November 27-30, 2000, Editors Balasubramaniam, A.S., Bergado, D.T., Der Gyey, L., Seah, T.H., Miura, K., Phien wej, N., and Nutalaya, P., Vol. 1, pp. 163-171.

Fellenius, B.H., and Infante, J-A, 2002. UniCone Version 1 Users Manual, UniSoft Ltd., Calgary, 33 p.

Fellenius, B.H., Harris, D., and Anderson, D.G., 2004. Static loading test on a 45 m long pipe pile in Sandpoint, Idaho. Canadian Geotechnical Journal 41(4) 613-628.

Fellenius, B.H. and Massarsch, K.M., 2008. Comments on the current and future use of pile dynamic testing. Keynote Lecture, The 8th International Conference on the Application of Stress Wave Theory to Piles. Edited by L.A. Santos, Lisbon September 8 10, 2008, pp. 7-17.

Fellenius, B.H. and Siegel, T.C, 2008. Pile design consideration in a liquefaction event. ASCE Journal of Geotechnical and Environmental Engineering, 132(9) 1312-1416.

Fellenius, B.H. and Ochoa, M., 2009. San Jacinto Monument Case History. Discussion. ASCE Journal of Geotechnical Engineering, 133(1) 162-167.

Fellenius, B.H. and Ochoa, M., 2009. Testing and design of a piled foundation project. A case history. Journal of the Southeast Asian Society 40(3).

Fellenius, B.H. and Tan, S.A., 2010. Combination of O-cell test and conventional head-down test. "Honoring Clyde Baker—the Art of Foundation Engineering Practice", ASCE Geotechnical Special Publication, Edited by M.H. Hussein, J.B. Anderson, and W. Camp, GSP.

Finno, R. J., 1989. Subsurface conditions and pile installation data. American Society of Civil Engineers, Proceedings of Symposium on Predicted and Observed Behavior of Piles, Evanston, June 30, ASCE Geotechnical Special Publication, GSP23, pp. 1 - 74.

Gilboy G., 1928. The compressibilty of sand-mica mixtures. Proceedings of ASCE Vol. 54, 555-568.

Goossens, D. and VanImpe, W.F., 1991. Long-term settlement of a pile group foundation in sand, overlying a clayey layer. Proceedings 10th European Conference on Soil Mechanics and Foundation Engineering, Firenze, May 26-30, Vol. I, pp. 425-428.

Goudreault P. A. and Fellenius, B.H., 2006. UniPile Version 4.0 Users Manual, UniSoft Ltd., Calgary, 76 p.

Goble, G. G., Rausche, F., and Likins, G.E., 1980. The analysis of pile driving—a state-of-the-art. Proceedings of the 1st International Seminar of the Application of Stress-wave Theory to Piles, Stockholm, Edited by H. Bredenberg, A. A. Balkema Publishers Rotterdam, pp. 131 - 161.

GRL, 1993. Background and Manual on GRLWEAP Wave equation analysis of pile driving. Goble, Rausche, Likins Associates, Cleveland.

GRL, 2002. Background and Manual on GRLWEAP Wave equation analysis of pile driving. GRL Engineers Inc., Cleveland.

Grozic, J.L.H., Lunne, T., and Pande, S, 2003. An oedometer test study of the preconsolidation stress of glaciomarine clays. Canadian Geotechnical Journal, 40(5) 857-872.

Hannigan, P.J. 1990. Dynamic monitoring and analysis of pile foundation installations. Deep Foundation Institute, Sparta, New Jersey, 69 p.

Hannigan, P.J., Goble, G.G., Likins, G.E., and Rausche, F. 2006. Design and Construction of Driven Pile Foundations. National Highway Institute Federal Highway Administration, U.S. Department of Transportation, Washington, D.C. 1,200 p.

Hansbo, S., 1960. Consolidation of clay with special reference to influence of vertical sand drains. Swedish Geotechnical Institute, Stockholm, Proceedings No. 18.

Hansbo, S., 1979. Consolidation of clay by band-shaped prefabricated drains. Ground Engineering, London, 12(5) 16-25.

Hansbo, S., 1981. Consolidation of fine-grained soil by prefabricated drains. 10th ICSMFE, Stockholm June 15-19, A.A. Balkema, Rotterdam, pp. 677-682.

Hansbo, S., 1994. Foundation Engineering. Elsiever Science B. V., Amsterdam, Developments in Geotechnical Engineering No. 75, 519 p.

Hansen, J.B., 1961. A general formula for bearing capacity. Ingeniøren International Edition, Copenhagen, Vol. 5, pp. 38 - 46. Also in Bulletin No. 11, Danish Geotechnical Institute Copenhagen, 9 p.

Hansen, J.B., 1963. Discussion on hyperbolic stress-strain response. Cohesive soils. ASCE Journal for Soil Mechanics and Foundation Engineering, 89(SM4) 241 - 242.

Harris, D., Anderson, D.G., Fellenius, B.H., Butler, J.J., and Fischer, G.S., 2003. Design of Pile Foundations for the Sand Creek Byway, Sandpoint, Idaho. Proceedings of Deep Foundation Institute Annual Meeting, Miami, October 23 - 26, 2003.

Holtz, R.D. and Wager, O., 1975. Preloading by Vacuum—Current Prospects. Transportation Research Record 548, pp. 26-29.

Holtz, R.D. and Kovacs, W.D., 1981. An introduction to geotechnical engineering. Prentice-Hall Inc., New York, 780 p.

Holtz, R.D., Jamiolkowski, M. B., Lancelotta, R., and Peroni, R., 1991. Prefabricated vertical drains: Design and Performance. Construction Industry Research and Information Association, CIRIA, London, 131 p.

Hong Kong Geo, 2006. Foundation design and construction. Hong Kong Geotechnical Control Office, No. 1/2006, 376 p.

Housel, W.S., 1956. Field and laboratory correlation of the bearing capacity of hardpan for the design of deep foundation. Proceedings American Society for Materials and Testing, ASTM, Vol. 56, pp. 1,320 - 1,346.

Huang, A.B., Huai, H.H., and Chang, J.W. 1999. The behavior of a compressible silty fine sand, Canadian Geotechnical Journal, 36(1) 88–101.

Hunter A.H and Davisson M.T., 1969. Measurements of pile load transfer. Proceedings of Symposium on performance of Deep Foundations, San Francisco, June 1968, American Society for Testing and Materials, ASTM, Special Technical Publication, STP 444, pp. 106 - 117.

Ismael, N.F., 1985. Allowable bearing pressure from loading tests on Kuwaiti soils. Canadian Geotechnical Journal, 22(2) 151-157.

Iwanowski, T. and Bodare, A., 1988. On soil damping factor used in wave analysis of pile driving. Third International Conference on Application of Stress-wave Theory to Piles, Ottawa, May 25 - 27, 1988, Edited by B.H. Fellenius, pp. 343 - 352.

Jaky, J. 1948. Earth pressure in silos. Proceedings 2nd International Conference on Soil Mechanics and Foundation Engineering, ICSMFE, Rotterdam, Vol. 1, pp. 103 - 107.

Jardine, J., Chow, F., Overy, R., and Standing, J., 2005. ICP design method for driven piles in sands and clays. Thomas Telford Publishing Ltd., London, 106 p.

Jamiolkowski, M., Ghionna, V.N, Lancelotta R, and Pasqualini, E. (1988). New correlations of penetration tests for design practice. Proceedings Penetration Testing, ISOPT-1, DeRuiter (ed.) Balkema, Rotterdam, ISBN 90 6191 801 4, pp 263 - 296.

Janbu, N., Bjerrum, L., and Kjaernsli B, 1956. Veiledning ved losning av fundamenteringsoppgaver. Norwegian Geotechnical Institute, Publication No. 16, 93 p. (in Norwegian).

Janbu, N., 1963. Soil compressibility as determined by oedometer and triaxial tests. European Conference on Soil Mechanics and Foundation Engineering, Wiesbaden, Vol. 1, pp. 19-25, and Vol. 2, pp. 17-21.

Janbu, N., 1965. Consolidation of clay layers based on non-linear stress-strain. Proceedings 6th International Conference on Soil Mechanics and Foundation Engineering, Montreal, Vol. 2, pp. 83-87.

Janbu, N., 1967. Settlement calculations based on the tangent modulus concept. University of Trondheim, Norwegian Institute of Technology, Geotechnical Institution, Bulletin 2, 57 p.

Janbu, N., 1998. Sediment deformations. University of Trondheim, Norwegian University of Science and Technology, Geotechnical Institution, Bulletin 35, 86 p.

Jardine, J., Chow, F., Overy, R., and Standing, J., 2005. ICP design method for driven piles in sands and clays. Thomas Telford Publishing Ltd., London, 105 p.

Jefferies, M.G., and Davies, M.P., 1991. Soil classification using the cone penetration test. Discussion. Canadian Geotechnical Journal, 28(1) 173-176.

Jones G.A., and Rust, E., 1982. Piezometer penetration testing, CUPT. Proceedings of the 2nd European Symposium on Penetration Testing, ESOPT-2, Amsterdam, May 24 - 27, Vol. 2, pp. 607-614.

Justason, M., Mullins, A.G., Robertson, D., and Knight, W. (1998). A comparison of static and Statnamic load tests in sand: a case study of the Bayou Chico bridge in Pensacola, Florida. Proc. of the 7th Int. Conf. and Exhibition on Piling and Deep Foundations, Deep Foundations Institute, Vienna, Austria, 5.22.2 - 5.22.7.

Justason, M. and Fellenius, B.H., 2001. Static capacity by dynamic methods for three bored piles. Discussion. ASCE Journal of Geotechnical Engineering, Vol. 127, No. 12, pp. 1081 - 1084.

Kany M., 1959. Beitrag zur berechnung von flachengrundungen. Wilhelm Ernst und Zohn, Berlin, 201 p. (as referenced by the Canadian Foundation Engineering Manual, 1985).

Karlsrud, K., Clausen, C.J.F., and Aas, P.M., 2005. Bearing capacity of driven piles in clay, the NGI approach. Proceedings of Int. Symp. on Frontiters in Offshore Geotehcnics, Perth, September 2005, A.A. Balkema, Publishers, pp. 775 - 782.

Kjellman, W. 1948a. Accelerating consolidation of fine-grained soils by means of cardboard wicks. Proc. 2nd International Conference on Soil Mechanics and Foundation Engineering, ICSMFE, Rotterdam, pp. 302 - 305.

Kjellman, W. 1948b. Consolidation of fine-grained soils by drain wells. Discussion. ASCE Transactions, Vol. 113, pp. 748 - 751.

Kondner, R.L., 1963. Hyperbolic stress-strain response. Cohesive soils. ASCE Journal for Soil Mechanics and Foundation Engineering 89(SM1) 115-143.

Kulhawy, F.H., 1984. Limiting tip and side resistance: fact or fallacy? Proceedings of the ASCE Symposium on Analysis and Design of Pile Foundations, R. J. Meyer, Editor, San Francisco, pp. 80 - 89.

Kulhawy, F.H. and Mayne, P.W., 1990. Manual on estimating soil properties for foundation design. Electric Power Research Institute, EPRI, 250 p.

Kusabe, O., Maeda, Y., and Ohuchi, M, 1992. Large-scale loading tests of shallow footings in pneumatic caisson. ASCE Journal of Geotechnical Engineering, 118(11) 1681-1695.

Ladd, C.C., 1991. Stability evaluation during staged construction. The Twenty-Second Terzaghi Lecture, ASCE Journal of Geotechnical Engineering 117(4) 540-615.

Larsson, R., and Mulabdic, M., 1991. Piezocone tests in clay. Swedish Geotechnical Institute, SGI, Report No. 42, 240 p.

Lunne, T., Eidsmoen, D., and Howland, J. D., 1986. Laboratory and field evaluation of cone penetrometer. American Society of Civil Engineers, Proceedings of In-Situ 86, ASCE SPT 6, Blacksburg, June 23 - 25, pp. 714 - 729.

Lunne, T. Robertson, P.K., and Powell, J.J.M., 1997. Cone penetration testing in goetechnical practice. Spon Press, London, 312p.

Massarsch, K.R., 1991. Deep Soil Compaction Using Vibratory Probes. American Society for testing and Material, ASTM, Symposium on Design, Construction, and Testing of Deep Foundation Improvement: Stone Columns and Related Techniques, Robert C. Bachus, Ed., London, ASTM Special Technical Publication, STP 1089, Philadelphia, pp. 297-319.

Massarsch, K.R., 1992. Static and Dynamic Soil Displacements Caused by Pile Driving, Keynote Lecture, Fourth International Conference on the Application of Stress-Wave Theory to Piles, the Hague, the Netherlands, September 21-24, 1992, pp.15-24.

Massarsch, K.R., (1994). Settlement Analysis of Compacted Fill. Proceedings, 13th International Conference on Soil Mechanics and Foundation Engineering, ICSMFE, New Delhi, Vol. 1, pp. 325 - 328.

Massarsch, K.R., Westerberg, E., and Broms, B.B., 1997. Footings supported on settlement-reducing vibrated soil nails. 15th International Conference on Soil Mechanics and Foundation Engineering, ICSMFE, Hamburg 97, Vol. 3, pp. 1533 - 1539.

Massarsch, K.M. and Fellenius, B.H., 2002. Dynamic compaction of granular soils. Canadian Geotechnical Journal 39(3) 695-709.

Massarsch, K.R., 2004. Vibrations caused by pile driving. Summer and Fall Featured Articles, Deep Foundation Institute Magazine, Hawthorne, 8 p.

Massarsch, K.R., 2005. Ground vibrations caused by impact pile driving. Keynote Lecture, Second International Conference on Prediction Monitoring, Mitigation, and Evaluation, September 20 - 22, Okayama University, Okayama, Taylor and Francis Group, London, pp. 369-379.

Massarsch, K.R. and Westerberg, E., 1995. The active design concept applied to soil compaction. Proceedings of Bengt B. Broms Symposium in Geotechnical Engineering, Singapore, December 13-15, pp. 262-276.

Massarsch, K.M., and Fellenius, B.H., 2008. Prediction of ground vibrations induced by impact pile driving, The Sixth International Conference on Case Histories in Geotechnical Engineering, Edited by S, Prakash, Missouri University of Science and Technology, August 12-16, 2008, Arlington, Virginia, 38 p.

Mayne, P.W., 2007. Cone penetation testing, a synthesis of highway practice. NCHRP Synthesis 368, Transportation Research Board, Washington, DC, 120 p.

Mayne, P.W., Kulhawy F, and Kay, J.N., 1990. Observations on the development of pore water pressure during piezocone penetration in clays. Canadian Geotechnical Journal 27(4) 418-428.

Mayne, P.W., Christopher, B.R., and DeJong, J. 2001. Geotechnical Site Characterization. Manual on Subsurface Investigations, National Highway Institute Publication No. FHWA NHI-01-031, FHWA, Washington, DC. 305 p.

Mayne, P.W, Christopher, B.R. and DeJong, J. 2002. Manual on Subsurface Investigations, Geotechnical Site Characterization. National Highway Institute Publication No. FHWA NHI-01-031, Federal Highway Administration, U.S. Department of Transportation, Washington, DC. 332 p.

McVay, M.C., Schmertmann, J., Townsend, F, and Bullock, P. (1999). Pile freeze, a field and laboratory study. Final Report, Florida Department of Transportation, Research Center, Contract No. B-7967, 1,314 p.

Meyerhof, G.G., 1951. The bearing capacity of foundations. Geotechnique 2(4) 301-332.

Meyerhof, G.G., 1963. Some recent research on bearing capacity of foundations. Canadian Geotechnical Journal 1(1) 16-26.

Meyerhof, G.G., 1976. Bearing capacity and settlement of pile foundations. The Eleventh Terzaghi Lecture, November 5, 1975. ASCE Journal of Geotechnical Engineering 102(GT3) 195-228.

Meyerhof, G.G., 1995. Development of geotechnical limit state design. Canadian Geotechnical Journal 32(1) 128-136.

Middendorp, P., Bermingham, P., and Kuiper, B. (1992). Statnamic loading test of foundation piles. Proc. 4th Int. Conf. on the Application of Stress Wave Theory to Piles, edited by B.J. Barends, Balkema, Rotterdam, The Netherlands, 581 - 588.

Middendorp, P., Beck, C., and Lambo, A., 2008. Verification of Statnamic load testing with static testing in a cohesive soil type in Germany. Proceedings of the 8th International Conference on the Application of Stress-wave Theory to Piles, pp. 531-536.

Moh, Z.C. and Lin, P.C., 2006. Geotechnical History of the development of the Suvarnabhumi International Airport. Special Issue of the Journal of South-East Asian Geotechnical Society, December 2006, 37(3) 143-170.

Mokwa, R.L., and Duncan, J.M., 2001. Experimental evaluation of lateral load resistance of pile caps. ASCE, Journal of Geotechnical and Geoenvironmental Engineering, 127(2) 185-192.

Moss, R.E.S., Seed, R.B., Kayen, R.E., Stewart, J.P., DerKiureghian, A., and Cetin, K.O., 2006. CPT-based probabilistic and deterministic assessment of in-situ seismic soil liquefaction potential. ASCE, Journal of Geotechnical and Geoenvironmental Engineering, 132(8) 1032-1051.

NAVFAC DM7, 1982. Design Manual for Soil Mechanics, Foundations, and Earth Structures. US Department of the Navy, Washington, DC.

Newmark, N.M., 1935. Simplified computation of vertical stress below foundations. Univ. of Illinois Engineering Experiment Station, Circular 24, Urbana, Illinois, 19 p. (as referenced by Holtz and Kovacs, 1981).

Newmark, N.M., 1942. Influence chart for computation of stresses in elastic foundations. University of Illinois Engineering Experiment Station, Bulletin Series 338, Vol. 61, No. 92, Urbana, Illinois, 28 p. (as referenced by Holtz and Kovacs, 1981).

Nishimura, S., Matsumoto, T., Kusakabe, O., Nishiumi, K., and Yoshizawa, Y., 2000. Case studies of Statnamic loading test in Japan. Proc. 6th Int. Conf. on the Application of Stress Wave Theory to Piles, Edited by S. Niyama and J. Beim, Balkema, Rotterdam, The Netherlands, 591 - 598.

Nordlund, R.L., 1963. Bearing capacity of piles in cohesionless soils. ASCE Journal of Soil Mechanics and Foundation Engineering 89(SM3) 1-35.

OHBDC, 1991. Ontario Highway Bridge Design Code, 3rd. Edition, Code and Commentary, Min. of Transp., Quality and Standards Division, Toronto.

Olsen, R.S., and Farr, V., 1986. Site characterization using the cone penetration test. American Society of Civil Engineers, Proceedings of In-Situ 86, ASCE SPT 6, Blacksburg, June 23 - 25, pp. 854 - 868.

Olsen, R.S., and Malone, P.G., 1988. Soil classification and site characterization using the cone penetrometer test. Proceedings of First International Symposium on Cone Penetration Testing, ISOPT-1, Orlando, March 22 - 24, Vol. 2, pp. 887 - 893.

Olsen, R.S., and Mitchell, J.K., 1995. CPT stress normalization and prediction of soil classification. Proceedings of International Symposium on Cone Penetration Testing, CPT95, Linköping, Sweden, SGI Report 3:95, Vol. 2, pp. 257 - 262.

Osterberg, J.O., 1998. The Osterberg load test method for drilled shaft and driven piles. The first ten years. Great Lakes Area Geotechnical Conference. 17 p. Seventh International Conference and Exhibition on Piling and Deep Foundations, Deep Foundation Institute, Vienna, Austria, June 15 - 17, 1998.

Peck, R.B., Hanson, W.E., and Thornburn, T. H., 1974. Foundation Engineering, Second Edition. John Wiley and Sons Inc., New York, 514 p.

Pecker, A.. 2004 Design and Construction of the Rion Antirion Bridge. Proceedings of the Conference on Geotechnical Engineering for Transportation Projects, , Geo-Trans, ASCE GeoInstitute, Los Angeles July 27 - 31, 2004, Ed. M.K. Yegian and E. Kavazanjian, Vol. 1 pp. 216 - 240.

Perloff W.H. and Baron W., 1976. Soil mechanics principles and applications. John Wiley and Sons, New York, 745 p.

Rausche, F., Moses, F., and Goble. G.G., 1972. Soil resistance predictions from pile dynamics. ASCE Journal of Soil Mechanics and Foundation Engineering 8(SM9) 17-937.

Rausche, F., Goble, G.G., and Likins, G.E., 1985. Dynamic determination of pile capacity. ASCE Journal of the Geotechnical Engineering Division 111(GT3) 367-383.

Riker, R.E. and Fellenius, B.H., 1992. A comparison of static and dynamic pile test results. Proceedings of the Fourth International Conference on the Application of Stress-Wave Theory to Piles, The Hague, September 21-24, pp. 143-152.

Robertson, P.K. Campanella, R.G., and Wightman, A., 1983. SPT-CPT correlations. ASCE Journal of the Geotechnical Engineering Division 109(GT11) 1449–1459.

Robertson, P.K. and Campanella, R.G., 1983. Interpretation of cone penetrometer tests, Part I sand and Part II clay. Canadian Geotechnical Journal, (20)4 718 - 733 and 734 - 745.

Robertson, P.K., and Campanella, R.G. 1985. Liquefaction potential of sands using the cone penetration test. Journal of Geotechnical Engineering, ASCE, 22(GT3) 298–307

Robertson, P. K., Campanella, R. G., Gillespie, D., and Grieg, J., 1986. Use of piezometer cone data. Proceedings of ASCE In-Situ 86 Specialty Conference, Edited by S. Clemence, Blacksburg, June 23 - 25, Geotechnical Special Publication GSP No. 6, pp. 1263 - 1280.

Robertson, P.K. and Campanella, R.G., 1986. Guidelines for use, interpretation, and application of the CPT and CPTU. Manual, Hogentogler & Company, Inc. 196 p.

Robertson, P.K., 1986. In-Situ testing and its application to foundation engineering. 1985 Canadian Geotechncial Colloquium, Canadian Geotechnical Journal 23(4) 573-594.

Robertson, P.K., 1990. Soil classification using the cone penetration test. Canadian Geotechnical Journal 27(1) 151-158.

Robertson, P.K. and (Fear) Wride, C.E., 1998. Evaluating cyclic liquefaction potential using the cone penetration test. Canadian Geotechnical Journal 35(3) 442-459.

Roscoe, K.H., Schofield, A.N., and Wroth, C.P. (1958). On the yielding of soils. Geotechnique 8(1) 22-53.

Salem, H.S, Lavergne, H.R., and Fellenius, B.H., 2008. Using dynamic pile testing to overcome surprising soil variations. Deep Foundations Institute, 33rd Annual Conference on Deep Foundations and 11th International Conference on Piling and Deep Foundations, October 15-17, 2008, New York, 7 p.

Sampaco, K., Pham, H., and Anderson, D. 2008. The Golden Ears Bridge design-build project: foundation design for segment 4 approach structures. Proceedings of the FHWA, and SCDOT Sixth National Seismic Conference on Bridges and Highways, Charleston, South Carolina, July 27-30, Paper 2B1-2, 12 p.

Sanglerat, G., Nhim, T.V., Sejourne, M., and Andina, R., 1974. Direct soil classification by static penetrometer with special friction sleeve. Proceedings of the First European Symposium on Penetration Testing, ESOPT-1, June 5 - 7, Stockholm, Vol. 2.2, pp. 337 - 344.

Schmertmann, J.H., 1970. Static cone to compute settlement over sand. ASCE Journal Soil Mechanics and Foundation Engineering 96(SM3) 1011-1043.

Schmertmann, J.H. 1975. Measurement of In-situ Shear Strength. Proceedings of ASCE Geotechnical Division, Specialty Conference on In-Situ Measurement of Soil Properties, June 1 - 4, 1974, Raleigh, NC, Vol. 2. pp. 57 - 138.

Schmertmann, J.H., 1978. Guidelines for cone penetration test, performance, and design. U.S. Federal Highway Administration, Washington, Report FHWA-TS-78-209, 145 p.

Seah, T.H., 2006. Design and construction of ground improvement works at Suvarnabhumi International Airport. Special Issue of the Journal of South-East Asian Geotechnical Society, December 2006, 37(3) 171-188.

Searle, I.W., 1979. The interpretation of Begemann friction jacket cone results to give soil types and design parameters. Proceedings of 7th European Conference on Soil Mechanics and Foundation Engineering, ECSMFE, Brighton, Vol. 2, pp. 265 - 270.

Seed, H.B., 1976. Evaluation of soil liquefaction effects on level ground during earthquakes. Liquefaction problems in Geotechnical Engineering, Proceedings of ASCE Annual Convention and Exposition, Philadelphia, pp. 1 - 104.

Senneset, K., Sandven, R., and Janbu, N., 1989. Evaluation of soil parameters from piezocone test. In-situ Testing of Soil Properties for Transportation, Transportation Research Record, No. 1235, Washington, D. C., pp. 24 - 37.

Shen Bao-Han and Niu Dong-Sheng, 1991. A new method for determining the yield load of piles. Proceedings of the Fourth International Conference on Piling and Deep Foundations, Deep Foundation Institute, Stresa April 7 - 12, Balkema Publishers, Vol. 1, pp. 531 - 534.

Smith, E.A.L., 1960. Pile driving analysis by the wave equation. Journal of the Soil Mechanics and Foundation Engineering Division, Proceedings ASCE 86(SM4) 35-61.

Stark, T.D., and Olsen, S.M. 1995. Liquefaction resistance using CPT and field case histories. Journal of Geotechnical Engineering, ASCE, 121(GT12) 856–869.

Stoll, M.U.W., 1961. Discussion on “New approach to pile testing” by T. Whitaker and R. W. Cooke, Proceedings 5th International Conference on Soil Mechanics and Foundation Engineering, Paris France, Vol. 3, pp. 279 - 281.

Swedish State Railways Geotechnical Commission, 1922. Statens Järnvägars Geotekniska Kommission – Slutbetänkande. Swedish State Railways, Bulletin 2 (in Swedish with English summary), 228 p.

Tanaka, H., Ritoh, F., and Omukai, N, 2002. Quality of samples retrieved from great depth and its influence on consolidation properties. Canadain Geotechnical Journal (39)6 1288-1301.

Taylor, D.W., 1948. Fundamentals of soil mechanics. John Wiley & Sons, New York, 700 p.

Tschebotarioff, G.P., 1951. Soil mechanics, foundations, and earth structures. McGraw-Hill Book Company Inc., New York, 655 p.

Terzaghi, K., 1943. Theoretical Soil Mechanics. John Wiley and Sons, New York, 511 p.

Terzaghi, K. and Peck, R.B., 1948. Soil Mechanics in Engineering Practice. John Wiley and Sons, New York, 566 p.

Terzaghi, K., 1954. Anchored bulkheads. ASCE Transactions, Vol. 119, pp. 1243 - 1324.

Terzaghi, K., 1955. Evaluation of coefficients of subgrade reaction. Geotechnique 5(4) 297-326.

Tomlinson, M.J., 1980. Foundation design and construction, Fourth Edition. Pitman Publishing Inc., London, 793 p.

Tumay, M. T., and Fakhroo, M., 1981. Pile capacity in soft clays using electric QCPT data. ASCE Cone Penetration Testing and Experience, St. Louis, October 26 30, pp. 434 455.

Vesic, A.S., 1973. Analysis of ultimate loads of shallow foundations. ASCE Journal of Soil Mechanics and Foundation Engineering 99(SM1) 45-73.

Vesic, A.S., 1975. Bearing capacity of shallow foundations. In Foundation Engineering Handbook, edited by H.F. Winterkorn and H-Y Fang, VanNostrand Reinhold Co., New York, pp. 121 - 147.

Vijayvergiya, V.N. and Focht, J.A. Jr., 1972. A new way to predict the capacity of piles in clay. Fourth Annual Offshore Technology Conference, Houston, Vol. 2, pp. 865 - 874.

Vos, J.D., 1982. The practical use of CPT in soil profiling, Proceedings of the Second European Symposium on Penetration Testing, ESOPT-2, Amsterdam, May 24 - 27, Vol. 2, pp. 933 - 939.

Westergaard, H.M., 1938. A problem of elasticity suggested by a problem in soil mechanics: A soft material reinforced by numerous strong horizontal sheets. In Contributions to the Mechanics of Solids, Stephen Timoshenko 60th Anniversary Volume, MacMillan, New York, pp. 260 - 277 (as referenced by Holtz and Kovacs, 1981).

Yang, Y., Tham, L.G., Lee, P.K.K., and Yu, F., 2006. Observed performance of long steel H-piles jacked into sandy soils. ASCE Journal of Geotechnical and Environmental Engineering 132(1) 24-35.

Youd, T.L., Idriss, I.M, Andrus, R.D., Arango, I., Castro, G., Christian, J.T., Dobry, R., Finn, W.D.L., Harder, L.F., Hynes, M.E., Ishihara, K., Koester, J.P., Liao, S.S.C., Marcuson, W.F., Martin, G.R., Mitchell, J.K., Moriwaki, Y., Power, M.S., Robertson, P.K., Seed, R.B., Stokoe, K.H. 2001. Liquefaction resistance of soils: Summary report from the 1996 NCEER and 1998 NCEER/NSF Workshops on evaluation of liquefaction resistance of soils, ASCE Journal of Geotechnical and Geoenvironmental Engineering 127(4) 297–313.

CHAPTER 15

INDEX